



This is a digital copy of a book that was preserved for generations on library shelves before it was carefully scanned by Google as part of a project to make the world's books discoverable online.

It has survived long enough for the copyright to expire and the book to enter the public domain. A public domain book is one that was never subject to copyright or whose legal copyright term has expired. Whether a book is in the public domain may vary country to country. Public domain books are our gateways to the past, representing a wealth of history, culture and knowledge that's often difficult to discover.

Marks, notations and other marginalia present in the original volume will appear in this file - a reminder of this book's long journey from the publisher to a library and finally to you.

### Usage guidelines

Google is proud to partner with libraries to digitize public domain materials and make them widely accessible. Public domain books belong to the public and we are merely their custodians. Nevertheless, this work is expensive, so in order to keep providing this resource, we have taken steps to prevent abuse by commercial parties, including placing technical restrictions on automated querying.

We also ask that you:

- + *Make non-commercial use of the files* We designed Google Book Search for use by individuals, and we request that you use these files for personal, non-commercial purposes.
- + *Refrain from automated querying* Do not send automated queries of any sort to Google's system: If you are conducting research on machine translation, optical character recognition or other areas where access to a large amount of text is helpful, please contact us. We encourage the use of public domain materials for these purposes and may be able to help.
- + *Maintain attribution* The Google "watermark" you see on each file is essential for informing people about this project and helping them find additional materials through Google Book Search. Please do not remove it.
- + *Keep it legal* Whatever your use, remember that you are responsible for ensuring that what you are doing is legal. Do not assume that just because we believe a book is in the public domain for users in the United States, that the work is also in the public domain for users in other countries. Whether a book is still in copyright varies from country to country, and we can't offer guidance on whether any specific use of any specific book is allowed. Please do not assume that a book's appearance in Google Book Search means it can be used in any manner anywhere in the world. Copyright infringement liability can be quite severe.

### About Google Book Search

Google's mission is to organize the world's information and to make it universally accessible and useful. Google Book Search helps readers discover the world's books while helping authors and publishers reach new audiences. You can search through the full text of this book on the web at <http://books.google.com/>





HARVARD UNIVERSITY



STUDENTS' ASTRONOMICAL  
LABORATORY

RESERVE  
LIBRARY















# THE ASTROPHYSICAL JOURNAL



**THE UNIVERSITY OF CHICAGO PRESS**  
**CHICAGO, ILLINOIS**

---

**THE CAMBRIDGE UNIVERSITY PRESS**  
**LONDON**

**THE MARUZEN-KABUSHIKI-KAISHA**  
**TOKYO, OSAKA, KYOTO, FUKUOKA, SENDAI**

**THE MISSION BOOK COMPANY**  
**SHANGHAI**

THE  
ASTROPHYSICAL JOURNAL

An International Review of Spectroscopy and  
Astronomical Physics

EDITORS

GEORGE E. HALE  
*Mount Wilson Observatory of the Carnegie  
Institution of Washington*

EDWIN B. FROST  
*Yerkes Observatory of the  
University of Chicago*

HENRY G. GALE  
*Ryerson Physical Laboratory of the  
University of Chicago*

COLLABORATORS

JOSEPH S. AMES, *Johns Hopkins University*; ARISTARCH BELOFOLSKY, *Observatoire de Poulkova*;  
WILLIAM W. CAMPBELL, *Lick Observatory*; HENRY CREW, *Northwestern University*; CHARLES  
FABRY, *Université de Marseille*; ALFRED FOWLER, *Imperial College, London*; CHARLES S.  
HASTINGS, *Yale University*; HEINRICH KAYSER, *Universität Bonn*; ALBERT A.  
MICHELSON, *University of Chicago*; HUGH F. NEWALL, *Cambridge University*;  
ERNEST F. NICHOLS, *Yale University*; ALFRED PEROT, *Paris*; CARL  
RUNGE, *Universität Göttingen*; HENRY N. RUSSELL, *Princeton  
University*; SIR ARTHUR SCHUSTER, *The University,  
Manchester*; FRANK SCHLESINGER, *Yale  
Observatory*

VOLUME LI  
JANUARY-JUNE, 1920



THE UNIVERSITY OF CHICAGO PRESS  
CHICAGO, ILLINOIS



**Published**  
**January, March, April, May, June, 1920**

**Composed and Printed By**  
**The University of Chicago Press**  
**Chicago, Illinois, U.S.A.**

# CONTENTS

## NUMBER I

	PAGE
OBSERVATIONS OF THE TOTAL SOLAR ECLIPSE OF MAY 29, 1919. C. G. Abbot and A. F. Moore . . . . .	I
BRIGHT NEBULAE AND STAR CLUSTERS IN SAGITTARIUS AND SCUTUM. John C. Duncan . . . . .	4
THE CHARACTERISTICS OF ABSORPTION SPECTRA PRODUCED BY THE ELECTRIC FURNACE. Arthur S. King . . . . .	13
REVISION OF THE SERIES IN THE SPECTRUM OF BARIUM. F. A. Saunders	23
THE SPECTRUM OF ELECTRICALLY EXPLODED WIRES. J. A. Anderson .	37
STUDIES BASED ON THE COLORS AND MAGNITUDES IN STELLAR CLUSTERS. XV. Harlow Shapley . . . . .	49
MINOR CONTRIBUTIONS AND NOTES: The Problem of the $\delta$ Cephei Variables. J. G. Hagen . . . . .	62

## NUMBER II

ANNIBALE RICCO, 1844-1919. Giorgio Abetti . . . . .	65
DIFFRACTION OF A TELESCOPIC OBJECTIVE IN THE CASE OF A CIRCULAR SOURCE OF LIGHT. H. Nagaoka . . . . .	73
ON COMET 1919b AND ON THE REJECTION OF A COMET'S TAIL. E. E. Barnard . . . . .	102
PRELIMINARY OBSERVATIONS OF THE ZEEMAN EFFECT FOR ELECTRIC FURNACE SPECTRA. Arthur S. King . . . . .	107
THE SPECTRUM OF NOVA OPHIUCHI 1919. Walter S. Adams and Cora G. Burwell . . . . .	121
REVIEWS: Theorie der Strahlung und der Quanten, Arthur March (A. C. Lunn), 127; Advanced Lecture Notes on Light, J. R. Eccles (F.), 128.	
NOTE CONCERNING RETIREMENT OF PROFESSOR KAYSER . . . . .	128

## NUMBER III

POLARIZATION OF RADIATION BY GRATINGS. L. R. Ingersoll . . .	129
STUDIES BASED ON THE COLORS AND MAGNITUDES IN STELLAR CLUSTERS. XVI. Harlow Shapley and Helen N. Davis . . . . .	140



	PAGE
OBSERVATIONS OF THE ELECTRIC FURNACE SPECTRA OF COBALT, NICKEL, BARIUM, STRONTIUM, AND CALCIUM IN THE REGION OF GREATER WAVE-LENGTH. Arthur S. King . . . . .	179
THE ORBITS OF THE SPECTROSCOPIC COMPONENTS OF BOSS 5026. W. E. Harper . . . . .	187
PREPARATION OF ABSTRACTS . . . . .	190
NOTICE TO CONTRIBUTORS . . . . .	192

---

#### NUMBER IV

THE ECLIPSING VARIABLE STAR, $\lambda$ TAURI. Joel Stebbins . . . . .	193
THE ELLIPSOIDAL VARIABLE STAR, $\pi^5$ ORIONIS. Joel Stebbins . . . . .	218
A MODIFICATION OF THE ELECTRON THEORY OF DISPERSION TO ACCOUNT FOR THE CHANGE OF THE REFRACTIVE INDEX WITH TEMPERA- TURE. E. O. Hulburt . . . . .	223
FINE STRUCTURE OF THE NEAR INFRA-RED ABSORPTION BANDS OF THE HALOGEN ACIDS. Walter F. Colby . . . . .	230
NOTE ON THE AIR LINES IN SPARK SPECTRA FROM $\lambda$ 5927 TO $\lambda$ 8719. Paul W. Merrill . . . . .	236
THE GOLD-POINT PALLADIUM-POINT BRIGHTNESS RATIO. Edward P. Hyde and W. E. Forsythe. . . . .	244
MINOR CONTRIBUTIONS AND NOTES: Five Oe5 Stars with Variable Radial Velocities, W. Carl Rufus, 252; The Parallax of the B-Star Boss 1517, J. Voûte, 254.	
PREPARATION OF ABSTRACTS . . . . .	255

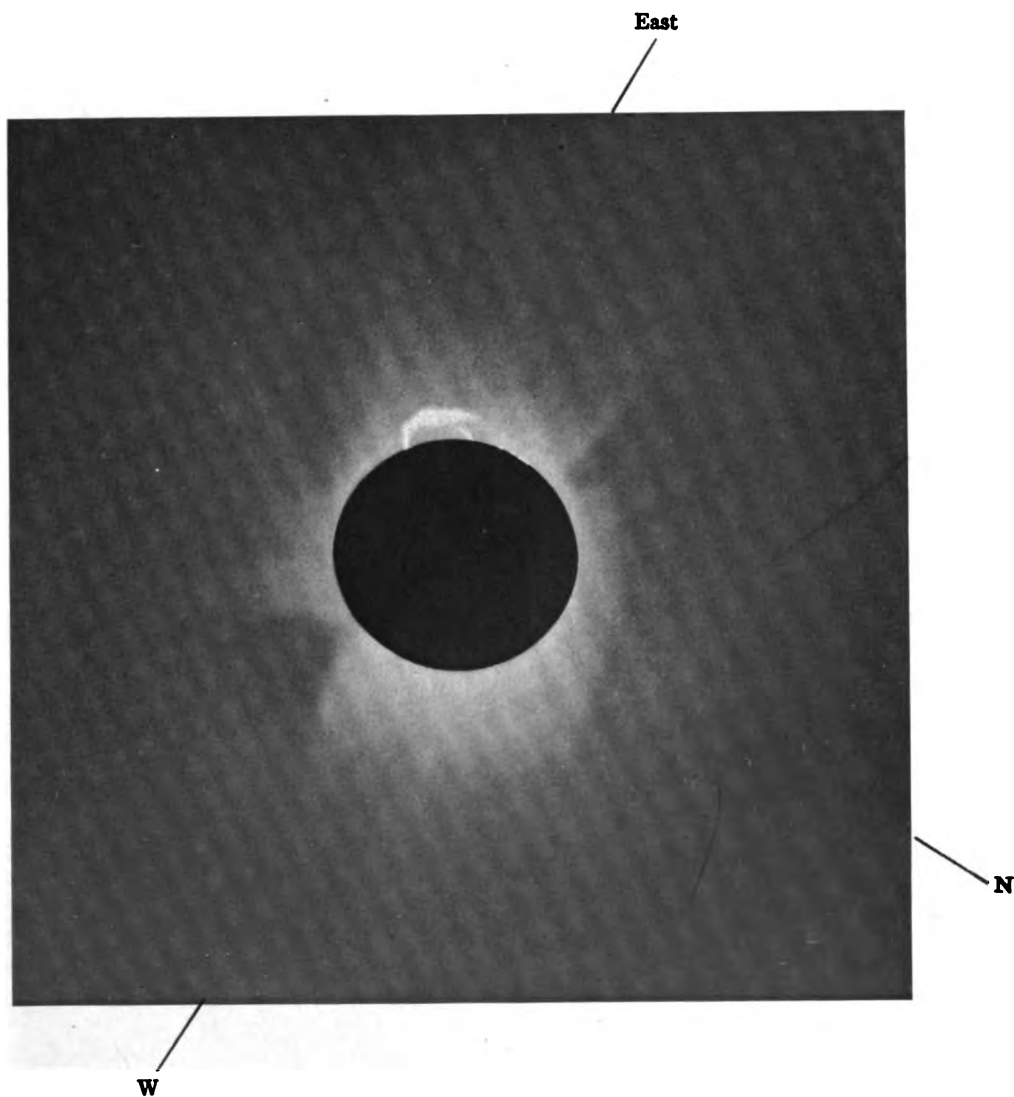
---

#### NUMBER V

ON THE APPLICATION OF INTERFERENCE METHODS TO ASTRONOMICAL MEASUREMENTS. A. A. Michelson . . . . .	257
APPLICATION OF MICHELSON'S INTERFEROMETER METHOD TO THE MEASUREMENT OF CLOSE DOUBLE STARS. J. A. Anderson . . . . .	263
PHOTOGRAPHS OF NEBULAE WITH THE 60-INCH REFLECTOR, 1917-1919. Francis G. Pease . . . . .	276
REVIEW: Problems of Cosmogony and Stellar Dynamics, J. H. Jeans (W. D. MacMillan) . . . . .	309
INDEX . . . . .	334



**PLATE I**



**TOTAL ECLIPSE OF MAY 29, 1919**

**As photographed at La Paz, Bolivia, by expedition from Smithsonian Observatory**

# THE ASTROPHYSICAL JOURNAL

AN INTERNATIONAL REVIEW OF SPECTROSCOPY  
AND ASTRONOMICAL PHYSICS

VOLUME LI

JANUARY 1920

NUMBER I

## OBSERVATIONS OF THE TOTAL SOLAR ECLIPSE OF MAY 29, 1919

By C. G. ABBOT AND A. F. MOORE

### ABSTRACT

*Solar corona, during the eclipse of May 29, 1919.*—The expedition from the Smithsonian Institution, stationed at El Alto, Bolivia, obtained two very good photographs of the corona, showing many narrow streamers extending nearly two diameters in almost every direction, and a great sickle-shaped *prominence* (see Plate I). The corona was of a type intermediate between that of a sun-spot maximum and that of a sun-spot minimum. A brief account of the expedition is given.

The Smithsonian Institution expedition to observe the eclipse consisted of C. G. Abbot and A. F. Moore. Abbot photographed the corona with twin telescopes of 7.6 cm (3 in.) aperture and 335 cm (11 ft.) focus, and Moore carried on pyranometer observations during the eclipse, as well as at the same time on the day preceding, and at intervals during the night preceding. The present note relates only to the photographic observations, and is mainly for the purpose of reproducing in the *Astrophysical Journal* the coronal photograph which was secured. The full publication of the work will be made in the *Smithsonian Miscellaneous Collections*.

The station was located at El Alto, Bolivia, on the rim of the canyon in which La Paz is situated. The approximate location of



El Alto is: latitude,  $16^{\circ}30'$  S.; longitude,  $4^{\text{h}}33^{\text{m}}$  W.; altitude, 4120 meters. Although at a high altitude the sky is rarely free from clouds, but very favorable conditions existed during the total and partial phases of the eclipse.

#### PHOTOGRAPHIC OBSERVATIONS

Owing to the shortness of the time available for preparation after the expected arrival of the party at La Paz, every possible arrangement had been made in advance to set up the photographic apparatus quickly. For this purpose each of the three boxes which contained the apparatus was designed in form and construction so as to act as a support to some of the photographic outfit when filled with stones and laid upon the floor of any room which might be found available for the observations. Also every detail of the apparatus was carried without any dependence on such lumber or other material as might ordinarily be available. It was very fortunate that this was so, for the expedition was delayed so that the apparatus was only set up two days before the eclipse.

The briefness of the time available for preliminary tests was unfortunate in one respect. Owing to the very low altitude of the sun (only twenty minutes after sunrise) when the eclipse took place, the refraction of the terrestrial atmosphere was continually changing at the time, so that the apparent motion of the sun in the sky was at a variable rate, not agreeing with that which prevailed later in the day. A test of the clock was made on the day preceding the eclipse, but owing to cloudiness it was not possible to follow quite up to the time of the eclipse. Such observations as were made on the preceding day, however, indicated that the clockwork moved a little too slowly and so the rate of the clock was increased about 3 per cent with the expectation of more exactly following the sun at the time of the eclipse. Unfortunately this proved to be too much of a correction so that the clock moved a little too fast during the eclipse, and the images of the moon are not as truly round as they should be.

The two camera telescopes were rigidly fastened together. Exposures were made by the removal of the two pasteboard boxes which covered the ends of the tubes but were separately mounted

on hinged supports independent of the cameras. As the requisite time of exposure was not accurately known, it was arranged to expose one of the telescopes for 1 minute 30 seconds, the other for 2 minutes 45 seconds.

The program was carried through without any accident, and upon developing the two negatives both were found to be very good, but the exposure of 1 minute 30 seconds seemed to show quite as much extension of the corona as that of 2 minutes 45 seconds. As less drift of the clock occurred during the shorter interval than during the longer we give in the accompanying illustration (Plate I) only the result of the shorter exposure.

There were a great number of sharp, relatively narrow coronal streamers extending nearly two diameters in almost every direction from the sun. Decided evidences occur of coronal streamers at the north and south poles similar to those which are found at times of sun-spot minimum. The corona on this occasion was of a type intermediate between that of a sun-spot maximum, equally extensive in all directions, and that of a sun-spot minimum, with relatively short polar streamers and long equatorial extensions. There was also on the following limb of the sun a great sickle-shaped prominence which extended up from the sun to about one-fourth of a radius, then turned sharply around with a very long extension parallel to the sun's surface. Later in the day this prominence was repeatedly photographed with spectroheliographs in the United States, and then extended as a complete arch of very great height and span.

Taking into account the great length and beauty of the coronal streamers, the splendid crimson prominence throwing its glory over all, and the fact that the eclipse was observed so near sunrise from so great an elevation as 14,000 feet, with a snow-covered range of mountains upward of 20,000 feet high as a background for the phenomenon, it seemed to the observers to be the grandest eclipse phenomenon which they had ever seen.

ASTROPHYSICAL OBSERVATORY  
SMITHSONIAN INSTITUTION  
WASHINGTON, D.C.  
December 1919

BRIGHT NEBULAE AND STAR CLUSTERS IN  
SAGITTARIUS AND SCUTUM  
PHOTOGRAPHED WITH THE 60-INCH REFLECTOR<sup>1</sup>

By JOHN C. DUNCAN

ABSTRACT

*Photographs* obtained with the 60-inch reflector are reproduced in five plates. They include the following interesting objects:

- In Sagittarius:* Nebula N.G.C. 6523 (Messier 8);  
Star Cluster N.G.C. 6530 (Messier 8);  
Globular Star Cluster N.G.C. 6656 (Messier 22).  
*In Scutum:* Star Cluster and Nebula N.G.C. 6611 (Messier 16);  
Swan Nebula N.G.C. 6618 (Messier 17).

The author refers to previous observations regarding these objects, calls attention to interesting details and identifies some of the brighter stars. Plate VI is the first large-scale photograph of the Globular Cluster (Messier 22) which has been published. On this plate there are about 75,000 stars, of which Shapley estimates that one-third are cluster stars.

*Dark markings* are clearly evident in the photographs of the nebulae N.G.C. 6523, 6611, and 6618.

*Spectrum of nebula N.G.C. 6611 (Messier 16).*—A spectrogram obtained by Slipher shows the nebulium lines weaker than the hydrogen series, and indicates that the nebula has a small radial velocity.

*Star Córdoba No. 12431.* The right ascension of this star seems to be incorrectly given in the Córdoba Observatory Catalogue.

Long-exposure photographs of nebulae and clusters made with the 60-inch reflector have been confined chiefly to objects north of the equator because of the better seeing at the high altitudes which they attain. It was the writer's privilege, during the summers of 1918 and 1919, to use this instrument on a number of nights, and the opportunity was utilized for photographing some of the more interesting of the objects that lie farther south. The four objects that form the subject of this article lie within a few degrees of each other in the rich region south of the bright star-cloud of Scutum Sobieskii, a region that includes also the Trifid nebula.

The photographs were made at the 25-foot focus of the 60-inch mirror, which was used at its full aperture. The plates were backed with a burnt-sienna mixture to prevent halation.

<sup>1</sup> *Contributions from the Mount Wilson Observatory*, No. 177.





PLATE II



MESSIER 8, CONSISTING OF THE NEBULA N.G.C. 6523 AND THE STAR CLUSTER N.G.C. 6530

Scale: 1 mm = 16".8

Enlargement 1.64

*Plate II.*—The chaotic Nebula N.G.C. 6523 and the Star Cluster N.G.C. 6530 (Messier 8), in Sagittarius. Center of plate (1900.0),  $\alpha = 17^h 57^m 9$ ,  $\delta = -24^\circ 21'$ . 1919, June 27. Exposure three hours. Seed 23 plate. Seeing very good. In preparing the positive for reproduction, the brightest part of the nebula was given a longer exposure than the remainder of the plate in order to bring out the detail.

The object known as Messier 8 is a bright open cluster (N.G.C. 6530) combined with a bright nebula (N.G.C. 6523), the combination being visible to the unaided eye as a hazy condensation in the Milky Way, not far from  $\mu$  Sagittarii. It is a little more than one degree south of the Trifid nebula, which the nebula of Messier 8 much resembles. Messier's description<sup>1</sup> is concerned chiefly with the cluster, his only reference to the nebula being the remark that near the cluster is a bright star ( $\eta$  Sagittarii) that is "surrounded by a very feeble light"; but modern instruments show that the nebula is one of the brightest and most extraordinary in the sky. Barnard<sup>2</sup> says of it that, "though seldom mentioned, it is far more remarkable than the celebrated Trifid." Sir John Herschel<sup>3</sup> gives a description and an elaborate drawing, and eloquent descriptions are also given in the catalogues of celestial objects of Smyth and Webb. Barnard has described the nebula in considerable detail,<sup>4</sup> and published photographs<sup>5</sup> of it made with the Willard lens. The only large-scale photograph that, to my knowledge, has appeared in any astronomical publication is the fine Crossley photograph<sup>6</sup> made by Keeler in 1899, although excellent plates have been obtained by Ritchey and Pease at Williams Bay, by Lampland at Flagstaff, and doubtless by others. Keeler<sup>7</sup> describes the spectrum as consisting of three bright lines. Lampland<sup>8</sup> has detected in the nebula eighteen variable stars.

The position given by Dreyer for N.G.C. 6523 is that of the brightest part of the nebula, at the left of the center of Plate II.

<sup>1</sup> Quoted by Flammarion, *L'Astronomie*, 32, 26, 1918.

<sup>2</sup> *Astronomy and Astrophysics*, 13, 792, 1894.

<sup>3</sup> *Cape Observations*, 1847, p. 116 and Plate I.

<sup>4</sup> *Loc. cit.* and *Astronomische Nachrichten*, 130, 234, 1892.

<sup>5</sup> *Publications of the Lick Observatory*, 11, 1913, Plates 51 and 52.

<sup>6</sup> *Ibid.*, 8, 1908, Plate 56. <sup>7</sup> *Ibid.*, 3, 205, 1904. <sup>8</sup> *Popular Astronomy*, 26, 32, 1919.

The center of the bright cluster appears on the right side of the plate, about  $10''$  farther west than Dreyer's position for N.G.C. 6530. Perhaps the most striking feature of the photograph is the dark rift that cleaves the nebula from northwest to southeast, passing between the cluster and the brightest part of the nebula. This rift is not perfectly dark, but contains certain bright filaments that recall the nebula about Merope in the Pleiades. This filamentous structure occurs also on the left side of the plate, east of the bright star  $\gamma$  Sagittarii. Besides the great rift, there are many smaller, irregular, sharply defined dark markings in all parts of the nebula, resembling the dark regions of the neighboring Milky Way which are interpreted by Barnard as due to obscuring matter. Some of these small dark markings occur in the very brightest part of the nebula; these, however, are not so dark as those in the fainter portions and would not be easily seen in the reproduction had not this part of the plate been given a longer exposure than the remainder in making the positive. Possibly the absorbing material is not perfectly opaque, but allows some light from the brightest nebulosity to pass through. The abrupt edge of the faint nebulosity on the north and south sides of the nebula may perhaps also be due to obscuring masses. The dark spots in Messier 8 suggested to Miss Clerke the name of "Lagoon";<sup>1</sup> but she seems to have found the name unsatisfactory, as it does not appear in the second edition of her book. Professor Ritchey applies the term "chaotic" to nebulae of this class.

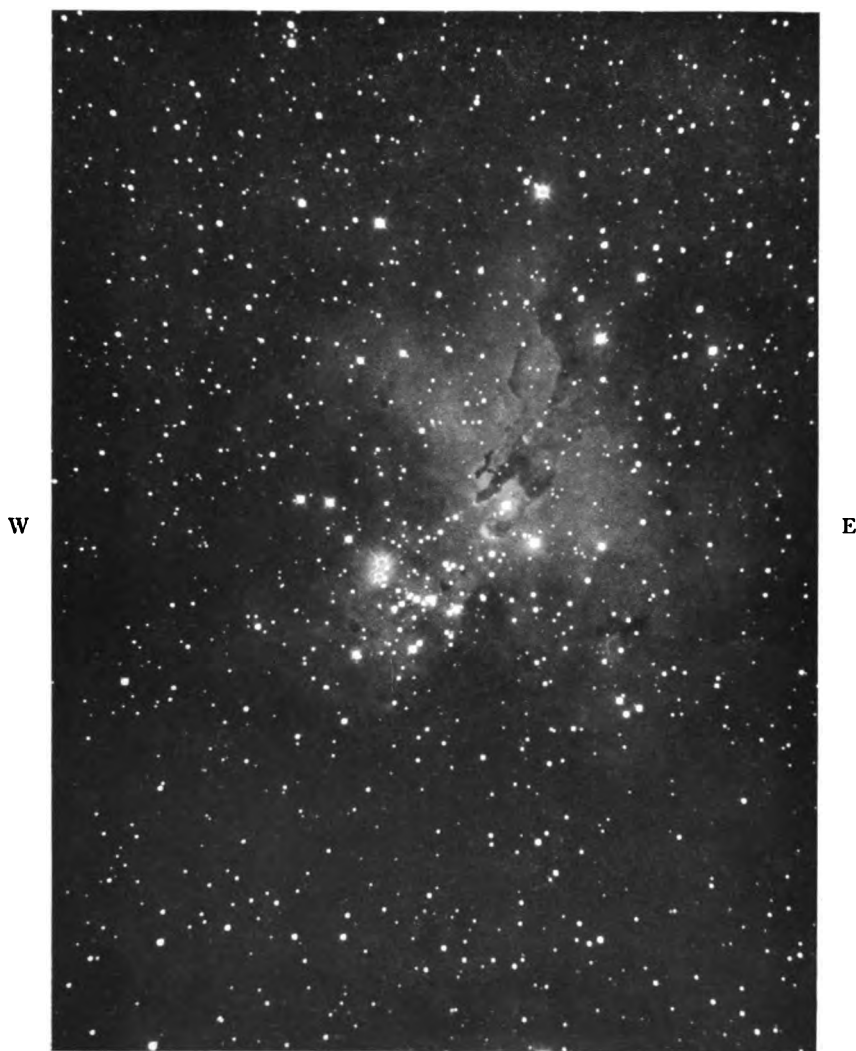
Two of the dark spots shown in Plate II are listed in Professor Barnard's "Catalogue of 182 Dark Markings in the Sky."<sup>2</sup> No. 88 of that catalogue is  $38$  mm from the right edge and  $39$  mm from the bottom, and No. 89 is  $13$  mm from the right and  $53$  mm from the top, near the bright star Córdoba 12446—not very well brought out in the engraving, though easily seen on the original plate. South of the stars Córdoba 12431 and 12437 and extending eastward almost to 12446 is a remarkable irregular bright line of nebulosity which suggests a thin fold turned edgewise to the observer. About  $3'$  west and  $1'$  south of Córdoba 12431 is a shorter, brighter line of

<sup>1</sup> *The System of the Stars*, first edition (1890), p. 284.

<sup>2</sup> *Astrophysical Journal*, 49, 16, 1919.



PLATE III



THE NEBULA AND STAR CLUSTER N.G.C. 6611=M 16

Scale: 1 mm=14".4      Enlargement 1.85



the same nature. In the upper right corner of the plate; about 7' south of Córdoba 12446, is a fainter line of the same general appearance. The appearance of slightly brighter nebulosity just below Córdoba 12466 is due to halation.

The positions and magnitudes of bright stars given in the following table were taken from the *Catálogo de 15,975 Estrellas* of the Córdoba Observatory.<sup>1</sup> The right ascension of No. 12431 as given in that catalogue seems to be in error, as the only star comparable with it in brightness appears on the photograph with about 2<sup>s</sup> less right ascension. It is stated in the notes at the end of the Córdoba publication that the position of this star rests on a single observation.

CÓRDOBA NO.	NAME	VISUAL MAG.	PLACE, 1900.0		DISTANCE IN MM FROM EDGE OF PLATE
			$\alpha$	$\delta$	
12383.....	7 Sagittarii	5.9	17 <sup>h</sup> 56 <sup>m</sup> 43 <sup>s</sup> .33	-24°16'53".1	L 4, B 50
12403.....		9.4	57 37.20	22 12.8	L 47, T 56
12407.....	9 Sagittarii	6.0	44.55	21 45.6	L 53, T 57
12411.....		8.1	49.02	18 52.7	L 57, B 57
12417.....		9.0	58 7.09	14 46.0	R 48, B 43
12418.....		9.6	7.42	5 41.3	R 48, B 11
12420.....		8.2	7.73	11 9.6	R 48, B 30
12430.....		8.0	17.84	23 22.2	R 40, T 52
12431.....		9.0	18.17(?)	26 27.3	R 42, T 41
12435.....		8.4	25.65	9 50.1	R 33, B 25
12437.....		8.8	27.89	27 2.4	R 31, T 39
12446.....	Piazzi 342	8.0	59 2.52	24 12.3	R 3, T 49

The following defects in Plate II might prove deceptive:

DESCRIPTION	DISTANCE IN MM FROM EDGE OF PLATE
Round, like faint star.....	R 31, B 58
Round, like faint star.....	R 22, B 64
Irregular, nebulous, 1 mm diameter.....	R 13, B 56

*Plate III.*—The Nebula and Star Cluster N.G.C. 6611 (Messier 16), in Scutum Sobieskii. Center of plate (1900.0),  $\alpha = 18^h 13^m 1^s$ ,  $\delta = -13^\circ 51'$ . 1919, August 25–26. Exposure 205 minutes. Seed 30 plate. Thick sky and poor seeing.

This object was discovered by Messier in 1764.<sup>2</sup> In the catalogues of Herschel, Webb, Smyth, and Dreyer it is described simply

<sup>1</sup> *Resultados del Observatorio Nacional Argentino en Córdoba*, 22, 1913.

<sup>2</sup> Captain W. H. Smyth, *A Cycle of Celestial Objects*, 2, 415, 1844.

as a star cluster, no mention being made of the nebula, though Messier says<sup>1</sup> the stars are "mixed with a feeble light." The nebula was detected photographically by Barnard<sup>2</sup> in 1895 and Roberts<sup>3</sup> in 1897. Though Messier seems to have been the only early observer to perceive the nebula visually, it is no more difficult than the nebula in the Pleiades, and I have seen it easily with the 12-inch refractor of the Whittin Observatory.

S. DM.	VISUAL MAG.	PLACE, 1855.0		DISTANCE IN MM FROM EDGE OF PLATE
		$\alpha$	$\delta$	
-13°49'14.....	9.5	18 <sup>h</sup> 9 <sup>m</sup> 49 <sup>s</sup> .1	-13°47'.9	L 10, B 49
15.....	9.2	52.6	35.8	L 13, B 1
17.....	9.5	55.2	39.7	L 14, B 15
-14 49'85.....	8.9	10 13.0	-14 7.7	L 31, T 4
86.....	9.1	13.8	2.7	L 33, T 26
-13 49'20.....	9.2	14.3	53.3	L 33, T 64
21.....	9.2	17.0	53.2	L 37, T 65
23.....	9.3	19.4	48.2	L 40, B 52
24.....	9.5	20.6	57.5	L 41, T 46
25.....	8.3	22.7	50.7	L 43, B 63
26.....	8.3	23.2	50.8	L 43, B 65
-14 49'88.....	8.5	23.4	-14 1.7	L 43, T 28
-13 49'27.....	9.2	27.1	-13 48.4	L 48, B 53
30.....	9.1	39.6	52.6	R 41, T 65
31.....	8.2	42.3	35.6	R 36, B 0
32.....	9.0	43.1	51.7	R 37, B 67
-14 49'91.....	8.2	45.0	-14 2.6	R 36, T 24
-13 49'33.....	9.8	51.8	-13 52.0	R 28, B 67
34.....	9.3	52.2	58.2	R 29, T 43
36.....	9.4	56.7	59.8	R 23, T 35
37.....	9.8	11 6.1	57.9	R 14, T 45

The large gap in the north side of the nebula led Barnard<sup>4</sup> to compare it to the nebula in Orion. The most interesting feature, however, as disclosed by the present photograph, is the system of sharply defined dark markings of which the most conspicuous is on the southeast side, extending inward beyond the center. This marking so resembles the result of irregular flow of developer that, when it appeared on an earlier negative, its reality was questioned until it was fully verified by the present plate. The nebulosity in a thin line lying along the northern rim of the great dark marking is brighter than elsewhere.

<sup>1</sup> C. Flammarion, *L'Astronomie*, 32, 239, 1918.

<sup>2</sup> *Publications of the Lick Observatory*, 11, 1913, Plate 57.

<sup>3</sup> *Celestial Photographs*, 2, 151, 1899. <sup>4</sup> *Astronomische Nachrichten*, 177, 233, 1908.

PLATE IV



THE SWAN NEBULA N.G.C. 6618=M 17

Scale: 1 mm = 19".5

Enlargement 1.4



PLATE V



CENTRAL PART OF THE SWAN NEBULA

Scale: 1 mm = 7".2

Enlargement 3.8





Dr. V. M. Slipher, of the Lowell Observatory, has written me that he obtained a spectrogram of this nebula in September, 1919, showing a spectrum "similar to that of the Trifid nebula and the outer parts of the Orion nebula, in that the Nebulium lines  $N_1$  and  $N_2$  are weaker than the Hydrogen series" and that, like the Trifid, the nebula has a small radial velocity.

The magnitudes and positions of bright stars given in the following table were taken from Schönfeld's Southern *Durchmusterung*.

*Plates IV and V.*—The Swan Nebula, N.G.C. 6618 (Messier 17), in Scutum Sobieskii. Center of Plate IV (1900.0),  $\alpha = 18^h 15^m 1$ ,  $\delta = -16^\circ 14'$ . 1919, July 29. Exposure three hours. Seed 23 plate. Seeing fair.

This nebula was discovered by Messier in 1764<sup>1</sup> and attracted considerable attention from observers throughout the last century. Drawings of it were made by Sir John Herschel in 1833<sup>2</sup> and 1837,<sup>3</sup> Lord Rosse in 1854,<sup>4</sup> Lassell in 1862,<sup>5</sup> Trouvelot and Holden in 1875,<sup>6</sup> and a number of others. It was photographed in 1893 by Roberts,<sup>7</sup> using his 20-inch reflector and giving an exposure of two hours, and in 1899 by Keeler<sup>8</sup> with the 36-inch Crossley reflector and an exposure of four hours. Huggins<sup>9</sup> described the spectrum as consisting of a single bright line ( $H\beta$  or  $\lambda 5007$ ?), together with a faint continuous spectrum when the image of the brightest part of the nebula was thrown upon the slit.

Messier perceived only a "train of light without stars, 5' or 6' in extent"<sup>10</sup>—evidently the brightest part shown in the photographs, lying northwest and southeast. Herschel, in his drawing of 1833, shows the bright, curved part extending southward

<sup>1</sup> Smyth, *A Cycle of Celestial Objects*, 2, 416, 1844.

<sup>2</sup> *Phil. Trans.*, 1833, p. 461 and Plate XII.

<sup>3</sup> *Cape Observations*, 1847, p. 7 and Plate II.

<sup>4</sup> *Observations of Nebulae and Clusters*, p. 151 and Plate VI.

<sup>5</sup> *Memoirs, R.A.S.*, 36, p. 49 and Plates VII and VIII, 1867.

<sup>6</sup> *American Journal of Science* (3), 11, 341, 1876.

<sup>7</sup> *Celestial Photographs*, 1, 101, 1893.

<sup>8</sup> *Publications of the Lick Observatory*, 8, Plate 58, 1908.

<sup>9</sup> *Phil. Trans.*, 156, 385, 1866.

<sup>10</sup> Flammarion, *L'Astronomie*, 32, 241, 1918.

from the west end of Messier's streak and giving the nebula, in Herschel's mind, the appearance of a capital  $\Omega$  with the right hook exaggerated. This appearance has led to the various names of Omega, Horseshoe, and Swan—the last applying more appropriately than the others, perhaps, to the view obtained with a moderate-sized telescope. Herschel's drawing of 1837 shows a second curve at the other end of Messier's streak, which explains the description "2-hooked" in the N.G.C. This is evidently the brightest part of the diffuse nebulosity shown near the center and eastern edge of Plate IV. Holden, in comparing his own observations with those of other observers, comes to the conclusion that conspicuous motion took place within the nebula between 1833 and 1875; but a comparison of the photographs shows that no

S. DM.	VISUAL MAG.	PLACE, 1855.0		DISTANCE IN MM FROM EDGE OF PLATE IV
		$\alpha$	$\delta$	
-16°48'13.....	9.4	18 <sup>h</sup> 11 <sup>m</sup> 47 <sup>s</sup> .6	-16° 4'3	L 13, B 17
15.....	9.5	12 2.0	0.3	L 22, B 5
16.....	9.6	5.7	15.7	L 26, B 53
17.....	10	9.4	22.6	L 30, T 26
18.....	9.4	13.4	14.2	L 31, B 47
19.....	9.7	22.5	8.6	L 38, B 32
21.....	9.2	25.8	21.0	L 41, T 31
22.....	9.2	26.3	5.6	L 41, B 21
23.....	10	29.4	0.9	L 44, B 6
26.....	9.6	41.8	4.9	L 52, B 19
27.....	9.5	44.5	8.3	L 54, B 29
28.....	9.1	49.5	4.0	R 52, B 17
29.....	8.7	52.2	26.2	R 49, T 16
30.....	8.9	57.7	26.4	R 45, T 16
32.....	9.3	13 5.0	5.0	R 41, B 19
34.....	9.3	8.4	0.6	R 39, B 8
35.....	9.5	12.8	16.3	R 34, B 52
36.....	7.8	26.5	23.0	R 24, T 25

changes on such a large scale occurred between 1893 and 1919, and it seems certain that the apparent changes noted by Holden were due to inaccuracies in drawing.

The photograph brings out much faint nebulosity that cannot be perceived visually, especially to the east and north of the region of Messier. This nebulosity is of a filamentous structure, somewhat remotely resembling that of the Network Nebula in Cygnus, N.G.C. 6992. Like M 8 and M 16, this nebula shows a



PLATE VI

South



THE GLOBULAR STAR CLUSTER N.G.C. 6656=M 22

Scale: 1 mm = 16".0

Enlargement 1.7

set of dark markings, but they seem of a different kind from those of the former nebulae. The most conspicuous is the square-cornered, sharply outlined space under the neck of the "swan," which is so devoid of light that its contrast with the bright part of the nebula at first gives the impression that it is blacker than the surrounding sky. This dark space is closed on the west by nebulosity which, though faint even on the photograph, was seen and drawn by Lassell. At the north edge of the faint northern extension of the nebula is a dark treelike structure (almost lost in the engraving). Most interesting of all are the dark streaks that cross the region of Messier and especially the head and neck of the swan. They are well shown in Plate V. Some of these seem to radiate from a point near the base of the swan's neck.

The magnitudes and positions of bright stars in the following table were taken from Schönfeld's Southern *Durchmusterung*. The nebula is S. DM.—16°4820.

*Plate VI.*—The Globular Star Cluster N.G.C. 6656 (Messier 22), in Sagittarius. Center of plate (1900.0),  $\alpha = 18^h 30^m 3$ ,  $\delta = -23^\circ 59'$ . 1918, August 6. Exposure three hours. Seed 23 plate. Seeing good. Part of the guiding for this photograph was by Mr. Hoge.

This cluster has been known since the early days of the telescope, and is one of the six "nebulae" in the list drawn up by Halley<sup>1</sup> (the others were the great nebulae of Andromeda and Orion and the star clusters  $\omega$  Centauri, M 11 and M 13). Smyth says,<sup>2</sup> "Halley ascribes the discovery of this in 1665 to Abraham Ihle, a German; but it has been thought this name should have been Abraham Hill, who was one of the first council of the Royal Society, and was wont to dabble with astronomy. Hevelius, however, appears to have noticed it previous to 1665 so that neither Ihle nor Hill can be supported."

Although one of the most magnificent clusters available to northern observers, appearing larger and brighter than even the great cluster in Hercules, it seems to have attracted comparatively little attention and no large-scale photographs have been published until now.

<sup>1</sup> *Phil. Trans.*, 29, 390; abridged edition, 4, 224, 1749.

<sup>2</sup> *Cycle of Celestial Objects*, 1844, p. 422.

Mr. Shapley<sup>1</sup> places the cluster at a distance of 8300 parsecs (or 27,000 light-years) from the sun and 1200 parsecs from the plane of the galaxy—nearer the galactic plane than any other known cluster. Its diameter is at least 30', so that the light of a star at one end of a diameter must require more than two hundred and forty years to travel to the other end. On the plate reproduced here, Miss Davis has counted about 75,000 stars, of which Shapley estimates that one-third are cluster stars, while the others belong to the Milky Way background. The faintest stars on the original plate are of about the twentieth magnitude, or, on the basis of Shapley's distance, between absolute magnitudes +5 and +6, about like the sun. From counts made on this plate and on others of shorter exposure, Shapley finds that the projection of the major axis of the cluster lies in position angle 25°, and is parallel to the galactic plane.

Two dark spots appear in the reproduction, one 13 mm from the left edge and 32 mm from the top, and the other 57 mm from the left and 34 mm from the top. These are defects due to insensitive spots in the original plate.

The following stars were identified in the Córdoba catalogue referred to in the discussion of Plate II.

CÓRDOBA NO.	VISUAL MAG.	PLACE, 1900.0		DISTANCE IN MM FROM EDGE OF PLATE
		$\alpha$	$\delta$	
12919.....	9.0	18 <sup>h</sup> 30 <sup>m</sup> 35 <sup>s</sup> .26	-24° 8' 38".7	R 44, T 26
12922.....	8.5	18 30 41.49	-23 50 42.0	R 38, B 27

I desire to record here my keen appreciation of the kindness of Mr. Hale and Mr. Adams in giving me a place among the Mount Wilson observers during two summers, and to Mr. Ritchey and Mr. Pease for practical suggestions and for allowing me the use of the 60-inch reflector on certain nights when that privilege would regularly have been theirs.

WHITIN OBSERVATORY  
WELLESLEY, MASS.  
October 1919

<sup>1</sup> *Mt. Wilson Contr.*, No. 160; *Astrophysical Journal*, 50, 42, 1919.



# THE CHARACTERISTICS OF ABSORPTION SPECTRA PRODUCED BY THE ELECTRIC FURNACE<sup>1</sup>

By ARTHUR S. KING

## ABSTRACT

*Absorption spectra of metallic vapors, produced by the electric furnace.*—By placing a short plug of graphite in the middle of a tube furnace, a continuous spectrum corresponding to the temperature of the plug was obtained as a background for a pure absorption spectrum due to the hot metallic vapor. *Barium, calcium, cobalt, iron, nickel, and titanium* were investigated.

*Relation of Absorptive Power to Temperature Class.*—The furnace demonstrates, more clearly than is possible with the arc, the fact that lines of the same intensity in the emission spectrum may differ greatly in absorptive power. This variation was found to be closely related to the behavior of the lines at different furnace temperatures. The lines relatively strong at low temperature are strongest in the absorption spectrum, these lines often being faint in the arc. As the temperature of the plug rises, lines appear in absorption which are given faintly in emission at lower temperature. The result is that the relative intensities in absorption correspond with those in the emission spectrum several hundred degrees lower.

*Mixed absorption and emission spectra of metallic vapors.*—By placing the graphite plug beyond the middle of the furnace tube, mixed spectra were obtained; for whether the heated vapor emits or absorbs more light of a given wave-length depends on the relative temperatures of the plug and the vapor. Thus the lines of either the low temperature or the higher temperature could be obtained in emission or in absorption or suppressed at will. Striking effects were obtained with *calcium* and *iron*. By adjusting the background, the author secured on the same spectrogram the high-temperature lines in emission, the low-temperature lines in absorption, and intermediate lines suppressed. These experiments may help to *explain stellar spectra containing both bright and dark lines*. Experiments are also described in which the incandescent vapor in the tube, without a plug, gave an absorption spectrum, consisting only of those lines which in the emission spectrum at lower temperature are self-reversed.

*Kirchhoff's law; application to the absorption spectra of metallic vapors in the electric furnace.* This is briefly discussed.

In former experiments with the electric furnace the writer has occasionally made use of the column of vapor inclosed in a graphite tube to produce absorption spectra, the incandescent background being given by the terminal of a carbon arc burning outside the furnace chamber. In this way the pressure-shifts<sup>2</sup> of absorption lines and the phenomena of anomalous dispersion<sup>3</sup> have been observed.

<sup>1</sup> *Contributions from the Mount Wilson Observatory*, No. 174.

<sup>2</sup> *Mt. Wilson Contr.* No. 60; *Astrophysical Journal*, 35, 183, 1912.

<sup>3</sup> *Mt. Wilson Contr.* No. 79; *Astrophysical Journal*, 45, 254, 1917.

In the work here described the furnace was made to supply its own continuous spectrum by placing in the middle of the tube, the heated portion of which was 20 cm long and 12.5 mm internal diameter, a short plug of graphite. The light from the plug passing through a metallic vapor filling the tube produces an absorption spectrum. The arrangement gives a close approach to black-body conditions, and is similar to that of Liveing and Dewar,<sup>1</sup> who studied the reversals of spectrum lines by passing a carbon rod into a carbon tube heated by an external arc.

1. *Relation of emissive and absorptive power.*—It was of special interest to see how the effects obtained may be interpreted as following from Kirchhoff's law, and also how the absorption spectrum compares with the emission spectrum of the furnace at the same temperature, obtained by simply removing the plug, thus leaving all conditions unchanged except the length of the column of vapor.

Kayser, discussing the application of Kirchhoff's law to absorbing vapors,<sup>2</sup> lays stress on the fact that lines in the same spectrum may differ in absorbing power, so that a given relation between the background and the absorbing vapor need not be expected to reverse all of the lines emitted by the latter. If for any given wave-length the emission of the plugged tube, practically that of a black body, be denoted by  $e$ , and that of a black body having the same temperature as the vapor in the tube by  $e'$ , then the emissive power of the vapor will be  $e'A$ , where  $A$  is its absorption coefficient for the given wave-length. The total emission from the tube filled with vapor will then be

$$e + e'A - eA = e - (e - e')A.$$

If an absorption line is to appear,  $(e - e')A$  must be above a minimum positive value, the darkness of the line increasing as this product becomes larger. Hence the emission of the vapor for the given wave-length must be less than that of the plug. If  $e - e'$  becomes 0, only the continuous spectrum of the plug will appear, a condition frequently obtained in my experiments, usually by

<sup>1</sup> *Proceedings of the Cambridge Philosophical Society*, 4, 256, 1882.

<sup>2</sup> *Handbuch der Spectroscopie*, 2, p. 53.

locating the plug in a cooler portion of the tube and thus reducing the value of  $e$ . The vapor may then absorb a given wave-length strongly and still no trace of the line will be seen, the large value of  $A$  being rendered ineffective by the zero value of the factor  $e - e'$ .

Assuming, however, a considerable difference in the emissive powers of the plug and the metallic vapor, the value of  $A$  determines whether a line will appear strong in absorption or be invisible as a result of  $A$  approaching 0. Kayser notes the well-known difference in reversibility of lines in the arc as evidence that the value of  $A$  is not the same for all lines. There is, however, a question as to whether the vapor producing a certain line is present in an appreciable quantity in the outer envelope of the arc, for the method of long and short lines shows that lines difficult to reverse are likely to be confined to the core. The furnace, on the other hand, supplies definite data. A photograph with no plug in the tube shows what lines are being emitted by the vapor. If under these conditions two of the lines are of about the same intensity, and if, when the plug is replaced, one of the lines appears strong in absorption and the other is weak or absent, a real difference in their absorptive powers is evident. Phenomena of this kind have regularly appeared in the absorption spectra to be described. There is a close connection between the absorptive effects and the class of a line as determined by the changes in its intensity at various furnace temperatures, and this relationship has been specially noted.

2. *Probable temperature differences.*—The difference of temperature between the graphite plug and the absorbing vapor is difficult to determine. Pyrometric measurements were made on a thin plug placed at intervals along the tube from near the open end to the middle. Close to the end, where the tube is cooled by the massive contact block, there is evidently a considerable drop in temperature, but for points more than 2.5 cm away from the block the temperature thus measured was surprisingly uniform. For a central temperature of 1800° C. the drop within this limit amounted to about 100°, but at 2400° the difference seemed to be not more than 25°. There is a question, however, as to how fully the inclosed vapor takes up the temperature of the wall of the tube, and as to

the influence, when the tube is very highly heated, of the rapid drop close to the end. There is also the consideration that if the radiation of metallic vapors in the furnace is due to temperature, the emission of a black body should be stronger than that of the vapor at the same temperature. This would give a virtual difference between  $e$  and  $e'$  at all times when the plug is in the hottest portion of the tube. Evidence in support of this latter point has been given in a previous paper,<sup>1</sup> in which it was noted that the continuous spectrum from a plugged tube extended at least 300 Å farther into the ultra-violet than the spectrum of iron vapor when the tube was excited to the same temperature. In any case, the emissive power of the vapor is less than that of the plug and the term  $e - e'$  will be greater than 0.

3. *General character of the absorption spectra.*—For the examination of absorption spectra several elements were selected whose emission spectra have previously been studied in detail with regard to temperature variations. These were iron, titanium, nickel, cobalt, calcium, and barium, the first two receiving the larger share of attention. It was evident at once that the absorption spectra differed greatly from those shown at the same temperature in emission. With titanium, no absorption lines showed at 2000°, though a large number of lines, listed in a former paper,<sup>2</sup> appeared at this temperature when there was no plug in the tube. When the temperature of the plugged tube was raised to 2400°, an absorption spectrum was brought out consisting of the same lines as are shown in emission at 2000°. These are the low-temperature lines, belonging to classes I and II, the difference between the classes being in the rate at which the lines strengthen with increasing temperature. Similar results with the other elements showed that the absorption spectrum corresponds with the emission spectrum at a temperature several hundred degrees lower. As a means of picking out low-temperature lines the absorption spectrum, obtained quickly at high temperature, is almost as reliable as the emission spectrum corresponding to the temperature at which the vapor begins to radiate and which often requires a

<sup>1</sup> *Mt. Wilson Contr.* No. 66; *Astrophysical Journal*, 37, 239, 1913.

<sup>2</sup> *Mt. Wilson Contr.* No. 76; *Astrophysical Journal*, 39, 139, 1914.

very long exposure to photograph. A different condition prevails in the ultra-violet, however, since in this region the emission spectrum ceases rather abruptly at a certain limit, depending on the temperature, while the easy reversal of ultra-violet lines causes a strong absorption spectrum which extends almost as far as the continuous ground given by the plug.

4. *Relation of absorptive power to temperature class.*—We may now take up the variation of  $A$  for different lines and its connection with the temperature classification. The difference in absorptive power of lines belonging to different temperature classes was very distinctly brought out. The strongest absorption lines are those of class I. The stronger lines of class II also show considerable intensity in absorption, but if two lines belonging respectively to classes I and II are of about the same intensity in emission (for example,  $\lambda\lambda$  4415 and 4427 of iron) that of class I will be stronger in absorption. Such lines of class III as appear faintly in emission at low temperatures can be obtained in absorption, but only with difficulty. For instance, in the iron spectrum at  $2000^\circ$ ,  $\lambda$  4260 (class III) is stronger in emission than  $\lambda$  4258 (class I A), but in absorption, with the tube at the same temperature,  $\lambda$  4258 becomes the stronger. Numerous other contrasting pairs of the same kind might be noted. The absorption spectrum of iron at  $2000^\circ$  is very similar in the blue and violet to the emission spectrum at  $1650^\circ$ , which is about the lower limit for the appearance of lines of class III. This results simply from the fact that at  $1650^\circ$  the lines of class I dominate the spectrum and, because of their higher absorptive power, they again dominate when a temperature stage is reached at which an absorption spectrum first appears. Lines of classes II and III, which are certainly being emitted by the vapor at this higher temperature, are deficient in absorbing power and either appear faintly or are quenched by the continuous spectrum. The same reasoning explains the absence in absorption, for the temperatures used in these experiments, of lines of classes IV and V and of all but the stronger lines of class III. On account of their relatively small absorbing power, a background of higher temperature would be required to show them in absorption.

It seems unnecessary to list the lines which have thus been obtained in absorption for iron and titanium, since they can at once be selected from the tables<sup>1</sup> of the furnace classification for these spectra. For lines of the same class the relative intensities in absorption are the same as for the furnace in emission, the differences between the two kinds of spectra showing a consistent connection with the class of the lines concerned.

The absorption spectrum of calcium is of interest on account of the variety of types of lines represented.  $\lambda 4227$  may have great width, depending on the amount of vapor present. H and K are narrow absorption lines, strengthening with the temperature, with little dependence on vapor density. The other calcium lines appearing in absorption within the range  $\lambda 3500$  to  $\lambda 5000$  correspond in strength with their furnace classes; the strong lines as usual are of class I, some lines of class II show faintly, while the lines of class III, usually of diffuse structure, are absent. The spectra of the other elements photographed showed a repetition of the conditions noted.

The difference between the arc spectrum and that of the absorption furnace is accentuated by the fact that, in the latter, lines of class I A are very strong and those of class III are weak or absent. In the arc, the reverse condition holds, I A lines being very faint while those of class III are among the strongest. The fact that the strong lines of class III, which fade out at lower temperature, are difficult to produce in absorption is in harmony with the observation of Liveing and Dewar that "it is by no means always the strongest lines which are most easily reversed, but those which are both persistent and strong."

5. *Variation of absorption effects with wave-length.*—The iron spectrum, which was examined in absorption and emission from  $\lambda 3000$  to  $\lambda 8200$ , furnishes an illustration of the change in the absorption spectrum with wave-length. A plug temperature of  $2600^\circ$  gave no iron lines in absorption beyond  $\lambda 5507$ . Iron lines of class I are few and relatively faint in the red. In the case of other elements, however, there is no difficulty in obtaining lines

<sup>1</sup> King, *Mt. Wilson Contr.* Nos. 66, 76; *Astrophysical Journal*, 37, 239, 1913; 39, 139, 1914.

of high absorptive power in this region, the potassium pair  $\lambda\lambda$  7765-99, for example, appearing readily in absorption. In the yellow and green the iron lines of class I absorb strongly, and a few of class II faintly. The strong lines of class III near  $\lambda$  4900 were absent in absorption, though they appear in emission at much lower temperatures. In the blue, besides a fairly complete spectrum of lines in classes I and II, a few of the strongest lines of class III appeared faintly in absorption. This condition extends into the ultra-violet, where in the emission furnace many lines reverse readily. As would be expected, their strength in absorption corresponds closely with the width of the self-reversal in emission. Presumably higher temperatures would bring out absorption lines of successively higher classes and show lines in the red which appear in emission at low and medium temperatures.

6. *Production of mixed absorption and emission spectra.*—By placing the graphite plug beyond the center of the tube away from the spectrograph, so that some of the metallic vapor is hotter than the plug, it is possible to obtain emission and absorption lines at the same time. The lines then showing in absorption are those of the low-temperature class. When the plug was not quite in the hottest portion of the tube, the pure absorption spectrum was replaced by one in which some of the lines, usually those of class II, appeared in emission on a continuous ground. Moving the plug to a still cooler portion caused a relative strengthening of the emission spectrum, and a position could be found such that the regular emission spectrum appeared complete, with the exception of the most easily absorbed lines of class I, which still appeared in absorption. Owing doubtless to the higher vaporization point of titanium, a mixture with iron showed the iron lines to be more easily absorbed. It is thus simply a matter of adjusting the intensity of the incandescent background to obtain in emission the higher temperature lines (including the enhanced lines when these are given by the furnace) while the low-temperature lines appear in absorption, a difference clearly due to the different absorbing power of lines belonging to different classes.

7. *Effects due to balancing of emission and absorption.*—I have experimented further in this way by placing the plug only 2 or 3 cm



from the farther end of the heated tube, thus causing its emission to be of about the same strength as that of the metallic vapor in the hottest portion. Some lines then appear in emission and others in absorption, according to their temperature class, while others, often among the strongest in the spectrum, are absent, being neutralized by the incipient absorption which they are undergoing. With calcium in the tube under these conditions, H and K appear in emission; and  $\lambda 4227$  in absorption, with no trace of any other lines from  $\lambda 3500$  to  $\lambda 5000$ . Some of the high-temperature lines are doubtless quenched by the continuous background on account of their weak emission by the vapor, but many strong low-temperature lines, such as the group of six near  $\lambda 4300$  and the series triplet  $\lambda\lambda 4425-55$ , disappear because they are beginning to reverse and are in the state where emission and absorption are nearly equal. With iron the effects were very striking. A condition was obtained such that the strongest lines in the blue region,  $\lambda\lambda 4271.9, 4308, 4326, 4384$ , were invisible, while most lines of classes II and III, weaker than these, showed in emission and many of the easily absorbed lines of class I in absorption. The absent line  $\lambda 4384$  is a member of a triplet of which the lines are always affected alike by changes in the source, but in this case its weaker companions  $\lambda\lambda 4404$  and  $4415$  show as emission lines. A change in the position of the plug evidently can be used to eliminate from the spectrum any set of lines having about the same absorbing power. In the case of stellar spectra, especially those containing both bright and dark lines, the principle here involved can hardly fail to be active in causing an apparent lack of certain lines whose absence is not easily explained by the temperature conditions of the star in question.

8. *Production of absorption spectra without the use of a plug.*—In connection with the results obtained with the plugged tube, a class of furnace spectra may be considered, numerous examples of which have been accumulated but which have been of no use in the regular comparison of spectra produced at various temperatures. These spectra appear when the temperature used is so high that the tube filled with vapor (without any plug) gives a strong continuous spectrum. This occurs with some vapors more

strongly than with others and is doubtless due in large measure to the long column of mixed metallic and carbon vapor, although probably the vapor particles reflecting light from the wall of the tube also contribute. The intensity of the continuous spectrum can be increased by operating the furnace at atmospheric pressure, but with high temperature it appears at the usual working pressure of a few millimeters, so that the well-known effect of high pressure in producing a continuous spectrum cannot be operative here. The presence of such a spectrum prevents any comparison of line-intensities with those corresponding to lower temperatures, for which the continuous background is less in evidence. For usable spectrograms, the continuous spectrum must be kept down, so that no faint lines may be quenched by it, and so that when lines reverse we have the normal self-reversal. Any increase in temperature which is accompanied by strong continuous emission brings about a radical change and a more or less complete transition to the absorption spectrum obtained with a plug at the center of the tube. The absorption lines are those of the low-temperature emission spectrum, and, at the highest stage used for temperature comparisons, are for the most part self-reversed. The lines of higher classes and low absorbing power are blotted out by the continuous ground. The result is that at a very high temperature only low-temperature lines are visible, though at a lower stage, before the continuous emission sets in, a spectrum of richness comparable with the arc is seen. The transition between the two is equivalent to an obliteration of the whole emission spectrum; what were formerly the centers of reversals then remain as absorption lines.

#### SUMMARY

1. By using a furnace tube obstructed by a graphite plug in its hottest portion, pure absorption spectra have been obtained.
2. The types of lines which in an absorption spectrum under given conditions may be expected to be the strongest have been identified. They are not necessarily those which are strongest in the emission spectrum. Instead, the selection is determined by the temperature class, low-temperature lines being most strongly absorbed, with successively higher classes appearing in absorption

as the temperature of the source of the continuous background rises. As a result, the absorption at each stage of temperature corresponds closely with the emission spectrum several hundred degrees lower.

3. Lines of the same temperature class follow the recognized rule for reversed lines, the lines of shorter wave-length appearing more readily in absorption.

4. When the plug is in a cooler portion of the tube, the spectrum consists of both bright and dark lines according to their temperature class; strong lines are then often neutralized through a balancing of emission and absorption.

5. Absorption spectra similar to those given by a plugged tube may be produced without a plug if the furnace contains vapor at very high temperature. The lines then showing are of the low-temperature classes, whose absorptive power is high, while those of smaller absorptive power are obliterated.

6. The phenomena studied in these experiments are those likely to appear when an extended mass of vapor containing temperature gradients is under examination. It is believed that their main characteristics may account for many conditions of line-intensity observed for such masses of vapor.

MOUNT WILSON OBSERVATORY  
November 1919

# REVISION OF THE SERIES IN THE SPECTRUM OF BARIUM

By F. A. SAUNDERS

## ABSTRACT

*Barium spectrum; series of triplets and single lines.*—The spectrum of barium contains three systems of series, the triplets, the single lines, and the pairs. After making a careful study of all available data, including recent unpublished observations by King, the author has revised and extended the previously recognized series of triplets and single lines and has identified the lines corresponding to one or more terms of each of several other series. Altogether about 135 lines are assigned to one or other of sixteen series, which include six series of triplets, eight series of single lines, and two inter-system combination series. Accurate constants for these series are given. The fundamental and diffuse series of triplets are unusually complex, and these and other series show curious irregularities both in the relative intensities of the terms and in the wave-lengths. No simple formula of the ordinary type will give the frequencies accurately. The paper includes a brief *explanation of the notation* used in designating the different series.

Recent experimental work has led to a considerable extension of our knowledge of the spectrum of barium. A. S. King<sup>1</sup> published some excellent measurements from plates covering the visible and ultra-violet portions of the spectrum, using a vacuum furnace as source. Since then he has extended the range of these photographs into the ultra-red and taken several plates especially to help in working out the series in this spectrum. All these he has generously turned over to me for study, and the results are here given. If they are of value, the credit should be given to Dr. King.

H. M. Randall<sup>2</sup> has made a careful study of the ultra-red, and Meggers<sup>3</sup> and Eder<sup>4</sup> have helped to fill in a gap between the visible and the ultra-red. Mention should also be made of the dissertations of Schmitz,<sup>5</sup> George,<sup>6</sup> Lorenser,<sup>7</sup> and Werner.<sup>8</sup>

<sup>1</sup> *Astrophysical Journal*, 48, 13, 1918.

<sup>2</sup> *Astrophysical Journal*, 42, 195, 1915.

<sup>3</sup> *Scientific Papers*, No. 312, Bureau of Standards, 1918.

<sup>4</sup> *Wiener Akad.*, 123, IIa, December 1914.

<sup>5</sup> *Zeitschrift für wissenschaftliche Photographie*, 11, 209, 1912.

<sup>6</sup> *Ibid.*, 12, 237, 1913.

<sup>7</sup> Tübingen, 1913.

<sup>8</sup> *Annalen der Physik*, 44, 289, 1914.

All these new observations have helped to fix the system of series in this spectrum with more certainty, and the present paper contains an accurate set of constants connected therewith, as well as several new series. A similar study of the spectra of Ca and of Sr, not yet quite finished, makes it possible to settle the nature of certain series in Ba on account of the close analogy with these spectra. The writer has also derived assistance in this task from some observations by S. Popow, made in the laboratory at Tübingen in the winter of 1913-14, under Paschen's direction, on the Zeeman effect in Ca, Sr, and Ba. These have not yet been published in full, but were used by Popow as the basis of one article.<sup>1</sup>

The full spectrum of Ba consists of three systems of series. Each system contains at least four different types of series, and there are combination series derived from these. The present paper is for the purpose of revising the series in the triplet and single-line systems; the pair system is large and important, but is reserved for a future communication.

The results are given in the form of a set of tables, one for each series, with explanatory notes. The notation used has been explained earlier,<sup>2</sup> and is almost identical with that used by Paschen. A brief explanation is here repeated. The best series formula is probably of the type

$$\frac{1}{\lambda} = \nu = L - \frac{N}{(m+a+R)^2},$$

where  $N$  is the so-called series constant, approximately constant for all elements;  $L$  is the limit of the particular series in question;  $m$  is the variable integer;  $a$  is a constant peculiar to this series;  $R$  is a "residual," which is itself a function of  $m$  and of other constants, which diminishes rapidly toward zero for the outer lines of a series ( $m$  large). In Rydberg's formula  $R$  is zero; in the formula of Møgendorff it has the value  $\frac{b}{m}$ ; but these simple values are by no means generally applicable.

The fraction  $\frac{n}{(m+a+R)^2}$  is called the "term," and is accurately known for any series as soon as the limit is found. The terms are

<sup>1</sup> *Annalen der Physik*, 45, 147, 1914.

<sup>2</sup> *Astrophysical Journal*, 41, 323, 1915.

represented by the symbols (*mp*), (*ms*), (*md*), and (*mf*) in the four types of series, the principal, sharp, diffuse, and fundamental, in the triplet system; (*mP*), (*mS*), (*mD*), (*mF*), likewise, for the single-line system.

#### TRIPLET SERIES SYSTEM

"*Fundamental*," or narrow series of triplets, (*1d*)—(*mf*).—This is now the most accurately measured series in Ba, due to the sharpness of the lines in the vacuum furnace, and the excellent results of King. On this account it is mentioned first. The list here given includes a few very faint lines not given in King's paper, but measured since then from his plates, either by him or by the writer. This series was first suggested some time ago<sup>1</sup> and three of its triplets correctly identified. The course of the rest of the series as then suggested proved, however, to be incorrect and was difficult to settle, chiefly because the second member of the series is abnormally

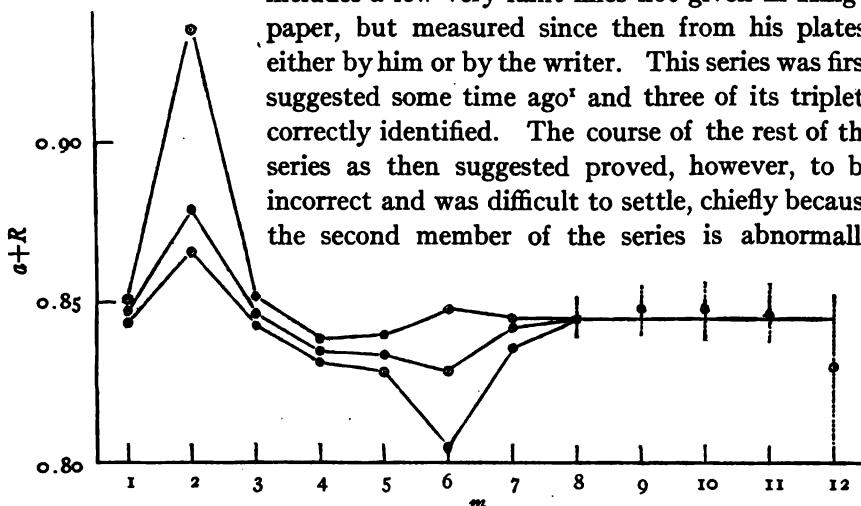


FIG. 1.—Variation of  $a+R$  with  $m$ . Dotted lines show estimated errors

faint. Unwilling as one might well be to admit the possibility of series in which the intensities run abnormally, there is now no doubt that they occur. Lorensen was not deterred by the abnormality referred to, and suggested an arrangement for the series which proves to be much nearer the truth. His second member is, however, wrong.

The series is complex, as are the corresponding ones in Ca and Sr, a feature which is, so far, rare in series of this type. It is, moreover, curiously irregular. In order to exhibit this irregularity three curves are given (Fig. 1), showing how the quantity  $a+R$

<sup>1</sup> *Astrophysical Journal*, 28, 228, 1908.

TABLE I  
FUNDAMENTAL SERIES OF TRIPLETS,  $(1d) - (mf)$

$$\begin{aligned}(1d_1) &= 32433.0 \\ (1d_2) &= 32814.1 \\ (1d_3) &= 32995.6\end{aligned}$$

$\lambda$	$\nu$	$\Delta\nu$	$\lambda$	$\nu$	$\Delta\nu$	$\lambda$	$\nu$	Terms ( $mf$ )	$m+e+R$	$n$
3997.92	25006.1	381.2	3937.88	25387.3	181.5	3909.92	25568.8	7426.8	3.8438	1
95.66	020.2	381.0	35.72	401.2				7412.8	3.8474	
93.40	034.4							7398.6	3.8511	
3596.33	27798.3	381.2	3547.70	28179.5	181.6	3524.97	28361.1	4634.6	4.8658	2
93.20	822.7	380.9	44.66	203.6				4610.4	4.8786	
79.67	927.7							4595.3	4.9352	
3421.48	29218.9*	381.4	3377.39	29600.3	181.6	3356.80	29781.9	3213.8	5.8432	3
21.01	222.9	381.0	76.98	603.9				3210.1	5.8466	
20.32	228.8							3204.2	5.8520	
3323.06	30084.3	381.0	3281.77	30462.8	181.8	3262.30	30644.6†	2351.2	6.8315	4
22.80	086.7		81.50	465.3				48.7	6.8552	
								46.3	6.8387	
3262.24	30045.2†	380.8	3222.44	31023.6	181.4	3203.70	31205.0	1790.5	7.8284	5
61.96	647.8		22.19	026.0†				88.0	7.8339	
								85.2	7.8401	
3222.28	31025.1†	381.3	3183.96	31398.6	182.0	3165.60	31580.6	1415.4	8.8049	6
21.63	031.4		83.16	406.4				07.8	8.8286	
								01.6	8.8481	
3193.97	31300.2	383.2	3155.67	31680.1	181.3	3137.70	31861.4	1134.2	9.836	7
93.91	300.8		55.34	683.4†				32.8	9.842	
								32.2	9.845	
3173.72	31499.7†	381.8	3135.72	31881.5	181.9	3117.94	32063.4	932.9	10.845	8
73.69	500.0†									
3158.54	31651.1‡	380.5	3121.02	32031.6				781.7	11.848	9
3146.90	31768.3	380.6	3109.63	32148.9				664.7	12.848	10
3137.80	31860.6							572.4	13.846	11
3130.6	31934							499	14.83	12

\* Much too strong; perhaps not a member of this series.

† This line may not belong to the series; this triplet irregular.

‡ One plate shows a suspicion of a wing on one side of these lines, but it yields a value of  $185$  for  $\Delta\nu$ , which is unsatisfactory.

† These lines somewhat doubtful, as they are not clearly resolved.

|| There is a faint line at  $3103.1$ , which may belong to the series, but it yields a value of  $185$  for  $\Delta\nu$ , which is unsatisfactory.

TABLE II  
DIFFUSE SERIES OF TRIPLETS,  $(1p) - (md)$   
 $(1p_1) = 28514.8$   
 $(1p_2) = 29392.8$   
 $(1p_3) = 29763.3$

$\lambda$	$\nu$	$\Delta\nu$	$\lambda$	$\nu$	$\Delta\nu$	$\lambda$	$\nu$	$\Delta\nu$	$\lambda$	$\nu$	Terms ( $md$ )	$m$
25515.7	3918.2	877.9	29223.9	3421.1	370.7	30933.8	3421.1	370.7	30933.8	3421.1	32433.0	1
23255.3	4299.0	878.0	27751.1	3602.6	370.6	5425.55	3602.6	370.6	5425.55	3602.6	32814.1	
22313.4	4486.6	878.2	5535.93	18058.9	370.6	18429.6	18058.9	370.6	18429.6	18058.9	32995.6	2
5818.91	17180.7	878.1	5519.12	113.9	370.7	4264.43	113.9	370.7	4264.43	113.9	11211.6	
5800.30	235.8	877.8	4332.96	23072.6	370.6	23443.3	23072.6	370.6	23443.3	23072.6	11279.0	
5777.70	303.2	877.8	4323.63	125.4	370.6	25696.0	125.4	370.6	25696.0	125.4	11333.9	3
4403.66	22247.6	878.3	3947.51	25325.4	370.6	3890.57	25325.4	370.6	3890.57	25325.4	6244.2	4
4489.00	270.6	878.3	3945.61	337.6	370.6	3719.92†	337.6	370.6	3719.92†	337.6	6267.3	
4087.31	24459.3†	878.2	3771.93	26504.1	370.6	26874.7	26504.1	370.6	26874.7	26504.1	4041.0	5
4084.87	473.8	878.2	3769.48	26521.5	370.6	2871.4	26521.5	370.6	2871.4	26521.5	4055.4	
3898.58	25043.3	878.2	3667.93	27255.7	370.6	2888.7	27255.7	370.6	2888.7	27255.7	4007.5	6
3894.34	671.0	878.2	3667.60	27258.1	370.6	2124.2	27258.1	370.6	2124.2	27258.1	2134.8	
3780.72	26379.89	878.0	3603.40	27743.7	370.6	1646.8	27743.7	370.6	1646.8	27743.7	2137.1	7
3788.18	390.6	878.0			370.6	1649.1		370.6	1649.1		1649.1	
3721.17	26865.7	878.0			370.6			370.6				
3720.85	26868.0	878.0			370.6			370.6				

\* Measured by Randall. This whole triplet occurs inverted in position. On this account in calculating its "terms" its frequency is to be taken as negative.  
† Probably there is a diffuse series line at  $\nu$  24459.4 and a sharp series line at  $\nu$  24459.1; not resolved.  
‡ King's plates show an iron line at 3719.93 from which the Ba line here given cannot be separated, when both are present. In one photograph, when a very small quantity of iron was present, this line showed unusual strength, and was then doubtless largely or entirely due to Ba.  
§ King's plates show an iron line at  $\lambda$  3618.77 which covers the faint Ba line to be expected there, due at 3618.72.



varies with  $m$  for each of the three lines, which together constitute the first "line" of each triplet. The curves show that  $R$  must be a complex function of  $m$ , or else that the true type of formula is quite different from that now accepted. They show, moreover, how curiously the structure of the triplet group opens out and closes again in passing along the series. The accuracy of the constant frequency differences makes it necessary to regard these abnormalities as real. Others of the same sort occur in Ca.

*Diffuse or first subordinate series of triplets,  $(1p) - (md)$ .*—The diffuse triplet series has been extended by one term and the accuracy of all wave-lengths greatly improved from King's plates. The limit used here was obtained indirectly, from the fundamental series, for greater accuracy. The curve of residuals for this series, though very far from complete, shows an abnormal course as far as it goes.

*Sharp or second subordinate series of triplets,  $(1p) - (ms)$ .*—King's plates show a few new lines of this series. The presence of bands makes it difficult to follow the series farther out.

TABLE III  
SHARP SERIES OF TRIPLETS,  $(1p) - (ms)$

$$(1p_1) = 28,514.8$$

$$(1p_2) = 29,392.8$$

$$(1p_3) = 29,763.3$$

$\lambda$	$\nu$	$\Delta\nu_1$	$\lambda$	$\nu$	$\Delta\nu_2$	$\lambda$	$\nu$	Terms ( $ms$ )	$m$
7905.80....	12645.5	878.2	7392.44	13523.7	370.6	7195.26	13894.3	15869.3	1
4902.90....	20390.5	878.2	4700.45	21268.7	370.5	4619.98	21639.2	8124.3	2
4239.56....	23580.0	878.4	4087.31	24459.3*	370.4	4026.30	24829.7	4934.0	3
3975.32....	25148.3	878.3	3841.15	26026.6	370.5	3787.23	26397.1	3366.5	4
3828.93....	26110.3	878.2	3704.23	26988.5†	.....	.....	.....	2404.5	5

\* See Table II, second note †.

† The last triplet is presented tentatively, as its faintness makes it very difficult to separate from the bands which are present.

*Principal series of triplets,  $(1s) - (mp)$ .*—This series is new and very incompletely observed. It is very faint and lies in the ultra-red. It forms combination series (see below) which are analogous to others in Ca and Sr; it is only by means of these that its course can be settled. The first triplet in the table belongs, in a mathematical sense at least, to this series, but is, physically speaking,

the first triplet of the sharp series. The third triplet cannot yet be checked by calculation from any combination and must be regarded as only provisionally located.

TABLE IV  
PRINCIPAL SERIES OF TRIPLETS,  $(1s)-(mP)$ .  $(1s)=15869.3$

$\lambda$	$\nu$	$\Delta\nu$	$\lambda$	$\nu$	$\Delta\nu$	$\lambda$	$\nu$	Terms ( $mP$ )	$m$
7195.26....	13894.3	370.6	7392.44	13523.7	878.2	7905.80	12645.5	28514.8 29392.8 29763.3	1
.....	4582.9 calc.	72.4 calc.	.....	4655.3 calc.	171.5 calc.	.....	4826.8 calc.	11042.5	2
.....	.....	.....	21477.2 obs.	4655.1 obs.	171.9 obs.	20712.0 obs.	4827.0 obs.	11214.0 11286.4	.....
10326.....	9682.4*	49.6	10272.9	9732.0	80.1	10189.1	9812.1	6057.2 6137.3 6186.9	3

\* Recently found by Randall.

#### SINGLE-LINE SERIES SYSTEM

*Principal series of single lines,  $(1S)-(mP)$ .*—This series has proved to be unexpectedly difficult to work out. After the corresponding series in Ca and in Sr were found, it was evident that

TABLE V  
PRINCIPAL SERIES OF SINGLE LINES,  $(1S)-(mP)$ .  $(1S)=42029.4$

$\lambda$	$\nu$	Terms ( $mP$ )	$m$
5535.53.....	18060.2	23969.2	1
3071.59.....	32547.2	9482.2	2
2702.65.....	36989.9	5039.5	3
2596.68.....	38499.5	3529.9	4
2543.2.....	39308	2721	5
2500.2.....	39985*	2044	6
2473.1.....	40423*	1606	7

\* Not positively identified as belonging to this series.

this series should occur in Ba also, and should begin with the flame line  $\lambda$  5535. In an earlier article<sup>1</sup> I remarked that  $\lambda$  2597 had exactly the right aspect for a member of this series. Later on,<sup>2</sup>

<sup>1</sup> *Astrophysical Journal*, 32, 155, 1910.

<sup>2</sup> *Physical Review*, 1, 332, 1913. The series SL<sub>2</sub> suggested at that time has proved, in the light of more accurate data, to be incorrect.

I gave the arrangement of the beginning of the series. Recently McLennan and Young,<sup>1</sup> using the method of self-reversal of the lines by the vapor of the metal, which had long been known to be useful in picking out lines of series of this type, have obtained a successful photograph clearly showing the later lines of the series. They also calculated the limit approximately. Their choice of lines for the series differs somewhat from mine. They include, for instance, two lines  $\lambda 3275$  and  $\lambda 2845$  for whose existence there is no other evidence. This region has been gone over very carefully by several observers, including King, who uses a furnace as source in which this series must surely appear complete, and in which, in fact, its first line is relatively stronger than usual. High precision is, of course, not claimed for their wave-lengths quoted above, but the known line nearest to  $\lambda 2845$  is 60 units away, and one must therefore suppose either that there was some error in identification in this case, or else that in a source particularly favorable to this series, and in which some of its lines are enhanced, others fail to appear. The latter assumption seems to me quite untenable.

The course of the series as suggested in the table receives support from the discovery of combination series derived from it, and presented below. The limit of the series has been accurately fixed by means of one of these,  $(1S) - (mp_2)$ , a combination between this series and the principal series of triplets.

The series is abnormal in the same sense that the fundamental series of triplets is abnormal; that is, the curve of residuals is not a simple one, and no simple formula will fit the series. The outer lines have not yet been measured with satisfactory precision, and therefore the full curve cannot yet be traced.

*Diffuse series of single lines,  $(1P) - (mD)$ .*—The experimental evidence necessary for the isolation of the lines of this series is still far from complete. Its limit  $(1P)$  is known from the principal series. The first term  $(1D)$  is probably  $30634.1$ , a conclusion which is reached by the considerations which follow. There are several pairs of lines in the Ba spectrum with a frequency difference of  $11395.3$  and one line of each of these belongs to a series

<sup>1</sup> *Proceedings of the Royal Society*, 95, 277, 1919.

ending at  $(1S)$ , or 42029.4. This indicates the existence of shifted series, ending at 42029.4-11395.3, or 30634.1. If this number is then a limit of one or more series, it must itself be a term of some other series. It cannot be a term of the sharp series, for  $(2S)$  would be far smaller. The same can be said for the fundamental series. It must therefore belong to the diffuse series and be the term  $(1D)$ . In this case one of the series ending at this limit is probably the fundamental series, and this is given below.

Having fixed the value of  $(1D)$ , the difference  $(1P)-(1D)$  should give the first line of the diffuse series.  $(1P)$  is 23969.2, and therefore the difference is a negative quantity. The occurrence of negative frequencies is not uncommon in series, but has not before been suggested for any diffuse single-line series. It occurs in others, however, e.g., in the diffuse series of pairs and of triplets in the Ba spectrum. Besides, in all sharp series, the first member is also the first member of the principal series, one of these being taken with a negative frequency, thus giving a close relationship in all elements between the series  $(1S)-(mP)$  and the series  $(1P)-(mS)$ . In the spectrum of Ba, and also in Ca and Sr, there exists this same relationship between  $(1D)-(mP)$  and  $(1P)-(mD)$ . The former of these two is the series formerly called  $SL_2$ , which is given for Ba below, as a combination series of principal type in the single-line system.

The difference  $(1P)-(1D)$ , ignoring the sign, leads to 6664.9, which hits a line of some strength, observed by Randall in the ultra-red. This is therefore at once the first line of the diffuse series and of the combination series. The term  $(2D)$  can be predicted by a formula, but not exactly; it indicates that the next line of the diffuse series is in the ultra-red, but further experiments are needed to settle this line exactly and to fix the others in the series. The rest of the series may, for instance, include  $\lambda\lambda$  9831.7, 6233.59, 5267.03, 4877.69, and 4663.60, and, if so, the combinations  $(1P_2)-(2D)$  and  $(1S)-(5D)$  appear to exist; but there is no definite evidence on hand on which to decide whether this selection is correct or not. Observations on the Stark effect in Ba should reveal this series, since it appears that diffuse series are as a class sensitive to the effects of electric fields.

*Sharp series of single lines,  $(1P) - (mS)$ .*—Both  $(1P)$  and  $(1S)$  being known, it ought to be possible to guess at  $(2S)$  by means of a formula without much ambiguity; but there are many lines in the expected region, the ultra-red, and the true one cannot be settled in this way alone. The term  $(2S)$  is, however, very likely to occur in combinations, such as  $(1S) - (2S)$ ,  $(2S) - (mP)$ , and perhaps others. I have found that if we assume  $(2S)$  to have the value of 16400.4, as it well may, according to any reasonable formula, then we get

$(1P) - (2S) = 7568.8$  calc.; 7569.8 observed as a strong line by Randall.

$(1S) - (2S) = 25629.0$  calc.; 25631.5 observed as a faint line.

$(2S) - (3P) = 11360.9$  calc.; 11360.9 observed as medium line.

$(2S) - (4P) = 12870.5$  calc.; 12871.8 observed as a weak line.

As these agreements are good, I feel that they are probably correct, and, if so,  $\lambda 13207$  ( $\nu 7569.8$ ) is the sharp series line in the ultra-red. The next line of this series cannot be picked out with certainty at present. There are several possible lines in the likely region.

*Fundamental series of single lines,  $(1D) - (mF)$ .*—As explained above, there are two series ending at the limit  $(1D)$ , and one of

TABLE VI  
FUNDAMENTAL SERIES OF SINGLE LINES,  $(1D) - (mF)$ .  $(1D) = 30634.1$

$\lambda$	$\nu$	Terms $(mF)$	$m$
5826.29.....	17158.9	13475.2	1
4080.93.....	24497.4*	6136.7	2
3789.74.....	26397.7†	4254.4	3

\* This line is almost exactly  $(1D) - (3F_2)$ , but as  $(1D) - (2F_2)$  does not occur this must be regarded as an accidental coincidence.

† This line almost coincides with a line of  $(1P) - (mF)$ ; it is doubtful which one was measured, or a blend of both.

these is of a new type, which cannot be either principal, diffuse, or sharp. Unless the spectrum contains more than four types, it is safe to call this the fundamental series. In accordance with the constant frequency shifts explained above, there is also the shifted series  $(1S) - (mF)$ . Lack of proper observations (which are very

difficult to make) prevents us from being quite positive about this series, but the course of it, as far as it is known, is shown in Table VI. This series is probably analogous to those formerly called  $SL_3$  in Ca and Sr.

COMBINATION SERIES IN THE TRIPLET SYSTEM

*Series (1d) - (mp).*—This combination is strong in Ca and Sr, and its course may be inferred from analogy. In the article by Popow already referred to, one term of the series is given, but in my opinion the identification is incorrect; his arrangement leads to a value of (2p) which is greater than (1s), so that the line (1s) - (2p) should have a negative frequency in Ba. (1s) - (1p) has, of course, a negative frequency, but no series has yet been shown to have two members of this sort, and I am reluctant to admit such a possibility. I have therefore rejected his arrangement.

Since both (1d) and (2p) are each triple, the differences (1d) - (2p) give us nine wave-numbers. Of these, three do not occur as real lines, and one which probably exists as a faint line, bracketed below, is "covered" by a very strong line of another series which occurs quite close to it. This group is arranged according to the Rydberg scheme in the following manner:

Group (1d) - (2p)			
			21709.0
			72.4
	21600.0	181.4	21781.4
		171.5	
21390.5	381.0	21771.5	[21953]

The identification of this group leads to the value of (2p) and hence to a triplet of the principal series in the ultra-red, given above, of which the third, and faintest, line has not yet been observed. An effort to find the next member of this series, (1d) - (3p), led to the discovery, in a photograph of the vacuum arc, taken by myself, of a very faint pair of lines, the first near  $\lambda$  3790.27, apparently the strongest of this group. This observation needs to be supported by observations of the other lines of the group.

*Series (2d) - (mf).*—This series occurs, to the extent of one term only, in the ultra-red of Ca. It probably occurs in Ba also.

The strongest line resulting from this combination is due at  $\nu$  3813.0 and Randall has observed a line at 3812.8.

#### COMBINATION SERIES IN THE SINGLE-LINE SYSTEM

*Series (1D) — (mP).*—This series is the one which was found in Ca and Sr and then<sup>1</sup> called SL<sub>2</sub>. It is a shifted series, an exact copy of the principal series, but shifted by a frequency difference of 11395.3 to the new limit, which has been identified above as (1D). An objection may be raised to this series, as the third line of it is fainter than the lines on either side. An abnormality of the same sort, however, occurs in the principal series, and the objection may not therefore be vital.

TABLE VII  
SERIES (1D) — (mP)

$\lambda$	$\nu$	Terms (mP)	$m$	Shift Number
15000.4.....	6664.9	23969.2	1	11395.3
4726.46.....	21151.7	9482.4	2	11395.5
3905.98.....	25594.7	5039.4	3	11395.2
3688.35.....	27104.5	3529.6	4	11395.0

*Series (1S) — (mF).*—This series is suggested tentatively, but as the three lines in the table give very accurate shift numbers I am disposed to regard it as real.

TABLE VIII  
SERIES (1S) — (mF)

$\lambda$	$\nu$	Terms (mF)	Shift Number	$m$
3501.12.....	28554.3	13475.1	11395.4	1
2785.26.....	35893.0	6136.4	11395.6	2
2646.50.....	37774.8	4254.6	11395.1	3

*Series (2S) — (mP).*—This series ought, by analogy with other elements, to occur in Ba. Two members are observed, fairly near their calculated places. The first, and supposedly strongest, member should lie in the ultra-red, and has not been observed; if this line is not found, the existence of the series will become somewhat precarious; but it must be said that all series involving

<sup>1</sup> *Astrophysical Journal*, 32, 156, 1910.

the terms ( $mP$ ) show an anomalous lack of intensity for  $m = 2$  or 3, and this one may have the same peculiarity.

TABLE IX  
SERIES ( $2S$ )—( $mP$ )

$\lambda$	$\nu$	$m$	Terms ( $mP$ )	Shift Number
.....	6918.2 calc.	2	[9482]	.....
8799.70.....	$\left\{ \begin{array}{l} 11360.9 \text{ calc.} \\ 11360.9 \text{ obs.} \end{array} \right\}$	3	5039	25629.0*
7766.80.....	$\left\{ \begin{array}{l} 12870.5 \text{ calc.} \\ 12871.8 \text{ obs.} \end{array} \right\}$	4	3528	25627.7

\* The calculated shift number is ( $1S$ )—( $2S$ ), which is 25629.0.

*Series ( $1P$ )—( $mF$ ).*—This is probably a very faint series. Only one line has been observed, which is ( $1P$ )—( $1F$ ); calculated  $\nu$  10494.1, observed  $\nu$  10493.6 ( $\lambda$  9527.0). Meggers reports this line as absent from his plates, but an inspection of the plate under the most favorable lighting, for which I was generously given an opportunity, showed the line as present, though faint. The next line of this series should be at  $\nu$  17833, but has not been found.

*Series ( $1S$ )—( $mS$ ).*—This combination is possible. It gives us  $\nu$  25629.0, and there is a faint line observed at  $\lambda$  3900.37, ( $\nu$  25631.5). The agreement is only fair.

#### INTER-SYSTEM COMBINATION SERIES

*Series ( $1S$ )—( $mp_2$ ).*—This series in the spectra of other elements has recently come into considerable prominence. It is strongly enhanced in the low-temperature oven spectra, and occurs in Ca and Sr. Some recent plates taken by Dr. King show that the only line in Ba which has this property and lies in the proper part of the spectrum for the line ( $1S$ )—( $1p_2$ ) is at  $\lambda$  7911. The proper region can be found by getting ( $1S$ ) approximately from the principal series of single lines by calculation, and then subtracting from it the better-known value of ( $1p_2$ ). In this way the line ( $1S$ )—( $1p_2$ ) is identified, and from its wave-number and the quantity ( $1p_2$ ) the value of ( $1S$ ) is redetermined with greater precision. This series fades away sharply in this group of elements. The second line should be a faint line and its calculated position is  $\lambda$  3244.20. King's plates show an iron line at 3244.18, and it has not been possible to resolve these two, or to get an



absolutely iron-free spectrum. One of his plates, in which Ba is very rich and Fe faint, shows this line relatively strong, compared with other Fe lines, and its position when measured came out exactly at 3244.20. As the dispersion on this plate is 1.86 Å per mm, the error of measurement is considerably less than 0.01 Å, so that this line is undoubtedly present. The next line of the series has not been found, on account of faintness.

*Series ( $1d_2$ )—( $mP$ ).*—This combination series is fairly strong. Like all the other series involving the terms ( $mP$ ), this series is somewhat abnormal in the intensities of its lines, the second line being faint. The two closely related series ( $1d_1$ )—( $mP$ ) and ( $1d_3$ )—( $mP$ ) might be expected to occur. There are two lines which might possibly be members of the series ( $1d_3$ )—( $mP$ ), but the agreement is not very good, and there is no other evidence in favor of the existence of these combinations.

TABLE X  
SERIES ( $1d_2$ )—( $mP$ )

$\lambda$	$\nu$	Terms ( $mP$ )	$m$	Shift Number
11304.20.....	8844.1	23970.0	1	9216.1*
4284.90.....	23331.2	9482.9	2	9216.0
3599.40.....	27774.9	5039.2	3	9215.2
3413.84.....	29284.3	3529.8	4	9215.2

\* The calculated shift number is  $(1S)-(1d_2)=9215.3$ .

#### SUMMARY

The spectrum of barium contains three systems of series, the triplets, the single lines, and the pairs. The first two systems are here shown to contain at least four types of series each, together with various combination series. In the triplet system the four type series are not new, but are here extended and revised; two combination series in this system are suggested. In the single-line system, the principal series is revised, and the other three type series in this system are shown in all probability to be present; several combination series in this system occur, including the series formerly called SL<sub>2</sub> and SL<sub>3</sub>; and two inter-system combination series are also found.

JEFFERSON PHYSICAL LABORATORY, HARVARD UNIVERSITY  
November 1919

# THE SPECTRUM OF ELECTRICALLY EXPLODED WIRES<sup>1</sup>

By J. A. ANDERSON

## ABSTRACT

*High-temperature absorption spectra*, such as those given by the sun and some stars, have not been reproduced fully in the laboratory. The absorption spectra obtained with the arc and the electric furnace have been limited to wave-lengths below  $0.56\ \mu$  for iron and have not included the high-temperature lines. The author has developed a *method of obtaining high-temperature absorption spectra*, which consists in electrically exploding a fine wire in a confined space. When the explosion occurs in air confined in a tube or slot, the flash gives a brilliant continuous spectrum crossed by the absorption lines of the elements composing the wire. The spectrograms reproduced show that for *iron* an absorption spectrum was obtained which extends to  $0.66\ \mu$  and includes all classes of lines except the pronounced enhanced lines. *Copper*, *nickel*, and *manganin* were also investigated. When the method has been more fully developed it may be possible to imitate stellar absorption spectra of the solar type.

*New laboratory source of light.*—By discharging a large condenser, charged to 26,000 volts, through a fine wire 5 cm long, about 30 calories of energy were dissipated in about  $10^{-5}$  sec. If all of this energy had gone into the 2 milligrams of wire it would have raised its temperature to about  $300,000^\circ$ . Actually, the brilliant flash which resulted had an intrinsic intensity corresponding to a temperature of about  $20,000^\circ$ , or about one hundred times the intrinsic brilliancy of the sun. The character of the spectrum and also the pressure developed depend, of course, upon the energy per unit mass and also upon the initial pressure and volume of the surrounding gas. When the wire was exploded within a tube or slot under a bell jar exhausted to 2 cm pressure, a *line emission spectrum* was obtained. As the air pressure was raised the continuous background increased in intensity and the spectrum became more and more an *absorption spectrum*. Because of the high temperature, the *continuous spectrum* extends far into the ultra-violet. This source should be useful in studying the *pressure shift* of lines, as pressures of 50 atmospheres can readily be obtained. The spectrograms already secured show the effect clearly. The *appearance* of the flash is shown by direct photographs. Its size corresponds to a speed of propagation in open air of about 3.3 km per second. Some striking *mechanical effects of the explosion* are briefly described.

*Meteorites falling into the sun.*—In a *theoretical discussion* the author points out that meteorites falling into the sun would be given a relatively enormous amount of energy in a short time and hence would be exploded by mechanical means much as his wires were exploded by electrical means.

*Fine wires.*—A *simple method of producing on a lathe* wires weighing down to 0.1 mg per cm was developed.

Laboratory investigations deal almost exclusively with emission spectra, that is, spectra consisting of bright lines on a more or less

<sup>1</sup> *Contributions from the Mount Wilson Observatory*, No. 178.

completely dark background. Absorption spectra such as are given by the sun and stars, not being readily produced in the laboratory, must be interpreted in terms of the knowledge derived from a study of emission spectra, which would not be a serious drawback if the mechanism of emission and of absorption were known; since, however, neither is at all well understood, one never feels absolutely sure of his ground in discussing solar or stellar spectra.

Absorption spectra are encountered in the laboratory: (1) in self-reversals of arc or spark lines; (2) by passing white light through cooler vapors or gases. In the arc or spark at atmospheric pressure only a small percentage of the lines are found to be reversed; in the spark at high pressures or in liquids more lines may be reversed, and in the experiments of Hale and Kent<sup>1</sup> at the highest pressure a fair absorption spectrum was produced, though the background was not quite uniform. Possibly at still higher pressures this method would yield a pure absorption spectrum. The high pressure required is, however, a disadvantage in more ways than one.

By passing white light through vapors or gases a pure absorption spectrum is obtained, but, since the hottest source of white light at our disposal is the crater of the arc, it has been found possible to reverse only those lines which are usually found self-reversed in the arc, and naturally very little can be done in the region beyond  $\lambda 2500$ . As an illustration consider the spectrum of iron, perhaps the most important element from the standpoint of the astrophysicist. The low-temperature lines (Groups *a* and *b* of Gale and Adams) are found self-reversed in the arc from the extreme ultra-violet up to about  $\lambda 5500$ , although reversals above  $\lambda 4500$  are not common. The same lines are also obtained as absorption lines in the electric furnace, either by passing white light from the crater of the arc through the furnace tube or by inserting a graphite plug near the middle of the tube;<sup>2</sup> but no lines beyond  $\lambda 5500$  have been reversed by this means. Liveing and Dewar mention  $\lambda 5615$  as having been reversed in one of their experiments, but

<sup>1</sup> *Publications of the Yerkes Observatory*, 3, Part II.

<sup>2</sup> A. S. King, *Mt. Wilson Contr.* No. 174; *Astrophysical Journal*, 51, 13, 1920.

this is the only case of reversal for iron in the region less refrangible than  $\lambda$  5500 that I have come across. The high-temperature lines, and in fact the great majority of iron lines, are nearly unknown as absorption lines except in the sun and stars.

In the course of the experiments described below the absorption spectrum of iron from  $\lambda$  2250 to  $\lambda$  6600 has been photographed; all classes of lines except the pronounced enhanced lines are present, as may be seen from the reproductions. Of course only a beginning has been made so far; but the results obtained are quite promising, and it seems reasonable to expect that when the method is fully developed we may be able to imitate successfully the spectra given by the sun and stars. The object of the present communication is to call attention to the method in the hope that other workers may be induced to aid in developing it as rapidly as possible.

It may be of interest to state briefly the idea which led to these experiments: Consider a meteoric particle falling into the sun or a similar center of attraction. Let its mass be  $m$  and its velocity  $v$ ; its kinetic energy is therefore  $\frac{1}{2} mv^2$ . With the sun as the center of attraction we have  $v = 6 \times 10^7$  cm/sec., and hence, for  $m = 1$  gram, the energy is  $1.8 \times 10^{15}$  ergs or about  $4 \times 10^7$  calories. How far such a particle would travel before being consumed will of course depend upon the density of the atmosphere through which it moves. In general the path would not be long; hence the time would be short, perhaps a second or, more probably, only a very small fraction thereof. The conditions thus indicate that *a very large quantity of energy is thrown into a small amount of matter in a short space of time*. The effects, spectroscopic and otherwise, of such conditions cannot of course be predicted; hence if any of the circumstances could be produced experimentally they might lead to interesting results.

The conditions to be satisfied are as just stated: to throw a large amount of energy into a small amount of matter in as short a time as possible. By purely mechanical means this does not appear to be easy, but by electrical methods it seemed worth trying.

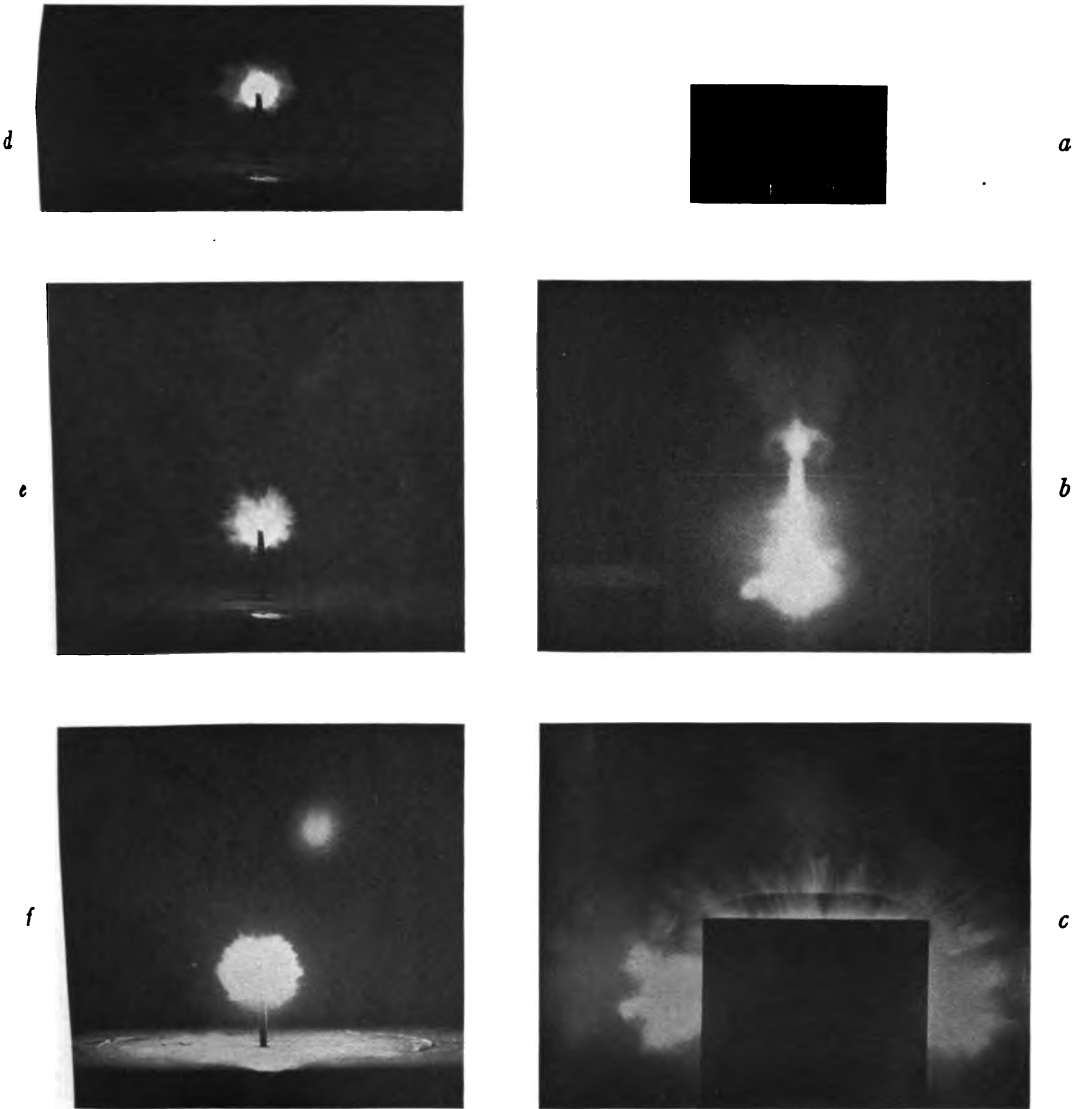
In the first attempts a small iron wire was inserted in a circuit containing two fair-sized 110-volt direct-current generators in

series. On closing the circuit, the wire blew up like an ordinary fuse with a blinding flash of light, the spectrum of which was easily photographed. On account of the large inductance of the circuit containing the armatures of the two generators, the duration of the flash was rather long and the amount of energy developed per gram per second not, therefore, very large. An estimate placed this at about  $10^5$  calories. A large storage battery would undoubtedly discharge at a much greater rate, but for obvious reasons this was not tried. Instead, a large glass plate condenser was built, which, when charged to about 25,000 volts, contains an amount of energy equal to 30 calories. When discharged through an iron wire 5 cm long and weighing 2 milligrams, this gives very good results. The circuit was so arranged that the frequency of the electrical oscillations as determined by a rotating mirror was 150,000 cycles per second, and the damping large enough to confine most of the energy to the first cycle. (See Plate VIIa, which is a photograph of the flash as seen in the rotating mirror.) If we assume that the effective time of a discharge is of the order of  $10^{-5}$  seconds and that the larger part of the energy of the condenser charge is expended in the exploding wire, we arrive at a rate of energy development per gram which is of the right order of magnitude. The discharge of this condenser was used throughout the present work.

#### DETAILS OF APPARATUS AND EXPERIMENTS

The condenser consists of 98 plates of single-strength window glass  $40 \times 50$  cm ( $16 \times 20$ ) inches having tin-foil coatings  $35 \times 43$  cm laid on with shellac. It is charged from a 500-watt, 26,000-volt transformer through a mechanical rectifier, the arrangement of the circuit being as shown in Figure 1. The difference of potential of the condenser plates can be regulated to some extent by varying the length of the series spark-gap  $S$ . When this is short, 2 mm approximately, and the gap  $W$  closed by a heavy conductor, sparks pass through  $S$  at the rate of 2 or 3 per second. When the gap  $S$  is lengthened to 2 cm, the sparks pass at the rate of one in about 2 seconds. The entire circuit  $CSW$  is made as short and compact as possible in order to keep the inductance low and the

# PLATE VII



## PHOTOGRAPHS OF ELECTRICALLY EXPLODED WIRES

- a* Explosion photographed by rotating mirror. Numbered divisions of scale correspond to one one-hundred-thousandth of a second
- b* Explosion in block of wood; end view
- c* Explosion in block of wood; side view
- d* Explosion in open air; aperture F/44
- e* Explosion in open air; aperture F/22
- f* Explosion in open air; aperture F/5.6. The faint image above is a ghost from the camera objective



frequency high. Since the capacity of the condenser is about 0.4 microfarad, and the frequency 150,000 cycles per second, it follows that the total inductance is only about  $\frac{1}{400}$  millihenry. The sparks are very noisy and the observer must not go too close without protecting his ears. This is especially true when a wire is exploded in the circuit. The sound-wave then sent out can be felt as a distinct sharp blow on the face or hands at a distance of 50 cm or more.

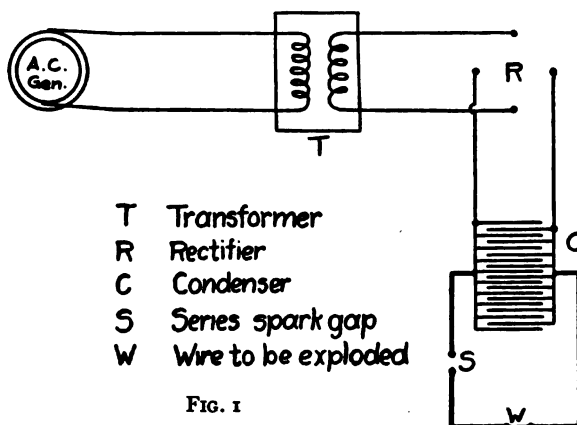


FIG. 1

The mechanical effects of exploding wires are interesting. Some of these have been described by Singer<sup>1</sup> and by F. E. Nipher.<sup>2</sup> If a glass tube with open ends be slipped over the wire the explosion breaks the tube into fragments, which are scattered all over the room; if the ends of the tube are closed by cork stoppers and the tube filled with water, the water disappears completely and the tube is broken into powder so fine that it is sometimes difficult to recognize it as glass. With the wire a few millimeters below the free surface of water in a large glass jar, the sound-wave transmitted through the water by the explosion thoroughly wrecks the containing vessel. The apparent absence of any heat effect is also quite striking. A No. 40 B. and S. gauge (0.080 mm) copper wire with double cotton insulation may be exploded, and in

<sup>1</sup> *Philosophical Magazine*, 46, 161, 1815.

<sup>2</sup> *Experimental Studies in Electricity and Magnetism*. Blakiston, 1914.



most cases the insulation remains nearly unchanged. Tissue paper wrapped tightly around the wire is torn into small bits, but not burned or even charred.

With the present condenser and voltage, it is not possible to obtain good effects with wires larger than No. 36 B. and S. gauge (0.127 mm), or longer than 8 cm; in fact smaller and shorter wires give better results. At first this was a great inconvenience, as it was found impossible to procure such small wires on the Pacific Coast. The difficulty was overcome by one of the mechanics, who found a neat way of making practically straight lathe turnings of any length, in sizes from less than 0.1 milligram per centimeter up.

In photographing the spectrum of the explosions a plane grating spectrograph was used. The collimator is a 12.5 cm (5 in.) Brashear telescope lens of 150 cm (60 in.) focus. The grating is a 10 cm (4 in.) Rowland, known as the "Kenwood grating," having bright second and third orders. The camera lens is a Bausch and Lomb Tessar Ic, F/4.5 of 39 cm (15  $\frac{3}{4}$  in.) focus. The second-order spectrum was used and the grating so inclined to the axis of the camera lens that the dispersion at the middle of the plate is 6 Å per millimeter. The ultra-violet region was photographed with a large Fuess quartz spectrograph, giving a scale at  $\lambda$  2300 of about 4.5 Å per millimeter.

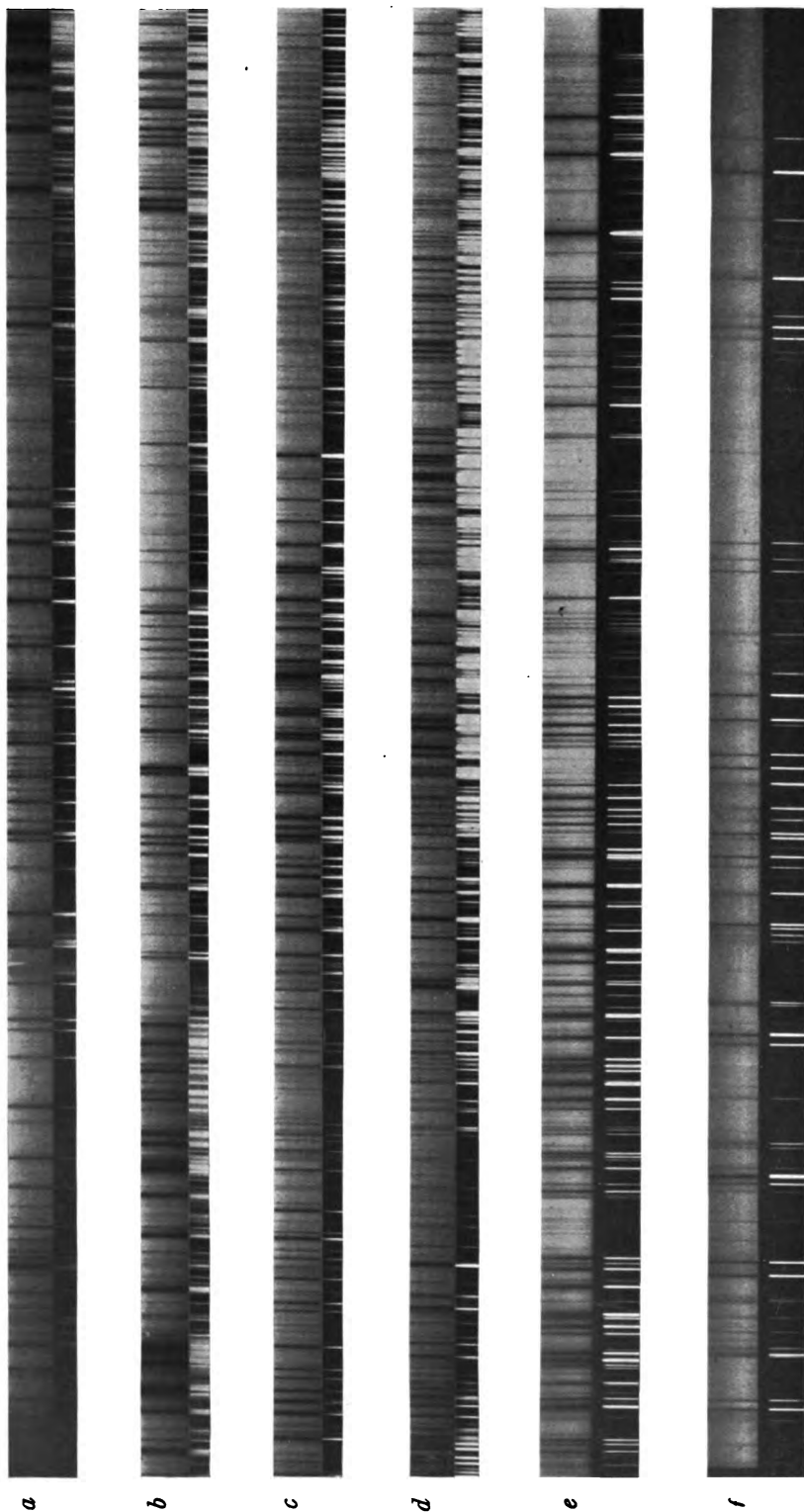
## RESULTS

The following are the general conclusions from the work up to the present time:

1. *Wire exploded in the open air.*—When viewed side on, the spectrum consists of bright lines, with faint self-reversals in the green region and more prominent reversals in the violet. There is a continuous background of increasing intensity toward shorter wave-lengths, but not very strong. Viewed end on, the reversals are more prominent throughout and the continuous background very much strengthened. At  $\lambda$  3700 the strength of the background is so great that this portion of the spectrum looks very much like a normal absorption spectrum. Open-air explosions were not studied in the region beyond  $\lambda$  3600.



# PLATE VIII



SPECTRA OF ELECTRICALLY EXPLODED IRON WIRES WITH IRON ARC COMPARISON

Quartz Spectrograph: *a*,  $\lambda$  2270 to  $\lambda$  2490; *b*,  $\lambda$  2472 to  $\lambda$  2764; *c*,  $\lambda$  2780 to  $\lambda$  3280; *d*,  $\lambda$  3216 to  $\lambda$  4075  
 Grating Spectrograph: *e*,  $\lambda$  3700 to  $\lambda$  4090; *f*,  $\lambda$  5143 to  $\lambda$  5645

2. *Wire surrounded by a wooden tube 1 cm in diameter and viewed end on.*—At atmospheric pressure the spectrum is perfectly continuous with absorption lines only, from  $\lambda$  2250 to above  $\lambda$  5700. To the violet of  $\lambda$  4500 the lines are in general quite narrow and sharp; to the red of  $\lambda$  4500 the flame lines are sharp, while lines of groups *d* and *e* are rather wide and diffuse. A spectrogram of the region  $\lambda$  6100– $\lambda$  6600 shows also a continuous spectrum with absorption lines, but there are faint traces of emission lines (enhanced iron lines). Using this arrangement under a bell jar, the region  $\lambda$  3600– $\lambda$  4200 was studied in air at pressures ranging from 2 cm to 20 cm. At 2 cm all lines were bright and very few showed self-reversals, except H and K (these came no doubt from the wood). From 5 cm to 13 cm pressure the continuous background increased rapidly in intensity; reversals became gradually more prominent, and the bright lines broadened and in general shifted toward longer wave-lengths, so that at 10 cm numerous lines showed as a fine absorption line in the normal position with a broad emission line lying wholly on its red side.

At 15 cm and 20 cm there was no trace of bright lines, the spectrum being perfectly continuous with the absorption lines in general very fine.

3. *Wire placed in a cut in a block of wood as indicated in Figure 2.*—The cut mostly used was 4 cm long, 2.5 cm deep, and 3 mm wide. This gives the same spectrum as that produced by the tube just

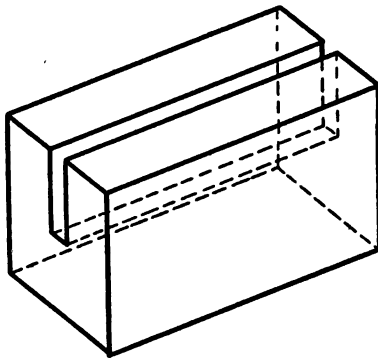


FIG. 2

described; it is, however, much easier to load, and is better adapted for projection on the slit of the spectroscope. The spectra reproduced in Plate VIII were taken with this arrangement, viewed end on.

4. *Brightness of the explosion as a source of light.*—Since the spectrum is continuous it becomes possible to compare the brightness of the source with that of the sun, for example, by merely

comparing the exposure-times which give the same density on the photographic plate, using the same spectroscope and projecting apparatus in both cases. The method is simply one of direct substitution. Such a comparison was made in the region  $\lambda$  3900– $\lambda$  4000, using both the quartz and grating spectrographs, and in the region of  $\lambda$  5500 using the grating instrument. The results are as shown in the accompanying table:

No. of Successive Explosions	Exposure to Sun for Equal Density	Region	Spectrograph
3.....	Sec. 1/200	$\lambda$ 3900– $\lambda$ 4000	Quartz
10.....	1/40	$\lambda$ 3900– $\lambda$ 4000	Grating
48.....	1/10	$\lambda$ 5200– $\lambda$ 5600	Grating

It remains to estimate the equivalent duration of an explosion. Plate VIIa shows that the total duration of light of sufficient intensity to affect the photographic plate exposed with the rotating mirror is not over 1/20,000 sec. It also shows that the greater part of this light is concentrated in the first half-cycle, the duration of which is 1/300,000 sec. Hence if we call the equivalent time 1/100,000 sec. we are overestimating rather than underestimating it. Using this value we find for the ratio of exposure to sun to that of the explosions for the three comparisons given above 167:1, 250:1, 200:1, respectively, or in the mean that it requires 200 times the exposure to the sun to produce the same density as that given by the explosions. The sunlight is of course considerably reduced in intensity in passing through the atmosphere, and there is an additional loss at the speculum mirror which reflects it into the projection system. If we say that only one-half of the light from the sun reached the projection system we still find this new source to be 100 times as bright as the solar surface.

5. *Direct photographs of the explosion.*—Plate VIIb shows an end view of the explosion in the block of wood, and Plate VIIc is a side view of the same. The contraction of the luminous column above the slot in the end view is evidently connected with the sharply defined “shadow” above the block in the side view. This apparent shadow is a little surprising and an explanation does not readily suggest itself.

Plate VII*d, e, f* shows end views of the explosion of a wire in the open air. They were taken with the camera lens stopped to F/44, F/22, and F/5.6, respectively, so as to get the effect of exposures of different "lengths." The F/44 exposure, together with a similar one taken side on (not reproduced), show plainly a central core of luminous vapor, having the form of a solid cylinder 22 mm in diameter and of a length somewhat greater than that of the wire used, the ends of the cylinder being roughly hemispherical caps. The remarkably sharp outer boundary of this cylinder indicates that it marks the limit reached by the expanding gases at the end of the first half-cycle, that is, at the end of  $1/300,000$  sec. The F/22 exposure shows clearly a fainter second cylinder outside the first, whose diameter is roughly 45 mm. Its outer boundary is, however, rather ragged in this exposure, and even in the F/5.6 exposure it is far from being as sharp as that of the inner cylinder. The outer cylinder probably marks the limit reached by the gases at the end of the first cycle, and its light is chiefly derived from the current during the second half-cycle, the greater part of which must have passed through the inner core.

The vapors undoubtedly go on expanding through the succeeding cycles, but partly on account of their rapid cooling due to expansion, and partly because of the great diminution of the current intensity, the corresponding cylinders fail to be registered on the photographs.

If the explanation just given is correct, we find for the velocity of the expanding gases 3.3 km per second, or about 10 times the velocity of sound in air at normal temperatures.

When the wire is exploded in the slot in the block of wood, the two regions corresponding to the two cylinders can still be seen quite well on the photographs, but they lack the sharp outline shown in the open air, perhaps owing to the resistance to motion offered by the confining walls of wood. It is clear, however, that the velocity in this case is considerably greater, measurements on one of the best plates giving 30 mm and 54 mm respectively, instead of 22 mm and 45 mm for the open air.

6. *Pressure in the gases of the explosion.*—The experiments of Hale and Kent, showing that a spark discharge in gases at a pressure

of 50 atmospheres or more gives a spectrum at least partially continuous, suggested that the cause of the continuous spectrum observed in these experiments may be a very high pressure in the gases formed by the explosion. An effort to estimate the order of magnitude of this pressure was made as follows: A hole 7 mm in diameter was bored through a block of wood weighing 130 grams. The block was then split into two parts by a cut passing through the axis of the hole. One-half was rigidly mounted, and the other suspended as a pendulum so as to hang in contact with the immovable half. The wire was mounted centrally in the hole and the velocity of the movable half produced by the explosion was measured and found to be 135 cm/sec. The mass of the movable block being 65 grams, its momentum was  $65 \times 135 = 8775$  gr. cm/sec. The wire in this case was a No. 36 B. and S. gauge (0.127 mm) nickel wire, 6 cm long, 48 mm being inside the opening in the split block. The mass of 48 mm of this wire is 4.8 mg. The momentum is of course equal to the product of the pressure, area, and the time. The pressure varies and is a function of the time. Not knowing the law of variation or the exact value of the time, only very rough estimates of the pressures could be made. The time in this case is of course not the same as the duration of the light, because the emission of light, being largely due to the flow of current through the gases, will cease after a few cycles; the gases, however, go on expanding until atmospheric pressure has been reached. If we assume the equivalent time to be that during which the maximum pressure would produce the momentum observed, we may reasonably suppose that its value would be somewhere between  $1/50,000$  and  $1/10,000$  sec., and probably nearer the latter figure. This gives, for the pressure, a value lying between 135 and 27 atmospheres, with the probability in favor of a value of 40 or 50 atmospheres. An independent method of estimating the pressure is as follows: Assume that the nickel wire is transformed into monatomic nickel vapor at a temperature of  $20,000^\circ \text{C.}$ , which is the order of temperature to be expected from the intensity of the light. The volume at atmospheric pressure would be 136 cu. cm, and if we neglect leakage through the open ends of the tube and merely divide by the volume of the tube, viz., 1.82 cu. cm,

we find 75 atmospheres as an upper limit for the pressure, which is in fair agreement with the estimate from the momentum of the block. We cannot be far from the truth if we say that in this experiment the pressure was of the order of 50 atmospheres.

The iron wires exploded in making the spectrograms accompanying this paper weighed only 0.4 as much as the nickel wire used in the experiment just described, and the volume of the slot in which the wires were placed was 2.5 cu. cm, or 1.4 times as great, so that in this case the pressure could hardly have been more than one-third of that just estimated, or of the order of 20 atmospheres. It seems reasonable to conclude, therefore, that the pressures developed in these explosions are not nearly as high as those which have often been used in spectroscopic investigations, and hence that *very high pressure in a gas is not at all necessary for the production of a continuous spectrum.*

7. *Experiments with other elements.*—A few spectrograms were made using copper, nickel, and manganin wires. With manganin the continuous spectrum has about the same brightness as with iron; with nickel it is brighter; while with copper it is very much fainter.

#### DISCUSSION

It may not be out of place to return for a moment to the idea which prompted these experiments. As stated above, this was to determine if possible the spectroscopic result of the fall of a meteoric particle of very high velocity into a resisting medium, such as the solar atmosphere. The general effect would be an extremely rapid vaporization of the materials forming the particle. In these experiments we have a rapid vaporization of a metal in the form of a thin wire. The analogy ends here, for in one case the vaporization is produced by mechanical, in the other by electrical, means. That the two methods would yield identical results is not to be expected; but on the other hand it is hard to advance any valid reason why they should be radically different. There is another difference, and an important one, in the amounts of energy available in the two cases. In our experiments the total energy of the condenser charge was 30 calories, and not all of this small amount went into the wire. The same wire falling into the sun



would develop 80,000 calories—in a longer time it is true, yet one cannot help feeling that an adequate imitation of what must happen in the sun requires much more energy than was available in the present work. The following general conclusions seem to be reasonable: A very small particle would be consumed in the extreme outer regions of the sun's atmosphere where the pressure is exceedingly low. The path of the particle would therefore be long and the rate of development of heat energy low. Under such conditions the spectrum would most likely consist of bright lines, with little if any continuous background. Particles large enough to reach a level where the pressure is appreciable would encounter an enormous resistance, and the development of heat energy would be extremely rapid, perhaps hundreds of times as rapid as in the present experiments. Here it seems likely that a continuous spectrum with absorption lines would be produced.

The experiments will be continued with a larger condenser and higher voltage. Attempts will also be made to observe the explosions in gases other than air; hydrogen, for example, should be interesting.

The author desires to express his thanks to Mr. Ellerman for help in some of the photographic work, and for his kindness in preparing the plates for reproduction. The author is also indebted to Mr. Sinclair Smith, who assisted throughout the experimental work.

#### SUMMARY

1. Fine wires exploded by a condenser discharge give a brilliant continuous spectrum crossed by the absorption lines of the element composing the wire.

2. The continuous spectrum extends into the extreme ultra-violet.

3. The intrinsic brightness of the explosion as a source of light is very high, being apparently much greater than that of the solar surface.

4. The pressure in the gases giving the continuous spectrum is not excessive, being at most of the order of 20 atmospheres.

MOUNT WILSON OBSERVATORY

December 1, 1919

# STUDIES BASED ON THE COLORS AND MAGNITUDES IN STELLAR CLUSTERS<sup>1</sup>

## FIFTEENTH PAPER: A PHOTOMETRIC ANALYSIS OF THE GLOBULAR SYSTEM MESSIER 68

By HARLOW SHAPLEY

### ABSTRACT

*Globular star cluster Messier 68.*—The paper contains the results of a characteristic *photometric analysis* of this hitherto unexplored typical cluster, based on fifteen photographs made at the primary focus of the 60-inch reflector. Twenty-eight *variable stars* were discovered, all but one of which appear to be typical, short-period, cluster variables. This cluster is poorer in *giant stars* than some others, as only 250 are brighter than the absolute magnitude zero. The magnitudes and colors of 56 of the brightest of these are tabulated. Most of them are red or yellow. The *distance* of the cluster as computed by three methods which give concordant results is about 55,000 light-years. The *form* is quite accurately circular as far as the two thousand brightest stars are concerned.

*Stellar clusters. Further evidence in support of the following general conclusions* is supplied by the analysis of M 68: (1) Cluster type *variables* are bluer at maximum than at minimum brightness. (2) Their mean brightness appears to be an astrophysical constant which is a little more than one magnitude fainter than the mean brightness of the 25 brightest stars of the cluster. (3) The fainter the *giant star*, the bluer is its color, on the average. (4) The brightest giant stars are always very red and have absolute photo-visual magnitudes between  $-4$  and  $-3$ . (5) The general *luminosity curve* for the stars of the cluster differs widely from a symmetrical probability curve. (6) The *distance* of such clusters can be computed from the diameter of the image of the cluster, or from the mean magnitude of the 25 brightest stars, or from the mean magnitude of the short-period variables.

The present paper reports on a characteristic photometric analysis of a typical globular cluster. The intention of the report, in addition to presenting explicit results that come out of the study of Messier 68, is to examine numerically some of the working hypotheses at the basis of earlier work on clusters,<sup>2</sup> and also to illustrate what astrophysical information can be derived from an inextensive survey of one of the globular systems. There is a considerable number of clusters no fainter than Messier 68 concerning whose structure little is now known.

<sup>1</sup> *Contributions from the Mount Wilson Observatory*, No. 175.

<sup>2</sup> For example, that relating to the general applicability of the adopted methods of determining parallax; cf. Section 5 on page 56.

1. *Earlier results.*—The position of Messier 68, = N.G.C. 4590 for 1900 is:

Right ascension =  $12^h 34^m 2$

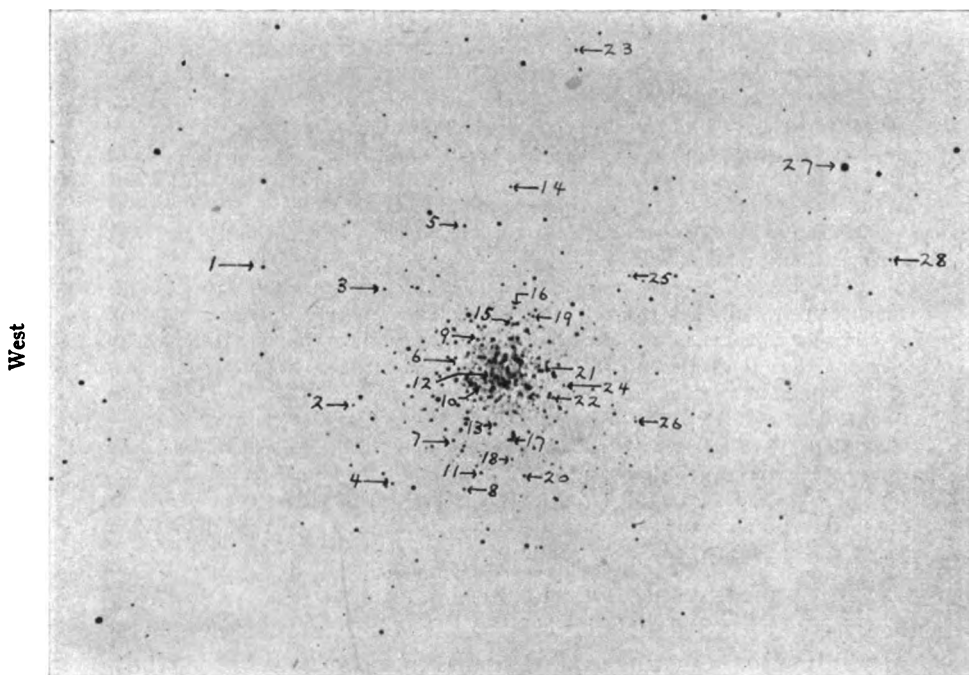
Declination =  $-26^\circ 12'$

Galactic longitude =  $268^\circ$

Galactic latitude =  $+36^\circ 6$

There are no early measures of magnitude for the individual stars, aside from roughly estimated limiting values by Bailey,<sup>1</sup> and no

North



THE VARIABLE STARS IN MESSIER 68

variable stars had been reported prior to our study. Holetschek's<sup>2</sup> integrated visual magnitude of the cluster is 8.2. The diameter estimated from the Franklin-Adams chart,  $5'.3$ , has led in *Mount Wilson Contribution* No. 152, to the parallax

$$\pi = 0''.000062, \quad (1)$$

<sup>1</sup> *Harvard Annals*, 60, 212, 1908; 76, 46, 1915.

<sup>2</sup> *Annalen der k.k. Universitäts Sternwarte in Wien*, 20, 114, 1907.

to which corresponds the linear galactic co-ordinates, in units of 100 parsecs,

$$\begin{aligned} R &= 161 \\ R \cos \beta &= 129 \\ R \sin \beta &= +97 \end{aligned}$$

2. *Mount Wilson photographs.*—The observations in Table I have all been made at the primary focus of the 60-inch reflector. The remarks in the last column show to what use the various plates have been put. Although the southern declination of this cluster greatly limits the working season with the 60-inch reflector and is also unfavorable to high accuracy in the comparison with polar standards, the plates are of good quality and the results appear to be trustworthy.

TABLE I  
PHOTOGRAPHS OF MESSIER 68 (N.G.C. 4590)

Plate Number	Date G.M.T.	Kind of Plate	Exposure Time	Remarks
4501*	1918, July 3.68	S 27	5 <sup>m</sup> , 5 <sup>m</sup> , 1 <sup>m</sup>	Variables
4842.....	1919, Feb. 24.91	S 27	15	Variables
4843*	1919, Feb. 24.92	S 27	1 1 1	Photographic magnitudes, variables
4844*	1919, Feb. 24.93	Isa + C	5 5 5	
4845*	1919, Feb. 24.95	S 27	1 1 1 1 <sup>m</sup>	
4855*	1919, Feb. 25.92	Isa + C	5 1 5	Photo-visual magnitudes
4856*	1919, Feb. 25.92	S 27	2 2 2	Photographic magnitudes, variables
4857*	1919, Feb. 25.93	S 27	10 10 2	Variables
4858*	1919, Feb. 25.94	Isa + C	15 15 2	Photo-visual magnitudes, variables
4859*	1919, Feb. 25.95	S 27	1 1 1	Photographic magnitudes, variables
4863.....	1919, Feb. 27.88	S 27	12	Variables, luminosity-curve
4864.....	1919, Feb. 27.90	S 27	35	Variables, chart
4911.....	1919, May 24.68	S 30	20	Variables
4924.....	1919, May 25.670	S 30	50	Variables, positions, ellipticity, luminosity-curve
4935.....	1919, May 26.68	S 30	20	Variables

\* Plates with multiple exposures are polar comparisons.

3. *Variable stars.*—By comparing the various plates in a stereocomparator, Miss Ritchie has found that the 28 stars listed in Table II undergo appreciable variation in light. The  $x$  and  $y$  co-ordinates in the second and third columns give the intervals of right ascension and of declination from the center;  $x$  is positive east, and  $y$  is positive north of the cluster. The positions are believed to be sufficiently accurate for identification. On the accompanying reproduction of Plate 4864 the variable stars are indicated by arrowheads.

The magnitudes have been determined as usual through the intermediary of polar comparison plates and by the measurement of some twenty comparison stars on all photographs listed in Table II. The last column of the table shows the differences between the photo-visual magnitude on Plate 4858 and the mean of the photographic magnitudes on Plates 4857 and 4859; these values of the variable color-index apply, of course, only to one phase of the light variation of each star. The bluish color for all but No. 27 indicates that the variables are of the usual cluster type. The observed ranges of light-variation and the similarity of the median magnitudes also support this view, although neither range nor median brightness is definitively determined.

A comparison of the magnitudes for any variable in Table II with the corresponding dates of observation in Table I shows that probably all except No. 27 have periods of less than a day. It appears reasonable to assume that these 27 stars belong to one or more of the sub-types<sup>1</sup> of Cepheid variables whose absolute photographic median magnitudes are approximately  $-0.2$  (*Mount Wilson Contribution* No. 151, p. 27).

The apparent photographic median magnitude cannot be derived with certainty for a given variable because of insufficient observations to determine the light-curve completely. The tabulated medians vary from 15.65 to 16.21; the average median is  $15.90 \pm 0.10$  (average deviation). Considering that all observations refer to a typical star, however, we derive the following fairly reliable mean value for the 27 variables:

$$\text{Median} = 15^m90 \pm 0.02 \text{ (p.e.)}. \quad (2)$$

As a further check of this value, the median of the means for the ten brightest and for the fifteen faintest<sup>2</sup> magnitudes in Table II is

$$(16.42 + 15.33)/2 = 15^m88.$$

<sup>1</sup> On the basis of the observed range and the relative number of bright and faint magnitudes, we infer that the variables numbered 4, 6, 8, 13, and 28 may belong to Bailey's sub-class *c*, for which the characteristics are very short period, small amplitude of variation, and light-curves practically symmetrical.

<sup>2</sup> For the average cluster-type star the duration of "brighter than median" is to the duration of "fainter than median" approximately as two to three.

TABLE II  
POSITIONS AND OBSERVATIONS OF 28 NEW VARIABLE STARS IN MESSIER 68

VARIABLE	POSITION		MAGNITUDES ON PHOTOGRAPHIC PLATES										OB- SERVED RANGE	MEDIAN MAGNI- TUDE	PROVI- SIONAL COLOR- INDEX
	$\alpha$	$\gamma$	4842	4843	4856	4857	4859	4863	4864	4911	4924	4935			
1.....	-4' 40"	+1' 49"	15.99	.....	16.03	15.88	.....	15.43	15.28	15.65	15.66	15.52	0.75	15.66	+0.07:
2.....	-2 48	-0 45	16.39	.....	16.24	16.02	16.11:	16.18	16.16	15.69	16.08	16.28	0.70	16.04	+0.34
3.....	-2 20	+1 31	16.34	.....	15.96	15.79	16.09:	15.76	15.54	15.93	15.93	15.86	0.80	15.94	+0.46
4.....	-1 57	-2 11	15.93	.....	16.02	15.70	15.77	15.84	15.65	15.08	15.56	16.01	0.46	15.79	+0.21
5.....	-0 56	+2 50	16.14	.....	15.85	15.76	15.90	15.62	15.51	15.69	15.77	15.91	0.63	15.82	+0.21
6.....	-0 54	+0 17	15.90	.....	16.00	15.64	15.71	15.73	15.77	15.65	15.93	16.03	0.39	15.84	+0.25
7.....	-0 50	-1 19	15.85	.....	15.87	15.56	15.65	15.78	15.48	15.65	16.16	15.94	0.68	15.82	+0.26
8.....	-0 38	-2 14	16.12	.....	16.03	15.79	16.00	15.84	15.82	15.69	16.14	15.74	0.45	15.92	+0.43
9.....	-0 31	+0 40	16.12	.....	16.07	16.10	.....	15.88	15.89	15.90	15.43	16.28	0.85	15.86	+0.40
10.....	-0 25	-0 16	16.62:	.....	15.93	16.20	15.84	16.21	15.28:	16.15	16.20	15.60	0.61	15.90	+0.47
11.....	-0 18	-1 52	15.93	.....	16.11	16.06	16.02	15.60	15.31	15.53	15.87	15.97	0.80	15.71	+0.33
12.....	-0 10	-0 1	16.23	.....	15.75	15.64	15.07	15.56	16.08	16.01	15.85	16.14	1.16	15.65	+0.27
13.....	-0 6	-0 56	15.90	.....	16.28	16.20	16.07	15.62	15.77	15.74	15.66	16.22	0.66	15.95	+0.24:
14.....	-0 4	+3 38	15.55	.....	16.29	16.10	.....	15.16	15.92	15.98	15.82	15.50	0.79	15.90	+0.29:
15.....	+0 9	+0 58	16.14	.....	15.89	15.69	15.65	15.76	16.08	16.36	16.08	15.78	0.71	16.00	+0.21
16.....	+0 11	+1 20	16.12	.....	15.89	15.74	15.71	15.73	15.95	16.43	16.16	15.86	0.72	16.07	+0.17
17.....	+0 16	-1 15	16.60:	.....	15.76	15.95	15.65	15.78	16.16	16.56	16.04	16.39	0.91	16.10	+0.50
18.....	+0 19	-1 36	16.28	.....	15.90	15.97	16.02	16.15	16.16	15.72	15.59	16.22	0.69	15.94	+0.29
19.....	+0 33	+1 10	16.21	.....	15.94	15.89	15.74	15.82	15.98	15.65	16.11	15.84	0.56	15.93	+0.24
20.....	+0 34	+1 54	15.82	.....	15.74	15.81	15.93	15.80	15.45	15.78	15.59	16.01	0.57	15.74	+0.45
21.....	+0 38	+0 8	16.60	.....	15.92	16.05	16.00	15.82	16.19	16.26	16.16	16.35	0.78	16.21	+0.57
22.....	+1 1	+0 22	16.52	.....	15.92	16.42	16.07	15.78	16.14	16.41	16.04	16.16	1.22	15.91	+0.46
23.....	+1 4	-0 20	16.34	.....	16.00	15.88	.....	15.76	15.85	15.78	15.08	16.16	1.26	15.71	+0.22
24.....	+1 14	-0 8	15.90	.....	16.09	16.10	16.00	16.11	16.01	16.34	16.00	15.74	0.60	16.04	+0.26
25.....	+2 21	+2 3	15.93	.....	15.77	16.07	.....	16.21	16.19	16.00	16.00	15.99	0.44	15.99	+0.39
26.....	+2 38	-0 44	15.68	.....	15.67	16.10	.....	16.11	15.89	16.09	16.35	15.72	0.68	16.01	+0.30
27.....	+6 20	+4 23	.....	.....	.....	.....	11.36	10.88	.....	14.89	15.04	14.94	4.0±	13.0±	+2.0±
28.....	+7 20	+2 40	15.93	.....	16.14	16.04	.....	15.67	15.62	16.04	15.66	15.97	0.52	15.88	+0.76
Means*															+0.34

\* Excluding No. 27.

Arranging the color-indices of Table II in order of the corresponding photographic magnitudes, we make the following tabulation, showing the anticipated increase of color-index with decreasing brightness, which is typical of this kind of variation (cf. Figs. 3, 4, and 5 of *Mount Wilson Contribution* No. 154).

Mean Pg. Magnitude	Number of Variables	Mean Color-Index
15.61.....	5	+0.23
15.80.....	5	0.32
15.91.....	5	0.29
16.05.....	6	0.41
16.12.....	6	+0.41

4. *Relation of absolute magnitude to color-index.*—From the polar comparison plates the magnitudes have been determined both for a series of selected comparison stars, to be used in studying the variables, and for a complete list of all the brighter stars (outside the central nucleus but within 3'.5 of the center), to be used in determining the parallax of the cluster and the upper limits of luminosity. Table III contains the positions, magnitudes, and colors of these stars. By accepting the value of the parallax adopted in a following section, the apparent photographic and photo-visual magnitudes may be transformed into absolute values by subtracting 16.15 from the magnitudes given in Table III. It is then seen that these stars are all giants, most of them red and yellow, but a few of the fainter ones blue.

The interdependence of color and magnitude among the giant stars is illustrated by Table IV and Fig. 1. The usual color law for giant stars in clusters, already found in several systems,<sup>1</sup> holds also in this case; that is, the fainter the giant, the bluer is the color, and, if the star is a Cepheid variable, the shorter is its period. The last group of Table IV (not plotted in Fig. 1) contains 27 variables; the next to the last group contains 3 stars, and the preceding groups contain 5 stars each. The variables agree perfectly with invariable stars in the relation of median color to absolute luminosity.

<sup>1</sup> *Mt. Wilson Communications*, No. 34, 1916.

TABLE III  
MAGNITUDES AND COLORS OF 56 STARS IN MESSIER 68

STAR	POSITION		MAGNITUDE		STAR	POSITION		MAGNITUDE		COLOR-INDEX
	$z$	$y$	Photo-graphic	Photo-visual		$z$	$y$	Photo-graphic	Photo-visual	
101†	-7' 25"	-5' 9"	12.06	11.06	129*	+0' 15"	+0' 58"	15.07	14.16	+0.91
102†	-2 48	-1 53	15.97	15.53	130*	+0 16	+0 43	14.85	13.98	+0.87
103	-2 39	-1 32	15.33	14.60	131*	+0 18	-1 10	14.92	14.02	+0.90
104*	-2 36	-0 35	14.35	13.12	132*	+0 22	+0 19	14.32	12.93	+1.39
105*	-2 29	-0 57	15.06	14.16	133*	+0 26	+0 54	14.76	13.80	+0.96
106†	-2 16	-0 4	15.92	15.20	134†	+0 28	-1 24	16.01	15.30	+0.71
107	-2 8	-2 2	15.60	14.56	135	+0 32	+2 24	15.02	14.18	+0.84
108†	-2 3	+0 2	16.18	16.0	136†	+0 36	+3 2	15.06	15.15	+0.65
109†	-2 2	+2 36	15.92	15.34	137*	+0 39	+4 19	15.80	14.41	+0.65
110*	-1 49	+0 24	14.75	13.69	138†	+0 54	+0 42	15.62	14.58	+1.04
111	-1 46	-0 20	15.84	15.11	139*	+0 58	+0 8	14.81	13.98	+0.83
112†	-1 41	+1 37	15.44	14.53	140*	+1 2	+2 24	15.58	14.99	+0.59
113	-1 34	+3 2	13.98	12.42	141*	+1 2	+0 3	14.45	13.29	+1.16
114	-1 34	-2 15	14.00	12.46	142*	+1 8	-1 13	15.67	15.36	+0.31
115†	-1 9	-0 33	13.86	12.38	143*	+1 9	-0 34	15.02	14.34	+0.68
116†	-1 6	+0 57	15.74	14.97	144*	+1 14	-2 19	14.99	14.11	+0.88
117*	-1 3	+0 4	15.07	14.26	145*	+1 17	+1 26	14.31	12.88	+1.43
118	-0 40	-1 28	15.40	14.39	146*	+1 24	+0 52	14.60	13.26	+1.34
119	-0 40	+1 7	13.99	12.40	147	+1 27	+1 16	14.08	12.66	+1.42
120*	-0 37	-0 57	15.08	13.98	148†	+1 52	-1 18	15.82	15.32	+0.50
121	-0 26	+0 20	15.66	15.32	149	+2 9	+0 10	15.80	15.66	+0.14
122†	-0 14	+2 53	14.63	13.56	150†	+2 9	+1 45	15.74	14.97	+0.77
123*	-0 13	+0 40	15.02	14.20	151*	+2 13	-0 37	15.02	14.15	+0.87
124*	-0 10	-0 15	14.67	13.70	152†	+2 26	-1 21	16.40	15.32	+1.08
125*	-0 10	-3 12	14.64	13.44	153†	+2 36	+1 57	15.20	15.56	+0.64
126	-0 8	+0 32	15.41	14.54	154†	+2 38	+0 42	15.82	15.61	+0.21
127†	-0 7	+1 44	16.32	15.48	155*	+2 47	+1 38	14.67	14.20	+0.47
128*	+0 6	-0 10	14.79	13.67	156†	+8 26	+4 50	12.87	11.78	+1.09

\* Bright stars used for the determination of distance.

† Comparison stars used for the study of variables.



5. *The distance of Messier 68.*—As described in *Mount Wilson Contribution* No. 151, Section 5, the mean apparent photographic magnitude of the bright stars can be used as a measure of distance.

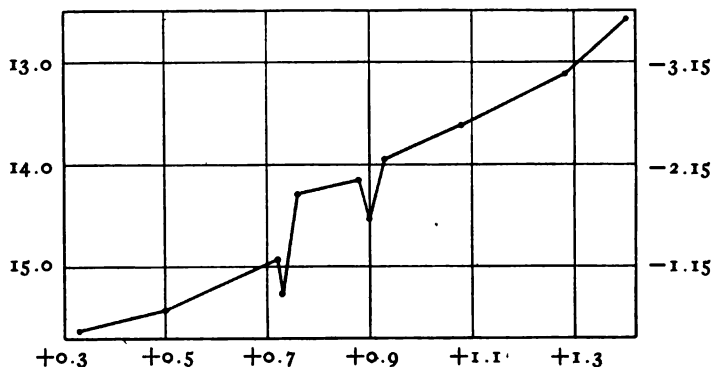


FIG. 1.—The color of giant stars in Messier 68. Abscissae are mean color indices; ordinates are apparent and absolute magnitudes.

Excluding the five brightest stars, we obtain from Table III for the next twenty-five stars in order of brightness the mean value of  $14.80 \pm 0.21$  (average deviation) with extremes of  $14^m.31$  and  $15^m.08$ .<sup>1</sup>

TABLE IV  
COLOR OF GIANT STARS

MEAN PHOTO-VISUAL MAGNITUDE		MEAN COLOR-INDEX
Apparent	Absolute	
12.59.....	-3.56	+1 <sup>m</sup> .40
13.12.....	-3.03	+1.28
13.61.....	-2.54	+1.08
13.95.....	-2.20	+0.93
14.15.....	-2.00	+0.88
14.28.....	-1.87	+0.76
14.52.....	-1.63	+0.90
14.93.....	-1.27	+0.72
15.26.....	-0.89	+0.73
15.41.....	-0.74	+0.50
15.61.....	-0.54	+0.33
15.57.....	-0.58	+0.34

If, as previously adopted, this mean value corresponds to absolute magnitude  $-1.5$ , we derive as the parallax of the cluster

$$\pi = 0''.000055. \quad (3)$$

<sup>1</sup> Cf. Table II of *Mt. Wilson Contr.* No. 152, 1917.

A better determination of the distance may be based on the variable stars, whose intrinsic luminosity is known with higher accuracy than that of the brighter stars. Accepting  $-0.23$  as the absolute value of the median photographic magnitude,<sup>1</sup> we compute from the observed value (2)

$$\pi = 0''.0000595. \quad (4)$$

These new determinations are of much higher weight than (1), which is based on the measured diameter alone. Assigning weights 1, 2, and 4 to (1), (3), and (4), respectively, we derive the definitive value

$$\pi = 0''.000059,$$

which differs from the earlier determination by less than 5 per cent. Corresponding to the adopted parallax, we have, in units of 100 parsecs,

$$\begin{aligned} R &= 170 \\ R \cos \beta &= 137 \\ R \sin \beta &= +102 \end{aligned}$$

and; to reduce from apparent to absolute magnitude, we compute the factor  $m - M = 16.15$ .

The difference Median *minus* "Mean of 25 Brightest,"  $+1.10$ , is somewhat small; but it differs by less than the adopted probable error from the mean value (derived from several clusters in *Contribution* 151) that was used in *Contribution* 152 for the determination of the distance of a considerable number of clusters in which variable stars are infrequent or unknown.

6. *The general luminosity-curve.*—The relation of the frequency of stars to absolute brightness is tabulated for two photographs in Table V. Numbers in parentheses show the frequencies when the known variable stars are excluded. On the plate of longer exposure, No. 4924, the magnitudes have been determined for more than 800 stars in representative selected areas that cover about one-fourth of the whole cluster; on Plate 4863 all stars in the cluster brighter than magnitude 17.5 were measured, excepting those within half a minute of arc of the center. Because of the

<sup>1</sup> *Mt. Wilson Contr.* No. 151, p. 27, 1917.

small apparent diameter and the fairly high galactic latitude of Messier 68, no correction for background stars has been considered necessary. The reduction of the measures has involved, however, the usual correction for irregularities of the measuring scale and for distance from the center of the plate, and also for the unlike magnitude intervals in Table V.

TABLE V  
LUMINOSITY AND FREQUENCY OF STARS

PLATE 4863		PLATE 4924	
Absolute Pg. Mag.	Number of Stars	Absolute Pg. Mag.	Number of Stars
-2.2.....	2.7	-2.4.....	0.7
-1.76.....	4.3	-2.06.....	1.4
-1.38.....	5	-1.64.....	1.4
-1.01.....	9	-1.25.....	3
-0.68.....	24 (23)	-0.86.....	6 (5)
-0.46.....	61 (55)	-0.56.....	11 (10)
-0.28.....	72 (65)	-0.28.....	14 (12)
-0.11.....	60 (53)	0.00.....	14 (12)
+0.11.....	31 (29)	+0.27.....	11 (10)
+0.4.....	24 (22)	+0.55.....	9
+0.7.....	25	+0.83.....	13
+1.0.....	41	+1.1.....	17
+1.3.....	70	+1.4.....	19
		+1.7.....	25
		+1.9.....	42
		+2.2.....	74
		+2.5.....	130
		+2.7.....	234

The relatively high frequency of stars near the median magnitude, Fig. 2, appears to be much the same in this cluster as in five other globular clusters previously studied.<sup>1</sup> With the variable stars omitted, the phenomenon of a secondary maximum is still distinctly shown. From these results it appears that the general luminosity-curve in a star cluster cannot be accepted as a symmetrical probability-curve. The computation by Schouten<sup>2</sup> and Coeberg<sup>3</sup> of the distance of clusters, on the basis of the relative frequency of stars of the brightest few magnitudes, is therefore

<sup>1</sup> *Mt. Wilson Contr.* No. 155, 1917.

<sup>2</sup> *Verslagen Koninklijke Akademie van Wetenschappen te Amsterdam*, 20, 1147, 1293, 1918.

<sup>3</sup> *Hemel en Dampkring*, November 1918.

open to serious objection because they assume the luminosities to be distributed according to a normal error-curve. The questionable assumption is obviously responsible for the anomalous results obtained by them for the absolute magnitudes of all stars in clusters.

7. *The maximum luminosity in Messier 68.*—The mean absolute magnitude of the five brightest cluster stars is  $-2.16$  photographic, and  $-3.55$  photo-visual. Variable No. 27 is excluded from this group as possibly not a member of the cluster; if a cluster star, its absolute photographic magnitude at maximum would be of the order of  $-5.0$ . The brightest blue star in the cluster appears to be No. 20 with the absolute photo-visual magnitude  $-0.5$ .

In Messier 68 there are about 250 stars brighter than the absolute magnitude zero; in Messier 13 and

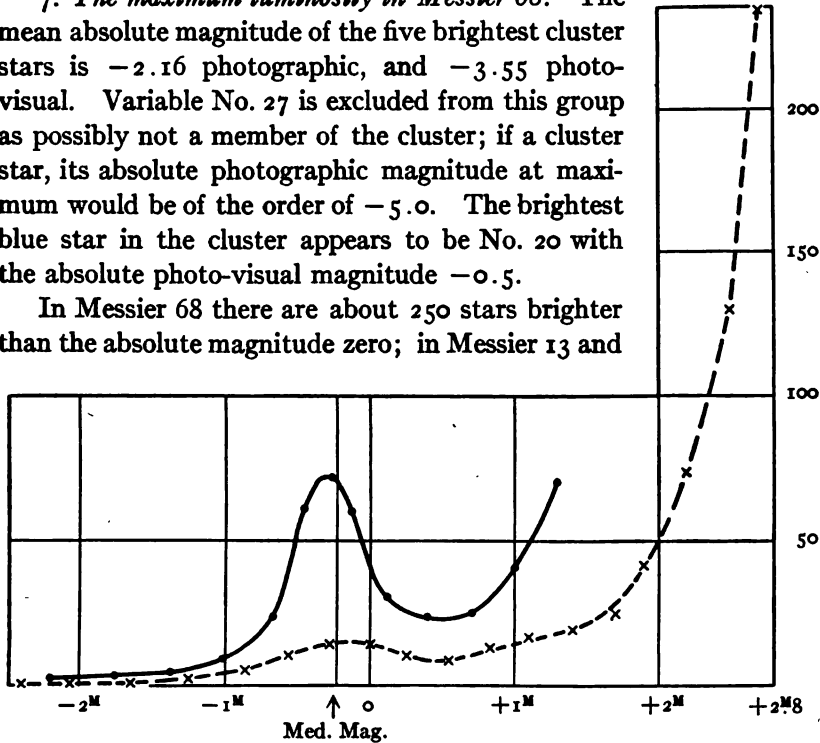


FIG. 2.—General luminosity-curves for Messier 68, from Plates 4863 (full line) and 4924; abscissae are absolute photographic magnitudes; ordinates, numbers of stars.

Messier 3 there are something like twice as many stars brighter than the same limit of absolute brightness.

8. *The form of the cluster.*—Using the system of superposed sectors and rings, described in earlier discussions of the ellipticity of clusters, we have counted 1700 stars brighter than absolute magnitude  $+2.7$  on Plate 4924. There is no appreciable deviation from perfect circularity. The results appear in Table VI, where opposite  $30^\circ$  sectors are combined to eliminate error in centering.

9. *Summary and conclusions.*—A. The results of a characteristic photometric study of Messier 68, a hitherto unexplored southern globular cluster, include the following items: (1) discovery of 28 variable stars, all but one of which appear to be typical cluster variables; (2) verification of the earlier result that cluster-type variables are characteristically bluer at maximum light than at minimum; (3) tabulation of the magnitudes and colors of the brightest giant stars of the cluster; (4) a new determination of the distance (55,000 light-years), based on diameter, variables, and bright stars, which differs very little from an earlier value based on

TABLE VI  
DISTRIBUTION OF STARS

POSITION ANGLE	NUMBER OF STARS	
	Distance from Center 0.5 to 5.0 mm	Distance from Center 1.0 to 4.0 mm
15° .....	293	205
45 .....	279	207
75 .....	284	212
105 .....	277	209
135 .....	280	208
165 .....	288	209
Mean .....	284	208

diameter alone; (5) proof of the circularity of the cluster, so far as the two thousand brightest stars are concerned; (6) discovery of a secondary maximum in the general luminosity-curve at about the median magnitude of the short-period variable stars; (7) evidence that this cluster, which is less concentrated to the center than usual, is much poorer in giant stars than some other globular systems.

B. The following general conclusions, resulting from previous studies of clusters, are directly supported by the evidence from Messier 68: (1) The general luminosity-curve for the stars in a cluster differs so widely from a symmetrical probability-curve that the former is of little value in determining the distance of clusters by the method tentatively suggested by Kapteyn (cf. Fig. 2). (2) The median brightness of the short-period variables in any

globular cluster appears to be an astrophysical constant whose value is a little more than one magnitude fainter than the mean of the magnitudes of the 25 brightest stars in the cluster; this result gives weight to the distances of clusters derived from measures of their brightest stars. (3) The diameter of the image of a globular cluster on a photographic chart is a valuable criterion of distance. (4) The brightest giant stars in globular clusters are always very red and have absolute photo-visual magnitudes between  $-4$  and  $-3$ . (5) With decreasing brightness, at least as far as absolute-magnitude zero, the average color-index of the giant stars decreases (cf. Fig. 1).

MOUNT WILSON OBSERVATORY  
October 1919

## MINOR CONTRIBUTIONS AND NOTES

### THE PROBLEM OF THE $\delta$ CEPHEI VARIABLES

#### ABSTRACT

*$\delta$  Cephei variables.* The author has recently suggested a *binary* theory which postulates that the variability of these stars is due to the action of satellites. If this is correct, we should expect to find variables of this type which undergo only slight variations of brilliancy as well as some which vary a full magnitude. The reason such variables have not been recognized may be that their properties do not facilitate discovery as much as the properties characteristic of known  $\delta$  Cephei variables. It is suggested that a careful study of eighteen stars recently listed by Adams and Joy might help to decide between the binary and pulsation theories of these variables.

In the *Publications of the Astronomical Society of the Pacific* (31, 184, 1919), a list of eighteen stars is given that have remarkable properties in common. According to Adams and Joy their spectral types all lie between F and K, their angular proper motions are less than  $0''.040$ , except one which is  $0''.100$ ; they are all within galactic latitude  $\pm 26^\circ$ , except two at  $+32^\circ$  and  $-43^\circ$ ; their absolute magnitudes, as indicated by spectroscopic determination, range from  $-1$  to  $-4$ .

1. The partial resemblance with the  $\delta$  Cephei type is striking; still the stars are not classified as belonging to that type, because a number of other qualities, supposed to be characteristic, have not yet been found. Only six of the stars have so far shown any variable velocity and no orbits have been computed. Furthermore no variation of light or of spectral type is observed, except that one star is suspected of variability.

Hitherto it was supposed that  $\delta$  Cephei stars had a light-range of at least half a magnitude, with a corresponding range of spectral type, and that the variable velocities, when computed on Doppler's principle, indicated a number of orbital peculiarities, such as small mass of the satellite, large eccentricity, and the periastron situated on the far side of the line of nodes.

2. Now it is suggested that these properties are not characteristic of the  $\delta$  Cephei class and that they only facilitate discovery.

The writer has tried to show this in an article which appeared under the title "Das Blinksternproblem."<sup>1</sup> The explanation starts from the binary theory and is based on the one very simple hypothesis, that the near approach of a satellite is capable of producing an eruption of light on the visible star, somewhat like the action of the sun on a comet.

The hypothesis entails a number of natural consequences: the luminous eruption is the stronger the nearer the approach of the satellite; it lags behind the passage through periastron; the decline of light will be slower than its eruption; the side of the variable star which turns toward the satellite is continually brighter than the opposite side.

3. This hypothesis being admitted, the properties mentioned in paragraph 1 are the very ones that facilitate discovery in that they are apt to increase the range of apparent light-variation.

a) Evidently the visible light-range is greatest when the angle  $i$  between the orbit and the tangent plane to the celestial sphere is nearly a right angle. The product  $m \sin i$ , in which  $m$  is the mass of the satellite, is always found to be a small number. Hence discovery is favored if the smallness of the product is not due to  $i$  but to  $m$ . This will account for the fact that the spectrum of the satellite does not show and that transits over the disks of the bright stars are not observed.

Another question is, Why should the product  $m \sin i$ , and consequently  $m$ , be always a small quantity? It is quite likely that a large satellite might distort the characteristic light-curve of the  $\delta$  Cephei stars and make its recognition difficult. Could not some variables that are classified among the eclipsing or  $\beta$  Lyrae stars be in reality of the  $\delta$  Cephei type?

b) That large eccentricities increase the range of light-variation and thus facilitate discovery needs no further comment.

c) The peculiar situation of the periastron beyond the line of nodes is no longer a puzzle because the eruption of light is best seen

<sup>1</sup> *Astronomische Nachrichten*, 209, 33, 1919.



when the satellite passes through periastron between the observer and the star.

4. The conclusion is that there may be  $\delta$  Cephei variables which have satellites of greater mass but which have not been recognized as such. Again there may be others which, on account of small orbital eccentricity, undergo only slight variation of brilliancy, and finally there may be such as vary to a full magnitude on the side turned away from the observer, periastron lying on our side of the nodes.

From this point of view the eighteen stars listed by Adams and Joy deserve the greatest attention and should be followed with photo-electric photometers and with spectrographs of high dispersion, in order to obtain light-curves and velocity-curves for intercomparison. The burning question between the binary and the pulsation theory of the  $\delta$  Cephei variables might then be brought nearer to a final solution.

J. G. HAGEN

VATICAN OBSERVATORY, ROME

December 25, 1919





ANNIBALE RICCÒ  
1844-1919

# THE ASTROPHYSICAL JOURNAL

AN INTERNATIONAL REVIEW OF SPECTROSCOPY  
AND ASTRONOMICAL PHYSICS

VOLUME LI

MARCH 1920

NUMBER 2

ANNIBALE RICCÒ, 1844-1919

By GIORGIO ABETTI

Annibale Riccò was born in Modena on September 14, 1844. He took his degree in mathematics at the University of Modena in the year 1866 and in civil engineering at the *Politecnico* of Milan in 1868; in the same year also the degree of doctor in natural science at the University of Modena.

He then began his scientific career as assistant in the small observatory of his birthplace (1868-77) and during this period took part in the International Meteorological Conference in Vienna (1873), visiting then the principal observatories in Austria and Germany. In 1878 he was called as professor of Technological Physics in the *Scuola superiore di applicazione* in Naples, but this was not the branch of science for which he had so strong an inclination and the next year he accepted the position of astronomer in the *Specola* of Palermo, Cacciatore being director. In 1890 Riccò was elected director of the two new observatories of Catania and Mount Etna (at 2943 meters' elevation) and of the geodynamical service of Sicily and surrounding islands. There especially he developed his enormous scientific activity, being also director of the *Società degli Spettroscopisti Italiani* and editor of the *Memorie*. He took part in three eclipse expeditions and in many conferences and meetings for astrophysics and geodynamics. Being in Rome

for the *Comitato antisismico* which had to decide on the construction of antiseismical buildings in the regions of Southern Italy more shaken by earthquakes, he suffered a violent attack of malaria. He was transferred to the *Policlinico* of that city and after a few days he died quietly on September 23, 1919, just when he was to retire from active service.

In these days when every branch of science covers so large a field that one can hardly keep up with the development of one's specialty, it is difficult to understand how Riccò was able to pursue such different and wide branches of science. But this was in his time almost a necessity, for lack of men and institutions, and was a consequence of the particular location in which an active and indefatigable energy must always be ready to follow the mysterious convulsions of nature.

In the *Memorie della Società degli Spettroscopisti Italiani*, the well-known journal of the society founded by Secchi and Tacchini in 1872, principally for the observations and study of the solar phenomena, we find the first signs of his scientific activity in the year 1875, with a note: "On the succession and persistence of the sensations of the colors." From that time we have an uninterrupted record of the activity of Riccò in these *Memorie* which, edited first by P. Tacchini in Palermo, then in 1879 in Rome, were transferred in 1899 to Catania under the direction of Riccò, who gave to them his most complete and careful attention.

The first regular series of solar observations, direct and spectroscopic, made by him at the Royal Observatory at Palermo with the Merz refractor of 25 cm aperture and 442 cm focal length and with a direct vision Tauber spectroscope with ten prisms, are printed in the *Memorie* for the year 1880, and from that time until a few days before his death, when he left Catania for his last journey to Rome, the series is uninterrupted, so that we have complete statistics and record of the activity of the sun during thirty-eight years. As a matter of fact, he observed the sun the very morning of his departure for Rome, and to friends who were visiting him at the hospital he was explaining how on that morning he had observed prominences of a peculiar filamentous appearance such as he "had never seen before." These were almost his last conscious words.

In 1804 the brothers Gemellaro had erected, for the study of the crater of Mount Etna, near the top of the volcano, a small refuge where, in conjunction with a station at the foot of the mountain, systematic meteorological and volcanologic observations were carried on from that date. It was not until after the establishment of the kingdom of Italy that, due to the interest of Tacchini, it was possible to begin, in 1879, the construction of the *Osservatorio Etneo*, enlarging the house of the Gemellaro; and shortly after, the observatory in the town was also established. In 1886 Tacchini, showing the perfect conditions of the sky in Catania, obtained permission for the observatory to take part in the international work of the *Carte photographique du Ciel* for the zone  $+47^{\circ}$  to  $+54^{\circ}$ . Since Tacchini, after the death of Father Secchi, had gone to the directorship of the observatory at the Collegio Romano, all the organization had to be done by Riccò who, with relatively small means, then had to provide for the installation of the instrument and for the work of observation, measurement, and reduction. These are well advanced, and some of the volumes of the astrographic catalogue containing the equatorial co-ordinates of the stars of that zone have been published by him and his collaborators.

But most of Riccò's attention was always given to the sun, and in this branch of astrophysics we find the greatest part of his work. Particular study was made by him of the relations between the sun-spots and the perturbations of terrestrial magnetism. He proves, with a number of observations, a retardation of the magnetic perturbation on the earth of  $45^h$  after the passage of the sun-spot across the central meridian, which would mean a velocity of propagation of the magnetic disturbance of about one thousand kilometers per second.

Attempts to photograph the solar corona without an eclipse were made by Riccò and Dr. G. E. Hale on Mount Etna in the summer of 1894. The collaboration of the two scientists is most interesting, although the experiments were not successful. Mr. Hale had decided on the expedition during Tacchini's visit to Chicago in August, 1893, hoping that the conditions of the sky on Mount Etna, and the opportunity to use there the 12-inch equatorial, would give him a better chance than on his first expedition to Pike's

Peak. But during his stay at Mount Etna in July of that year, as Riccò writes, there was "unfortunately just at this time a certain increase in the activity of the central crater which was probably the prelude of the disastrous earthquakes on the eastern slope of the volcano which occurred on the 7th and 8th of August. The volume of smoke rising from the great crater was carried by the prevailing northwest wind over the observatory." The observations after the departure of Dr. Hale were continued by Riccò, who proved that, except at an eclipse, it was not possible to photograph any part of the corona.

Long after, in 1910, Riccò was able to obtain funds, to which the William E. Hale Fund contributed a notable part for the construction of a spectroheliograph to be attached to the Merz refractor of 30 cm aperture and 557 cm focal length, so that, from that time, daily spectroheliograms of the sun were a part of the regular observations made at Catania.

Special consideration was given to the statistics of the prominences and the study of their structure in the period 1880 to 1912, and the results presented by Riccò at the Fifth Conference of the International Solar Union establish important conclusions, as, for instance, the progressive decrease of the production of the prominences in the successive cycles of the activity of the sun and that the duration of the cycles of the prominences is approximately equal to that of the spots. There are two distinct kinds of prominences: those on the zone of the spots, very active, very variable, with hydrogen, helium, calcium, and other metals, on the one hand; and those of hydrogen only, quiescent, which appear in latitudes increasing from a maximum to the following one. Professor Schwarzschild, at the close of the report of Riccò, said: "I want to point out again the important result of Professor Riccò that the height in the frequency-curve of the sun-prominences is decreasing steadily. This means that also in the prominences there is an indication of great super-periods of the activity of the sun-spots. Such a result can be reached only with a continuous observation during a whole lifetime, as Professor Riccò has done."

The study of the prominences and dark filaments observed with the spectroheliograph on the surface of the sun brings Riccò to

this conclusion: "There cannot be any more doubt that the filaments and dark flocculi are due to absorption and obscuration of the light of the photosphere due to the prominences which exist on the solar disk at the moment of the spectroheliographic observation." This was suspected also by Hale and Ellerman from their first spectroheliograms taken at the Yerkes Observatory in 1903 and lately confirmed again with a splendid series of pictures taken in June, 1917, with the 13-foot spectroheliograph at Mount Wilson by Ellerman, which shows the dark patches carried by the sun's rotation to the limb and becoming prominences.

Riccò took part in three eclipse expeditions, in Algeria for that of May 28, 1900, at Alcalà de Chivert (Spain), August 30, 1905, and at Teodosia (Crimea), August 21, 1914. For the last two expeditions that he directed we find especially interesting reports in the *Memorie*. In Spain he observed the white prominences first discovered by Tacchini in 1883 and he noted then that "probably they are objects of intermediate nature between the prominences and the coronal streamers; that is, they are like a line of conjunction between these two classes of phenomena."

In the eclipse observed in Russia he did not find any white prominences, but in some of the prominences the "prevailing radiations of calcium because of their faint violet coloration give images white or almost white."

In the eclipse of 1905, when the solar activity was at its maximum, he obtained good photographs with the prismatic camera of the flash spectrum with the green coronal line  $\lambda 5303$ ; in that of 1914, the sun being almost at the minimum of activity, he photographed, always with the prismatic camera, a new red band, confirmed by the observations of the other expeditions to the same eclipse, at  $\lambda 6374$ , which does not correspond to any known substance; he did not find any trace of the green coronal line.

Numerous observations were made by Riccò on the comets and their spectra, especially of the comets Morehouse and Halley. These observations gave him the occasion to discuss the hypothesis expressed by Professor Righi in his lecture on the physical constitution of the comets, which reaches the conclusion that we



have in them electric and optical phenomena analogous to those produced in the physical laboratories with the discharge tubes containing highly rarefied gases; analogous conditions to those of the comets which are constituted of matter extremely rarefied, wandering in the vacuum of sidereal space.

In the field of geodesy and geophysics Riccò made important observations for the determination of the relative gravity in Sicily, dividing the work with the geodesist, Professor Venturi, so that with their combined work they were able to make a chart of the anomalies of gravity in these interesting regions. Riccò determined the gravity with pendulum observations in 43 places in eastern Sicily, thus establishing relations between the anomalies of the terrestrial magnetism and those of the gravity and the seismic activity of those regions. Besides that, he was always a most intelligent observer of the phenomena of the volcanoes, and notable is his contribution to the researches on the eruption of Mount Etna in 1910, with a study of the central crater from 1892 to 1910.

After the death of Tacchini in 1906, he was invited to become a collaborator of this *Journal*, and was always interested in the intercourse between this paper and the *Memorie degli Spettroscopisti* and between the American and Italian scientists. He was one of the most active members of the International Union for Co-operation in Solar Research, and took part in the fourth conference held at Mount Wilson in 1910. After this visit he made a long report of the great development of astrophysics in the United States, describing the equipment and the lines of research followed in the American observatories, especially at Mount Wilson. He was present, too, at the fifth conference of the Union at Bonn in 1913, when he extended the invitation of the Italian government, accepted unanimously, that the next conference should be held in 1916 in Rome. This meeting, deferred by the obvious circumstances, will be held there in the near future, but the Union will regret the absence of one of its most distinguished members.

Considering all the various and indefatigable activity of Riccò one can see that his faculties of organization have been most successful in establishing the study of astrophysics and continuing

the fine traditions of Secchi, Donati, and Tacchini, and this is appreciated the more by those who know the limited means that he had at his disposal. Summing up the work done by him and his collaborators at the observatory of Catania, whether in establishing the observatory, or in its scientific production, it is really astonishing how much could be done with such small means, always obtained by hard efforts and with difficulty.

The scientific production of Riccò is collected chiefly in the *Memorie degli Spettroscopisti*, also in the *Comptes Rendus* of the French Academy, in the *Memorie* and *Atti* of the *Accademia dei Lincei*, of which he was elected national member in 1911, in the *Atti* of the *Accademia Gioenia*, of which he was elected president in 1899, in the *Rivista di Astronomia*, the *Astrophysical Journal*, and for geodynamics and meteorology in the Annals of the Italian weather bureau.

He received many Italian and foreign honors and prizes. In 1910 the *Accademia dei Lincei* awarded him the royal prize for astronomy. He was a member of numerous national and foreign academies and took part in many international meetings; the last one was that held at Brussels in July of this year under the auspices of the International Research Council, where the new International Astronomical Union was established. He was elected president of the section of volcanology.

He was for two years (1898-1900) rector of the Royal University of Catania and for eight years dean of the faculty of science at the same university. The gold medal for astrophysics of the French Academy and the Janssen medal were awarded to him, and he was Knight of the Crown of Italy and of S.S. Maurizio and Lazzaro.

The two events which marked the close of the scientific life of Riccò happened shortly before his death. The faculty of science of the University of Catania met on May 5, 1919, to deliberate upon the report of Riccò and others of his colleagues on the new Volcanologic Institute for Mount Etna, planned since 1910, which had to provide a chair for these studies separate from the one for astrophysics. He understood well that the two branches had so grown in a relatively small number of years that

independent institutes and workers were necessary for the development of each. The other event was the close of his official career and of his lectures at the university in July, 1919, when, having reached his seventy-fifth year, according to the Italian law, he had to retire. All his colleagues and students brought to him on that occasion their affectionate manifestations of esteem.

Always in good health and of great physical strength, he bore until his last days the fatigue of studies and of his many duties. He had a beloved and numerous family to whom he gave all his care and devoted affection. To science and his family he dedicated all of his life,

*cui laboro et fraudo animam meam bonis?—Ecclesiaste iv. 8.*

He knew well how and for what purpose he had to give all his wealth of mind and labor.

As a tragic circumstance, his wife, succumbing to the same illness during the same days in Catania, two days after followed him to the better life. They both live and will live in the memory of their sons and of all their numerous and sincere friends.

ROME

December 1919

# DIFFRACTION OF A TELESCOPIC OBJECTIVE IN THE CASE OF A CIRCULAR SOURCE OF LIGHT

By H. NAGAOKA

## ABSTRACT

*Diffraction of a telescope objective; distribution of intensity in the image of a circular object and of a combination of circular objects.*—Many astronomical observations involve the question of the effect of diffraction on the images of circular objects. This problem is exhaustively treated in this paper. After deriving the general expression for the intensity of any part of the image of a circular source, in the form of an integral of a combination of cylinder functions and elliptic integrals, the author evaluates it for various parts of the image: the center, the periphery, and points just inside and outside the periphery. The results obtained for the intensity near the periphery, called the marginal intensity, are of particular interest. They enable diagrams to be constructed which show the isophotes for various stages of the following phenomena: (1) the transit of a bright point over a bright disk (Fig. 5); (2) the transit of one bright disk over another (Fig. 6); (3) the transit of a dark disk over a larger bright one (Fig. 7). The isophotes of a *luminous lune* are also given (Fig. 8).

*Telescopic observation of transits; effect of diffraction phenomena.*—The diagrams just mentioned show (1) that a luminous point approaching a luminous disk appears to enter the disk before it really is in line with the periphery, and (2) that the moment of contact of two disks is difficult to judge on account of the gradual transition of the isophotes. In the case of such occultation and transit phenomena, therefore, the time observations may vary with the instrument used.

In studying the diffraction phenomena produced by different forms of apertures, we generally assume a point source of light. This is, however, a rough approximation from a practical point of view; as regards the resolving power and the explanation of some astronomical observations, we have to assume a finite source of light. The diffraction of a circular aperture due to a point source was treated by Airy<sup>1</sup> and afterward perfected by Lommel.<sup>2</sup> For a finite source of light, the discussion was given by Rayleigh,<sup>3</sup> André,<sup>4</sup> H. Struve,<sup>5</sup> Strehl,<sup>6</sup> and Lommel.<sup>7</sup> In a former paper,<sup>8</sup> I was led to

<sup>1</sup> *Trans. Phil. Soc. (Cambridge)*, 6, 1838.

<sup>2</sup> *Abhand. Bayer. Akad.*, 15, 1884.

<sup>3</sup> "Wave Theory of Light," *Encyc. Brit.*, 9th edition.

<sup>4</sup> *Ann. l'Ecole Norm. Sup.*, 5, 1876; 10, 1881.

<sup>5</sup> *Mem. P. Acad. St. Petersbourg*, 30, 1882.

<sup>6</sup> *Theorie des Fernröhre* (Leipzig), 1894.

<sup>7</sup> *Abhand. Bayer. Akad.*, 19, 1897.

<sup>8</sup> *Jour. Coll. Sci. (Tokyo)*, 9, 1898; *Phil. Mag.*, January 1898.

an approximate solution of the problem for a circular source of light, and obtained results which account for the drop formation during the ingress and the egress of the planets over the sun's disk. In the present discussion most of the difficulties hitherto encountered are overcome, and the result is made to apply to the practical solutions of problems concerning the distribution of light over a luminous disk as observed by means of a telescope. The result here obtained can be extended to the discussion of problems relating to the distribution of light, when bright disks are nearly in contact, or when a dark disk passes over a bright disk, and to questions of similar nature.

*General formula.*—In studying the diffraction due to a finite source of light, we start from the supposition that the independent sources of light do not give rise to interference effects. Dividing the source into elements, each of them sends out coherent waves which produce interference effects, but waves from any two of them do not interfere. The observed effect is therefore the sum of separate effects due to different elements of the source. A diffraction pattern due to a point source, such as a fixed star, produced by a circular aperture, consists of a system of concentric rings; when the source is of a finite area, the intensity of light in the focal plane of the observing telescope is an integral effect due to all the elements of the source. The problem is to find the intensity of the image of a uniform luminous disk, and then to proceed to find the effect of superposing luminous and dark disks, and combinations of similar nature.

The problem to be discussed naturally belongs to Fraunhofer's diffraction phenomena, as the source is placed at an infinite distance and the telescope is focused to it. Taking the plane of the aperture of the telescope for the  $xy$ -plane, denote the cosines of the angles which the incident ray makes with the  $x$ - and  $y$ -axes by  $\alpha$  and  $\beta$  and those for the diffracted ray by  $\alpha'$  and  $\beta'$ ; then putting

$$r = \frac{2\pi\sqrt{(\alpha - \alpha')^2 + (\beta - \beta')^2}}{\lambda} R,$$

where  $R$  denotes the radius of the objective, and  $\lambda$  the wave-length of light, the intensity of the diffracted ray in the focal plane of the telescope is proportional to

$$\frac{J_1^2(r)}{r^2},$$

where  $J_1(r)$  denotes the cylinder function of the first kind and of order 1, with argument  $r$ . For normal incidence  $\alpha = \beta = 0$ , and

$$r = \frac{2\pi R \sin \phi}{\lambda},$$

where  $\phi$  is the angle made by the diffracted ray with the axis of the telescope. For  $R = 1$  cm,  $\lambda = 0.5 \mu$ ,  $\phi = 1'$ , the value of  $r = 36.55$ , so that for most of the telescopes  $r$  becomes tolerably large even for small angles of diffraction; in practical application the limits for  $r$  lie between 0 and a large value, which will be denoted by  $a$ . For a finite source of light we have to consider  $\alpha$  and  $\beta$  as variables, corresponding to the diffracted ray in direction  $\alpha'$ ,  $\beta'$ , and integrate the effects due to all elements of the luminous disk. Thus the intensity is proportional to

$$\int \frac{J_1^2(r)}{r^2} d\sigma, \quad (1)$$

where  $d\sigma$  is a surface element of the source. Expressed in polar co-ordinates  $r$ ,  $\theta$ , the above integral becomes

$$c \int \int \frac{J_1^2(r)}{r} dr d\theta.$$

To fix the factor of proportionality,  $c$ , we shall assume the intensity due to an infinite disk of uniform brightness to be unity. Since

$$\begin{aligned} \frac{J_1^2(r)}{r} &= -\frac{1}{2} \frac{d}{dr} (J_0^2(r) + J_1^2(r)) \\ \int_0^r \int_0^r \frac{J_1^2(r)}{r} d\theta dr &= \frac{1}{2} \int (1 - J_0^2(r) - J_1^2(r)) d\theta, \end{aligned}$$

the value of the integral at the center of a circular disk of infinite radius and of uniform brightness

$$\int_0^{2\pi} \int_0^\infty \frac{J_1^2(r)}{r} d\theta dr = \pi.$$

Consequently, the factor of proportionality is  $\frac{I}{\pi}$  and the intensity

$$I = \frac{I}{2\pi} \int (1 - J_0^2(r) - J_1^2(r)) d\theta. \quad (2)$$

To find the intensity of light at any point  $P$  in the plane of the disk, let  $AP = r$ ,  $OA = a$ ,  $OP = \nu a$ , where  $OP/OA = \nu \leq 1$ , as  $P$  lies inside or outside the disk. Then on account of the geometrical condition

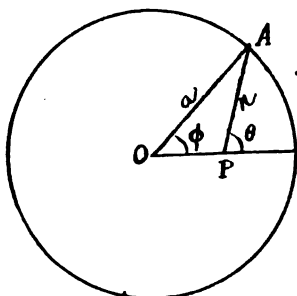


FIG. 1

$$r^2 = a^2(1 - 2\nu \cos \phi + \nu^2)$$

and

$$a \cos \theta = \nu a + r \cos \theta,$$

we have

$$d\theta = \left( \frac{1 - \nu \cos \phi}{1 - 2\nu \cos \phi + \nu^2} \right) d\phi;$$

consequently the expression for the intensity becomes

$$I = \frac{I}{2\pi} \int_0^{2\pi} [1 - J_0^2(r) - J_1^2(r)] \frac{1 - \nu \cos \phi}{1 - 2\nu \cos \phi + \nu^2} d\phi. \quad (3)$$

Putting

$$\phi = \pi - 2\psi, \quad \cos \phi = 2 \sin^2 \psi - 1,$$

we have

$$r = a(1 + \nu) \sqrt{1 - k^2 \sin^2 \psi} = a \sqrt{1 - k^2 \sin^2 \psi}, \quad (4)$$

where

$$k^2 = \frac{4\nu}{(1+\nu)^2}, \quad \text{and } a = a(1+\nu),$$

and

$$1 - k^2 = k'^2 = \left( \frac{1-\nu}{1+\nu} \right)^2.$$

For points inside the disk

$$k' = \frac{1-\nu}{1+\nu}, \quad (5)$$

and outside it

$$k' = \frac{\nu-1}{\nu+1}. \quad (5')$$

For points near the margin,  $\nu$  is nearly equal to 1, and we shall put

$$\nu = 1 - \epsilon, \quad (5'')$$

where  $\epsilon$  is generally a small quantity. We remark that for marginal points

$$k' = \frac{\epsilon}{2} \quad (5''')$$

and

$$k = 1$$

nearly, neglecting small terms of higher order.

Further

$$\frac{1 - \nu \cos \phi}{1 - 2\nu \cos \phi + \nu^2} = \frac{1}{2} \left( 1 \pm \frac{k'}{1 - k^2 \sin^2 \psi} \right) \quad (6)$$

where the  $+$  sign is to be taken for internal, and the  $-$  sign for external, points.

For simplifying the expression, put

$$u = \int_0^\psi \frac{d\psi}{\sqrt{1 - k^2 \sin^2 \psi}}$$



and  $u=K$  for  $\psi=\frac{\pi}{2}$ ,  $K$  denoting a complete elliptic integral of the first kind. Borrowing the notation of the elliptic functions

$$\sqrt{1-k^2 \sin^2 \psi} = \operatorname{dn} u$$

and

$$\frac{k'}{\operatorname{dn} u} = (\operatorname{dn} u + K),$$

we obtain for (4) and (6)

$$r = a(1+\nu) \operatorname{dn} u = a \operatorname{dn} u \quad (4')$$

$$\frac{1-\nu \cos \phi}{1-2\nu \cos \phi + \nu^2} d\psi = \frac{1}{2} [\operatorname{dn} u \pm \operatorname{dn}(u+K)] du, \quad (6')$$

and the expression for the intensity (3) becomes

$$I = \frac{1}{\pi} \int_0^K \{1 - J_0^2(a \operatorname{dn} u) - J_1^2(a \operatorname{dn} u)\} [\operatorname{dn} u \pm \operatorname{dn}(u+K)] du. \quad (7)$$

Thus the present problem is reduced to the evaluation of  $I$  in (7), and the proper interpretation of the result thus obtained.

It is convenient to discuss the result in four steps: (1) the intensity at the center of the disk; (2) the intensity at the periphery of the disk; (3) the intensity at points internal and external to the disk; (4) the intensity near the margin.

*Intensity at the center of the disk.*—For finding the intensity at the center of the disk, we have to put  $\nu=0$ , whence  $k=0$ , and  $\operatorname{dn} u=1$ ,  $\operatorname{dn}(u+K)=1$ ,  $a=a$ , and  $K=\frac{\pi}{2}$ .

Thus

$$I_0 = 1 - J_0^2(a) - J_1^2(a). \quad (8)$$

The above value can be found directly from (2) without having recourse to (7).

Since  $J_0$  and  $J_1$  are fluctuating functions,  $J_0^2 + J_1^2$  have several singular characteristics, which were discussed in my former paper.

Plotting the curve

$$y = J_0^2(x) + J_1^2(x) \quad (9)$$

we find that it shows a succession of steps at nearly equal horizontal intervals (Fig. 2a); the height of the consecutive steps becomes smaller and the rate of decrease diminishes as we recede from the axis of  $y$ . The mean curve for values of  $x$  greater than the first root  $x_1 = 3.8317$  of  $J_1(x)$  is approximately a rectangular hyperbola

$$xy = \frac{2}{\pi}. \quad (9')$$

This comes from the following property of the function.  $y$  defined by (9) is less than 1, for all values of  $x$ , except for  $x=0$ ; it gradually diminishes with increasing values of  $x$ . Points corresponding to the roots of  $J_1(x)=0$  are points of inflexion and have tangents parallel to the  $x$ -axis; these points occur at nearly equal intervals of the abscissae little greater than  $\pi$ , for values of  $x$  greater than the first root  $x_1$ ; the consequence is that the curve has neither maximum nor minimum, excepting the point  $x=0, y=1$ , as shown in Fig. 2b.

To calculate the numerical value of the intensity at the center, we have to evaluate  $J_0^2(a) + J_1^2(a)$ . For small values of  $a$ , we find by expanding

$$J_0^2(a) + J_1^2(a) = \frac{2}{\pi} \int_0^\pi J_0(2a \sin \omega) \cos^2 \omega \, d\omega$$

in power series,

$$J_0^2(a) + J_1^2(a) = \sum_0 \frac{(-1)^n \Pi(2n)}{2^{2n} (\Pi n)^3 \Pi(n+1)} a^{2n} = \sum_0 A_n a^{2n} \quad (10)$$

where  $A_0 = 1$ ;  $A_1 = \frac{1}{2}$ ;  $A_2 = \frac{5}{36}$ ;  $A_3 = \frac{7}{288}$ ;  $A_4 = \frac{7}{2400}$ ;  $A_5 = \frac{11}{43200}$ ;  $A_6 = \frac{143}{8467200}$ ;  $A_7 = \frac{2 \cdot 5 \cdot 11 \cdot 13}{(8!)^2}$ ;  $A_8 = \frac{2 \cdot 11 \cdot 13 \cdot 17}{(9!)^2}$ ;  $A_9 = \frac{4 \cdot 13 \cdot 17 \cdot 19}{(10!)^2}$ ;  $A_{10} = \frac{2 \cdot 7 \cdot 13 \cdot 17 \cdot 19}{(11!)^2}$ . For large values of  $a$ , the semi-convergent expansion

$$J_0^2(a) + J_1^2(a) = \frac{2}{\pi a} \left( 1 + \frac{1}{8a^2} - \frac{\cos 2a}{2a} - \frac{\sin 2a}{8a^2} + \dots \right) \quad (11)$$

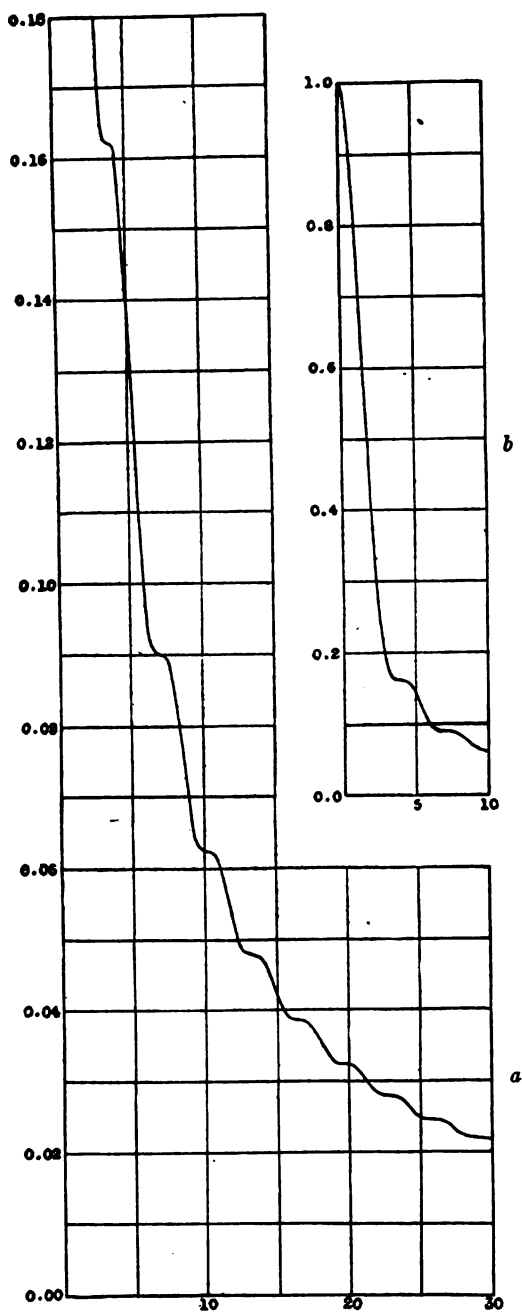


FIG. 2

is rapidly convergent, and can be conveniently used for values of  $a$  greater than the first root  $x_1$  of  $J_1(x)=0$ ; for this value of  $a$ , the above expression is accurate to the fourth decimal place. (9') follows at once from (11). Other expressions for  $y$  can be deduced, but they are simply of mathematical interest, so that they will be omitted in the present paper.

As to the intensity at the center of the disk, we remark that by dividing the disk into a series of zones bounded by circles whose radii are equal to the roots of  $J_1(a)=0$ , we find for the first circle ( $a=3.8317$ )  $I=0.83778$ ; for the second circle ( $a=7.0156$ )  $I=0.90994$ ; for the third circle ( $a=10.1735$ )  $I=0.93765$ ; and so on at a decreasing rate. The difference in intensity between successive circles gradually diminishes with the increasing value of  $a$ , and the intensity at the center of a large disk is given by the approximate expression

$$I_0 = 1 - \frac{2}{\pi a}, \quad (12)$$

which is the natural consequence of equation (11). As already noticed,  $a$  is generally large in practical applications, so that (12) is useful for comparing the intensity of a bright disk with that of an infinite extent. The numerical values are given in Table I later on; in it will be found the values of  $1-I_0$ , which is nearly equal to  $\frac{2}{\pi a}$ . The conclusion is that the intensity at the center of a circular disk is very little smaller than that of an infinite plate of the same intrinsic brightness.

*Intensity at the periphery.*—The intensity at the periphery of the disk can be found by putting  $\nu=1$  in (7). This case corresponds to  $k=1$ ,  $k'=0$ ,  $\text{dn}u = \cos \psi$ ,  $\text{dn}(u+K)=0$ , and  $a=2a$ ; thus  $r=2a \cos \psi$  and

$$\begin{aligned} I_p &= \frac{1}{\pi} \int_0^{2a} [1 - J_0^2(r) - J_1^2(r)] \frac{dr}{\sqrt{4a^2 - r^2}} \\ &= \frac{1}{2} - \frac{1}{\pi} \int_0^{2a} [J_0^2(r) + J_1^2(r)] \frac{dr}{\sqrt{4a^2 - r^2}}. \end{aligned} \quad (13)$$

As we assume  $a$  to be tolerably large, the integral is to be divided into two parts, the limits of the first integral being from 0 to  $x_1 = 3.8317$ , which is the first root of  $J_1(x) = 0$ ; in this integral  $J_0^2 + J_1^2$  is to be expanded in power series. In the second integral, in which the limits lie between  $x$  and  $2a$ , we may conveniently employ the semi-convergent series (11) for  $J_0^2 + J_1^2$  and effect the

TABLE I

$a$	$I_0$	$1 - I_0$	$1 - I_1$	$I_1$
20.....	0.9676	0.0324	0.0306	0.4694
25.....	0.9750	0.0250	0.0254	0.4746
30.....	0.9784	0.0216	0.0218	0.4782
35.....	0.9820	0.0180	0.0191	0.4809
40.....	0.9841	0.0159	0.0171	0.4829
45.....	0.9858	0.0142	0.0154	0.4846
50.....	0.9874	0.0126	0.0141	0.4859
60.....	0.9895	0.0105	0.0121	0.4879
70.....	0.9909	0.0091	0.0106	0.4894
80.....	0.9920	0.0080	0.0094	0.4906
90.....	0.9929	0.0071	0.0085	0.4915
100.....	0.9936	0.0064	0.0078	0.4922
150.....	0.9958	0.0042	0.0055	0.4945
200.....	0.9968	0.0032	0.0042	0.4958
250.....	0.9975	0.0025	0.0035	0.4965
300.....	0.9979	0.0021	0.0030	0.4970
400.....	0.9984	0.0016	0.0023	0.4977
500.....	0.9987	0.0013	0.0019	0.4981
600.....	0.9989	0.0011	0.0016	0.4984
700.....	0.9991	0.0009	0.0014	0.4986
800.....	0.9992	0.0008	0.0012	0.4988
900.....	0.9993	0.0007	0.0011	0.4989
1000.....	0.9994	0.0006	0.0010	0.4990
1500.....	0.9996	0.0004	0.0007	0.4993
2000.....	0.9997	0.0003	0.0005	0.4995
2500.....	0.9997	0.0003	0.0004	0.4996
3000.....	0.9998	0.0002	0.0004	0.4996

integration. After a somewhat tedious process of expansion and integration, we find that for the first part of the integral

$$\frac{1}{\pi} \int_0^{x_1} [J_0^2(r) + J_1^2(r)] \frac{dr}{\sqrt{4a^2 - r^2}} = \frac{0.302117}{a} + \frac{0.093952}{a^3} + \frac{0.12142}{a^5} + \dots \quad (14a)$$

For the second part we use the expansion (11) in (13); thus the integral sought consists of the following parts:

$$\begin{aligned} \frac{2}{\pi^2} \int_{x_1}^{2\pi} \frac{dr}{r\sqrt{4a^2-r^2}} &= -\frac{1}{\pi^2 a} \log n \frac{x_1}{4a} - \frac{x_1^2}{16\pi^2 a^3} + \dots \\ &= \frac{0.004355}{a} + \frac{0.233301}{a} \log_{10} a - \frac{0.09297}{a^3} \end{aligned} \quad (14b)$$

$$\frac{1}{4\pi^2} \int_{x_1}^{2\pi} \frac{dr}{r^3\sqrt{4a^2-r^2}} = \frac{0.000431}{a} + \frac{0.003645}{a^3} \log_{10} a - \frac{0.00086}{a^3} + \dots \quad (14c)$$

The oscillating term gives

$$-\frac{1}{\pi^2} \int_{x_1}^{2\pi} \frac{\cos 2r}{r^2\sqrt{4a^2-r^2}} dr = \frac{0.0749}{\pi^3 a} + \dots = \frac{0.00242}{a} + \dots \quad (14d)$$

This last integral is rather difficult to evaluate, as  $x_1$  is not a multiple of  $\frac{\pi}{2}$ ; we have to evaluate first the integral from  $x_1$  to  $\frac{3\pi}{2}$ , and then through successive intervals of  $\pi$ . The formula (14d) is only applicable when  $a$  is tolerably large. The integral coming from the term  $\frac{\sin 2r}{4\pi r^3}$  in the expansion of  $J_0^2 + J_1^2$  is negligibly small. Adding (14a, b, c, d), we find for the intensity at the periphery of a circular disk

$$I_p = \frac{1}{2} - \left( \frac{0.3093}{a} + \frac{0.2333}{a} \log_{10} a + \frac{0.0036}{a^3} \log_{10} a - \dots \right) \quad (15)$$

The expansion (15) shows that the peripheral intensity for a large disk is nearly half the intensity at the center. The following table gives the intensity at the center of different disks  $I_0$ , and that at the periphery  $I_p$ , and shows how the foregoing conclusion is a close approximation. Graphically represented, the curve takes the form given in Fig. 3 for  $\epsilon = 0.000$ .

*Intensity inside and outside the disk.*—For finding the value of the intensity at points neither near the center nor the margin of the disk, whose radius  $a$  is tolerably large, the integral can be reduced in the following manner.

Since  $a$  is large, and  $\operatorname{dn} u > 0$ , we can expand  $J_0^2 + J_1^2$  and retain the first term. Thus

$$J_0^2(\operatorname{adnu}) + J_1^2(\operatorname{adnu}) = \frac{2}{\pi a \operatorname{adnu}} \text{ or } = \frac{2(\operatorname{dn} u + K)}{\pi a k'}. \quad (16)$$

The integral (7) thus becomes

$$I = \frac{1}{\pi} \int_0^K \left( 1 - \frac{2}{\pi a \operatorname{adnu}} \right) [\operatorname{dn} u \pm \operatorname{dn}(u+K)] du. \quad (17)$$

Evaluating the integral, we find the intensity in terms of the complete elliptic integrals of the first and second kind,  $K$  and  $E$  respectively.

$$\begin{aligned} I_i &= 1 - \frac{1}{\pi^2 a} \left( \frac{E}{k'} + K \right) \\ &= 1 - \frac{2}{\pi^2 (1+\nu) a} \left( \frac{E}{k'} + K \right) \end{aligned} \quad (18)$$

for points *internal* to the disk.

$$I_e = \frac{2}{\pi^2 (1+\nu) a} \left( \frac{E}{k'} - K \right) \quad (18')$$

for points *external* to the disk. The expansion is correct to three or four decimal places for values of the argument  $\operatorname{adnu}$  greater than the first root  $x_1$  of  $J_1(x) = 0$ ; thus for practical purposes the approximation here introduced is generally sufficient, as the fourth decimal is of little significance for the present problem.

For small values of  $k'$  we can conveniently utilize the approximate expressions for the elliptic integrals.

$$\begin{aligned} K &= \log \frac{4}{k'} + \frac{1}{4} k'^2 \left( \log \frac{4}{k'} - 1 \right) + \dots \\ \frac{E}{k'} &= \frac{1}{k'} + \frac{1}{2} k' \left( \log \frac{4}{k'} - \frac{1}{1.2} \right) + \dots \end{aligned} \quad (19)$$

Substituting in (18) and (18') and noticing that  $\frac{1}{k'} = \frac{1+\nu}{1-\nu}$ , we obtain for the intensities at points inside and outside the disk under the form

$$\begin{aligned} I_i &= 1 - \frac{2}{\pi^2(1+\nu)a} \left\{ \left(1 + \frac{k'}{2}\right) \log \frac{4}{k' - \frac{k'}{4}} \right\} - \frac{2}{\pi^2(1-\nu)a} \\ I_e &= \frac{2}{\pi^2(1+\nu)a} \left\{ \left(1 - \frac{k'}{2}\right) \log \frac{4}{k' + \frac{k'}{4}} \right\} - \frac{2}{\pi^2(1-\nu)a} \end{aligned} \quad (20)$$

In finding the intensity for values of  $k$  not near 1, we can easily utilize Landen's transformation. Putting

$$k_1 = \frac{1-k'}{1+k'} = \nu \dots \dots \text{for internal point,}$$

$$= \frac{1}{\nu} \dots \dots \text{for external point;}$$

$$k_2 = \frac{1-k'_1}{1+k'_1} = \left( \frac{\nu}{1+\sqrt{1-\nu^2}} \right)^2 \text{ for internal point,}$$

$$= \left( \frac{1}{\nu+\sqrt{\nu^2-1}} \right)^2 \text{ for external point;}$$

we know from the theory of elliptic functions that

$$K = \frac{\pi}{2}(1+k_1)(1+k_2) \dots \dots$$

$$E = \left\{ (1-k)^2 + \frac{1}{2}k^2 \left( 1 - \frac{1}{2}k_1 - \frac{1}{2}k_1k_2 + \dots \dots \right) \right\} K.$$

Consequently, the terms entering into the expressions for the intensity (18) and (18') become

$$\frac{E}{k'} + K = \left( \frac{1+k'}{2k'} \right)^2 \left\{ 1 - \frac{k_2^2}{2} \left( 1 + \frac{1}{2}k_2 \right) \right\} K \quad (21)$$

and

$$\frac{E}{k'} - K = \frac{(1-k')^2}{4k'} \left( 1 - \frac{k_2}{2} \right) K \quad (21')$$



nearly. These substituted in (18) and (18') give the intensities not very near the margin.

Tables II and III give the values of  $\frac{2}{\pi^2(1+\nu)}\left(\frac{E}{k'}+K\right)$  for finding  $I_i$ , and  $\frac{2}{\pi^2(1+\nu)}\left(\frac{E}{k'}-K\right)$  for  $I_e$ , and the values of the constituent two terms multiplied by  $a$  for  $\nu$  very near unity are also given. These can be used only for large values of  $a$ , such that  $a\epsilon$  is less than  $x_1$ .

TABLE II

	$\epsilon$	$\frac{2}{\pi^2(1+\nu)}\left\{\left(1+\frac{k'}{2}\right)\log\frac{4}{k'}-\frac{k'}{4}\right\}$	$\frac{2}{\pi^2(1-\nu)}$	$\frac{2}{\pi^2(1+\nu)}\left(\frac{E}{k'}+K\right)$
0.990.....	0.010	0.682	20.264	20.946
0.991.....	0.009	0.692	22.516	23.208
0.992.....	0.008	0.704	25.330	26.034
0.993.....	0.007	0.717	28.949	29.666
0.994.....	0.006	0.732	33.774	34.506
0.995.....	0.005	0.750	40.528	41.478
0.996.....	0.004	0.772	50.661	51.433
0.997.....	0.003	0.801	67.547	68.348
0.998.....	0.002	0.841	101.321	102.162
0.999.....	0.001	0.911	202.642	203.553
0.9999.....	0.0001	1.144	2026.4	2027.6
	$-\epsilon$	$\frac{2}{\pi^2(1+\nu)}\left\{\left(1-\frac{k'}{2}\right)\log\frac{4}{k'}+\frac{k'}{4}\right\}$	$-\frac{2}{\pi^2(1-\nu)}$	$\frac{2}{\pi^2(1+\nu)}\left(\frac{E}{k'}-K\right)$
1.010.....	0.010	-0.673	20.264	19.591
1.009.....	0.009	-0.684	22.516	21.832
1.008.....	0.008	-0.696	25.330	24.634
1.007.....	0.007	-0.710	28.949	28.239
1.006.....	0.006	-0.726	33.774	33.048
1.005.....	0.005	-0.745	40.528	39.783
1.004.....	0.004	-0.768	50.661	49.893
1.003.....	0.003	-0.798	67.547	66.749
1.002.....	0.002	-0.839	101.321	100.482
1.001.....	0.001	-0.910	202.642	201.732
1.0001.....	0.0001	-1.144	2026.4	2025.3

From the tables it is evident that the intensity is very nearly equal to 1 over the surface of the disk; only when  $\nu=1-\epsilon$  is near unity, or when  $\epsilon$  is very small, is its variation considerable. Thus the intensity diminishes to the value  $\frac{1}{2}$  near the margin of the disk. On passing the periphery to the outside ( $\epsilon < 0$ ), the change in inten-

sity is quite rapid and tends toward zero. Instead of giving the values of the intensity for different  $\epsilon$ , it is shown graphically in Fig. 3. The numerals under each curve give the values of  $\epsilon$ , the radii  $a$  of the disk, calculated according to the formula already given, being indicated by the abscissae and the intensities by the ordinates. For a given radius of the disk, the intensities at different points inside and outside it are found by cutting the curve by a straight line parallel to the ordinate through the abscissa corresponding to  $a$ . Figure 4 shows how the intensity varies from inside to outside for different values of the radius  $a$ .

TABLE III

$\epsilon$	$a$	$\frac{2}{\pi(1+\epsilon)} \left( \frac{E}{k} + K \right)$	$\epsilon$	$-a$	$\frac{2}{\pi(1+\epsilon)} \left( \frac{E}{k} - K \right)$
0.05.....	0.95	0.6378	1.01.....	0.01	19.591
0.10.....	0.90	0.6414	1.02.....	0.02	9.533
0.15.....	0.85	0.6476	1.03.....	0.03	6.199
0.20.....	0.80	0.6565	1.04.....	0.04	4.542
0.25.....	0.75	0.6683	1.05.....	0.05	3.554
0.30.....	0.70	0.6836	1.1.....	0.1	1.6077
0.35.....	0.65	0.7027	1.2.....	0.2	0.6779
0.40.....	0.60	0.7266	1.3.....	0.3	0.3898
0.45.....	0.55	0.7562	1.4.....	0.4	0.2560
0.50.....	0.50	0.7930	1.5.....	0.5	0.1813
0.55.....	0.45	0.8392	1.6.....	0.66	0.1349
0.60.....	0.40	0.8980	1.7.....	0.7	0.1040
0.65.....	0.35	0.9746	1.8.....	0.8	0.0824
0.70.....	0.30	1.0773	1.9.....	0.9	0.0667
0.75.....	0.25	1.2214	2.0.....	1.0	0.0549
0.80.....	0.20	1.4369	3.0.....	2.0	0.0135
0.85.....	0.15	1.7936	4.0.....	3.0	0.0053
0.90.....	0.10	2.4994	5.0.....	4.0	0.0027
0.95.....	0.05	4.5838	10.0.....	9.0	0.003
0.96.....	0.04	5.617	100.0.....	99.0	0.0000
0.97.....	0.03	7.332			
0.98.....	0.02	10.747			
0.99.....	0.01	20.947			

From Fig. 3 we see that for  $\epsilon$  nearly equal to zero, the curves of intensity are much curved for small values of  $a$ . To obtain the exact value, we must have recourse to another method of expansion, which is semi-convergent and can be expressed in terms of a cylinder function of the first kind and of different orders. The expansion was given by Lommel in his theory of twilight, for which the diffraction aperture is of the order of a micron, representing the dimension

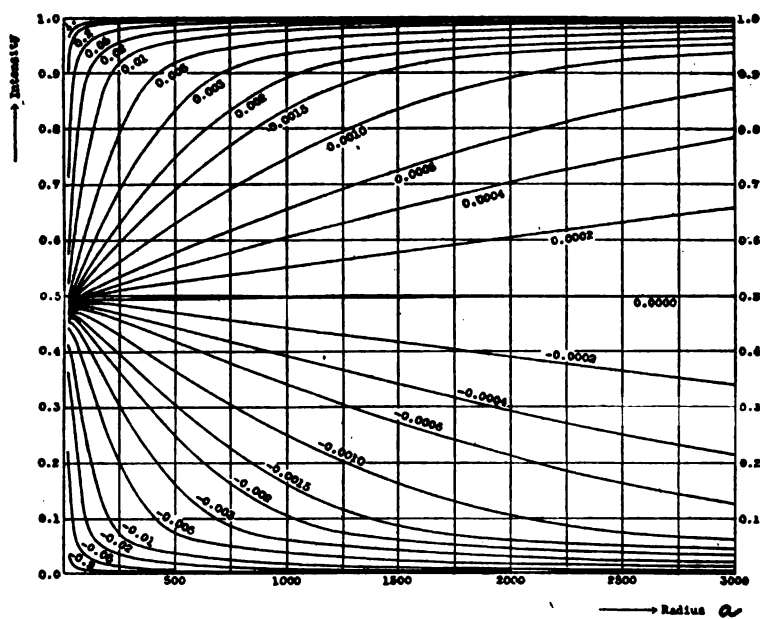


FIG. 3

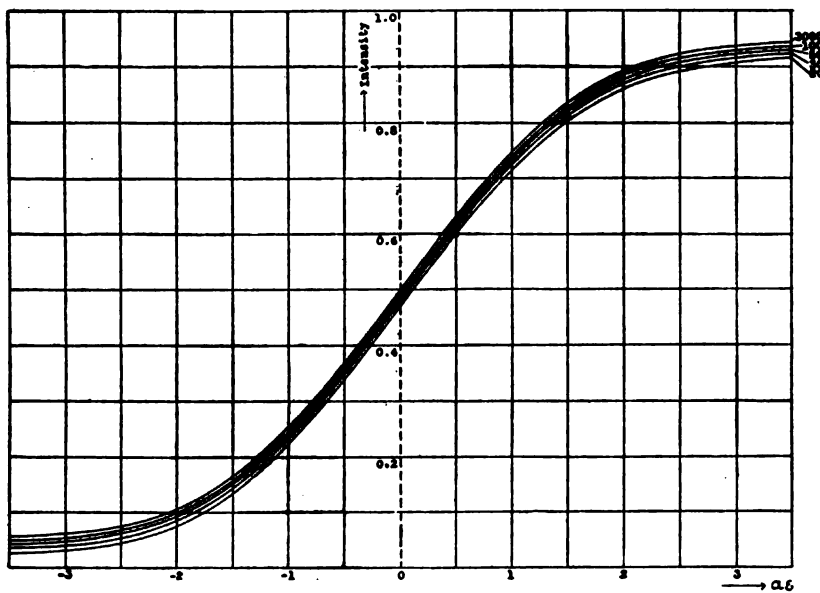


FIG. 4

of a dust particle. Such a case is never met with in telescopes and consequently the discussion is omitted in the present paper.

*Marginal intensity.*—As noticed above, the intensity near the periphery, which we shall call the marginal intensity, is of great interest in the diffraction phenomena of telescopic objectives. The expression is, however, most difficult to evaluate, and the numerical calculation somewhat tedious. In the papers hitherto published, several approximate expressions were obtained, sometimes expanded in series and sometimes evaluated by means of mechanical quadratures. In spite of these difficulties I found that the marginal intensity can be obtained by separating the integral giving the intensity into several parts, of which the principal consists of the peripheral intensity of a bright disk whose radius is somewhat smaller than that in question.

In the first place, it is to be remarked that in the general expression for the intensity

$$I = I_1 + I_2 = \frac{1}{\pi} \int_0^K \{1 - J_0^2(adnu) - J_1^2(adnu)\} [dnu \pm (dnu + K)] du \quad (7)$$

$k$  is very nearly equal to 1 near the margin; consequently  $dnu = \sqrt{1 - k^2 \sin^2 \psi} = \cos \psi$  to a close approximation. To take an example, for  $\epsilon = 0.02$ ,  $k' = 0.01$ , and  $k = 0.99995$ .

The first part of the integral (7) thus reduces to

$$I_1 = \frac{1}{\pi} \int_0^{\frac{\pi}{2}} \{1 - J_0^2(a \cos \psi) - J_1^2(a \cos \psi)\} d\psi, \quad (21)$$

which is the value of the peripheral intensity of the disk of radius  $\frac{a}{2} = \frac{a(1+\nu)}{2}$  and may be expressed by

$$I_1 = I_p\left(\frac{a}{2}\right) = I_p\left(\frac{a(1+\nu)}{2}\right). \quad (22)$$

As already noticed,  $I_p$  is nearly equal to  $\frac{1}{2}$  when  $a$  is tolerably large and can be found from Table I; the deviation from the peripheral

intensity is given by the second term affected with  $\pm$  sign, where  $+$  refers to internal points and  $-$  to the external.

The second integral is equivalent to

$$I_2 = \frac{1}{\pi} \int_0^{\frac{\pi}{2}} \left\{ 1 - J_0^2(a(1+\nu)\sqrt{1-k^2 \sin^2 \psi}) - \frac{J_1^2(a(1+\nu)\sqrt{1-k^2 \sin^2 \psi})}{1-k^2 \sin^2 \psi} \right\} \frac{k' d\psi}{1-k^2 \sin^2 \psi} \quad (23)$$

We shall separate the integral into two parts, such that the limits lie between 0 to  $\phi_1$  with respect to  $\phi$ , where  $\phi = \frac{\pi}{2} - \psi$ , and 0 to  $\frac{\pi}{2} - \phi_1$  with respect to  $\psi$ ,  $\phi_1$  being a small angle defined by the relation

$$a\sqrt{k'^2 + k^2 \phi_1^2} = x_1, \quad (24)$$

where  $x_1$  has the usual meaning. Then

$$\begin{aligned} & \frac{1}{\pi} \int_0^{\frac{\pi}{2}} \left\{ 1 - J_0^2(a\sqrt{1-k^2 \sin^2 \psi}) - J_1^2(a\sqrt{1-k^2 \sin^2 \psi}) \right\} \frac{k' d\psi}{1-k^2 \sin^2 \psi} \\ &= \frac{1}{\pi} \int_0^{\phi_1} \left\{ 1 - J_0^2(a\sqrt{k'^2 + k^2 \phi^2}) - J_1^2(a\sqrt{k'^2 + k^2 \phi^2}) \right\} \frac{k' d\phi}{k'^2 + k^2 \phi^2} \\ &+ \frac{1}{\pi} \int_{\frac{\pi}{2}-\phi_1}^{\frac{\pi}{2}} \left\{ 1 - J_0^2(a\sqrt{1-k^2 \sin^2 \psi}) - J_1^2(a\sqrt{1-k^2 \sin^2 \psi}) \right\} \frac{k' d\psi}{1-k^2 \sin^2 \psi} \end{aligned} \quad (25)$$

The first integral can be easily expressed by putting

$$a\sqrt{k'^2 + k^2 \phi^2} = x,$$

so that

$$x dx = a^2 k^2 \phi d\phi$$

and

$$\frac{d\phi}{k'^2 + k^2 \phi^2} = \frac{a dx}{kx \sqrt{x^2 - a^2 k'^2}}.$$

Consequently the integral becomes

$$\frac{ak'}{\pi} \int_{ak'}^{x_1} \{1 - J_0^2(x) - J_1^2(x)\} \frac{dx}{kx\sqrt{x^2 - a^2 k'^2}} = S. \quad (26)$$

Expanding the expression in parenthesis in powers of  $x$ , and integrating by parts, we obtain

$$S = \frac{k'a}{2\pi k} \sqrt{x_1^2 - k'^2 a^2} \left\{ 0.31845 - 0.47814 \left(\frac{k'a}{4}\right)^2 - 0.46770 \left(\frac{k'a}{4}\right)^4 \right. \\ \left. - 0.29870 \left(\frac{k'a}{4}\right)^6 + 0.13284 \left(\frac{k'a}{4}\right)^8 - 0.04339 \left(\frac{k'a}{4}\right)^{10} + \dots \right\}$$

Remembering that  $a = 2a$  and  $k' = \frac{\epsilon}{2}$ ,  $k = 1$  nearly,

$$S = \frac{a\epsilon}{\pi} \sqrt{14.682 - a^2 \epsilon^2} \left\{ 0.15923 - 0.23907 \left(\frac{a\epsilon}{4}\right)^2 + 0.23385 \left(\frac{a\epsilon}{4}\right)^4 \right. \\ \left. - 0.14935 \left(\frac{a\epsilon}{4}\right)^6 - 0.06642 \left(\frac{a\epsilon}{4}\right)^8 - 0.0217 \left(\frac{a\epsilon}{4}\right)^{10} + 0.0054 \left(\frac{a\epsilon}{4}\right)^{12} \right. \\ \left. - 0.00107 \left(\frac{a\epsilon}{4}\right)^{14} + 0.0002 \left(\frac{a\epsilon}{4}\right)^{16} - \dots \right\} \quad (27)$$

$S$  is given in Table IV for values of  $a\epsilon$  from 0 to  $x_1$ .

As to the second integral, we remark that the first term gives

$$\frac{k'}{\pi} \int_0^{\frac{\pi}{2} - \phi_1} \frac{d\psi}{1 - k^2 \sin^2 \psi} = \frac{k'}{\pi} \int_0^{\frac{\pi}{2}} \frac{d\psi}{1 - k^2 \sin^2 \psi} - \frac{k'}{\pi} \int_{\frac{\pi}{2} - \phi_1}^{\frac{\pi}{2}} \frac{d\psi}{1 - k^2 \sin^2 \psi} \\ = \frac{1}{2} - \frac{1}{\pi k} \cos^{-1} \frac{k'a}{x_1} \\ = \frac{1}{2} - \frac{1}{\pi} \cos^{-1} \frac{a\epsilon}{x_1} \quad (28)$$

nearly. The values of  $\cos^{-1} \frac{a\epsilon}{x_1}$  are given in Table V.

TABLE IV

$\alpha$	$S$	$\alpha$	$S$
0.0.....	0.0000	2.0.....	0.2334
0.1.....	0.0194	2.1.....	0.2320
0.2.....	0.0387	2.2.....	0.2300
0.3.....	0.0576	2.3.....	0.2268
0.4.....	0.0761	2.4.....	0.2225
0.5.....	0.0941	2.5.....	0.2171
0.6.....	0.1113	2.6.....	0.2109
0.7.....	0.1276	2.7.....	0.2037
0.8.....	0.1432	2.8.....	0.1958
0.9.....	0.1576	2.9.....	0.1868
1.0.....	0.1709	3.0.....	0.1770
1.1.....	0.1830	3.1.....	0.1663
1.2.....	0.1939	3.2.....	0.1545
1.3.....	0.2034	3.3.....	0.1418
1.4.....	0.2117	3.4.....	0.1276
1.5.....	0.2185	3.5.....	0.1117
1.6.....	0.2241	3.6.....	0.0933
1.7.....	0.2284	3.7.....	0.0700
1.8.....	0.2311	3.8.....	0.0344
1.9.....	0.2327	3.8317.....	0.0000

TABLE V

$\alpha$	$\frac{1}{\pi} \cos^{-1} \frac{\alpha}{x_1}$	$\alpha$	$\frac{1}{\pi} \cos^{-1} \frac{\alpha}{x_1}$
0.0.....	0.5000	2.0.....	0.3252
0.1.....	0.4917	2.1.....	0.3154
0.2.....	0.4834	2.2.....	0.3053
0.3.....	0.4751	2.3.....	0.2951
0.4.....	0.4667	2.4.....	0.2845
0.5.....	0.4583	2.5.....	0.2737
0.6.....	0.4490	2.6.....	0.2626
0.7.....	0.4415	2.7.....	0.2511
0.8.....	0.4332	2.8.....	0.2391
0.9.....	0.4245	2.9.....	0.2267
1.0.....	0.4160	3.0.....	0.2137
1.1.....	0.4073	3.1.....	0.2000
1.2.....	0.3986	3.2.....	0.1854
1.3.....	0.3898	3.3.....	0.1697
1.4.....	0.3809	3.4.....	0.1526
1.5.....	0.3720	3.5.....	0.1334
1.6.....	0.3629	3.6.....	0.1112
1.7.....	0.3537	3.7.....	0.0837
1.8.....	0.3443	3.8.....	0.0410
1.9.....	0.3349	3.8317.....	0.0000

For the rest of the integral between the limits  $x_1$  and  $a$ , we make use of the expansion

$$J_0^2(adnu) + J_1^2(adnu) = \frac{2}{\pi adnu} + \dots,$$

leaving out of account the fluctuating terms, which are generally very small on integration.

We have to find the integral

$$\frac{2k'}{\pi^2 a} \int_0^{K-u(x_1)} \frac{du}{dn^2 u}, \quad (29)$$

where  $u(x_1)$  denotes the value of  $u$  corresponding to  $adnu = x_1$ ; in other words,  $a\sqrt{k'^2 + k^2 \phi_1^2} = x_1$ , or  $\phi_1 = \frac{\sqrt{x_1^2 - a^2 \epsilon^2}}{2a}$  nearly. Evidently

$$k^2 \frac{d}{du} \left( \frac{\sin u \operatorname{cn} u}{dn u} \right) = dn^2 u - \frac{k'^2}{dn^2 u};$$

whence

$$\begin{aligned} \int \frac{du}{dn^2 u} &= \frac{1}{k'^2} \int dn^2 u du - \frac{k^2}{k'^2} \frac{\sin u \operatorname{cn} u}{dn u} \\ &= \frac{E\left(\frac{\pi}{2} - \phi_1, k\right)}{k'^2} - \frac{k^2}{k'^2} \frac{\sin \phi_1 \cos \phi_1}{\sqrt{1 - k^2 \sin^2 \phi_1}} \end{aligned} \quad (30)$$

following Legendre's notation.

Since

$$E\left(\frac{\pi}{2} - \phi_1, k\right) = \int_0^{\frac{\pi}{2} - \phi_1} \sqrt{1 - k^2 \sin^2 \psi} d\psi = \int_0^{\frac{\pi}{2}} - \int_{\frac{\pi}{2} - \phi_1}^{\frac{\pi}{2}}, \quad (31)$$

we find

$$\begin{aligned} \int_{\frac{\pi}{2} - \phi_1}^{\frac{\pi}{2}} \sqrt{1 - k^2 \sin^2 \psi} d\psi &= \int_0^{\phi_1} \sqrt{k'^2 + k^2 \phi^2} d\phi \\ &= -\frac{\phi_1}{2} \sqrt{k'^2 + k^2 \phi_1^2} + \frac{k'^2}{2k} \log \left\{ \phi_1 + \frac{\sqrt{k'^2 + k^2 \phi_1^2}}{k} \right\} + \frac{k'^2}{2k} \log \frac{k'}{k}. \end{aligned}$$



Further

$$\frac{1}{k'} E\left(\frac{\pi}{2}, k\right) = \frac{1}{k'} + \frac{k'}{2} \left( \log \frac{4}{k'} - \frac{1}{2} \right)$$

Since  $k' = \frac{\epsilon}{2}$  nearly, we have

$$\begin{aligned} \frac{E\left(\frac{\pi}{2} - \phi_1, k\right)}{k'} &= \frac{2}{\epsilon} - \frac{x_1 \sqrt{x_1^2 - a^2 \epsilon^2}}{4a^2 \epsilon} + \frac{\epsilon}{4} \left\{ \log 4 - \frac{1}{2} - \log \left( \frac{x_1 + \sqrt{x_1^2 - a^2 \epsilon^2}}{2a} \right) \right\} \\ \frac{k^2 \sin \phi_1 \cos \phi_1}{k' \sqrt{k'^2 + k^2 \phi_1^2}} &= \frac{2 \sqrt{x_1^2 - a^2 \epsilon^2}}{x_1 \epsilon}. \end{aligned}$$

Consequently the expression sought becomes after reduction

$$\begin{aligned} \frac{2}{\pi^2 a} \left( \frac{E\left(\frac{\pi}{2} - \phi_1, k\right)}{k'} - \frac{k^2 \sin \phi_1 \cos \phi_1}{k' \sqrt{k'^2 + k^2 \phi_1^2}} \right) &= \frac{1}{\pi^2} \left\{ \frac{2a\epsilon}{x_1(x_1 + \sqrt{x_1^2 - a^2 \epsilon^2})} \right. \\ &\quad \left. - \frac{x_1 \sqrt{x_1^2 - a^2 \epsilon^2}}{4\pi a^3 \epsilon} + \frac{\epsilon}{4a} \left( \log 4 - \frac{1}{2} - \log \frac{x_1 + \sqrt{x_1^2 - a^2 \epsilon^2}}{2a} \right) \right\} \end{aligned}$$

nearly. In most cases  $a\epsilon$  is very small compared with  $4a$ , so that the value of the integral turns out to be simply

$$\frac{1}{\pi^2} \cdot \frac{2a\epsilon}{x_1(x_1 + \sqrt{x_1^2 - a^2 \epsilon^2})} \quad (31)$$

which is given in Table VI.

From the quantities given in Tables IV, V, and VI we obtain the value of the integral which enters the expression of the marginal intensity. Table VII gives that part of the integral, which is to be added for internal points, and subtracted for the external, from the peripheral intensity given by (22), which is to be found from Table I. The diffraction phenomena, which appear quite striking, are usually observed near the margin of a luminous disk, when

TABLE VI

$g_4$	$\frac{2g_4}{\pi^2 z_1 (z_1 + \sqrt{z_1^2 - g_4^2})}$	$g_4$	$\frac{2g_4}{\pi^2 z_1 (z_1 + \sqrt{z_1^2 - g_4^2})}$
0.0.....	0.0000	2.0.....	0.0149
0.1.....	0.0007	2.1.....	0.0158
0.2.....	0.0014	2.2.....	0.0167
0.3.....	0.0020	2.3.....	0.0176
0.4.....	0.0028	2.4.....	0.0186
0.5.....	0.0035	2.5.....	0.0196
0.6.....	0.0042	2.6.....	0.0207
0.7.....	0.0049	2.7.....	0.0218
0.8.....	0.0056	2.8.....	0.0230
0.9.....	0.0063	2.9.....	0.0242
1.0.....	0.0070	3.0.....	0.0255
1.1.....	0.0078	3.1.....	0.0270
1.2.....	0.0085	3.2.....	0.0285
1.3.....	0.0092	3.3.....	0.0302
1.4.....	0.0100	3.4.....	0.0321
1.5.....	0.0108	3.5.....	0.0344
1.6.....	0.0116	3.6.....	0.0370
1.7.....	0.0124	3.7.....	0.0405
1.8.....	0.0132	3.8.....	0.0465
1.9.....	0.0140	3.8317.....	0.0529

TABLE VII

$$I_2 = \int_0^\pi \left( 1 - J_0^2[a(1+\nu)\sqrt{1-k^2 \sin^2 \psi}] - J_1^2[a(1+\nu)\sqrt{1-k^2 \sin^2 \psi}] \right) \frac{k' d\psi}{1-k^2 \sin^2 \psi}$$

$g_4$	$I_2$	$g_4$	$I_2$
0.1.....	0.0270	2.1.....	0.4008
0.2.....	0.0539	2.2.....	0.4080
0.3.....	0.0806	2.3.....	0.4141
0.4.....	0.1066	2.4.....	0.4194
0.5.....	0.1323	2.5.....	0.4238
0.6.....	0.1571	2.6.....	0.4276
0.7.....	0.1812	2.7.....	0.4308
0.8.....	0.2045	2.8.....	0.4336
0.9.....	0.2268	2.9.....	0.4359
1.0.....	0.2479	3.0.....	0.4378
1.1.....	0.2679	3.1.....	0.4393
1.2.....	0.2868	3.2.....	0.4406
1.3.....	0.3044	3.3.....	0.4419
1.4.....	0.3208	3.4.....	0.4430
1.5.....	0.3357	3.5.....	0.4439
1.6.....	0.3496	3.6.....	0.4450
1.7.....	0.3623	3.7.....	0.4458
1.8.....	0.3736	3.8.....	0.4469
1.9.....	0.3839	3.8317.....	0.4471
2.0.....	0.3933		

another luminous point or disk comes nearly in contact with it, or when a dark disk passes over a luminous disk. We have therefore to lay special stress on the treatment of this particular case. The difficulty hitherto encountered was principally in the evaluation of (27) and (31), and especially of the latter. By the simplification here obtained, the different aspects of the phenomena can be easily studied from the tables of the numerical quantities involved in the problem.

*A luminous point and a bright disk.*—Having solved the problem in four steps, we can proceed to the discussion of several cases of interest in observations with telescopes.

Suppose a luminous point is situated on the margin of a bright disk. The intensity of the diffracted image due to a point source is given by  $\left(\frac{2J_1(r)}{r}\right)^2$ , and the lines of equal intensity or the isophotes are concentric circles, whose position is easily given by the tables calculated by Lommel. If we superpose on this system of isophotes those belonging to a bright disk, we can graphically obtain a system of isophotes due to a luminous point and a bright disk. The diagrams are given in Figs. 5*a*, *b*, and *c*; the intensity of the point and that of the disk ( $a=50$ ) at the center is taken to be unity. The actual position of the point and the periphery of the disk are shown by an asterisk and a dotted line respectively, while the isophotes are shown in full lines, the numbers indicating the intensities. The normal distance between the point and the periphery being given by  $d$ , the inspection of the figures indicates that with the approach of the point to the disk the place of maximum intensity is gradually shifted toward the disk; when the point comes exactly in contact with the periphery of the disk the luminosity is most intense a short way inside the disk; the consequence is that the point apparently enters the surface of the disk before it is actually covered by coming behind the disk, if it lay farther away.

*Two bright disks.*—By a procedure similar to the foregoing we can easily draw the isophotes for two bright disks nearly in contact. The isophotes are shown in Figs. 6*a* and *b*, which are drawn on the supposition that the intensities for both disks are equal. It

will be easily seen from the course of the isophotes that the contact of two disks is difficult to judge on account of the gradual transition of the isophotes, which depend mainly on the aperture of the telescopic objective. Thus there may be some difference in the

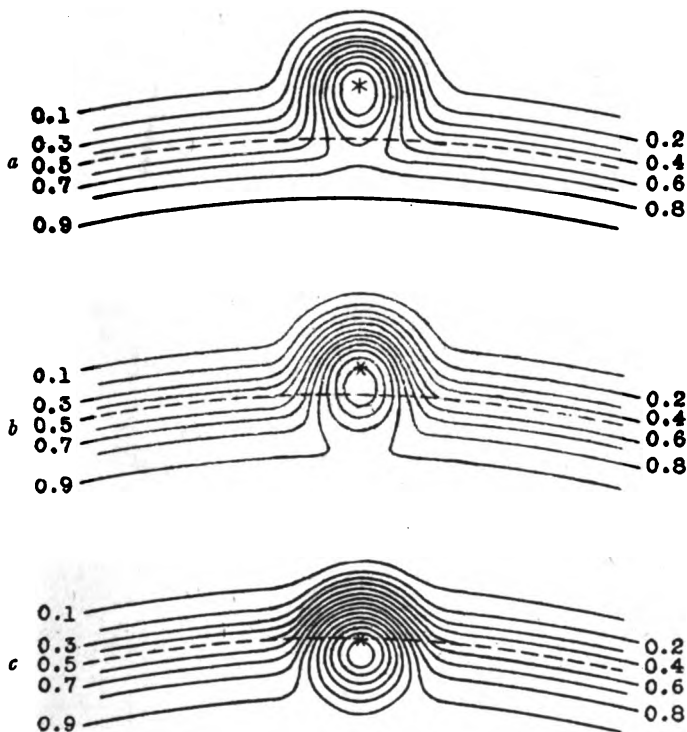


FIG. 5.—Luminous point and bright disk,  $a = 50$

a.  $d = -2$

b.  $d = -1$

c.  $d = 0$

measurement of the moment of contact of a disk either with a luminous point or with a bright disk according to the instrument of observation.

*A dark disk in a bright disk.*—The case presenting much interest is the case of a bright disk partly covered by a dark disk; this corresponds in astronomical phenomena to the transit of the inferior planets over the sun's disk.

Constructing the isophotes in the same manner as the preceding, by superposing the intensity with positive sign due to the bright disk on that with negative sign due to the dark disk, we find various transitions of the isophotes, as the dark disk gradually covers a portion of the bright disk. The various stages of progress

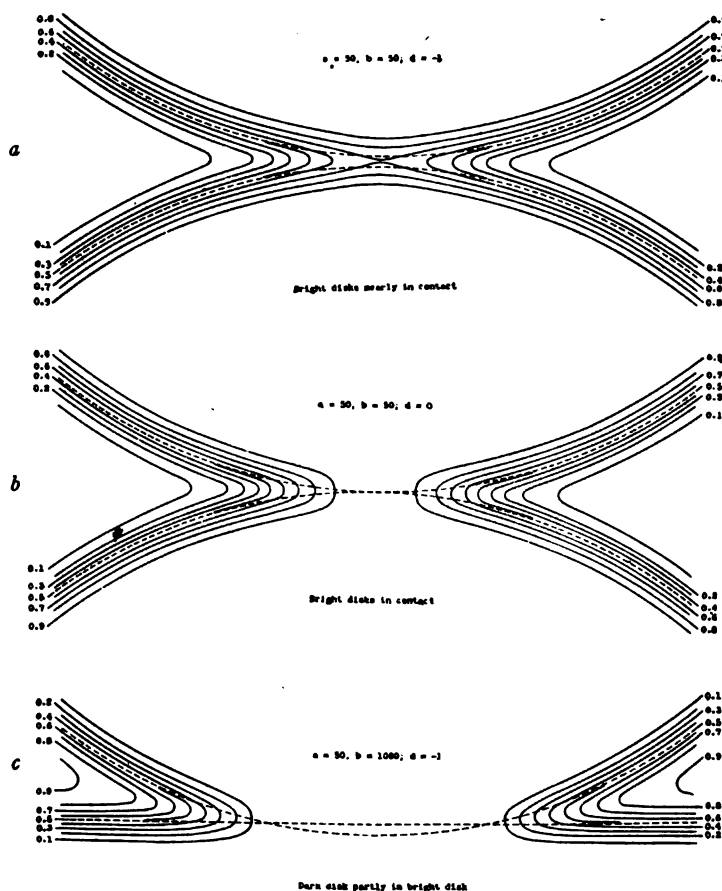


FIG. 6

are shown in Fig. 6c and Fig. 7, the radius of the dark disk being  $a = 50$  and that of the bright disk  $b = 1000$ .

When the dark disk is partially in the bright disk and when they are in contact, the dark surface is apparently connected with the region external to the bright disk. The isophotes show curious

trends, so that the space bounded by them resembles a dark drop. When the shortest distance between the disks  $d=0.38$ , in the diagram here given, the isophote of intensity 0.1 surrounding the

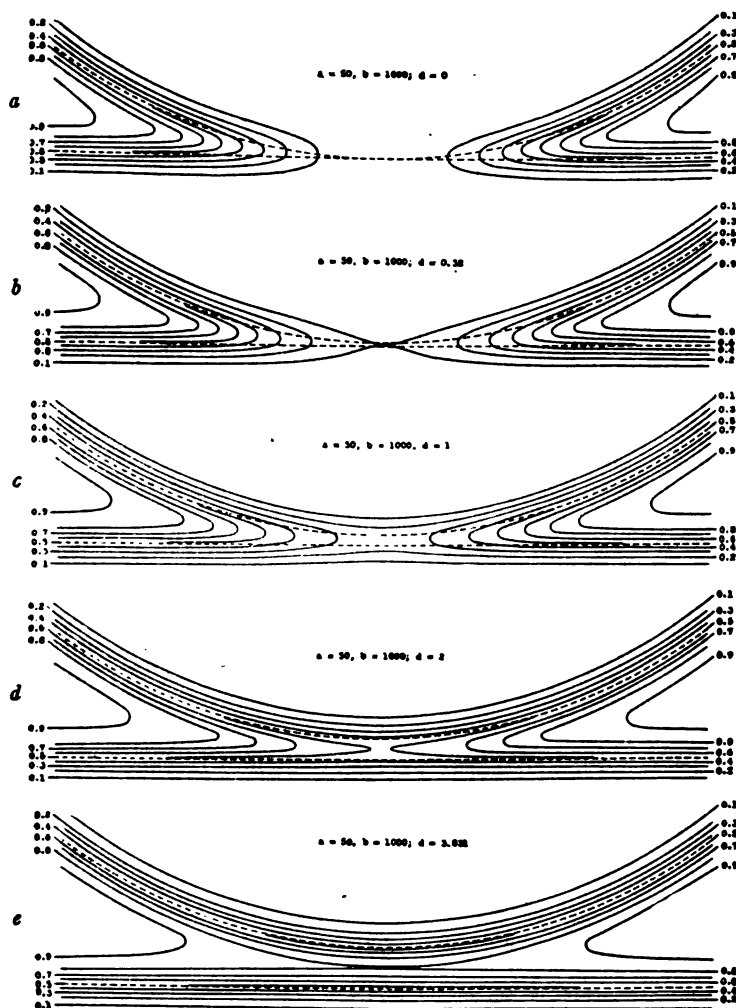


FIG. 7.—Dark disk in bright disk

dark disk comes nearly in contact with that of the same intensity outside the bright disk (Fig. 7*b*); the curve shows a small protuberance, and the dark ligament which connects the dark space

inside and outside the bright disk is on the verge of disappearing. On passing this curious transient state, the protuberance gradually

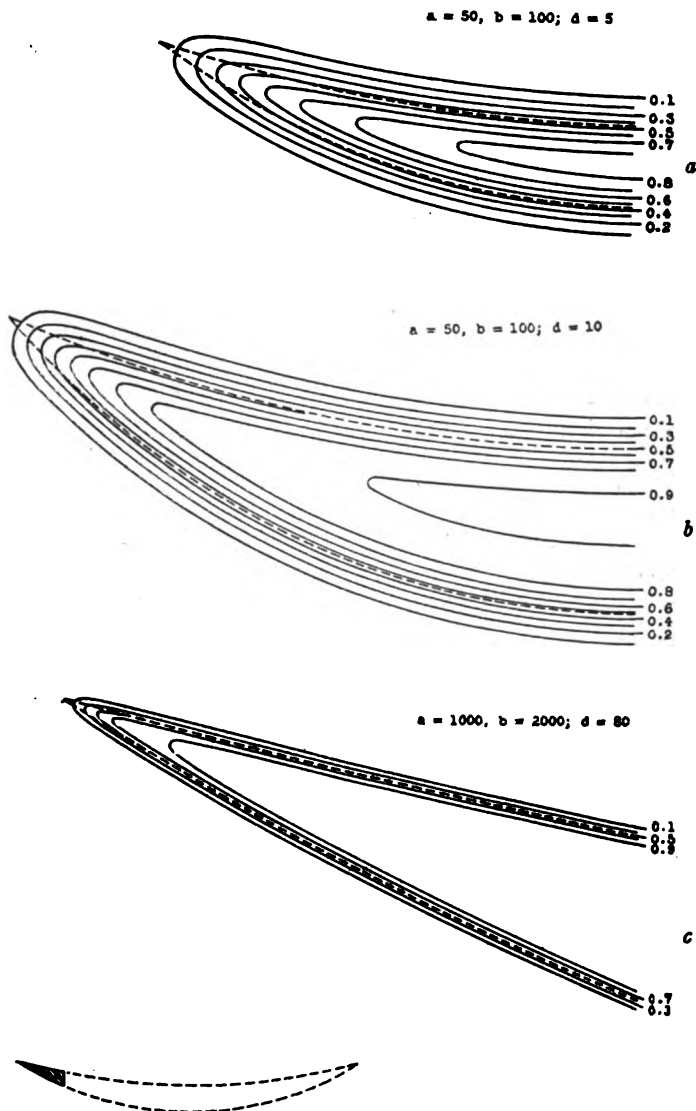


FIG. 8

disappears, and the dark disk assumes a circular shape as it enters deeper into the bright disk, until the deformation in the contour

of both disks becomes indistinct, as a glance at the isophotes in Figs. 7*c*, *d*, and *e* for  $d=1, 2, 3.83$ , will show. Some of these curves have already been given in my former paper, but as the method of calculating the isophotes was extremely tedious, the transient stages could not be followed closely as here given.

It is needless to remark that when  $a=b$ , and the radius is made very large, while  $d$  is small, the distribution of the intensity will approach that in the image of a long slit. The intensity lacks uniformity toward the edge, as can be easily conceived from the construction of Fig. 7*e*.

*Lune*.—A similar process leads to the construction of isophotes in a luminous lune. As will be easily conceivable, the distribution of the isophotes in and about the lune differs with the radii of the bounding circles. When they are small and the lune thin, the isophotes are as shown in Fig. 8*a* ( $a=50, b=100, d=5$ ), while for double the above-mentioned thickness, they are given in Fig. 8*b*. For very large radii and corresponding increase in thickness ( $a=1000, b=2000, d=80$ ), only a small portion of the boundary is affected, as shown in Fig. 8*c*, of which a shaded portion in the annexed figure is given. It will be seen that the effect of diffraction is to round the extremities of the lune, so as to change them into curves having finite curvature. Thus the effect will be strongly felt, when the radii of the bounding circles are small.

*Conclusion*.—Examples of like nature can be multiplied by considering various other cases, but it will be sufficient to indicate the variation in the image of the luminous surface caused by the diffraction of the observing telescope. In the actual observation, physiological effects such as irradiation may cause further modification of the observed image, but it is outside the scope of the present investigation. What I want to show is the rôle played by the diffraction of the telescopic objective in forming the image of a circular source.

In preparing the present paper my thanks are due to Mr. Sadazo Sakurai, assistant in the Institute for Physical and Chemical Research, for carrying out complicated numerical calculations and for verifying various formulae in the present paper.

PHYSICAL INSTITUTE, TOKYO IMPERIAL UNIVERSITY

August 1919



## ON COMET 1919*b* AND ON THE REJECTION OF A COMET'S TAIL

By E. E. BARNARD

### ABSTRACT

*Comet 1919b*, which is a return of Brorsen's comet V of 1847, is interesting both from a historical standpoint and because of its tails. During September and October, 1919, it was visible to the naked eye as a dim, hazy star without any tail, with a maximum *brightness* corresponding to about magnitude 4.5. Twelve *photographs* were taken. The first ones showed only a slender tail several degrees long, but later the comet became fairly active and about October 20 *discarded its tail* and developed a new one which made an angle of  $12^\circ$  with the old.

*Rejection of a comet's tail.*—The *instances* of this phenomenon which have been observed previously are the following: Borrelly's comet in 1903, Morehouse's comet in 1908, and Halley's comet in 1910. The case of *Morehouse's comet* on October 15, 1908, is particularly interesting, for the photographs when combined and viewed with the stereoscope clearly show that the rejection was associated with a cyclonic disturbance. Other features characteristic of the *various stages* of the phenomenon, the true nature of which the author was the first to recognize, are briefly described.

The first of the two comets discovered in August, 1919, by Metcalf was shown by Leuschner to be a return of Brorsen's comet V of 1847, which was originally discovered by Brorsen at Altona, Germany, on July 20, 1847, and passed perihelion about September 9 of that year.<sup>1</sup> At its present return the comet passed perihelion on October 16, 1919. It seems to belong to the Neptunian family of comets,<sup>2</sup> of which group Halley's is the best-known member. Photographs of it, therefore, are interesting from a historical standpoint, if from no other.

At the apparition of 1847 it was a rather faint object and apparently did not attain naked-eye visibility. Various orbits were computed from the observations of 1847 (the best of which was one by B. A. Gould), but though they showed the comet to be certainly periodic the periods assigned were discordant and unsatisfactory.

<sup>1</sup> *Astronomische Nachrichten*, 26, 87, 155, 1847.

<sup>2</sup> In the *Scientific American* for November 1, 1919, Professor H. N. Russell has shown that Neptune could not be responsible (like Jupiter for his comet family) for the grouping of these comets. Though Neptune may not have been responsible for their capture, the term "Neptunian comet family" may still hold through courtesy.

At the present return this object was visible to the naked eye for over a month as a dim hazy star without any tail. The greatest brightness seemed to be at about  $4\frac{1}{2}$  magnitude on the Harvard scale. For a while it was above the horizon throughout the night, and later it could be seen both in the evening and in the morning, and later still only in the morning sky just before dawn.

#### NAKED-EYE VISIBILITY OF THE COMET

Following are some of the notes made while the comet was visible to the naked eye:

1919 Sept. 15, 7<sup>h</sup>45<sup>m</sup> Central Standard Time. Distinctly visible to the naked eye as a hazy spot. Comparisons with 5 Canum Venaticorum made the comet's magnitude 5.4. With the field glass and the image out of focus comparisons with the above-mentioned star made its magnitude 5.0. At 8<sup>h</sup>0<sup>m</sup> to the naked eye the comet was very slightly brighter than the Andromeda Nebula, but very much smaller.

Sept. 19, 8<sup>h</sup>0<sup>m</sup>. Just visible to the naked eye.

Oct. 5, 16<sup>h</sup>20<sup>m</sup>. Visible to the naked eye as a small hazy spot of light. By comparison with several stars its magnitude was 4.0, but its light was mixed up with that of 93 Leonis, and the magnitude given is probably too bright.

Oct. 6, 16<sup>h</sup>40<sup>m</sup>. Visible to naked eye;  $4\frac{1}{2}$  magnitude.

Oct. 7, 16<sup>h</sup>30<sup>m</sup>. Not visible to the naked eye because of moonlight.

Oct. 12, 16<sup>h</sup>30<sup>m</sup>. Too much moonlight to see it with the naked eye. Brightly condensed in the 5-inch guiding telescope but with no trace of tail on the bright sky.

Oct. 16, 16<sup>h</sup>30<sup>m</sup>. Not visible to the naked eye on account of moonlight.

Oct. 20, 16<sup>h</sup>50<sup>m</sup>. Faintly visible to the naked eye; 5.6 magnitude. In the 5-inch guiding telescope there was some tail.

The magnitudes are on the Harvard scale.

#### PHOTOGRAPHS OF THE COMET

During most of the time that the comet was present the Bruce telescope was not available for photographing it, but later, especially in the morning sky when near perihelion, photographs were obtained with the 6-inch and 10-inch lenses of this instrument. But the

exposures were short from moonlight and dawn. Bad weather also interfered with the observations during the most important period. Some of the photographs, however, are valuable. They suggest that had better conditions prevailed the results would have been extremely interesting.

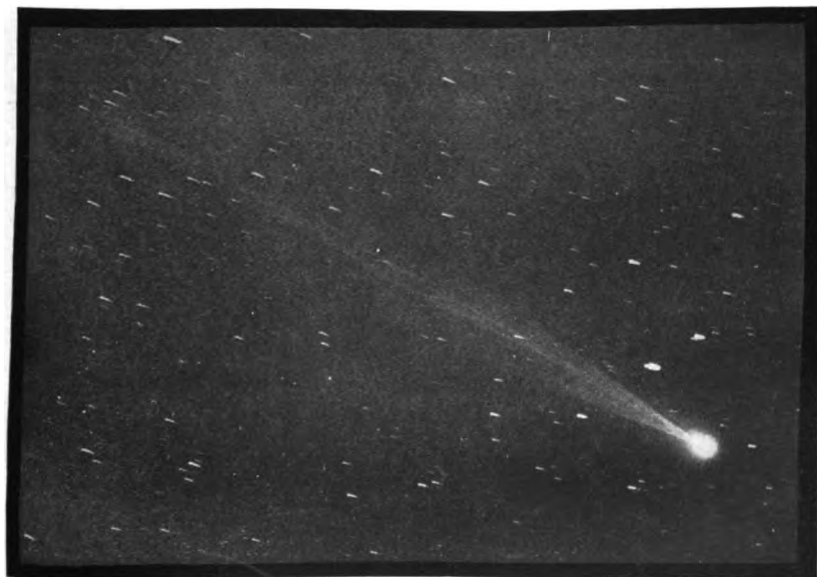
The first photographs, in September, showed only a slender tail several degrees long and of no special interest. The later pictures, however, when, unfortunately, short exposures only were possible, are quite interesting and show that the comet finally became fairly active, especially when past perihelion. This was strikingly the case on or about October 22, when the tail was discarded and a new one formed. The table gives a complete list of the photographs which were secured by the writer with the Bruce telescope. The approximate position angles and length of the tail are also given:

Date	C. S. T.	Exposure	Length of Tail	Position Angle
1919 Sept. 21..	16 <sup>h</sup> 27 <sup>m</sup>	0 <sup>h</sup> 7 <sup>m</sup>	$\frac{1}{2}^{\circ}$	2°
22..	7 37	0 28	$\frac{1}{2}$	.....
22..	16 5	0 45	3	5
24..	7 33	0 47	$\frac{1}{2}$	9
Oct. 5..	16 20	0 41	3	328
6..	16 14	0 57	7	328
7..	16 26	0 41	7	331 $\frac{1}{2}$
12..	16 33	0 43	5	315
16..	16 27	0 50	8 $\frac{1}{2}$	312
20..	16 50	0 33	7	307 $\frac{1}{2}$
22..	16 51	0 24	6	307 nearer part, or new tail
28..	16 50	0 40	5	302

In some of these plates the tail is very faint toward its end. The rejected part, in the photographs of October 22, makes an angle of 12° with the new tail. The nearest point of this drifting tail is 51' from the head. October 23 was cloudy here so that no photographs could be made. This was unfortunate, as material for the motion of the particles of the tail would have undoubtedly been obtained. The photographs of October 20 may show an earlier stage of this separation. On that date the tail proper seemed disconnected from the head. The rearward portion, which

# PLATE X

North



*a*

North



*b*

COMET 1919*b* (METCALF-BROSEN)

Scale: 1 cm = 36'

- a.* 1919, October 5, 16<sup>h</sup>20<sup>m</sup> C.S.T. Exposure, 0<sup>h</sup>41<sup>m</sup>
- b.* 1919, October 6, 16<sup>h</sup>14<sup>m</sup> C.S.T. Exposure, 0<sup>h</sup>57<sup>m</sup>



# PLATE XI

North

*a*



*b*



COMET 1919*b* (METCALF-BRORSEN)

Scale: 1 cm = 36'

- a.* 1919, October 20, 16<sup>h</sup>50<sup>m</sup> C.S.T. Exposure, 0<sup>h</sup>33<sup>m</sup>  
*b.* 1919, October 22, 16<sup>h</sup>51<sup>m</sup> C.S.T. Exposure, 0<sup>h</sup>24<sup>m</sup>



was sharply pointed, was 9'.6 from the head, while a new and widening tail filled the space between it and the head. If these parts of the tail were the same on the two dates, the recession of the particles was at the rate of 21' a day. Photographs made elsewhere will probably decide this question. On the photograph of October 20 a brighter condensation about 2° long is shown in the tail 2°30' back from the head. Four of these pictures of the comet, on the dates October 5, 6, 20, and 22, made with the 10-inch lens of the Bruce telescope, are reproduced in Plates X and XI.

This discarding of the entire tail of a comet is not a new feature, though I believe it was unknown previous to the successful introduction of photography to the study of comets. The first known case really occurred in 1903, when on July 24 Borrelly's comet discarded its tail and at once formed a new one. On that date the comet's tail presented a puzzling appearance. It seemed to be split diagonally into two tails. To explain this phenomenon the present writer suggested<sup>1</sup> that the comet had discarded its entire tail and had formed a new one at a slightly different angle and that the old tail was drifting away bodily into space. Though this explanation was somewhat antagonistic to the then received ideas of a comet's tail, it proved to be the true one. It has been amply verified since then by Morehouse's comet on several dates, by Halley's comet on June 6, 1910, and by comet 1919b. In the various cases of this kind a new tail (and sometimes a system of tails) is always sent out at once by the comet, generally in a somewhat different direction from that of the rejected tail.

Perhaps the most interesting case of rejection is that of Morehouse's comet on October 15, 1908, when the nearer end of the receding tail presented a twisted or knotted appearance. Fortunately photographs on that date were secured at a number of observatories, both in this country and in Europe. My own photographs of it cover a period of over seven hours. Thus a fairly full record of these changes was obtained. I have combined for the stereoscope several sets of my own pictures of the comet at that time. The results are very interesting. They clearly show the gradual transformation of the near end of the old tail. At

• <sup>1</sup> *Astrophysical Journal*, 18, 213, 1902.



first it was twisted or cyclonic in form, as if it had received some twisting motion when it left the head. It slowly formed into a thickish fragment of a ring, from all parts of which streams of particles swept back to form the old tail, giving it the appearance of part of an open sack, or a partly opened scroll, with irregular sides. Without the aid of the stereoscope one would never have guessed the real form of the tail. It seems that immediately after the separation of the tail from the head a new and slender tail was shot out from the head at a different angle from that of the receding one. In the stereoscope this new tail is seen to pass behind the old one—away from us and toward the background of the stars. It was moving out much faster than the rear portion of the old tail—a peculiarity that seems to be always present in the general process of forming a new tail. This fact was very strongly shown in the case of Borrelly's comet of 1903. It would therefore seem that the rear part of a receding tail is made up of the more sluggish, or larger, particles and is not moving as fast as the other parts of the rejected tail. Measurements of this part will therefore give the minimum velocity of the tail-forming particles.

In *Popular Astronomy*, 17, for November 1909, Plate IX, I have given two photographs of Morehouse's comet on 1908 October 15, that form a stereoscopic view, which beautifully shows the earlier stages of the separation of the tail from the head.

YERKES OBSERVATORY, WILLIAMS BAY, WIS.

January 16, 1920

# PRELIMINARY OBSERVATIONS OF THE ZEEMAN EFFECT FOR ELECTRIC FURNACE SPECTRA<sup>1</sup>

By ARTHUR S. KING

## ABSTRACT

*Zeeman effect for furnace spectra of iron and vanadium.*—Hitherto Zeeman effect observations have been almost exclusively confined to spark spectra. Because the electric furnace emits or absorbs strongly many lines which are weak or absent in spark spectra, and because it is desirable to compare the effects of a magnetic field on spectra from different sources, the present investigation was undertaken. The furnace tube was placed parallel to the lines of force, in a field varying from 6500 gauss in the center to 9000 gauss near the ends, and it was heated to a maximum temperature of 2200°. To obtain the inverse effect, a carbon plug was placed so as to supply a continuous high-temperature spectrum as a background. Spectrograms were taken with a concave grating giving a scale of about 1.83 Å per mm. Table I contains the observed separations for both the direct and the inverse effects, viewed along the lines of force, for 100 iron furnace lines together with the corresponding separations obtained with the spark as source. Table II contains similar data for the direct effect for 90 vanadium lines. Twenty of the iron lines and eleven of the vanadium lines had not previously been investigated. It was found that the character and magnitude of the separations for the  $n$ -components of furnace lines both in emission and in absorption agree closely with those of the corresponding spark lines, reduced to the same field intensity; that is, the effect is independent of the source used. Since these three methods give identical results for each line, they may be used to supplement each other in studying the effect. Among other advantages of the furnace, the non-uniformity of the magnetic field enables the location and temperature of the active centers of absorption or emission for various lines to be determined. Spectrograms are reproduced in Plates XII and XIII.

*Zeeman effect for the D-lines of the sodium spectrum.*—The author suggests a possible explanation of a variation of the effect with the source of light, which was observed by Woltjer.

On account of the difficulty of maintaining an arc in the magnetic field, investigations of the Zeeman effect have thus far been carried out almost exclusively with the electric spark as the source of light. While the spark is satisfactory for much work of this kind, certain disadvantages make it desirable to supplement the spark experiments with those from a source quite different in character. Two features of the spark spectrum are especially

<sup>1</sup> Contributions from the Mount Wilson Observatory, No. 180.

troublesome. First, many lines characteristic of the low-temperature sources, and important in sun-spot spectra, are faint or absent in the spark, though, on the other hand, the spark emits strongly the enhanced lines and others requiring high excitation. Second, the condensed spark in air, made more disruptive by the magnetic field, is an unfavorable source for obtaining the sharp Zeeman components required for measurements of high precision. A sharpening of the lines by the use of self-induction, which also removes the disturbing air lines, is accompanied by a reduction in the luminosity of the spark.

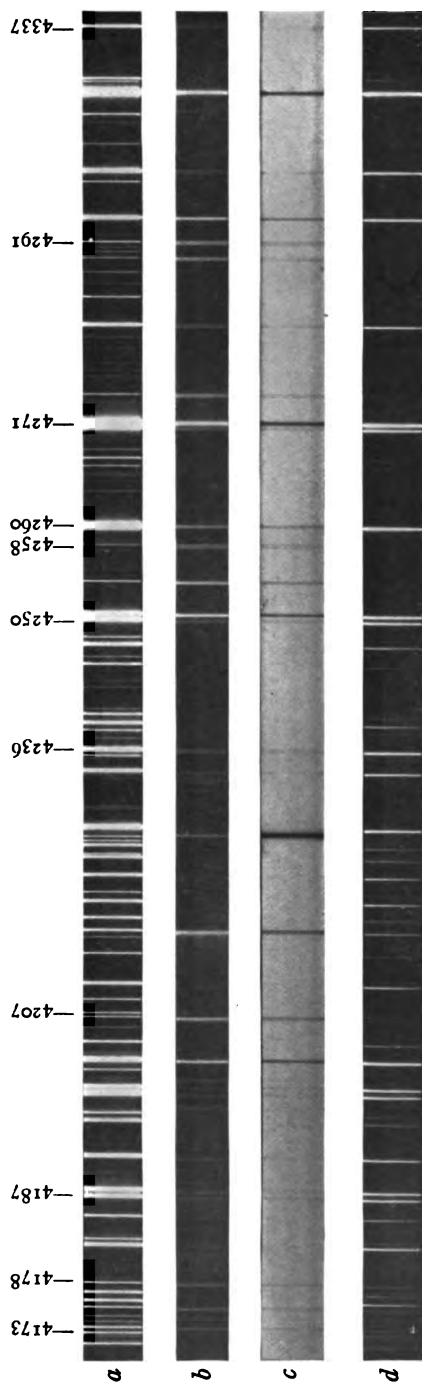
The electric furnace is especially effective in emitting the lines which are weak in the spark. When inclosed in a vacuum chamber, the furnace lines can be made extremely sharp, and, unlike the sources involving an electric discharge, neither the action of the furnace nor the character of its spectrum undergoes material modification when operated *in vacuo*. A third useful feature of the furnace is the unique facilities afforded for the study of the inverse Zeeman effect by the production of absorption spectra when a diaphragm of graphite is placed at the center of the tube. The absorption spectra produced in the regular furnace by this means were described in a recent paper.<sup>1</sup>

The obvious disadvantage of the furnace when used with the usual type of electromagnet is its relatively large size, which prevents the use of high magnetic fields. While an equipment designed to overcome this difficulty is being prepared, it seemed desirable, by operating a small furnace between the poles of a Weiss electromagnet, to examine the character of the magnetic separations given by the moderate field available. The possibilities of the furnace for this work could thus be determined and it could be seen whether any decided peculiarities appeared for a source very different from the spark.

This investigation has been limited to the spectra of iron and vanadium, with the addition of a few impurity lines, but the material is sufficient to show clearly the nature of the magnetic separations for the furnace spectrum.

<sup>1</sup> *Mt. Wilson Contr.*, No. 174; *Astrophysical Journal*, 51, 13, 1920.

## PLATE XII

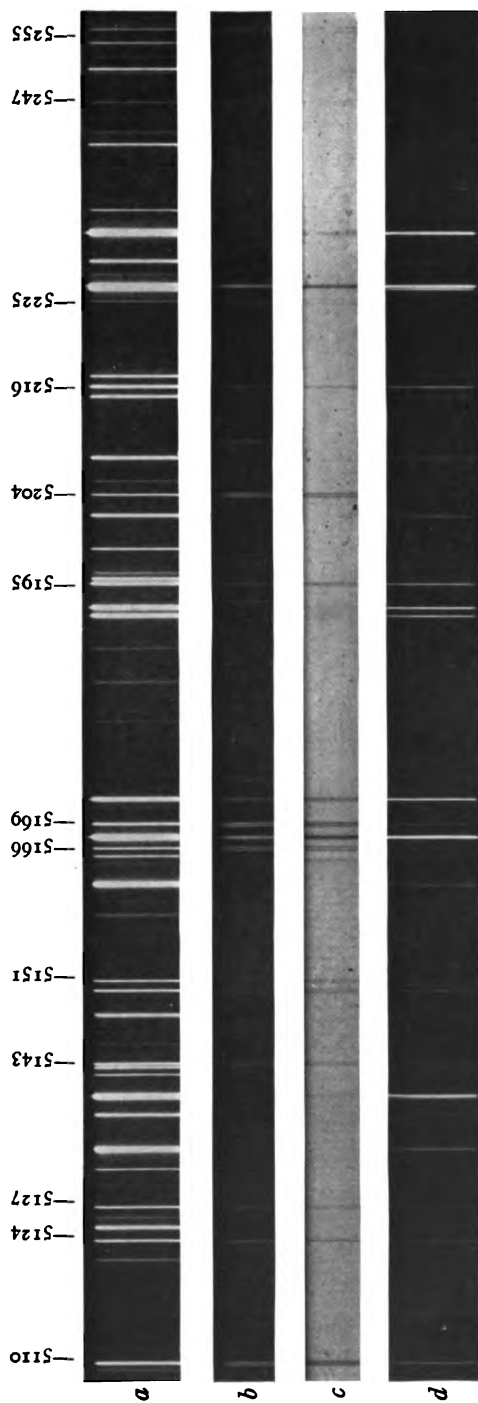


EFFECT OF A MAGNETIC FIELD ON THE ELECTRIC FURNACE SPECTRUM OF IRON

- a, d.* Comparison arc spectra of iron without field
- b.* Emission spectrum of furnace in magnetic field
- c.* Absorption spectrum of furnace in magnetic field



# PLATE XIII



EFFECT OF A MAGNETIC FIELD ON THE ELECTRIC FURNACE SPECTRUM OF IRON

- a, d. Comparison arc spectra of iron without field
- b. Emission spectrum of furnace in magnetic field
- c. Absorption spectrum of furnace in magnetic field



## EXPERIMENTAL METHOD

A graphite tube 10 cm long, of 6 mm internal and 12.5 mm external diameter, was placed axially between the poles of a large Weiss electromagnet. The latter was provided with pole-pieces 5.1 cm in diameter, one of which was perforated to enable the light from the furnace tube to pass through the hollow core to the spectrograph. The tube was clamped at each end in a graphite bushing 12.5 mm wide held in a brass ring of the same width, the two halves of which were bolted tightly together. This ring was of rectangular cross-section and made hollow to permit of water-cooling. The alternating current, at potentials of 5 to 20 volts, was led to the clamping rings by flexible copper tubes, also water-cooled, from the massive transformer terminals some 2 meters distant. The portion of the furnace tube between the clamps was turned down to a slightly smaller diameter, varying in different experiments, and, since no vacuum chamber was used, it was surrounded by a protecting jacket. Various jacketing methods were tried, but the most satisfactory was to inclose the furnace tube in a thick-walled graphite tube, with an air space of 2 to 3 mm between, and to cool this outer tube with a tubular water-jacket of brass.

A magnetic gap of about 10.5 cm was required to allow space for the furnace. The field in this gap, when the magnet was fully excited, was measured with a bismuth spiral as 6500 gauss at the center, and increased to 9000 gauss 1 cm from the pole, which, however, was considerably beyond the heated portion of the tube. The bearing of this field variation on the observed phenomena of the furnace will be noted later.

The material to be vaporized, either iron filings or powdered vanadium, was placed in the central part of the tube when the emission spectrum was desired, or in front of a graphite plug placed at the center when the absorption spectrum was to be observed. The metal was fused at a moderate temperature before the field was turned on. This, in the case of the iron, which sticks to the graphite when melted, prevented the metal from being drawn out of the tube. The largest current usable with the rather fragile



tube was 800-900 amperes, the temperature attained, judging from the spectrum, being in the neighborhood of  $2200^{\circ}\text{C}$ . The fact that the current passed through the contact blocks for a short distance at right angles to the field caused a vibration which, in spite of fairly rigid clamping in a wooden frame, eventually broke the tube. The limited exposures possible on this account were sufficient to allow photographing with the first order of the 30-foot plane-grating spectrograph and the second order of the 15-foot concave grating, the scales being about  $1\text{ mm} = 1.83\text{ \AA}$  and  $1\text{ mm} = 1.86\text{ \AA}$ , respectively.

#### • OBSERVATIONS OF THE ZEEMAN EFFECT

1. *Character of the separations*.—As the spark has hitherto been the only source extensively used in studies of the Zeeman effect, it cannot be assumed without proof that a source so different in its action as the furnace would show no differences in the magnetic behavior of spectrum lines as compared with the spark. The present investigation has therefore had as one of its chief objects a comparison of the furnace and spark material extensive enough to show whether for a given field-strength the number of components and the amount of their separation is the same for the two sources. Since the observations were made entirely along the lines of force, the data collected are for the  $n$ -components only. Measurements of the spark separations for iron have been published by the writer,<sup>1</sup> and those for vanadium by Mr. Babcock,<sup>2</sup> for fields of 16,000 and 20,000 gauss, respectively. These have furnished comparisons of furnace and spark separations for nearly all of the lines except those which are strong in the furnace as compared with the arc or spark. These are chiefly 1A lines of the furnace classification and in most cases the measurements given here are the first that have been made for such lines.

A large variety is found in the appearance of the lines emitted by the furnace in the magnetic field, but this is readily explained in every case by the data at hand on the temperature class and the character of the magnetic separations shown for the spark in high

<sup>1</sup> *Papers of the Mt. Wilson Observatory*, 2, Part I, 1912.

<sup>2</sup> *Mt. Wilson Contr.*, No. 55; *Astrophysical Journal*, 34, 209, 1911.

fields. For lines of triplet separation, the furnace shows a pair of sharp  $n$ -components, their sharpness when viewed along the varying field in which the furnace is placed indicating that the particles emitting them are rather definitely localized in the tube. Many cases of blurred components occur, the line sometimes appearing as a diffuse patch. These are found to be either complex lines in which the four or more  $n$ -components are not resolved by the low field, or low-temperature lines whose components are self-reversed, or sometimes a combination of both effects. Interesting cases are observed in which a line has the same appearance as a triplet when viewed at right angles to the lines of force, there being a sharp middle component twice as strong as either side component. This is caused by reversals of the two  $n$ -components for which the amount of separation and the width of reversal happen to be such that the red side of one reversed component falls exactly upon the violet side of the other. The furnace results, including the absorption spectra to be discussed later, supply ample evidence that reversed magnetic components, when observed along the lines of force, show no peculiarities as compared with unreversed components of the same lines. A certain amount of evidence on this point has appeared in work with the spark, the difficulty of obtaining some of the ultra-violet iron lines with unreversed components having been noted by the writer.<sup>1</sup>

Lines such as  $\lambda\lambda$  5124 and 5435 of iron, which show no separation for high fields with the spark, are sharp also in the furnace spectrum. Several lines which give a quartet of  $n$ -components in the spark show the same resolution in the furnace, and the iron line  $\lambda$  5497 is resolved into five  $n$ -components in both sources. The field used with the furnace was too low to separate the more complex types, but in every case of lines common to both, the appearance of the furnace line is explained by the character of its separation in the spark.

2. *The inverse effect.*—Experiments on the magnetic separation of absorption lines were carried out for the iron spectrum to a sufficient extent to show what may be expected of the furnace when operated in this way. The absorption lines obtained with

<sup>1</sup> *Papers of the Mt. Wilson Observatory*, 2, Part I, p. 19, 1912.

a plug in the center of the tube and their dependence on temperature class were discussed in a former paper.<sup>1</sup> It was shown there that successive classes of lines appeared as the temperature was raised, so that the production of narrow absorption lines for a given class is a matter of temperature adjustment. With the absorption furnace in the magnetic field, the components follow closely the character of the no-field absorption line, so that a proper temperature must be chosen for the desired set of lines. Proceeding according to this principle, a large part of the iron lines for which the direct Zeeman effect had been observed were obtained with their components in absorption. Complete similarity as to character and number of components was found for the direct and inverse effects. The absorption method is useful for obtaining low-temperature lines with short exposures, this requiring, as for the no-field spectrum, a higher temperature than that needed for the same lines in emission. For the regular work of obtaining measurable lines under the special conditions supplied by the furnace, the direct effect—adjusting the temperature and vapor-density to the character of various groups of lines—will probably be more used than the inverse effect. The absorption method, however, will have its place in many problems, especially in those connected with solar spectra. For the  $n$ -components observed along the lines of force, the present results show that the character of the magnetic resolution is the same for the two effects, so that the components in absorption may be studied by this means when it is of advantage to do so.

3. *Magnitude of furnace separations.*—The separations measured for iron and vanadium are recorded in Tables I and II. A field measurement was first made by selecting a number of lines, each of which has a pair of sharp  $n$ -components in both furnace and spark. A comparison of the separations gave for the direct effect a strength of 6400 gauss for the field generally used with the furnace, while a value of slightly less than 6500 gauss was given by a bismuth spiral placed midway between the poles. There is thus excellent agreement of furnace and spark separations, provided the furnace components are emitted by vapor near the center

<sup>1</sup> *Mt. Wilson Contr.*, No. 174; *Astrophysical Journal*, 51, 13, 1920.

of the tube. This is probably the case, as the lines compared were as a rule furnace lines of moderate strength which the central vapor should emit most strongly, the strongest low-temperature lines being usually either overexposed or complex. In Tables I and II, therefore, the spark values, so far as they are available for the given lines, are reduced to a field of 6400 for comparison with the furnace separations.

A comparison of the inverse and direct effects for the same lines showed the separation of the absorption components to be consistently larger than in emission, the separations of the best lines being in the ratio of 1 to 0.87, a result repeated on a number of plates for which the same field was used. This indicated a larger field-strength in the part of the tube where the absorbing vapor was effective. Measurements along the pole-gap with the bismuth spiral brought out the interesting fact that at about 25 mm from the center the field increased to the value indicated by the absorption lines. It follows that the absorbing particles were centered about a position at this distance from the plug. The distance probably varies for different sets of lines; the field and dispersion now used are not sufficient to test this point.

Besides explaining the larger separations of the absorption components in the present experiments, this result suggests a method of locating the section of the furnace tube in which any line is emitted or where the vapor absorbs the line most strongly, and from this the corresponding temperature. A knowledge of the variation of field-strength along the axis of the magnet would be required, and also the temperature-gradient along the tube, which can be measured by moving a plug from end to center and recording its temperature at different points. A high precision in the measurement of the magnetic separations should then give valuable information as to the origin of different groups of lines.

4. *Comparison with spark separations.*—The list of iron lines in Table I gives in the second column the temperature class, in the third the emission separations as measured, in the fourth the absorption separations reduced by the factor required on account of the larger field apparently operating in this case, and in the fifth the

TABLE I  
SEPARATION OF IRON LINES IN MAGNETIC FIELD

$\lambda$	CLASS	$\Delta\lambda$		
		Emission	Absorption	Spark
3940.885.....	IA	.....	.186	.184
4100.745.....	IA	.176	.185	.....
4147.675.....	I	.231	.220	.270
4152.176.....	IA	.114	.....	.....
4172.748.....	IA	.....	.116	.....
4174.917.....	IA	.....	.116	.150
4177.598.....	IA	.....	.142	.....
4206.696.....	IA	.....	.191	.135
4216.185.....	I	.....	.188	.183
*4222.225.....	III	.174	.....	.190
4232.724.....	IA	.317	.....	.....
*4235.953.....	II	.174	.180	.181
4250.134.....	III	.163	.157	.153
4258.386.....	IA	.264	.285	.....
*4260.489.....	III	.173	.185	.160
*4271.171.....	III	.161	.161	.158
4282.406.....	II	.150	.150	.124
4291.472.....	IA	.233	.250	.....
*4299.254.....	II	.172	.161	.162
4315.092.....	III	.216	.216	.207
4337.052.....	II	.097	.....	.106
4347.239.....	IA	.182	.....	.....
4352.740.....	II	.178	.....	.166
*4375.934.....	I	.....	.180	.170
4389.251.....	IA	.....	.166	.....
*4427.313.....	I	.....	.193	.172
4430.622.....	II	.304	.....	.288
4435.154.....	IA	.174	.176	.....
4442.349.....	III	.193	.....	.194
4447.727.....	II	.244	.....	.234†
4459.128.....	II	.200	.....	.180
*4461.658.....	I	.....	.182	.174
4466.557.....	I	.180	.172	.137
4482.176.....	I	.....	.186	.160
4489.744.....	IA	.178	.190	.....
4494.571.....	II	.134	.128	.121
4528.624.....	II	.147	.....	.143
4531.155.....	I	.147	.....	.159
4592.658.....	I	.152	.....	.166
4602.946.....	I	.224	.....	.226
*4678.226.....	III	.455	.....	.437
4939.689.....	I	.221	.....	.232
4957.612.....	III	.181	.....	.200
4994.133.....	I	.234	.211	.232
*5012.073.....	I	.212	.222	.215
5041.079.....	I	.232	.228	.199
5041.763.....	III	.223	.221	.200
*5051.643.....	I	.209	.206	.208
5079.742.....	I	.337	.321	.295
5083.344.....	I	.196	.200	.190
5110.414.....	I	.238	.260	.216

TABLE I—Continued

$\lambda$	CLASS	$\Delta\lambda$		
		Emission	Absorption	Spark
5127.364.....	I	.257	.254	.270
5142.934.....	I	.238	.231	.231
5150.845.....	I	.246	.256	.252
5166.288.....	IA	.293	.301	.....
5167.492.....	II	.173	.181	.185
5168.904.....	IA	.260	.266	.....
*5171.601.....	II	.209	.214	.208
*5194.950.....	I	.177	.175	.183
5204.585.....	IA	.293	.284	.....
5216.277.....	II	.094	.104	.122
5225.533.....	IA	{ .506 .260	.....	.....
5227.187.....	II	.169	.171	.163
5232.954.....	III	.....	.204	.223
5247.052.....	IA	.349	.341	.....
5250.212.....	IA	.513	.506	.....
5254.956.....	IA	.400	.381	.....
*5270.357.....	II	.120	.117	.120
5328.539.....	II	.217	.217	.195
5397.135.....	I	.....	.260	.252
5429.701.....	I	.....	.240	.243
5497.521.....	I	{ .568†† .288	.....	{ .556†† .277
5501.471.....	I	.368	.....	.400
5506.785.....	I	.404	.....	.410
5615.663.....	IV	.239	.....	.234
5658.836.....	IV	.280	.....	.290
5701.555.....	III	.224	.....	.243
*6137.704.....	III	.254	.....	.262
6173.346.....	III	.605	.....	.636
*6191.568.....	II	.191	.....	.216
6213.440.....	III	.456	.....	.480§
6219.290.....	III	.396	.....	.396
*6230.732.....	III	.299	.....	.307
*6252.567.....	III	.213	.....	.233
*6254.266.....	III	.355	.....	.381
6265.145.....	III	.392	.....	.388
6280.622.....	IA	.359	.....	.....
6301.524.....	IV	.404	.....	.425
6322.696.....	III	.389	.....	.386
6335.341.....	III	.288	.....	.266
6358.684.....	IA	.447	.....	.298
6393.609.....	III	.213	.....	.237
*6421.361.....	III	.389	.....	.397
6430.859.....	III	.310	.....	.....
*6494.993.....	II	.258	.....	.273
6546.251.....	III	.209	.....	.234
*6592.928.....	III	.262	.....	.280
6663.452.....	IV	.411	.....	.435
*6678.001.....	III	.292	.....	.315

† Mean of two pairs.

†† Five  $\pi$ -components. Measurements for outer and inner pairs.

§ Mean of two pairs.

spark values reduced to the furnace field. Table II, for vanadium, is similar, except that the absorption method was not used for this element.

These lists include the lines for which more or less sharply defined doublets could be measured. When the furnace components were not sharp, those of the spark showed a pronounced widening or a resolution into an inner and an outer pair. Many strong furnace lines, whose complex character allowed no resolution in this field, are omitted.

A general close agreement of the furnace and spark separations in the tables indicates that the action of the field is the same for the two sources. In Table I the iron lines which in the spark show two sharp  $n$ -components and yield measurements of high weight are marked with an asterisk. The agreement for these lines is good. For the other lines, the furnace and spark values often agree closely, and when different show no systematic variation. The mean separations of 67 iron doublets measured for both furnace and spark are 0.2516 and 0.2537 respectively for the two sources. A similar comparison of 79 vanadium doublets gives means of 0.3083 and 0.3100. In the few cases where the discrepancy is considerable, the line is invariably found to be especially difficult to measure in one or both sources, usually owing to a shading of the complex  $n$ -components toward one side or the other. The vanadium lines of Table II are usually less difficult to measure than those of iron, the only notable discrepancies being for lines of complex structure.

This observational material is presented in some detail on account of the difficulty in handling magnetic-field data if the character or magnitude of the separations depends upon the nature of the source. No indication of such a dependence in the iron or vanadium spectrum has appeared. The field possible with the present form of furnace has not enabled me to check the observations of Woltjer<sup>1</sup> on the components of the D lines of sodium. He examined these lines as emitted by a vacuum tube and as given in absorption by the oxy-acetylene flame, and found that while the spacing remained the same, the relative intensities of the five

<sup>1</sup> *Amsterdam Dissertation*, 1914; (Abstract) *Physikalische Zeitschrift*, 15, 918, 1914.

TABLE II  
SEPARATIONS OF VANADIUM LINES IN MAGNETIC FIELD

$\lambda$ (EXNER AND HASCHKE)	CLASS	$\Delta\lambda$	
		Furnace	Spark
5176.95.....	III	.178	.177
5193.20.....	III	.230	.245
5193.84.....	III	.197	.165
5195.65.....	III	.245	.204
5213.82.....	III	.208	.....
5216.76.....	IV	.279	.260
5225.90.....	III	.256	.260
5234.26.....	III	.156	.153
5241.03.....	III	.188	.184
5353.56.....	III	.198	.....
5402.17.....	III	.174	.175
5415.47.....	III	.197	.193
5487.42.....	III	.219	.237
5488.10.....	III	.182	.217
5517.40.....	IIA	.342	.....
5542.91.....	IIA	.182	.....
5546.13.....	IIIA	.357	.361
5547.26.....	II	.342	.344
5574.20.....	IIA	.208	.....
5584.77.....	I	.290	.299
5586.21.....	III	.200	.214
5592.63.....	I	.290	.300
5601.60.....	III	.208	.216
5604.41.....	IV	.204	.....
5605.18.....	II	.327	.362
5627.85.....	I	.271	.288
5640.29.....	II	.342	.360
5657.70.....	II	.290	.309
5668.55.....	II	.297	.305
5683.37.....	III	.226	.232
5725.80.....	III	.215	.219
5733.29.....	IV	.193	.191
5734.21.....	III	.189	.199
5737.25.....	II	.234	.256
5743.66.....	II	.260	.273
5747.92.....	III	.200	.228
5749.05.....	III	.222	.185
5786.43.....	III	.230	.210
5807.38.....	III	.197	.180
5826.83.....	III	.200	.....
5850.57.....	IIIA	.301	.325
5979.11.....	IIIA	.241	.229
5981.02.....	IIIA	.238	.227
6002.89.....	IIA	.416	.457
6008.90.....	IIIA	.331	.280
6018.16.....	IIIA	.301	.....
6025.64.....	IIIA	.222	.209
6039.95.....	I	.332	.331
6087.70.....	IIIA	.312	.....
6090.45.....	I	.272	.286
6111.90.....	II	.294	.293



TABLE II—Continued

$\lambda$ (EXNER AND HASCHKE)	CLASS	$\Delta\lambda$	
		Furnace	Spark
6119.70.....	I	.239	.240
6150.32.....	I	.280	.282
6170.55.....	IA	.286	.269
6189.55.....	IIA	.244	.240
6199.40.....	I	.355	.351
6214.04.....	I	.355	.359
6216.52.....	I	.337	.352
6224.70.....	I	.356	.357
6230.92.....	I	.336	.339
6233.31.....	IA	.356	.349
6240.30.....	IIA	.357	.364
6245.35.....	IIA	.359	.359
6252.02.....	I	.376	.378
6257.03.....	IIA	.394	.396
6258.73.....	IIA	.797	.785
6261.39.....	IIA	{.743 .181	{.770 .190
6266.49.....	IIA	.508	.503
6268.98.....	IIA	.458	.469
6274.80.....	I	{.587 .303	{.607 .308
6285.32.....	I	.379	.385
6293.02.....	I	.380	.371
6296.69.....	I	.368	.377
6327.00.....	III	.268	.278
6339.23.....	III	.257	.260
6349.61.....	III	.238	.234
6357.47.....	III	.186	.196
6358.99.....	III	.297	.278
6430.68.....	III	.370	.330
6433.37.....	IIIA	.279	.269
6452.55.....	IIA	.394	.384
6488.22.....	IV	.249	.292
6504.38.....	IIA	.348	{.582 .464
6531.65.....	II	.433	.421
6543.71.....	IIIA	.456	.....
6566.10.....	IIIA	.732	.708
6606.22.....	IIIA	.388	.368
6608.06.....	IIIA	.264	.....
6625.10.....	IIIA	.407	.375

$n$ -components of  $D_2$  were quite different in the two cases. This difference Woltjer provisionally ascribes to temperature. The results of the writer's recent study of absorption spectra<sup>1</sup> with the furnace may, however, have some bearing on this case. Instances were there noted of the weakening of spectral lines through a

<sup>1</sup> *Loc. cit.*

partial balancing of emission and absorption. The effect of large differences in furnace temperatures on the magnetic separations has not been fully tested, owing to the long exposures required at low temperature, but a temperature difference of at least  $400^{\circ}$  produced no perceptible changes other than those clearly due to reversals at the higher stage.

5. *Magnetic characteristics of Class IA lines.*—This class, especially in the iron spectrum, presents interesting features. It is an important group of lines for which the magnetic data must depend largely on furnace observations, since these lines are very difficult in the spark when they can be measured at all. In number they include 23 per cent of the lines given in Table I. The sharpness of the components in a large majority of cases indicates a greater prevalence of the triplet type than is found among the lines of other classes. In the blue the average separation of IA lines is about the same as for others, but in the green it is nearly twice as great. Simple and often large separations appear to be characteristic of these lines, which are strong in the low-temperature furnace, and very faint in the arc and spark.

Other large groups of lines, for which the furnace is not so necessary as for those of Class IA, are yet relatively strong in the furnace and their Zeeman components appear with less difficulty than with the spark. For a large proportion of the lines in a spectrum the usefulness of the furnace in observations supplementary to those of the spark seems thus to be assured.

#### DESCRIPTION OF THE PLATES

Plates XII and XIII illustrate the results obtained for both emission and absorption spectra. Arc spectra with long and short exposures, respectively, are given above and below for each section, with the furnace spectra between. The plates selected for reproduction favor the weaker furnace lines so that many of the strong lines are overexposed, some of these showing in the negative the apparent triplet structure resulting from the reversal of both  $n$ -components. It will be noted that numerous lines, well defined in the furnace, are scarcely visible in the lower arc exposure, which is a normal one for the stronger arc lines. The very strong arc

spectrum above is necessary to show these IA lines for which the furnace is especially effective.

#### SUMMARY

1. The action of a magnetic field on the furnace spectrum has been examined both for the direct and inverse effects.

2. The character and magnitude of the separations for the  $n$ -components of furnace lines in emission agree closely with those of the spark in a corresponding field. Self-reversed components are frequent and follow the character of the no-field line.

3. The use of a plug in the furnace tube gives the Zeeman components in absorption. The effects agree with those obtained for emission, except that uniformly larger separations for absorption components indicate that the absorption particles are localized in a part of the tube having a higher field-strength.

4. The large class of lines which are relatively strong in the furnace spectrum makes this source especially useful in supplementing the results for the spark in the magnetic field. For the more pronounced type of these lines, not usually obtainable with the spark, the furnace provides an effective method of increasing the data on magnetic separations.

The writer is indebted to Miss Brayton, of the Computing Division, for assistance in measuring a part of the spectrograms.

MOUNT WILSON OBSERVATORY  
December 1919

# THE SPECTRUM OF NOVA OPHIUCHI 1919<sup>1</sup>

BY WALTER S. ADAMS AND CORA G. BURWELL

## ABSTRACT

*Spectrum of Nova Ophiuchi.*—The paper reports in detail measurements of a spectrogram obtained with the 100-inch reflector on November 2. Although the star had reached its maximum brightness over six weeks before, the general features of the spectrum are characteristic of novae at a comparatively early stage of development. The strong continuous background is crossed by bright bands, with absorption lines forming their violet edges, which correspond mainly to hydrogen and calcium lines and to the enhanced lines of iron and titanium. The middle of each band is displaced about 1 Å to the red, while the absorption lines are displaced from 4.5 to 5.5 Å to the violet. The shifts for the various lines are proportional to the wavelength and are about half the width of the associated bands. The radial velocity indicated by the calcium absorption lines is about +6 km.

*Spectra of novae; a simple interpretation of the observed displacements.*—The fact that for Nova Persei, Nova Geminorum No. 2, Nova Aurigae and Nova Ophiuchi the displacement of the absorption lines is in each case about twice the width of the corresponding bands, suggests that both phenomena are mainly Doppler effects, and lends some support to the hypothesis of a shell of gas moving rapidly out from each star.

The spectrum of the nova in Ophiuchus discovered by Miss Mackie on photographs made at the Harvard College Observatory<sup>2</sup> was observed at Mount Wilson on the nights of November 1 and 2. The magnitude of the star was estimated at about 8.0, and for this reason and because of its low altitude it was necessary to use a spectrograph of small dispersion. For the first photograph the 60-inch reflector and the Cassegrain spectrograph with one prism and a camera of 18 cm focal length were employed; the second spectrogram was made with the 100-inch reflector and a spectrograph containing one prism and a camera with a focal length of 46 cm. The latter negative obtained with an exposure time of 110 minutes was most satisfactory, and the results given in this communication are based upon its measurement.

<sup>1</sup> *Contributions from the Mount Wilson Observatory*, No. 179.

<sup>2</sup> *Harvard College Observatory Bulletin*, No. 696.

The general features of the spectrum are those characteristic of novae at a comparatively early stage of development. This is in itself remarkable, since the maximum of light of the star apparently occurred about September 13, over six weeks previous to these observations. The continuous spectrum is strong and a large number of fairly well-defined absorption lines are present. In many cases these are associated with bright bands upon the side of longer wave-length. These bands, as has been found in other novae, are due to hydrogen, calcium, and the more prominent enhanced lines of iron, titanium, and other elements. It is probable that all the absorption lines are accompanied by bright bands, but unless the latter are rather strong it is not possible to distinguish them with certainty against the continuous background. There is little difficulty in identifying essentially all of the absorption lines with the enhanced or the stronger arc lines of various elements. The lines present are nearly identical with those found in the spectrum of Nova Aquilae No. 3 a few days after maximum of light, but their displacement is only about  $-4.7$  angstroms at  $\lambda 4500$ , against a displacement of  $-23$  angstroms in Nova Aquilae.

#### RADIAL VELOCITY

A bright band is present in the position of the calcium line K and another band is made up of calcium H and the hydrogen line H $\epsilon$ . Across these bands are dark lines due to calcium, the measurement of which affords a means of determining the radial velocity of the star. The lines are somewhat stronger than in most novae, but the measurements are subject to considerable uncertainty because of the inferior focus in this part of the spectrum. The mean of the determinations by two observers, after correction for the earth's motion, is  $+6$  km.

#### ABSORPTION LINES

The principal dark lines measured in the spectrum are given in Table I. Successive columns show the wave-length, as taken from Rowland's table, of the line with which the stellar line is identified, the element to which it is due, the wave-length in Nova Ophiuchi, the displacement, and the corresponding displacement

TABLE I

SUN	ELEMENT	NOVA OPHIUCHI	DISPLACEMENT	
			Nova Oph.	Nova Aquilae
			A	A
3900.68.....	Enh. Ti	3895.79	-4.9	.....
3913.61.....	Enh. Ti	3909.08	4.5	.....
3933.82.....	Ca	3928.94	4.9	-19.5
3970.25.....	He	3965.17	5.1	20.9
4012.54.....	Enh. Ti	4007.94	4.60	20.45
4028.50.....	Enh. Ti	4024.24	4.26	19.28
4101.90.....	H $\beta$	4097.57	4.33	20.54
4163.82.....	Enh. Ti	4159.33	4.49	20.68
4172.84.....	Enh. Ti, Fe	4168.29	4.55	20.41
4179.02.....	Enh. Fe	4174.01	5.01	20.86
4184.47.....	Enh. Ti	4180.03	4.44	20.59
4226.90.....	Ca	4222.38	4.52	20.96
4233.33.....	Enh. Fe	4228.78	4.55	21.44
4247.00.....	Enh. Sc	4242.52	4.48	21.10
4290.38.....	Enh. Ti	4285.74	4.64	21.60
4294.20.....	Enh. Ti	4289.61	4.59	21.58
4296.74.....	Enh. Fe	4292.31	4.43	22.09
4300.21.....	Enh. Ti	4295.59	4.62	21.61
4308.08.....	Fe, Enh. Ti	4303.30	4.78	21.48
4314.09.....	Enh. Ti	4309.68	4.41	21.31
4321.12.....	Enh. Ti	4315.92	5.20	21.62
4325.94.....	Fe	4321.37	4.57	21.98
4340.63.....	H $\gamma$	4336.03	4.60	21.68
4352.01.....	Cr, Mg.	4347.21	4.80	21.69
		4363.83		
4375.10.....	.....	4370.28	4.82	21.84
4385.55.....	Enh. Fe.	4380.57	4.98	20.14
4395.20.....	Enh. Ti	4390.49	4.71	21.98
4399.94.....	Enh. Ti	4395.66	4.28	21.50
		4401.51		
4417.43.....	Enh. Fe, Ti	4412.33	5.10	21.20
4443.98.....	Enh. Ti	4439.22	4.76	22.12
4468.66.....	Enh. Ti	4463.89	4.77	22.27
4489.06.....	Enh. Ti, Fe	4484.09	4.97	22.47
4501.44.....	Enh. Ti	4496.56	4.88	22.36
4508.46.....	Enh. Fe	4503.36	5.10	22.45
4515.51.....	Enh. Fe	4510.13	5.38	22.39
4520.40.....	Enh. Fe	4515.48	4.92	22.82
4522.80.....	Enh. Fe	4517.94	4.86	22.35
4528.80.....	Fe	4523.70	5.10	.....
4534.14.....	Enh. Ti	4529.44	4.70	22.50
4549.77.....	Enh. Fe, Ti	4544.57	5.20	22.79
4563.94.....	Enh. Ti	4558.92	5.02	22.65
4572.16.....	Enh. Ti	4567.16	5.00	22.39
4576.51.....	Enh. Fe	4571.98	4.53	.....
4584.02.....	Enh. Fe	4579.06	4.96	23.15
4805.29.....	Enh. Ti	4800.58	4.71	23.86
4861.53.....	H $\beta$	4855.88	5.65	.....
4924.11.....	Enh. Fe	4918.44	5.67	24.86
5018.63.....	Enh. Fe	5011.6	7.0	24.97

in the spectrum of Nova Aquilae on June 11, 1918, the date on which the spectrum was most nearly comparable with that of Nova Ophiuchi. The wave-lengths at the beginning and end of the table are less accurate than the others. Corrections have been applied for radial velocity.

The well-known proportionality between displacement and wave-length characteristic of the spectra of novae is marked in these results. Thus if we form means for each 200 angstrom units beginning at  $\lambda$  4000 we find the following displacements:

$$\lambda 4120 -4.52 \quad \lambda 4320 -4.65 \quad \lambda 4520 -4.95 \quad \lambda 4900 -5.76$$

These values are satisfied by the equation  $\Delta\lambda = 0.00110 \lambda$  with the following residuals, weights being assigned according to the number of lines:

$$\lambda 4120 0.00 \quad \lambda 4320 -0.09 \quad \lambda 4520 -0.01 \quad \lambda 4900 +0.38$$

The ratio of the displacement of the absorption lines in Nova Ophiuchi to that in Nova Aquilae as obtained from Table I is 1 to 4.53. A similar comparison of the displacements in Nova Aurigae, Nova Persei, Nova Geminorum No. 2, and Nova Aquilae, was made by Adams,<sup>1</sup> and attention was called to the remarkably close agreement of the ratios with the integer numbers 1, 2, and 3, the largest value belonging to the more refrangible component of the hydrogen lines. The corresponding value in the case of Nova Ophiuchi should apparently be 4, and the departure from the whole number is too large to come within the limits of error of the determination. Although the relationship found for the four earlier novae may well be regarded as a coincidence, attention should be called to the fact that in the case of at least one, Nova Aquilae, the displacement varied with the interval after maximum of light. Accordingly, results obtained at the same relative light-phase should be used, and no strict comparison can be made between the displacements found in the case of Nova Ophiuchi six weeks after apparent maximum and those in Nova Aquilae only three days after maximum.

One other possible effect may be referred to. As will appear later, the bright bands in Nova Ophiuchi are displaced about

<sup>1</sup> *Proceedings of the National Academy of Sciences*, 4, 355, 1918.

one angstrom toward the red, and those in Nova Aquilae the same amount toward the violet. If these displacements are in any way related to those of the absorption lines, allowance should be made for the difference.

## BRIGHT BANDS

A list of the bright bands measured in the spectrum is given in Table II. The values for the first few bands are necessarily uncertain.

TABLE II

Sun	Element	Center of Band	Width in A	Displacement in A
3889.2.....	H $\epsilon$	3890	.....	+1
3933.8.....	Ca	3935	7	+1
3970.2.....	He	3971	8	+1
4028.5.....	Enh. Ti	4029.7	7.3	+1.2
4101.9.....	H $\delta$	4102.9	7.6	+1.0
4233.3.....	Enh. Fe	4233.8	8.0	+0.5
4340.6.....	H $\gamma$	4341.7	8.8	+1.1
4417.4.....	Enh. Fe, Ti	4418.5	8.6	+1.1
4444.0.....	Enh. Ti	4444.9	9.1	+0.9
4468.7.....	Enh. Ti	4469.6	8.7	+0.9
4481.4.....	Enh. Mg.	4482.1	.....	+0.7
		4513		
4522.8.....	Enh. Fe	4523.8	8.9	+1.0
4584.0.....	Enh. Fe	4585.7	10.7	+1.7
		4633		
4861.5.....	H $\delta$	4863.2	9.2	+1.7
4924.1.....	Enh. Fe	4925.7	10.1	+1.6
5018.6.....	Enh. Fe	5020	11	+1

It is clear from these results that there is a displacement of the center of these bands of the order of one angstrom unit to the red. It also seems probable that both the displacement and the width of the bands increase in proportion to the wave-length. This result is well known in the case of previous novae. The following summary shows the values of the width and displacement at  $\lambda$  4500 for the four principal stars of this character:

	Width of Bands in A	Displacement in A
Nova Persei .....	48	+1.0
Nova Geminorum .....	25	+1.2
Nova Aquilae.....	49	-1.0
Nova Ophiuchi.....	9	+1.1



The displacement to the violet in the case of Nova Aquilae is of especial interest. It is well established from the observations of Harper at Ottawa<sup>1</sup> and from the Mount Wilson measurements.

A comparison of the widths of the bands in these stars shows that their ratio is closely the same as that between the displacements of the absorption lines, and that in each case the width is very nearly twice that of the corresponding displacement. The absorption lines, therefore, may be regarded as marking definitely the violet edges of the bright bands, and the conclusion is obvious that the cause which produces the displacements of the dark lines must be mainly responsible for the widening of the bright bands. This would favor the view that the Doppler effect is the principal agent involved, since in such laboratory investigations as that of the spectrum of the spark in liquids and under high pressures, in which a slight degree of resemblance to the spectra of novae has been attained, the dark lines and the bright bands have been very differently affected. The hypothesis of a shell of gas moving rapidly outward from the star may, accordingly, be regarded as receiving some slight degree of support from these results.

In conclusion the suggestion may be made that the displacements of the absorption lines and the widths of the bright bands are to some extent an indication of the disturbances present in the star, and so perhaps form a rough measure of its absolute magnitude. From this point of view Nova Ophiuchi would be of especial interest as being intrinsically the faintest of the last five prominent novae.

MOUNT WILSON OBSERVATORY  
December 15, 1919

<sup>1</sup> *Journal of the Royal Astronomical Society of Canada*, 12, 494, 1918.

## REVIEWS

---

*Theorie der Strahlung und der Quanten.* Von ARTHUR MARCH.

Leipzig: Barth, 1919. Pp. 182, figs. 36. 12 marks.

This book seems designed to be a general introduction to the study of various aspects of the theory of quanta, with chief attention to the mathematical developments. Experimental data are referred to in the briefest way sufficient to show the physical bearing of the theories. The topics chosen are in the main those whose investigation may be called somewhat mature. These are perhaps the reasons for omitting consideration of photo-electric phenomena and the quantum relations of cathode particles and X-rays.

About half of the space is given to the classical laws of thermal radiation and Planck's successive deductions of his formula for the spectral distribution of energy. This part is similar in content to Planck's lectures and the order of thought is naturally much the same, even to methods of proof, though more concise. There is a brief chapter on the quantum hypothesis in relation to the statistical theory of entropy, and one on the Einstein and Debye theories of specific heat.

The long fourth chapter is devoted to the relation of quantum theory to spectroscopy and resulting speculations on the structure of atoms. It presents in outline Bohr's theory of the Balmer series and the analogous Moseley X-ray spectra, together with the relativity corrections and Sommerfeld's theory of the details of structure of individual lines. There is no reference to the possibility of a modified theory of the Zeeman effect, but the Stark effect as explained by Epstein and Schwarzschild is treated at some length.

The quantum theory raises many troublesome questions because of its dubious relation to older theories, whose range of success is wide and which as yet it can claim to supplant only in a limited and ill-defined region. Through ignoring these questions and in other ways the present work has unfortunately at times the air of special pleading, but if read with due care it will give a very fair and vivid idea of the remarkable suggestiveness and positive achievements of the new theory.

A. C. LUNN

*Advanced Lecture Notes on Light.* By J. R. ECCLES. Cambridge: The University Press, 1919. American agents, G. P. Putnam's Son's. Pp. 141. \$2.50.

This is a handsome book of size  $21 \times 25$  cm, printed in large type, on one side of the page, with margins that give no suggestions of economy of paper. There are no illustrations. The Preface states that the book was first printed for private circulation, we must infer among the science masters of secondary schools. The title conveys an entirely erroneous impression for American teachers, because "advanced" merely distinguishes this from an earlier and still more elementary work by its author. The book covers what would be expected of students in a good high school or preparatory school in the United States, or for a beginner's course in optics in college. Only arithmetic and algebra are involved, except for the occasional use of a trigonometric function, as in the case of the law of refraction. The titles of the sections are as follows: "Rainbows," "Magnifying Power," "Chromatic Aberration," "Spherical Aberration," "Wave Theory of Light," "Interference," "Diffraction," "Polarization of Light." The mode of derivation and presentation of formulae is conventional and the book seems to be free from misprints. There is no index.

F.

---

#### NOTE

We are informed that our esteemed collaborator Professor Heinrich Kayser has recently resigned his position as professor of physics and director of the laboratory at the University of Bonn, on account of poor health and advancing years. He intends, however, to continue some work in spectroscopy. A second and wholly re-written edition of the first volume of his monumental work *Handbuch der Spectroscopie* was ready for publication at the beginning of the war, but it is now uncertain when the printing can be resumed, if ever.

The high reputation of the laboratory at Bonn as a center of spectroscopic research will be maintained by the appointment of Professor F. Paschen, of Tübingen, as successor to Professor Kayser.

# THE ASTROPHYSICAL JOURNAL

AN INTERNATIONAL REVIEW OF SPECTROSCOPY  
AND ASTRONOMICAL PHYSICS

VOLUME LI

APRIL 1920

NUMBER 3

## POLARIZATION OF RADIATION BY GRATINGS

By L. R. INGERSOLL

### ABSTRACT

*Polarizing effect of gratings.*—(1) *Reflected radiation.* After a brief review of previous investigations, both theoretical and experimental, the author points out that while the Rayleigh-Voigt theory predicts an anomalous effect for a wave-length equal to the grating space, no experimental investigation of polarization effects for a range of wave-lengths which includes the grating space has been made. Accordingly the author tested four *speculum gratings*, whose grating space varied from 1.2 to 2.7  $\mu$ , with plane polarized light of wave-length 0.5 to 2.3  $\mu$ , and obtained the reflecting power of the ruled surface relative to the polished unruled surface for normal incidence. With the polarization (electric vector) perpendicular to the rulings, a sharp minimum was found at a wave-length equal to the grating space and also, in some cases, for approximately one-half and one-third this value. Observations made with an incidence of  $7^\circ$  gave two minima at wave-lengths equal to the grating space multiplied by  $(1 \pm \sin \theta)$ . As the curves show, the polarizing action depends not only on the wave-length but also on the particular grating used; and since polishing the gratings resulted in practically no change the effect must depend upon the groove form. (2) *Transmitted radiation.* The author also tested some *collodion replica gratings* with spaces of either 1.0 or 1.6  $\mu$ . The transmitted light was found to be partially polarized at right angles to the rulings; also the polarizing effect showed maxima for wave-lengths equal to the grating space and to half that value. (3) *Radiation diffracted tangentially* from the *speculum gratings* showed a marked polarization at right angles to the rulings. (4) *Conclusions.* These experiments show that the excess of perpendicularly polarized energy present in light tangentially diffracted from a reflecting grating is accompanied by a deficiency in radiation of this polarization in the directly reflected beam; thus they tend to confirm the Rayleigh-Voigt theory.

*Use of gratings in studying polarization phenomena.*—The results of these experiments suggest that it would be advisable to avoid angles of incidence at which the light being studied is tangentially diffracted in any higher order.

The present work is a study of the polarization of the undiffracted, i.e., directly reflected, light from ordinary speculum metal gratings for the range of wave-length  $0.5 \mu$  to  $2.3 \mu$ . The directly transmitted beam has also been studied for a number of collodion replica gratings.

Polarization by gratings, as well as the related case of polarization by slits, has been extensively investigated both theoretically and experimentally but will be only very briefly<sup>1</sup> reviewed here. The observation of Fizeau<sup>2</sup> that light is more readily transmitted by a very narrow ( $0.1 \mu$ ) slit when its polarization<sup>3</sup> is such that the electric vector vibrates in a direction perpendicular to the edges has been verified by Ambronn<sup>4</sup> and others, and is in agreement with the theory of Rayleigh<sup>5</sup> for narrow openings in a thin screen. For slightly wider slits ( $> \frac{1}{3} \lambda$ ), vibrations parallel to the slit are transmitted somewhat better than the others. The theory is not applicable when the slit-width approaches equality with the wave-length.

Wire gratings show polarization effects somewhat analogous to narrow slits. When the wave-length is larger than the grating space—the Hertzian case—vibrations perpendicular to the wires are more readily transmitted. This case has been theoretically investigated by J. J. Thomson,<sup>6</sup> H. Lamb,<sup>7</sup> and others, while on the experimental side Du Bois and Rubens,<sup>8</sup> using a wide spectral region including some long *Reststrahlen*, found for fine wire gratings a Hertzian polarization for wave-lengths longer than a certain

<sup>1</sup> For a more extended list of references see paper by Du Bois and Rubens, *Philosophical Magazine* (6), 22, 322, 1911.

<sup>2</sup> *Annales de Chimie et de Physique*, 63, 385, 1861.

<sup>3</sup> Following recent practice, the direction of polarization, as referred to in the present paper, will always be that of the electric vector.

<sup>4</sup> *Wiedemann's Annalen*, 48, 717, 1893.

<sup>5</sup> *Proceedings of the Royal Society (A)*, 89, 194, 1913.

<sup>6</sup> *Recent Researches in Electricity and Magnetism*, p. 425 (Oxford, 1893).

<sup>7</sup> *Proceedings of the Mathematical Society of London*, 29, 523, 1893.

<sup>8</sup> *Wiedemann's Annalen*, 49, 593, 1893; *Philosophical Magazine* (6), 22, 322, 1911.

fraction of the grating space. For shorter wave-lengths an inversion occurred and the polarization changed sign, reaching a maximum in the neighborhood of  $1\ \mu$ .

Rayleigh<sup>1</sup> has developed a theory applicable to ordinary reflecting gratings and this has been extended by Voigt,<sup>2</sup> account being taken of the optical constants of the metal on which it is ruled. Voigt and Collet<sup>3</sup> and Pogany<sup>4</sup> have carried out experiments in support of this theory, measuring amplitude and phase relations in the diffracted light. Of the earlier work on grating polarization, perhaps that of Fröhlich<sup>5</sup> is the most extensive.

An interesting point in the Rayleigh-Voigt theory, and one with which we shall be somewhat concerned in the present work, is a prediction to the effect that when a given wave-length in the spectrum of any order is just passing (tangentially) off the grating, the same wave-length in lower orders will be abnormally increased in intensity. This effect, however, is confined to the electric vector vibrating in a direction perpendicular to the rulings, while the light which is just passing off tangentially is completely polarized in this sense. This seems to explain some of the anomalies found by Wood,<sup>6</sup> particularly with gratings ruled on silver. These effects were profoundly modified, however, by even the slightest rubbing with soft chamois skin, so that they are apparently due to the sharp ridges rather than the bottoms of the grooves.

*Present investigation.*—It may be remarked that previous investigations in this line have, in general, been limited to radiation somewhat shorter in wave-length than the grating space, or else very much longer. An exception is the work of DuBois and Rubens; but with *Reststrahlen* it is of course impossible to secure a continuous series of wave-lengths. It seemed worth while, then, to investigate the polarization effects for a range of wave-lengths which included the grating space. While the analogy of the slit is perhaps not a

<sup>1</sup> *Proceedings of the Royal Society (A)*, 79, 399, 1907.

<sup>2</sup> *Göt. Nachr. Math. Phys. Kl.* (1911), p. 40.

<sup>3</sup> *Ibid.*, 4, 385, 1912.

<sup>4</sup> *Annalen der Physik*, 37, 257, 1912.

<sup>5</sup> *Wiedemann's Annalen*, 13, 133, 1881, and 15, 587, 1882.

<sup>6</sup> *Philosophical Magazine* (6), 3, 396, 1902, and 23, 310, 1912. See also Rayleigh, *ibid.* (6), 14, 60, 1907.

very good one, the fact that the theory of the transmission of radiation in this case breaks down for a wave-length equal to the width of the opening would seem to make it of interest to study gratings in this same spectral region.

*Method and apparatus.*—The apparatus<sup>1</sup> used was that developed by the writer in connection with preceding experiments<sup>2</sup> on various polarization phenomena in the early infra-red spectrum,

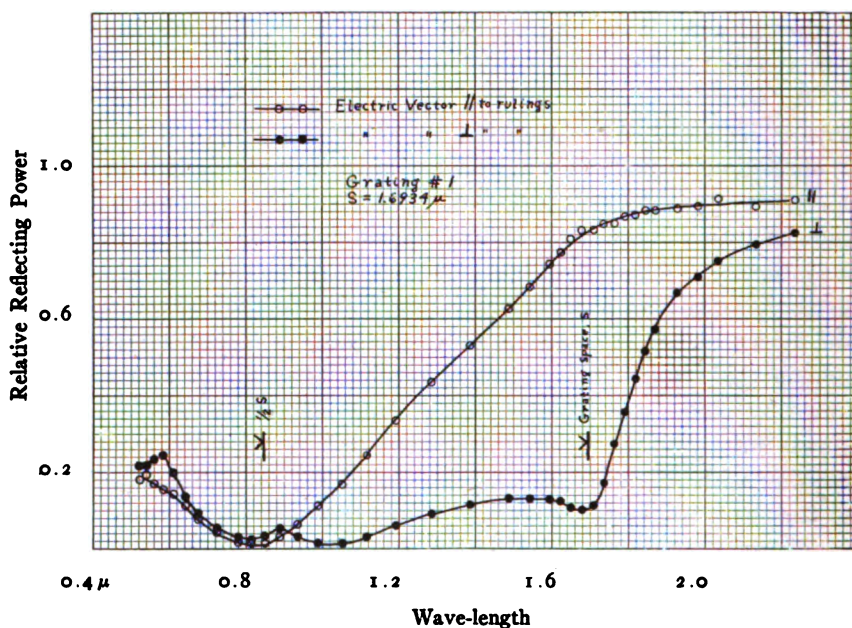


FIG. 1.—Reflection-curves for grating No. 1

although a somewhat simpler arrangement might have served equally well in the present investigation. Light from a flat filament tungsten lamp<sup>3</sup> was plane polarized at an angle of  $45^\circ$  with the vertical plane and allowed to fall on the grating, the incidence

<sup>1</sup> Acknowledgment is due the Rumford Fund for assistance in purchasing part of this apparatus some time ago.

<sup>2</sup> *Physical Review*, 35, 312, 1912, and (2), 9, 257, 1917; *Astrophysical Journal*, 32, 265, 1910.

<sup>3</sup> These lamps were specially made and furnished through the courtesy of the Nela Research Laboratory.

being as nearly normal as possible. After reflection from the grating and then from a silver surface, also at nearly normal incidence, it passed through a large double-image prism whose planes of transmission were vertical and horizontal, respectively, and the two beams, after dispersion by a large mirror and prism spectrometer, fell on the two strips of a special bolometer already described in previous papers.<sup>1</sup> The grating was mounted in a holder which

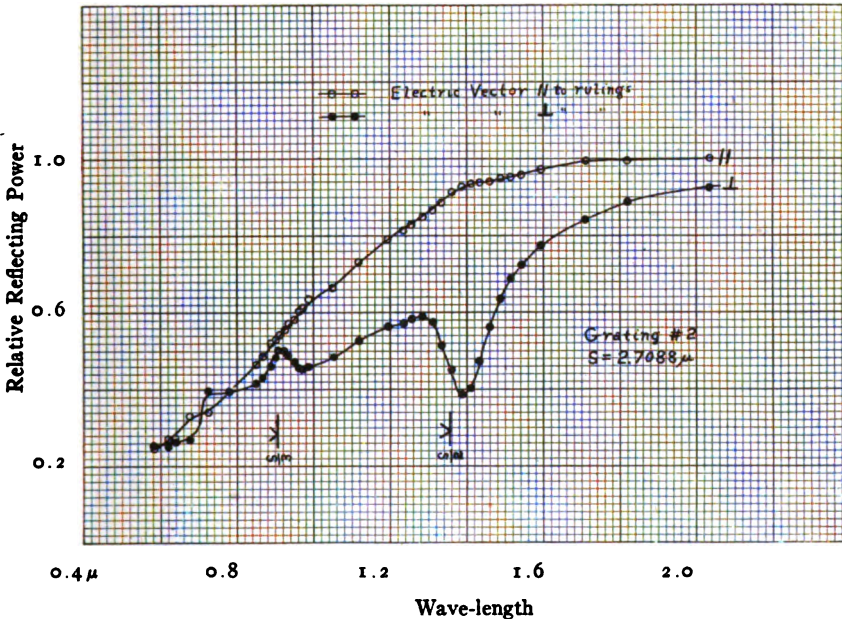


FIG. 2.—Reflection-curves for grating No. 2

allowed it to be shifted in the plane of the surface, so that the light could be alternately reflected from the ruled portion and from the polished unruled surface and the two intensities compared. The incidence obviously could not be made exactly normal, but the grating was set with the rulings parallel to the plane of incidence, save in a special case, which will be noted later, and the angle of incidence was always small—from  $5^\circ$  to  $9^\circ$ .

Measurements were made of the energy reflected from the ruled and unruled portions of the grating surface for both azimuths

<sup>1</sup> *Philosophical Magazine* (6), 18, 74, 1909.



of polarization and for a series of wave-lengths from  $0.5 \mu$  to  $2.3 \mu$ . When the area of each part of the surface was sufficiently large the light was allowed to fall on the grating in a parallel beam. Otherwise it was converged to a focus near the grating surface, the cone of rays in this case subtending an angle of perhaps  $3^\circ$ . The phenomena observed were substantially the same in each case. The measurements in the present case were limited to the amplitude

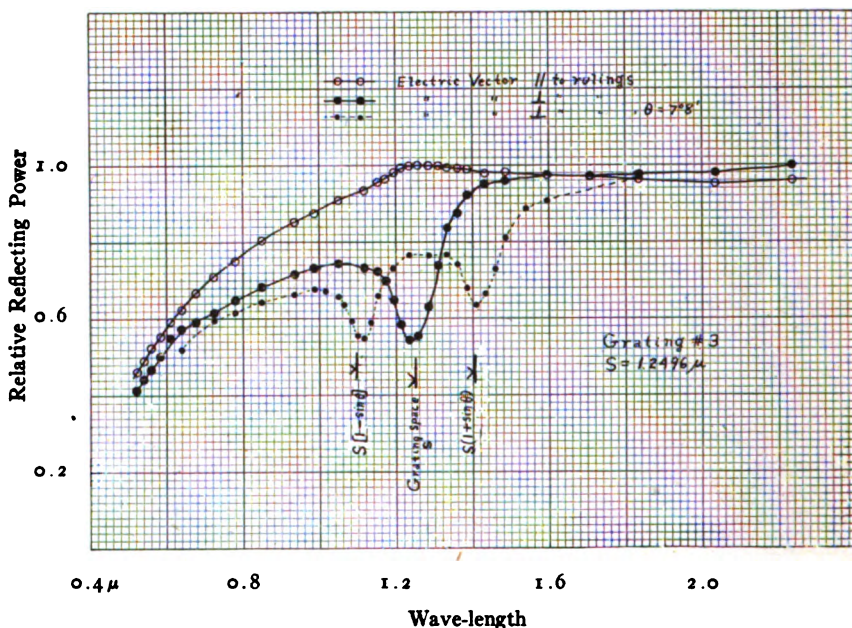


FIG. 3.—Reflection-curves for grating No. 3

(intensity) relation; the phase changes on reflection at such a surface are difficult to measure in this region of the spectrum, although the writer hopes to be able to accomplish this in a continuation of the present research.

*Gratings.*—Four plane reflecting gratings were tested in this way. They were:

1. A large Rowland grating of 15,000 lines to the inch—grating space  $S=0.0016934$  mm. This was loaned through the courtesy of Professor J. S. Ames. Part of the surface of this grating was

cross-ruled and not usable, but the remainder was ample in area for the purposes of this investigation. This grating showed a fairly bright first-order spectrum on one side and a very bright second-order spectrum on the same side. The central image was very faint.

2. A piece of Michelson grating of space  $0.0027088$  mm. This showed a bright first-order spectrum on one side as well as bright second- and third-order spectra.

3. A Michelson grating of space  $0.0012496$  mm. This showed bright first-order spectra, one slightly more intense than the other,

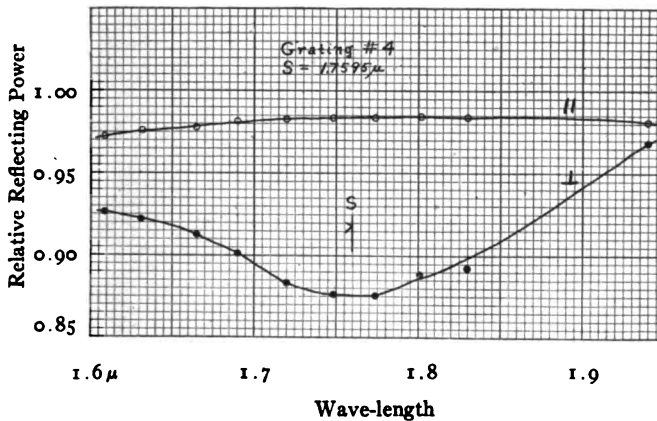


FIG. 4.—Reflection-curves for grating No. 4

and faint second-order spectra. For these last two gratings I am indebted to the kindness of Professor Gale.

4. A Rowland grating of space  $0.0017595$  mm, showing a bright first-order spectrum on one side. The second-order spectrum on this same side was extremely faint.

In all of the above-mentioned gratings the light diffracted tangentially showed a marked polarization with vibration perpendicular to the rulings, although this was somewhat less noticeable in grating No. 1 than in the three others.

*Results.*—These are shown in the curves of Figures 1-4, where the ratio of the energy reflected from the ruled surface divided by that from the unruled—i.e., the reflecting power of the ruled

relative to the polished surface—is plotted against wave-length for each azimuth of polarization. As might be expected, the curves all show an upward trend with increasing wave-length, and for wave-lengths longer than the grating space the reflecting power of the ruled portion is scarcely less than that of the unruled. This is reasonable, since in this case no energy can be dissipated in diffracted spectra.

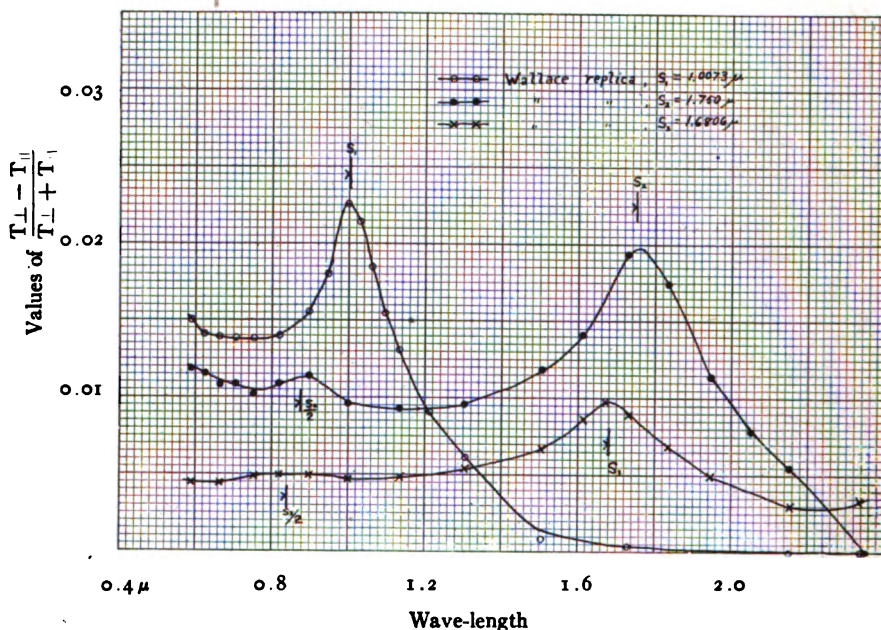


FIG. 5.—Curves showing polarization on transmission for three Wallace replica gratings.

The most striking thing about the curves, however, is the sharp minimum which occurs when the polarization (electric vector) is perpendicular to the rulings, for a wave-length equal to the grating space and in some cases for (approximately) one-half and one-third this value. For light at normal incidence and a wave-length equal to the grating space, the first-order spectrum is just disappearing tangentially from the grating. If we can assume, then, that there is a compensation whereby the excess of perpendicularly polarized energy which is coming off almost tangentially

is taken from the directly reflected light, we shall have an explanation of the foregoing effect. The same reasoning applies to the second-order spectra for a wave-length of half the grating space and a similar explanation holds for the third order. This is well illustrated by the curves of Figures 1-4. The agreement is not so good in the case of grating No. 2, but this was the least satisfactory one to work with, inasmuch as it was only a broken fragment with no unrulings and the reflecting power had to be measured relative to another surface.

A *rather critical* test may be applied to the foregoing reasoning by tilting the grating slightly so that the angle of incidence—the grating now being turned so that the plane of incidence is normal to the rulings—is  $6^\circ$  or  $8^\circ$ . Under these conditions, then, the particular wave-length in the first-order spectrum on one side, which is just coming off tangentially, will be somewhat shorter than the grating space; while on the other side it will be a corresponding amount longer, the exact values being given by

$$\lambda_1 = S(1 - \sin \theta) \text{ and } \lambda_2 = S(1 + \sin \theta)$$

respectively. We should then expect to find the minimum at  $\lambda = S$  in the perpendicular azimuth curve replaced by two somewhat smaller minima at these two wave-lengths. This experiment was tried for an angle of incidence of  $\theta = 7^\circ 8'$ , and the dotted curve of Figure 3 shows how well the foregoing prediction is justified. The slight difference in magnitude of the drop in the curve in the two minima probably indicates the relative energy in the two first-order spectra.

A point of some interest in this connection is that cleaning the gratings with ammonia, and even vigorous polishing (parallel to the rulings) with Vienna lime on chamois skin, failed to alter the phenomena in any material respect. It would seem, then, that this is a general characteristic of all gratings of this type, and is presumably dependent upon the form of the groove as a whole; that is to say, it is not determined merely by the thin edge of the ruling, as is probably the case in the silver grating experimented on by Wood. Such slight changes as were observed upon polishing were mostly confined to the visible spectrum, as might be expected.

It may be noted in this connection that, as shown by curves 1-3, the polarizing action of such gratings in the visible spectrum is a very variable quantity and dependent on the exact wave-length and particular grating tested. In the near infra-red, however, they would give in the central image, if illuminated with unpolarized light, an excess of radiation polarized parallel to the rulings. This is particularly true in the case of grating No. 1, where at  $\lambda = 1.05 \mu$  the reflected light would be 90 per cent polarized in this sense. Beyond  $\lambda = S$  the polarizing action has largely disappeared.

*Transmission gratings.*—Some experiments were also tried on Wallace replica transmission gratings of 14,500 to 25,100 lines to the inch. These gratings show a slight polarization in the Hertzian sense, i.e., higher transmission for electric vector perpendicular to the rulings, but the effect is considerably smaller than for most reflection gratings. The measurements plotted in the curves of Figure 5 are not those of transmission through the ruled space of the grating relative to the unruled, but were obtained by simply rotating the grating in its plane through  $90^\circ$ . This gave at once the difference of the two transmissions divided by the sum, a quantity which is proportional to the percentage of polarized light which would be found in the directly transmitted beam if unpolarized light fell on the grating. The maxima at the grating space and half the grating space are very distinct, but experiments aimed at showing which vector was chiefly concerned in producing this maximum were rather unsatisfactory, although the weight of the evidence seemed to be in favor of the perpendicular vibration. As such gratings have somewhat less practical interest and have not been as carefully investigated theoretically as the others, this part of the subject has not been followed farther.

*Conclusions.*—The results of the present work show that the excess of perpendicularly polarized (electric vector) energy present in light tangentially diffracted from a reflecting grating is made up for by a deficiency in radiation of this polarization in the directly reflected beam. While not affording any direct proof<sup>1</sup> of the prediction of the Rayleigh-Voigt theory regarding abnormalities

<sup>1</sup> The writer hopes shortly to be able to investigate the polarization characteristics of the diffracted radiation in the near infra-red spectrum for a series of gratings.

in intensity of spectra of lower orders for this state of polarization, the deficiency in the central image noted above is more than sufficient to account for the energy for such abnormalities as well as for the effects found by Wood.<sup>1</sup>

From a practical standpoint, the evidence for the generality of such an effect as predicted by Raleigh and Voigt seems strong enough to make it advisable for observers of polarization phenomena, such as the Zeeman effect, to avoid it. This is easily done by keeping clear of such angles of incidence that the particular wave-length used is just passing from the grating in any higher order.

PHYSICAL LABORATORY  
UNIVERSITY OF WISCONSIN  
January 24, 1920

<sup>1</sup> *Philosophical Magazine* (6), 23, 314, 1912.

# STUDIES BASED ON THE COLORS AND MAGNITUDES IN STELLAR CLUSTERS <sup>1</sup>

## SIXTEENTH PAPER: PHOTOMETRIC CATALOGUE OF 848 STARS IN MESSIER 3

BY HARLOW SHAPLEY AND HELEN N. DAVIS

### ABSTRACT

*Globular cluster Messier 3.*—The paper reports in detail measurements of 14 photographic plates taken at the primary focus of the 60-inch reflector during 1915 and 1917. Table II is a *photometric catalogue of 848 stars*, giving the photographic and photo-visual magnitudes and the color-index of each. Of these stars, 750 are suitable for statistical work. The known variables are omitted, but it appears from a comparison of the different plates that at least 17 others are probably *variable stars*. As for the *distribution of stars of various magnitudes and color-type*, a statistical study of the measurements shows that stars of all types and magnitudes are very well mixed, at least for angular distances from the center greater than 2'. The *spectral curve*, omitting variables, shows a maximum frequency near color-class  $f_5$  and differs from the corresponding curve for Messier 13 in being without a secondary maximum for the blue stars (Fig. 1). The *magnitude curve* shows a maximum frequency for photo-visual magnitude 15.5 which is near absolute magnitude zero, as computed on the basis of the previously determined *parallax* of 0".000072; the curve, as usual, is far from being symmetrical. The *relation of color-index to magnitude* shows the usual decrease of index with decreasing brightness (Fig. 3). In general these results corroborate those yielded by the previous analysis of Messier 13. The *position co-ordinates of 370 stars* which were not listed by von Zeipel are given in Table III.

An extended investigation of the photographic and photo-visual magnitudes of stars in the globular cluster Messier 13 is described in the second paper of this series, *Mt. Wilson Contr.* No. 116. The study yielded results of sufficient novelty and importance to justify the detailed corroborative analysis of another globular cluster. For this purpose the bright northern system Messier 3 was chosen because of the excellent catalogue of positions by von Zeipel<sup>2</sup> and the published and unpublished studies of variable stars at Harvard<sup>3</sup> and Mount Wilson.<sup>4</sup> The work was begun in

<sup>1</sup> *Contributions from the Mount Wilson Observatory*, No. 176.

<sup>2</sup> *Annales de l'Observatoire de Paris, Mémoires*, 25, F1-101, 1908.

<sup>3</sup> *Harvard Annals*, 78, 1-98, 1913.

<sup>4</sup> *Mt. Wilson Contr.*, No. 154, 1917; *Mt. Wilson Communications*, No. 47, 1917; *Publications of the Astronomical Society of the Pacific*, 29, 110, 140, 1917.

1915 and completed nearly two years ago, some of the results appearing meanwhile in *Mt. Wilson Contr.* Nos. 151 and 152, and particularly in *Mt. Wilson Contr.* No. 155. An illustrated discussion of the dimensions of Messier 3 was printed in *Publications of the Astronomical Society of the Pacific*, 29, 245, 1917.

Stars in the central part of Messier 3 have not been measured for magnitudes because of the uncertainties introduced by the Eberhard effect into photographic work in crowded regions. Between distances 1'8 and 11'3, however, the survey is practically complete to photo-visual magnitude 16.8, and about 140 fainter stars have also been measured. Altogether the catalogue contains 848 stars, less than 100 being within 2' of the center.

The catalogue of Messier 13 (Table IX, *Mt. Wilson Contr.* No. 116) contains 616 stars, all more distant than 2' from the center of the cluster, and complete to photo-visual magnitude 15.6, approximately. Because of the greater distance of Messier 3, the gain of 1.2 in apparent magnitude is partly lost when absolute magnitudes are considered. Thus, using the parallaxes given in *Mt. Wilson Contr.* No. 152, we have

	Messier 3	Messier 13
Parallax	0".000072	0".000090
<i>m</i> - <i>M</i>	15.72	15.23
Limit of Abs. Mag.	+1.08	+0.37

1. *Observational data.*—The photographs used in the present work are described in Table I. All were made at the primary focus of the 60-inch reflector. In addition to these plates more than eighty others have been made at Mount Wilson, largely for work on variable stars. The ten thousand measures of magnitude for the photometric catalogue are mainly the work of Miss Davis. Miss Ritchie has assisted in preparing the tables and figures for the press.

2. *Description of the catalogue.*—The numbers in the first column are those of von Zeipel's catalogue. Postscript letters are assigned to stars fainter than those listed by him. Miss Ritchie has measured position co-ordinates on photographic enlargements of the cluster for the identification of the 370 postscript stars,



referring each object to two or more stars of von Zeipel's catalogue. The results appear in Table III. The center of the cluster is

$$\left. \begin{array}{l} \text{R. A.} = 13^{\text{h}}37^{\text{m}}35^{\text{s}} \\ \text{Decl.} = +28^{\circ}52'56'' \end{array} \right\} 1900.0$$

according to the determination by von Zeipel. Approximate galactic co-ordinates are: Longitude =  $8^{\circ}$ , Latitude =  $+77^{\circ}$ .

TABLE I  
LIST OF PLATES

PLATE		DATE	LENGTH OF EXPOSURE	No. EXPOSURES ON FOLE	USE
Number	Kind				
2371...	Iso	1915, Apr. 16	10 <sup>m</sup>	2	Photo-visual magnitudes
2372...	S 27	Apr. 16	2	2	Comparison stars
2462...	Iso	June 7	10	1	Photo-visual magnitudes
2463...	S 27	June 7	3	2	Photographic magnitudes
2505...	Iso	July 6	20	1	Photo-visual magnitudes
2506...	S 27	July 6	3	2	Photographic magnitudes
3678...	Iso	1917, Mar. 28	5	2	Photo-visual zero point
3679...	S 27	Mar. 28	3	2	Photographic magnitudes
3680...	S 27	Mar. 28	2	2	Photographic magnitudes
3684...	Iso	Apr. 19	120, 20	0	Photo-visual magnitudes
3774...	Iso	May 27	52, 10	0	Photo-visual magnitudes
3775...	Iso	May 27	90, 15	0	Photo-visual magnitudes
3846...	S 27	July 25	4	2	Postscript stars, photographic
3847...	S 27	July 25	5	2	Postscript stars, photographic

An asterisk following the number in the first column indicates that the deduced magnitude is uncertain because of duplicity, bad image, or similar cause. Such stars are excluded from the statistical discussion. A dagger following the number indicates a comparison star used at Harvard and Mount Wilson for the study of variable stars. The magnitudes for these stars, collected in Table VI, depend upon a rather extensive discussion, which will be described in a later contribution dealing with the variables. The three stars marked with a double dagger, Nos. 612, 752, 982, were measured by Miss Ritchie after the completion of the catalogue and are not included in the following discussion; their spectra have been determined by Mr. Sanford and will be reported by him in another place.

\* Corrections to von Zeipel's catalogue: No. 502 is about 10" south of catalogued declination, which refers to our 502a; No. 1227 (on our chart made in 1915) is about 4" north of the catalogued position; No. 184 is not found on Mount Wilson plates.

The second column contains the distance from the center of the cluster in minutes of arc. The final photographic and photo-visual magnitudes in the third and fifth columns, and the color-index in the last, are followed by colons when special uncertainty has affected the measurements; these doubtful results are also excluded from the statistical treatment. A few stars impossible of accurate measurement (brighter than photo-visual magnitude 17 and outside distance 1'8) may have been omitted entirely, but it is very unlikely that any of the omissions noted above have prejudiced the general interpretation of the observations.

For all determinations of a star's brightness the residuals from the mean are given in hundredths of a magnitude in the fourth and sixth columns of the catalogue. The photographic residuals refer, in order of the sub-column, to Plates 2463, 2506, 3679, and 3680, respectively, except that when in parentheses in the first two sub-columns the residuals refer to Plates 3846 and 3847. Similarly, the photo-visual residuals refer to Plates 2371, 2462, 2505, and 3684, respectively, with residuals for Plates 3774 and 3775 appearing in parentheses in the first two sub-columns. The letter "m" indicates that the tabulated magnitude depends upon only one plate. An asterisk following the photo-visual magnitude (six instances) means that the star was also measured on Plate 3678, but the residual for that plate is not entered in the following column; its value is the algebraic sum of the residuals there given with sign changed. Occasionally, in forming mean magnitudes, uncertain values were given half-weight; such cases are shown by the residuals; for example, see No. 926a.

To eliminate errors as far as possible, all color-indices less than  $-0.30$  or greater than  $+1.40$  have been independently re-determined from special series of measures, and all magnitude determinations showing residuals greater than  $0.20$  have been re-examined. Some corrections to the catalogue resulted from this supplementary work; its main outcome, however, is the conviction that many of the stars, whose magnitudes are similar to those of the variables, undergo slight variations of light. (Cf. discussion of their residuals in *Mt. Wilson Contr.* No. 155, p. 5.) The following

17 stars have photographic residuals greater than 0.25 and in most cases are probably variable stars:

251	845	1241
357	935	1244
603	962	1374
606	1146	1437
632	1170	1439
665	1214	

There are 49 stars, including the comparison star *h*, with photographic residuals between 0.20 and 0.25. All of these stars will be included in future investigations of the variables.

The photographic and photo-visual residuals are summarized for the principal plates in Tables IV and V.<sup>1</sup> The systematic errors are satisfactorily small and no serious divergence of scale has been found. The average probable error of the final magnitudes is  $\pm 0.04$ , which is of the same order of accuracy as that attained in the comparable study of Messier 13.

The contents of the catalogue (which does not include any of the 150 known variable stars) may be summarized as follows:

	Number of Stars
With asterisks . . . . .	27
With no color-index . . . . .	21
Color-index with colon (uncertain) . . . . .	10
Fainter than 16.99 (Pv. mag.) . . . . .	64
Supplementary . . . . .	3
Suitable for statistical work (Tables VII, VIII, etc.)	750
Total . . . . .	875
Subtract for duplicate listing . . . . .	27
Net total in catalogue . . . . .	848

3. *Statistical tables and diagrams.*—Tables VII and VIII are in the usual form for the correlation of magnitude, color, number, and distance. Tables IX and X give convenient summaries or rearrangements of the larger tables. From the various tables, and from the figures illustrating these tabular results, it is clear that distance from the center<sup>2</sup> plays no very important part in the

<sup>1</sup> Some stars were measured after the tables were formed, so that altogether more than 3600 residuals appear in the catalogue.

<sup>2</sup> This does not apply to distances less than 1'.5.

interrelations of color, magnitude, and number of stars. This conclusion supports the earlier one that the stars of all types and absolute magnitudes are very well mixed in a globular cluster.

The spectral curve of Messier 3 (Fig. 1) has its maximum near color-class  $f_5$ , in that respect agreeing with Messier 13; but the form of the curve as it now stands differs conspicuously in the absence of a preliminary maximum for the blue stars. If colors for the 100 variables, within our present limits of distance from

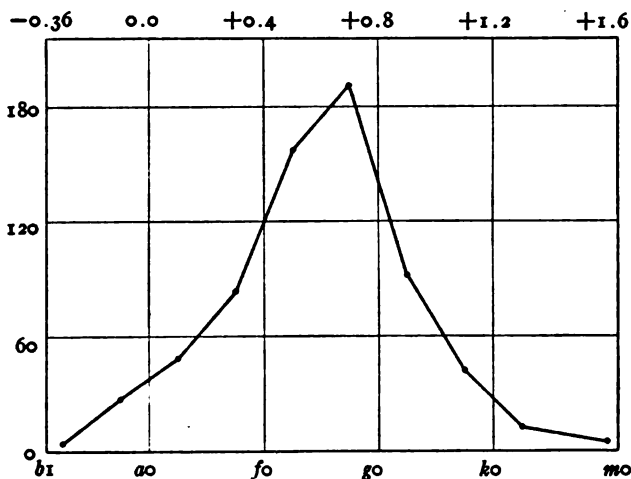


FIG. 1.—Spectral curve of giant stars in Messier 3; ordinates are numbers of stars in each half color-class; abscissae are color-indices and color-classes. Variable stars are not included; there are about 100 within the region studied, and their average median color-index, which varies with the light, is probably  $+0.25$ . (Cf. *Contribution*, No. 154, Fig. 4.)

the center, were also included in the diagram, it is probable that this dissimilarity between Messier 3 and Messier 13 would largely disappear. As noted before,<sup>1</sup> the many blue stars of Messier 13 appear to be represented in Messier 3 by cluster-type variables.

The photographic and photo-visual luminosity-curves for Messier 3 have been fully discussed in *Mt. Wilson Contr.* No. 155. The maximum frequency of stars in the vicinity of absolute magnitude zero is conspicuously shown, for all intervals of distance from the center, by the numbers in the last column of Table VIII. The

<sup>1</sup> *Mt. Wilson Contr.*, No. 155, p. 12, 1917.

wide divergence of these observed luminosity-curves from a symmetrical probability-curve again points to the inadvisability of assuming them comparable for the purpose of estimating the distances of clusters.<sup>1</sup>

Although the galactic latitude of Messier 3 is so high that superposed foreground stars are few, there may be some evidence in the shape of the curves in Fig. 2, of the influence of non-cluster stars on mean magnitude and color at distances greater than 7'.

• It is more likely, however, that the brighter average magnitudes

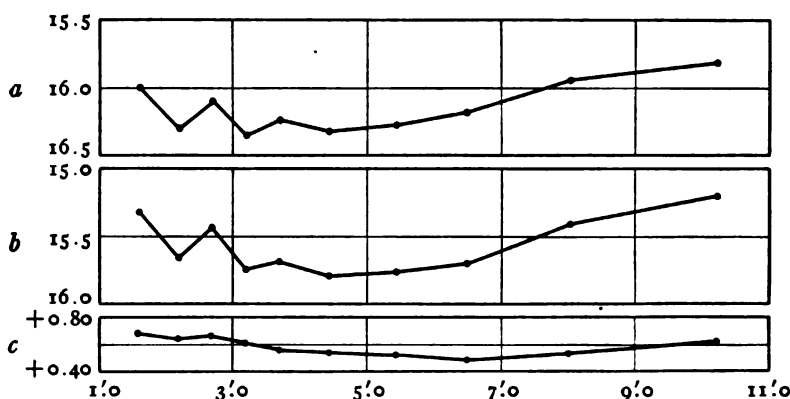


FIG. 2.—Average magnitudes and colors for different distances from the center: a) photographic magnitude; b) photo-visual magnitude; c) color-index. Abscissae are distances in minutes of arc.

at the greatest distances, and also near the center, are due to incompleteness of the catalogue to the seventeenth photo-visual magnitude in those regions.

Figure 3a illustrates for Messier 3 the decrease of color-index with decreasing brightness, which has been found to be a typical characteristic of the giant stars in globular clusters. A similar diagram for Messier 13 based on data given in *Mt. Wilson Contr.* No. 116 is given in Fig. 3b. In both cases the mean absolute magnitudes are derived from the parallaxes given earlier in this paper.

<sup>1</sup> Cf. *Mt. Wilson Contr.*, No. 175, 1919.

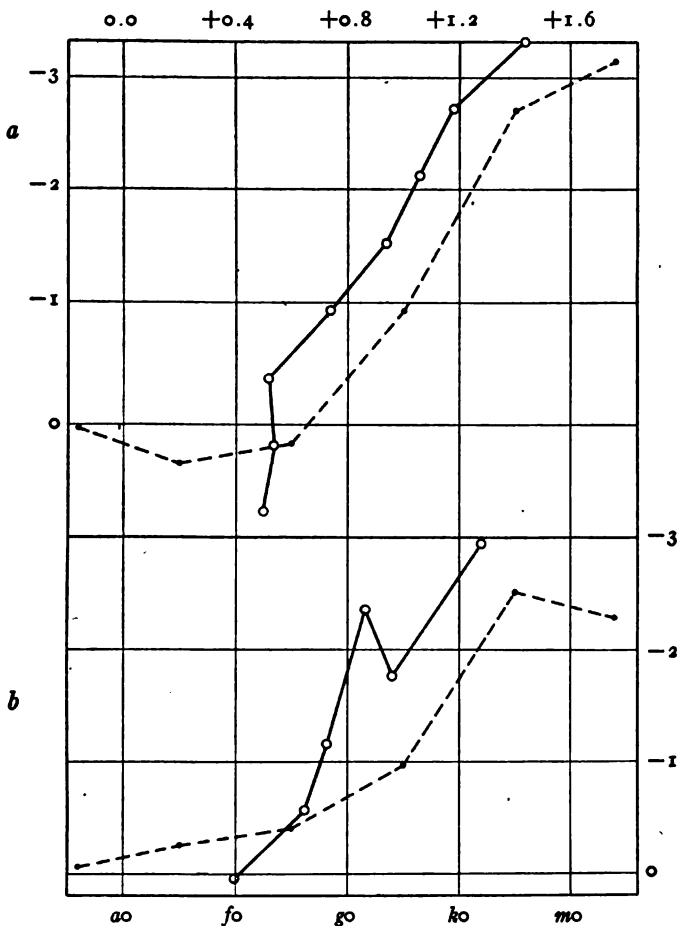


FIG. 3, *a* and *b*

*a*) The color of giant stars in Messier 3 (distance  $\approx 2'$ ). The circles indicate the mean color-index for equal intervals of magnitude (Table X); the dots indicate mean magnitudes for equal intervals of color-index (Table IX). Abscissae are color-classes and color-indices; ordinates are absolute photo-visual magnitudes. The form of the broken curve is of course affected by the absence from the catalogue of stars fainter than photo-visual magnitude 17. The continuous curve, however, accurately represents the change of average color with brightness down to photo-visual magnitude 16.8; fainter stars are not included.

*b*) Similar representation of the color of giant stars in Messier 13 (distance  $\approx 2'$  except for *m* stars).

TABLE II  
PHOTOMETRIC CATALOGUE OF 848 STARS IN MESSIER 3

NUM- BER	DIS- TANCE	PHOTOGRAPHIC		PHOTO-VISUAL		COLOR- INDEX
		Mag.	Residuals	Mag.	Residuals	
145...	11.4	15.84	+ 8, - 7, . . . . .	16.02	(-15, +14) . . . . .	-0.18
145...	9.8	15.12	- 4, + 5, . . . . .	14.52	. . . . . m, . . . . .	+0.60
157...	9.7	15.48	- 9, + 8, . . . . .	15.52	(+ 6, - 5) . . . . .	-0.04
157a...	0.8	17.17	(+ 4, - 4) . . . . .	16.68	(-11, +10) . . . . .	+0.49
157b...	8.9	16.18	(+ 2, - 1) . . . . .	15.42	( 0, 0) . . . . .	+0.76
157c...	8.9	17.42	(. . . . . m) . . . . .	16.39	( m, . . . . . ) . . . . .	+1.03
158...	9.8	15.82	+ 4, - 5, . . . . .	15.37	(- 5, + 5) . . . . .	+0.45
162...	9.2	15.10	+ 5, - 1, - 3, . . . . .	14.63	(. . . . . - 2) + 2, . . . . .	+0.47
164...	9.0	14.54	+ 7, + 7, -13, . . . . .	13.62	0, . . . . . 0, . . . . .	+0.92
164a...	8.8	16.71	(+ 1, - 1) . . . . .	16.16	(- 4, + 4) . . . . .	+0.55
164b...	9.2	16.78	(- 6, + 7) . . . . .	16.16	(. . . . . m) . . . . .	+0.62
164c...	9.4	16.82	(- 6, + 7) . . . . .	16.12	(+ 6, - 6) . . . . .	+0.70
166...	9.0	16.00	- 2, + 4, - 2, . . . . .	15.30	(- 3, + 3) . . . . .	+0.70
167...	8.4	15.68	+ 2, - 3, . . . . .	14.97	(+ 3, - 3) . . . . .	+0.71
168...	9.4	16.36	- 4, + 5, . . . . .	15.62	(+ 2, - 1) . . . . .	+0.74
168a...	9.1	16.78	(+ 1, - 1) . . . . .	16.06	(- 6, + 7) . . . . .	+0.72
169...	9.6	14.90	+ 1, - 1, . . . . .	13.86	(+19, -20) . . . . .	+1.04
174...	13.0	. . . . .	. . . . .	11.11?	m, . . . . .	. . . . .
175...	8.4	15.85	- 9, + 5, + 3, . . . . .	15.36	(- 1, 0) . . . . .	+0.49
175a...	8.6	16.94	(+ 6, - 5) . . . . .	16.64	(-11, +11) . . . . .	+0.30
177...	7.8	14.45	- 8, +11, - 2, . . . . .	13.45	+ 5, . . . . . - 5, . . . . .	+1.00
177a...	7.4	16.19	(- 1, + 1) . . . . .	15.58	(+ 3, - 2) . . . . .	+0.61
177b...	6.9	17.13	(+12, -12) . . . . .	16.72	(- 2, + 3) . . . . .	+0.41
179...	7.6	14.98	0, - 1, . . . . .	14.53	. . . . . m, . . . . .	+0.45
179a...	7.3	16.74	(- 2, + 3) . . . . .	16.30	( 0, - 1) . . . . .	+0.44
180...	9.3	16.08	+ 4, - 4, . . . . .	15.03	( 0, 0) . . . . .	+1.05
180a...	11.0	16.80	(+ 6, - 7) . . . . .	16.50	(- 7, + 8) . . . . .	+0.30
180b...	10.6	16.94	(- 1, + 2) . . . . .	15.76	(-12, +11) . . . . .	+1.18
181a...	7.4	17.02	(+ 8, - 9) . . . . .	. . . . .	. . . . .	. . . . .
181b...	7.9	16.68	(+ 2, - 2) . . . . .	16.18	(- 6, + 5) . . . . .	+0.50
181c...	8.2	17.08	( 0, + 1) . . . . .	16.58	(+ 3, + 4) . . . . .	+0.50
182...	10.2	15.39	-17, +17, . . . . .	15.42	( 0, 0) . . . . .	-0.03
187...	9.1	15.80	+ 3, - 3, . . . . .	15.00	(- 2, + 3) . . . . .	+0.80
188...	7.2	15.12	- 1, + 1, . . . . .	14.55	. . . . . m, . . . . .	+0.57
188a...	7.0	16.92	( 0, + 1) . . . . .	16.60	(-10, + 9) . . . . .	+0.32
188b...	7.8	16.80	(- 1, + 1) . . . . .	16.33	(+13, -13) . . . . .	+0.47
188c...	6.7	17.18	(+ 6, - 5) . . . . .	16.74	(- 4, + 4) . . . . .	+0.44
188d...	6.3	16.36	(- 6, + 5) . . . . .	15.68	(+ 4, - 4) . . . . .	+0.68
189...	6.5	15.92	+ 3, - 2, . . . . . 0	15.24	(+11, -10) . . . . .	+0.68
190...	6.6	15.57	- 3, + 8, . . . . . - 6	15.42	(- 5, + 5) . . . . .	+0.15
190a...	6.5	17.16	(- 2, + 1) . . . . .	16.56	(- 3, + 4) . . . . .	+0.60
191...	8.5	15.49	+ 9, +12, -14, - 8	15.40	(- 3, + 2) . . . . .	+0.09
192...	6.2	14.65	+10, - 4, - 1, - 4	13.80	. . . . . - 2, + 1, . . . . .	+0.85
193...	9.6	15.36	-14, +15, . . . . .	14.54	. . . . . + 3, - 2, . . . . .	+0.82
193a...	9.3	16.64	(- 2, + 2) . . . . .	16.06	(- 3, + 4) . . . . .	+0.58
194...	7.0	14.59	- 2, +18, -10, - 5	13.64	- 1, - 5, + 5, . . . . .	+0.95
195...	8.8	16.20	- 5, + 6, . . . . .	15.80	(-13, +13) . . . . .	+0.40
196...	8.0	15.49	- 6, +12, - 5, - 1	15.40	(+ 5, + 7) . . . . . -11	+0.09
198...	7.6	16.42	+ 5, - 5, . . . . .	15.73	(- 6, + 6) . . . . .	+0.69
199...	6.0	15.50	0, +11, -13, + 4	14.78	(- 1, + 1) . . . . .	+0.72

TABLE II—Continued

NUM- BER	DIS- TANCE	PHOTOGRAPHIC		PHOTO-VISUAL		COLOR- INDEX
		Mag.	Residuals	Mag.	Residuals	
200...	7.1	15.68	- 1, - 3, + 15, - 10	14.87	(..., + 13) - 13, ...	+0.81
202...	6.0	15.61	+ 6, + 12, - 6, - 13	15.34	(- 2, + 2).....	+0.27
203...	7.0	15.45	+ 1, + 20, - 24, + 3	15.37	(+ 5, + 8)....., - 14	+0.08
204...	7.7	15.71	+ 21, - 2, - 3, - 16	15.74	(- 7, + 7).....	-0.03
205...	6.2	13.81	- 3, - 23, + 20, + 6	12.72*	+ 2, - 2, - 9, ...	+1.09
205a...	6.0	16.78	(- 2, + 3).....	16.10	(- 13, + 13).....	+0.68
206...	7.4	11.27	..., - 2, ..., + 2	10.26*	+ 7, - 3, - 6, ...	+1.01
206a...	7.5	16.90	(- 11, + 11).....	16.26	(+ 1, 0).....	+0.64
208...	8.2	16.76	- 1, + 1, ...	16.22	(- 4, + 4).....	+0.54
208a*	8.3	17.25	(m, ...)	16.65:	(m, ...)	+0.60:
210...	5.5	15.40	- 1, + 11, - 19, + 11	15.53	(0, 0).....	-0.13
210a...	5.7	16.82	(- 3, + 3).....	15.96	(- 15, + 14).....	+0.86
210b...	5.7	17.28	(- 3, + 2).....	16.64	(+ 1, - 1).....	+0.64
211...	5.5	15.86	+ 18, + 4, ..., - 21	15.33	(- 6, + 3)....., + 4	+0.53
211a...	5.5	16.06	(- 8, + 8).....	15.26	(- 9, + 10).....	+0.80
211b...	5.2	17.27	(+ 1, - 1).....	16.74	(- 9, + 10).....	+0.53
212...	6.3	16.15	+ 5, + 3, - 10, + 1	15.40	(+ 5, - 4).....	+0.75
212a...	5.8	17.28	(- 3, + 2).....	16.88	(0, 0).....	+0.40
212b...	6.3	17.36	(- 18, + 18).....	16.76	(- 15, + 15).....	+0.60
213...	7.1	15.48	+ 9, + 8, - 18, + 3	15.44	(+ 3, + 6)....., - 10	+0.04
215...	5.4	16.74	- 2, + 1, ...	16.25	(+ 2, - 2).....	+0.49
215a...	5.4	17.42	(..., m).....	16.61	(m, ...)	+0.81
216...	9.1	14.77	+ 14, + 8, - 10, - 12	13.83	0, - 2, + 1, ...	+0.94
217...	5.7	16.25	+ 2, + 5, ..., - 7	15.64	(+ 5, - 5).....	+0.61
218...	5.7	15.04	- 2, + 1, - 2, + 3	14.51	..., + 9, - 9, ...	+0.53
219...	7.2	16.02	+ 10, - 12, + 3, 0	15.15	(- 7, + 7)....., - 1	+0.87
220...	8.2	16.46	+ 6, - 5, ...	15.71	(- 2, + 2).....	+0.75
225...	5.2	15.62	- 8, + 20, - 7, - 4	14.74	..., m, ...	+0.88
227...	5.0	15.25	- 1, - 9, - 2, + 10	14.60	..., - 8, + 9, ...	+0.65
228...	10.0	15.78	- 11, + 12, ...	15.10	(- 5, + 5).....	+0.68
229...	5.8	15.30	- 11, + 8, - 9, + 11	14.58	..., m, ...	+0.72
230...	9.0	15.74	- 4, + 3, ...	15.34	(- 7, + 8).....	+0.40
230a...	9.3	16.56	(+ 6, - 6).....	15.66	(+ 1, - 2).....	+0.90
230b...	9.6	17.19	(+ 2, - 2).....	16.72	(..., m).....	+0.47
230c...	10.0	16.60	(+ 6, - 7).....	16.03	(0, 0).....	+0.57
231...	5.5	15.43	0, + 18, - 18, ...	14.78	..., - 11, ..., + 11	+0.65
232...	8.7	15.87	+ 5, - 5, ...	15.22	(+ 3, - 2).....	+0.65
233...	6.4	16.78	+ 2, - 3, ...	16.11	(- 5, + 5).....	+0.67
235...	7.5	15.53	+ 21, - 2, - 12, - 6	15.50	(+ 3, - 3).....	+0.93
236...	5.3	15.87	- 10, + 8, + 1, + 1	15.36	(- 4, - 3)....., + 8	+0.51
237...	6.6	14.33	- 15, - 10, + 10, + 16	13.91	+ 10, - 6, - 3, ...	+0.42
238...	4.5	14.27	- 16, + 3, ..., + 12	12.48*	+ 14, ..., + 6, ...	+1.79
238a...	4.3	16.82	(- 12, + 11).....	16.16	(- 4, + 4).....	+0.66
238b...	4.5	16.72	(0, + 1).....	16.22	(- 1, + 2).....	+0.50
240...	4.7	15.34	+ 9, + 9, - 19, + 1	14.68	..., + 14, - 13, ...	+0.66
241...	5.6	15.55	- 20, + 18, ..., + 3	15.18	(- 10, + 10).....	+0.37
245...	4.6	15.65	+ 2, + 8, - 7, - 4	15.63	(+ 15, + 10)....., - 24	+0.02
247...	4.2	15.74	+ 2, + 12, ..., - 13	15.43	(- 8, + 7)....., 0	+0.31
247a...	4.0	16.76	(- 29, + 29).....	16.50	(+ 3, - 4).....	+0.26
248...	5.4	15.86	+ 6, + 4, - 11, ...	15.54	(+ 1, - 1).....	+0.32
249a...	5.0	17.36	(- 5, + 6).....	16.99	(- 11, + 11).....	+0.37
249b...	5.1	16.99	(- 2, + 2).....	16.41	(+ 9, - 9).....	+0.58



TABLE II—Continued

NUMBER	DISTANCE	PHOTOGRAPHIC		PHOTO-VISUAL		COLOR-INDEX
		Mag.	Residuals	Mag.	Residuals	
250†..	5.2	14.81	+ 4,+ 7,- 5,- 6	13.91	- 1, 0,+ 2,...	+0.90
250a..	5.4	16.78	(+ 1,- 1).....	16.22	(+ 5,- 6).....	+0.56
251...	4.4	15.78	+32,- 5,- 10,- 17	14.89	....., - 9,- 10,...	+0.89
					(+19,.....)	
251a..	4.3	17.09	(-12,+12).....	16.60	(+15,-14).....	+0.49
253a..	5.2	16.76	( 0,+ 1).....	16.17	(+ 1,- 1).....	+0.59
255...	5.6	15.11	- 7,- 6,.....,+13	14.11	- 6,+10,- 4,....	+1.00
255a..	5.5	17.16	(+ 2,- 3).....	16.63	(- 6,+ 6).....	+0.53
256...	9.7	16.07	+ 3,- 3,.....	14.98	( 0,- 1).....	+1.09
257...	4.7	16.21	- 4,+ 5,....., 0	15.60	(+ 1,- 1).....	+0.61
258†..	4.3	15.52	+15,+ 6,.....,-21	15.54	(- 4,+ 5).....	-0.02
258a..	4.1	17.27	(-19,+19).....	16.84	(+ 4,- 3).....	+0.43
259...	3.9	15.82	+ 4,+13,.....,-17	15.46	(+ 4,- 4).....	+0.36
260...	3.9	16.59	- 7,+ 7,.....	15.75	(- 6,+ 6).....	+0.84
260a..	3.7	17.32	(+ 3,- 2).....	16.97	(-13,+13).....	+0.35
261...	5.7	15.90	+ 8,- 8,.....	15.30	(- 3,+ 3).....	+0.60
261a..	6.1	17.17	(- 9,+ 9).....	16.74	(- 4,+ 4).....	+0.43
262...	4.5	15.84	- 1,+ 2,.....	15.33	(+12,+ 6).....,-17	+0.51
262a..	4.8	16.76	(- 6,+ 5).....	16.19	(- 1,+ 1).....	+0.57
263†..	4.1	14.53	+ 7,- 10,- 7,+11	13.41	-10,+ 7,+ 2,....	+1.12
265...	5.0	14.29	-22,+18,+ 4,....	13.15	- 5,+ 3,+ 3,....	+1.14
266...	5.1	16.22	+ 3,- 4,.....	15.61	(+ 8,- 8).....	+0.61
268...	5.7	16.34	- 2,- 4,.....,+ 7	15.60	(+ 4,- 4).....	+0.74
270...	3.9	16.16	+ 9,- 8,.....	15.29	(- 4,+ 4).....	+0.87
272...	5.1	16.56	- 2,+ 1,.....	15.84	(- 3,+ 3).....	+0.72
273...	3.7	16.00	- 8,+ 4,.....,+ 5	15.22	(- 7,+11).....,- 5	+0.78
276...	3.5	16.24	+ 8,- 6,.....,+ 1	16.42	(- 6,+ 7).....	-0.18
277...	3.6	15.17	- 2,- 4,.....,+ 7	14.55	....., m,....	+0.62
280*	4.2	.....	.....	17.41	(....., m).....	.....
281...	4.8	14.61	- 4,+ 4,....., 0	13.42	- 6,+ 6,+ 1,....	+1.19
281a..	4.5	17.01	(....., m).....	16.98	(+18,-17).....	+0.03
282...	4.1	15.90	+ 5,- 4,.....	14.99	(+11,- 5).....,- 6	+0.91
283...	3.3	16.55	- 8,+ 5,.....,+ 2	15.92	(- 2,+ 1).....	+0.63
285...	3.3	16.59	+ 8,+ 4,.....,-13	16.05	(- 5,+ 5).....	+0.54
286...	3.2	15.77	- 1,+ 9,.....,- 9	15.11	(- 1,+ 1).....	+0.66
289...	3.3	15.24	+ 5,- 11,.....,+ 7	14.40	....., m,....	+0.84
290...	8.0	15.74	-11,+ 8,- 2,+ 4	15.41	(- 4,+ 4).....	+0.33
290a..	8.0	17.12	(- 4,+ 5).....	16.84	(-19,+19).....	+0.28
290b..	8.0	16.98	(+10,-10).....	16.46	(-10,+10).....	+0.52
291...	3.1	14.85	+16,- 8,.....,- 9	14.06	+ 4,- 3,- 1,....	+0.79
291a..	3.0	17.02	(- 2,+ 3).....	16.32	(- 2,+ 3).....	+0.70
291b..	3.4	17.30	(- 5,+ 4).....	16.76	(+12,-11).....	+0.54
291c..	3.7	17.26	(- 5,+ 4).....	16.90	(- 6,+ 5).....	+0.36
292...	3.5	15.60	0,+13,-12,....	15.58	( 0,+ 1).....	+0.02
293...	3.1	15.50	+ 4,- 3,.....	14.61	.....,+ 5,- 5	+0.89
296a..	3.2	17.42	(- 4,+ 4).....	17.11	(-23,+23).....	+0.31
296b..	3.4	17.38	(- 3,+ 4).....	17.17	(....., m).....	+0.21
297...	7.4	14.14	-13,+17,- 3,....	12.82	0,-12,+11,....	+1.32
298...	4.2	16.50	0,+ 1,.....	15.78	(- 6,+ 6).....	+0.72
299...	7.0	16.14	+ 3,- 3,.....,- 1	15.38	(- 6,+ 7).....	+0.76
300...	3.0	16.64	+ 2,- 1,.....	15.90	(- 6,+ 6).....	+0.74
301...	4.5	15.85	+10,+10,.....,-20	15.42	(-10,+11).....,- 2	+0.43
301a..	4.5	17.16	(+12,-11).....	16.62	(+ 3,- 4).....	+0.54

TABLE II—Continued

NUM- BER	DIS- TANCE	PHOTOGRAPHIC		PHOTO-VISUAL		COLOR- INDEX
		Mag.	Residuals	Mag.	Residuals	
301b..	4.8	16.68	(- 6,+ 5).....	15.94	(-13,+12).....	+0.74
301c..	5.2	17.13	(-13,+13).....	16.78	(+ 6,- 6).....	+0.35
301d..	5.3	17.24	(- 6,+ 6).....	17.14	(...., m).....	+0.10
302*	3.4	14.95	m,.....	.....	.....	.....
303...	2.8	16.51	+ 3,+ 3,....,- 7	15.82	(+ 8,- 9).....	+0.69
303a..	2.9	17.02	(- 2,+ 3).....	16.42	(- 3,+ 4).....	+0.60
304...	2.8	15.49	+14,+ 2,-17,...	15.53	(- 3,+ 3).....	-0.04
305a..	4.6	17.16	(- 2,+ 1).....	16.46	( m,....).....	+0.70
306...	2.7	16.12	- 5,- 1,+ 5,...	15.22	( o, o).....	+0.90
307...	3.8	15.96	- 4,+12,- 8,...	15.16	(- 1,+ 1).....	+0.80
307a..	3.9	16.70	(+ 9,- 8).....	16.06	(-13,+14).....	+0.64
307b..	4.1	16.96	(+ 4,- 3).....	16.58	(-12,+11).....	+0.38
308...	3.0	15.80	+15,-15,....	15.66	(+ 6,- 5).....	+0.14
308a..	2.7	16.60	(-17,+17).....	15.88	(+ 5,- 4).....	+0.72
308b..	3.4	17.22	(+16,-17).....	17.02	(-14,+15).....	+0.20
309...	2.7	14.37	-24,+ 6,....,+17	13.18*	(-12,+ 7,-11,...	+1.19
310...	2.8	16.92	+ 3,- 4,....	15.78	(- 6,+ 6).....	+1.14
310a..	2.8	17.22	(-12,+12).....	16.74	(+ 5,- 5).....	+0.48
311...	3.6	15.45	+ 1,+20,-20,...	15.52	(+ 3,- 2).....	-0.07
311a..	3.5	16.82	( o,- 1).....	16.02	(- 9,+ 8).....	+0.80
311b..	3.4	17.08	(- 4,+ 5).....	16.51	(+ 2,- 2).....	+0.57
312...	2.7	15.98	+ 3,+ 6,-10,...	14.97	(+ 6,- 6).....	+1.01
313...	2.7	16.59	- 7,+ 7,....	15.84	(+ 6,- 5).....	+0.75
314...	4.8	15.34	+ 1,+22,-22,...	14.40	....., m,....	+0.94
315...	3.3	15.49	+11,+12,-24,...	14.77	....., m,....	+0.72
317...	3.0	15.92	+15,-15,....	15.90	( o, o).....	+0.02
319...	3.6	16.48	- 6,+ 6,....	15.73	(+14,-14).....	+0.75
320...	6.3	16.66	-10,+ 9,....	15.95	(+ 8,- 8).....	+0.71
320a..	6.3	17.24	(- 3,+ 2).....	16.72	(-15,+16).....	+0.52
320b..	6.2	16.98	(+ 6,- 5).....	16.68	(- 3,+ 4).....	+0.30
322...	2.9	17.04	- 9,+10,....	16.65	(- 4,+ 4).....	+0.39
322a..	2.9	17.38	(- 7,+ 8).....	16.76	(- 1,+ 2).....	+0.62
323...	2.7	15.35	+ 8,-14,....,+ 6	14.39	....., o, o,....	+0.96
325...	3.8	15.98	+ 3,+13,-15,...	15.40	(+ 7,- 7).....	+0.58
326...	2.8	15.64	- 1,+ 5,....,- 3	14.68	.....,-11,+11,...	+0.96
326a..	3.0	17.30	(- 5,+ 4).....	16.77	(- 7,+ 7).....	+0.53
326b..	3.0	17.26	(...., m).....	16.57	( m,....).....	+0.69
326c..	3.2	17.08	(+13,-12).....	16.20	(- 2,+ 3).....	+0.88
327...	3.2	15.82	+ 1,+ 8,....,-10	15.44	(-12,- 2).....,+15	+0.38
329...	4.4	15.93	-10,+11,- 2,...	15.12	(- 2,+ 2).....	+0.81
330...	2.5	16.39	- 7,+ 2,....,+ 5	15.62	(+ 2,- 1).....	+0.77
331...	6.2	15.45	- 6,+16,....,-10	15.40	(- 5,+ 5).....	+0.05
332...	3.9	15.85	- 6,+ 5,+ 1,....	15.26	(- 9,+ 7).....,+ 3	+0.59
332a..	4.1	17.26	(- 5,+ 4).....	16.82	(-17,+17).....	+0.44
332b..	3.9	17.34	(- 3,+ 3).....	16.86	(- 2,+ 2).....	+0.48
334...	2.6	14.27	-14,+12,+ 1,....	13.14	- 2,+15,-13,...	+1.13
335...	3.6	16.10	+ 7,+ 5,- 2,- 8	15.44	(- 9,+10).....	+0.66
336...	2.9	15.07	+ 4,+ 2,- 6,....	14.05	+13,- 7,- 6,....	+1.02
336a..	3.0	17.17	(+ 4,- 4).....	.....	.....	.....
337...	2.4	15.54	+19,- 3,-22,+ 7	15.60	(+ 1,- 1).....	-0.06
339...	2.9	15.49	-17,+24,....,- 8	14.76	.....,+ 5,- 6	+0.73
340...	2.7	16.65	-15,+15,....	15.88	(- 1,+ 2).....	+0.77

TABLE II—Continued

NUM- BER	DIS- TANCE	PHOTOGRAPHIC		PHOTO-VISUAL		COLOR- INDEX
		Mag.	Residuals	Mag.	Residuals	
341...	3.5	15.55	-12, +22, ..., -10	14.69	..., ..., m, ...	+0.86
342...	5.5	15.75	+4, +7, ..., -10	15.40	(-3, +2)...	+0.35
343...	2.6	15.40	+6, -6, ..., +1	15.26	(-11, +7)...	+0.14
345...	3.0	14.61	-4, +8, -5, ...	13.35	+2, +2, -4, ...	+1.26
345a...	3.1	17.30	(-12, +12)...	16.78	(+10, -11)...	+0.52
347...	2.8	16.13	-1, +2, 0, ...	15.42	(-7, +8)...	+0.71
348...	2.3	14.76	-4, +1, ..., +4	13.88	+10, -2, -8, ...	+0.88
348a...	2.2	16.76	(+3, -3)...	16.14	(-5, +6)...	+0.62
349...	3.6	15.89	+21, -7, -14, ...	14.96	(+12, -11)...	+0.93
350...	3.0	16.46	-16, +17, ...	15.60	(+1, +1)...	+0.86
350a...	2.9	17.36	(-1, +1)...	16.76	(-6, +5)...	+0.60
352...	2.3	15.24	+1, -11, ..., +11	14.28	-6, +2, +5, ...	+0.96
354...	6.5	15.76	+3, -3, ...	15.47	(m, ...)...	+0.29
355a...	2.4	16.87	(+10, -10)...	16.24	(-3, +2)...	+0.63
357...	2.4	15.20	+26, +14, -40, ...	14.45	(-3, +3)...	+0.75
360...	2.1	15.82	-3, +17, ..., -14	15.02	(+6, -5)...	+0.80
360a...	2.1	16.03	(+2, -2)...	15.50	(-3, +3)...	+0.53
360b...	2.1	16.93	(0, 0)...	16.19	(-7, +7)...	+0.74
360c...	2.1	17.10	(0, -1)...	16.52	(+9, -8)...	+0.58
360d...	2.2	17.46	(-8, +8)...	16.89	(-10, +10)...	+0.57
364...	2.1	15.75	-21, +24, ..., -3	15.78	(+9, -8)...	-0.03
364a...	2.1	16.84	(+2, -3)...	15.90	(+3, -3)...	+0.94
365...	2.1	15.62	+8, +3, -11, ...	15.54	(+4, -4)...	+0.08
367...	2.3	15.10	+5, +3, -9, ...	13.96	-6, +2, +3, ...	+1.14
369...	2.0	15.08	+3, +5, -9, ...	14.40	..., ..., m, ...	+0.68
370...	1.9	16.85	-13, +13, ...	16.24	(0, -1)...	+0.61
371...	6.6	15.11	+4, -10, -7, +13	14.81	(-1, +1)...	+0.30
372...	2.5	15.63	+4, +6, ..., -9	14.71	..., ..., m, ...	+0.92
373...	2.3	16.22	-15, +15, ...	15.46	(+12, -13)...	+0.76
375...	1.9	15.49	+11, +7, -19, ...	14.77	..., ..., m, ...	+0.72
376...	1.9	16.06	-2, +2, ...	15.41	(-1, +1)...	+0.65
376a...	1.9	16.80	(-4, +5)...	16.32	(..., m)...	+0.48
377...	2.1	15.92	+12, +7, -20, ...	15.26	(+1, -1)...	+0.66
378a...	4.0	17.40	(-2, +2)...	16.99	(-15, +15)...	+0.41
379a...	2.4	17.45	(-7, +7)...	16.96	(+8, -8)...	+0.49
379c...	2.4	17.34	(..., m)...	16.58	(+8, -8)...	+0.76
380...	1.9	16.05	-1, +10, ..., -10	15.24	(-7, +6)...	+0.81
380a...	2.1	16.88	(+2, -3)...	16.08	(-11, +12)...	+0.80
380b...	2.2	17.34	(+1, 0)...	16.98	(-5, +5)...	+0.36
381...	2.1	15.22	+7, -9, ..., +2	14.22	(-7, +10, -2, ...)	+1.00
381a...	2.0	17.02	(+2, -1)...	16.45	(+1, -1)...	+0.57
381b...	2.0	17.38	(+4, -4)...	17.12	(-8, +8)...	+0.26
382*	2.0	15.48	-2, +21, -18, ...	15.10	(+22, -22)...	+0.38
383...	2.3	16.40	+2, -3, ...	15.58	(-13, +12)...	+0.82
385...	2.0	15.36	+24, -23, ...	14.06	(-4, +5)...	+1.30
385a...	2.1	17.46	(-8, +9)...	16.94	(-1, +1)...	+0.52
385b...	2.0	17.36	(-11, +10)...	16.92	(-8, +7)...	+0.44
386...	3.4	15.94	+13, +5, -19, ...	15.40	(-10, +10)...	+0.54
386a...	3.5	17.44	(-2, +2)...	16.96	(+2, -1)...	+0.48
387...	2.1	14.75	+4, -2, ..., -3	13.85	(-3, +1, +3, ...)	+0.90
387a...	2.1	16.86	(+14, -13)...	16.06	(-9, +10)...	+0.80
389...	1.8	15.46	0, -3, ..., +2	14.62	(..., +2) - 1, ...	+0.84

TABLE II—Continued

NUM- BER	DIS- TANCE	PHOTOGRAPHIC		PHOTO-VISUAL		COLOR- INDEX
		Mag.	Residuals	Mag.	Residuals	
392...	2.9	16.30	- 3,+ 7,...,- 4	15.60	(- 5,+ 4).....	+0.70
393...	8.1	15.55	-12,+ 6,+ 7,...	14.63	(...,+ 1)- 1,...	+0.92
394...	1.7	15.94	+ 7,+14,...,-22	15.38	(- 8,+ 7).....	+0.56
394a...	1.8	16.40	(- 1,+ 1).....	15.70	(- 1, 0).....	+0.70
396a...	2.7	16.83	(-13,+13).....	15.97	(-19,+19).....	+0.86
397a...	1.6	15.49	(+ 1,- 1).....	15.61	(... , m).....	-0.12
398...	3.0	14.32	-19,- 5,+11,+12	13.19*	- 7,- 4,...	+1.13
399...	3.3	16.45	-20,-11,+23,+ 7	15.84	(+ 3,- 3).....	+0.61
400...	1.6	15.90	+ 5,+ 9,...,-15	15.34	(-12,+11).....	+0.56
401...	2.1	16.16	+ 1,- 1,...	15.18	(- 1,+ 2).....	+0.98
403...	1.6	15.42	+ 8,- 8,...	15.32	(+ 8,- 7).....	+0.10
403a...	1.7	16.47	(- 8,+ 8).....	15.78	(+ 9,- 8).....	+0.69
403b...	1.7	16.28	(- 6,+ 7).....	15.60	(- 5,+ 4).....	+0.62
403c...	1.5	15.96	(- 8,+ 8).....	15.38	(+ 2,- 2).....	+0.58
403d...	1.7	17.34	(-20,+21).....	16.99	(... , m).....	+0.35
403e...	1.7	17.44	(+ 1,- 2).....	17.45	(... , m).....	-0.01
403f...	1.6	17.41	(+ 4,- 4).....	17.24	(... , m).....	+0.17
403g...	1.6	17.44	(- 9,+ 8).....	16.78	(... , m).....	+0.66
406...	2.6	16.53	- 6,- 5,+ 5,+ 4	15.71	(+ 7,- 7).....	+0.82
411a...	4.8	16.96	(+ 1, 0).....	16.53	(+12,-12).....	+0.43
412...	3.1	15.59	- 5,+14,...,- 8	15.56	(... , m).....	+0.03
414...	2.5	16.38	- 4,+ 3,...	15.70	(- 1, 0).....	+0.68
417...	1.6	14.09	- 2,+ 2,...	12.94	+ 8,- 5,- 3,...	+1.15
417a...	1.7	15.04	(- 6,+ 7).....	15.21	(- 1,+ 1).....	-0.17
417b...	1.7	16.42	(- 3,+ 2).....	16.05	(- 8,+ 8).....	+0.37
417c...	1.8	17.04	(- 4,+ 5).....	16.25	(- 1,+ 1).....	+0.79
417d...	1.9	17.42	(- 4,+ 4).....	16.48	(- 2,+ 3).....	-0.06
418...	2.1	15.60	+16,+13,-28,...	15.44	(- 2,+3).....	+0.16
418a*	2.1	.....	.....	16.64	(+20,-20).....	.....
419...	2.6	15.63	-13,+14,...,- 2	15.46	(- 4,+ 4).....	+0.17
419a*	2.6	17.04	(+ 4,- 3).....	16.14	(-14,+15).....	+0.90
420*	1.4	13.59	m,.....	13.40	+ 7,- 6,- 1,...	+0.19
422...	2.4	15.55	+12,+10,-23,...	15.48	(- 8,+ 8).....	+0.07
422a...	2.3	17.24	(+14,-15).....	16.54	(-15,+15).....	+0.70
423...	10.6	14.92	- 1,- 7,+ 9,...	14.60	(...,+ 7)- 6,...	+0.32
425a...	1.8	16.18	(- 6,+ 5).....	15.46	(-16,+15).....	+6.72
426...	11.2	14.85	+ 2,- 4,+ 1,...	13.75	..... , m,.....	+1.10
433...	2.9	15.92	- 3,+12,...,-10	15.84	(-12,+12).....	+0.08
434...	2.4	16.90	- 5,+ 4,...	16.10	(- 1, 0).....	+0.80
435...	6.7	15.84	+ 8,- 7,...	15.00	(- 2,+ 3).....	+0.84
436...	2.1	16.66	0, 0,...	15.84	(- 3,+ 3).....	+0.82
444...	2.5	15.39	+18,- 1,-16,...	15.42	(+ 3,- 3).....	-0.03
450...	2.1	16.86	- 4,+ 5,...	16.10	(-10,+10).....	+0.76
452...	1.9	15.34	+ 1,-13,...,+11	14.44	(-11,+11).....	+0.90
452a...	2.1	17.38	( 0,- 1).....	16.64	(+11,-10).....	+0.74
452b...	2.2	16.94	(- 8,+ 7).....	16.25	(+ 2,- 2).....	+0.69
452c...	1.9	17.38	(- 7,+ 8).....	16.78	(+10,-11).....	+0.60
454...	2.5	16.92	-22,+22,...	16.20	(- 2,+ 3).....	+0.72
455a...	5.7	17.52	( 0, 0).....	16.99	(-15,+15).....	+0.53
457...	2.7	16.80	-10,+11,...	16.52	(+ 1,- 1).....	+0.28
463...	2.4	14.25	-21,+ 2,...,+19	13.12*	(- 4,- 3,- 8,...	+1.13
464...	1.9	16.22	- 7,+12,...,- 4	15.40	(-18,+19).....	+0.82

TABLE II—Continued

NUMBER	DISTANCE	PHOTOGRAPHIC		PHOTO-VISUAL		COLOR-INDEX
		Mag.	Residuals	Mag.	Residuals	
465...	2.5	15.01	+ 7, - 4, ..., - 3	14.01	+ 5, - 2, - 2, ...	+1.00
467...	2.7	15.75	- 8, + 20, - 9, - 4	15.67	(- 3, + 3).....	+0.08
467a...	2.6	17.36	(+ 2, - 2).....	16.66	(- 9, + 9).....	+0.70
467b...	2.7	17.28	(- 3, + 2).....	16.76	(+ 8, - 9).....	+0.52
471...	3.4	16.14	+ 23, - 24, .....	15.77	(+ 1, - 1).....	+0.37
471a...	3.5	16.70	(- 4, + 3).....	15.94	(- 7, + 6).....	+0.76
472...	1.9	14.76	+ 11, - 20, + 10, ...	14.45	..., m, .....	+0.31
473...	3.0	16.33	- 1, + 1, .....	15.60	(+ 1, - 1).....	+0.73
474...	1.7	15.73	- 10, + 17, ..., - 8	15.61	(- 3, + 3).....	+0.12
480...	3.3	16.28	- 3, + 2, .....	15.49	(- 7, + 7).....	+0.79
480a...	3.7	17.05	(- 8, + 8).....	16.50	(+ 3, - 4).....	+0.55
480b...	4.0	17.52	(..., m).....	17.16	(0, + 1).....	+0.36
482...	2.2	15.92	+ 6, - 6, .....	15.57	(- 2, + 2).....	+0.35
482a...	2.1	16.50	(- 13, + 12).....	15.70	(- 9, + 9).....	+0.80
482b...	2.1	16.39	(- 2, + 2).....	15.66	(+ 3, - 2).....	+0.73
484...	9.2	16.13	+ 9, - 9, .....	15.43	(+ 4, - 4).....	+0.70
490...	2.0	14.13	+ 5, - 14, + 10, ...	12.33	0, + 3, - 2, ...	+1.80
499...	3.4	16.26	- 1, 0, .....	15.62	(+ 2, - 3).....	+0.64
499a...	3.5	17.24	(+ 11, - 11).....	16.87	(- 8, + 8).....	+0.37
499b...	4.0	17.01	(- 8, + 8).....	16.56	(- 3, + 2).....	+0.45
499c...	4.1	17.34	(- 3, + 3).....	16.83	(- 8, + 8).....	+0.51
499d...	3.9	17.46	(..., m).....	17.31	(..., m).....	+0.15
499e...	3.9	...	...	17.48	(..., m).....	...
499f...	3.9	17.44	(..., m).....	17.31	(..., m).....	+0.13
499g...	4.0	17.19	(- 11, + 11).....	16.88	(- 4, + 3).....	+0.31
499h...	4.0	17.59	(..., m).....	17.21	(- 17, + 17).....	+0.38
502...	2.4	16.14	+ 3, - 3, .....	15.21	(- 1, + 1).....	+0.93
502a...	2.3	16.20	(0, 0).....	15.64	(+ 3, - 3).....	+0.56
512...	5.0	15.79	+ 4, + 7, - 11, ...	14.94	(+ 14, - 15).....	+0.85
513...	2.2	16.03	+ 9, + 1, ..., - 11	15.18	(- 6, + 7).....	+0.85
513a...	2.3	17.19	(- 11, + 11).....	16.40	(- 7, + 6).....	+0.79
514...	2.9	15.44	+ 2, - 1, .....	14.58	..., m, ...	+0.86
522...	3.1	16.54	- 7, + 6, .....	15.76	(- 7, + 8).....	+0.78
522a...	3.2	16.72	(- 6, + 5).....	16.14	(- 5, + 6).....	+0.58
522b...	3.0	16.94	(- 1, + 2).....	16.34	(+ 2, - 2).....	+0.60
522c*	3.0	...	...	16.79	(m, ...).....	...
530...	2.4	16.98	- 16, + 16, .....	16.50	(- 14, + 15).....	+0.48
539*	1.8	15.16	- 18, + 22, ..., - 3	14.98	(m, ...).....	+0.18
550...	1.8	15.99	+ 11, + 9, ..., - 20	15.10	(- 2, + 2).....	+0.89
550a...	1.8	17.36	(- 18, + 19).....	16.86	(+ 12, - 11).....	+0.50
564...	1.9	15.94	+ 16, + 5, - 22, ...	14.97	(+ 3, - 6)....., + 3	+0.97
566...	2.4	16.13	- 1, - 2, ..., + 3	15.17	(0, 0).....	+0.96
568...	3.9	16.16	- 6, + 2, + 5, ...	15.44	(+ 1, - 2).....	+0.72
573...	3.4	15.28	- 3, - 7, ..., + 10	14.62	..., - 17, + 5, ...	+0.66
573a...	3.3	17.19	(- 11, + 11).....	16.67	(+ 21, - 21).....	+0.52
578...	2.0	16.18	+ 4, - 3, .....	15.28	(+ 2, - 6)....., + 4	+0.90
581...	1.6	16.35	- 1, + 2, - 2, ...	15.34	(+ 3, - 4).....	+1.01
589...	1.5	13.71	0, 0, .....	12.80	- 2, + 13, - 10, ...	+0.91
590...	3.5	16.00	- 14, + 22, ..., - 8	15.17	(- 5, + 5).....	+0.83
590a...	3.7	17.11	(- 3, + 2).....	16.61	(- 11, + 11).....	+0.50
594...	10.4	15.39	- 17, + 17, .....	14.85	(- 3, + 3).....	+0.54
595...	7.9	15.54	- 15, + 15, .....	15.40	(- 8, + 7).....	+0.14

TABLE II—Continued

NUM- BER	DIS- TANCE	PHOTOGRAPHIC		PHOTO-VISUAL		COLOR- INDEX
		Mag.	Residuals	Mag.	Residuals	
595b*	7.4	17.37:	(..., m).....	16.92	-22,+22,.....	+0.45:
596...	2.0	15.80	+6,+10,.....-15	15.12	( 0, 0).....	+0.68
603...	1.8	15.69	+17,+17,-34,...	15.60	(- 2,+ 1).....+ 2	+0.09
605...	2.3	15.86	+ 6,+ 9,-14,...	15.31	(+11,-11).....	+0.55
605a...	2.3	17.10	(- 6,+ 7).....	16.48	(+ 2,- 2).....	+0.62
606...	1.9	15.64	+22,+ 9,- 32,...	15.47	( 0,- 5).....+ 6	+0.17
609†...	4.1	15.66	- 4,+ 7,.....- 2	15.70	(- 3,+ 3).....	-0.04
609a...	4.0	17.42	(-11,+10).....	16.94	(- 1,+ 1).....	+0.48
609b...	4.3	17.53	(- 5,+ 2).....	17.31	(+ 9,- 4).....	+0.21
612†...	1.3	13.96	....., - 2,+ 2	12.58	....., - 9,.....	+1.38
621...	3.1	15.07	+ 1,+ 2,.....- 2	13.97	+ 3,+ 1,- 4,...	+1.10
621a...	3.2	16.92	(- 2,+ 1).....	16.26	(- 2,+ 3).....	+0.66
621b...	3.2	17.15	(-11,+11).....	16.80	(- 5,+ 4).....	+0.35
621d...	3.2	17.79:	(- 4,+ 4).....	17.38	(..., m).....	+0.41:
628...	1.6	16.37	- 3, 0,+ 4,...	15.52	(+ 6,- 7).....	+0.85
628a...	1.6	16.34	(+ 3,- 2).....	15.38	(+15,-16).....	+0.96
632...	5.1	15.62	+ 5,+20,-25,...	15.38	(+ 9,-10).....	+0.24
639...	2.1	16.06	- 2,+ 9,.....- 8	15.18	(- 6,+ 7).....	+0.88
640†...	2.7	14.40	- 1,+16,-11,- 3	13.22	-10,+ 1,+ 9,...	+1.18
640a...	3.0	17.15	(+ 6,- 6).....	16.85	(- 6,+ 6).....	+0.30
640b...	3.2	17.05	(+16,-16).....	16.48	(+ 2,- 2).....	+0.57
640c...	3.0	17.50	(-15,+15).....	16.98	(- 5,+ 5).....	+0.52
640d...	3.1	17.32	(- 1,+ 2).....	16.98	(-23,+22).....	+0.34
640e...	3.2	17.30	(-12,+12).....	17.04	(-16,+16).....	+0.26
640f...	2.8	17.42	(- 7,+ 7).....	17.17	(..., m).....	+0.25
649...	4.1	15.98	+14,- 3,- 10,...	15.35	(+ 2,- 2).....	+0.63
649a...	4.3	17.02	(+ 2,- 1).....	16.71	(- 1,+ 1).....	+0.31
649b...	4.3	17.16	(- 2,+ 1).....	16.82	(- 3,+ 2).....	+0.34
649c...	3.8	17.17	(- 9,+ 9).....	16.74	(+10,- 9).....	+0.43
659...	4.0	15.52	- 6,+ 4,.....+ 2	15.49	(- 7,+ 7).....	+0.03
665...	2.0	15.88	+10,+16,-26,...	15.84	(+ 6,- 5).....	+0.04
665a...	2.1	17.28	(- 3,+ 2).....	16.90	(+14,-15).....	+0.38
667*	1.5	16.14	- 4,.....+ 3,...	.....	.....	.....
674...	1.8	16.24	+21,-20,.....	15.53	( m, ...).....	+0.71
675...	2.5	15.79	+ 4,+ 7,.....-11	16.03	(-13,+13).....	-0.24
680...	1.6	14.75	+ 4,- 2,.....- 3	13.66	- 2,-13,+16,...	+1.09
680a...	1.6	15.80	-11,+12,.....	15.58	(+ 6,- 5).....	+0.22
680b...	1.6	15.78	( 0,- 1).....	15.58	(- 5,+ 6).....	+0.20
680c...	1.7	16.37	(+ 2,- 2).....	15.60	(- 5,+ 4).....	+0.77
700a...	2.4	16.40	(- 3,+ 4).....	15.76	(+ 8,- 9).....	+0.64
701...	5.0	16.45	+14,-15,.....+ 1	15.68	(- 7,+ 8).....	+0.77
701a...	6.0	16.72	(- 2,+ 1).....	16.08	(- 5,+ 5).....	+0.64
701b...	5.2	17.33	(- 2,+ 2).....	16.88	(- 4,+ 3).....	+0.45
701c...	5.0	17.35	(- 7,+ 7).....	17.06	(-18,+18).....	+0.29
701d...	5.0	17.36	(-11,+10).....	16.94	(-15,+16).....	+0.42
706...	1.5	14.06	-14,+ 5,.....+10	12.90	+14,- 1,-12,...	+1.16
707...	1.8	16.73	+12,- 1,.....-11	15.84	(- 3,+ 3).....	+0.89
708...	1.9	15.30	+16,-17,.....- 1	15.43	(-16,+16).....	-0.13
709...	11.4	14.26	-16,+16,.....	14.13	(+ 7,- 7).....	+0.13
713a...	9.0	.....	.....	16.64	(-14,+14).....	.....
724...	2.1	16.74	- 2,+ 3,.....	16.03	(-10,+10).....	+0.71
730...	1.6	16.14	.....,+ 1,- 1,...	15.15	(+ 2,-15).....,+13	+0.99

TABLE II—Continued

NUMBER	DISTANCE	PHOTOGRAPHIC		PHOTO-VISUAL		COLOR-INDEX
		Mag.	Residuals	Mag.	Residuals	
730a...	1.6	17.70	(-14,+13).....	16.94	(-10,+9).....	+0.76
738...	1.6	16.70	-11,+10,.....	16.76	(+12,-13).....	-0.06
739...	4.9	15.55	-12,+14,.....-1	15.50	(-5,+6).....	+0.05
739a...	4.7	16.64	(-2,+2).....	16.12	(+6,-6).....	+0.52
739b...	5.2	16.81	(0,0).....	16.32	(+11,-12).....	+0.49
740†...	3.5	14.10	-8,+4,+2,+1	13.40	-13,+6,+6,....	+0.70
740a...	3.3	17.24	(-14,+14).....	17.25	(-27,+13).....	-0.01
740b...	3.3	17.40	(-2,+2).....	17.14	(-16,+17).....	+0.26
752...	1.2	13.96	.....,-6,+7	12.54	.....-7,.....	+1.42
753...	1.5	15.09	-11,+4,.....+8	13.95	-2,+1,+2,....	+1.14
758...	1.6	16.07	+3,+8,-12,....	15.04	(+8,-16).....+9	+1.03
758a...	1.7	17.58	(-10,+11).....	17.10	(-22,+21).....	+0.48
759a*...	2.2	.....	.....	16.51	(-5,+5).....	.....
767...	2.0	15.89	-10,+19,.....-10	15.42	(-12,+11).....	+0.47
777...	2.4	16.94	-1,0,.....	16.42	(+4,-4).....	+0.52
801...	1.3	15.59	+1,+23,-24,....	15.47	(+11,-11).....	+0.12
801a...	1.4	17.06	(-2,+3).....	16.25	(-1,+1).....	+0.81
801b...	1.4	17.47	(+1,-1).....	17.14	(-10,+10).....	+0.33
801c...	1.5	.....	.....	17.24	(.....,m).....	.....
805...	1.6	15.57	-3,-1,.....+4	15.57	(-4,+4).....	0
810...	2.2	16.06	+1,-2,.....	15.98	(-8,+8).....	+0.08
811...	1.6	15.88	+19,-15,.....-3	15.14	(+8,-8).....	+0.74
832...	2.8	15.23	-8,+2,.....+5	14.47	(.....-5,.....	+0.76
					(.....,+5)	
837...	3.9	13.83	-8,-17,+20,+4	12.47	+4,+9,-12,....	+1.36
837b...	4.0	17.13	(-13,+13).....	16.75	(0,0).....	+0.38
841...	5.6	15.59	-16,+6,+13,-1	15.36	(+6,-6).....	+0.23
845...	1.8	15.62	+14,+28,-41,....	15.58	(+6,+3).....-8	+0.04
845a...	1.8	17.26	(-16,+16).....	16.52	(+13,-14).....	+0.74
853...	4.0	14.56	-19,+21,-2,....	13.63	-8,0,+7,....	+0.93
872...	3.4	15.18	-7,-5,-3,+13	14.40	-17,-8,0,....	+0.78
					(.....,+27)	
879...	1.5	15.58	-8,+7,.....,0	15.10	(+20,.....)-19,....	+0.48
882...	1.7	15.99	+16,0,-16,....	15.14	(+3,.....).....-3	+0.85
883...	3.7	16.00	-2,-1,+17,-15	15.40	(+7,-7).....	+0.60
885...	1.9	14.47	-6,+9,-4,....	13.27	-6,+2,+4,....	+1.20
885a...	2.0	17.22	(-8,+8).....	16.54	(+3,-3).....	+0.68
900...	2.1	16.24	+1,-2,.....	15.28	(-3,+2).....	+0.96
900a...	2.4	16.98	(+6,-5).....	16.44	(+9,-9).....	+0.54
900b...	2.5	17.41	(+4,-4).....	17.20	(.....,m).....	+0.21
902...	2.4	15.85	+4,+10,.....-13	15.26	(-1,+2).....	+0.59
902a...	2.4	17.34	(-3,+3).....	16.68	(+7,-8).....	+0.66
902b...	2.3	17.50	(-12,+13).....	17.02	(-4,+5).....	+0.48
925...	2.8	14.29	-11,-2,+14,....	12.95	-11,-2,+12,....	+1.34
925a...	2.8	16.28	(+2,-2).....	15.54	(-4,+5).....	+0.74
925b...	2.9	17.66	(-18,+17).....	17.24	(-2,+3).....	+0.42
925c...	3.0	17.46	(-8,+9).....	16.92	(-15,+15).....	+0.54
925d*...	2.9	17.31	(-3,+3).....	16.96	(-21,+21).....	+0.35
925e...	2.9	17.38	(-7,+8).....	17.11	(-18,+9).....	+0.27
926*...	4.2	14.65	m,.....	14.43	(.....-5,+5,....	+0.22
926a...	4.2	17.10	(-6,+7).....	16.74	(+14,-28).....	+0.36
935...	10.0	15.77	+27,-12,-15,....	14.70	(.....,+12)-11,....	+1.07

TABLE II—Continued

NUMBER	DISTANCE	PHOTOGRAPHIC		PHOTO-VISUAL		COLOR-INDEX
		Mag.	Residuals	Mag.	Residuals	
945..	1.6	16.36	- 2, + 1, .....	15.50	(+ 8, - 8)....., 0	+0.86
945a.	1.6	16.12	( 0, - 1).....	15.21	(+ 1, - 1).....	+0.91
945b.	1.7	16.60	(+ 2, - 2).....	15.58	( 0, + 1).....	+1.02
952..	1.7	16.16	- 4, + 6, ....., - 3	16.19	(- 7, + 7).....	-0.03
953..	1.5	15.84	-11, +11, .....	15.22:	(...., + 8) - 17, ...	+0.62:
955..	10.1	14.92	+12, - 7, - 4, ...	14.55	(...., 0) 0, ...	+0.37
962..	10.0	15.79	+31, -14, -17, ...	14.86	(...., + 8) - 8, ...	+0.93
969..	8.5	16.15	0, 0, .....	15.76	(- 7, + 8).....	+0.39
974..	7.7	16.10	0, + 1, .....	14.97	(+ 6, - 6).....	+1.13
974a.	7.0	16.78	(+ 1, - 1).....	16.26	(-11, + 6).....	+0.52
982.	1.3	15.98	...., ....., - 9, + 9	15.32	...., ....., .....	+0.66
1000..	3.0	14.08	-20, - 9, +15, +12	12.83	+13, - 7, - 5, ...	+1.25
1000a.	2.8	17.45	(-14, +14).....	16.88	( 0, 0).....	+0.55
1009..	4.0	15.67	- 4, +19, -16, ...	15.76	(+ 2, - 3).....	-0.09
1012..	1.7	15.72	- 2, + 1, ....., 0	15.64	( 0, 0).....	+0.08
1014..	1.9	15.69	+ 4, +13, -18, ...	14.96	(+12, -11).....	+0.73
1017..	6.6	16.39	+ 9, + 2, ....., -12	15.96	(-15, +14).....	+0.43
1022..	2.0	16.66	-16, +16, .....	16.44	(+ 2, - 3).....	+0.22
1022a.	2.1	16.82	(- 3, + 3).....	16.97	(-13, +13).....	-0.15
1028..	2.3	15.66	-12, +11, .....	14.73	...., - 6, + 8, ...	+0.93
					(...., - 3)	
1028a.	2.3	17.27	(+18, -18).....	16.92	(+12, -11).....	+0.35
1028b.	2.2	16.54	(-17, +16).....	15.96	(- 6, + 7).....	+0.58
1028c.	2.2	17.46	(...., m).....	17.07	(...., m).....	+0.39
1039..	2.0	15.02	+ 2, - 9, ....., + 7	13.96	-11, + 5, + 5, ...	+1.06
1047..	1.8	15.95	0, + 4, ....., - 3	14.99	(- 1, + 1).....	+0.96
1050..	1.6	15.38	+16, -17, .....	14.17	...., ....., m, ...	+1.21
1055†.	4.6	15.95	- 7, + 7, ....., + 1	15.26	(+14, -14).....	+0.69
1061..	2.1	16.64	-14, +13, .....	15.88	(- 1, + 2).....	+0.76
1062..	1.8	15.35	+19, - 6, -14, ...	14.60	(...., - 5) + 5, ...	+0.75
1063..	2.2	16.08	- 7, + 3, ....., + 5	15.14	(+ 3, - 2).....	+0.94
1064..	1.8	16.23	-13, +14, ....., - 2	15.25	(- 5, + 5).....	+0.98
1070..	2.1	16.19	- 7, + 3, ....., + 4	16.20	(- 5, + 6).....	-0.01
1076..	1.8	16.12	- 2, + 3, .....	15.56	(- 9, + 8).....	+0.56
1076a.	1.9	17.08	(- 8, + 9).....	16.16	(-10, +10).....	+0.92
1086..	2.0	16.42	- 8, + 9, .....	15.66	(- 2, + 1).....	+0.76
1089..	2.2	15.18	+ 7, + 3, -11, ...	14.09	...., ....., m, ...	+1.09
1090a.	2.1	17.08	(- 8, + 9).....	16.48	(+13, -13).....	+0.60
1090b.	2.3	17.08	( 0, + 1).....	16.47	(+ 6, - 6).....	+0.61
1090c.	2.3	16.34	(- 4, + 4).....	15.60	(- 5, + 4).....	+0.74
1098..	1.8	16.48	+ 4, - 3, .....	15.64	(...., m).....	+0.84
1101..	4.4	15.90	- 1, 0, .....	14.88	(+15, -15).....	+1.02
1120..	2.2	16.12	+ 5, - 4, .....	15.96	(- 6, + 7).....	+0.16
1120a.	2.3	17.02	(- 2, + 3).....	16.58	(-12, +11).....	+0.44
1123..	2.5	15.52	- 2, +21, -20, ...	15.52	(+ 9, -10).....	0
1123a.	2.5	17.32	(- 1, + 2).....	17.03	(...., m).....	+0.29
1123b.	2.5	17.24	(+11, -11).....	16.76	(+ 8, - 7).....	+0.48
1123c.	2.4	17.56	( m, ....).....	17.02	(- 4, + 5).....	+0.54
1127..	1.6	13.92	- 9, + 7, ....., + 3	12.62	...., - 1, 0, ...	+1.30
1127a.	1.7	16.52	(-13, +14).....	15.80	(- 5, + 4).....	+0.72
1128..	3.6	14.08	-20, - 5, +15, +12	14.68	...., -17, + 1, - 1	-0.60
					(...., +17)	



TABLE II—Continued

NUM- BER	DIS- TANCE	PHOTOGRAPHIC		PHOTO-VISUAL		COLOR- INDEX
		Mag.	Residuals	Mag.	Residuals	
1128a.	3.5	17.08	(- 4, + 5).....	16.51	(+ 2, - 2).....	+0.57
1128b.	3.4	17.32	(+ 3, - 2).....	16.82	(+ 6, - 7).....	+0.50
1128c.	3.8	.....	.....	17.12	(+10, - 5).....	.....
1130..	3.2	15.53	- 3, +12, ..., - 8	15.44	(-12, +12).....	+0.09
1131†.	4.0	15.81	- 3, + 7, - 9, + 5	15.48	(- 6, + 5).....	+0.33
1131a.	4.0	17.30	(+ 1, 0).....	16.80	(-15, +15).....	+0.50
1131b.	3.9	17.31	(- 6, + 6).....	16.72	(+ 3, - 3).....	+0.59
1137..	2.2	17.05	m, .....	16.62	(-23, +22).....	+0.43
1140..	4.4	15.89	+12, - 7, ..., - 4	15.06	(+ 2, - 3).....	+0.83
1140a.	4.5	16.96	(-20, +21).....	16.54	(+11, -10).....	+0.42
1140b.	4.3	17.34	(+ 4, - 4).....	17.02	(-14, +15).....	+0.32
1140c.	4.5	17.38	(- 3, + 4).....	17.10	(..., m).....	+0.28
1140d.	4.5	17.29	(- 8, + 8).....	16.84	(..., m).....	+0.45
1141..	3.0	16.21	- 4, - 3, + 8, ...	15.31	(+19, - 3)....., -15	+0.90
1143..	2.2	15.71	-11, +15, ..., - 3	15.02	(+ 6, - 5).....	+0.69
1146..	2.9	15.64	+25, + 9, -34, ...	15.58	(0, + 3)....., - 2	+0.06
1147..	4.6	16.10	+ 5, + 1, ..., - 5	15.53	(- 3, + 3).....	+0.57
1148..	2.6	15.86	+ 3, + 9, ..., -11	15.28	(- 1, 0).....	+0.58
1149..	2.0	16.50	-16, +13, ..., + 4	15.70	(+ 5, - 6).....	+0.80
1149a.	2.0	17.58	(-16, +16).....	17.14	(..., m).....	+0.44
1149b.	1.9	17.54	(-11, + 5).....	16.56	(+ 1, - 2).....	+0.98
1149c.	2.1	17.37	(-12, +12).....	16.87	(+ 6, - 6).....	+0.50
1149d.	2.1	17.38	(+ 4, - 4).....	16.84	(+ 9, - 9).....	+0.54
1149e.	2.2	17.46	(- 1, 0).....	16.96	(- 8, + 7).....	+0.50
1149f*	2.3	.....	.....	17.24	(..., m).....	.....
1149g*	2.3	.....	.....	17.20	(..., m).....	.....
1154..	2.5	15.89	+15, + 6, ..., -21	15.38	(-11, +12).....	+0.51
1154a.	2.5	17.21	+ 4, - 4, .....	16.44	(+ 9, - 9).....	+0.77
1158..	6.2	16.80	..., m, .....	16.56	(- 3, + 2).....	+0.24
1162..	7.7	16.08	- 4, + 3, ..., + 2	15.30	(+ 2, - 2).....	+0.78
1168*.	2.0	16.12	+ 3, +18, -21, ...	14.87	(..., - 9, + 6, ...	+1.25
					(..., + 4)	
1170*.	2.0	15.57	+19, +12, -32, ...	14.54	(..., + 5, - 6, ...	+1.03
1172..	2.8	15.49	- 6, + 2, ..., + 5	14.62	(..., - 1) + 2, ...	+0.87
1172a.	2.9	16.31	(- 1, + 1).....	15.56	(- 3, + 3).....	+0.75
1172b.	3.0	17.28	(- 7, + 6).....	16.68	(+ 2, - 1).....	+0.60
1172c.	2.8	17.08	(0, + 1).....	16.41	(- 5, + 5).....	+0.67
1173..	2.4	15.35	0, +16, -17, ...	14.69	..., m, .....	+0.66
1174..	1.8	16.56	- 6, + 7, .....	15.66	(- 2, + 1).....	+0.90
1175..	2.7	15.37	+ 9, + 1, -10, ...	14.34	(..., - 8) + 9, ...	+1.03
1175a.	2.7	17.00	(0, + 1).....	.....	.....	.....
1178..	5.3	16.22	+ 3, - 4, .....	15.60	(+ 7, - 7).....	+0.62
1178a.	5.0	17.09	(-12, +12).....	16.87	(- 8, + 8).....	+0.22
1178b.	4.8	17.01	(- 4, + 4).....	16.62	(+ 3, - 2).....	+0.39
1178c.	5.4	16.96	(+ 4, - 3).....	16.62	(-19, +19).....	+0.34
1178d.	5.4	17.21	(+ 4, - 4).....	17.20	(..., m).....	+0.01
1181a.	3.0	17.32	(-11, +10).....	16.66	(-16, +15).....	+0.66
1181b.	3.1	17.10	(- 2, + 3).....	16.48	(+ 2, - 2).....	+0.62
1182..	2.2	16.18	+ 2, - 3, .....	15.14	(+ 3, - 2).....	+1.04
1186..	2.4	16.01	- 3, +10, ..., - 6	15.32	(+ 8, - 7).....	+0.69
1192..	2.0	16.22	- 5, + 4, ..., + 1	15.39	(..., m).....	+0.83
1199..	2.8	15.55	- 1, - 4, ..., + 6	14.76	(..., + 6) - 6, ...	+0.79

TABLE II—Continued

NUMBER	DISTANCE	PHOTOGRAPHIC		PHOTO-VISUAL		COLOR-INDEX
		MAG.	Residuals	MAG.	Residuals	
1201a.	3.6	17.49:	(..., m).....	16.98	( 0,+ 1).....	+0.51:
1201b.	3.6	17.48	(- 3,+ 1).....	17.05	(-26,+26).....	+0.43
1201c*	3.5	17.04:	( m,...).....	17.31:	(..., m).....	-0.27:
1201d*	3.5	17.35:	( m,...).....	17.10	(-22,+21).....	+0.25:
1203..	2.7	14.40	-14,- 1,...,+14	13.08	+ 4,- 3,- 2,...	+1.32
1204..	2.6	16.02	...,..., m,...	15.22	(- 2,+ 3).....	+0.80
1205..	2.2	16.86	- 9,+ 8,...	16.68	(+ 7,- 8).....	+0.18
1205a.	2.3	.....	...,...,...	17.00	(- 2,+ 3).....	.....
1206..	1.8	16.15	-11,+11,.....	15.20	(- 3,+ 2).....	+0.95
1206a.	1.8	17.00	( 0,+ 1).....	16.08	(-11,+12).....	+0.92
1206b.	1.7	16.32	(- 2,+ 3).....	15.40	(+ 5,- 4).....	+0.92
1206c.	1.8	16.04	(- 6,+ 7).....	15.36	(+ 1, 0).....	+0.68
1208..	2.0	14.40	-14,+ 3,...,+11	13.17	0,+ 2,- 2,...	+1.23
1210..	6.4	16.00	+ 4,- 5,...	15.57	(+ 4,- 4).....	+0.43
1211..	1.9	15.82	+13,-14,+ 9,-10	15.12	(+10,- 9).....	+0.70
1212..	2.0	15.34	+16,- 5,-11,...	14.57	...,+ 2,+13,...	+0.77
1213..	2.0	15.36	+10,+ 2,-13,...	15.12	(+13,-12).....	+0.24
1214..	1.8	14.40	-27,+12,+14,...	13.18	+ 9,-13,+ 4,...	+1.22
1215..	1.9	16.02	+ 2,- 3,...	15.75	( m,...).....	+0.27
1216..	1.9	16.61	-14,+14,.....	15.86	(- 2,+ 1).....	+0.75
1217..	1.8	14.86	+12,-17,+ 1,+ 5	13.69	..., m,...	+1.17
1218..	2.5	16.70	-11,+10,.....	15.08	(- 5,+ 5).....	+0.72
1218a.	2.5	17.30	(- 5,+ 4).....	16.65	(- 4,+ 4).....	+0.65
1218b.	2.4	17.31	(- 6,+ 6).....	16.84	(+ 9,- 9).....	+0.47
1219..	1.9	14.04	- 3,-12,+16,...	12.64	+11,-13,+ 2,...	+1.40
1222a.	2.0	17.40	(- 9,+ 9).....	16.65	(+14,-14).....	+0.75
1222b.	2.1	17.22	(-12,+12).....	16.44	(+ 2,- 3).....	+0.78
1222c.	2.2	17.36	(+ 9,-10).....	17.03	(..., m).....	+0.33
1223..	5.3	16.61	+ 9,- 1,...,- 7	15.82	(- 4,+ 5).....	+0.79
1223a.	5.1	17.10	(-10,+11).....	16.90	(- 2,+ 1).....	+0.20
1223b.	5.4	17.28	(+ 7,- 7).....	16.92	(-27,+28).....	+0.36
1224..	2.9	14.78	+ 5,- 9,...,+ 5	13.57	+ 4,- 5,+ 1,...	+1.21
1225..	1.9	15.33	+ 6,- 4,- 3,...	14.46	..., - 8,+11,...	+0.87
1225a.	2.0	17.04	(- 4,+ 3).....	16.44	(+ 6,- 6).....	+0.60
1225b.	2.0	17.01	(- 8,+ 8).....	16.36	(+10,-10).....	+0.65
1225c.	1.9	17.18	(- 8,+ 7).....	16.50	( m,...).....	+0.68
1226..	2.1	16.02	- 1,+ 2,...	15.47	(+11,-11).....	+0.55
1227*	4.0	16.36	+ 6,- 6,...	15.57	(- 2,+ 2).....	+0.79
1227a.	4.1	16.98	(+ 6,- 5).....	16.31	(-10,+10).....	+0.67
1227b.	4.1	17.28	(- 3,+ 2).....	17.00	(+ 4,- 5).....	+0.28
1227c.	4.0	17.40	(- 5,+ 6).....	16.94	(- 1,+ 1).....	+0.46
1227d.	3.8	17.34	(- 9,+ 8).....	17.12	(- 2,+ 2).....	+0.22
1229..	2.1	15.63	- 9,+ 9,...	14.64	(...,+ 3)- 3,...	+0.99
1230..	2.3	16.71	+ 6,-11,...,+ 6	16.03	(-13,+13).....	+0.68
1235..	2.2	16.31	- 4,+ 4,...	15.24	(- 4,+ 4).....	+1.07
1236..	2.0	15.35	+15,- 6,- 8,...	14.32	(...,+ 1) 0,...	+1.03
1236a.	1.9	16.52	(+10,-11).....	15.71	(+ 1,- 1).....	+0.81
1238..	2.1	15.78	- 8,+ 8,...	15.64	( 0, 0).....	+0.14
1239..	2.2	15.24	+ 1,+ 5,- 6,...	14.56	...,..., - 6,+ 7	+0.68
1240..	3.0	15.84	-11,+11,.....	15.22	(- 5,+ 6).....	+0.62

TABLE II—Continued

NUM- BER	DIS- TANCE	PHOTOGRAPHIC		PHOTO-VISUAL		COLOR- INDEX
		Mag.	Residuals	Mag.	Residuals	
1241*	2.1	15.00	+ 8,+21,-29,....	13.70	....., - 4,+ 5,....	+1.30
1242..	2.1	15.98	+ 3,+ 5,- 7,....	15.77	(+ 7,- 7).....	+0.21
1242a.	2.3	16.55	(+11,-11).....	15.68	(+ 4,- 4).....	+0.87
1243..	2.8	16.37	-10,- 7,+15,+ 1	15.60	(- 5,+ 4).....	+0.77
1243a.	2.8	16.67	(+ 5,- 5).....	16.24	( 0,- 1).....	+0.43
1244*	2.1	15.79	- 3,+25,-21,....	14.59	.....,-32,+ 2,....	+1.20
					(.....,+14)	
1244a.	2.1	17.16	(- 2,+ 1).....	16.42	(- 3,+ 4).....	+0.74
1246..	2.5	15.01	0, 0,.....	14.01	+ 4,- 3,- 2,....	+1.00
1247..	2.2	15.81	-14,+14,.....	15.70	(- 1, 0).....	+0.11
1247a.	2.4	16.94	(+ 6,- 5).....	16.34	(- 7,+ 7).....	+0.60
1247b.	2.3	17.04	( 0,+ 1).....	16.40	(- 7,+ 6).....	+0.64
1249..	2.4	16.18	+ 4,- 3,.....	16.13	(-10,+10).....	+0.05
1250a.	5.6	16.94	(- 8,+ 7).....	16.28	(-10,+10).....	+0.66
1251..	7.1	16.50	0,+ 1,.....	15.74	(- 2,+ 2).....	+0.76
1254..	7.4	15.82	+ 1, 0,.....	15.57	(+ 4,- 4).....	+0.25
1254a.	7.5	16.01	(- 7,+ 7).....	15.62	(- 1,+ 2).....	+0.39
1255..	2.4	15.61	+ 6,-14,.....,+ 7	15.48	(- 3,+ 2).....	+0.13
1258..	2.1	15.21	+ 4,+ 8,-12,....	14.26	(.....,- 1)+ 1,....	+0.95
1260..	2.2	15.80	+ 6,- 7, 0,....	15.24	(- 2,+ 1).....	+0.56
1261..	3.2	15.30	+13,-13,- 7,+ 8	14.58	(.....,+ 2)- 3,....	+0.72
1261a.	3.4	15.98	(- 7,+ 6).....	15.52	(+ 1,- 2).....	+0.46
1262..	2.2	15.43	- 8,+22,-13,....	15.30	(+ 2,- 2).....	+0.13
1263..	7.3	15.35	+ 4,-10,+ 6,....	15.38	(- 8,+ 9).....	-0.03
1264..	8.2	15.98	+ 8,- 8,.....	15.36	(- 4,+ 3).....	+0.62
1265a.	3.4	16.84	(-12,+12).....	16.37	(- 1,+ 1).....	+0.47
1265b.	3.4	16.45	(- 8,+ 8).....	15.82	(+ 2,- 3).....	+0.63
1265c.	3.4	17.28	(- 7,+ 6).....	16.88	(- 4,+ 3).....	+0.40
1265d.	3.5	17.42	(- 7,+ 7).....	16.94	(- 6,+ 5).....	+0.48
1265e.	3.7	16.76	(- 6,+ 5).....	16.24	(+ 3,- 4).....	+0.52
1265f.	3.6	17.30	(+ 5,- 4).....	17.12	(-19,+19).....	+0.18
1265g.	3.5	15.96	(- 2,+ 1).....	15.08	(-10,+ 9).....	+0.88
1269..	6.0	14.73	+ 8,+ 8,-14,- 1	13.86	- 9,.... + 9,....	+0.87
1270..	6.5	14.85	-24,+20,....,+ 5	13.86	+ 1,- 5,+ 5,....	+0.99
1270a.	6.4	17.21	(-13,+13).....	16.84	(- 5,+ 4).....	+0.37
1270b.	6.4	17.02	(+ 6,- 6).....	16.84	(- 5,+ 4).....	+0.18
1271..	2.7	15.69	+20, 0,-18,- 1	14.68	.....,+10,.....	+1.01
					(.....,- 9)	
1271a.	2.8	16.64	(+ 2,- 2).....	15.06	(- 6,+ 7).....	+0.68
1273..	2.8	14.53	-20,+ 3,+ 1,+15	13.29	+ 3, 0,- 4,....	+1.24
1274..	2.6	15.24	+ 1,- 7,- 6,+14	14.57	.....,- 2,- 3,....	+0.67
					(.....,+ 4)	
1275..	5.1	16.22	- 2,- 7,+ 7,+ 1	15.37	(-10,+10).....	+0.85
1278..	2.4	16.24	- 7,+ 6,.....	15.29	(-14,+ 4).....,+11	+0.95
1278a.	2.3	17.61	(+17,- 9).....	17.24	(....., m).....	+0.37
1279..	2.4	15.94	- 5,....,+ 4,....	15.09	(-11,+11).....	+0.85
1280..	3.1	16.75	+ 5,+ 2,....,- 7	16.34	(+ 2,- 2).....	+0.41
1280a.	3.0	17.36	(- 5,+ 6).....	16.84	(-14,+15).....	+0.52
1280b.	2.9	17.36	(- 1,+ 1).....	17.21	(+ 1,- 1).....	+0.15
1283..	2.6	16.04	- 6,+ 7,- 2,....	15.03	(+12,-12).....	+1.01
1283a.	2.7	16.67	(+ 5,- 5).....	16.08	(-15,+15).....	+0.59
1285..	2.8	15.97	- 8,+ 7,+ 1,+ 1	15.96	(+ 1, 0).....	+0.01

TABLE II—Continued

NUM- BER	DIS- TANCE	PHOTOGRAPHIC		PHOTO-VISUAL		COLOR- INDEX
		Mag.	Residuals	Mag.	Residuals	
1285a.	3.1	17.35	(- 7, + 7).....	17.23	(+ 6, - 6).....	+0.12
1285b.	3.2	17.34	(- 3, + 3).....	17.08	(-10, + 9).....	+0.26
1286..	2.5	16.30	- 3, + 4,.....	15.57	(- 7, + 4)....., + 2	+0.73
1287..	4.4	15.89	+ 6, + 1, - 6,...	15.50	(+ 3, + 6)....., -10	+0.39
1287a.	4.4	17.13	(+ 8, - 8).....	16.82	(- 3, + 2).....	+0.31
1289..	3.2	16.24	-14, + 6,....., + 8	15.38	(-11, +12).....	+0.86
1289a.	3.1	16.34	( 0, + 1).....	15.94	(- 7, + 6).....	+0.40
1290..	2.8	15.46	+17, + 1, -19,...	14.62	0, - 1).....	+0.84
1290a.	3.0	17.34	(- 9, + 8).....	16.90	(- 2, + 1).....	+0.44
1290b.	3.0	17.48	( 0, + 1).....	16.84	(- 5, + 4).....	+0.64
1292a.	2.5	17.36	(+ 2, - 2).....	16.86	(+18, -17).....	+0.50
1292b.	2.5	17.49	(+ 3, - 3).....	17.22	(- 6, + 5).....	+0.27
1293..	3.8	16.24	+10, - 9,.....	15.54	(- 1, + 2).....	+0.70
1293b.	3.9	17.34	(- 3, + 3).....	16.94	(-10, + 9).....	+0.40
1293c.	3.9	16.27	(+10, -10).....	15.58	( 0, + 1).....	+0.69
1294..	4.4	15.76	- 9, +10,....., - 1	15.25	(- 3, + 3).....	+0.51
1294a.	4.3	17.24	(- 6, + 6).....	16.81	(+ 7, - 7).....	+0.43
1294b.	4.1	17.38	(- 3, + 4).....	17.05	(-12, +12).....	+0.33
1294c.	4.1	17.64	(+ 1, - 1).....	17.12	(-14, +15).....	+0.52
1296..	2.5	15.34	(+16, - 9, - 7,...	15.18	(+ 7, - 6).....	+0.16
1296a.	2.5	15.81	( 0, 0).....	15.84	( 0, 0).....	-0.03
1296b.	2.7	17.45	(- 7, + 7).....	17.20	(..., m).....	+0.25
1296c.	2.7	17.42	(- 4, + 4).....	17.10	(..., m).....	+0.32
1299..	4.0	15.78	- 8, - 9, +17, + 1	15.37	(- 5, + 5).....	+0.41
1299a.	4.1	16.92	(- 2, + 1).....	16.36	(- 9, + 8).....	+0.56
1300..	2.7	15.98	+ 9, + 6, -15,...	15.32	(- 5, - 4)....., + 8	+0.66
1301..	3.4	15.35	-10, -10,....., +19	14.57	(- 4, + 4).....	+0.78
1302..	2.9	16.84	- 2, + 1,.....	16.03	(-13, +13).....	+0.81
1303..	4.7	15.98	0, 8, + 7,...	15.00	(+10, - 6)....., - 3	+0.98
1303a.	4.4	16.22	(- 2, + 1).....	15.52	(- 2, + 1).....	+0.70
1304..	2.8	16.33	(- 1, + 1).....	15.61	(..., m).....	+0.72
1304a.	2.9	16.59	(-37, +37).....	16.08	(-15, +15).....	+0.51
1304b.	2.9	17.31	(-10, +21).....	16.96	(-12, +11).....	+0.42
1304c.	2.8	17.15	(-15, +15).....	16.64	(-14, +14).....	+0.51
1304d*	2.9	17.38	(-28, +27).....	17.17	(..., m).....	+0.21
1305..	4.6	15.22	- 4, -13, + 2, +15	14.50	(..., + 4) - 5,...	+0.72
1306..	6.6	15.92	0, - 2, + 3,...	15.50	0, 0).....	+0.42
1307a.	3.3	17.38	(-13, +14).....	17.20	(+ 4, - 3).....	+0.18
1309..	3.4	16.07	+ 5, -12, + 6,...	16.00	(-13, +13).....	+0.07
1309a.	3.6	17.16	(+12, -11).....	17.00	(-21, +20).....	+0.16
1310..	3.0	15.48	-13, +13,.....	14.64	(+ 4, - 6) + 3,...	+0.84
1312..	4.1	16.11	- 4, - 7,....., +12	15.32	(+ 3, - 4).....	+0.79
1313..	3.0	14.90	- 3, - 1, + 3,...	13.86	(- 6, + 7, - 1,...	+1.04
1313a.	2.9	16.98	(+ 6, - 5).....	16.68	(+16, -17).....	+0.30
1314..	10.5	15.86	- 3, + 4,.....	15.22	(-10, +11).....	+0.64
1315..	3.2	15.25	+ 4, 0, - 4,...	14.43	(+12, -12).....	+0.82
1315a.	3.4	17.34	(- 3, + 3).....	16.90	(- 2, + 1).....	+0.44
1316..	3.5	15.90	+ 2, 0, - 2,...	15.46	(+ 1, - 1).....	+0.44
1318..	8.0	15.68	-22, - 3, +20, + 4	15.72	(-11, +12).....	-0.04
1318a.	7.8	16.38	(-18, +17).....	15.82	(- 7, + 8).....	+0.56
1319..	3.1	15.94	+ 4, + 1, - 6,...	15.48	(-11, + 2)....., + 8	+0.46
1319a.	3.0	17.32	(-14, +14).....	17.02	(- 4, + 5).....	+0.30

TABLE II—Continued

NUM- BER	DIS- TANCE	PHOTOGRAPHIC		PHOTO-VISUAL		COLOR- INDEX
		Mag.	Residuals	Mag.	Residuals	
1319b.	3.0	17.24	(- 3,+ 2).....	16.82	(-12,+13).....	+0.42
1322..	6.7	15.62	+ 1,+11,-11,....	15.81	(- 6,+ 6).....	-0.19
1323..	3.4	16.08	+ 4,- 4,.....	15.24	(+ 1,- 2).....	+0.84
1324..	5.5	15.64	- 1,+ 1,.....+ 1	15.74	(- 7,+ 7).....	-0.10
1324a.	5.6	17.12	(- 2,+ 1).....	16.86	(- 2,+ 2).....	+0.26
1324b.	5.5	16.99	(- 2,+ 2).....	16.63	(- 6,+ 6).....	+0.36
1324c.	5.8	16.96	(+ 4,- 3).....	16.78	(- 3,+ 3).....	+0.18
1324d.	6.2	17.31	(- 3,+ 3).....	16.98	(-19,+19).....	+0.33
1325..	5.0	15.23	+ 9,- 6,- 2,....	14.45	..... m,....	+0.78
1327f.	5.9	16.17	- 7,- 5,.....+11	15.49	(- 4,+ 4).....	+0.68
1329..	3.4	15.93	+11,-11,.....	15.50	(- 8,+ 9).....	+0.43
1329a.	3.2	17.04	(+ 4,- 3).....	16.46	( 0, 0).....	+0.58
1329b.	3.2	17.32	(- 4,+ 5).....	17.15	(- 5,+ 5).....	+0.17
1331..	9.3	15.89	+ 3,- 3,.....	15.15	(- 7,+ 7).....	+0.74
1331a.	9.5	16.06	(+ 6,- 5).....	15.46	(- 1,+ 1).....	+0.60
1332..	5.1	15.60	-10,+13,.....- 2	14.82	(- 5,+ 6).....	+0.78
1333..	3.9	16.48	-14,+15,.....	15.74	(-10,+10).....	+0.74
1334..	3.8	16.12	+ 3,- 4,.....	15.40	(- 3,+ 2).....	+0.72
1335..	3.5	15.60	- 6,+ 5,.....	15.53	(- 8,+ 8).....	+0.07
1336..	4.3	16.26	+ 1, 0,.....	15.56	(- 1, 0).....	+0.70
1338..	3.5	15.48	+15,-14,.....	14.70	(- 8,- 9).....+17	+0.78
1338a.	3.6	17.40	(- 5,+ 6).....	17.14	(- 4,+ 3).....	+0.26
1339..	5.9	15.90	+11,- 8,- 2,....	15.08	( 0,+ 1).....	+0.82
1339a.	5.6	17.30	(+18,- 9).....	16.96	(-17,+18).....	+0.34
1340..	5.9	15.68	- 9,+ 9, 0,....	15.58	(- 3,+ 3).....	+0.10
1340a.	6.5	17.07	(-10,+10).....	16.81	(+ 7,- 3).....	+0.26
1340b.	6.4	17.08	( 0,+ 1).....	16.91	(-16,+16).....	+0.17
1342..	5.2	15.03	+ 8,+ 2,-10,....	14.08	- 5,+13,- 7,....	+0.95
1343a*	10.1	16.17	(....., m).....	16.69	(....., m).....	-0.52
1343b.	9.6	17.08	( 0,+ 1).....	16.74	(- 4,+ 4).....	+0.34
1344*	4.2	16.48	-16,+15,.....	16.98	(- 5,+ 5).....	-0.50
1344a*	4.2	.....	.....	17.27	(....., m).....	.....
1345..	4.1	14.76	+ 7,- 7,.....	13.62	- 9,.....+10,....	+1.14
1345a.	4.4	17.16	(-19,+18).....	16.78	(+ 1, 0).....	+0.38
1346..	10.0	11.80	+ 3,- 4,.....	10.57	+36,- 5,-30,....	+1.23
1346a.	9.6	16.92	(-16,+17).....	16.51	(-12,+12).....	+0.41
1346b.	10.4	16.93	(- 3,+ 3).....	16.48	(-12,+12).....	+0.45
1347..	5.5	15.48	- 9,- 1,.....+10	15.50	(+ 5,- 5).....	-0.02
1347a†	5.7	16.79	- 2,+ 2,.....	16.38	(- 2,+ 3).....	+0.41
1350..	4.1	15.89	+ 6,+ 1,+16,-24	15.29	(+ 1,- 1).....	+0.60
1352..	4.4	15.97	+ 4,- 2,- 1,....	16.02	(-15,+14).....	-0.05
1352a.	4.0	17.20	(- 2,+ 1).....	16.66	(-13,+12).....	+0.54
1354..	9.0	16.02	+ 8,- 7,.....	15.42	(- 2,+ 3).....	+0.60
1354a.	9.0	17.20	(- 6,+ 6).....	16.76	(-23 +23).....	+0.44
1356*	6.8	16.22	0, 0,.....	16.10	(+51,-51).....	+0.12
1360..	4.4	14.73	+ 6,- 4,+ 2,- 5	13.69	-12,.....+12,....	+1.06
1360a.	4.1	17.40	(- 2,+ 2).....	17.26	(- 4,+ 5).....	+0.14
1360b.	4.0	17.22	(-14,+15).....	16.85	(-10,+10).....	+0.37
1361..	9.8	16.86	-11,+12,.....	16.91	(....., m).....	-0.05
1362..	6.3	14.72	+ 3,-11,-10,+18	13.75	-10,+ 4,+ 6,....	+0.97

TABLE II—Continued

NUM- BER	DIS- TANCE	PHOTOGRAPHIC		PHOTO-VISUAL		COLOR- INDEX
		Mag.	Residuals	Mag.	Residuals	
1363..	4.5	15.21	+ 1, - 4, + 2, ...	14.45	..., ..., m, ...	+0.76
1363a.	5.0	16.74	(- 4, + 3) ..., ...	16.37	(- 1, + 1) ..., ...	+0.37
1363b.	4.9	17.17	(+ 4, - 4) ..., ...	16.56	(- 6, + 7) ..., ...	+0.61
1364..	4.7	15.96	- 7, - 19, + 18, + 6	15.31	(- 16, + 16) ..., ...	+0.65
1364a.	4.6	17.05	(+ 9, - 9) ..., ...	16.54	(+ 11, - 10) ..., ...	+0.51
1365..	4.7	15.64	+ 3, - 3, ..., ...	15.63	(+ 4, - 4) ..., ...	+0.01
1365a.	5.2	16.98	(+ 2, - 2) ..., ...	16.62	(- 1, + 1) ..., ...	+0.36
1365b.	4.5	17.27	(+ 1, - 1) ..., ...	17.17	..., m, ...	+0.10
1366..	9.6	15.85	- 2, - 12, + 3, + 10	15.09	(+ 3, - 3) ..., ...	+0.76
1367..	4.7	16.54	- 12, + 12, ..., ...	15.70	(- 1, 0) ..., ...	+0.84
1368..	6.1	16.20	+ 2, - 2, ..., ...	15.54	(+ 1, - 1) ..., ...	+0.66
1369..	5.0	15.94	+ 4, - 4, ..., ...	16.16	(- 4, + 4) ..., ...	-0.22
1371..	5.8	15.36	+ 7, - 7, ..., ...	15.32	(+ 5, - 4) ..., ...	+0.04
1371a.	5.6	17.38	(- 7, + 8) ..., ...	16.94	(- 15, + 16) ..., ...	+0.44
1372..	5.6	15.27	+ 12, - 22, - 5, + 15	14.45	(+ 1, - 1) ..., ...	+0.82
1372a.	5.7	16.42	(+ 13, - 13) ..., ...	15.99	(- 15, + 14) ..., ...	+0.43
1372b†	6.6	16.43	+ 9, - 12, ..., + 2	15.78	(- 14, + 15) ..., ...	+0.65
1373a.	6.7	17.02	(+ 12, - 13) ..., ...	17.04:	(m, ...) ..., ...	-0.02:
1374..	6.3	15.30	+ 5, - 25, + 11, + 8	14.68	(- 2, + 2) ..., ...	+0.62
1375..	12.1	...	..., ..., ..., ...	12.68	..., m, ...	...
1376..	5.9	14.63	+ 2, - 2, + 1, ...	13.52	- 5, - 4, + 9, ...	+1.11
1376a.	5.1	15.66	(- 1, + 1) ..., ...	15.72	(- 3, + 4) ..., ...	-0.06
1376b.	4.6	17.07	(- 10, + 10) ..., ...	16.63	(- 2, + 2) ..., ...	+0.44
1377..	5.5	16.55	- 11, + 11, ..., ...	15.76	(- 7, + 8) ..., ...	+0.70
1378..	6.2	16.02	- 1, + 2, ..., ...	15.52	(- 2, + 1) ..., ...	+0.50
1379..	5.6	16.68	+ 4, - 5, ..., ...	16.00	(- 13, + 13) ..., ...	+0.68
1380a.	7.7	16.08	(+ 1, 0) ..., ...	15.46	(+ 7, - 7) ..., ...	+0.62
1381..	5.6	16.54	- 4, + 3, ..., ...	15.84	(- 3, + 3) ..., ...	+0.70
1382..	5.7	16.01	+ 6, - 11, + 4, ...	15.53	(0, 0) ..., ...	+0.48
1383..	8.3	15.04	+ 15, - 15, ..., ...	13.91	..., ..., m, ...	+1.13
1383a.	8.2	16.99	(+ 1, - 1) ..., ...	16.13	(- 13, + 13) ..., ...	+0.86
1385..	7.4	16.24	+ 6, - 6, ..., ...	15.50	(0, 0) ..., ...	+0.74
1386a.	5.6	17.00	(0, + 1) ..., ...	16.56	(- 13, + 13) ..., ...	+0.44
1387..	9.6	15.56	- 10, + 9, ..., ...	14.96	(- 11, + 10) ..., ...	+0.60
1388a.	6.8	17.00	(0, 0) ..., ...	16.36	(0, - 1) ..., ...	+0.64
1389..	9.6	15.58	- 8, + 7, ..., ...	...	..., ..., ..., ...	...
1390..	6.0	15.85	+ 13, - 8, + 15, - 20	15.46	(- 6, + 7) ..., ...	+0.39
1391..	6.1	15.12	- 1, - 7, 0, + 9	14.13	(..., + 9) - 9, ...	+0.99
1391a.	6.4	16.90	(0, - 1) ..., ...	16.32	(- 2, + 3) ..., ...	+0.58
1391b.	6.1	17.02	(+ 6, - 6) ..., ...	16.72	(- 2, + 3) ..., ...	+0.30
1392..	8.1	14.14	- 16, - 11, + 11, + 18	12.92	- 12, + 7, + 4, ...	+1.22
1392a.	7.5	17.01	(- 8, + 8) ..., ...	16.82	(- 7, + 6) ..., ...	+0.19
1393..	6.5	15.57	+ 3, - 1, - 2, ...	15.53	(- 8, + 8) ..., ...	+0.04
1393a.	6.6	16.80	(+ 6, - 7) ..., ...	16.48	(- 9, + 10) ..., ...	+0.32
1393b.	6.5	17.24	(- 10, + 10) ..., ...	16.80	(- 10, + 11) ..., ...	+0.44
1393c.	6.4	16.68	(- 6, + 5) ..., ...	16.38	(+ 1, 0) ..., ...	+0.30
1393d.	6.0	17.45	(m, ...) ..., ...	...	..., ..., ..., ...	...
1396..	9.9	16.07	+ 3, - 3, ..., ...	15.36	(- 4, + 3) ..., ...	+0.71
1396a.	9.2	16.86	(0, 0) ..., ...	16.61	(- 11, + 11) ..., ...	+0.25
1396b.	9.1	16.96	(+ 1, 0) ..., ...	16.69	(..., m) ..., ...	+0.27
1397..	7.4	14.29	- 7, + 2, + 4, ...	12.60	- 6, - 11, + 17, ...	+1.69
1397a.	7.1	16.90	(- 4, + 3) ..., ...	16.58	(- 1, 0) ..., ...	+0.32

TABLE II—Continued

NUM- BER	DIS- TANCE	PHOTOGRAPHIC		PHOTO-VISUAL		COLOR INDEX
		Mag.	Residuals	Mag.	Residuals	
1401..	8.8	15.32	- 7, + 6, .....	15.44	(- 2, + 1) .....	-0.12
1402..	9.6	13.44	-29, +30, .....	12.78	....., m, .....	+0.66
1403..	10.6	16.60	- 6, + 6, .....	16.14	(- 5, + 6) .....	+0.46
1403a.	10.5	16.96	(+ 1, 0) .....	16.60	(-21, +20) .....	+0.36
1405..	7.1	16.26	-11, +11, .....	15.47	( 0, 0) .....	+0.79
1405a.	6.8	17.10	(-10, +11) .....	16.61	(- 8, + 8) .....	+0.49
1408..	9.6	15.91	+ 1, - 1, .....	15.12	(- 4, + 5) .....	+0.79
1408a.	9.2	17.01	(....., m) .....	16.35	(....., m) .....	+0.66
1412..	7.6	15.72	+ 4, - 3, .....	14.87	(+ 5, - 5) .....	+0.85
1412a.	8.6	16.82	(- 3, + 3) .....	16.48	(- 2, + 3) .....	+0.34
1412b.	8.1	16.98	(+ 2, - 2) .....	16.78	(-17, +17) .....	+0.20
1413..	7.7	15.68	+ 5, -11, +21, -13	15.50	(+ 3, - 3) .....	+0.18
1417..	9.6	16.24	-17, +17, .....	15.82	(-13, +14) .....	+0.42
1417a.	9.4	16.66	(- 4, + 4) .....	16.20	(- 8, + 9) .....	+0.46
1418..	8.3	15.44	- 5, -10, +14, .....	14.55	(+ 1, - 1) .....	-0.11
1420..	9.4	14.92	+ 6, - 7, + 1, .....	14.14	(+12, -11) .....	+0.78
1422b.	8.3	17.10	(-10, +11) .....	16.81	(....., m) .....	+0.29
1422c.	8.5	16.70	(+ 9, - 8) .....	16.34	(-10, +10) .....	+0.36
1423..	10.0	15.01	0, 0, .....	14.35	(+ 7, - 7) .....	+0.66
1426..	9.7	15.28	+15, -23, + 9, .....	14.55	(+ 9, - 9) .....	+0.73
1426a.	8.8	16.72	( 0, + 1) .....	16.25	(- 1, + 1) .....	+0.47
1429..	10.4	15.73	-13, +13, .....	15.38	(- 1, + 1) .....	+0.35
1433..	9.5	16.30	+ 4, - 4, .....	15.72	(- 3, + 4) .....	+0.58
1435..	9.6	15.92	+ 9, -10, .....	15.36	(+ 4, - 3) .....	+0.56
1437..	10.7	12.10	+12, -28, +13, + 2	11.75	(- 7, + 7) .....	+0.35
1439..	10.7	13.61	-26, +10, +16, .....	12.86	(-11, +10) .....	+0.75
1441..	10.5	16.75	-19, +19, .....	15.93	( 0, 0) .....	+0.82
1441a.	10.6	16.98	(+ 6, - 5) .....	16.64	(-11, +11) .....	+0.34
1448..	11.3	16.70	+ 2, - 1, .....	16.32	(-26, +26) .....	+0.38
1449..	11.3	14.18	-14, +13, .....	12.78	- 9, .....	+1.40
					(+ 9, .....	

TABLE III  
CO-ORDINATES OF POSTSCRIPT STARS (1900.0)

No.	R.A.	Decl.	No.	R.A.	Decl.
	13 <sup>h</sup>	28°		13 <sup>h</sup>	28°
157a....	36 <sup>m</sup> 50 <sup>s</sup> .9	54' 58"	290b...	37 <sup>m</sup> 26 <sup>s</sup> .4	60' 36"
157b....	36 55.1	54 30	291a...	37 21.1	52 47
157c....	36 55.1	54 40	291b...	37 19.4	52 55
164a....	36 55.2	52 58	291c...	37 20.8	52 54
164b....	36 52.8	52 37	296a...	37 20.8	52 15
164c....	36 52.0	52 37	296b...	37 20.0	52 19
168a....	37 0	57 56	301a...	37 23.3	56 29
175a....	36 57.7	50 20	301b...	37 22.4	56 39
177a....	37 1.8	51 23	301c...	37 21.7	57 4
177b....	37 4.2	51 9	301d...	37 20.8	57 5
179a....	37 1.6	52 38	303a...	37 22.0	52 41
180a....	37 56.2	45 52	305a...	37 23.0	49 9
180b....	36 58.8	45 53	307a...	37 22.6	50 4
181a....	37 2.3	54 26	307b...	37 22.1	50 0
181b....	37 0.7	55 26	308a...	37 24.2	51 38
181c....	36 59.2	55 17	308b...	37 20.8	51 33
188a....	37 7.6	49 18	310a...	37 22.7	51 58
188b....	37 2.1	49 38	311a...	37 23.8	50 27
188c....	37 6.4	50 35	311b...	37 23.9	50 32
188d....	37 8.0	50 29	320a...	37 21.1	47 31
190a....	37 7.2	54 49	320b...	37 21.0	47 24
193a....	37 7.4	59 52	322a...	37 22.7	51 51
205a....	37 10.0	55 10	326a...	37 22.8	54 12
206a....	37 9.6	57 53	326b...	37 22.8	54 19
208a....	37 6.7	47 25	326c...	37 22.6	54 28
210a....	37 10.0	53 58	332a...	37 23.7	56 4
210b....	37 10.0	54 8	332b...	37 23.2	55 44
211a....	37 10.3	52 23	336a...	37 23.6	51 16
211b....	37 11.9	52 12	345a...	37 24.1	50 55
212a....	37 12.4	55 56	348a...	37 25.2	53 25
212b....	37 11.7	56 21	350a...	37 25.2	54 44
215a....	37 10.6	52 49	355a...	37 25.1	52 0
230a....	37 12.3	60 52	360a...	37 25.3	52 54
230b....	37 11.6	61 1	360b...	37 25.3	52 51
230c....	37 11.3	61 15	360c...	37 25.3	52 44
238a....	37 15.5	52 55	360d...	37 24.8	52 56
238b....	37 14.7	52 55	364a...	37 25.7	53 14
247a....	37 17.1	53 37	376a...	37 26.4	53 20
249a....	37 15.4	55 17	378a...	37 27.6	49 19
249b....	37 14.7	55 14	379a...	37 27.0	51 18
250a....	37 16.0	49 30	379c...	37 27.3	51 10
251a....	37 16.8	51 10	380a...	37 26.1	53 33
253a....	37 15.3	55 52	380b...	37 25.7	53 41
255a....	37 18.1	56 55	381a...	37 27.2	53 58
258a....	37 18.4	54 48	381b...	37 27.4	53 59
260a....	37 18.5	52 15	385a...	37 26.9	51 44
261a....	37 18.4	48 12	385b...	37 27.2	51 54
262a....	37 17.2	50 12	386a...	37 26.7	49 56
281a....	37 20.7	56 8	387a...	37 27.3	54 9
290a....	37 21.5	60 21	394a...	37 26.9	53 7



TABLE III—Continued

No.	R.A.	Decl.	No.	R.A.	Decl.
	13 <sup>h</sup>	28°		13 <sup>h</sup>	28°
396a....	37 <sup>m</sup> 27 <sup>s</sup> .6	55' 4"	640a....	37 <sup>m</sup> 32 <sup>s</sup> .8	49' 56"
397a....	37 27.8	52 53	640b....	37 32.4	49 49
403a....	37 27.4	52 38	640c....	37 33.2	49 52
403b....	37 27.2	52 37	640d....	37 33.3	49 47
403c....	37 27.9	52 43	640e....	37 33.6	49 41
403d....	37 27.2	52 29	640f....	37 32.4	50 6
403e....	37 27.5	52 31	649a....	37 32.8	48 34
403f....	37 27.7	52 33	649b....	37 32.5	48 34
403g....	37 27.9	52 34	649c....	37 33.7	49 4
411a....	37 28.3	48 19	665a....	37 33.3	50 48
417a....	37 28.0	52 15	680a....	37 33.0	54 24
417b....	37 27.7	52 20	680b....	37 32.5	54 27
417c....	37 27.5	52 12	680c....	37 33.0	54 30
417d....	37 26.8	52 10	700a....	37 33.5	50 29
418a....	37 28.4	51 25	701a....	37 33.7	58 52
419a....	37 28.5	55 3	701b....	37 31.3	57 59
422a....	37 28.8	51 0	701c....	37 31.0	57 50
425a....	37 27.9	53 54	701d....	37 30.7	57 49
452a....	37 27.8	54 15	713a....	37 37.1	43 46
452b....	37 27.8	54 26	730a....	37 34.1	51 16
452c....	37 29.2	51 14	730b....	37 31.4	57 30
455a....	37 28.8	58 27	739b....	37 35.1	57 63
467a....	37 30.6	55 18	740a....	37 35.4	49 34
467b....	37 30.5	55 22	740b....	37 35.0	49 35
471a....	37 29.4	49 34	758a....	37 34.3	51 10
480a....	37 30.1	56 22	759a....	37 34.1	55 7
480b....	37 30.0	56 46	801a....	37 35.0	51 24
482a....	37 30.2	51 2	801b....	37 35.8	51 24
482b....	37 30.9	51 1	801c....	37 36.3	51 20
499a....	37 27.5	55 59	837b....	37 36.5	56 49
499b....	37 25.1	56 10	845a....	37 36.2	51 4
499c....	37 24.9	56 19	885a....	37 35.5	51 4
499d....	37 24.8	56 4	900a....	37 36.8	50 32
499e....	37 24.9	56 2	900b....	37 36.3	50 26
499f....	37 25.1	56 4	902a....	37 36.0	55 16
499g....	37 24.4	56 8	902b....	37 35.7	55 12
499h....	37 24.3	56 8	925a....	37 36.4	50 6
502a....	37 30.5	50 46	925b....	37 37.1	49 59
513a....	37 31.1	55 3	925c....	37 36.8	49 54
522a....	37 30.5	55 53	925d....	37 36.6	50 1
522b....	37 30.2	55 40	925e....	37 38.2	50 3
522c....	37 30.0	55 44	926a....	37 36.8	57 5
550a....	37 32.1	54 39	945a....	37 37.6	51 20
573a....	37 32.3	56 8	945b....	37 38.1	51 15
590a....	37 32.0	56 29	974a....	37 35.1	45 48
595b....	37 30.3	60 10	1000a....	37 37.5	55 36
605a....	37 32.6	50 36	1022a....	37 38.3	50 55
609a....	37 32.0	56 51	1028a....	37 38.4	55 4
609b....	37 32.5	57 9	1028b....	37 37.8	55 4
621a....	37 34.2	56 4	1028c....	37 37.4	55 5
621b....	37 33.9	56 5	1076a....	37 39.2	51 14
621d....	37 32.4	55 58	1090a....	37 39.5	54 45
628a....	37 32.3	51 22	1090b....	37 40.0	54 54

TABLE III—Continued

No.	R.A.	Decl.	No.	R.A.	Decl.
	13 <sup>h</sup>	28°		13 <sup>h</sup>	28°
1090c...	37 <sup>m</sup> 39 <sup>s</sup> .5	54' 58"	1227c...	37 <sup>m</sup> 42 <sup>s</sup> .2	49' 9"
1120a...	37 40.8	51 0	1227d...	37 41.7	49 25
1123a...	37 39.7	50 38	1236a...	37 43.6	52 34
1123b...	37 39.1	50 32	1242a...	37 44.4	52 11
1123c...	37 38.7	50 36	1243a...	37 46.3	54 53
1127a...	37 40.9	54 7	1244a...	37 44.6	53 29
1128a...	37 39.8	56 10	1247a...	37 45.5	53 42
1128b...	37 41.2	55 58	1247b...	37 45.2	53 42
1128c...	37 42.6	56 21	1250a...	37 44.0	58 15
1131a...	37 39.5	56 50	1254a...	37 44.3	45 47
1131b...	37 38.7	56 44	1261a...	37 45.9	50 29
1140a...	37 39.9	57 15	1265a...	37 43.8	55 44
1140b...	37 39.8	57 2	1265b...	37 43.1	55 49
1140c...	37 43.4	57 0	1265c...	37 42.6	55 54
1140d...	37 44.9	56 48	1265d...	37 43.0	55 59
1149a...	37 41.0	54 20	1265e...	37 45.8	55 46
1149b...	37 40.6	54 19	1265f...	37 45.3	55 45
1149c...	37 41.8	54 24	1265g...	37 45.8	55 34
1149d...	37 41.2	54 28	1270a...	37 45.8	58 49
1149e...	37 42.1	54 29	1270b...	37 46.7	58 46
1149f...	37 43.7	54 16	1271a...	37 46.3	54 13
1149g...	37 43.5	54 19	1278a...	37 45.8	53 1
1154a...	37 41.4	54 59	1280a...	37 45.5	50 51
1172a...	37 41.0	55 33	1280b...	37 45.1	50 55
1172b...	37 41.1	55 29	1283a...	37 46.7	51 54
1172c...	37 41.0	55 34	1285a...	37 47.8	54 22
1175a...	37 41.4	50 37	1285b...	37 47.8	54 28
1178a...	37 40.7	48 4	1287a...	37 46.6	49 19
1178b...	37 42.8	48 20	1289a...	37 46.2	54 54
1178c...	37 42.7	47 48	1290a...	37 47.4	51 30
1178d...	37 41.8	47 40	1290b...	37 47.0	51 28
1181a...	37 42.6	55 28	1292a...	37 46.6	52 51
1181b...	37 42.7	55 31	1292b...	37 46.7	52 53
1201a...	37 41.4	49 35	1293b...	37 48.0	50 11
1201b...	37 41.0	49 34	1293c...	37 48.4	50 20
1201c...	37 41.4	49 38	1294a...	37 47.4	56 16
1201d...	37 41.1	49 39	1294b...	37 46.9	56 6
1205a...	37 43.3	51 24	1294c...	37 47.1	56 1
1206a...	37 42.8	53 36	1296a...	37 46.2	52 17
1206b...	37 42.3	53 43	1296b...	37 47.2	52 20
1206c...	37 42.5	53 46	1296c...	37 47.4	52 23
1218a...	37 43.5	51 11	1299a...	37 48.1	55 50
1218b...	37 43.2	51 18	1303a...	37 48.1	49 26
1222a...	37 43.5	53 50	1304a...	37 48.2	53 26
1222b...	37 43.9	53 51	1304b...	37 47.5	53 24
1222c...	37 44.0	53 59	1304c...	37 48.0	53 12
1223a...	37 43.0	57 40	1304d...	37 48.4	53 16
1223b...	37 44.0	57 52	1307a...	37 47.6	54 42
1225a...	37 44.3	53 18	1309a...	37 48.8	50 51
1225b...	37 43.9	53 22	1313a...	37 48.4	52 36
1225c...	37 43.7	53 9	1315a...	37 48.9	51 26
1227a...	37 43.8	49 16	1318a...	37 48.9	60 5
1227b...	37 44.1	49 20	1319a...	37 49.0	52 26

TABLE III—*Continued*

No.	R.A.	Decl.	No.	R.A.	Decl.
	13 <sup>h</sup>	28°		13 <sup>h</sup>	28°
1319b...	37 <sup>m</sup> 48.8	52' 31"	1372a...	37 <sup>m</sup> 59.3	54' 55"
1324a...	37 49.0	57 33	1372b...	38 1.2	56 11
1324b...	37 47.3	57 37	1373a...	37 58.4	57 7
1324c...	37 48.0	58 0	1376a...	37 55.7	50 36
1324d...	37 49.0	58 15	1376b...	37 54.0	50 51
1329a...	37 49.4	53 23	1380a...	38 1.3	48 1
1329b...	37 49.5	53 31	1383a...	37 56.8	46 13
1331a...	37 48.4	43 42	1386a...	38 0.8	53 8
1338a...	37 51.3	52 16	1388a...	38 0.3	49 1
1339a...	37 50.5	48 19	1391a...	38 4.1	53 45
1340a...	37 53.9	47 49	1391b...	38 2.0	54 39
1340b...	37 54.8	48 13	1392a...	38 1.1	57 44
1343a...	37 44.4	42 57	1393a...	38 3.7	50 51
1343b...	37 44.0	43 29	1393b...	38 3.1	50 46
1344a...	37 52.4	54 52	1393c...	38 3.4	51 16
1345a...	37 53.9	54 34	1393d...	38 1.9	51 31
1346a...	37 53.9	61 45	1396a...	38 4.2	59 53
1346b...	37 55.6	62 20	1396b...	38 2.8	60 1
1347a...	37 54.7	56 35	1397a...	38 4.9	50 5
1352a...	37 53.2	53 32	1403a...	38 5.2	61 7
1354a...	37 52.7	44 36	1405a...	38 6.4	53 16
1360a...	37 54.1	53 2	1408a...	38 8.2	59 3
1360b...	37 53.2	52 57	1412a...	38 13.1	55 20
1363a...	37 57.6	53 21	1412b...	38 9.2	56 16
1363b...	37 57.2	53 29	1417a...	38 12.1	58 1
1364a...	37 55.2	54 1	1422b...	38 12.6	51 3
1365a...	37 58.4	51 56	1422c...	38 13.6	51 34
1365b...	37 55.2	51 59	1426a...	38 13.0	49 36
1371a...	37 54.0	56 12	1441a...	38 21.8	56 10

TABLE IV  
PHOTOGRAPHIC RESIDUALS

	PLATE NUMBER						
	2463	2506	3679	3680	3846	3847	All
Number of Magnitudes.....	466	465	186	188	332	332	1969
Systematic Deviation.....	0.00	+0.02	-0.05	0.00	-0.03	+0.03	0.00
Average Deviation.....	±0.08	±0.08	±0.11	±0.07	±0.06	±0.06	±0.075

TABLE V  
PHOTO-VISUAL RESIDUALS

	PLATE NUMBER						
	2371	2462	2505	3684	3774	3775	All
Number of Magnitudes.....	64	80	85	39	661	661	1569
Systematic Deviation.....	-0.01	-0.01	+0.01	0.00	-0.02	+0.02	0.00
Average Deviation.....	±0.07	±0.05	±0.06	±0.07	±0.067	±0.067	±0.066

TABLE VI  
COMPARISON STARS

DESIGNATION		PHOTOGRAPHIC MAGNITUDE		COLOR-INDEX
Bailey	Von Zeipel	Harvard	Mt. Wilson	
a.....	740	13.50	14.04	+0.70
b.....	238	13.58	14.05	+1.79
c.....	640	13.98	14.57	+1.18
d.....	263	14.22	14.53	+1.12
e.....	250	14.50	14.81	+0.90
f.....	218	14.98	15.06	+0.53
g.....	227	15.28	15.22	+0.65
h*.....	258	15.70	15.53	-0.02
k.....	609	16.00	15.63	-0.04
l.....	1131	16.23	15.83	+0.33
m.....	1055	16.49	15.94	+0.69
n.....	1327	16.82	16.16	+0.68
o.....	1372b	17.15	16.37	+0.65
p.....	1347a	17.63	16.84	+0.41

TABLE VII  
COLOR-CLASS AND DISTANCE

DISTANCE	TABULATED QUANTITY	COLOR-CLASS						ALL COLORS
		<i>b</i>	<i>a</i>	<i>f</i>	<i>g</i>	<i>k</i>	<i>m</i>	
1'3 to 1'5	No. Stars....	0	1	2	4	0	0	7
	Av. C. I.....	+0.12	+0.12	+0.53	+1.00	.....	.....	+0.74
	Av. Pv. mag.	15.47	15.47	15.24	13.98	.....	.....	14.55
1'6.....	No. stars....	2	4	4	9	2	0	21
	Av. C. I.....	-0.09	+0.13	+0.68	+0.98	+1.26	.....	+0.69
	Av. Pv. mag.	16.18	15.51	16.05	14.86	13.40	.....	15.20
1'7.....	No. stars....	2	4	5	3	0	0	14
	Av. C. I.....	-0.10	+0.23	+0.67	+0.93	.....	.....	+0.49
	Av. Pv. mag.	15.70	16.07	15.63	15.37	.....	.....	15.71
1'8.....	No. stars....	0	2	9	10	1	0	22
	Av. C. I.....	+0.06	+0.68	+0.93	+0.93	+1.22	.....	+0.77
	Av. Pv. mag.	.....	15.59	15.76	15.21	13.18	.....	15.38
1'9.....	No. stars....	2	3	9	8	2	0	24
	Av. C. I.....	-0.10	+0.25	+0.66	+0.88	+1.30	.....	+0.67
	Av. Pv. mag.	15.96	15.22	15.77	15.37	12.96	.....	15.35
2'0.....	No. stars....	0	3	11	5	2	1	22
	Av. C. I.....	.....	+0.17	+0.64	+0.92	+1.26	+1.80	+0.75
	Av. Pv. mag.	.....	15.80	15.87	14.93	13.62	12.33	15.28
2'1.....	No. stars....	3	5	16	13	0	0	37
	Av. C. I.....	-0.06	+0.19	+0.65	+0.89	.....	.....	+0.62
	Av. Pv. mag.	16.32	15.86	16.20	15.17	.....	.....	15.80
2'2.....	No. stars....	0	7	9	5	0	0	21
	Av. C. I.....	.....	+0.20	+0.59	+1.00	.....	.....	+0.56
	Av. Pv. mag.	.....	16.02	15.96	14.96	.....	.....	15.74
2'3.....	No. stars....	0	1	11	6	0	0	18
	Av. C. I.....	.....	+0.35	+0.64	+0.93	.....	.....	+0.72
	Av. Pv. mag.	.....	16.92	16.08	14.68	.....	.....	15.66
2'4.....	No. stars....	1	3	14	6	0	0	24
	Av. C. I.....	-0.06	+0.08	+0.61	+0.94	.....	.....	+0.60
	Av. Pv. mag.	15.60	15.70	16.03	15.00	.....	.....	15.71
2'5.....	No. stars....	3	2	10	3	0	0	18
	Av. C. I.....	-0.10	+0.08	+0.65	+0.97	.....	.....	+0.52
	Av. Pv. mag.	15.76	15.35	16.12	14.24	.....	.....	15.66
2'6.....	No. stars....	0	2	3	4	0	0	9
	Av. C. I.....	.....	+0.16	+0.65	+0.94	.....	.....	+0.67
	Av. Pv. mag.	.....	15.36	15.50	14.78	.....	.....	15.15
2'7.....	No. stars....	0	2	6	8	1	0	17
	Av. C. I.....	.....	+0.18	+0.67	+1.02	+1.32	.....	+0.81
	Av. Pv. mag.	.....	16.10	15.96	14.50	13.08	.....	15.12

TABLE VII—Continued

DISTANCE	TABULATED QUANTITY	COLOR-CLASS						ALL COLORS
		b	a	f	g	h	m	
2'8.....	{No. stars....	1	1	13	4	2	0	21
	{Av. C. I.....	-0.04	+0.01	+0.65	+0.95	+1.29	.....	+0.71
	{Av. Pv. mag.	15.53	15.96	15.85	14.92	13.12	.....	15.41
2'9.....	{No. stars....	0	4	8	3	1	10	16
	{Av. C. I.....	.....	+0.21	+0.62	+0.90	+1.21	.....	+0.60
	{Av. Pv. mag.	.....	16.19	16.11	14.89	13.57	.....	15.74
3'0.....	{No. stars....	0	3	15	5	2	.....	25
	{Av. C. I.....	.....	+0.15	+0.60	+0.95	+1.26	.....	+0.67
	{Av. Pv. mag.	.....	16.14	16.49	14.52	13.09	.....	15.78
3'1.....	{No. stars....	0	2	7	2	0	0	11
	{Av. C. I.....	.....	+0.18	+0.57	+1.00	.....	.....	+0.58
	{Av. Pv. mag.	.....	16.27	15.83	14.29	.....	.....	15.63
3'2.....	{No. stars....	0	3	6	3	0	0	12
	{Av. C. I.....	.....	+0.27	+0.63	+0.85	.....	.....	+0.60
	{Av. Pv. mag.	.....	15.89	15.84	15.34	.....	.....	15.73
3'3.....	{No. stars....	0	0	6	1	0	0	7
	{Av. C. I.....	.....	.....	+0.64	+0.84	.....	.....	+0.66
	{Av. Pv. mag.	.....	.....	15.79	14.40	.....	.....	15.59
3'4.....	{No. stars....	0	2	14	1	0	0	17
	{Av. C. I.....	.....	+0.22	+0.56	+0.84	.....	.....	+0.54
	{Av. Pv. mag.	.....	15.88	15.84	15.24	.....	.....	15.81
3'5.....	{No. stars....	1	3	7	4	0	0	15
	{Av. C. I.....	-0.18	+0.15	+0.60	+0.84	.....	.....	+0.52
	{Av. Pv. mag.	16.42	15.99	15.70	15.24	.....	.....	15.68
3'6 and 3'7.....	{No. stars....	2	2	8	1	0	0	13
	{Av. C. I.....	-0.34	+0.36	+0.62	+0.93	.....	.....	+0.46
	{Av. Pv. mag.	15.10	16.94	15.71	14.96	.....	.....	15.75
3'8 and 3'9.....	{No. stars....	0	1	12	3	1	0	17
	{Av. C. I.....	.....	+0.36	+0.61	+0.84	+1.36	.....	+0.68
	{Av. Pv. mag.	.....	15.46	15.97	15.40	12.47	.....	15.64
4'0 and 4'1.....	{No. stars....	2	7	16	4	0	0	29
	{Av. C. I.....	-0.06	+0.29	+0.54	+1.02	.....	.....	+0.51
	{Av. Pv. mag.	15.73	16.36	16.31	13.91	.....	.....	15.95
4'2 and 4'3.....	{No. stars....	1	4	5	0	0	0	10
	{Av. C. I.....	-0.02	+0.33	+0.60	.....	.....	.....	+0.43
	{Av. Pv. mag.	15.54	16.42	16.18	.....	.....	.....	16.21
4'4 and 4'5.....	{No. stars....	1	4	9	5	0	1	20
	{Av. C. I.....	-0.05	+0.28	+0.54	+0.92	.....	+1.79	+0.61
	{Av. Pv. mag.	16.02	16.52	15.80	14.73	.....	12.48	15.52

TABLE VII—*Continued*

DISTANCE	TABULATED QUANTITY	COLOR-CLASS						ALL COLORS
		<i>b</i>	<i>a</i>	<i>f</i>	<i>g</i>	<i>h</i>	<i>m</i>	
4'6 and	{ No. stars....	0	2	10	2	0	0	14
4'7.....	{ Av. C. I.....	.....	+0.02	+0.61	+0.91	.....	.....	+0.57
	{ Av. Pv. mag.....	.....	15.63	15.66	15.35	.....	.....	15.61
4'8 and	{ No. stars....	0	2	4	2	0	0	8
4'9.....	{ Av. C. I.....	.....	+0.22	+0.59	+1.06	.....	.....	+0.62
	{ Av. Pv. mag.....	.....	16.06	16.30	13.91	.....	.....	15.64
5'0 and	{ No. stars....	2	5	8	3	0	0	18
5'1.....	{ Av. C. I.....	-0.14	+0.28	+0.66	+0.95	.....	.....	+0.52
	{ Av. Pv. mag.....	.....	15.94	16.50	15.54	14.49	.....	15.68
5'2 and	{ No. stars....	0	2	7	3	0	0	12
5'3.....	{ Av. C. I.....	.....	+0.36	+0.58	+0.91	.....	.....	+0.62
	{ Av. Pv. mag.....	.....	16.70	16.13	14.24	.....	.....	15.75
5'4 and	{ No. stars....	3	5	6	2	0	0	16
5'5.....	{ Av. C. I.....	-0.08	+0.35	+0.59	+0.80	.....	.....	+0.42
	{ Av. Pv. mag.....	.....	15.59	16.22	15.83	15.94	.....	15.92
5'6 and	{ No. stars....	0	4	14	3	0	0	21
5'7.....	{ Av. C. I.....	.....	+0.30	+0.56	+0.89	.....	.....	+0.56
	{ Av. Pv. mag.....	.....	16.09	16.01	14.84	.....	.....	15.86
5'8 and	{ No. stars....	0	3	3	2	0	0	8
5'9.....	{ Av. C. I.....	.....	+0.32	+0.60	+0.96	.....	.....	+0.51
	{ Av. Pv. mag.....	.....	15.89	15.65	14.30	.....	.....	15.40
6'0 and	{ No. stars....	0	3	5	2	0	0	10
6'1.....	{ Av. C. I.....	.....	+0.32	+0.63	+0.93	.....	.....	+0.60
	{ Av. Pv. mag.....	.....	15.84	15.85	14.00	.....	.....	15.48
6'2 and	{ No. stars....	0	4	7	3	0	0	14
6'3.....	{ Av. C. I.....	.....	+0.23	+0.63	+0.97	.....	.....	+0.59
	{ Av. Pv. mag.....	.....	16.40	15.82	13.42	.....	.....	15.47
6'4 and	{ No. stars....	1	7	5	1	0	0	14
6'5.....	{ Av. C. I.....	-0.58	+0.23	+0.56	+0.99	.....	.....	+0.35
	{ Av. Pv. mag.....	.....	16.32	16.40	16.06	13.86	.....	16.09
6'6 to	{ No. stars....	1	5	10	2	0	0	18
7'0.....	{ Av. C. I.....	-0.19	+0.23	+0.52	+0.90	.....	.....	+0.44
	{ Av. Pv. mag.....	.....	15.81	15.74	15.92	14.32	.....	15.69
7'1 to	{ No. stars....	1	6	7	3	1	1	19
7'5.....	{ Av. C. I.....	-0.03	+0.20	+0.65	+0.90	+1.32	+1.69	+0.60
	{ Av. Pv. mag.....	.....	15.38	15.92	15.63	13.43	12.60	15.05
7'6 to	{ No. stars....	2	5	8	3	0	0	18
8'0.....	{ Av. C. I.....	-0.04	+0.20	+0.57	+0.99	.....	.....	+0.47
	{ Av. Pv. mag.....	.....	15.73	15.71	15.73	14.43	.....	15.51

TABLE VII—Continued

DISTANCE	TABULATED QUANTITY	COLOR-CLASS						ALL COLORS
		<i>b</i>	<i>a</i>	<i>f</i>	<i>g</i>	<i>h</i>	<i>m</i>	
8'.1 to 8'.5.....	{No. stars.... Av. C. I..... Av. Pv. mag.	1 -0.11 14.55	5 +0.27 16.22	6 +0.60 15.70	3 +0.97 14.89	1 +1.22 12.92	0 .....	16 +0.56 15.46
8'.6 to 9'.0.....	{No. stars Av. C. I..... Av. Pv. mag.	1 -0.12 15.44	2 +0.32 16.56	9 +0.55 15.74	2 +0.98 15.00	0 .....	0 .....	14 +0.53 15.73
9'.1 to 9'.5.....	{No. stars.... Av. C. I..... Av. Pv. mag.	0 ..... .....	1 +0.25 16.61	12 +0.65 15.64	4 +0.92 14.88	0 .....	0 .....	17 +0.69 15.52
9'.6 to 10'.0.....	{No. stars.... Av. C. I..... Av. Pv. mag.	2 -0.04 16.22	1 +0.34 16.74	16 +0.59 15.34	5 +0.99 14.59	1 +1.23 10.57	0 .....	25 +0.64 15.12
10'.1 to 11'.4.....	{No. stars Av. C. I..... Av. Pv. mag.	2 -0.10 15.72	9 +0.32 15.16	6 +0.58 14.98	3 +1.03 15.15	1 +1.40 12.78	0 .....	21 +0.51 15.05



TABLE VIII  
FREQUENCY OF PHOTO-VISUAL MAGNITUDES FOR EACH COLOR-CLASS  
DISTANCE FROM CENTER 1'3 TO 1'9

Limits of Photo-visual Magnitude	< b <sub>5</sub>	b <sub>5</sub> to a <sub>0</sub>	a <sub>0</sub> to a <sub>5</sub>	a <sub>5</sub> to f <sub>0</sub>	f <sub>0</sub> to f <sub>5</sub>	f <sub>5</sub> to g <sub>0</sub>	g <sub>0</sub> to g <sub>5</sub>	g <sub>5</sub> to h <sub>0</sub>	h <sub>0</sub> to h <sub>5</sub>	> h <sub>5</sub>	All Colors
12.60-.79.....									1	1	2
.80-.99.....							1	2			3
13.00-.19.....									1		1
.20-.39.....									1		1
.40-.59.....											
.60-.79.....								2			2
.80-.99.....								1			1
14.00-.19.....									1		1
.20-.39.....											
.40-.59.....				1			2				3
.60-.79.....						2	1				3
.80-.99.....						1	2				3
15.00-.19.....					1	2	3	1			7
.20-.39.....		1	1		3	1	5	1			12
.40-.59.....		1	4	2	1	3	4	1			16
.60-.79.....		1	3	1		4	3				12
.80-.99.....						2	1				3
16.00-.19.....		1		1			2				4
.20-.39.....					1	2	1				4
.40-.59.....		1				2	1				4
.60-.79.....		1				2					3
.80-.99.....				1	1	1					3
Total.....	0	6	8	6	7	22	26	8	4	1	88

DISTANCE FROM CENTER 2'0 TO 2'9

12.20-.39.....										1	1
.40-.59.....											
.60-.79.....											
.80-.99.....									1		1
13.00-.19.....								3	2		5
.20-.39.....								1	1		2
.40-.59.....									1		1
.60-.79.....											
.80-.99.....							2	2			4
14.00-.19.....								4	1		5
.20-.39.....							3	3			6
.40-.59.....						6	1				7
.60-.79.....						3	6	1			10
.80-.99.....								1			1
15.00-.19.....			1	1		2	7	2			13
.20-.39.....			2		5	3	7	1			18
.40-.59.....		2	7	1	3	5	1				19
.60-.79.....		2	3	1	1	9	4	1			21
.80-.99.....		1	5		1	7	3				17
16.00-.19.....	1		1		2	5	4				13
.20-.39.....		1			1	5					7
.40-.59.....				2	6	14					22
.60-.79.....			1	2	5	7					15
.80-.99.....		1		3	11						15
Total.....	1	7	20	10	35	66	38	19	6	1	203

TABLE VIII—Continued

DISTANCE FROM CENTER 3'.0 TO 3'.9

Limits of Photo- visual Magnitude	< b <sub>5</sub>	b <sub>5</sub> to a <sub>0</sub>	a <sub>0</sub> to a <sub>5</sub>	a <sub>5</sub> to f <sub>0</sub>	f <sub>0</sub> to f <sub>5</sub>	f <sub>5</sub> to g <sub>0</sub>	g <sub>0</sub> to g <sub>5</sub>	g <sub>5</sub> to h <sub>0</sub>	h <sub>0</sub> to h <sub>5</sub>	> h <sub>5</sub>	All Colors
12.40-.59.....									I		I
.60-.79.....											I
.80-.99.....									I		I
13.00-.19.....								I			I
.20-.39.....									I		I
.40-.59.....						I					I
.60-.79.....											
.80-.99.....								2			2
14.00-.19.....						I					I
.20-.39.....											
.40-.59.....						4	2				6
.60-.79.....	I					3	3				7
.80-.99.....							I				I
15.00-.19.....						I	3				4
.20-.39.....					I	2	4				7
.40-.59.....		I	4	2	6	7					20
.60-.79.....			I	I		5	2				9
.80-.99.....			I		I	5					7
16.00-.19.....			I		2	I	I				5
.20-.39.....					3	3	I				7
.40-.59.....		I			5	2					8
.60-.79.....					7	2					9
.80-.99.....				6	12	I					19
Total.....	I	2	7	9	37	38	17	3	3	0	117

DISTANCE FROM CENTER 4'.0 TO 5'.9

Limits of Photo- visual Magnitude	< b <sub>5</sub>	b <sub>5</sub> to a <sub>0</sub>	a <sub>0</sub> to a <sub>5</sub>	a <sub>5</sub> to f <sub>0</sub>	f <sub>0</sub> to f <sub>5</sub>	f <sub>5</sub> to g <sub>0</sub>	g <sub>0</sub> to g <sub>5</sub>	g <sub>5</sub> to h <sub>0</sub>	h <sub>0</sub> to h <sub>5</sub>	> h <sub>5</sub>	All Colors
12.40-.59.....										I	I
.60-.79.....											
.80-.99.....											
13.00-.19.....								I			I
.20-.39.....											
.40-.59.....								3			3
.60-.79.....							I	2			3
.80-.99.....							I				I
14.00-.19.....							I	I			2
.20-.39.....											
.40-.59.....					I	4	2				7
.60-.79.....						3	I				4
.80-.99.....						I	3	I			5
15.00-.19.....				I			4				5
.20-.39.....			I	2	5	6	2				16
.40-.59.....		3	3	5	3	4					18
.60-.79.....		4	2			8	I				15
.80-.99.....					I	4	I				6
16.00-.19.....	I	I			3	2					7
.20-.39.....				I	6	2					9
.40-.59.....				2	6	2					10
.60-.79.....			I	9	6	I	I				18
.80-.99.....			I	10	14						25
Total.....	I	8	8	30	45	37	18	8	0	I	156

TABLE VIII—Continued  
DISTANCE FROM CENTER  $\geq 6'.0$

Limits of Photo- visual Magnitude	< $b_5$	$b_5$ to $a_0$	$a_0$ to $a_5$	$a_5$ to $f_0$	$f_0$ to $f_5$	$f_5$ to $g_0$	$g_0$ to $g_5$	$g_5$ to $h_0$	$h_0$ to $h_5$	> $h_5$	All Colors
< 12.00				1				1	1		3
12.00-19											
20-39											
40-59											
60-79						1		1		2	4
80-99						1			2		3
13.00-19											
20-39											
40-59								1			1
60-79							3	1			4
80-99					1		4	2			7
14.00-19			1			1	1				3
20-39						1					1
40-59		1		1	2	2	1				7
60-79				1	1	2	1	1			6
80-99				1	1	2	3	2			9
15.00-19						4	3	1			8
20-39		1	1	2	4	8					16
40-59			3	9	4	3	10				29
60-79			2	2	1	6	1	1			13
80-99		1			4	1	1				7
16.00-19		1			5	6	1				13
20-39	1			3	6	3		1			14
40-59				5	4	1					10
60-79				9	8	1					18
80-99		1	3	5	1						10
Total	1	10	14	34	41	50	19	12	3	2	186

DISTANCE FROM CENTER  $2'.0$  TO  $11'.3$

Limits of Photo- visual Magnitude	< $b_5$	$b_5$ to $a_0$	$a_0$ to $a_5$	$a_5$ to $f_0$	$f_0$ to $f_5$	$f_5$ to $g_0$	$g_0$ to $g_5$	$g_5$ to $h_0$	$h_0$ to $h_5$	> $h_5$	All Colors
< 12.00				1				1	1		3
12.00-19											
20-39										1	1
40-59									1	1	2
60-79						1		1		2	4
80-99						1			4		5
13.00-19								5	2		7
20-39								1	2		3
40-59						1		4	1		6
60-79							4	3			7
80-99					1		7	6			14
14.00-19			1			2	2	5	1		11
20-39						1	3	3			7
40-59		1		1	3	16	6				27
60-79	1			1	1	11	11	2			27
80-99				1	1	3	7	4			16
15.00-19			1	2		7	17	3			30
20-39		1	4	4	15	19	13	1			57
40-59			9	23	12	15	26	1			86
60-79			8	6	4	2	28	8	2		58
80-99		2	6		7	17	5				37
16.00-19	2	2	2		12	14	6				38
20-39	1	1		4	16	13	1	1			37
40-59		1		9	21	19					50
60-79			2	20	26	11	1				60
80-99		2	4	24	38	1					69
Total	4	27	49	83	158	191	92	42	12	4	662

TABLE IX  
COLOR-CLASS, DISTANCE, AND PHOTO-VISUAL MAGNITUDE  
(Summary of Table VII)

INTERVAL OF DISTANCE	COLOR-CLASS							ALL COLORS	AVERAGE COLOR-INDEX
	b	a	f	g	h	m			
1'3-1'9.....	15.95(6)	15.62(14)	15.75(29)	15.02(34)	13.18(5)	.....	15.32(88)	+0.68	
2'0-2'4.....	16.14(4)	15.94(19)	16.05(61)	14.99(35)	13.62(2)	12.33(1)	15.66(122)	+0.64	
2'5-2'9.....	15.70(4)	15.85(11)	15.96(40)	14.64(22)	13.22(4)	.....	15.44(81)	+0.66	
3'0-3'4.....	.....	16.04(10)	16.03(48)	14.74(12)	13.09(3)	.....	15.74(72)	+0.61	
3'5-3'9.....	15.54(3)	16.22(6)	15.83(27)	15.26(8)	12.47(1)	.....	15.68(45)	+0.56	
4'0-4'9.....	15.76(4)	16.30(19)	16.04(44)	14.45(13)	.....	12.48(1)	15.70(81)	+0.54	
5'0-5'9.....	15.73(5)	16.27(19)	15.88(38)	14.71(13)	.....	.....	15.76(73)	+0.52	
6'0-7'0.....	16.06(2)	16.14(19)	15.91(27)	13.84(8)	.....	.....	15.70(56)	+0.48	
7'1-9'0.....	15.37(5)	16.02(18)	15.70(30)	14.39(11)	12.87(2)	12.60(1)	15.41(67)	+0.54	
9'1-11'3.....	15.97(4)	15.44(11)	15.38(34)	14.82(12)	11.68(2)	.....	15.20(63)	+0.61	
1'3-11'3.....	15.79(37)	16.01(146)	15.86(378)	14.78(168)	12.99(18)	12.47(3)	15.57(750)	+0.59	
Outside Distance $\alpha'$ .....	15.76(31)	16.06(132)	15.89(349)	14.71(134)	12.91(13)	12.47(3)	15.61(662)	+0.58	

TABLE X  
THE COLOR OF GIANT STARS

Interval of Photo-visual Magnitude	Number of Stars	Average Color-Index
12.0-12.6.....	3	+1.43
12.6-13.2.....	16	+1.18
13.2-13.8.....	16	+1.06
13.8-14.4.....	32	+0.94
14.4-15.0.....	70	+0.74
15.0-15.6.....	173	+0.52
15.6-16.2.....	133	+0.54
16.2-16.8.....	147	+0.50

MOUNT WILSON OBSERVATORY  
October 1919

# OBSERVATIONS OF THE ELECTRIC FURNACE SPECTRA OF COBALT, NICKEL, BARIUM, STRONTIUM, AND CALCIUM IN THE REGION OF GREATER WAVE-LENGTH<sup>1</sup>

By ARTHUR S. KING

The material presented in this paper was collected during a series of experiments designed to extend as far as possible into the infra-red several furnace spectra which had previously been studied through the range  $\lambda$  3000 to  $\lambda$  7000.<sup>2</sup>

Since photographic emulsions stained with dicyanin are sensitive far beyond the red limit of the visible spectrum, it is possible to observe the characteristics of infra-red lines without extraordinary difficulties. For the weaker light-sources, however, faster plates than those now available are highly desirable, and this lack of speed has been much felt in the photography of furnace spectra. It has been noted repeatedly in former furnace investigations that the region of greater wave-length is relatively weak in the furnace. The present study of the infra-red bears out this observation, and long exposures were often required to bring out the spectra that have been obtained. It has been possible, however, to photograph the spectrum to about  $\lambda$  9200 and to classify the lines which the furnace was able to emit within this range.

Seed "23" plates or Eastman Portrait Films were treated with a dicyanin bath according to the method recommended by Merrill.<sup>3</sup> The plates were used for the first-order spectrum of the 15-ft. concave grating to about  $\lambda$  8250, while the films exposed with a 1-meter concave grating gave the extension farther into the infra-red.

The tube-resistance furnace was operated as usual *in vacuo*, and photographs were made for three temperature stages selected according to the element under examination. This treatment

<sup>1</sup> *Contributions from the Mount Wilson Observatory*, No. 181.

<sup>2</sup> *Mt. Wilson Contr.*, Nos. 108, 150; *Astrophysical Journal*, 42, 344, 1915; 48, 13, 1918.

<sup>3</sup> *Bulletin of the Bureau of Standards*, 14, 487, 1919.

brought out the groups of lines appearing at the successive temperatures and showed the relative changes in line intensity as the temperature rises.

The resulting classification is given in the last column of Tables I-IV and follows the method of previous work. Lines of Classes I and II appear at low temperatures; those of Class II strengthen more rapidly at higher temperatures and are usually strong arc lines. Class III lines appear at medium temperature, while those of Classes IV and V are high-temperature lines. Those lines which are especially characteristic of the furnace spectrum and are relatively faint in the arc are denoted by "A" after the class number. The predominating lines of this type are those of Classes I A and III A.

#### COBALT

The cobalt lines obtained in this investigation are listed in Table I, the wave-lengths (and also those of Table II) being the measures of Meggers and Kiess,<sup>1</sup> which are on the international system. The metal used in the furnace was a purified powder prepared by Kahlbaum.

The results are presented in the usual form, with intensities for the arc and three furnace temperatures. The latter were approximately 2400°, 2100°, and 1900° C. Some of the low-temperature lines as far as  $\lambda$  7085 were also listed in the former tables.<sup>2</sup> The classification of these lines remains the same, but the relative intensities are changed owing to the use of dicyanin plates. The low-temperature spectrograms required long exposure, and, in order to make sure that all possible lines for this temperature were recorded, the results with the 15-ft. spectrograph were checked by a strongly exposed film taken with the 1-meter concave grating.

The variety of types observed for the visible spectrum continues in the region of longer waves. A number of moderately strong arc lines did not appear in the furnace and are placed in Class V. Two very faint arc lines  $\lambda\lambda$  7250 and 7437 are relatively strong in the furnace. The low-temperature spectrum ceases at  $\lambda$  7417, but

<sup>1</sup> *Bulletin of the Bureau of Standards*, 14, 637, 1919.

<sup>2</sup> *Mt. Wilson Contr.*, No. 108; *Astrophysical Journal*, 42, 344, 1915.

that for medium temperature holds up to the end of the list at  $\lambda$  8094.

TABLE I  
TEMPERATURE CLASSIFICATION OF COBALT LINES

$\lambda$ (MEGGERS AND KIRSS)	ARC INTENSITY	FURNACE INTENSITIES			CLASS
		High Temperature	Medium Temperature	Low Temperature	
6678.84.....	5	5	4	2	II
6771.05.....	50	50	40	40	I
6814.99.....	40	40	30	25	I
6872.42.....	40	40	30	20	I
6937.85.....	4	2	1	.....	III
6997.30*.....	4	.....	.....	.....	V
7004.82.....	3	3	2	.....	III
7016.65.....	35	35	25	25	I
7027.86.....	6	tr	.....	.....	V
7052.84.....	60	60	40	50	I
7054.08.....	10	8	5	.....	III
7084.99.....	100	80	80	80	I
7094.64.....	1	1	.....	.....	IV
7113.74.....	5	.....	.....	.....	V
7124.45.....	1	1	1	.....	III
7134.37.....	5	.....	.....	.....	V
7154.71.....	8	8	6	2	II
7159.23.....	6	.....	.....	.....	V
7193.63.....	4	.....	.....	.....	V
7250.09.....	1	3	2	.....	III A
7285.29.....	4	1	.....	.....	IV
7354.61.....	3	4	2	.....	III
7388.66.....	5	2	1	.....	III
7417.40.....	10	10	5	2	II
7437.15.....	1	2	1	.....	III A
7457.43.....	6	.....	.....	.....	V
7533.52.....	1	1	.....	.....	IV
7554.04.....	4	1	.....	.....	IV
7590.60.....	2	2	1	.....	III
7606.30.....	2	.....	.....	.....	V
7610.29.....	2	1	.....	.....	IV
7712.68.....	6	5	2	.....	III
7838.18.....	3	.....	.....	.....	V
7869.92.....	2	.....	.....	.....	V
7871.43.....	2	.....	.....	.....	V
7908.75†.....	6	3?	3?	.....	III?
7926.59.....	3	.....	.....	.....	V
7987.38.....	5	5	3	.....	III
8007.34.....	5	.....	.....	.....	V
8043.33.....	2	.....	.....	.....	V
8056.03.....	2	.....	.....	.....	V
8094.03.....	8	4	2	.....	III

\* Probably double.

† Furnace line may be due to carbon.



## NICKEL

The nickel lines listed in Table II were obtained for about the same temperature stages as the cobalt lines in Table I. The

TABLE II  
TEMPERATURE CLASSIFICATION OF NICKEL LINES

$\lambda$ (MEGGERS AND KIESS)	ARC INTENSITY	FURNACE INTENSITIES			CLASS
		High Temperature	Medium Temperature	Low Temperature	
6842.10.....	8	.....	.....	.....	V
6876.77.....	2	2	.....	.....	IV
6914.60.....	50	50	20	15	II
6955.10.....	3	.....	.....	.....	V
7001.55.....	1	1	.....	.....	IV
7024.76.....	3	.....	.....	.....	V
7030.10.....	3	.....	.....	.....	V
7034.42.....	1	.....	.....	.....	V
7110.08.....	3	15	8	.....	III A
7122.31*.....	100	4?	2?	.....	IV?
7182.06.....	8	.....	.....	.....	V
7197.07.....	5	15	5	.....	III A
7261.94.....	3	8	3	.....	III A
7291.30.....	1	3	1	.....	III A
7385.23†.....	1	1?	.....	.....	IV?
7386.24†.....	1	3?	2?	.....	III A?
7393.67.....	10	2	1	.....	III
7409.35.....	8	1	.....	.....	IV
7414.51.....	2	6	4	.....	III A
7422.34.....	15	4	3	.....	III
7522.87.....	3	2	1	.....	III
7525.18.....	2	1	tr	.....	III
7555.67.....	5	2	2	.....	III
7574.10.....	1	.....	.....	.....	V
7617.02.....	5	2	1	.....	III
7619.24.....	1	1	tr	.....	III
7714.27.....	3	8	8	6	I A
7727.68.....	3	1	.....	.....	IV
7748.94.....	3	tr	.....	.....	IV
7788.95.....	2	6	6	.....	III A
7797.66.....	3	.....	.....	.....	V

\* Difficult on account of strong carbon spectrum. Line, if present, is faint in furnace.

† Furnace lines may be due to carbon.

metallic nickel was a purified preparation from Kahlbaum. In some cases cobalt and nickel were used together in the furnace.

The low-temperature stage, at which many lines appear in the visible spectrum, shows in the region now studied only  $\lambda\lambda$  6915 and 7714. About one-fourth of the lines in Table II, however, are relatively strong in the furnace as compared with the arc. The

most notable of this type is the I A line  $\lambda$  7714, the others belonging to Class III A. This feature causes the occurrence of various contrasting pairs of neighboring lines, one of which is a decided arc line and the other a furnace line. Such pairs are  $\lambda\lambda$  7111 and 7122, 7414 and 7422, 7714 and 7728, 7789 and 7798. The relative intensities of the members of any of these pairs in a given source will decide its resemblance to the furnace or the arc.

## BARIUM

The barium lines in Table III were obtained at temperatures of 2400°, 2000°, and 1650° C. for the three stages. Desiccated

TABLE III  
TEMPERATURE CLASSIFICATION OF BARIUM LINES

$\lambda$	MEASURED BY	ARC INTENSITY	FURNACE INTENSITIES			CLASS
			High Temperature	Medium Temperature	Low Temperature	
6772.07.....	H	2n	1	1	.....	III
6865.93.....	H	3o	10	6	3	II
6868.04*.....	H	8n	2	?	.....	IV?
7060.26†.....	H	4oor	200R	100	40	II
7090.51.....	H	5n	5	3	.....	III
7120.73.....	H	200	100	40	20	II
7153.72.....	S	5	5	2	.....	III
7195.71.....	H	8o	40	30	4	III
7208.50.....	H	1n	1	1	.....	III
7213.83.....	H	1	6	4	.....	III A
7229.40.....	H	25	10	5	.....	III
7280.58.....	H	15or	100R	40	15	II
7359.67.....	H	1	4	2	.....	III A
7376.10.....	H	2n	2	1	.....	III
7392.83.....	H	3o	15	12	4	II
7410.6.....	S	1	1	.....	.....	IV
7417.80.....	H	5	6	5	2	II
7460.27†.....	H	5n	5	2	.....	III
7488.38.....	H	10	10	10	8	I
7610.50.....	M	2	4	4	.....	III A
7636.88.....	M	2n	3	2	.....	III
7642.92.....	M	4n	4	2	.....	III
7672.12.....	M	25f	20r	15	12	I
7706.58.....	M	1n	1	1	.....	III
7780.49.....	M	10	10	8	7	I
7905.80.....	M	6	6	6	1	III
7911.36.....	M	3	3	6	10	I A
8210.28†.....	M	4	3	2	?	III?
8559.90.....	M	4	3	2	2	I

\* Difficult at medium temperature on account of band.

† Intensities much affected by vapor density.

‡ May be concealed by band at low temperature.

barium chloride was used in the furnace. First-order plates taken with the 15-ft. concave grating supplied the data except for the last two lines, which were photographed on films with the 1-meter concave grating.

The wave-lengths are those measured by Hermann,<sup>1</sup> by Saunders,<sup>2</sup> and by Meggers,<sup>3</sup> as indicated by the initials in the second column. The values of Meggers are on the international system.

The low-temperature spectrum yields a considerable number of lines in this region. Besides the strong arc lines of Class II, which are present at low temperature, there is an important set of five Class I lines, of which the I A line  $\lambda$  7911 is the most interesting. This line widens at high temperature and its low density may be due to incipient reversal, but the high intensity of this weak arc line at low temperature is very striking. Several lines just visible in the arc with moderate exposure attain considerable strength at the high and medium furnace temperatures and are placed in Class III A. Lines which in the arc show a diffuse structure are indicated by "n" after the arc intensity. Some of these are shaded toward red or violet. In all such cases the vacuum furnace gives a sharply defined line. Three lines,  $\lambda\lambda$  7060, 7281, 7672, are reversible both in the arc and in the high-temperature furnace. The reversals are narrow, however, compared with those of the potassium pair  $\lambda\lambda$  7665, 7699, which, though given merely by an impurity, often appear widely reversed.

#### STRONTIUM

The strontium lines in Table IV were obtained with the dried chloride in the tube at the same temperatures as were used with barium. No lines showed a higher relative intensity in the furnace than in the arc.  $\lambda$  6892.62 is the most conspicuous low-temperature line, the only one falling in Class I. The other strong lines fade rapidly at low temperature.  $\lambda$  7153.08 seems usually to have been ascribed to barium, which has a line at  $\lambda$  7153.72,

<sup>1</sup> *Tübingen Dissertation*, 1904; *Annalen der Physik* (4), 16, 684, 1905.

<sup>2</sup> *Astrophysical Journal*, 32, 153, 1910.

<sup>3</sup> *Bulletin of the Bureau of Standards*, 14, 371, 1918.

but the two lines are clearly shown by these photographs to be distinct.

TABLE IV  
TEMPERATURE CLASSIFICATION OF STRONTIUM LINES

$\lambda$ (MEGERS)	ARC INTENSITY	FURNACE INTENSITIES			CLASS
		High Temperature	Medium Temperature	Low Temperature	
6791.08.....	100	20	20	5	II
6878.36.....	300	40	30	10	II
6892.62.....	50	50†	50	50	I
7070.15.....	400	100	100	30	II
7153.08*.....	5	1?	.....	.....	IV?
7167.24†.....	50	10	4	.....	III
7232.24‡.....	20	6	2	.....	III
7287.44.....	1	1	.....	.....	IV
7309.47.....	70	15	10	1	III
7621.54.....	10	4	2	.....	III
7673.11§.....	15	4	1	.....	III

\* Furnace line may be due to carbon.

† Widens to red in arc.

‡ Widens to red in arc.

§ Widens to violet in arc.

#### CALCIUM

Spectrograms were made with metallic calcium in the furnace for the same temperatures as were used with barium and strontium. The lines measured by Meggers at  $\lambda\lambda$  7148.15, 7202.21, 7326.12 were obtained with the furnace. These come within the range covered in the former investigation.<sup>1</sup> Numerous attempts were made to photograph the lines  $\lambda\lambda$  8497.98, 8542.06, 8662.10, but these, while strong in the arc, did not appear with certainty in the furnace, though a trace of the strongest may have been present. These lines are of special interest as in the solar spectrum they are the strongest in that part of the infra-red at present reached by photography. This high solar intensity and the fact that they are stronger in the spark than in the arc are features which they have in common with the H and K lines. They are, however, enhanced lines of a more pronounced type than H and K, the latter appearing even at low temperatures in the furnace, while those of the infra-red triplet belong clearly in Class V.

<sup>1</sup> *Mt. Wilson Contr.*, No. 150; *Astrophysical Journal*, 48, 13, 1918.

## SUMMARY

1. By means of plates bathed with dicyanin, a study of the cobalt, nickel, barium, strontium, and calcium spectra extending into the infra-red has been made for three temperatures of the electric furnace.

2. The lines of the arc spectrum, above a certain minimum intensity, appear for the most part in the furnace. Some strong arc lines, however, were not obtained in the furnace, and, on the other hand, a number of examples appear of lines strong in the furnace which are faint in the arc,

3. Besides these features, the same variety as to rate of increase of line intensity with temperature was observed as for the visible spectrum, and the resulting classification is based on the differing response to varying temperature.

MOUNT WILSON OBSERVATORY  
January 1920

# THE ORBITS OF THE SPECTROSCOPIC COMPONENTS OF BOSS 5026

By W. E. HARPER

## ABSTRACT

*Spectroscopic binary* Boss 5026 (mag. 6.3; type F5). A series of twenty-nine plates secured during the summer has enabled the *elements of both orbits* to be determined with considerable accuracy. The results are given in a table and are also shown graphically. The period is 7.638 days; the *masses* are nearly equal, 1.854 and 1.827  $\odot$ ; the *velocity of the system* is about  $-15.6$  km.

This star (1900:  $\alpha = 19^h 36^m 4$ ;  $\delta = +50^\circ 44'$ ; photographic magnitude 6.3; type F5) was found to be a binary from the double lines shown on the first plate made. Twenty-nine plates were secured during the summer, all but four of which have been used in the present solution. These four, taken before the approximate period was known, fall at a phase in the orbit where the spectra are partially superposed and hence are unmeasurable. Of the remaining twenty-five, all but four have both components measurable, so that the determination of the orbit rests on the equivalent of forty-six plates. All were made on Seed 30 emulsion with the single-prism spectrograph which has a dispersion at the central ray  $\lambda 4200$  of 25.7 angstroms per millimeter.

The spectra of the two components are quite similar, the difference in intensities being barely sufficient to enable one to tell from inspection to which component each set of lines belongs. The lines of both components are fuzzy in nature, but as about a dozen on the average were measured in each case, a fairly reliable result was obtained, the probable error of a plate for component 1 (the one with the more intense lines) being  $\pm 2.1$  and for the other  $\pm 2.5$  km per sec. The masses, as may be expected, are very nearly equal, component 2 having a mass 0.986 times that of component 1.

The period was obtained early in the observations, thus avoiding to a large extent useless plates at phases where the lines would be hopelessly mixed. In addition, this knowledge of the general

form of the curve made possible the securing of separated spectra close to the crossing points by narrowing the collimator slit from its usual width of 0.051 mm. Nicely resolved lines were secured where the difference in velocity was of the order of 70 km per sec., and in one case a difference of 60 km gave lines clearly double in the violet region.

From the preliminary elements given later, observation equations were built up according to the notation of Lehmann-Filhés, modified to suit cases of double spectra,<sup>1</sup> and a least-squares solution effected. As no early observations existed whereby the preliminary value of the period might be corrected, this term was

TABLE OF ELEMENTS

Element	Preliminary	Final
Period.....P	7.635 days	7.6383 days $\pm 0.0019$ days
Eccentricity.....e	0.55	0.527 $\pm 0.006$
Longitude of apse..... $\omega_1$	48°	46° 74' $\pm 0^{\circ} 81'$
Longitude of apse..... $\omega_2$	228°	226° 74' $\pm 0^{\circ} 81'$
Velocity of system..... $\gamma$	-16.26 km	-15.59 km $\pm 0.36$ km
Semi-amplitude primary...K <sub>1</sub>	92 km	89.81 km $\pm 0.69$ km
Semi-amplitude secondary...K <sub>2</sub>	92 km	91.12 km $\pm 0.71$ km
Periastron passage.....T	J.D. 2,422,201.405	J.D. 2,422,398 $\pm 0.007$
Semi-major axis..... $a_1 \sin i_1$	.....	8,017,000 km
Semi-major axis..... $a_2 \sin i_2$	.....	8,134,000 km
Mass primary..... $m_1 \sin i_1$	.....	1.854 $\odot$
Mass secondary..... $m_2 \sin i_2$	.....	1.827 $\odot$

also included in the solution. This practically necessitated treating all the observations separately, and only where they were taken on one night or where they fell on a smooth part of the curve was this principle departed from. In this connection the four plates showing single lines, which group themselves symmetrically about one of the crossing points, were formed into one normal place. Thus a set of thirty-five observation equations involving the seven unknowns were built up, whose solution gave small corrections to the preliminary elements, as may be noted in the foregoing table. One solution was seen to be sufficient, as judged by the agreement of the ephemeris residuals and those obtained by substituting directly in the observation equations. The sum

<sup>1</sup> *Dominion Observatory Publications*, 1, 327.

of the squares of the residuals for the normal places was reduced from 527 to 386, about 27 per cent.

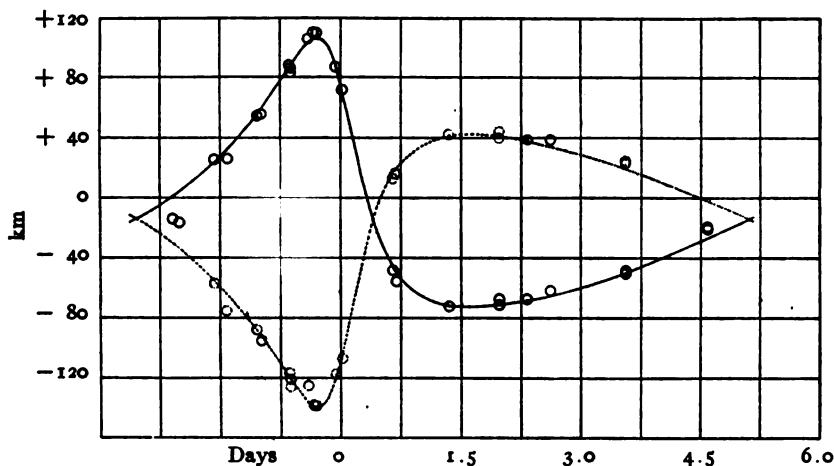


FIG. 1.—Radial velocity curves of Boss 5026 showing individual observations

The graph shown represents the final elements, the continuous curve being that of the so-called component 1, the dotted curve that of the other. Individual observations are plotted.

DOMINION ASTROPHYSICAL OBSERVATORY  
VICTORIA, B.C.  
November 7, 1919



## PREPARATION OF ABSTRACTS

Every article in the *Astrophysical Journal*, however short, is to be preceded by an abstract prepared by the author and submitted by him with the manuscript. The abstract is intended to serve as an aid to the reader by furnishing an index and brief summary or preliminary survey of the contents of the article; it should also be suitable for reprinting in an abstract journal so as to make a reabstracting of the article unnecessary. Therefore, *the abstract should summarize the information completely and precisely*, and also, in order to enable a reader to tell at a glance what the article is about and to enable an efficient index of the subject-matter of the abstract to be readily prepared, *the abstract should contain a set of subtitles which together form a complete and precise index of the information contained in the article.*

In the preparation of abstracts, authors should be guided by the following rules, which are illustrated by the abstracts appearing in the *Astrophysical Journal* for January and March 1920.<sup>1</sup> First the new information contained in the article should be determined by a careful analysis; then the subtitles should be formulated; and finally the text should be written and checked.

### RULES

1. *Material not new* need not be analyzed or described; a valuable summary of previous work, however, should be noted.
2. *The subtitles should together include all the new information*; that is, every measurement, observation, method, improvement of apparatus, suggestion, and theory which is presented by the author as new and of value in itself.
3. *Each subtitle should describe the corresponding information so precisely* that the chance of any investigator's being misled into thinking the article contains the particular information he desires when it does not, or vice versa, may be small. "Zeeman effect for electric furnace spectra" is too broad unless all metals have been studied, for an investigator may be interested, at the time, in only one metal; but "Infra-red arc spectrum of iron to  $3\mu$ " evidently satisfies this rule. It is particularly desirable that ranges of variation of temperature, wave-length, pressure, etc., be given.
4. *The text should summarize the author's conclusions and should transcribe all numerical results of general interest*, including all that might be looked for in a table of astronomical and physical constants, with an indication of the

<sup>1</sup> The rules and illustrative abstracts were prepared by G. S. Fulcher, of the National Research Council.

accuracy of each. It should give all the information that anyone, not a specialist in the particular field involved, might care to have in his notebook.

5. *The text should be divided into as many paragraphs* as there are distinct subjects concerning which information is given. Parts of subtitles may be scattered through the text but the subject of each paragraph must be indicated at the beginning.

6. *Complete sentences* should be used except in the case of subtitles. The abstract should be made as readable as the necessary brevity will permit.

## NOTICE TO CONTRIBUTORS

There is occasionally published in the *Astrophysical Journal* a Standing Notice (for instance, on pages 179-180 of the number for September 1917). This is principally intended to guide contributors regarding the manuscript, illustrations, and reprints. This notice contains the following paragraph:

Where unusual expense is involved in the publication of an article, on account of length, tabular matter, or illustrations, arrangements are made whereby the expense is shared by the author or by the institution which he represents, according to a uniform system.

The present sheet has been printed for amplifying further that paragraph.

The "uniform system" according to which "arrangements are made" is as follows: The cost of composition in excess of \$50, and of stock, presswork, and binding of pages in excess of 40 pages, for any one article shall be paid by the author or by the institution which he represents at the current rates of the University of Chicago Press. When four articles from one institution or author have appeared in any one volume, on which the cost of composition has amounted to \$50 each, or when the total cost of composition incurred by the *Astrophysical Journal* on articles for one institution has reached the sum of \$200, the entire cost of the composition, stock, presswork, and binding of any additional articles appearing in that volume shall be paid by the author or by the institution which he represents.

As to illustrations, the arrangement cannot be quite as specific, but it may be generally assumed that not more than three half-tone inserts can be allowed without payment by the author. The cost of paper, presswork, and binding for each full-page insert is about \$8.00, aside from the cost of the half-tone itself. In the matter of zinc etchings, considerable latitude has to be allowed, as in many cases diagrams take the place of more expensive tables. It may be assumed, however, that it will seldom be possible for the *Journal* to bear an expense of over \$25 for diagrams and text illustrations in any one article.

Contributors should notice that since January 1917 it has been impossible to supply any free reprints of articles.

Reprints of articles, with or without covers, will be supplied to authors at cost. No reprints can be furnished unless a request for them is received before the *Journal* goes to press.

Some of the foregoing arrangements have been in effect for several years; others have been reluctantly, but necessarily, adopted by the Editors and Publishers on account of the grave difficulties in publishing an international journal during war times. At the beginning of the war three-fifths of the subscribers to this *Journal* were resident outside of the United States. The University authorities have loyally continued their generous subsidy of about one-half the expense of publication, but it has not been possible to increase this during the present time. It is hoped that the reasonableness of the foregoing "arrangements" will be appreciated by our valued contributors.

THE EDITORS

# THE ASTROPHYSICAL JOURNAL

AN INTERNATIONAL REVIEW OF SPECTROSCOPY  
AND ASTRONOMICAL PHYSICS

VOLUME LI

MAY 1920

NUMBER 4

## THE ECLIPSING VARIABLE STAR, $\lambda$ TAURI

By JOEL STEBBINS

### ABSTRACT

*Eclipsing variable star,  $\lambda$  Tauri; photometric study.*—Two series of observations made with a sensitive photo-electric photometer during 1916–1917 and 1917–1918 have enabled the *light-curve* of this third-magnitude star to be determined (Fig. 1, Table IX). It is found to be a normal eclipsing system with two minima and continuous variation between eclipses. A comparison of the times of minima with those computed from spectroscopic studies shows a satisfactory agreement. *No light effect due to the third body*, whose existence was shown by Schlesinger to account for the observed spectroscopic orbit, is clearly evident, although a few observations, discordant up to 0<sup>m</sup>.1, occurred at such dates as to suggest they might be caused by this body. Because of the undetermined light of the third body and because of the small range of about 0<sup>m</sup>.4 in a partial eclipse, *the elements for this system* can be determined, as yet, only roughly. Plausible values for the *sizes, densities*, and relative *brightness* of the bodies, and for the *inclination* and *ellipsoidal constants*, are given in Table X and Fig. 3. The *difference in brightness of opposite sides of the second body* is probably chiefly due to the heating effect of the intense radiation from the first body. The author calls attention to a systematic discrepancy of 0<sup>m</sup>.01 between the two series of observations of 1916–1917 and 1917–1918, which is unexplained.

*Stars of Class B,  $\pi^1$  Orionis,  $\xi$  Tauri,  $\epsilon$  Tauri,  $\mu$  Tauri.*—These stars were used for comparison in the above series of photo-electric measurements and none was observed to vary by as much as 0<sup>m</sup>.05, although variables are common in this class.

*Photo-electric photometer for stellar observations.*—After a large number of trials, a potassium photo-electric cell of fused quartz has been developed which makes the photometer much more sensitive than the former selenium photometer and which enables sixth-magnitude stars to be studied with a 12-inch telescope.

The variability of  $\lambda$  Tauri was established by Baxendell<sup>1</sup> in 1848, this being the third discovery of an eclipsing star, following

<sup>1</sup> *Monthly Notices*, 9, 37, 1848.

Algol and S Cancri, while with a magnitude of 3.3  $\lambda$  Tauri ranks in brightness next to Algol among the older known stars of this class. Although it was immediately found that  $\lambda$  Tauri has a period of 3.95 days, there has been no good determination of the light-curve in the sixty years since the discovery of the variation, observers recording irregularities in the times of minima amounting to several hours. Apparently because of the small range of variation and few suitable comparison stars this variable is unusually difficult for visual estimates.

In 1897 Belopolsky found  $\lambda$  Tauri to be a spectroscopic binary, and the orbit has since been well determined at Allegheny. Schlesinger<sup>1</sup> has shown that the anomalies in the orbital motion can be explained by the presence of a third body which revolves about the eclipsing system in a period of 34.6 days. He was unable to detect the spectrum of more than one component on the plates, though there were certain peculiarities in the lines. The third body might account for large disturbances of the four-day eclipsing pair, though the spectroscopic results for the short-period orbit show no great discrepancies.

When the study of Algol with the selenium photometer was completed in 1910, the next bright eclipsing star available was  $\lambda$  Tauri, but the change to a whole magnitude fainter than Algol made this star, especially at minimum, entirely too faint for satisfactory observation, and attempts at measures were postponed until the apparatus could be improved. After several years the selenium photometer was discarded in favor of the new photo-electric cell made in our physics laboratory by Dr. Jakob Kunz and myself, and finally in 1916 the photo-electric photometer was in such a stage of development that stars considerably fainter than  $\lambda$  Tauri could be observed. A comparison of the relative performances of the selenium and photo-electric instruments is somewhat difficult, but it is safe to say that with the new device, attached to the same 12-inch refractor, stars at least three magnitudes fainter can be observed than with the selenium photometer. In fact, a careful comparison might show a difference of five magnitudes, or a one-hundred fold improvement, as the present

<sup>1</sup> *Publications of the Allegheny Observatory*, 3, 167, 1915.

measures of fifth-magnitude stars are better than the measures of any stars whatever with selenium. The present practical limit is about magnitude 6.0 for stars of spectrum class A. The "color equation" of the installation, that is, the measured difference of two stars of classes A and K of the same visual brightness, is  $0^m.86$ .

I hope sometime to publish a detailed description of the photometer and the method of observing with it. No great changes have been introduced in the instrument since the work in 1915 on  $\beta$  Lyrae,<sup>1</sup> but the one important new feature is the potassium photo-electric cell which is of fused quartz. This substitution of quartz for glass in the cell wall has eliminated most of the so-called "dark current," and the particular cell now in use, our number QK99, is far superior to any cell which we had previously made. Its number indicates that it was the ninety-ninth cell which was enough of a success to be given a number, failures not being counted.

The observations of  $\lambda$  Tauri were begun here in October, 1916, using  $\xi$  Tauri as the principal comparison star, but also  $\pi^4$  Orionis and  $\pi^5$  Orionis. It was not long before the discrepancies indicated that  $\pi^5$  Orionis is a variable, going through its changes in the spectroscopic period of 3.70 days, and the results for this star are given in the following article in this *Journal*. It was not possible to secure enough observations for a definitive light-curve of  $\lambda$  Tauri during the first season, but the main characteristics of the variation were established, there being primary and secondary eclipses as expected, and also continuous variation between minima, due to ellipticity of the components and to radiation effect. Toward the end of the season it was suspected that certain anomalies were repeated in the period of 34.6 days, showing an effect of the third body, and it was therefore determined to observe the star carefully the following year. In the meantime we had begun the practice of using neutral shade glasses to cut down the light of bright stars, and two fainter comparison stars were added,  $\epsilon$  Tauri and  $\mu$  Tauri. In these observations the light of  $\lambda$  Tauri was reduced to approximate equality with the comparison star. Only one of the five comparison stars,  $\epsilon$  Tauri, is

<sup>1</sup> *Lick Observatory Bulletin*, 8, 186, 1916.

not in the list of spectroscopic binaries, and it is just among these stars of class B that variables are to be expected, but I have succeeded in establishing a light-curve only in the case of  $\pi^s$  Orionis.

TABLE I  
COMPARISON STARS

H.R.	Star	Spectroscopic Period	Spectrum	Visual Magnitude	Shade Used on $\lambda$ Tauri	Photo-electric Reduction to $\xi$ Tauri
1239....	$\lambda$ Tauri	$3^d952941$	B <sub>3</sub>	Var.	.....	.....
1038....	$\xi$ Tauri	Unknown	B <sub>8</sub>	3.75	.....	.....
1174....	$\epsilon$ Tauri	.....	B <sub>3</sub>	5.03	$1^d56$	$0^m215$
1320....	$\mu$ Tauri	Unknown	B <sub>5</sub>	4.32	0.86	0.250
1552....	$\pi^s$ Orionis	9.5191	B <sub>3</sub>	3.78	.....	0.120
1567....	$\pi^s$ Orionis	3.70045	B <sub>3</sub>	3.87	.....	Var.

In Table II are the observations of  $\lambda$  Tauri made with the photo-electric photometer. The first date of Series I is October 22, 1916, and of Series II, September 10, 1917. The phase in the second column is computed from the elements:

$$\text{Minimum} = \text{J.D. } 2421194.573 + 3^d952941 \cdot E,$$

the period being that of v. Aretin.<sup>1</sup> The phase for the monthly period is based upon the hypothetical eclipse times from Schlesinger's elements:

$$\text{Minimum} = \text{J.D. } 2417831.30 + 34^d60 \cdot E.$$

In computing the phases the times were reduced to the sun. The difference of magnitude is referred to  $\xi$  Tauri as standard, using the corrections for the other comparison stars as given in the last column of Table I, except in the case of  $\pi^s$  Orionis, the corrections for which are in Table III. Each magnitude is usually the mean of three sets of measures, a set consisting of two measures of the comparison star, four of the variable, and then two of the comparison star, the rate of observing being about six sets per hour. The residuals were taken in part graphically from the final light-

<sup>1</sup> *Vierteljahrsschrift der Astronomischen Gesellschaft*, 48, 365, 1913.

TABLE II  
OBSERVATIONS OF  $\lambda$  TAURI  
SERIES I

Date, G.M.T.	$3^{d}95$ Phase	$3^{d}96$ Phase	Difference of Magnitude	Residual	Com- pari- son Star	Remarks
2421159.776..	0 <sup>d</sup> 785	6 <sup>d</sup> 88	0 <sup>m</sup> 334	-0 <sup>m</sup> 003	$\epsilon$	
.810..	0.819	6.92	.347	+ .007	$\epsilon$	
1163.733..	0.780	10.84	.329	- .008	$\epsilon$	
.756..	0.812	10.86	.327	- .012	$\epsilon$	
1164.696..	1.754	11.80	.320	- .014	$\epsilon$	
.718..	1.774	11.82	.317	- .010	$\epsilon$	
.785..	1.841	11.89	.279	- .021	$\epsilon$	
.857..	1.913	11.96	.282	+ .012	$\epsilon$	
.929..	1.985	12.03	.266	+ .005	$\pi^5$	
1168.692..	1.795	15.80	.323	+ .004	$\epsilon$	
.710..	1.813	15.82	.314	+ .003	$\epsilon$	
.765..	1.868	15.87	.282	- .006	$\epsilon$	
.830..	1.933	15.94	.257	- .008	$\epsilon$	
.909..	2.012	16.01	.283	+ .019	$\pi^5$	
1169.698..	2.801	16.80	.365	- .001	$\epsilon$	
.726..	2.829	16.83	.371	+ .006	$\epsilon$	
.797..	2.900	16.90	.347	- .015	$\epsilon$	Readings discordant
.830..	2.933	16.94	.375	+ .015	$\epsilon$	
.902..	3.005	17.01	.375	+ .020	$\pi^5$	
1170.691..	-0.159	17.80	.067	- .001	$\epsilon$	
.718..	-0.132	17.82	.000	- .013	$\epsilon$	
.776..	-0.074	17.88	(- .138)	(- .043)	$\epsilon$	Rejected
.801..	-0.049	17.91	- .127	+ .003	$\epsilon$	
.841..	-0.009	17.95	- .177	- .015	$\epsilon, 2$	
.865..	+0.015	17.97	- .151	+ .009	$\pi^5$	
.885..	0.035	17.99	- .192	- .048	$\pi^5, 2$	Readings discordant, half-weight
.909..	0.059	18.02	- .112	+ .006	$\pi^5, 2$	
1172.692..	1.842	19.80	+ .276	- .023	$\epsilon$	
.710..	1.860	19.82	.285	- .006	$\epsilon$	
.753..	1.905	19.86	.245	- .028	$\epsilon$	
.772..	1.922	19.88	.273	+ .005	$\epsilon$	
.794..	1.944	19.90	.270	+ .006	$\epsilon$	
.813..	1.963	19.92	.271	+ .009	$\epsilon$	
.867..	2.017	19.97	(.286)	(+ .021)	$\pi^5$	
.885..	2.035	19.99	(.300)	(+ .030)	$\pi^5$	Probably smoke
1178.781..	0.026	25.89	- .154	- .002	$\epsilon$	
.800..	0.045	25.91	- .128	+ .006	$\epsilon$	
.850..	0.095	25.96	- .063	- .006	$\pi^5$	
.882..	0.127	25.99	+ .022	+ .019	$\pi^5$	
.908..	0.153	26.01	.041	- .016	$\pi^5, 2$	
1179.719..	0.964	26.82	.371	+ .016	$\epsilon$	
.742..	0.987	26.85	.372	+ .015	$\epsilon$	
1182.663..	-0.045	29.77	(- .112)	+ .022	$\epsilon$	
.687..	-0.021	29.79	(- .134)	+ .022	$\epsilon$	
.708..	0.000	29.81	(- .165)	- .002	$\epsilon$	
.739..	+0.031	29.84	(- .130)	+ .018	$\epsilon$	
.758..	0.050	29.86	(- .111)	+ .018	$\epsilon$	
.782..	0.074	29.89	(- .073)	+ .022	$\epsilon$	
.842..	0.134	29.95	(+ .001)	- .016	$\pi^5$	
.874..	0.166	29.98	(+0.093)	+0.011	$\pi^5$	



TABLE II—Continued

Date, G.M.T.	<sup>3495</sup> Phase	<sup>3496</sup> Phase	Difference of Magnitude	Residual	Com- pari- son Star	Remarks
2421183.731..	1.023	30.84	0.363	+0.003	$\xi$	No effect from third body
.747..	1.030	30.85	.359	— .002	$\xi$	
1185.765..	3.057	32.87	.339	— .009	$\xi$	
.783..	3.075	32.89	.348	+ .002	$\xi$	
.848..	3.140	32.95	.337	— .001	$\pi^s$	
.868..	3.160	32.97	.325	— .011	$\pi^s$	
1186.632..	—0.029	33.74	— .141	+ .009	$\xi$	
.648..	—0.013	33.75	— .172	— .012	$\xi, 2$	
.683..	+0.022	33.79	— .158	— .003	$\xi, 2$	
.699..	0.038	33.80	— .157	— .016	$\xi$	
.733..	0.072	33.84	— .086	+ .012	$\xi, 2$	
.755..	0.094	33.86	— .057	+ .002	$\xi$	
.770..	0.109	33.88	— .035	— .004	$\xi$	
.783..	0.122	33.89	+ .014	+ .020	$\xi, 2$	
.842..	0.181	33.95	.095	— .016	$\pi^s$	
.857..	0.196	33.96	.143	+ .004	$\pi^s, 2$	
.870..	0.209	33.98	.160	.000	$\pi^s, 2$	
1187.622..	0.961	0.13	.354	— .001	$\xi$	
.641..	0.980	0.15	.354	— .002	$\xi$	
.711..	1.050	0.22	.353	— .009	$\xi$	
.739..	1.078	0.24	.354	— .010	$\xi$	
.840..	1.179	0.35	.374	+ .006	$\pi^s$	
1192.644..	2.030	5.15	.258	— .010	$\xi$	Smoke?
.666..	2.052	5.17	.248	— .027	$\xi$	
.696..	2.082	5.20	.285	— .002	$\xi$	
.714..	2.100	5.22	.296	+ .002	$\xi$	
.741..	2.127	5.25	.310	+ .005	$\xi$	
.759..	2.145	5.26	.305	— .008	$\xi$	
1194.608..	0.041	7.11	— .127	+ .011	$\xi$	
.628..	0.061	7.13	— .112	+ .003	$\xi$	
.647..	0.080	7.15	— .077	+ .007	$\xi$	
.744..	0.177	7.25	+ .110	+ .007	$\xi$	
.762..	0.195	7.27	.146	+ .009	$\xi$	
.807..	0.240	7.31	.209	.000	$\pi^s$	
.831..	0.264	7.34	.225	— .014	$\pi^s$	
1197.655..	3.088	10.16	.351	+ .007	$\xi$	
.671..	3.104	10.18	.355	+ .012	$\xi$	
1202.743..	0.260	15.25	.240	— .005	$\pi^s$	
.759..	0.285	15.26	.229	— .033	$\pi^s, 2$	
.777..	0.303	15.28	.260	— .012	$\pi^s, 2$	
.817..	0.345	15.32	.283	+ .005	$\pi^s, 2$	
1203.620..	1.146	16.13	.375	+ .008	$\xi$	
.682..	1.208	16.19	.367	— .001	$\xi$	
.744..	1.270	16.25	.358	— .010	$\pi^s$	
1207.695..	1.268	20.20	.363	— .005	$\xi$	
1211.701..	1.321	24.21	.375	+ .007	$\xi, 2$	
1213.622..	3.242	26.13	.326	.000	$\xi$	Smoke?
.645..	3.265	26.15	.347	+ .024	$\xi$	
1222.575..	0.337	0.48	.261	— .016	$\xi$	
.606..	0.368	0.51	.290	+ .009	$\xi$	
1230.555..	0.410	8.46	.287	+ .002	$\xi$	
.636..	0.491	8.54	0.287	—0.010	$\xi, 2$	

TABLE II—Continued

Date, G.M.T.	$3^{d}95$ Phase	$3^{d}96$ Phase	Difference of Magnitude	Residual	Com- pari- son Star	Remarks
2421232.575..	2 <sup>d</sup> 430	10 <sup>d</sup> 48	0 <sup>m</sup> .373	+0 <sup>m</sup> .010	$\xi$	Third body?
1234.560..	0.462	12.46	(.325)	+ .033	$\xi$	
1237.531..	3.433	15.44	.303	+ .002	$\xi$	
1247.512..	1.554	25.42	.355	— .007	$\xi$	
.536	1.578	25.44	.351	— .010	$\xi$	
.558..	1.600	25.46	.358	— .003	$\xi$	Third body?
.660..	1.702	25.56	.346	— .005	$\pi^4, 2$	
.676..	1.718	25.58	.322	— .024	$\pi^4$	
1252.522..	2.610	30.43	(.441)	+ .074	$\xi$	
.542..	2.630	30.45	(.429)	+ .061	$\xi$	
1253.668..	—0.197	31.57	.138	— .003	$\pi^4, 2$	Through smoke, rough test only
1256.577..	2.712	34.48	(.353)	(— .015)	$\xi$	
.600..	2.735	34.50	(.359)	(— .008)	$\pi^4$	
.639..	2.774	34.54	(.328)	(— .039)	$\pi^4$	
.654..	2.780	34.56	(.353)	(— .013)	$\pi^4$	
1258.508..	0.690	1.81	.306	— .019	$\xi$	Third body?
1259.511..	1.693	2.81	.344	— .010	$\xi$	
.562..	1.744	2.86	.330	— .007	$\xi$	
.617..	1.799	2.92	.318	+ .002	$\pi^4$	
.632..	1.814	2.93	.286	— .024	$\pi^4, 2$	
1265.537..	—0.188	8.84	.152	+ .028	$\xi, 1$	Third body?
.563..	—0.162	8.86	.088	+ .014	$\xi, 1$	
1269.547..	—0.131	12.85	(— .107)	— .118	$\xi, 2$	
.609..	—0.069	12.92	(— .168)	— .054	$\pi^4$	
1281.537..	—0.001	24.84	— .161	+ .002	$\pi^4$	
.581..	+0.043	24.88	— .138	— .002	$\pi^4$	Poor sky
1296.541..	3.143	5.24	.301	— .037	$\pi^4$	
1307.547..	2.289	16.24	.342	— .015	$\pi^5$	Smoke, rough test only
1321.562..	0.491	30.26	(0.323)	(+0.026)	$\pi^5$	

TABLE II—*Continued*

## SERIES II

Date, G.M.T.	<sup>14</sup> <sub>05</sub> Phase	<sup>14</sup> <sub>46</sub> Phase	Difference of Magnitude	Residual	Com- pari- son Star	Remarks
2421482.856..	-0.279	18.56	0.251	-0.009	e	
.895..	-0.240	18.60	.226	+ .014	ξ	
.935..	-0.200	18.64	.144	- .003	ξ	
1483.835..	0.700	19.54	.350	+ .014	e	
.872..	0.737	19.57	.351	+ .009	ξ	
1484.807..	1.672	20.51	.365	- .002	e	
.872..	1.737	20.57	.363	+ .015	ξ	
.924..	1.789	20.63	.338	+ .009	e	
1485.849..	2.714	21.55	.400	+ .022	e	
.894..	2.759	21.60	.391	+ .014	e	
1486.803..	-0.285	22.50	.281	+ .015	e	
.860..	-0.228	22.56	.222	+ .029	e	
.881..	-0.207	22.58	.160	+ .001	ξ	
.918..	-0.170	22.62	.102	+ .012	e, 2	
.936..	-0.152	22.64	.056	+ .001	ξ, 2	
1487.864..	0.776	23.57	.347	.000	e, 4	Smoke
1488.808..	1.720	24.51	.352	- .001	e	
.860..	1.772	24.56	.343	+ .007	e	
.917..	1.829	24.62	.318	+ .006	ξ	
1489.858..	2.770	25.56	.368	- .009	e	
.900..	2.812	25.60	.364	- .012	ξ, 2	
1490.799..	-0.242	26.50	.212	- .002	e, 2	Poor sky
1493.842..	2.801	29.54	.377	+ .001	ξ	
.905..	2.864	29.61	.380	+ .006	e	
1494.797..	-0.196	30.50	(.163)	+ .023	e	
.816..	-0.177	30.52	(.127)	+ .023	e	
.836..	-0.157	30.54	(.101)	+ .036	e	
.862..	-0.131	30.56	(+.006)	- .005	ξ	Third Body?
.880..	-0.113	30.58	(-.019)	+ .004	ξ	
.901..	-0.092	30.60	(-.071)	- .011	e	
.919..	-0.074	30.62	(-.110)	- .016	e	
1495.798..	0.805	31.50	.347	- .002	e	Poor sky
.818..	0.825	31.52	.353	+ .002	e	
1496.923..	1.930	32.63	.291	+ .016	e, 2	Poor sky
.937..	1.944	32.64	.246	- .027	e, 2	
1499.832..	0.886	0.94	.340	- .018	ξ	
1500.778..	1.832	1.88	.328	+ .017	e	
.847..	1.901	1.95	.290	+ .007	ξ	
.893..	1.947	2.00	.280	+ .007	e	
.937..	1.991	2.04	.263	- .009	e, 2	Readings discordant
1501.842..	2.896	2.94	.371	- .001	ξ	
.861..	2.915	2.96	.373	+ .002	ξ	
1502.877..	-0.112	3.89	- .032	- .007	ξ	
.815..	-0.084	3.92	- .072	+ .006	ξ	
.841..	-0.058	3.94	- .102	+ .013	ξ	Probably smoke on this date
.862..	-0.037	3.96	- .138	- .001	ξ	
.879..	-0.020	3.98	- .176	- .026	ξ	
.899..	0.000	4.00	- .174	- .021	ξ	
1506.860..	+0.009	7.96	- .135	+ .015	ξ	
.891..	0.040	7.99	- .133	- .009	ξ	
1507.835..	0.984	8.94	0.364	-0.003	ξ	

TABLE II—Continued

Date, G.M.T.	3 <sup>45</sup> Phase	3 <sup>46</sup> Phase	Difference of Magnitude	Residual	Com- pari- son Star	Remarks
2421510.780..	-0 <sup>0</sup> .021	11 <sup>4</sup> .88	-0 <sup>M</sup> .132	+0 <sup>M</sup> .017	e	
.803..	+0.002	11.91	-.154	-.002	ε	
.825..	0.024	11.93	-.137	+.003	ε	
.842..	0.041	11.95	-.111	+.012	ε	
.860..	0.059	11.96	-.110	-.009	ε	
1514.755..	-0.002	15.86	-.132	+.021	e	
.776..	+0.019	15.88	-.126	+.018	e	
.800..	0.043	15.90	-.127	-.006	ε	
.819..	0.062	15.92	-.094	+.003	ε	
.839..	0.082	15.94	-.067	-.006	ε	
.866..	0.109	15.97	-.010	+.001	e	
.889..	0.132	15.99	+.023	-.011	e	
.916..	0.159	16.02	.098	+.010	μ	
.942..	0.185	16.05	.138	.000	μ	
1517.783..	3.026	18.89	.353	-.008	ε	
1522.810..	0.148	23.92	.052	-.015	ε	
.883..	0.221	23.99	.222	+.024	μ	
1529.700..	3.091	30.81	(.293)	-.060	e, 2	Third body? Rejected
.778..	3.163	30.88	(.327)	-.018	e, 2	
1534.799..	0.278	1.30	(.339)	(+.070)	ε	Readings discordant
.842..	0.321	1.35	.264	-.022	e	
.894..	0.373	1.40	.308	+.016	μ	
1535.790..	1.269	2.29	.390	+.012	ε	
.816..	1.295	2.32	.378	.000	e	
.853..	1.332	2.35	.363	-.014	e	
.880..	1.359	2.38	.392	+.015	μ	
.904..	1.383	2.41	.376	.000	μ	
1536.756..	2.235	3.26	.345	-.013	ε	
.771..	2.250	3.28	.337	-.026	ε	
.800..	2.279	3.30	(.317)	(-.050)	e	No apparent reason for discrepancy
.817..	2.296	3.32	(.317)	(-.051)	e	
.861..	2.340	3.37	.367	-.003	μ	
.881..	2.360	3.39	.345	-.026	μ	
.902..	2.381	3.41	.351	-.020	μ	
1537.728..	3.207	4.23	.343	+.003	ε	
.753..	3.232	4.26	.350	+.013	e	
1538.731..	0.257	5.24	.247	.000	ε	
.751..	0.277	5.26	.270	+.002	e	
.774..	0.300	5.28	.288	+.006	ε	
.795..	0.321	5.30	.282	-.004	ε	
.809..	0.335	5.31	.296	+.009	e	
.830..	0.362	5.34	.262	-.028	e	
.862..	0.388	5.37	.292	-.001	μ	
.885..	0.411	5.39	.291	-.005	μ	
.911..	0.437	5.42	.299	-.001	μ	
1548.749..	2.370	15.26	.374	+.003	ε	
.774..	2.395	15.28	.368	-.004	e	
1549.705..	3.326	16.21	.318	-.007	e	Poor sky
.724..	3.345	16.23	.332	+.009	ε	
.887..	3.508	16.39	.304	+.005	μ	
1551.687..	1.356	18.19	.367	-.010	ε	
1553.692..	3.361	20.20	0.328	+0.007	ε	

TABLE II—*Continued*

Date, G.M.T.	3 <sup>d</sup> 05 Phase	3 <sup>d</sup> 46 Phase	Difference of Magnitude	Residual	Com- pari- son Star	Remarks
2421553.716..	3 <sup>d</sup> 385	20 <sup>d</sup> 22	0 <sup>m</sup> .337	+0 <sup>m</sup> .020	e	Cell near glowing point
1573.628..	3.531	5.53	.272	— .024	ξ	
1574.612..	0.562	6.52	.333	+ .015	ξ, 2	
.637..	0.587	6.54	.354	+ .032	e	
1579.610..	1.607	11.52	.354	— .017	ξ	
.637..	1.634	11.54	.358	— .011	e	
1580.623..	2.620	12.53	.303	— .015	e	
1583.562..	1.606	15.47	.375	+ .004	e	
.597..	1.641	15.50	.349	— .020	ξ	
1588.665..	2.756	20.57	.305	— .012	ξ	
1592.603..	2.741	24.51	.380	+ .003	e	No effect from third body
1596.589..	2.773	28.49	.388	+ .012	ξ	
.607..	2.791	28.51	.395	+ .019	e	
1598.561..	0.792	30.46	.347	— .001	e	
.579..	0.810	30.48	.354	+ .004	ξ	
1601.594..	—0.128	33.50	— .010	— .016	ξ	Readings discordant
1603.549..	1.827	0.85	.307	— .006	ξ	
1612.567..	2.938	9.87	.390	+ .021	ξ	
1613.534..	—0.048	10.84	— .129	— .003	ξ	
.581..	—0.001	10.88	— .143	+ .010	e	
1622.693..	1.205	20.00	.398	+ .020	μ	
1626.535..	1.094	23.84	.390	+ .015	ξ	
1628.567..	3.125	25.87	.370	+ .021	e	
.687..	3.245	25.99	.365	+ .030	μ	
1631.677..	2.282	28.98	.302	— .005	μ	
.701..	2.306	29.00	.380	+ .012	μ	
1635.531..	2.183	32.83	.338	— .002	ξ	
.550..	2.202	32.85	.323	— .024	e	
.569..	2.221	32.87	.356	+ .002	e	
.591..	2.243	32.89	.356	— .004	μ	
1663.569..	2.547	26.27	.370	— .007	μ	
1669.576..	0.647	32.27	.345	+ .016	μ	
1670.569..	1.640	33.27	0.369	0.000	μ	

curve. When less than three sets of measures were averaged the number is indicated by the figure following the comparison star. Where both the difference of magnitude and corresponding residual are in parentheses it indicates that the observation was entirely rejected; where the difference of magnitude only is in parenthesis the observation was not used in determining the short-period light-curve, but was used in the test for the third body.

In Table III are shown the reductions of the observations with  $\pi^5$  Orionis. The light-curve of  $\pi^5$  was referred to  $\pi^4$  Orionis, and the correction on account of the variation of  $\pi^5$  is given in the fourth column. The adopted values in the last column are

the sums of the corresponding numbers in the third and fourth columns plus 0.120 magnitude, the difference between  $\pi^4$  Orionis and  $\xi$  Tauri.

TABLE III  
COMPARISONS OF  $\lambda$  TAURI WITH  $\pi^5$  ORIONIS

Date, G.M.T.	$\pi^4$ Phase	Observed Difference of Magnitude	Reduction to $\pi^4$ Orionis	Adopted Referred to $\xi$ Tauri
2421164.929....	0 <sup>d</sup> 770	+0 <sup>m</sup> 138	+0 <sup>m</sup> 008	+0 <sup>m</sup> 266
1168.909....	1.049	+ .154	+ .009	+ .283
1169.902....	2.042	+ .289	- .034	+ .375
1170.865....	3.005	- .274	+ .003	- .151
.885....	3.025	- .313	+ .001	- .192
.909....	3.049	- .232	.000	- .112
1172.867....	1.307	+ .174	- .008	+ .286
.885....	1.325	+ .190	- .010	+ .300
1178.850....	3.589	- .145	- .038	- .063
.882....	3.621	- .059	- .039	+ .022
.908....	3.647	- .040	- .039	+ .041
1182.842....	0.181	- .084	- .035	+ .001
.874....	0.213	+ .006	- .033	+ .093
1185.848....	3.187	+ .228	- .011	+ .337
.868....	3.207	+ .217	- .012	+ .325
1186.842....	0.480	- .012	- .013	+ .095
.857....	0.495	+ .035	- .012	+ .143
.870....	0.508	+ .051	- .011	+ .160
1187.840....	1.478	+ .276	- .022	+ .374
1194.807....	1.044	+ .080	+ .009	+ .209
.831....	1.068	+ .097	+ .008	+ .225
1202.817....	1.653	+ .197	- .034	+ .283
1307.547....	2.771	+0.211	+0.011	+0.342

In Table IV are given the normal magnitudes on the basis of the period of 3.952941 days, together with the residuals from the final light-curve. In forming these normals it was desirable, especially for Series I, not to mix up in the same normal observations with different comparison stars, one of which is known to be a variable. Each normal usually comprises six sets or more, but when fewer than five sets were averaged that fact is indicated by the figure which follows the comparison star. The systematic corrections, which were applied to Series II before forming the normals, will be discussed later.

The normal magnitudes of Table IV are shown graphically in Figure 1, where open circles represent the results of Series I, and barred circles those of Series II. The normals of the first series which were of low weight, and also those referred to  $\pi^4$  or  $\pi^5$  Orionis, are indicated by crosses.

From the residuals in Table II there follow for the probable errors of a single observation: Series I,  $\pm 0^m.008$ ; Series II,  $\pm 0^m.009$ . In computing these probable errors all poor observations were given full weight, and the residuals include all unknown variations of the comparison stars and outstanding errors of the light-curve. Treating the residuals of Table IV likewise as all of equal weight, the probable error of one normal is  $\pm 0^m.006$  for each series.

## TEST FOR THE THIRD BODY

In view of the discordances which observers have reported for  $\lambda$  Tauri, it was expected that the photo-electric measures would show either large perturbations of the eclipse times, or actual

TABLE IV  
NORMAL MAGNITUDES  
SERIES I

Phase	Difference of Magnitude	Residual	Comparison Stars	Phase	Difference of Magnitude	Residual	Comparison Stars
$-0^d.197$	$+0^m.138$	$-0^m.003$	$\pi^1, 3$	$1^d.064$	$+0^m.354$	$-0^m.009$	$\xi$
$- .175$	$+ .120$	$+ .020$	$\xi, 2$	$1.177$	$.371$	$+ .003$	$\xi$
$- .159$	$+ .067$	$- .001$	$\xi, 3$	$1.224$	$.366$	$- .002$	$\pi^1, \pi^5$
$- .132$	$.000$	$- .013$	$\xi, 3$	$1.294$	$.369$	$+ .001$	$\xi$
$- .039$	$- .134$	$+ .006$	$\xi$	$1.577$	$.355$	$- .006$	$\xi$
$- .011$	$- .174$	$- .012$	$\xi, 4$	$1.710$	$.334$	$- .014$	$\pi^1, 4$
$- .001$	$- .161$	$+ .002$	$\pi^1, 3$	$1.718$	$.337$	$- .009$	$\xi$
$+ .022$	$- .165$	$- .009$	$\pi^5$	$1.763$	$.318$	$- .013$	$\xi$
$.024$	$- .156$	$- .002$	$\xi$	$1.804$	$.318$	$+ .004$	$\xi$
$.041$	$- .137$	$+ .001$	$\xi$	$1.805$	$.305$	$- .009$	$\pi^1$
$.051$	$- .125$	$+ .003$	$\pi^1, \pi^5$	$1.842$	$.278$	$- .021$	$\xi$
$.066$	$- .099$	$+ .009$	$\xi$	$1.864$	$.284$	$- .005$	$\xi$
$.087$	$- .067$	$+ .004$	$\xi$	$1.908$	$.264$	$- .008$	$\xi$
$.111$	$- .020$	$+ .007$	$\pi^5$	$1.928$	$.265$	$- .001$	$\xi$
$.114$	$- .015$	$+ .006$	$\xi$	$1.954$	$.270$	$+ .007$	$\xi$
$.167$	$+ .068$	$- .016$	$\pi^5$	$1.998$	$.274$	$+ .012$	$\pi^5$
$.186$	$.128$	$+ .008$	$\xi$	$2.041$	$.253$	$- .018$	$\xi$
$.202$	$.152$	$+ .003$	$\pi^5, 4$	$2.089$	$.289$	$- .001$	$\xi$
$.252$	$.217$	$- .008$	$\pi^5$	$2.136$	$.308$	$- .001$	$\xi$
$.275$	$.236$	$- .015$	$\pi^1$	$2.289$	$.342$	$- .015$	$\pi^5, 3$
$.318$	$.272$	$- .003$	$\pi^1, \pi^5, 4$	$2.430$	$.373$	$+ .010$	$\xi, 2$
$.352$	$.276$	$- .002$	$\xi$	$2.815$	$.368$	$+ .002$	$\xi$
$.459$	$.287$	$- .005$	$\xi$	$2.922$	$.366$	$+ .005$	$\xi$
$.768$	$.326$	$- .009$	$\xi$	$3.066$	$.344$	$- .003$	$\xi$
$.816$	$.337$	$- .003$	$\xi$	$3.078$	$.353$	$+ .007$	$\pi^5$
$.962$	$.360$	$+ .005$	$\xi$	$3.096$	$.353$	$+ .010$	$\xi$
$.982$	$.360$	$+ .003$	$\xi$	$3.254$	$.336$	$+ .011$	$\xi$
$1.031$	$+0.361$	$+0.001$	$\xi$	$3.433$	$+0.303$	$+0.002$	$\xi, 3$

TABLE IV—*Continued*

## SERIES II

Phase	Difference of Magnitude	Residual	Comparison Stars	Phase	Difference of Magnitude	Residual	Comparison Stars
-0.277	+0.256	+0.003	$\epsilon$	0.813	+0.340	+0.001	$\epsilon$ , $\xi$
- .236	+ .211	+ .008	$\epsilon$ , $\xi$	0.993	.355	- .002	$\xi$
- .213	+ .181	+ .014	$\epsilon$ , $\xi$	1.280	.370	+ .002	$\epsilon$ , $\xi$ , $\mu$
- .180	+ .113	+ .004	$\epsilon$ , $\xi$	1.371	.362	- .005	$\xi$ , $\mu$
- .135	+ .013	- .006	$\xi$	1.621	.352	- .008	$\epsilon$ , $\xi$
- .093	- .062	- .001	$\xi$	1.656	.348	- .010	$\epsilon$ , $\xi$ , $\mu$
- .048	- .126	+ .005	$\xi$	1.748	.343	+ .007	$\epsilon$ , $\xi$
- .024	- .145	+ .009	$\epsilon$ , $\xi$	1.820	.311	+ .003	$\xi$
- .006	- .164	- .001	$\epsilon$ , $\xi$	1.893	.293	+ .015	$\epsilon$ , $\xi$
+ .005	- .168	- .005	$\epsilon$ , $\xi$	1.962	.257	- .005	$\epsilon$
.011	- .154	+ .008	$\xi$	2.207	.329	- .008	$\epsilon$ , $\xi$
.027	- .142	+ .009	$\epsilon$ , $\xi$	2.244	.336	- .013	$\xi$ , $\mu$
.045	- .132	+ .002	$\xi$	2.271	.334	- .022	$\xi$ , $\mu$
.056	- .128	- .006	$\xi$	2.340	.344	- .016	$\mu$
.077	- .090	- .001	$\xi$	2.387	.351	- .010	$\epsilon$ , $\xi$ , $\mu$
.125	- .004	- .004	$\epsilon$	2.632	.364	- .004	$\epsilon$ , $\mu$
.159	+ .060	- .008	$\xi$ , $\mu$	2.757	.369	+ .002	$\epsilon$ , $\xi$
.208	.160	+ .001	$\mu$	2.783	.374	+ .008	$\epsilon$ , $\xi$
.272	.248	.000	$\epsilon$ , $\xi$	2.831	.364	- .001	$\epsilon$ , $\xi$
.319	.268	- .007	$\epsilon$ , $\xi$	2.921	.368	+ .007	$\xi$
.362	.275	- .004	$\epsilon$ , $\mu$	3.124	.345	+ .005	$\epsilon$ , $\xi$
.417	.274	- .012	$\mu$	3.273	.331	+ .009	$\epsilon$ , $\mu$
.604	.331	+ .018	$\epsilon$ , $\xi$ , $\mu$	3.369	.322	+ .012	$\epsilon$ , $\xi$
0.743	+0.339	+0.007	$\epsilon$ , $\xi$	3.521	+0.277	-0.011	$\xi$ , $\mu$

occulting effects of the third body. During the first season, however, no discrepancy was noted until J.D. 2421252, January 23, 1917, when two observations of three sets each, with  $\xi$  Tauri as comparison star, made  $\lambda$  Tauri unusually bright, the residuals later being determined as 0.074 and 0.061.  $\xi$  Tauri was promptly compared with  $\pi^4$  Orionis, and this measure made  $\xi$  Tauri only 0.014 fainter than usual. There was nothing apparent in the observing conditions which could account for this sudden brightening up of  $\lambda$  Tauri, and the discordance was some seven or eight times the probable error of an observation.

The next large discordance was on J.D. 2421269, February 9, 1917, when two comparison stars were used. The mean of two sets with  $\xi$  Tauri made  $\lambda$  Tauri faint by 0.118, while three sets with  $\pi^4$  Orionis gave a residual of 0.054 in the same direction. As these measures were taken during the primary eclipse of the close pair, a careful search has been made for an error in the



recorded times or in the reductions, but the results are apparently correct.

At the end of that season when all of the results were arranged on the 34.6-day phase, it was seen that the discrepancies had occurred at two places in the cycle, separated by about half the period. These were at the approximate phases 13 and 30.5 days, zero phase being counted from the hypothetical time of the third

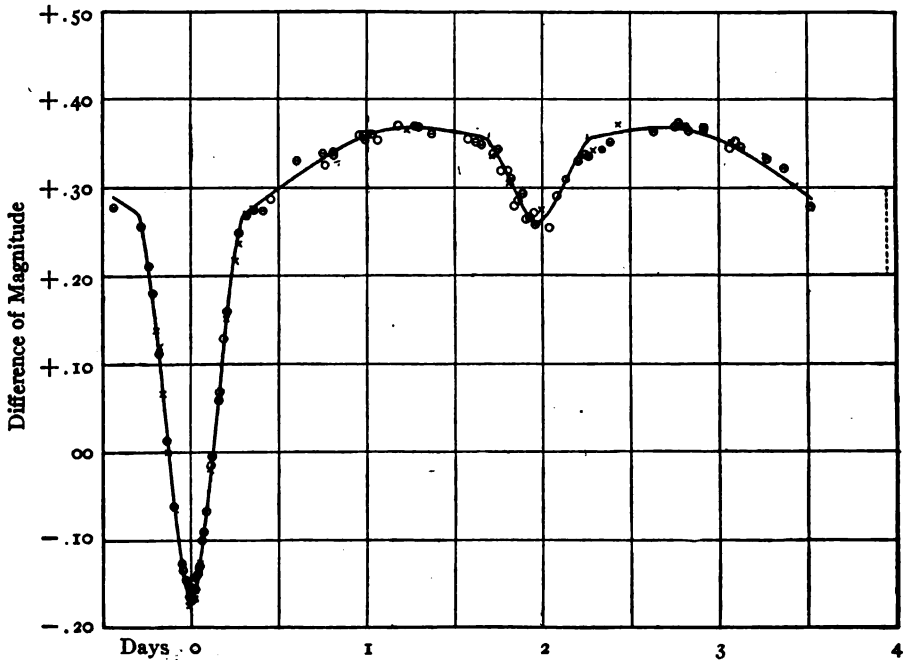


FIG. 1.—The light-curve of  $\lambda$  Tauri

body eclipsing the center of mass of the close system, as computed from the spectroscopic elements. Therefore, if we could assume that the third body was about four days ahead of its predicted place, we should have a clue to the cause. A triply eclipsing system would present interesting observational difficulties, as the eclipses of the close components by the distant member would each be displaced over a range of several days due to the motion about the center of mass. I have no idea, however, as to what

would cause the total light of the system to be increased by 6 or 7 per cent when the third body is nearly in front of the others, though at the present writing I have suspicions of a similar brightening up at the beginning and end of the eclipses of another star. The observations of  $\lambda$  Tauri were carried through the second season with the special object of detecting the effect of the third body, but also to polish up the light-curve for the close pair.

The residuals of Table II have been arranged according to the phase of the longer period, combining observations only on the same night, and the result of this test is shown in Figure 2. As before, open circles indicate the observations of Series I, barred circles those of Series II, while crosses indicate the means of fewer

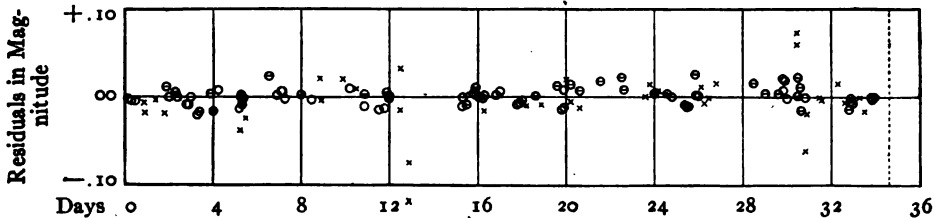


FIG. 2.—Test for the third body of  $\lambda$  Tauri; period = 34.6 days

than five sets for either series. There are apparently four nights involved in the larger discrepancies, two when the system was faint and two when it was bright, also one or two other nights near the same phase when the light was changing abnormally. On the other hand there are about an equal number of observations in the vicinity of phase 30–31 days where nothing unusual was noted.

My conclusion is that at best we have here only a suspicion of an effect due to a third body, which in any event must be small, and it is not worth while to continue the search further. After spending two seasons on the attempt I am willing to let someone else try his hand at detecting discrepancies of less than a tenth of a magnitude, which come at intervals of seventeen days, and which if they exist at all must be subject to large irregularities.

## COMPARISON WITH THE SPECTROSCOPIC ELEMENTS

A further test of the anomalies in this system is given by a comparison of the photometric results with the spectroscopic orbit, since on the simple eclipse theory the epoch of primary minimum should be when the bright body is  $90^\circ$  from the node.

TABLE V  
TIMES OF MINIMA

Source	Elements	Computed Minimum	Difference
		J.D.	
Spectroscopic orbit.....		2417945.240	.....
v. Aretin.....	J.D. 2399607.527+3 <sup>d</sup> 952941·E	7945.220	-0 <sup>d</sup> 020
Photometric 1916, Series I.....	2421194.573+3 <sup>d</sup> 952941·E	7945.255	+ .015
Photometric 1917, Series II.....	2421506.850+3 <sup>d</sup> 952941·E	7945.250	+ .010
Photometric 1917, with corrected period.....	2421506.850+(3.952952·E)	7945.240	( 0.000)

An inspection of the available data leads to the following conclusion. The difference of fourteen minutes between the observed time of minimum in 1917 and that required by the spectroscopic elements from plates taken in 1907-1914, corresponds to an error of 1 km/sec. in the velocity-curve, of 0<sup>m</sup>02 in the light-curve, or of one second in the adopted period. It will therefore require more evidence than we have at present to establish any real discordance between the photometric and spectroscopic results.

THEORY OF THE SYSTEM OF  $\lambda$  TAURI

In deriving the elements of the system of  $\lambda$  Tauri the method and notation of Russell have been used. The first step was to derive the law of variation between eclipses. Using the normals farther than 0.35 day from the times of primary and secondary minima, there was found:

$$\left. \begin{aligned} \text{Series I, Magnitude} &= 0^{\text{m}}3576 - 0^{\text{m}}0474 \cos \theta - 0^{\text{m}}0542 \cos^2 \theta \\ &\quad \pm 13 \quad \pm 25 \quad \pm 47 \\ \text{Series II, Magnitude} &= 0^{\text{m}}3740 - 0^{\text{m}}0420 \cos \theta - 0^{\text{m}}0710 \cos^2 \theta \\ &\quad \pm 17 \quad \pm 20 \quad \pm 41 \end{aligned} \right\} (1)$$

where  $\theta$  is the phase angle, and the magnitude is referred to  $\xi$  Tauri. The difference between the first terms could be due to a progressive variation of the total light of the system or to a change in the comparison star from one year to the next. The coefficients of  $\cos \theta$  agree within half a hundredth of a magnitude. The difference between the coefficients of  $\cos^2 \theta$  could be interpreted to mean a change in the ellipticity of figure of the components, but the discrepancy of 30 per cent is too large to be considered in this connection. By inspection of the graphs of both series it was seen that by a shift of a hundredth of a magnitude the curve between minima for Series II would fit the observations of Series I very well; and it was independently found that during the primary eclipse a systematic difference of a hundredth of a magnitude in the same direction also existed. It was therefore thought best to apply the correction of  $0^m.010$  to all magnitudes of Series II. It was also found graphically that the time of primary minimum for Series II was 0.005 day early on the basis of the times computed from the first season. The two series were treated therefore as follows:

*Series I.*—Original observations in Table II and all normals were unchanged.

*Series II.*—Original phases and magnitudes in Table II were unchanged, but corrections of  $+0.005$  day to the phases and  $-0^m.010$  to the observed differences of magnitude were applied before forming the normals in Table IV. The residuals for Series II, given in Table II, were derived after the corrections had been applied.

The normal magnitudes for the two seasons were thus made homogeneous, and the next step was to rectify the magnitudes during the eclipses, which was accomplished from (1) by adding  $0^m.0542 \cos^2 \theta$  to the observed magnitudes, then reducing to light and adding  $0.0418 (1 + \cos \theta)$  in light units. At primary minimum the normals before and after zero phase were combined on one branch of the curve. The observations near secondary minimum were used only to determine the minimum light at that phase, as the form of the curve, with less than a tenth of a magnitude range, was of no service in deriving the elements.

The spectroscopic eccentricity of 0.060 gives 2.010 days for the phase of the secondary minimum, but as the photometric results are not sufficient to establish an accurate time in this part of the curve it has seemed sufficient to neglect the eccentricity and assume the central phase of the secondary to be at the phase equal to one-half of the period, or 1.976 days.

TABLE VI  
COMBINED NORMALS, PRIMARY MINIMUM

Phase	Observed Magnitude	Rectified Light	Residual Light	Series
0.006.....	-0.166	0.705	-0.002	II
0.008.....	- .170	.703	- .006	I
0.021.....	- .147	.716	+ .006	II
0.023.....	- .159	.709	- .003	I
0.040.....	- .138	.721	+ .001	I
0.046.....	- .129	.726	+ .003	II
0.057.....	- .113	.735	+ .006	I
0.066.....	- .109	.738	- .001	II
0.095.....	- .051	.773	+ .005	I
0.109.....	- .033	.785	- .002	II
0.121.....	- .009	.799	- .001	I
0.147.....	+ .036	.828	- .007	II
0.167.....	+ .085	.862	+ .001	I
0.193.....	+ .136	.899	+ .003	I
0.194.....	+ .136	.899	+ .001	II
0.224.....	+ .196	.943	+ .011	II
0.264.....	+ .226	.964	- .013	I
0.274.....	+0.252	0.984	+0.002	II

TABLE VII  
RECTIFIED CURVE

	Magnitude	Range	Light	Loss of Light
Maximum.....	0.405	.....	1.000	.....
Primary minimum.....	+0.029	0.376	0.707	0.293
Secondary minimum.....	0.315	0.090	0.920	0.080

The combined normals for primary minimum, using both branches of the curve, are given in Table VI. After some trials the constants of the curve were adopted as in Table VII. These constants with the combined rectified normals are the basis of the elements.

It is obvious at the outset that  $\lambda$  Tauri furnishes a case where the elements will be poorly determined, first because of the small

range of about  $0.4$  in a partial eclipse, and second because of the undetermined light of the third body. In allowing for the effect of the ellipsoidal figure of the bodies, we have from the last term of (1)  $0.0542$  in magnitude  $= 0.0487$  in light, and hence

$$z = 2 \times 0.0487 = 0.097.$$

But this value of  $z$  is too small if there is light from the third body, which would reduce the apparent variation of the eclipsing pair from whatever cause. In view of this uncertainty, and for convenience, all computations have been on the basis:

$$z = 0.10.$$

In Russell's method for a partial eclipse, we have to find the function  $\chi(k, a_0, \frac{1}{4})$  which is derived from the form of the curve at primary minimum. If we consider the total light at any time as coming from a pair of overlapping disks plus the light of the third body, the effect would be the same if we should extinguish the third member and give its light to the uneclipsed member of the close pair. The  $\chi$  function is therefore independent of the light of the third body.

In using the secondary minimum to determine the elements we have for two bodies

$$a_0(L_1 + L_2) = 1 - \lambda_1 + \frac{1 - \lambda_2}{k^2},$$

but with the third body, if  $L_1 + L_2 + L_3 = 1$ , there follows

$$a_0 = \frac{1}{1 - L_3} \left( 1 - \lambda_1 + \frac{1 - \lambda_2}{k^2} \right).$$

We now determine  $a_0$  and  $k$  by the intersection of the curve

$$\chi(k, a_0, \frac{1}{4}) = \text{constant},$$

and the system of curves

$$a_0 = \frac{1}{1 - L_3} \left( 0.080 + \frac{0.293}{k^2} \right)$$

which may be drawn for different assumed values of  $L_3$ . As there is no way of determining  $L_3$ , the elements must remain uncertain within certain limits, between zero and a quantity such that  $L_2$  and  $L_3$  together shall not be large enough for their combined spectra to show on the plates. This limit of  $L_2 + L_3$  is assumed to be one-third of  $L_1$ , or

$$0 < L_3 < \frac{L_1}{3} - L_2.$$

When the first approximate solution was made, it was found that  $L_3$  must be as large as 0.13 for the curves giving  $a_0$  and  $k$  to intersect. Thus with only two eclipsing bodies a solution was impossible, but it was possible on the assumption of a third body giving 0.13 of the total light. This was a striking case of the "astronomy of the invisible," but a critical examination shows that the material is not sufficient to establish the light effect of the third body in this way. It was found that any value of the  $\chi$  function between 1.76 and 1.84 would satisfy the observations about equally well. Even if  $\chi$  could be determined there is a large range of the values for each element of the system, as is shown in Table VIII, which is computed for  $C=0.125$ ,  $D=0.0695$ ,  $C/D=\chi=1.80$ .

TABLE VIII  
ELEMENTS FOR  $\chi$  ( $a_0, k, \frac{1}{2}$ ) = 1.80

	0.641	0.625	0.65	0.70	0.75	0.80	0.90	1.00
$k$ .....	1.00	.95	.84	.73	.655	.60	.52	.45
$a_0$ .....	.71	.79	.83	.82	.796	.76	.70	.65
$L_1$ .....	.08	.09	.10	.11	.122	.13	.15	.18
$L_2$ .....	.21	.12	.07	.07	.082	.11	.15	.17
$L_3/(L_2+L_3)$ .....	2.4	3.8	4.9	4.6	3.9	3.2	2.3	1.9

From Table VIII it is seen that  $k$  may range from 0.6 to 0.8, but that for  $k=0.9$ ,  $L_1$  would be only 2.3 times  $(L_2+L_3)$ , and the additional spectra should be detected. Similar tables were made for  $\chi=1.76$  and 1.84. For  $\chi=1.76$  there is a solution for  $k=0.6$ , and no solutions for larger values of  $k$ , except that there is just a possibility for  $k=1.0$ . For  $\chi=1.84$  the least

value of  $L_3$  would be 0.20, and any solution would give too much light for the two fainter bodies. The possibility of the large body being in front at primary minimum seems to be entirely excluded, as this would also give too great a value for  $L_2+L_3$ . Taking the various combinations, the plausible range of the different quantities is

$$\begin{aligned} k &= 0.6 - 1.0 \\ a_0 &= 0.4 - 1.0 \\ L_1 &= 0.75 - 0.9 \\ L_2 &= 0.1 - 0.2 \\ L_3 &= 0.0 - 0.15 \\ L_1/(L_2+L_3) &= 3 - 10. \end{aligned}$$

The value  $k=0.75$  is therefore probably correct within 20 per cent, and on this basis, with  $\chi=1.80$ , the remaining elements will give a fair idea of the nature of the system. Using Russell's formulae there are found for the radii of the bodies and the inclination:

$$\begin{aligned} a_1 &= 0.299 \\ ka_1 &= 0.224 \\ \cos i &= 0.202 \end{aligned}$$

From the ellipsoidal constant  $z=0.10$  we have, following Russell, for the axes of the ellipsoids

$$a:b:c = 1.00:0.95:0.92.$$

The effect of the polar flattening is too small to consider as changing the computed inclination.

The final light-curve during eclipse was computed both by Russell's method, using the constants  $a_0$ ,  $k$ ,  $C$ , and  $D$ , and also independently from the elements by an adaptation of Harting's method, using Blazko's table.<sup>1</sup> The necessary changes because of elliptical disks were of course taken into account.

The graph in Figure 1 shows a satisfactory agreement of the curve with the observations, the only outstanding discordance being near the beginning and end of the secondary minimum, where a lowering of the curve by about a hundredth of a magnitude

<sup>1</sup> *Annales de l'observatoire astronomique de Moscou*, 5, 104, 1911.



would make a better agreement. This error is largely due to the adoption of the curve between minima as wholly from Series I, but in view of the systematic difference between measures of the two seasons, and the fundamental uncertainty in the final elements, it was not considered worth while to go through the work again. Likewise there appears no advantage in a case like this in making a solution for disks darkened at the limb.

TABLE IX  
LIGHT-CURVE OF  $\lambda$  TAURI

Phase	Difference of Magnitude	Phase	Difference of Magnitude
0 <sup>d</sup> .00.....	-0 <sup>m</sup> .163	1 <sup>d</sup> .80.....	0 <sup>m</sup> .316
$\pm$ 0.05.....	- .129	1.85.....	.295
$\pm$ 0.10.....	- .048	1.90.....	.275
$\pm$ 0.15.....	+ .051	1.95.....	.263
$\pm$ 0.20.....	.146	1.976.....	.261
$\pm$ 0.25.....	.222	2.00.....	.262
$\pm$ 0.30.....	.271	2.05.....	.274
$\pm$ 0.307.....	.273	2.10.....	.294
+0.40.....	.284	2.15.....	.315
0.50.....	.298	2.30.....	.334
0.75.....	.333	2.25.....	.351
1.00.....	.358	2.282.....	.357
1.25.....	.368	2.50.....	.365
1.273.....	.368	2.680.....	.368
1.50.....	.363	2.75.....	.367
1.669.....	.357	3.00.....	.355
1.70.....	.352	3.25.....	.326
1.75.....	0.335	3.50.....	0.291

In his discussion of the system of  $\lambda$  Tauri, Schlesinger has shown that the relative distances of the second and third bodies from the brightest one can be closely estimated, and on the assumption that the primary has 2.5 times the mass of the eclipsing satellite he finds the distances of the three bodies from the centroid of  $m_1$  and  $m_2$  to be respectively 3,200,000 km, 8,000,000 km, and 50,000,000 km. He used  $\sin i = 0.96$ , which is near enough the present value, 0.98. On this basis and the sun's radius of 695,500 km, there follow when the sun's mass, radius, and density are each taken as unity

$$m_1 = 2.5$$

$$a_1 = 4.8$$

$$\rho_1 = 0.025$$

$$m_2 = 1.0$$

$$a_2 = 3.6$$

$$\rho_2 = 0.024$$

$$m_3 = 0.4$$

$$\rho_0 = 0.025$$

The mean density of the close pair,  $\rho_0$ , follows from the values of the period and of  $a_1$  and  $k$ , and it is only by a coincidence that the independent assumption of the relative masses gives nearly equal densities for the two components. Lacking eclipse measurements of the third body, we have no clue as to its diameter and density. In Figure 3 the close system is drawn to scale, and in spite of the uncertainties this probably gives a rough idea of the conditions and dimensions of the two stars.

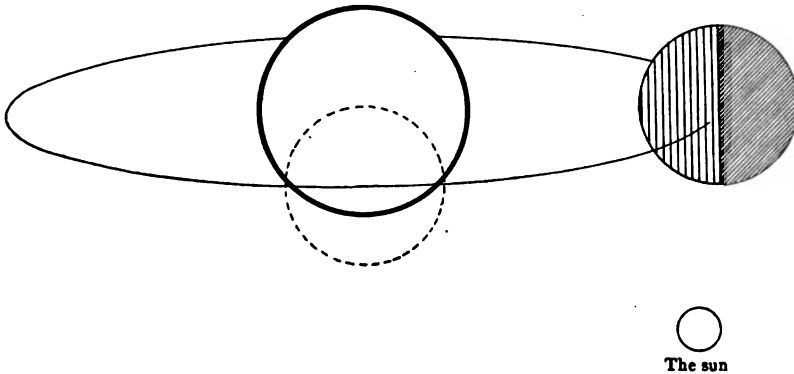


FIG. 3.—The four-day system of  $\lambda$  Tauri

The second body in the system of  $\lambda$  Tauri is similar to the companion of Algol in being brighter on the side toward the primary, in fact this radiation effect is apparently present in all close systems where the bodies are of unequal brightness. Using the formula<sup>1</sup> for the value of the albedo,  $\mu$ , on the basis of Lambert's law of reflection there follows

$$\mu = 2.7.$$

The corresponding albedo with the reflection law of Seeliger has been computed with an unpublished formula which I have derived or:

$$\mu = 3.8.$$

The conclusion from these figures, which is also plausible from other considerations, is simply that since theoretically the albedo cannot exceed unity the extra light from one side of the second body must be due in large part to the heating effect of the intense radiation from the primary.

<sup>1</sup> *Astrophysical Journal*, 33, 397, 1911.

## SUMMARY

We may now bring together the principal results of this paper, emphasizing some points which have not been brought out before.

1. A thorough study of  $\lambda$  Tauri has been made with the photo-electric photometer, and it is found that this star is a normal eclipsing system, with two minima and continuous variation between eclipses. (Fig. 1, Table IX.)

2. Of the five comparison stars used, all of which are of spectral class B, only one,  $\pi^5$  Orionis, has been established as a regular variable. (Tables I, III; also next article in this *Journal*.)

3. The probable errors of an observation comprising three sets of four readings each on the variable and a comparison star are  $\pm 0^m.008$  and  $\pm 0^m.009$  respectively for two seasons. This accordance indicates no large anomalies for either the variable or the other stars. (Table II.)

4. There were, however, some half-dozen nights when the measures of  $\lambda$  Tauri were systematically discordant up to a tenth of a magnitude, and an attempt was made to trace these discrepancies to an effect of the third body. Although the anomalies occur at two places in the 34.6-day cycle which are separated by half the period, we have at best only a suspicion that the third body is the cause. (Fig. 2.)

5. A comparison of the four-day light-curve with the Allegheny spectroscopic elements shows a good agreement of the eclipse times within the errors of the observed data. (Table V.)

6. There is a systematic difference of about a hundredth of a magnitude between the light of  $\lambda$  Tauri as measured in 1916-1917 and in 1917-1918. This may be ascribed to a change in the total light of the variable, in the light of the comparison star  $\xi$  Tauri, or to an unsuspected instrumental change; but there is not enough evidence at hand to make a decision on this matter. (Table II, Series I and II, also [1] Series I and II, also (1).)

7. Subject to the unavoidable uncertainties and with the assumptions which have been made, the plausible elements for the triple system of  $\lambda$  Tauri for uniform disks are as follows.

It is a pleasure to make acknowledgment of the work of various persons whose collaboration has made possible the results in this paper. The development of the photo-electric cells has been due

to Dr. Jakob Kunz, of our department of physics of the University. It happened that the particular quartz cell described was made with Dr. Kunz's apparatus during his absence by Mr. L. A. Welo, with some assistance from myself. I am indebted to Dr. Elmer Dershem for various improvements in the photometer, and for

TABLE X  
SUMMARY OF ELEMENTS OF  $\lambda$  TAURI

		Adopted	Range
From the Light-Curve			
Ratio of radii of first and second bodies.....	$k$	0.75	0.6 — 1.0
Area of second body obscured at minimum....	$a_0$	0.655	0.4 — 1.0
Light of first body.....	$L_1$	0.796	0.75 — 0.9
Light of bright side of second body.....	$L_2$	0.122	0.1 — 0.2
Light of faint side of second body.....	$L_2 - 2b$	0.038	0.0 — 0.12
Light of third body.....	$L_3$	0.082	0.0 — 0.15
Ratio of surface brightness of bright sides of first and second bodies.....	$J_1/J_2$	3.7	.....
Major radius of first body.....	$a_1$	0.299	.....
Major radius of second body.....	$a_2$	0.224	.....
Cosine of inclination.....	$\cos i$	0.202	.....
Ellipsoidal constant.....	$z$	0.10	.....
Ratio of axes of ellipsoids.....	$b/a$	0.95	.....
	$c/a$	0.92	.....
Mean density of close pair, sun = 1.....	$\rho_0$	0.025	.....
Computed albedo of second body, Lambert's law.....	$\mu$	2.7	.....
Computed albedo of second body, Seeliger's law.....	$\mu$	3.8	.....
From Allegheny Spectroscopic Elements			
Assumed, $m_1 = 2.5 \ m_2$		Sun = 1	
Mass of first body.....	$m_1$	2.5	.....
Mass of second body.....	$m_2$	1.0	.....
Mass of third body.....	$m_3$	0.4	.....
Major radius of first body.....	$a_1$	4.8	.....
Major radius of second body.....	$a_2$	3.6	.....
Density of first body.....	$\rho_1$	0.025	.....
Density of second body.....	$\rho_2$	0.024	.....

about half of the observations in 1917-1918; also to various students, in particular to Mr. P. H. Lucas, for assistance in observing, to Miss Iva Hamlin for reductions, and to Mr. L. L. Steimley for check computations.

This work is a portion of that accomplished under two grants of three hundred dollars each from the Draper fund of the National Academy of Sciences.

UNIVERSITY OF ILLINOIS OBSERVATORY  
February 1920

## THE ELLIPSOIDAL VARIABLE STAR, $\pi^5$ ORIONIS

By JOEL STEBBINS

### ABSTRACT

*Ellipsoidal variable star,  $\pi^5$  Orionis.*—The *light-curve* for this variable has been determined with reference to  $\pi^4$  Orionis by a series of observations made with a photo-electric photometer in 1916–1918. The results, corrected for atmospheric extinction, show that this star is a continuous variable with a double period equal to the time of revolution in the spectroscopic orbit, 3.70 days (Fig. 1). No eclipses are apparent. The evidence indicates that the variation is due entirely to the ellipsoidal shape of the components, resulting from their mutual attraction. The elongation of the brighter component, computed from the amplitude of light variation, must be something more than 5 per cent. This is the first case where ellipsoidal variation unaccompanied by eclipses has been detected by the author.

*Spectroscopic binary,  $\pi^4$  Orionis.*—The photo-electric photometric observations indicate that the *light variation* of this binary is little or none.

During the winter of 1916–1917, in the first series of measures of  $\lambda$  Tauri with the photo-electric photometer, it was found that one of the comparison stars,  $\pi^5$  Orionis, was giving discordant results, and it was natural to suspect that this star was itself variable.<sup>1</sup> At the same time  $\pi^5$  Orionis was being used as a standard in light-tests of the spectroscopic binary  $\pi^4$  Orionis.<sup>2</sup> Through an oversight the reference to the spectroscopic orbit of  $\pi^5$  Orionis had been missed, and it was not until the light variation was well established that Lee's orbit<sup>3</sup> was found. As some of the comparisons of  $\lambda$  Tauri with  $\pi^5$  Orionis had been made during primary minima of  $\lambda$  Tauri when no other comparison star was available, it was decided to determine the light-curve of  $\pi^5$  with  $\pi^4$  Orionis as standard, and then on the basis of this curve to use  $\pi^5$  for  $\lambda$  Tauri. In the sequel it turned out that  $\pi^4$  has little or no light variation, but even if it had the problem of determining both light-curves by comparison of two spectroscopic binaries of known periods could easily be solved by successive approximations.

<sup>1</sup> *Publications of the American Astronomical Society*, 3, 272, 1916.

<sup>2</sup> Baker, *Publications of the Allegheny Observatory*, 1, 110, 1908.

<sup>3</sup> *Astrophysical Journal*, 38, 180, 1913.

In Table I are the observations. The first date is October 31, 1916, and it will be noted that sixteen observations were made in 1916-1917, and nine in 1917-1918. Each difference of magnitude is the mean of three sets of four readings on each star, except where a different number is noted in the remarks. The differences are in the sense indicated, a plus sign meaning that  $\pi^4$  was brighter than  $\pi^5$ . The correction for atmospheric extinction in the third column was derived by multiplying the tabular visual extinction by the factor in the fourth column. This factor was determined

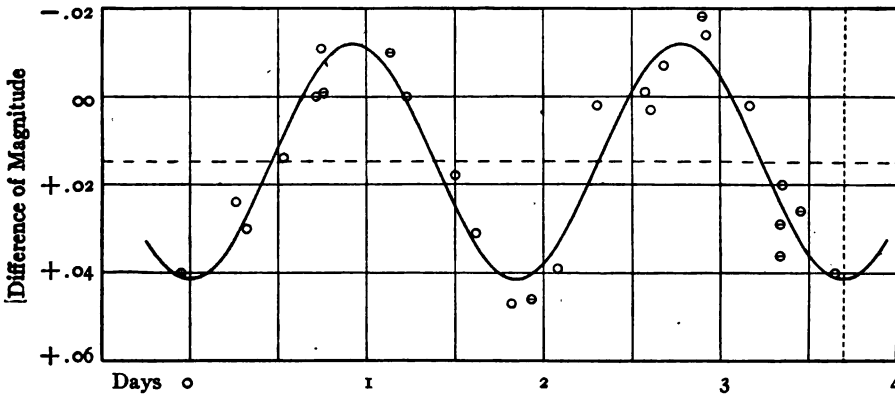


FIG. 1.—The light-curve of  $\pi^5$  Orionis

as a matter of routine for each night, the adopted value being found from measures of stars of known relative brightness; from the absolute light effects from standard stars, the instrumental conditions being constant over long intervals; and from the observer's estimate of the quality of the sky. The adopted factor was more or less arbitrary but was formed without reference to its effect upon the accordance of the results.

The phases for  $\pi^4$  and  $\pi^5$  are counted from the hypothetical eclipse times computed from the respective orbits.

$$\pi^4, \text{ minimum} = \text{J.D. } 2418287.584 + 9^d 5191 \cdot E$$

$$\pi^5, \text{ minimum} = \text{J.D. } 2417922.565 + 3^d 70045 \cdot E$$

In Figure 1 the differences of magnitude are plotted according to the phase of  $\pi^5$ , and it is seen that this star is a continuous

TABLE I  
OBSERVATIONS OF  $\pi^4$  AND  $\pi^5$  ORIONIS

Date, G.M.T.	$\pi^4 - \pi^5$ , Observed	Extinction	Factor	$\pi^4$ Phase	$\pi^5$ Phase	$\pi^4 - \pi^5$ , Corrected	Residual	Remarks
J.D. 2421159.932	$+\alpha^M_{018}$	$-\alpha^M_{020}$	1.7	7 <sup>h</sup> 09.9	3 <sup>h</sup> 17.4	$-\alpha^M_{002}$	$-\alpha^M_{011}$	4 sets
1186.889	$+.046$	$-.032$	2.0	5.499	0.527	$+.014$	$+.005$	2 sets, poor
1197.728	$+.048$	$-.024$	2.0	6.818	0.265	$+.024$	$+.007$	
.783	$+.050$	$-.020$	2.0	6.873	0.320	$+.030$	$+.003$	
1199.769	$+.019$	$-.017$	1.7	8.859	2.396	$+.002$	$+.013$	5 sets
1202.787	$+.060$	$-.029$	2.6	2.358	1.623	$+.031$	$-.003$	
1203.743	$+.017$	$-.018$	1.8	3.314	2.579	$-.001$	$+.005$	
.774	$+.021$	$-.018$	1.8	3.345	2.610	$+.003$	$+.011$	
1207.782	$+.010$	$-.024$	2.2	7.353	2.918	$-.014$	$-.005$	
1230.713	$+.058$	$-.018$	1.6	1.727	3.646	$+.040$	$-.001$	
1247.646	$+.057$	$-.018$	1.8	9.141	2.077	$+.039$	$+.005$	
1253.691	$+.025$	$-.025$	1.8	5.667	0.721	$+.000$	$+.006$	
.708	$+.018$	$-.029$	1.8	5.684	0.738	$-.011$	$+.004$	
1269.592	$+.065$	$-.018$	1.8	7.434	1.820	$+.047$	$+.006$	
1281.556	$+.011$	$-.018$	1.8	4.975	2.683	$-.007$	$+.004$	
1302.578	$+.060$	$-.042$	2.5	6.958	1.502	$+.018$	$+.007$	
1550.769	$+.032$	$-.033$	3.0	6.053	0.703	$-.001$	$+.007$	
1554.833	$+.019$	$-.029$	2.6	1.198	1.127	$-.010$	$+.004$	
1596.748	$+.065$	$-.029$	2.2	6.036	3.337	$+.036$	$.013$	
1603.710	$+.006$	$-.024$	2.1	3.479	2.898	$+.018$	$+.008$	
1611.670	$+.046$	$-.020$	1.8	1.920	3.457	$+.026$	$+.007$	6 sets, discordant
1622.653	$+.053$	$-.024$	2.2	3.384	3.336	$+.029$	$+.006$	
.669	$+.042$	$-.022$	1.8	3.400	3.354	$+.020$	$+.005$	
1628.647	$+.065$	$-.019$	1.6	9.378	1.932	$+.046$	$+.006$	6 sets, discordant
1631.649	$+.039$	$-.039$	3.0	2.861	1.233	$0.000$	$-.001$	

variable with double period equal to the time of revolution in the spectroscopic orbit. There are apparently no eclipses, and since the two minima are approximately equal and the spectrum is single, the variation is due entirely to the ellipsoidal shape of the components. The light variation is expressed by

$$\begin{aligned} \text{Difference of magnitude} = & +0^m.0146 + 0^m.0267 \cos 2\theta, \\ & \pm 10 \qquad \qquad \pm 14 \end{aligned}$$

where  $\theta$  is the phase angle, and the coefficients and their probable errors were derived by a least-squares solution from the twenty-five observations. The probable error of one observation of Table I is  $\pm 0^m.0048$ . Since the mean difference between  $\pi^4$  and  $\pi^5$  has been measured as  $0^m.0146$  with a probable error of a thousandth of a magnitude, it is worth while to examine the measures and see if this apparent accuracy is not illusory. A test of the accordance is given by averaging the results for the two seasons separately, which gives  $0^m.0142$  and  $0^m.0154$ , a discrepancy of  $0^m.0012$ , which is small enough to indicate that neither  $\pi^4$  nor  $\pi^5$  is changing progressively at a rapid rate. However, an inspection of the extinction correction in Table I shows that with corrections ranging from  $0^m.017$  to  $0^m.042$  the agreement between the two seasons must be in part accidental. The mean values of the extinction for the two seasons are  $0^m.022$  and  $0^m.027$ , and it could easily happen that there is a systematic error of several thousandths in either season. These two stars do not give a favorable case for the elimination of the extinction, as  $\pi^4$  is always higher in the sky than  $\pi^5$ , but if we take two nearly equal stars of the same spectral type, close together and near the zenith, the mean of twenty-five observations with the photo-electric photometer ought to have a probable error as small as  $0^m.001$ , assuming, of course, that the stars are not variable.

The coefficient of  $2\theta$  gives readily a measure of the least ellipticity of figure of the components of  $\pi^5$  Orionis.

$$\begin{aligned} 2 \times 0^m.0267 &= 0^m.0534 = 0.048 \text{ in light,} \\ \text{Ratio of axes, } b/a &= 0.952. \end{aligned}$$



We conclude that the two bodies are elongated by mutual attraction by something more than 5 per cent, though of course this measure probably refers only to the brighter component. This is the first case in the tests of spectroscopic binaries where I have detected the ellipsoidal variation without there also being eclipses, and there must of course be many other such objects awaiting discovery.

The results in this paper were secured with the same assistance and support that were acknowledged in the preceding paper on  $\lambda$  Tauri.

UNIVERSITY OF ILLINOIS OBSERVATORY  
February 1920

# A MODIFICATION OF THE ELECTRON THEORY OF DISPERSION TO ACCOUNT FOR THE CHANGE OF THE REFRACTIVE INDEX WITH TEMPERATURE

By E. O. HULBURT

## ABSTRACT

*Dispersion formula involving temperature, according to a modified electron theory.*—Various observers have found that the decrease of refraction index with increasing temperature is approximately linear. To explain this fact, the author has modified the Lorentz dispersion formula by introducing the *assumption* that, for the range of spectrum involved, the variation with temperature is determined by electrons of a single type, upon which the medium acts only with a *restoring force which increases linearly with the absolute temperature*, as is to be expected from the law of equipartition of energy. The new formula has four arbitrary constants (equation 6). The *agreement with observed results* for a number of transparent liquids is within 0.2 per cent for a considerable range of wave-length and temperature and clearly indicates that the above assumption is a step in the right direction, though it is too simple to correspond accurately with the facts.

1. *Introductory.*—Measurements of the refractive indices of liquids at various temperatures and for various wave-lengths of monochromatic radiation are recorded in the Landolt-Börnstein physical tables. More recently K. G. Falk<sup>1</sup> has made a systematic study of the refractive index of fourteen organic liquids for four wave-lengths of light in the visible region of the spectrum for temperatures between 15° and 75° C. Most of the observers have concluded that within the error of experiment the refractive index increased linearly with decrease in temperature. Forch and Kucera<sup>2</sup> have given the results of their determinations of the refractive indices of six liquids at temperatures below 0° C. for sodium light in the form of empirical equations which, in addition to the first power, contained higher powers of the temperature. The numerical coefficients of the higher powers were, however, small, showing that the deviations from the linear relation were slight.

No previous attempt has been made to explain quantitatively these facts on the basis of any of the theories of dispersion.

<sup>1</sup> *Jour. Amer. Chem. Soc.*, 31, 86 and 806, 1909.

<sup>2</sup> *Physikalische Zeitschrift*, 3, 132, 1901-1902.

In the present paper an assumption is made concerning the mechanism of the dispersing medium which leads to a modification of the dispersion formula, enabling the refractive index at various temperatures to be computed.

2. *Theoretical*.—In the following discussion we shall consider only isotropic, transparent media, for the experimental data at hand preclude consideration of any but the simplest cases. It is assumed that the only force due to the medium which acts on the dispersion electron is of an elastic nature. Therefore there is no frictional force (i.e., absorption) and no external magnetic field. We use the electron theory of dispersion as given by H. A. Lorentz,<sup>1</sup> and write the equation of motion of the dispersion electron of a single type

$$m \frac{d^2\xi}{dt^2} = \sqrt{4\pi} e (E_x + \sigma \sqrt{4\pi} e N \xi) - f\xi. \quad (1)$$

$\xi$  and  $E_x$  are the X-components of the displacement of the electron from its equilibrium position and the electric force on the electron, respectively. There are similar equations for the Y- and Z-components.  $f$  is a certain positive constant which depends upon the structure and properties of the particle or molecule in which the electron is situated, such that  $-f\xi$  is the X-component of the elastic force or the force of restitution. The charge on the electron in c.g.s. electrostatic units is  $e$ , its mass is  $m$ .  $N$  is the number of such electrons per unit volume.  $\sigma$  is a constant which Lorentz has shown to be approximately  $1/3$  for isotropic media.

Let  $e$  be the base of natural logarithms, and let all dependent variables of (1) contain the time only in the factor  $e^{i\frac{2\pi c}{\lambda}t}$ , where  $\frac{2\pi c}{\lambda}$  is the frequency,  $\lambda$  the wave-length of the vibration, and  $c$  the velocity of light *in vacuo*. The solution of (1) gives the refractive index  $\mu$  as determined by the relation

$$\frac{1}{\sigma + \frac{1}{\mu^2 - 1}} = \frac{4\pi N \frac{e^2}{m}}{\frac{f}{m} - \frac{4\pi^2 c^2}{\lambda^2}}. \quad (2)$$

<sup>1</sup> *Theory of Electrons*, 1909, p. 132.

This equation expresses  $\mu$  in terms of the constants of a single type of dispersion electron. There may be other types of dispersion electrons in the medium with constants peculiar to the type, so that in the more general case the right-hand member of (2) becomes a summation of similar terms, one term for each type. For this case the complete dispersion formula is

$$\frac{1}{\sigma + \frac{1}{\mu^2 - 1}} = \sum \frac{C_s}{\frac{f}{m} - \frac{4\pi^2 c^2}{\lambda^2}}, \quad (3)$$

where  $C_s = 4\pi N_s \frac{e^2}{m}$ , and the subscript  $s$  denotes the  $s$ th type of electron.

We assume we are dealing with a region of the spectrum in which the change of refractive index with wave-length is determined by the electrons of a single type, so that in the summation of (3) all the terms except one may be replaced by a quantity  $q_1$  which is independent of  $\lambda$ . Then (3) becomes

$$\frac{1}{\sigma + \frac{1}{\mu^2 - 1}} = q_1 + \frac{C_1}{\frac{f}{m} - \frac{4\pi^2 c^2}{\lambda^2}}. \quad (4)$$

We now consider the effect of temperature-changes upon  $\mu$  as expressed by (4). It is assumed that  $\sigma$  and  $q_1$  remain constant throughout any temperature-change.  $C_1$  is a function of the temperature, but as it is proportional to the number of electrons per unit volume, and hence to the density, its changes with temperature may be calculated from a knowledge of the density of the substance at various temperatures.

There remains for consideration the quantity  $f$ , which is the elastic force of restitution acting on the electron.  *$f$  is assumed to increase linearly with the absolute temperature.* This assumption may be interpreted to result logically from the law of the equipartition of energy. This law states that during the temperature-change of a substance the energy associated with each degree of freedom within the substance varies proportionally with the

absolute temperature. When the law of equipartition is applied to a substance composed of molecules which have no internal modes of motion, it has been shown that the kinetic energy of the molecule is proportional to the absolute temperature. If the molecule possesses internal modes of motion, as will be the case if it contains movable electrons, the same law of equipartition of energy may be assumed to dictate the distribution of energy among these modes, and it follows in a particular case that the force of restitution of the electron is a positive linear function of the absolute temperature. We then write

$$f = f_0 (1 + \beta\theta), \quad (5)$$

where  $\theta$  is the temperature Kelvin,  $f_0$  is the value of  $f$  at the zero of temperature, and  $\beta$  is a positive constant.

Introducing (5) into (4), the dispersion formula becomes finally

$$\frac{1}{\sigma + \frac{1}{\mu^2 - 1}} = q_1 + \frac{C_1}{\frac{f_0}{m} (1 + \beta\theta) - \frac{4\pi^2 c^2}{\lambda^2}}. \quad (6)$$

3. *Application to observation.*—Since formula (6) contains no term denoting absorption, its application is limited to substances which are transparent to the wave-lengths in the region of the spectrum concerned. Furthermore, the refractive index of the substance at constant temperature must conform to the relation of refractive index and wave-length given by equation (4).

The application of the dispersion formula (6) to several substances gave the same general results. The case of benzaldehyde is discussed in detail below. The method of computation and the results for this substance are typical of those for all the substances examined.

The refractive index of benzaldehyde for wave-lengths 434, 486, 589.3, and 656  $\mu\mu$ , from the observations of Falk<sup>1</sup> for a range of temperature between 20° and 70° C., are shown by the straight lines of Figure 1. The density of the substance was also measured throughout this range of temperature. The determination of  $\mu$  was

<sup>1</sup> *Loc. cit.*

accurate to about 0.0001, and Falk considered that a straight line represented the variation of  $\mu$  with  $\theta$ , when  $\lambda$  is constant, within the error of experiment.

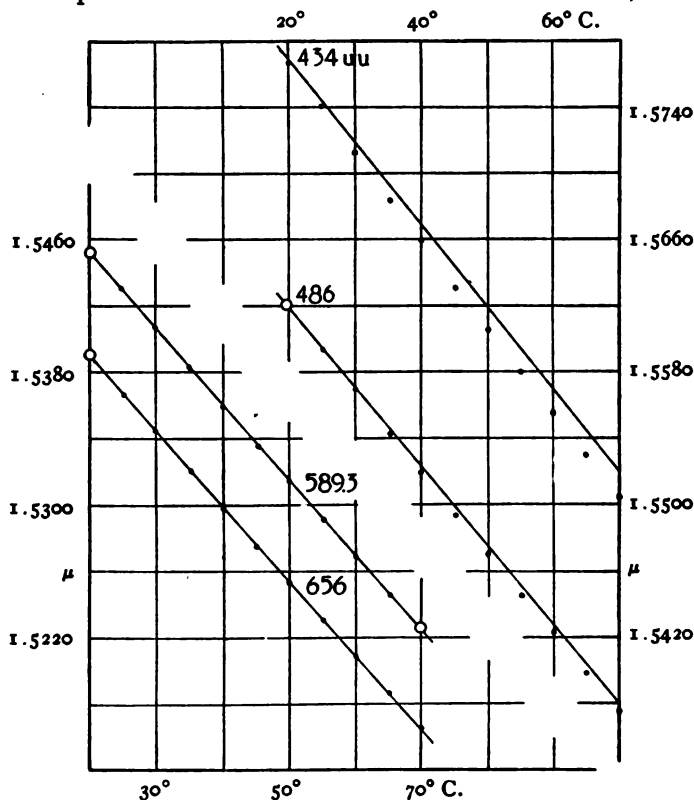


FIG. 1.—Refractive index of benzaldehyde

Introducing the values of the wave-length and of the corresponding refractive index from Figure 1 at 20° C., namely,

$\lambda$ 486 $\mu\mu$	589.3	656
$\mu$ 1.5621	1.5453	1.5391

and at 70° C., namely,  $\lambda = 589.3 \mu\mu$  and  $\mu = 1.5225$ , into the dispersion formula (6) to determine the four constants, we find

$$\begin{aligned}
 q_1 &= 0.50887 & C_1 &= 40.931 \times 10^{30} \text{ at } 20^\circ \text{ C.} \\
 \beta &= 7.8778 \times 10^{-4} & \frac{f_0}{m} &= 83.882 \times 10^{30}
 \end{aligned}$$

In the computations it is to be remembered that  $\sigma$  is  $\frac{1}{2}$ , and that for any temperature  $C_1$  is proportional to the density. With the above values for the constants of (6)  $\mu$  has been computed for various temperatures from 20° to 70° C. for the four wave-lengths given in Figure 1. The computed values of  $\mu$  are shown by dots in the figure; the four values of  $\mu$  used to determine the constants are shown by circles. The temperature-change in  $\mu$  as given by (6) is linear to a first approximation, and it is seen that the computed  $\mu$ - $\theta$  lines have but slight curvature for all the wave-lengths. For the longer wave-lengths the agreement between the observed and computed  $\mu$ - $\theta$  lines is good, but for the shorter wave-lengths it is seen from Figure 1 that the observed and computed lines differ in slope, and that the difference in slope increases with decreasing wave-length.

Similar computations for carbon disulphide, acetylacetone, and  $\alpha$ -monobromnaphthalene yielded results similar to those for benzaldehyde, namely, equation (6) gave good agreement between the observed and computed  $\mu$ - $\theta$  lines for the longer wave-lengths, with increasing deviations as the wave-length was decreased.

4. *Discussion.*—The accuracy with which equation (6) expresses the observations, though none too great, is still sufficient to lead to the belief that the assumption given by (5), which possesses certain physical significance, is a step in the right direction. Manifestly substances do not conform very exactly to the several assumptions underlying the dispersion formula (6), and only approximate agreement might be expected. Without attempting to discuss all the assumptions, there are two which deserve further mention. In the first place, the assumption that the absorption is zero, and hence that the change of absorption with temperature has a negligible effect upon the refractive index, is questionable. In the second place, changes in  $q_1$  due to temperature have been assumed to produce no noticeable changes in  $\mu$ . Such an assumption is also hardly permissible. Undoubtedly  $q_1$  does change with the temperature, since it is the contribution to the dispersion equation (6) from the other types of electrons, and in view of the fact that in all the cases examined  $q_1$  was nearly as large as one-half of the refractive index its temperature variations probably affect

$\mu$  appreciably. However, the quantitative data on the absorption of the substances and on the refractive index and its temperature-changes are hardly numerous enough to justify more extended numerical computations.

5. *Summary.*—In order to explain the observed temperature variations of the refractive index of transparent isotropic substances, the assumption has been made that the force of restitution acting on the dispersion electron increases linearly with the absolute temperature. This assumption when introduced into the dispersion equation deduced from the electron theory of Lorentz resulted in an equation for the refractive index which was found to express the results of observation with a certain degree of exactness.

JOHNS HOPKINS UNIVERSITY  
December 1919



# FINE STRUCTURE OF THE NEAR INFRA-RED ABSORPTION BANDS OF THE HALOGEN ACIDS

By WALTER F. COLBY

## ABSTRACT

*Absorption spectra of diatomic gases; a quantum theory of the fine structure of the infra-red bands.*—The postulate of Bjerrum, that the fine structure of these bands is due to the rotation of the molecules in stationary states corresponding to the quantum relation, has proved very fruitful. The purpose of the present paper is to test the hypothesis by comparing the *theoretical results for the simplest molecular model of the Bohr type* with the experimental results recently obtained by Imes for the *halogen acids*. For HF, HCl, and HBr, the observed interatomic vibration frequencies come out respectively 18, 40, and 47 per cent less than the theoretical, while the computed separations of the pairs of nuclei are respectively 38, 54, and 59 per cent less than the values given by Imes. The variation with mass is explained as a screening effect which has been neglected in the elementary theory. The agreement between theory and experiment is sufficient to lend support to the Bjerrum hypothesis, and suggests the importance of developing a more adequate theory involving fewer simplifying assumptions.

Recent experimental work in the fine structure of absorption spectra in the near infra-red has been greatly stimulated by the very fruitful postulate of Bjerrum<sup>1</sup> concerning the mechanism of this absorption. He explains the structure of the bands in this region as due to the vibration of the atoms in the molecule modified by the rotation of the molecule as a whole about an axis normal to the line of vibration. Following the requirements of the quantum theory, the molecule is assumed to be capable of stationary states of rotation defined by the equation

$$\omega = nh/2\pi I.$$

$n$  indicates successive integers. The rotational frequencies are thus

$$\nu_r = nh/4\pi^2 I.$$

Calling the interatomic vibration frequency  $\nu_0$ , the foregoing theory states that absorption will occur at frequencies given by the equation

$$\nu = \nu_0 \pm \nu_r.$$

<sup>1</sup> *Nernst Festschrift*, p. 90, 1912.

Assuming that  $\nu_0$  is not modified by the rotational velocity and consequently not a function of  $n$ , this equation would require a series of absorption lines symmetrically grouped about  $\nu_0$ . The series would have two regions of maximum intensity symmetrically placed, corresponding to the most probable value of  $\omega$ . A small variation of  $\nu_0$  with  $\omega$  would cause a crowding of the bands on one side and a separation on the other. Considerable experimental evidence has been obtained to verify the original hypothesis in these details. It is apparently applicable likewise in the study of band spectra, a success which will greatly strengthen its present position.

The first experimental work which presented these absorption regions with sufficient dispersion to show the fine structure was done by Eva von Bahr in 1913.<sup>1</sup> She used a prism spectrometer and was able to distinguish and measure a considerable number of lines in the bands of a group of diatomic and triatomic gases. The separation of the lines in the simpler spectra gave rotation frequencies which it was possible to identify with absorption lines in the far infra-red, and moments of inertia computed from these and the quantum relation were of the order of magnitude demanded by the kinetic-gas theory. With low dispersion these regions appear as doublets. With these and also with the fine structure slightly resolved, von Bahr was able to measure relative intensities and find that the rotation velocities approximated a Maxwellian distribution. When the temperature was raised the doublet separated and its members became flatter and broader. The maximum shifted outward according to the requirements of the Maxwell law for change of most probable velocity with temperature. The recent work, especially that of Sleator<sup>2</sup> and Imes<sup>3</sup> in this laboratory and of Kemble and Brinsmade<sup>4</sup> at Harvard, has extended the dispersion and resolution of the fine structure very materially. Work now in progress confirms qualitatively the earlier statement that the rotational velocities conform quite closely to a Maxwellian distribution, even broken up as they are into the discrete

<sup>1</sup> *Verhandlungen der deutschen Physikalischen Gesellschaft*, 15, 710, 1913.

<sup>2</sup> *Astrophysical Journal*, 48, 125, 1918.

<sup>3</sup> *Ibid.*, 50, 251, 1919.

<sup>4</sup> *Proceedings of the National Academy of Sciences*, 3, 420, 1917.

regions of preferred velocities. The great contribution of the new work, however, has been in pushing the resolution to its apparent limit and in determining so precisely the frequencies of these ultimate members. The effect of rise of temperature of the absorbing gas now appears very definitely not to displace these individual lines but simply to sweep the position of maximum intensity outward toward higher values of  $n$ . Present work is also using this means of assembling data on the higher members.

The work of Imes has presented the absorption of three of the halogen acids with remarkable precision. It is the object of the present paper to make use of this data in checking the order of magnitude of the variation of  $\nu_0$  with  $n$  as shown by a molecular model of the Bohr type and to see whether it is possible to express  $\nu_0$  for such a model by as strikingly simple a function of  $n$  as Imes has found it to be. It will be possible also to check the variation of  $I$  with  $n$ .

The simplest model of the Bohr type is that first proposed by him,<sup>1</sup> which has the great advantage of being electrically symmetrical. HCl has been chosen as a type, since the results are most complete for that gas. The chlorine atom is assumed to contribute one electron only to the valence ring. The hydrogen atom also contributes one. The H nucleus and the Cl nucleus with remaining electrons are then treated as point charges, an assumption which may depart considerably from the details of the model, but which is sufficiently near for a first treatment. The nuclei thus each possess one positive charge and differ only in mass. Bohr has written the equilibrium conditions for such a system and for this problem it is only necessary to add one term to take care of the molecular rotation. This term is in fact of the same type as the one Bohr has used to indicate the centrifugal force on the electrons in the valence ring.  $2x$  indicates the distance between the nuclei,  $y$  the radius of the valence ring,  $M$  is the reduced mass of the rotating system [ $I = M(2x)^2$ ], other symbols have their usual significance. The equations are

$$\begin{aligned} n^2 h^2 / 4\pi^2 (2x)^3 M + e^2 / (2x)^2 &= 2e^2 x / (x^2 + y^2)^{3/2} \\ h^2 / 4\pi^2 y^3 m + e^2 / (2y)^2 &= 2e^2 y / (x^2 + y^2)^{3/2}. \end{aligned}$$

<sup>1</sup> *Phil. Mag.*, 26, 857, 1913.

The first term in each equation gives the centrifugal force and recognizes the fact that the angular momentum  $=nh/2\pi$ . For the electrons,  $n$  is set equal to unity. The influence of the molecular rotation on the electrons is neglected. A slight computation shows that the electrons have no appreciable effect on the reduced mass and also that the centrifugal force on the electrons is of a much lower order of magnitude than the electric forces on them parallel to the molecular axis. The equations are easier to discuss if one replaces  $y$  by a new variable  $a$  by means of the substitution

$$y = x \tan a.$$

It is possible then to solve for  $x$  and  $n^2$  in terms of  $a$ . For  $n^2=0$ ,  $a=60^\circ$ .  $a$  decreases slightly as  $n^2$  grows and becomes  $59^\circ 27'$  for  $n^2=104$ . Although it has not been possible to form a closed expression for  $x$  in terms of  $n^2$ , a curve of corresponding values shows the relation to be very nearly linear for  $n^2 < 100$ . One may express these quantities as a series in ascending powers of the very small quantity  $(60^\circ - a)$ . These series are rapidly convergent and easily obtained. They contribute nothing new to the present discussion but are convenient tools for future work. The following values of the constants were used.

$$\begin{aligned} M &= 1.613 \times 10^{-24} \\ h &= 6.55 \times 10^{-27} \\ e &= 4.77 \times 10^{-10} \\ m &= 9.01 \times 10^{-28} \end{aligned}$$

The linearity between  $x$  and  $n^2$  is then given by

$$x = 2.917 \times 10^{-9} + 1.23 \times 10^{-12} n^2.$$

Imes gives at  $n=0$ ,  $x=6.4 \times 10^{-9}$ . This agreement is not close, but one must note that Imes obtains in the case of HF  $x=4.7 \times 10^{-9}$  and for HBr,  $x=7.1 \times 10^{-9}$ , and that our equations do not involve  $M$  when  $n=0$ . The observed variation must therefore be due to the screening effect of the inner electrons in the halogen atom. In this calculation the foregoing model should consequently be more nearly checked by HF, which we find to be the case. The centroid of this group of molecules lies always very near the halogen nucleus. We should expect, therefore, that many variations with atomic

number must be explained rather by this screening effect than by difference of mass. A model which is otherwise satisfactory but assumes as we have done that the halogen atom may be replaced electrically by a point charge will yield limiting values which the experimental data will approach as the atomic number decreases. As soon as this material is extended and completed the dependence of these frequencies on atomic number can be more satisfactorily studied.

Imes has found an apparent linearity between  $x^2$  and  $n$ . It is very difficult to establish a relation here since the variation is so extremely small. He finds that the variation of  $x$  from the first to the tenth member is about  $50 \cdot 10^{-12}$ . Our formula gives  $123 \cdot 10^{-12}$ .

To investigate the vibration frequency we shall assume that the amplitudes involved in the absorption in this region are small enough so that we may set the restoring force proportional to the displacement.  $\nu_0$  is then given by  $\frac{1}{2\pi} \sqrt{F/M}$ , where

$$F = d/d(2x)(n^2 h^2 / 32\pi^2 M x^3 + e^2 / 4x^2 - 2e^2 \cos^3 a / x^2).$$

A differentiation of the second of the equilibrium equations allows an evaluation of  $da/dx$ . Although the calculation is fairly laborious, it is straightforward. One can obtain an expression of  $\nu_0$  in terms of  $a$ , and with the help of the previous relation between  $a$  and  $n^2$  a graphical solution is possible for  $\nu_0$  in terms of  $n^2$ . Here again the curve is surprisingly closely approximated by a straight line, the equation of which may be written

$$\nu_0 = 1.4485 \cdot 10^{14} - 4.63 \cdot 10^{10} n^2.$$

Imes's equation reads

$$\nu_0 = 0.8661 \cdot 10^{14} - 0.9 \cdot 10^{10} n^2.$$

We must note again that the observed variation of the constants of this equation with atomic number of the halogen is much too great to be due to difference of mass alone.

$$\text{For HF } \nu_0 = 1.1887 \cdot 10^{14} - 6.20 \cdot 10^{10} n^2.$$

$$\text{HCl } \nu_0 = 0.8661 \cdot 10^{14} - 0.90 \cdot 10^{10} n^2.$$

$$\text{HBr } \nu_0 = 0.7677 \cdot 10^{14} - 0.69 \cdot 10^{10} n^2.$$

The assumed model may again be thought of as an idealization of the halogen acid molecule, which one may expect the actual cases to approach as the atomic number decreases. The discussion of the influence of atomic number will be resumed here also as more measurements are made.

To show that the centers of these line pairs are subject to a variation of the same magnitude as the supposed molecular model would suffer with rotation is striking evidence of the authenticity of the assumption that the fine structure of these bands is due to this rotation. Work is now satisfactorily in progress to extend the number of observed lines of the HCl absorption region at  $3.4 \mu$  by raising the temperature of the absorbing gas. It is hoped thus to test these variations with much more material. The second absorption region at slightly less than double this frequency is also being extended and we may hope it to yield more information as to the possibility of a second stationary amplitude of vibration.

A second treatment will endeavor to remove at least some of the foregoing simplifying assumptions. This would consist in using the more satisfactory Kossel model, the at least partial recognition of the space-configuration of the halogen atom, and, most important, the scrutiny of the validity of assuming simple harmonic motion. In respect to this last point, if one assumes an equation of motion involving the square of the displacement the Sommerfeld phase integral still allows a definite statement of the problem of stationary states. By inspecting the standard solution of this new equation of motion one may foresee that the foregoing results will be changed in the right direction. The more complicated solution requires some ingenuity of treatment but may prove valuable in accounting for the higher frequency regions which apparently share the same structure.

PHYSICAL LABORATORY, UNIVERSITY OF MICHIGAN  
January 1920

## NOTE ON THE AIR LINES IN SPARK SPECTRA FROM $\lambda$ 5927 TO $\lambda$ 8719<sup>\*</sup>

By PAUL W. MERRILL

### ABSTRACT

*Air lines in condensed spark spectra,  $\lambda$  5927 to  $\lambda$  8719.*—As an essential preliminary to the investigation of spark spectra in this region, a study of the air lines has been begun by comparing spectra obtained with different elements as electrodes, both in air and in oxygen. (1) The *wave-lengths* of 58 air lines, so determined, are given in Table I with an accuracy which is limited by the fact that the lines are usually ill-defined and sometimes broad and hazy. Twenty of them correspond to known H, N, O, or A lines, including six lines of the *red spectrum of argon* and four *oxygen lines* which had not previously been observed in spark spectra. Except for two more, which are probably due to oxygen, the rest have not, as yet, been identified. (2) All of the identified lines are found to be *shifted with reference to vacuum tube spectra*; the increase of wave-length is about 0.1 Å for the *oxygen lines* and two *nitrogen lines*, 0.3 Å for three other N lines, 0.6 Å for the *argon lines*, and 0.7 Å for *hydrogen alpha* and for three other N lines. (3) The *effect of adding self-inductance* is to weaken the two *nitrogen lines*,  $\lambda\lambda$  6482 and 6610.

*Spectrum of condensed spark in oxygen.*—Several identifications of oxygen and nitrogen lines by previous observers using vacuum tubes are confirmed and the doubtful identification of  $\lambda$  7157 as due to oxygen is strengthened.

In the spectrum of the condensed spark in air there appear numerous lines which are to be ascribed to the gases of the surrounding atmosphere rather than to the material of the electrodes. These lines may be stronger and more numerous than the electrode lines. They are usually ill-defined and often broad and nebulous. Lines of nitrogen, oxygen, hydrogen, and argon are present in the spectrum of the disruptive discharge in ordinary air.

Very little information in regard to spark spectra beyond  $\lambda$  6600 is available at present, although the need for it is becoming pressing. The recognition of the air lines is an essential preliminary to the investigation of spark spectra in a new region; and since it is always of interest to study spectral lines as produced under different modes of excitation, the observation of the air lines in spark spectra is desirable for the additional reason that many of

<sup>\*</sup> *Contributions from the Mount Wilson Observatory*, No. 183.

these lines occur both in vacuum tube discharges and in the tube-arc.<sup>1</sup> Moreover, certain of these lines are present in astronomical spectra. The best-known examples are the hydrogen lines, but the presence of the spark lines of oxygen and nitrogen in stellar spectra has been recognized for some time.

In the present investigation fifty-eight lines which are thought to be due to air have been observed in spark spectra from  $\lambda$  5927 to  $\lambda$  8719. These lines have all been photographed in the spectrum of the spark between electrodes of at least two elements, carbon and aluminum. Most of them have been photographed with several other elements also. For the region of wave-length greater than  $\lambda$  7000 the air lines are the most striking features of the spectra of all the elements observed, including Al, C, Ca, Co, Cu, Fe, Ni, Ti, so that the photographed infra-red spark spectra of these elements appear much alike.

*Wave-length measurements.*—The lines which have been measured in the present investigation appear in the first column of Table I. Their relative intensities are in the second column. All the lines are more or less hazy and diffuse; those which are especially so are marked "h." The voltage employed was 8000, the capacity about 0.1 microfarad. No auxiliary spark-gap was used. No special temperature control was provided for the electrodes but care was taken that they did not become excessively hot, for in that case the characteristic spark features are weakened and the spectrum tends to become like that of the arc.

At  $\lambda$  6456 and 6950 are broad hazy patches which cannot be accurately measured.  $\lambda$  7479 is a curious feature extending from  $\lambda$  7476.7 to  $\lambda$  7482.1. It is markedly unsymmetrical, being stronger toward the violet. Presumably it is composed of several ill-defined lines completely blended. Most of the other lines are fairly symmetrical, though lack of symmetry was especially noted for  $\lambda$  7424, 7442, and 7468. With high dispersion the lines of the oxygen triplet  $\lambda$  7772, 7774, 7775 appear slightly unsymmetrical.

All the lines have been measured with a dispersion of 16.8 Å per mm; the stronger ones with 3.7 Å per mm, and  $\lambda$  6482 and

<sup>1</sup> Arthur S. King and Paul W. Merrill, "Recent Observations of Tube-Arc Spectra Especially in the Infra-Red," *Physical Review*, 14, 271, 1919.



TABLE I  
AIR LINES IN SPARK SPECTRA

I. A.	Int.	Probable Error	Previous Observers	Probable Error	Vacuum Tubes
5927.83.....	5	.02	5927.88	.03	5927.57 N
5931.78.....	7	.02	5931.85	.04	5931.50 N
5941.54.....	11	.02	5941.65	.05	5941.49 N
5952.33.....	4	.02	5952.48	.03	5952.20 N
6160.72.....	1h	(.04)			
6171.0.....	3h	(.4)	6170.4	.1	
6284.22.....	1	(.03)	6284.4	(.2)	6283.29 N
6358.13.....	oh	(.08)			6356.78 N
6370.92.....	oh	(.06)			
6379.52.....	3h	.03	6379.7	(.2)	6378.79 N
6456.....	vh				O
6482.054.....	7	.004	6482.045	.01	6481.34 N
6563.5.....	12vh	.06	6563.3	.1	6562.79 H
6610.39.....	8	.007	6610.41	.04	6610.06 N
6640.7.....	o	(.3)			
6654.78.....	2	.05			
6721.25.....	1	.02			
6811.9.....	o	(.3)			
6864.....	oo				
6887.61.....	1	(.06)			
6950.....	vh				
6965.95.....	1	.04			6965.43 A
7067.6.....	o	(.08)			7067.22 A
7157.36.....	9	.01			7157. O
7384.53.....	1	(.04)			7383.98 A
7424.04.....	8	.02			
7432.9.....	o	(.1)			
7442.70.....	10	.01			
7458.7.....	o	(.1)			
7468.72.....	14	.02			(7474. O)?
7479.....					
7504.84.....	o	(.04)			7503.87 A
7515.16.....	o	(.07)			7514.65 A
7635.70.....	1	(.07)			7635.11 A
7772.07.....	10	.01			7771.97 O
7774.33.....	7	.01			(7774.00)O
7775.60.....	6	.01			(7775.67)O
7947.83.....	4	.01			
7951.10.....	3	(.06)			
7952.3.....	2	(.2)			
8185.26.....	4	(.02)			
8188.42.....	4	(.02)			
8200.72.....	1	(.03)			
8211.12.....	2	(.02)			
8216.72.....	7	(.02)			
8223.48.....	4	(.02)			
8230.20.....	o	(.05)			
8242.80.....	4	(.03)			
8440.84.....	5	(.03)			8446.42 O
8594.....	oo				
8630.02.....	o	(.04)			

TABLE I—*Continued*

I. A.	Int.	Probable Error	Previous Observers	Probable Error	Vacuum Tubes
8680.63.....	2	(.04)	.....	.....	.....
8683.70.....	1	(.04)	.....	.....	.....
8686.41.....	0	(.04)	.....	.....	.....
8692.....	$\infty$	.....	.....	.....	.....
8703.8.....	$\infty$	(.2)	.....	.....	.....
8712.00.....	0	(.1)	.....	.....	.....
8719.2.....	$\infty$	(.2)	.....	.....	.....

6610 with 1.8 A per mm in addition, first-order grating spectra being used in every observation. The spectra having 16.8 A per mm and some of those having 3.7 A per mm were obtained on films, the remainder on glass plates. The wave-lengths were determined in most cases by reference to iron-arc comparison spectra, usually in the second order, but on some plates in the first order. Wherever possible, however, lines in the spark spectra themselves were used as standards. For this purpose the exposures to the calcium and copper sparks were especially suitable. The wave-lengths of the metallic lines were taken from *Scientific Papers of the Bureau of Standards*, Nos. 312 and 324.

In the fourth column appear the mean wave-lengths found by previous observers.<sup>1</sup> In the third and fifth columns are the probable errors; those in parentheses, depending on a small number of determinations, have been estimated; the others have been computed from the residuals in the usual way.

*Hydrogen.*—The hydrogen line  $H\alpha$  which appears on all of the photographs is exceedingly diffuse and difficult to measure. Measurements on a considerable number of exposures, however, have given the wave-length  $\lambda$  6563.5, with a probable error of 0.06 A. The effective wave-length thus found is 0.7 A greater

<sup>1</sup> The principal sources from which these wave-lengths have been taken are Otto Schulemann, "Das Funkenspektrum des Indiums," *Zeitschrift für wissenschaftliche Photographie*, 10, 263, 1911-1912; Franz Joseph Kasper, "Messungen am Silberspektrum," *ibid.*, p. 53; A. Kretzer, "Untersuchungen über das Antimonspektrum," *ibid.*, 8, 45, 1909-1910; Wilhelm Schwetz, "Die Spektren des Wismuts," *ibid.*, p. 301; Matthias Aretz, "Über den langwelligen Teil des Kupferfunken- und Kupferbogenspektrum," *ibid.*, 9, 256, 1910-1911; J. M. Eder and E. Valenta, "Wellenlängenmessungen im roten Bezirke der Funkenspektren," *Sitzungsberichte Akad. der Wiss. Wien, Math-naturw. Kl.*, 118, IIa, 511, 1909.

than that obtained from vacuum tubes.<sup>1</sup> The values of previous observers give a slightly smaller displacement, 0.5 Å. The interpretation of this apparent displacement should be considered in connection with the similar displacements shown by the lines of nitrogen and argon.

*Nitrogen and oxygen.*—Most of the air lines are due to nitrogen and oxygen. The vacuum tube wave-lengths of nitrogen are by Porlezza,<sup>2</sup> those of oxygen are by Runge and Paschen,<sup>3</sup> reduced to the international system.<sup>4</sup>

Confirmation of several of the identifications was obtained by operating the spark in an atmosphere of oxygen. The oxygen used was a commercial product and probably was not free from nitrogen, as the nitrogen lines were not eliminated from the spectrum and in fact were not greatly reduced in intensity. When the exposures in oxygen were so timed as to give the same general intensity as exposures in air, only two lines were found to be certainly weakened, namely  $\lambda\lambda$  6482.054 and 6610.39. The following lines were strengthened in an atmosphere of oxygen:  $\lambda\lambda$  6158, 6456, 7003, 7157.36, 7772.07, 7774.33, 7775.60, 8446.84. The lines at  $\lambda\lambda$  6158, 6456, and 7003 are very wide and diffuse. The first and third are absent or very weak in air and do not appear in Table I.  $\lambda\lambda$  6158 and 6456 probably correspond to triplets, and  $\lambda$  7003 to a single line, all observed by Runge and Paschen in the series spectrum of oxygen. The last four lines are well-known oxygen lines; and  $\lambda$  7157.36 is probably due to oxygen. A line at approximately this wave-length was observed in an oxygen tube by Runge and Paschen, though not included by them in their table of oxygen lines.

The exposures with the spark in oxygen did not give sufficiently great changes in the relative intensities of the remaining lines in

<sup>1</sup> W. E. Curtis, "Wave-Lengths of Hydrogen Lines and Determination of the Series Constant," *Proceedings of the Royal Society*, A90, 605, 1914.

<sup>2</sup> C. Porlezza, "Lo Spettro a righe dell'azoto in tubo di Geissler," *Atti R. Accademia dei Lincei*, Serie 5, 20, 584, 1911.

<sup>3</sup> Runge and Paschen, *Annalen der Physik*, 61, 641, 1897; Paschen, *Annalen der Physik*, 27, 562, 1908.

<sup>4</sup> K. W. Meissner, "Untersuchungen und Wellenlängenbestimmungen im roten und infraroten Spektralbezirk," *Annalen der Physik*, 50, 713, 1916.

Table I to make it possible to assign their origins. They may be due to nitrogen, but this is not certain except for those of shorter wave-length corresponding to lines found by previous observers in nitrogen tubes. The identification of the remaining lines must await further work with the spark in atmospheres of pure gases or with vacuum tubes containing pure gases.

Comparison of the spark wave-lengths of nitrogen lines with those by Porlezza in the vacuum tube shows a large positive displacement. For eight lines the mean displacement is  $0.43 \pm 0.08$  Å, the probable error being computed as though the shift were actually of the same amount for all lines. This is not necessarily

TABLE II  
WAVE-LENGTHS OF OXYGEN LINES

SPARK	TUBE RUNGE AND PASCHEN*	ARC		SUN MEISSNER†
		Meissner*	Meggers and Kees†	
7772.07.....	7771.97	7771.98	7771.93	7771.97
7774.33.....	7774.00	7774.19	7774.14	7774.20
7775.60.....	7775.67	7775.42	7775.43	7775.42
8446.84.....	8446.42	$\begin{Bmatrix} 8446.36 \\ 8446.76 \end{Bmatrix}$	8446.42	$\begin{Bmatrix} 8446.38 \\ 8446.78 \end{Bmatrix}$

\* K. W. Meissner, *Annalen der Physik*, 50, 713, 1916.

† *Bulletin of the Bureau of Standards*, 14, 637, 1918.

the case, but even so the displacement is more than five times the probable error. Including one more line ( $\lambda$  6358), poorly determined, gives  $0.53 \pm 0.1$  Å. Using values of previous observers for eight lines we get a displacement of  $0.52 \pm 0.08$  Å. The chance that these displacements are due to accidental errors is negligible, and it would be surprising if systematic errors to the amount of 0.4 or 0.5 Å should exist in either series.

The wave-lengths of four oxygen lines as found in various sources are collected in Table II. The spark lines seem to be displaced toward longer wave-lengths as compared with other sources, though by smaller amounts than occur in the similar displacements shown by the lines of hydrogen, nitrogen, and argon. The vacuum-tube values of Runge and Paschen for the second and third lines are admittedly inaccurate.

These four infra-red oxygen lines are essentially spark lines. They are faintly present in the arc<sup>1</sup> and are fairly strong in the solar spectrum.<sup>2</sup> A preliminary photograph by Mr. Ellerman and the writer indicated that the triplet at  $\lambda\lambda$  7772-7775 is much weakened in the spot spectrum as compared with the disk. This is conclusively shown by an excellent photograph secured by Mr. Brackett. It would not be surprising if this triplet were found to be strong in the spectra of certain stars of types B and A.

*Argon.*—The photographs show six faint lines near the positions of six of the strongest lines of the so-called "red" spectrum of argon. Lines of wave-length 4000-5000 in the "blue" argon spectrum have been previously observed in spark spectra,<sup>3</sup> but the writer is not familiar with any record of observation of lines of the "red" spectrum in the spark. As these lines are produced in the vacuum tube without capacity, it seems somewhat peculiar that they should appear in the condensed spark. Their effective wave-lengths in the spark appear to be greater than the vacuum-tube values.<sup>4</sup> The six lines give a mean displacement of  $0.59 \pm 0.06$  Å.

*Self-induction.*—A few exposures were made with about 0.1 millihenrys self-induction in the electric circuit. The only striking change in the appearance of the spectrum is the pronounced weakening of the nitrogen lines  $\lambda\lambda$  6482 and 6610, though many of the lines probably become narrower.

#### SUMMARY

1. Fifty-eight air lines have been photographed in spark spectra from  $\lambda$  5927 to  $\lambda$  8719 and their wave-lengths determined with varying degrees of accuracy.

2. The lines which can be identified at present are due to argon, hydrogen, nitrogen, and oxygen.

<sup>1</sup> An unpublished observation by Mr. Babcock to which he kindly permits reference in this connection shows that the three lines at  $\lambda\lambda$  7772, 7774, and 7775 are quite strong at the *poles* of the iron arc, especially at the positive pole, as would be expected of spark lines.

<sup>2</sup> That  $\lambda\lambda$  7772, 7774, and 7775 are not caused by the earth's atmosphere, but are true solar lines, was shown by St. John (*Annual Report of the Director of Mount Wilson Observatory for 1911*).

<sup>3</sup> See discussion by A. S. King, *Astrophysical Journal*, 21, 344, 1905.

<sup>4</sup> K. W. Meissner, *Annalen der Physik*, 51, 115, 1916.

3. An attempt to distinguish between the nitrogen and oxygen lines by operating the spark in an atmosphere of oxygen confirmed several previous identifications, but was inconclusive in regard to most of the new lines.

4. The effective wave-lengths of the lines of argon, hydrogen, and nitrogen appear to be greater in the spark than in vacuum tubes by several tenths of an angstrom unit. The oxygen lines show the same effect to a smaller degree.

5. Self-induction in the spark circuit causes a relative weakening of the nitrogen lines  $\lambda\lambda$  6482.054 and 6610.39.

In conclusion it may be noted that this investigation is preliminary and incomplete. Further work on the apparent displacement of the lines is required in order that its true character and interpretation may be found. Chemical identifications should be established for the unknown lines by operating the spark in very pure atmospheres of oxygen, nitrogen, and argon.

MOUNT WILSON OBSERVATORY  
February 1920

# THE GOLD-POINT PALLADIUM-POINT BRIGHTNESS RATIO

BY EDWARD P. HYDE AND W. E. FORSYTHE

## ABSTRACT

*Gold-point palladium-point brightness ratio.*—The authors have determined this ratio within less than 1 per cent by two sets of readings. (1) Ten determinations made with an ordinary pyrometer give  $R=76.9$  for  $\lambda=0.6663\ \mu$ , hence  $\lambda \log R=1.2566\ \mu$ ; (2) three determinations made with a spectral pyrometer give  $R=122.2$  for  $\lambda=0.6018\ \mu$ , hence  $\lambda \log R=1.2560\ \mu$ . Taking the gold point as  $1336^\circ\text{K}$ , these results enable either the palladium point or  $c_2$  to be computed if the other is known. Assuming  $c_2$  to be  $14350\ \mu\text{ deg.}$ , the *palladium point* comes out  $1828^\circ.5\text{ K}$ ; while assuming the Day and Sosman value for the palladium point,  $1823^\circ\text{K}$ , the *radiation constant*  $c_2$  comes out  $14470\ \mu\text{ deg.}$

*Double-platinum-wound black-body furnaces* are described, which give a very uniform temperature and may be used at the palladium point repeatedly without appreciable deterioration.

Four quantities are related by the gold-point palladium-point brightness ratio, and if three of them are known, the fourth can be calculated. These four quantities (the two temperatures, the ratio of brightness, and  $c_2$ ) are connected by the following relation from Wien's equation:

$$\log R = \frac{c_2}{\lambda} \log e \left( \frac{1}{T_1} - \frac{1}{T_2} \right),$$

where  $R$  is the ratio of brightness for the wave-length interval whose center is at  $\lambda$ ;  $T_1$  and  $T_2$  the two temperatures, on the absolute centigrade scale, in this case the gold and palladium points; and  $c_2$  a constant of Wien's equation. Wien's equation

$$\left[ E_\lambda = c_1 \lambda^{-5} e^{-\frac{c_2}{\lambda T}} \right]$$

is used for such work rather than Planck's form

$$\left[ E_\lambda = \frac{c_1 \lambda^{-5}}{\left( e^{\frac{c_2}{\lambda T}} - 1 \right)} \right],$$

which has been shown by experiment to represent the facts quite well, because for the visible spectrum and not too high temperatures the two equations give practically the same values and the former is easier to use in calculation. It can be seen from the form of the two equations that the value of the product  $\lambda T$  is the important factor in determining the difference between them. By calculation the relation shown in Table I between the two equations for different values of  $\lambda T$  ( $\lambda$  expressed in  $\mu$ ) can be obtained.

TABLE I

$\lambda T$	$E_P/E_W$
2000	1.0008
2500	1.003
3000	1.008
4000	1.028
5000	1.056

This table shows the ratio between Planck's and Wien's equations for different values of  $\lambda T$ , where  $E_W$  is the brightness as determined from Wien's equation and  $E_P$  from Planck's equation. Thus, for optical pyrometry where the wave-length is always less than  $0.7\mu$  Wien's equation gives a negligibly small error over a wide range of temperature.

For two known temperatures, if the brightness ratio is measured for a particular wave-length the value of  $c_2$  can be calculated. On the other hand, if one temperature is known, and a value for  $c_2$  accepted, the other temperature can be calculated. The palladium melting-point in this way can be determined from the melting-point of gold and  $c_2$ . Since the value of the constant  $c_2$  is better known than the melting-point of palladium, it seems better to use the measured ratio to determine this melting-point than to determine the value of  $c_2$ .

In the work described in this paper three different platinum-wound black-body furnaces were used. Two of these were of the same size and of the regular form with fixed diaphragms, one being made of marquardt porcelain and the other of alundum. The tubes were about 3.5 cm outside diameter and 30 cm long. The diaphragm forming the front of the uniformly heated cavity or



black body had an opening  $1\frac{1}{2}$  cm in diameter. This cavity as usual was located in the center of the tube. These inner heater tubes were uniformly wound with platinum ribbon, 2 cm wide and 0.01 mm thick, the distance between the different windings being as small as it was possible to wind them and avoid short circuits. This heater tube was slipped into another tube (inside diameter about 5 cm) and the space between the two tubes filled and packed tightly with very pure aluminum oxide. The aluminum oxide was held in place at the ends by two bushings made of alundum that just fitted inside of the outer tube and easily slipped over the end of the inner tube. The outside tube, which projected several centimeters beyond the inner tube, was also wound with platinum ribbon of the same size, but in this case the windings were spaced farther apart at the center of the tube in order to correct for end cooling. After a few trials a spacing for the windings was found so that with the allowable range of current through these two sets of windings the heating of the inner tube was quite uniform. The outside heater tube thus served two purposes: first to enable the platinum-wound furnace to be operated at as high a temperature as the palladium point, and, second, to correct for the end cooling. A diagram of this furnace is shown in Figure 1. The third black-body furnace was made up in the Laboratory by fitting diaphragms into a marquardt porcelain tube with an internal diameter of about  $1\frac{1}{2}$  cm. This heater tube was wound and mounted in exactly the same manner as the larger tubes.

Each of these furnaces contained a thermocouple inserted from the back into the central heated part in the usual manner. This was used as an indicator in holding the temperature of the furnace constant at any definite point. In this Laboratory a black-body furnace thus wound and mounted has been heated to the temperature of melting palladium as many as a dozen different times, held there for several hours each time, and is still in good working order.

The sample of gold or palladium was mounted between platinum wires supported by two porcelain tubes in such a manner that the central part of the sample could not touch either of these

two tubes. This mounting was necessary as it has sometimes been found that if a single tube is used the melted metal will touch and cling to the end of the tube so that the electric circuit through the two platinum wires and the sample used to give a signal when the sample melted would not be broken at the instant of melting and thus a high value would be obtained. With the central part of the sample free the circuit would without doubt be broken at the instant of melting. The authors have heard it stated that this method, with the sample in the form of very fine wires, gives high values, but in this case the effect could only be differential, as

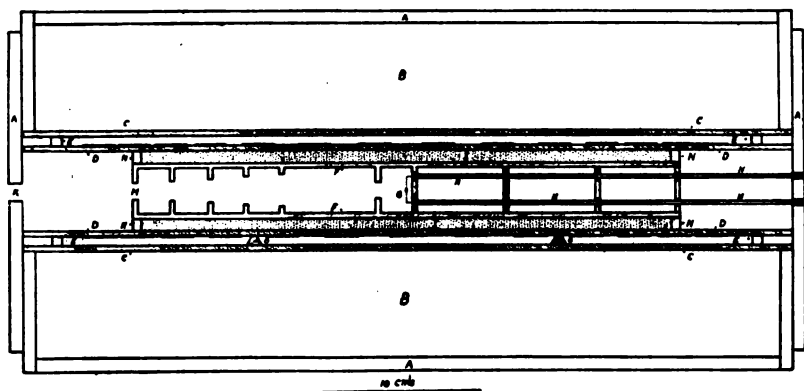


FIG. 1.—Diagram of black-body furnace tubes F and D wound with platinum ribbon, tube F uniformly and tube D about as shown to aid in correcting for end cooling. The space between these two tubes is filled and packed with very pure aluminum oxide. To prevent sagging, tube D is supported at two points, as shown, by supports O. Space outside of tubes (B) filled with infusorial earth.

the same method was used for each metal. Furthermore, as the samples were mounted in several different ways and no difference was detected, it is thought that such errors, if they exist, are very small when care is used in the mounting. Two sets of samples of both gold and palladium were used. They were obtained from the American Platinum Works at different times, about two and one-half years apart. In ordering these samples it was specified that the purest Heraeus metals for melting-point determinations were to be furnished. No differences could be detected between the two samples of gold or the two samples of palladium.

Values of this ratio were measured by two different forms of pyrometer; first, the ordinary pyrometer where a red glass is used as the monochromatic screen, and, second, a spectral pyrometer.

When values of the ratio of brightnesses of a black body between two temperatures are measured, using an optical pyrometer, the wave-length is determined from the effective wave-length of the red glass used in the eyepiece. In using the ordinary optical pyrometer, it is the integral luminosities through the red glass screen that are compared, for which reason the effective wave-length of red glass screen for a certain temperature interval has been defined as the wave-length, such that the ratio of its radiation intensities for these two temperatures equals the ratio of the integral luminosities through the particular screen used.

Knowing the spectral transmission of the red glass, it is possible to calculate the effective wave-length,  $\lambda_e$ , for the temperature interval by means of the following equations:

$$\left[ \frac{J(\lambda T_1)}{J(\lambda T_2)} \right]_{\lambda_e} = \frac{\int_0^{\infty} \tilde{J}(\lambda T_1) \iota'_R V_\lambda d\lambda}{\int_0^{\infty} \tilde{J}(\lambda T_2) \iota'_R V_\lambda d\lambda}$$

where  $J(\lambda T)d\lambda$  is the energy as given by Wien's equation for the wave-length interval from  $\lambda$  to  $\lambda+d\lambda$ ;  $\iota'_R$  is the spectral transmission of the red glass; and  $V_\lambda$  is the visibility. These integrals can be computed by the step-by-step method (each step  $0.005 \mu$ ) with sufficient accuracy for this purpose. To determine the temperature of the palladium point to better than one degree requires that the wave-length be known a little better than one part in six hundred. By the foregoing method of calculation the effective wave-length can be determined to about one or two parts in six thousand.

By the use of a spectral pyrometer a determination of this brightness ratio can be made, and, at the same time, if proper precautions are taken, the wave-length easily determined. This instrument differs from the ordinary pyrometer in that a spectro-

scope is used in place of the ordinary eyepiece. If, with this spectral pyrometer, care is taken to correct for the slit-widths in the regular manner, or to avoid such corrections by using very narrow slits, both for the collimator and the eyepiece, the wavelength used will be very definitely known. In the spectral pyrometer used to determine this ratio, a Hilger constant-deviation spectroscope was used for the eyepiece and such values used for the slit-widths (each slit 0.3 mm, which transmitted a range of wavelength amounting to about  $0.005 \mu$  for  $\lambda = 0.6 \mu$ ) that the error due to this source was negligible.

When making the foregoing determinations of this brightness ratio with either pyrometer, the brightness for each melt was measured in terms of the current through the pyrometer filament. The sample was melted inside the black-body cavity of the furnace. The temperature of the latter was raised very slowly and the E.M.F. of the thermocouple very carefully followed by the observers and thus the values were obtained at the exact time of melt. By the use of an electrical bell which rang when the sample melted, the observer was able to give his attention to following the changes in the E.M.F. of the thermocouple and at the same time to be sure when the sample melted. A very high resistance relay was inserted in the circuit so as to avoid heating the sample with the current used. The E.M.F. of the thermocouple at the time of melt was employed as an indicator and thus the furnace was held at this temperature as long as was necessary to measure this brightness with the pyrometer. In this manner several melts were made and the brightness measured with one metal and then the temperature of the furnace was changed and several melts were made and the brightness also measured with the other metal.

When the black body was at the temperature of the palladium point proper sector disks were used to give an apparent brightness just above and just below that of the black body at the temperature of melting gold. By interpolation, using the logarithms of the current and the relative brightness as obtained from the reading with these and other sectors (since the logarithms of current and brightness give nearly a linear relation), the value of the ratio corresponding exactly to the gold-point brightness was found.

The sectors used had been very carefully calibrated in this Laboratory by a photometric method by Mr. Cady. The six-degree sector used was calibrated on a circular dividing engine by the Bureau of Standards and a value found that agreed very closely with that found by the method used in this Laboratory.

In Table II are given the results for the two different pyrometers. The values for the palladium point were calculated from the ratios found from the value of  $1336^{\circ}$  K for the gold point and from  $c_2 = 14350 \mu$  deg. The range of values of the ratio found by means of the ordinary optical pyrometer is from 1 per cent above to the same amount below the mean value given in Table II. This range in the ratio corresponds to about  $\frac{1}{15}$  of 1 per cent in the value for the melting-point of palladium. Thus the range due to this error is about  $\pm 1.5^{\circ}$  K. The range for the value using the spectral pyrometer was about the same, being in this case somewhat less than 1 per cent. As a result of this work the laboratories of the General Electric Company have decided, for the time being, to accept  $1828^{\circ}$  K as the palladium point.

TABLE II  
SUMMARY OF RESULTS OF MEASUREMENTS OF THE GOLD-POINT PALLADIUM-POINT  
BRIGHTNESS RATIO

METHOD	NUMBER OF SEPARATE DETERMINA- TIONS	NUMBER OF MELTS		$\lambda$	AVERAGE OF RATIO FOUND	RESULT FOR THE PALLADIUM POINT
		Pd.	Au.			
Ordinary Pyrometer*....	10	45	45	0.6663	76.9	$1828^{\circ}.6$ K
Spectral Pyrometer.....	3	13	12	0.6018	122.2	$1828^{\circ}.3$ K

\* A statement of these results was published several years ago (*Astrophysical Journal*, 42, 300, 1915), but at that time the values were used to determine  $c_2$  rather than the palladium point.

The value found for the melting-point of palladium from the measured ratio and the value accepted for the value of  $c_2$  is about  $5^{\circ}$  C. higher than the value given by Day and Sosman in their extended work with the gas thermometer. These experimenters allow an error of  $\pm 2^{\circ}$  C. There has been no chemical analysis of the palladium used in this work but it is doubtful if this is the cause

of the difference. More extended work should be done in order to settle this point. No attempt has been made to refer to all the work that has been done on this point. An excellent review of the field is found in a paper by Waidner and others in the *Report of the Symposium on Pyrometry* soon to be issued by the American Institute of Mining and Metallurgical Engineers.

NELA RESEARCH LABORATORY, CLEVELAND, OHIO  
March 1920

## MINOR CONTRIBUTIONS AND NOTES

### FIVE Oe5 STARS WITH VARIABLE RADIAL VELOCITIES

#### ABSTRACT

*Class Oe5 stars with variable radial velocities.*—As in the case of most of the stars of this spectral class which have been investigated, it has been found that *9 Sagittae*, *A Cygni*, *B.D.+37°1146*, *B.D.+44°3639*, and *B.D.+56°2617* have variable velocities and therefore probably belong to binary or multiple systems. Measurements of twenty-nine plates, scattered over a period of several years, are given in a table and show variations for the different stars amounting to from 20 to 160 km/sec., variations which are from 8 to 60 times the probable error. In addition, variations of about 10 km/sec. were found for *B.D.+52°726* and *19 Cephei*.

During the progress of a radial velocity program at the Detroit Observatory of stars of spectral class Oe5 the following were found by the writer to have variable velocities. The table is self-explanatory. The radial velocity is reduced to the sun.

The lines measured for the radial velocity determination include hydrogen  $\beta$ ,  $\gamma$ ,  $\delta$ ,  $\epsilon$ ,  $\zeta$ , the  $\zeta$  Puppis series  $\gamma'$ ,  $\delta'$ ,  $\epsilon'$ ,  $\zeta'$ , helium  $\lambda\lambda$  4713, 4388, 4144, 4026, 4009, and the four lines whose wavelengths were determined by Frost<sup>1</sup> in *10 Lacertae*, a star of the same spectral class,  $\lambda\lambda$  4685.90, 4116.33, 4097.55, 4089.12. The H and K lines of calcium were also measured, but in general their range of displacement is small.

The width of the hydrogen lines, the diffuse character of the  $\zeta$  Puppis series, changes in the relative intensities of various lines, and apparent shifts in the center of absorption make the determination of velocity rather difficult. Some of the lines of the third plate of *A Cygni* appeared to be doubled, but consistent velocities could not be obtained. The radial velocities referred to the sun have been determined to the nearest tenth of a kilometer per second, although the probable error for a single plate based upon the agreement of the lines used is about two or three kilometers. Two

<sup>1</sup> *Astrophysical Journal*, 40, 268, 1914.

other stars of the program, B.D. +52°726 and 19 Cephei, gave ranges of ten kilometers on five plates each, only two kilometers less than the range in the case of 10 Lacertae.

Including six other stars of class Oe5 having variable radial velocities,  $\xi$  Persei,  $\theta^*$  Orionis (C),  $\iota$  Orionis, S Monocerotis,  $\tau$  Canis

Star Position 1900 Phot. Magnitude	Date	Julian Day	Radial Velocity	Quality of Plate
B.D. +37°1146	Oct. 13, 1917	<sup>242</sup> 1,515.824	km - 2.3	Weak
	Dec. 11, 1917	574.755	-20.3	Fair
5 <sup>h</sup> 14 <sup>m</sup> 0	Feb. 1, 1919	991.733	- 2.8	Fair
+37°20'	Feb. 5, 1919	995.653	- 1.8	Fair
6.71	Feb. 18, 1919	2,008.599	+ 0.3	Fair
	Mar. 27, 1920	2,411.656	- 8.9	Weak
	Mar. 29, 1920	2,413.635	-10.4	Fair
9 Sagittae	June 18, 1918	1,763.760	+ 9.7	Good
	July 8, 1918	783.674	+17.1	Fair
10 <sup>h</sup> 47 <sup>m</sup> 9	July 12, 1918	787.764	- 7.9	Fair
+18°25'	Aug. 3, 1918	809.726	- 2.1	Fair
6.29	Aug. 5, 1918	811.692	- 2.5	Fair
B.D. +44°3639	July 19, 1918	1,794.762	-17.5	Fair
	July 25, 1918	800.736	-12.9	Fair
20 <sup>h</sup> 53 <sup>m</sup> 1	Aug. 2, 1918	808.726	+22.2	Weak
+44°33'	Aug. 5, 1918	811.762	+ 9.2	Good
6.01	Aug. 9, 1918	815.687	+16.4	Fair
	Aug. 10, 1918	816.740	+17.1	Fair
A Cygni	Nov. 8, 1915	0,810.635	+28.8	Fair
	Aug. 3, 1919	1,809.793	-27.9	Fair
21 <sup>h</sup> 14 <sup>m</sup> 8	Aug. 5, 1918	811.816	?	Fair
+43°31'	Aug. 7, 1918	813.683	+ 7.	Poor
6.06	Aug. 12, 1918	818.703	-54.0	Fair
B.D. +56°2617	Nov. 9, 1915	0,811.600	+92.6	Good
	July 20, 1918	1,795.858	-57.2	Fair
21 <sup>h</sup> 35 <sup>m</sup> 9	July 25, 1918	800.812	-30.4	Fair
+57°2'	Aug. 7, 1918	813.753	+56.5	Poor
5.64	Aug. 10, 1918	816.792	+87.5	Fair
	Aug. 12, 1918	818.758	-65.2	Fair

Majoris, and 10 Lacertae, it appears that a very large proportion of the stars of this class that have been investigated have variable velocities; and a star of class Oe5 with a constant velocity may prove to be the exception rather than the rule.

It is interesting to note also that eight out of fourteen Oe5 stars here observed belong to well-known visual binary or multiple systems,  $\lambda$  Orionis,  $\theta^1$  Orionis,  $\delta$  Orionis, S Monocerotis,  $\tau$  Canis



Majoris, B.D. +56°2617, 19 Cephei, and 10 Lacertae. Including the two mentioned above with velocity ranges of ten kilometers and interpreting variable radial velocity stars as spectroscopic binaries, the entire number, fourteen, belong to binary or multiple systems.

W. CARL RUFUS

DETROIT OBSERVATORY  
ANN ARBOR, MICH.  
April 16, 1920

### THE PARALLAX OF THE B-STAR BOSS 1517

#### ABSTRACT

*The parallax of the B-Star Boss 1517 has been recomputed. The result is*

$$\pi = +0''.048 \pm 0''.021.$$

In the *Observatory* for July 1919 (42, 281) Mr. A. J. Roy gives  $-2''.3$  as the corrected Boss proper motion in right ascension for the B-star Boss 1517. With this proper motion I have recomputed my parallax plates and get

$$\pi = +0''.048 \pm 0''.021.$$

This is still a large parallax for a star of spectral class B and in better agreement with the hypothetical parallax of  $0''.033$  computed by Professor Kapteyn (*Astrophysical Journal*, 47, 104, 1918).

J. VOÛTE

MET. OBSERVATORIUM  
WELTEVREDEN, JAVA  
February 14, 1920

## PREPARATION OF ABSTRACTS

Every article in the *Astrophysical Journal*, however short, is to be preceded by an abstract prepared by the author and submitted by him with the manuscript. The abstract is intended to serve as an aid to the reader by furnishing an index and brief summary or preliminary survey of the contents of the article; it should also be suitable for reprinting in an abstract journal so as to make a reabstracting of the article unnecessary. Therefore, *the abstract should summarize the information completely and precisely*, and also, in order to enable a reader to tell at a glance what the article is about and to enable an efficient index of the subject-matter of the abstract to be readily prepared, *the abstract should contain a set of subtitles which together form a complete and precise index of the information contained in the article.*

In the preparation of abstracts, authors should be guided by the following rules, which are illustrated by the abstracts appearing in the *Astrophysical Journal* for January and March 1920.<sup>1</sup> First the new information contained in the article should be determined by a careful analysis; then the subtitles should be formulated; and finally the text should be written and checked.

### RULES

1. *Material not new* need not be analyzed or described; a valuable summary of previous work, however, should be noted.

2. *The subtitles should together include all the new information*; that is, every measurement, observation, method, improvement of apparatus, suggestion, and theory which is presented by the author as new and of value in itself.

3. *Each subtitle should describe the corresponding information so precisely* that the chance of any investigator's being misled into thinking the article contains the particular information he desires when it does not, or vice versa, may be small. "Zeeman effect for metallic furnace spectra" is too broad unless all metals have been studied, for an investigator may be interested, at the time, in only one metal; but "Infra-red arc spectrum of iron to  $3\mu$ " evidently satisfies this rule. It is particularly desirable that ranges of variation of temperature, wave-length, pressure, etc., be given.

4. *The text should summarize the author's conclusions and should transcribe all numerical results of general interest*, including all that might be looked for in a table of astronomical and physical constants, with an indication of the

<sup>1</sup>The rules and illustrative abstracts were prepared by G. S. Fulcher, of the National Research Council.

accuracy of each. It should give all the information that anyone, not a specialist in the particular field involved, might care to have in his notebook.

5. *The text should be divided into as many paragraphs* as there are distinct subjects concerning which information is given. Parts of subtitles may be scattered through the text but the subject of each paragraph must be indicated at the beginning.

6. *Complete sentences* should be used except in the case of subtitles. The abstract should be made as readable as the necessary brevity will permit.

# THE ASTROPHYSICAL JOURNAL

AN INTERNATIONAL REVIEW OF SPECTROSCOPY  
AND ASTRONOMICAL PHYSICS

VOLUME LI

· JUNE 1920

NUMBER 5

## ON THE APPLICATION OF INTERFERENCE METHODS TO ASTRONOMICAL MEASUREMENTS<sup>1</sup>

By A. A. MICHELSON<sup>2</sup>

### ABSTRACT

*An interference method of measuring extremely small angles and changes of angle.—*Thirty years ago the author called attention to the possibility of measuring such minute angles as the *diameters of planetoids and satellites* and the *distance between the components of double stars* by observing the interference fringes produced at the focus of a telescope when only two portions of the objective, located on the same diameter, are used; for it was shown that as the distance apart of the apertures is increased the visibility of the fringes reaches a minimum for a distance equal to  $1.22 \lambda/a$ , or  $0.5 \lambda/a$ , for a disk or double star respectively, when  $\lambda$  is the effective wave-length and  $a$  is the desired angle. This beautiful and simple method was applied successfully by the author in 1891 to the accurate measurement of the size of Jupiter's satellites but was not tested on stellar objects, probably because it was supposed to require ideal seeing conditions. Last year, however, the author discovered by tests at Yerkes Observatory and at Mount Wilson that even when the "seeing" was bad, clear and relatively steady fringes could be obtained; and Anderson, using the 100-inch reflector, has recently measured the separation of the components of Capella,  $0''.0545$ , within less than 1 per cent by the application of this method. In fact the 100-inch could measure with accuracy separations as small as  $0''.025$ . But to determine the *diameter of a fixed star*, a distance between apertures of at least 10 meters would be required; so that an interferometer arrangement would have to be substituted for the telescope. The author also suggests that by the use of prisms to superpose the fringe systems of two stars, small *relative motions* and *parallaxes* could be measured.

*Relative brightness of components of double stars* may also be determined from the relative visibility of the focal fringes at minimum and maximum visibility.

<sup>1</sup> *Contributions from the Mount Wilson Observatory*, No. 184.

<sup>2</sup> Research Associate of the Carnegie Institution of Washington, Mount Wilson Observatory.

In the number of the *Philosophical Magazine* for July 1890 (30, 1) a method was described for the measurement of the angular magnitude of astronomical objects such as the diameter of planetoids and satellites and the distance between double stars, when these are beyond the powers of the largest telescopes, and the hope was there expressed that it might not be impossible thus to measure the diameter of the fixed stars.

Briefly, the process consists in utilizing only the two portions of a large objective at opposite ends of a diameter. The interference fringes at the focus under these conditions will be a series of equidistant interference bands which are most distinct with a source subtending an infinitesimal angle. For an object presenting an appreciable angle the visibility is less and may become zero—the exact relation being readily expressed for any given distribution of light in the source. Thus if  $\phi(a)da$  represent the intensity of a strip of the source of angular width  $da$ , and  $s$  the distance between the apertures (supposed small compared with  $s$ ), and

if  $P = \int \phi(a)da$ ,  $C = \int \phi(a)da \cos 2\pi \frac{s}{\lambda} a$ , and  $S = \int \phi(a)da \sin 2\pi \frac{s}{\lambda} a$ ,

then the visibility of the interference bands is

$$V = \frac{\sqrt{C^2 + S^2}}{P}.$$

Thus for a double star, the brightness of whose components is in the ratio  $1:r$  and whose angular distance  $= a$ ,

$$V = \frac{\sqrt{1+r^2+2r \cos 2\pi \frac{s}{\lambda} a}}{1+r}.$$

For equal components this reduces to  $\cos \frac{\pi sa}{\lambda}$ , which vanishes for  $a = \frac{1}{2} \frac{\lambda}{s}$ . Accordingly this angle can be accurately measured when it is only half of the limit of resolution of the full-apertured telescope.

Again, by comparing the visibility at maximum and at minimum, the ratio of the brightness of the component stars may be found by

$$r = \frac{V_1 - V_2}{V_1 + V_2}.$$

For a uniformly illuminated disk

$$V = \int_0^1 \sqrt{1+\omega^2} \cos \omega nd\omega$$

where  $n = \pi \frac{sa}{\lambda}$ ,  $a$  being the angular diameter. For such an object the fringes vanish for an angular diameter  $a = 1.22 \frac{\lambda}{s}$ .

A series of observations was taken on the satellites of Jupiter at the Lick Observatory the following year with results which amply confirmed the practicability and accuracy of the method.

It is clear, however, that as in all probability the stars present an angular diameter less than one-hundredth of a second, it would be almost hopeless to make such measurements, utilizing the largest telescope in existence; for it would require a distance between the apertures of at least 10 meters to observe the vanishing of the fringes.<sup>1</sup> While such a large telescope would be entirely out of question, the interferometer arrangements figured in the article referred to may serve the purpose, as there is theoretically no limit to the effective base line and practically only that which depends on the atmospheric disturbances.

With a view to testing the effect of these, a trial was made (August 25, 1919) with the 40-inch refractor at Yerkes Observatory, using two apertures 4 inches by 5 inches at opposite ends of a diameter. The result was very encouraging, the interference bands being remarkably steady, notwithstanding the relatively poor "seeing"—2 to 3 on a scale of 5.

On invitation from Dr. George E. Hale the test was applied (September 18, 1919) to the 60-inch reflector of the Mount Wilson Observatory and then to the 100-inch reflector, and in both cases the experience at the Yerkes Observatory was confirmed.

In the case of the 60-inch telescope the apertures were applied, as in the case of the 40-inch, to the objective; while for the 100-inch, it was found quite as effective and far more convenient to use a small screen with two apertures near the eyepiece, the distance and orientation being thus much more readily controlled while the effective size and separation of the two interfering pencils remain the same.

<sup>1</sup> A diminution in visibility, however, might be observed with a diameter of 2 meters.

The interference fringes in both observations remained remarkably clear and steady, notwithstanding the excessive "boiling" of the highly magnified images corresponding to "seeing" 2 on a scale of 10.

Subsequent observations showed that the interference bands remain visible even when the seeing is so poor that the usual type of observation is impracticable.

A statement of results obtained by this method by Dr. J. A. Anderson of the staff of the Mount Wilson Observatory from observations of the spectroscopic binary Capella is herewith appended.

STATEMENT OF RESULTS FROM OBSERVATIONS OF CAPELLA WITH THE MICHELSON INTERFEROMETER

Date of Observation	Distance	Position Angle	Remarks
December 30.6 1919	0".0418	(153°.9)	P.A. calculated. Only the distance observed accurately*
February 13.6 1920	0.0458	5.0	
February 14.6 1920	0.0451	1.0	
February 15.6 1920	0.0443	356.4	
March 15.6 1920	0.0505	242.0	
April 23.6 1920	(0.0439)	107.0	Distance calculated. Only the position angle observed accurately†

\* The rough observation of position angle was  $148^\circ \approx 10^\circ$ .

† Observation made in strong daylight. The blue background shifted the effective wave-length to the red, causing the observed distance of 0".0402 to be much too low. The background could not affect the position angle.

Using the following elements<sup>1</sup> for the orbit, these observations are satisfied as indicated:

$$\begin{aligned}
 a_1 + a_2 &= 0".05249 & (a_1 + a_2) \sin i &= 83,277,900 \text{ km} \\
 e &= 0.016 \\
 \omega &= 117^\circ 3' \\
 i &= 140^\circ 30' \\
 \text{Position angle of } \Omega &= 45^\circ 55' \\
 T &= \text{J.D. } 2,422,387.9 & \text{ or } P &= 104.006 \text{ days}
 \end{aligned}$$

<sup>1</sup> See orbit by H. M. Reese, *Astrophysical Journal*, 14, 263, 1901, for values of  $(a_1 + a_2) \sin i$ , of  $e$ , and of  $\omega$ .  $a_1$  and  $a_2$  are the semi-major axes;  $e$ , the eccentricity (same for each orbit);  $\omega$  is the distance of periastron from the ascending node in the plane of the orbit;  $i$  is the inclination of the orbit to the line of sight;  $\Omega$  is the symbol for the ascending node and is here equivalent to the position angle on the tangential plane.

Date	$t-T$	$a$	$i$	$r$	Position Angle
1. December 30.6 1919	39 <sup>d</sup> .7	1 and 5 0.05249	180°-39°31'	0.04180	153.9
2. February 13.6 1920	84.7	2 and 5 0.05250	-39 36	0.04583	4.6
3. February 14.6 1920	85.7	3 and 5 0.05248	-39 22	0.04506	1.0
4. February 15.6 1920	86.7	4 and 5 0.05249	-39 31	0.04430	357.3
5. March 15.6 1920	11.7	.....	-39 30	0.05050	242.4
6. April 23.6 1920	50.7			0.04391	107.2
		Means 0.05249	180°-39 30		

Parallax of Capella 0.0600.

It appears from a comparison of these results with the orbit that an order of accuracy of one ten-thousandth of a second of arc is attainable in the case of Capella with a base line of 100 inches.

In these observations the distance between the apertures was fixed, and the vanishing of the fringes was observed at the appropriate position angle.

The complete disappearance of the interference bands showed that the component stars are of equal brightness; otherwise the visibility would have a minimum from which the ratio of the brightness may be obtained as indicated above.

For this, however, it would be necessary to measure the visibility, or at least to calibrate the eye estimates.

This may be effected by adjusting the relative width of two auxiliary apertures so that the resulting visibility of a single comparison star (or of the double star in a direction perpendicular to the plane of the components) is the same as that which is actually observed.

If the ratio of the width of the apertures is  $\rho$ , then when the visibilities are equal in the two systems of fringes

$$V = \frac{2}{\rho + \frac{1}{\rho}}.$$

Other problems which involve the comparison of two stars, such as the measurement of stellar parallax, proper motion, variation of latitude, etc., may also be undertaken by a modification of the interference method. For this two prisms or prism couples are similarly placed in front of the apertures, with the plane of refraction parallel with that passing through the two apertures



and the axis. This plane is rotated until the direction coincides with that of the stars to be compared. The refraction by the prisms is then altered (by rotating the single prisms in the same plane, or by equal and opposite rotations of the elements of the prism couples) until the two systems of fringes are superposed. Any change in the relative position of the stars is accompanied by a corresponding alteration in the appearance of the fringes, which is then compensated by rotation of the prisms, from which the change in position may be determined.

Preparations are now under way at Mount Wilson for testing the possibilities of the interferometer method with a base line of 18 to 20 feet.

RYERSON PHYSICAL LABORATORY

June 1920

# APPLICATION OF MICHELSON'S INTERFEROMETER METHOD TO THE MEASUREMENT OF CLOSE DOUBLE STARS<sup>1</sup>

By J. A. ANDERSON

## ABSTRACT

*Michelson interference method of measuring close double stars.*—It is surprising that this method of accurately measuring angles as minute even as half the limit of resolution of the telescope used has heretofore been applied only to Jupiter's satellites. But after Michelson found by tests last year at the Yerkes Observatory and at Mount Wilson that clear and relatively steady fringes can be obtained even when the "seeing" is bad, steps were taken to apply the method to the measurement of the separation of the components of Capella. The *arrangement of apparatus* adopted is described in full. The apertures were placed near the focus instead of at the objective and set at a fixed distance apart, somewhat greater than the distance for minimum visibility, and were then rotated and the four position angles which gave minimum visibility were determined. After the *effective wave-length* for a G-type star had been found by laboratory experiments with sunlight to be about  $0.550 \mu$ , the position readings gave both the angular separation of the components and the direction of the line joining them. The *effect of atmospheric dispersion* is in general to shift the center of the system. Two methods of compensating for this effect are suggested. A method of determining the *relative brightness of components* when the ratio is not more than 1.5 is described and illustrated.

*Accuracy.*—In the case of Capella, the separation, about  $0''.05$ , was determined within 1 per cent. As to the *limits of applicability of the 100-inch reflector* in such measurements, the theoretical resolution limit with the interferometer is  $0''.025$ , and double stars down to about the eleventh magnitude should be measurable under ordinary observing conditions.

*Elements for Capella as determined by the Michelson interference method.*—Observations made on six dates, December 1919 to April 1920, give the following results:  $a = 0''.05249$ ;  $T = \text{J.D. } 2422387.9$ ;  $i = 140^\circ 30'$ . These combined with spectroscopic elements give:  $P = 104.006$  days;  $a_1 + a_2 = 130,924,000$  km;  $m_1 = 4.62 \odot$ ;  $m_2 = 3.65 \odot$ .

*Interference method of measuring atmospheric dispersion*, by its effect on the fringe systems of stars at various zenith distances, is suggested by the author as likely to prove very sensitive.

The astronomical applications of the interferometer have been discussed by Professor Michelson in a number of papers.<sup>2</sup> He

<sup>1</sup> *Contributions from the Mount Wilson Observatory*, No. 185.

<sup>2</sup> *Philosophical Magazine* (5), 30, 1, 1890; (5), 31, 338, 1891; (5), 34, 280, 1892; *American Journal of Science* (3), 39, 115, 1890.

explains how the diameters of stars can be measured, considered as uniformly luminous disks; and, in case there is darkening toward the limb, how the amount of darkening can be determined. Further, if a celestial object is not circular in apparent shape, he explains how its exact shape may be found. Special cases, such as double stars, are fully treated.

In view of the great beauty and simplicity of the method, it is rather surprising to find that the only application it has had up to the present time is to the determination of the diameters of Jupiter's satellites, and this was done by Professor Michelson himself. It is possible that astronomers who in general are so much troubled by the phenomena of "bad seeing" have had a feeling that an instrument so extraordinarily sensitive as the interferometer is known to be could hardly, if ever, be used, especially with the larger telescopes.

On September 18, 1919, Professor Michelson made a final test of this point by applying the interferometer to the 60-inch and 100-inch telescopes of the Mount Wilson Observatory, and found that the interference fringes were easily observed, although the seeing at the time was rated about 2 on a scale of 10. He had on August 25 found similar results with the 40-inch refractor of the Yerkes Observatory. Accordingly, it was decided to give the method a trial with the 100-inch reflector, and Mr. Hale requested the writer to undertake the experiments described below.

As it appeared probable that an aperture much larger than 100 inches would be required for effective work in measuring stellar diameters, it was decided to apply the method to the measurement of some double star, if possible, to one too close to be measured with the usual method. Capella was selected, because an estimate of the separation of its components, based on knowledge of its spectroscopic orbit and parallax, places this around  $\frac{1}{10}$  second of arc, which should be easy to measure with the interferometer applied to the 100-inch telescope.

A preliminary observation (by Mr. Pease and the writer) was made on December 30, 1919, the chief object of which was to learn just how the interferometer should be constructed in order that it might be suited to the measurement of double stars. This obser-

vation gave the distance between the components of Capella with a probable error of about 1 per cent; a reading of the position angle was also made, but it was so very rough that it might easily be in error by  $10^\circ$  either way. Regular observations with the improved form of apparatus were made on February 13, 14, and 15, March 15, and April 23, 1920.

As shown in the diagram (Fig. 1) the interferometer consists simply of a plate (A) having two apertures in it, placed in the

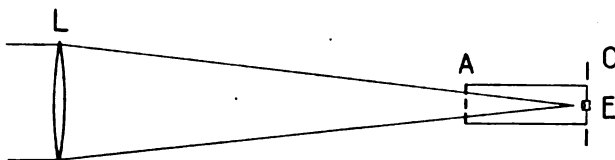


FIG. 1

converging beam of light coming from the telescope objective or mirror. The interference fringes formed in the focal plane are viewed with a high-power eyepiece *E*. The entire interferometer can be rotated about the telescope axis so as to vary the position of the line joining the centers of the two apertures; and the apertures themselves are so arranged that their distance apart can be varied, the actual separation being read on a scale at the eye end of the instrument, where the circle is also located from which the position angle of the apertures is read. The plate carrying the apertures can also be moved entirely out of the beam of light to facilitate the accurate centering of the star to be observed.

The method of making the measurements differs slightly from that described by Professor Michelson,<sup>1</sup> and will therefore be described in sufficient detail to be clear even without reference to any previous work.

Let the light from a star fall upon two apertures placed (for simplicity) in front of the telescope objective or mirror. Let the width of each aperture measured along the line joining their centers be  $d$ ; let the distance between their centers be  $D$ . The

<sup>1</sup> *Philosophical Magazine* (5), 30, 1, 1890.

shape of the diffraction pattern seen in the focal plane of the telescope will depend upon that of the apertures; but we are here concerned only with its dimension in the direction of the line joining the two apertures, and this, in angular measure, as seen from a distance equal to the equivalent focal length of the telescope, is  $\alpha = 2C\lambda/d$ . The intensity, being, say, unity at the center of the pattern, falls to the first zero value at an angle  $\alpha/2$  from this point.  $C$  is a factor depending on the shape of the apertures. For rectangular slits,  $C = 1$ ; for circular apertures,  $C = 1.22$  nearly. Upon the diffraction pattern will appear the interference fringes, these being at right angles to the line joining the two apertures. The angular distance between two bright fringes is  $\lambda/D$ . Hence the number of fringes which can be seen on the central diffraction disk depends on the ratio  $D/d$ , and is equal to  $2CD/d$ . If this number is greater than 10, the fringes farthest from the center will, in general, be invisible in white light, because of the overlapping of the different colors.

Now assume that this arrangement is pointed at a double star, the angular separation of its components being  $\beta$ . If  $\beta$  is larger than  $2C\lambda/d$ , two separate diffraction patterns will be seen, each with its own system of interference fringes. When  $\beta$  is less than  $2C\lambda/d$  the patterns will overlap more or less; and if  $\beta$  is just equal to  $\lambda/2D$  and the position angle of the double star is the same as that of the line joining the two apertures, the conditions are such that a bright fringe due to one component falls on a dark fringe due to the other component, or we may say that the two fringe systems are out of step by just one-half a fringe; and hence, if the two component stars are of the same intensity the visibility of the fringes near the center of the pattern will be zero. (It is, of course, clear that minima of visibility will occur for  $\beta = N\lambda/2D$ , where  $N$  is any odd integer.) Hence we may say that the interferometer "resolves" two stars whose angular separation is  $\lambda/2D$ , just as a circular telescope objective of diameter  $D$  will resolve two stars whose separation is  $1.22\lambda/D$ ; that is, the resolving power of the interferometer is somewhat more than twice that of a telescope of the same aperture. It should also be borne in mind that useful measurements may be made with the interferometer

even when the angular separation is much less than  $\lambda/2 D$ , as will be discussed more fully below.

Let  $D_0$  denote the smallest value of  $D$  which will cause the fringes to disappear for a double star having equal components. If we choose  $D$  a little larger than  $D_0$ , so that  $D_0 = D \cos \theta$ , it is evident that the fringes will be visible when the position angle of the apertures is the same as that of the double star. If now the interferometer be rotated through an angle  $\pm \theta$ , the fringes will just disappear; and the same thing will happen when the instrument is rotated through an angle  $180^\circ \pm \theta$ . For any value of  $D$  greater than  $D_0$  there are, therefore, four values of the position angle, for each of which the fringes disappear, or have minimum visibility, according as the two components of the double star are of equal or of unequal intensity. From these four position angles and the known value  $D$  one can obviously find the value of  $D_0$  and the position angle of the double star. There will, of course, be two possible position angles differing by  $180^\circ$ , but, as will be explained presently, unless the two components have exactly the same intensity and the same color, even this uncertainty may be removed.

The method just described was employed in the present work on Capella. As a rule, a complete observation included three complete rotations of the interferometer for each of three values of  $D$ , making a total of thirty-six readings of position angle. The values of  $D$  were so chosen that  $\theta$ , as defined above, should lie between  $30^\circ$  and  $50^\circ$ . Under these conditions and with reasonably good seeing the probable error of a single reading should not exceed  $3^\circ$ . It is the author's opinion that with a little practice a good observer will be able to reduce the probable error of a single setting to about  $1^\circ$ . The corresponding error in the distance is about 1.8 per cent. The time required for a complete observation was about one hour, but it is reasonable to expect that when one becomes accustomed to observations of this kind no more than fifteen minutes will be required.

Given a suitable arrangement for measuring the "visibility" of the fringes, the following method of observation may be used. Choose a value of  $D$  smaller than  $D_0$ . Determine the visibility

at position angles differing from each other by, say,  $15^\circ$  all the way around the circle. If the object is a double star, the visibility will show two maxima and two minima in a revolution. (This will also be true if the object has the form of a luminous surface longer in one dimension than at right angles thereto. Further measures will, however, readily distinguish between this case and that of a double star.) Repeat twice, using two other values of  $D$ . The data thus obtained should be sufficient to determine both position angle and distance of the double star, with a high degree of accuracy, and without requiring a value of  $D$  as large as  $D_0$ .

Having found  $D_0$  as explained above, we need to know only  $\lambda$  in order to compute  $\beta$ , since  $\beta = \lambda/2 D_0$ . The value of  $\lambda$  for the sun was found from laboratory measures, using as an artificial double star two small round holes illuminated by sunlight reflected from freshly silvered mirrors. The constants of the apparatus were determined by direct measurements, and also by observations on the artificial double star illuminated by very nearly monochromatic light of known wave-length. The results from two series of observations with sunlight were 5498 Å and 5500 Å. It seems safe, therefore, to use for a G-type star  $\lambda = 0.0000550$  cm, and this value was employed in reducing the observations of Capella.

In this connection it is important to bear in mind the rôle played by the background on which the interference pattern is observed. On April 23 an observation of Capella was made in full daylight. The observation was very easy to make, but on being reduced, using the value of  $\lambda$  given above, the distance between the components came out approximately 10 per cent too small. A little consideration shows that this might have been predicted, for the skylight, being relatively very rich in blue light, would reduce the visibility of the blue fringes much more than that of the yellow or red fringes, thus resulting in a considerable increase in the value of the effective wave-length.

#### EFFECTS OF ATMOSPHERIC DISPERSION

When observations are made at some distance from the zenith it is found that for certain position angles of the interferometer

the center of the fringe system does not fall on the center of the diffraction pattern and may even be displaced to such an extent that the fringes cannot be seen at all. This happens when the line joining the apertures is perpendicular to the horizon. The cause of the phenomenon is atmospheric dispersion, as became evident from a series of observations on a star at zenith distances between  $50^\circ$  and  $20^\circ$ . The phenomenon is well known to physicists who have used interferometers. For completeness, however, the explanation will be reproduced here.

To fix ideas, let us consider a star at zenith distance  $45^\circ$ . As seen on the sky it is really a short spectrum, the violet end above and the red end pointing down toward the horizon. Set the interferometer at right angles to this spectrum, that is, with the line joining the apertures parallel to the horizon. The fringe system will be seen central on the diffraction pattern, but the fringes will be closer together at the upper edge than at the lower, for the former are in violet light, the latter in red light. Hence the fringe system is fan-shaped, very much as indicated in the diagram (Fig. 2). Now, if we rotate the interferometer through



FIG. 2

an angle of  $90^\circ$ , the central fringe will no longer be white, but colored—a spectrum whose width is equal to the length of the little stellar spectrum seen on the sky. The order of colors in this fringe is violet above, red below. The angular width of this fringe for the case we are considering ( $z=45^\circ$ ) is about  $0.8''$ , and is therefore equal to about ten times the distance between two bright fringes when  $D=113$  cm. Consequently, in this part of the system the fringes overlap to such an extent that the result is perfectly uniform illumination. Let us for a moment imagine the atmospheric dispersion removed, all other conditions being the same. The diffraction pattern will then show a perfectly normal fringe system, the central fringe being white, the others being spectra whose dispersion increases linearly with the distance from the central fringe. For convenience let us number the fringes, calling the central fringe 0; then  $+1$ ,  $+2$ ,  $+3$ , etc., upward, and  $-1$ ,  $-2$ ,  $-3$ , etc., downward. The order of colors in the  $+$  fringes is red above, violet below, this order being just the reverse for the  $-$  fringes. Since the dispersion



increases with the order, it is evident that we can find some fringe which will have a given width, say  $0.8$ , and hence will be an inverted duplicate of the central fringe as seen with atmospheric dispersion. This will evidently be one of the  $+$  fringes, say the  $+p$ th. If we now introduce atmospheric dispersion, the  $+p$ th fringe will be white or very approximately so, and will accordingly be regarded as the center of the system. Indeed, the fringes  $p-1$ ,  $p-2$ , etc., will be violet above, red below, while the fringes  $p+1$ ,  $p+2$ , etc., will be violet below, red above, as they should be. Now if  $p$  is greater than  $CD/d$ , the new central fringe will be off the diffraction pattern, in the direction away from the horizon.

We may calculate  $p$  as a function of  $D$  and the zenith distance as follows: Let the limits of the spectrum be taken as  $\lambda_{4500}$  and  $\lambda_{6500}$ . Let the width of the  $+1$ st fringe be  $w$ , and its distance from the  $0$  fringe be  $W$ . The width of the  $p$ th fringe will be  $pw$ , or since  $w/W = 4/11$ , the width of the  $p$ th fringe is  $4pW/11$ . In angular measure  $W = \lambda/D$  or, in seconds of arc,  $W = 11''.3/D$ . Hence the width of the  $p$ th fringe in seconds of arc is  $45''.2 p/11 D$  where  $D$  is, of course, in centimeters.

The mean atmospheric refraction in seconds of arc for zenith distances less than about  $70^\circ$  is given to a sufficient approximation by  $r'' = 60 \tan z$ . The atmospheric dispersion between the wavelength limits chosen is  $0.0138$  times this, according to the values given in *Bulletin of the Bureau of Standards*, 14, No. 4, 697-740, 1919. Hence the dispersion will be given by  $\delta'' = 0.83 \tan z = 45''.2 p/11 D$ , whence  $p = 0.22 D \tan z$ . Taking  $D = 150$  cm,  $z = 45^\circ$ , we have  $p = 33$ , which indicates that with good conditions of seeing this should be a very sensitive method for the actual determination of atmospheric dispersion.

In order to make observations at all zenith distances, it is necessary to be able to compensate for this effect of atmospheric dispersion. The method thus far used is not entirely satisfactory. Two plates of plane parallel glass of exactly the same thickness are mounted, one in front of each of the apertures of the interferometer. The normals to the plane faces of these plates make an angle of about  $5^\circ$  with the axis of the telescope, and hence, by tilting one of the plates slightly so as to vary the angle, one of

the two beams can be retarded or accelerated with respect to the other sufficiently to bring the fringe system back to the center of the diffraction disk. Unfortunately, as the interferometer is rotated, one must constantly vary the tilt of the movable plate, and this is annoying, especially with bad seeing, when the fringes are none too easy to observe anyway. A much better way, which, however, has not been tried yet, would be to place a prism with a variable angle in front of the interferometer, but mounted so as not to rotate with the latter. By maintaining its refracting edge always downward it would then only be necessary to vary the refracting angle with the zenith distance. It should be easy to arrange the mounting so that the adjustments would be made automatically by the action of gravity.

#### SIZE OF APERTURES AND BRIGHTNESS

The apertures which were used with the 100-inch reflector measure  $18.3 \times 27.5$  cm as seen in projection on the telescope mirror. Their distance apart was varied from about 120 to 200 cm. On the average, then,  $D = 160$  cm, and  $d = 0.12 D$ . With  $d$  as small as this, the diffraction disk is, of course, quite large compared to the size of the fringe system. A relatively small amount of light is admitted by the small apertures, and this is spread over a rather large area in the focal plane; hence the intensity is low. A little consideration will show that doubling the size of the apertures will result in a 16-fold increase in the intensity of the image; consequently, if we are interested in faint stars, we must use apertures as large as possible. In the present work on Capella this question was of no importance, for with such a bright star there is plenty of light for observations with small apertures even in daytime. Sufficient data were gathered, however, both with the large telescope and from laboratory experiments, to enable us to see pretty clearly just what can be done.

With  $d = 0.12 D$  it was found possible with the 100-inch reflector to observe stars down to the seventh magnitude, the seeing being usually 1 on a scale of 10. With good seeing perhaps one might reach a magnitude fainter. Laboratory experiments showed that there is practically no loss in the distinctness of the fringes when  $d$

is as large as  $0.5 D$ , which would increase the intensity two hundred and fifty-six times, or about six magnitudes. Hence with an instrument as large as the 100-inch, one might be able to observe stars down to the thirteenth magnitude, and there should be no difficulty in reaching the eleventh magnitude under ordinary conditions of observing. It is, of course, important to bear in mind that, as  $d$  is increased, the size of the diffraction disk decreases according to theory only if the seeing is very good. A small

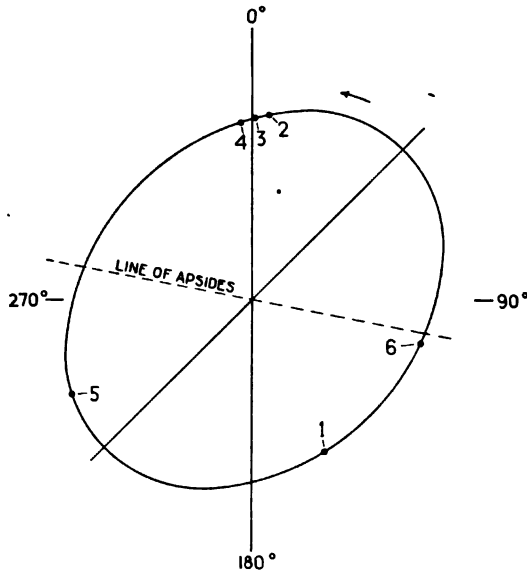


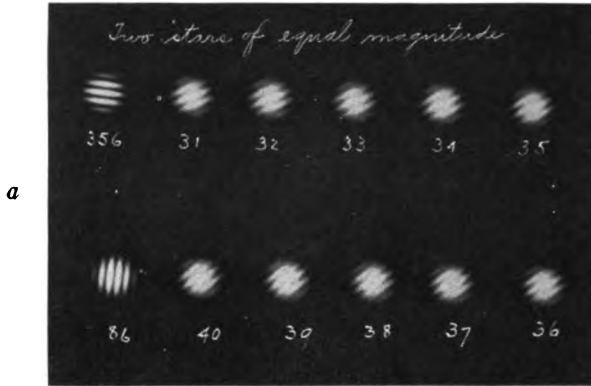
FIG. 3.—Apparent orbit of Capella

instrument will, therefore, be much more likely to reach the theoretical limiting magnitude than one as large as the 100-inch.

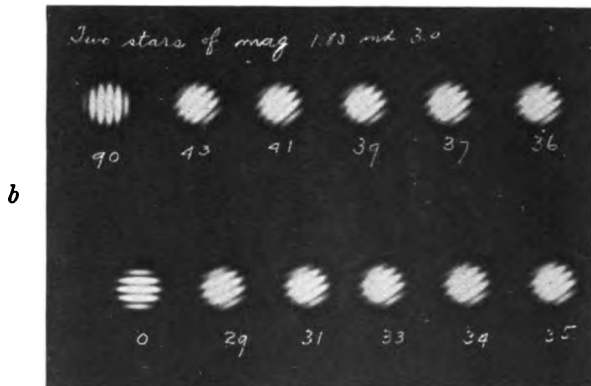
When  $d$  is greater than  $0.3 D$ , so that the fringe system covers all of the diffraction disk, the normal phase-changes over the latter begin to produce an appreciable effect. If, for example, two stars of equal intensity are observed,  $d$  being greater than  $0.3 D$ , and  $D$  being so chosen that the fringes should just disappear, one finds that although they do disappear at the center of the disk, they may still be seen at the ends of a diameter parallel to the line



# PLATE XIV



Position Angle of Stars  $266^{\circ}$



Position Angle of Stars  $270^{\circ}$

APPEARANCE OF INTERFERENCE SYSTEM FROM ARTIFICIAL STARS  
IN THE LABORATORY

joining the two stars. If, say, the star on the right side is brighter than that on the left, the fringes will be visible at the center, but will disappear at some point between the center and the left side. These phenomena are beautifully shown if  $D$  is so chosen that  $\theta$  is around  $45^\circ$ , the fringes being inclined at  $45^\circ$  to the line joining the two stars. Plate XIV is reproduced from two series of photographs made to illustrate this point. The position angle of the artificial double star used in Plate XIV *a* was  $266^\circ$ , and the two stars had the same magnitude. The number under each image shows the position angle of the interferometer when the photograph was made. Plate XIV *b* shows a similar set for two stars in position angle  $270^\circ$ , their magnitudes differing by 1.17. It will be observed that in each set the image made at  $35^\circ$  shows the fringes on the right side out of step by half a fringe with the fringes on the left side. In *a*, however, the two systems meet in a vertical line across the center of the image, while in *b* this line is near the left edge. From this it is clear that if one uses a relatively large value of  $d$ , and the seeing is good enough to enable one to see the phenomena just described, there should be no difficulty in estimating the difference in brightness of the components, provided this does not exceed say 1.5 mag., or in removing completely the uncertainty of  $180^\circ$  in the value of the position angle. Experience also shows that with a pattern such as shown in Plate XIV the probable error of a single setting for  $\theta$  is not greater than  $1^\circ$ ; in fact, the probable error of the mean of 10 settings seldom exceeded  $0^\circ.15$ . The observed co-ordinates of Capella are as follows:

## RESULTS FOR CAPELLA

Observation	Date G.M.T.	Distance	Position Angle	Remarks
1.....	1919 Dec. 30.6	$0''.0418$	$148^\circ \pm 10^\circ$	Position angle only roughly estimated
2.....	1920 Feb. 13.6	$0.0458$	5.0	
3.....	Feb. 14.6	$0.0451$	1.0	
4.....	Feb. 15.6	$0.0443$	356.4	Observed distance ( $0''.0402$ ) greatly in error on account of daylight
5.....	Mar. 15.6	$0.0505$	242.0	
6.....	Apr. 23.6	.....	107.0	

The following spectroscopic elements for Capella are taken from Campbell's *Second Catalogue of Spectroscopic Binaries*:<sup>1</sup>

$P$	$T$	$\omega$	$e$	$a \sin i$	$a \sin^2 i$
104.022	J.D. 2414899.5	117.3 (297.3)	0.016	36,847,900 km 46,430,000 km	0.19 0.94

Adding 72  $P$  to  $T$ , we have  $T' = \text{J.D. } 2422389.1$  as a convenient time of periastron for our calculations. The data are not well distributed and indeed are insufficient for a complete revision of the elements; but a slight change in  $P$  is, of course, allowable, and for purposes of fitting the observed and calculated positions we may regard  $T'$  as variable with limits of  $\pm 2$  days.

Let  $\rho$  and  $v$  be the radius vector and true anomaly in the orbit plane. Let  $r$  and  $\phi$  be the radius and angle from the node in the apparent orbit. Then

$$\begin{aligned}\rho \cos (v+\omega) &= r \cos \phi \\ \rho \sin (v+\omega) \cos i &= r \sin \phi\end{aligned}$$

Since the eccentricity is small, we may set  $\rho = a(1 - e \cos v)$  so that

$$\begin{aligned}r^2 &= a^2(1 - e \cos v)^2[\cos^2(v+\omega) + \sin^2(v+\omega) \cos^2 i] \\ &= a^2(1 - e \cos v)^2[1 - \sin^2(v+\omega) \sin^2 i]\end{aligned}$$

Combining the fifth observation with each of the first four we can derive four values of  $a$ . With the mean value of  $a$  we can then find five values of  $i$ . The values of  $a$  and  $i$  thus obtained should agree except for errors in the observations or in the given elements. We have assumed that the given elements are all accurate except  $P$ , as indicated above. Using  $T' = 2422389.1$  we derive:

Observation	$t - T'$	$M$	$v$	$a$	$i$
1.....	38 <sup>d</sup> .5	133 <sup>o</sup> .25	134 <sup>o</sup> .59	0.05334	137° 51'
2.....	85.5	289.00	287.27	.05394	132 49
3.....	84.5	292.45	290.75	.05377	134 2
4.....	85.5	295.92	294.27	.05368	134 42
5.....	10.5	36.34	37.43	.....	134 42
6.....	49.5	171.32	171.60	.....	.....
Mean				0.05368	

<sup>1</sup> *Lick Observatory Bulletin*, No. 181.

Reducing  $T'$  by 0.9 and then by 1.2 days we have:

Observation	$t-T'$	$a$	$i$	$t-T'$	$a$	$i$
1.....	39 <sup>d</sup> .4	0".05270	139° 56'	39 <sup>d</sup> .7	0".05249	140° 29'
2.....	84.4	.05280	138 46	84.7	.05250	140 24
3.....	85.4	.05276	139 11	85.7	.05248	140 38
4.....	86.4	.05276	139 6	86.7	.05249	140 29
5.....	11.4	.....	139 14	11.7	.....	140 30
	Mean	0.05275	.....	Mean	0.05249	140 30

By subtracting 1.2 days from  $T$ , we arrive at a remarkable constancy in the values of  $a$  and  $i$ , and conclude that the observations to date are best represented by

$$T' = \text{J.D. } 2422387.9, \quad a = 0".05249, \quad i = 140^\circ 30'$$

Computing the distance and position angle with these values we have:

Observation	$r$ (Observed)	Pos. Ang. (Observed)	$r$ (Calc.)	Pos. Ang. (Calc.)	O-C	
					$r$	Pos. Ang.
1.....	0".0418	148° ± 10°	0".04180	153° 54'	0".00000	.....
2.....	.0458	5.0	.04583	4 34	-0.00003	+0°.4
3.....	.0451	1.0	.04506	1 0	+0.00004	0.0
4.....	.0443	356.4	.04430	357 18	0.00000	-0.9
5.....	.0505	242.0	.05050	242 26	0.00000	-0.4
6.....	.....	107.0	0.04391	107 12	.....	-0.2

The agreement is, perhaps, better than we have any reason to expect, due possibly to the fact that the number of observations is small. However, taking the results as they stand, we can substitute in the elements as given by Campbell and derive:

$$P = 104.006 \text{ days. } a_1 + a_2 = 130,924,000 \text{ km.}$$

$$\pi = 0".0600; \quad m_1 = 4.62 \odot; \quad m_2 = 3.65 \odot.$$

It remains to be seen whether recent spectroscopic observations are in agreement with this new value of the period.

MOUNT WILSON OBSERVATORY  
June 1920



# PHOTOGRAPHS OF NEBULAE WITH THE 60-INCH REFLECTOR, 1917-1919<sup>1</sup>

By FRANCIS G. PEASE

## ABSTRACT

*Photographs of nebulae with the 60-inch reflector.*—About 330 of the nebulae found on the 66 plates taken by the author during the years 1917-1919 are listed or described in this article, and 27 of these are illustrated on the 18 plates reproduced. The most remarkable are: N.G.C. 2146, Camelopardus, with its handlike dark marking, a spiral with an abnormal center; N.G.C. 3379, resembling an unresolved star cluster; N.G.C. 3384, with a dual, Saturn-like nucleus and symmetrical wings; N.G.C. 4395-4399-4400-4401, which together form a remarkable spiral; N.G.C. 4656-4657, which constitute a single right-handed spiral without a well-defined nucleus; and I.C.II 5146 Cygnus, a unique array of light and dark markings. In addition the following are described: (1) Spirals: N.G.C. 48, 1186, 1699, 2290, 2291, 2964, 2968, 3310, 3367, 3389, 3395-3396, 3786, 3788, 5257, 5258, 5278-5279, 5544, 5545, 6014 (?), 6906, 6928, 6930, 7722; I.C.II 1441, 2233. (2) Round or elongated: N.G.C. 49, 51, 1700, 2274, 2275, 2288, 2289, 2970, 3377, 3391, 5557, 5868, 5869, 6017, 6927, 7240, 7242, 7435, 7436, 7611, 7615, 7617, 7619, 7621, 7623, 7627, 7631; I.C.I 922, 928; I.C.II 5192, 5194, 5195. (3) Misc.: N.G.C. 955, 2294 (spindles); 1491, 1555, 2024, 2245, 2247, 2359, 2403, 2537, 6820, 6888, 7023 (irregular); 3357 (stellar); 6703(?), 7048 (planetary); I.C.I 931 (stellar); 1470 (irregular); I.C.II 5191 (spindle). (4) Uncatalogued nebulae numbering 255. *Variations from N.G.C.*—The positions for N.G.C. 48, 49, 51, 2247, 5544, 5545, 6927, 6928, and 6930 were given incorrectly. N.G.C. 5865, 5871, and 7433 were not found. N.G.C. 6823 is a cluster and N.G.C. 6846 is a group of stars. In four cases, indicated above by dashes, two or more nebulae seem to form parts of a single system. *Variable nebulae.*—The changes in N.G.C. 1555 are described and also possible differences in the nuclear region of N.G.C. 2245, which will be investigated further. Other nebulae, N.G.C. 955, 1186, 2024, and 7023, showed no change.

*Spectra of two nebulae.*—N.G.C. 1700 is of type Go or later and has a large radial velocity. The spectrum of the nucleus of N.G.C. 3379 is Go or later and the radial velocity is +850 km per sec.

This series of observations of nebulae covers the writer's work in direct photography with the 60-inch reflector during the years 1917-1919. The program included (a) peculiar nebulae, e.g., N.G.C. 3395-3396; (b) groups of nebulae with a view to future measurement, e.g., N.G.C. 48, 49, 51; I.C.I 922, etc.; (c) variable nebulae such as N.G.C. 1555; (d) previously observed nebulae requiring additional photographic data, these being indicated with

<sup>1</sup> Contributions from the Mount Wilson Observatory, No. 186.

an asterisk thus: N.G.C 955\*; (e) a few objects for special purposes, and several affording data for classification photographed during intervals in the regular program. In addition a search for spirals was made along the Milky Way among the smaller nebulae with no success thus far.

Trails for orientation were made on practically all the plates. Many of the measures have been made with a polar co-ordinate machine; and while this serves admirably for the determination of orientation and distances, the magnification (12) is too high for use in determining the size of the objects. For these data recourse was had to the polar co-ordinate réseau and a low-power magnifier. Many objects appearing near the edges of the plates have been listed; but it is to be remembered that at 10' from the center of the field a star image is oval, and at 15' it is comate or arrow-shaped, although poor seeing rounds out these forms, with some increase in size. The smaller nebulae not listed in the N.G.C., or the *Index Catalogue*, are listed as *a*, *b*, *c*, etc., in order of their right ascension.

The descriptions apply to a particular plate or to the general results from a number of plates of the same object, and are not co-ordinated into a homogeneous series of intensities corresponding to the N.G.C. The nebulae have been separated into four orders of brightness: faint, F; medium faint, MF; medium bright, MB; bright, B. The following abbreviations have also been used in the descriptions: R, round; Irr., irregularly; gbM, gradually brighter in the middle; lbM, little brighter in the middle; Nu., nucleus; sbM, suddenly brighter in the middle. All illustrations are placed with N at the top, *p* on the right.

As before, the positions are those of the N.G.C. brought forward to the year 1920. A number of these have been found incorrect, and recourse has been had to Bigourdan's *Observations des Nebuleuses et d'Amas Stellaires* to obtain the correct data.

Photographs of several objects taken with the 100-inch reflector have been used in this paper and are designated with the prefix 100—. Several of Mr. Shapley's photographs showing nebulae have been used in compiling the descriptions. These are designated as *Shapley* 2968, etc.

TABLE I  
NEGATIVES WITH THE 60-INCH REFLECTOR

N.G.C.	$\alpha$ 1920	$\delta$ 1920	Constellation	G.C.	H and Others	$h$	Type	Plate No.	Illustration	Remarks
48.....	$0^h 13^m 32^s$	$+47^\circ 47'.8$	Lacerta	.....	Barnard	.....	Spl.	309		8 additional
49.....	$0 10 40$	$48.0$	Lacerta	.....	A.N.	.....	Elong.	309		Nebulae on plate
50.....	$0 10 40$	$48.0$	Lacerta	.....	.....	.....	Elong.	309		
932*	$2 0 16$	$-1 27.0$	Cetus	.....	.....	.....	Spl.	310	XVd	15 additional
1132*	$3 0 31$	$+42 39.6$	Perseus	531	IV 278	229	Elong.	310	XVc	20 additional
1555*	$4 17 17$	$+51 55.1$	Taurus	539	IV 258	281	Spl.	310		
1555*	$4 17 17$	$+19 52.8$	Taurus	539	Hind	.....	Var.	312, 322		
1655*	$4 53 1$	$-4 50.3$	Eridanus	.....	.....	.....	Spl.	314, Hogg 3		
1700.....	$5 37 0$	$-1 53.6$	Orion	632	V 32	336	R	314, Hogg 3		
2024.....	$5 37 0$	$+78 31$	Camelopardus	1227	IV 32	.....	R	314, Hogg 3		
2146.....	$6 1 53$	$+10 13.2$	Camelopardus	5157	Winnecke	II	Err.	316	XVf	
2245.....	$6 28 17$	$+10 13.2$	Monoceros	1425	IV 303	393	Fan.	631, 320	XVla	
2247.....	$6 28 15$	$+10 21.7$	Monoceros	.....	Ld. R. Swi	.....	Err.	321, 320		
2274.....	$6 43 2$	$+33 30.0$	Gemini	1448	II 614	406	R	313		
2275.....	$6 43 3$	$20.1$	Gemini	1440	Ld. R	407	R	313		
2288.....	$6 45 28$	$20.1$	Gemini	1455	.....	.....	R	311, 315		
2289.....	$6 45 20$	$30.9$	Gemini	1456-7	II 808	410	Elong.	311, 315		
2290.....	$6 45 33$	$27.7$	Gemini	5369	III 807?	.....	Spl.	311, 315	XVla	12 additional
2291.....	$6 45 35$	$33.0$	Gemini	1458	III 807?	409	Spl.	311, 315		
2294.....	$6 45 47$	$33.2$	Gemini	1460	Ld. R	.....	Spl.	311, 315		
2350.....	$7 13 59$	$-13 4.1$	Canis Major	1511	V 21	307.5	.....	320	XVlb	
2403*	$7 20 7$	$+65 46.5$	Canis Major	1541	V 44	.....	.....	307		
2537.....	$8 7 35$	$+46 14$	Lynx	1541	.....	.....	Err.	359, Sh. 2968		
2603.....	$0 27 30$	$+21 51.2$	Leo Major	1861	I 56	6041	Single	282		No text given
2605.....	$0 27 41$	$+21 52.3$	Leo Major	1863	I 57	6042	Spl.	.....		15 additional
2604.....	$0 38 11$	$+32 12.8$	Leo Minor	1866	I 114	622	Spl.	321, 324		
2608.....	$0 38 28$	$+32 17.7$	Leo Minor	1869	II 491	624	El. Spl.	321, 324		
2670.....	$0 38 28$	$+32 20.7$	Leo Minor	1901	.....	627	Elong.	321, 324		
3310.....	$10 33 48$	$+53 55.1$	Ursa Major	2158	IV 60	731	Spl.	356		
3357.....	$10 40 6$	$+14 30.3$	Ursa Major	5533	.....	.....	Neb. Star	201	XVe	No text given
3367.....	$10 42 21$	$+14 10.2$	Ursa Major	2193	II 78	748	Spl.	280, 327		9 additional
3377.....	$10 43 28$	$+13 44.4$	Ursa Major	2201	II 99	754	Elong.	280, 327		4 additional
3379.....	$10 43 37$	$+12 0.2$	Ursa Major	2203	I 17	757	R	290, 334		
3384.....	$10 44 4$	$+12 3.1$	Ursa Major	2207	I 18	758	Elong.	290, 334	XVlla	See text 3377
3391.....	$10 44 14$	$+12 57.0$	Ursa Major	2211	II 41	761	Spl.	290, 334		
3391.....	$10 44 14$	$+14 38.6$	Ursa Major	5535	.....	.....	Elong.	280, 327	XVlla	
3395.....	$10 45 23$	$+33 24.4$	Ursa Major	2216	I 116	765	Double	286, 332		
3396.....	$10 45 28$	$+33 24.9$	Ursa Major	2217	I 117	766	Spiral	337, 338	XVb	26 additional
3786.....	$11 35 29$	$+32 21.8$	Ursa Major	2470	.....	.....	Spiral	330-331, 333	XVllb	
3788.....	$11 35 32$	$+32 22.8$	Ursa Major	2480	.....	.....	Single	.....		
4395.....	$12 21 51$	$+33 59.4$	Canes Venatici	2958	V 29.1	1252	.....	.....		
4399.....	$12 22 31$	$+34 34$	Canes Venatici	2959	V 29.2	.....	.....	.....		
4400.....	$12 22 31$	$+34 34$	Canes Venatici	2960	Ld. R	.....	.....	.....		
4401.....	$12 22 1$	$+33 57.5$	Canes Venatici	2962	Ld. R	.....	.....	.....		

4956	12 40 5	+32 36.2	Canes Venatici	3189	I	176	1414	Single	336, 339	XVIIIb	11 additional
4957	12 40 14	+32 39.4	Canes Venatici	3190	I	177	1415	Spl.	345	XIXb	
5257	13 35 40	+1 14.7	Virgo	3624	II	805	1654	Spl.	345	XIXa	
5258	13 35 53	+1 14.3	Virgo	3625	II	806	1655	Spl.			
5278	13 38 40	+56 4.3	Ursa Major	3630	Ld. R	798	1665	Single	341, 342		
5279	13 38 45	+56 4.3	Ursa Major		Ld. R	419	1771	Spl.	127, 260, 261	XXb	13 additional
554*	14 13 40	+36 56.5	Bootes	3833	II	684	1776	Spl.	127, 260, 261		
554*	14 13 41	+36 56.8	Bootes	3834	Ld. R	90		Spl.	127, 260, 261		
5557	14 15 5	+36 51.6	Bootes	3843	I	684		Elong.	328, 335		Not on plate
5865	15 5 43	+0 48.	Serpens	4027	II			R	328, 335		Not on plate
5868	15 5 44	+0 48.	Serpens	4060	II	545	1908	Elong.	328, 335		
5869	15 5 45	+0 46.6	Serpens	4061	II		1908	Elong.	328, 335		
5871	15 5 57	+0 40.1	Serpens		II		1908	Elong.	328, 335		
6014	15 52 1	+6 9.7	Serpens	4148	II		1940	Spl?	325		
6017	15 53 10	+6 13.6	Serpens	4159	II		1941	Elong.	325		
6020	15 53 10	+45 27.7	Lyra	5931	II		1941	Plan?	344		
6820	19 39 3	+22 53.3	Vulpecula	5945	II		2049	Cluster	298		10 additional
6823	19 39 48	+23 6.5	Vulpecula	4512	VII	18		Group of stars	298		
6846	19 53 22	+32 8.4	Cygnus	5948	IV	72		Group of stars	295	XXc	
6888	20 9 33	+38 9.1	Cygnus	4561	IV	40		Sp.	352		
6906	20 19 36	+6 12.3	Sagitta	5936	m			Elong.	347, 350		4 additional
6927	20 28 46	+9 38.6	Delphinus	5962	m			Spl.	347, 350		
6928	20 28 58	+9 30.2	Delphinus	5963	IV			Spl.	347, 350		
6930	20 29 7	+9 34.6	Delphinus	5964	IV	74		Spl.	343		
7023*	21 0 37	+07 51.	Dr ...	4634	IV			Plan.	296		
7028	21 11 23	+45 57.4	Cygnus		St. IV			Elong.	292, 354, 357		19 additional
7240	22 11 53	+36 52.7	Lacerta	6033	St. V			Elong.	292, 354, 357		Star on plate
7242	22 12 10	+36 53.7	Lacerta	6035	St. V			Elong.	292, 354, 357		Not on plate
7431	22 53 47	+25 44.2	Pegasus		Bigourdan			R	293		14 additional
7433	22 54 2	+25 43.2	Pegasus	4872	Ld. R	243	2105	R	293		
7435	22 54 6	+25 42.2	Pegasus	4873	Ld. R			Elong.	293		
7436	22 54 6	+25 42.2	Pegasus	4871	Ld. R			Elong.	351		
7011	23 15 33	+7 22.5	Pegasus	4934	III		2229	Elong.	351		
7015	23 15 53	+7 22.5	Pegasus	4935	III			Elong.	351		
7017	23 16 2	+7 58.5	Pegasus	4936	III			Elong.	351		
7019	23 16 12	+7 46.	Pegasus	4937	III	439	2230	R	351		
7021	23 16 20	+7 55.7	Pegasus	4938	III	574		Elong.	351		
7023	23 16 27	+7 57.5	Pegasus	4938	III	435	2231	R	351		
7026	23 16 39	+7 57.5	Pegasus	4940	III	440	2233	R	351		
7031	23 17 24	+7 46.7	Pegasus	4942-3	Ld. R			Elong.	351		
7722	23 34 41	+15 31.0	Pegasus	6216				Spl.	353		
922	13 40 47	+50 0.4	Ursa Major	Barnard					341, 342	72 additional	
928	13 40 43	+50 1.2	Ursa Major	AN							
931	13 40 43	+50 1.3	Ursa Major								
1441	22 11 47	+30 53.8	Lacerta	4136	Bigourdan				292	XXa	See text N.G.C. 7240
1470	23 1 51	+59 48.9	Cassiopeia	Spatzier 62	Barnard 3110			Irr.	297		
2233	23 1 51	+45 50.5	Lynx					Spl.	297		
5146	21 50 25	+45 50.5	Cygnus	Espan	Wolf			Irr.	276, 349	XIXc	See text N.G.C. 7240
5191	22 12 7	+30 52.8	Lacerta						292		
5192	22 12 7	+30 52.8	Lacerta								
5194	22 12 11	+30 53.8	Lacerta								
5195	22 12 11	+30 53.8	Lacerta								

To increase their sensitiveness, the plates were given a preliminary exposure. Before use at the telescope they were exposed to an 8 c. p. red lamp at a distance of six feet. The amount varied from twenty to forty seconds, depending upon the length of exposure to be given at the telescope.

Mr. W. P. Hoge, Mr. J. C. Duncan, Mr. Hugo Benioff, and Mr. Milton Humason have assisted in making the plates, and to them the writer wishes to express his gratitude for the help rendered. I am indebted to Mr. Ellerman for the preparation of the positives for the half-tones.

#### N.G.C. 48, 49, and 51, *Lacerta*

N.G.C. 48	$\alpha = 0^h 9^m 52^s$ , $\delta = +47^\circ 47' 8''$	} (1920); $\lambda = 84^\circ$ , $\beta = -14^\circ$
N.G.C. 49	$\alpha = 0^h 10^m 13^s$ , $\delta = +47^\circ 48' 0''$	
N.G.C. 51	$\alpha = 0^h 10^m 26^s$ , $\delta = +47^\circ 48' 9''$	

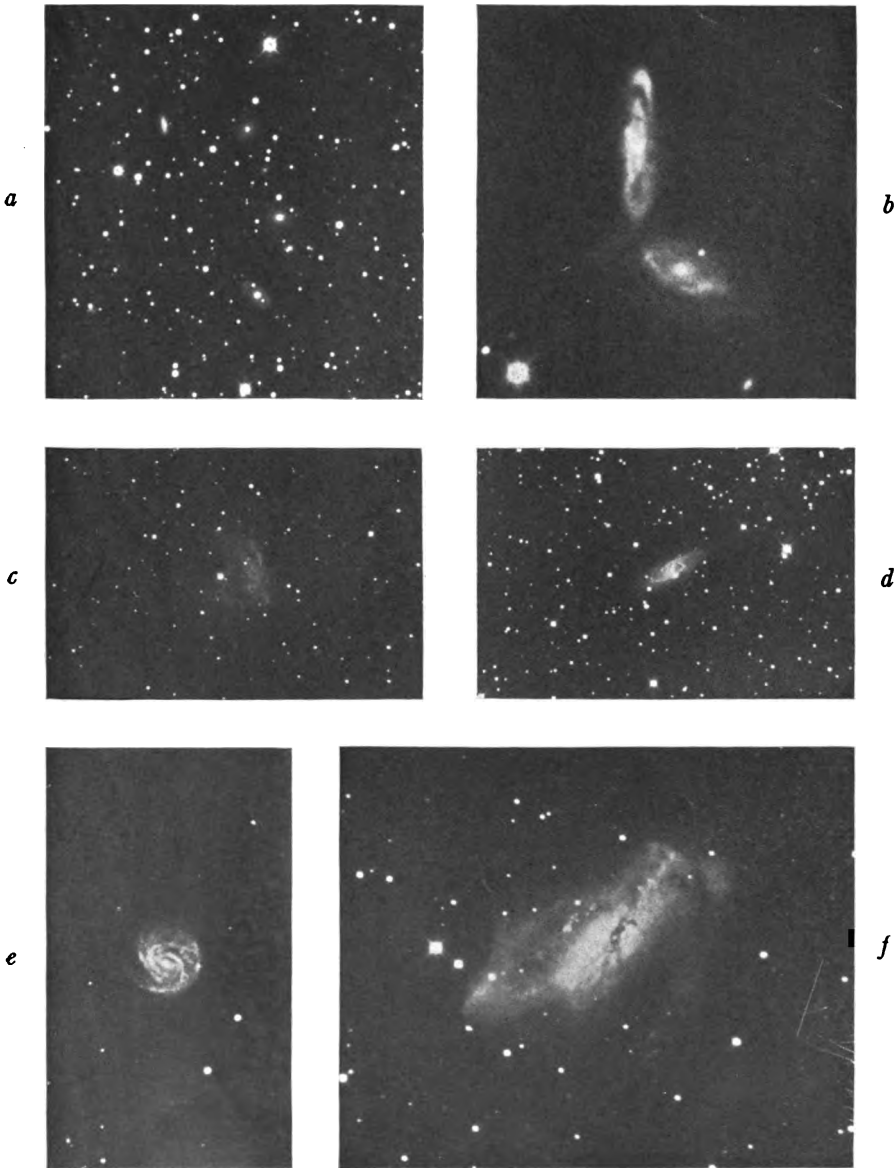
Plate No. 309, 1917, November 16, 130<sup>m</sup>. Images large

A group of eleven nebulae, six of which are described by Barnard in *A.N.* 4136. Eight are elliptical in shape, the other three irregularly round. Two have distinct spiral structure, four have strong bright almost stellar nuclei. Two are medium-faint, almost uniform spindles, and the remainder, faint patches with slightly brighter middle.

The positions given in the N.G.C. are not correct, those above being obtained from Barnard's corrected values. The following is a description of the nebulae, measures being referred to the nucleus of N.G.C. 51.

<i>a</i> , <i>p</i>	250°	<i>d</i>	15'5	MF	12"×6", <i>p</i> 161°.
<i>b</i> ,	234		10.5	MB	20"×10", <i>p</i> 65°, almost stellar Nu.; Barnard No. 1.
<i>c</i> ,	227		8.7	MB	Spiral, 45"×15", <i>p</i> 168°, gbM, vs almost stellar Nu.; Barnard No. 2.
<i>d</i> ,	257		5.7	MB	Spiral, 45"×30", <i>p</i> 11°, N.G.C. 48, Barnard No. 3.
<i>e</i> ,	202		7.3	MF	9" diameter with almost stellar Nu., Barnard No. 4.
<i>f</i> ,	308		2.7	F	10" diameter gbM.
<i>g</i> ,	256		2.1	MF	12"×9", <i>p</i> 161°, gbM, B almost stellar Nu., N.G.C. 49, Barnard No. 5.
<i>h</i> ,		0		MB	30"×18", <i>p</i> 59°, B, almost stellar Nu. on sp edge of central B patch 10" diameter, N.G.C. 51, Barnard No. 6.

# PLATE XV



- |   |  |
|---|--|
| a. N.G.C. 2288, 2289, 2290, 2291, 2294. | Exposure, 210 <sup>m</sup> S 27, Enlargement, 1.9, 1 mm = 14.4 |
| b. N.G.C. 3786, 3788                    | Exposure, 135 S 27, Enlargement, 5.6, 1 mm = 4.9               |
| c. N.G.C. 1491                          | Exposure, 160 S 23, Enlargement, 1.9, 1 mm = 14.4              |
| d. N.G.C. 1186                          | Exposure, 220 S 27, Enlargement, 1.9, 1 mm = 14.4              |
| e. N.G.C. 3367                          | Exposure, 150 S 30, Enlargement, 2.4, 1 mm = 11.2              |
| f. N.G.C. 2146                          | Exposure, 258 S 23, Enlargement, 3.5, 1 mm = 7.8               |



PLATE XVI

*a*



*b*

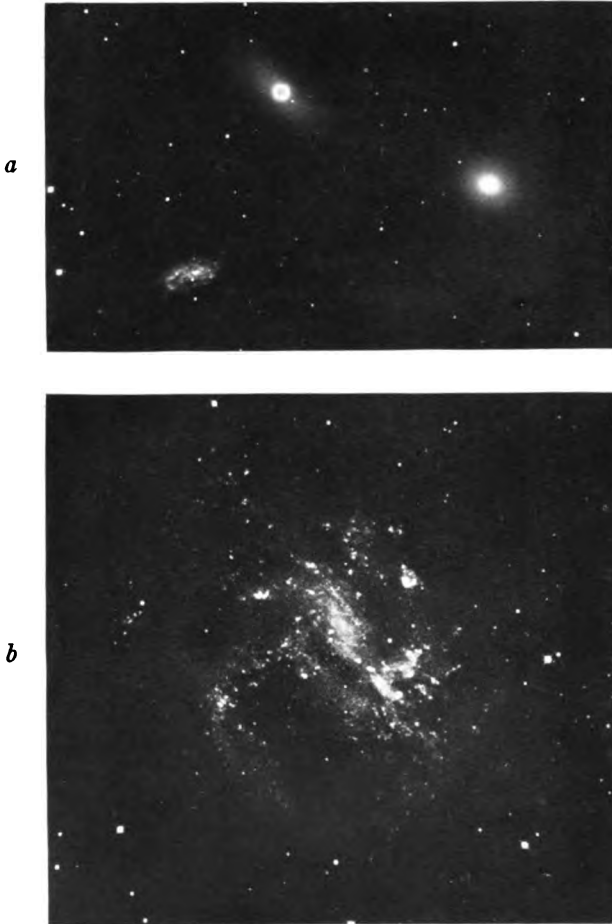


- a.* N.G.C. 2245, 2247, Exposure, 95<sup>m</sup> S 30, Enlargement, 1.9, 1 mm = 14".4  
*b.* N.G.C. 2359, Exposure, 210 S 23, Enlargement, 2.5, 1 mm = 11.0





PLATE XVII



*a.* N.G.C. 3379, 3384, 3389, Exposure, 120<sup>m</sup> S 23, Enlargement, 1.9, 1 mm = 14".4  
*b.* N.G.C. 4395, 4399, 4400, 4401, Exposure, 450 S 30, Enlargement, 2.0, 1 mm = 13.3



PLATE XVIII

*a*



*b*



- a.* N.G.C. 3395-96, Exposure, 120<sup>m</sup> S 23, Enlargement, 5.6, 1 mm = 4".9  
*b.* N.G.C. 4656-57, Exposure, 240 S 30, Enlargement, 1.9, 1 mm = 8.5 (100-inch)



# PLATE XIX

*a*



*b*



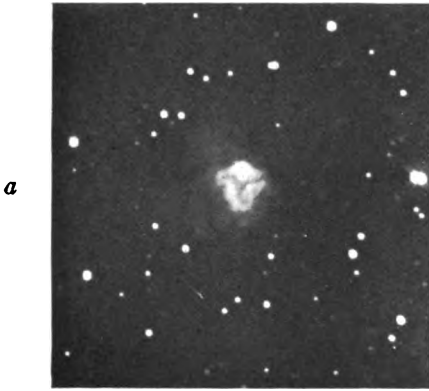
*c*



- a.* N.G.C. 5278-79, Exposure, 160<sup>m</sup> S 30, Enlargement, 3.5, 1 mm = 7".8  
*b.* N.G.C. 5257, 5258, Exposure, 50 S 30, Enlargement, 3.5, 1 mm = 7.8  
*c.* I.C. II 5146, Exposure, 300 S 23, Enlargement, 1.9, 1 mm = 14.4



# PLATE XX



- a.* I.C. I 1470, Exposure, 190<sup>m</sup> S 23, Enlargement, 5.5, 1 mm = 5.0  
*b.* N.G.C. 5544, 5545, Exposure, 360 S 27, Enlargement, 5.5, 1 mm = 5.0  
*c.* N.G.C. 6888, Exposure, 300 S 30, Enlargement, 2.4, 1 mm = 11.2





<i>i</i> ,	0	8.0	F	Patch 10" diameter.
<i>j</i> ,	13	6.4	MF	Patch 10" gbM.
<i>k</i> ,	18	10.7	MF	Spindle 30"×6", <i>p</i> 19°, gbM.

**N.G.C. 955,\* Cetus**

$$\alpha = 2^{\text{h}}26^{\text{m}}29^{\text{s}}, \quad \delta = -1^{\circ}27'8'' (1920); \quad \lambda = 138^{\circ}, \quad \beta = -54^{\circ}$$

Plate No. 319, 1917, December 17, 30<sup>m</sup>; 18, 65<sup>m</sup>. Total 95<sup>m</sup>. Images large

A so-called variable nebula, but thought by Dreyer to be unchanging. This plate was made for comparison with No. 229. It is stronger than the 1913 plate; the general dimensions are increased to 113"×10", but there is no change of relative intensity in the different parts of the nebula. Many small nebulae are shown on both plates; 15 of the more important ones are as follows, the measures referring to the nucleus of N.G.C. 955:

<i>a</i> , <i>p</i>	249°, <i>d</i>	16'3	Nebulous spot.	
<i>b</i> ,	346	15.1	F, uniform, 8" diameter.	
<i>c</i> ,	214	4.9	F, spindle, 20"×4", <i>p</i> 32°, BM.	
<i>d</i> ,	31	8.2	F, sliver, 10"×2", <i>p</i> 15°.	
<i>e</i> ,	35	6.9	MF, spindle, 12"×3", <i>p</i> 115°, gbM.	
<i>f</i> ,	162	13.6	MF, spindle, 20"×6", <i>p</i> 44°, gbM, Nu.	
<i>g</i> ,	156	16.0	MF, spindle, 5" diameter, gbM, Nu.	
<i>h</i> ,	59	7.9	F, sliver, uniform, 15"×3", <i>p</i> 30°.	
<i>i</i> ,	88	8.5	MF, uniform 12" diameter, with Nu. 2" diameter elongated 143°.	
<i>j</i> ,	146	14.3	F, uniform, 6" diameter.	
<i>k</i> ,	146	20.0	MF, 8" diameter, gbM.	
<i>l</i> ,	84	16.5	MF, spindle, 10"×4", <i>p</i> 63°, gbM, Nu.	
<i>m</i> ,	61	20.5	MB, spindle, 13"×6", <i>p</i> 40°, gbM, Nu. (edge of plate).	
<i>n</i> ,	94	17.8	F, 8" diameter gbM (edge of plate).	
<i>o</i> ,	98	19.2	MF, 10" diameter gbM (edge of plate).	

**N.G.C. 1186,\* Perseus**

$$\alpha = 3^{\text{h}}0^{\text{m}}16^{\text{s}}, \quad \delta = +42^{\circ}30'9'' (1920); \quad \lambda = 115^{\circ}, \quad \beta = -13^{\circ}$$

Plate No. 310, 1917, November 16, 220<sup>m</sup>. S 27.

Images large. Illustrated Plate XVd

This photograph was made for comparison with No. 245, taken in 1914. This supposedly variable nebula has undergone no relative change since 1914. The longer exposure brings out, however, the spiral structure more clearly and shows the nebulosity extending to 2'5×0'8. The arrangement of the arm is not regular.

Many small nebulae are on the plate, among them the following. The measures refer to the nucleus of N.G.C. 1186, and not to the star.

<i>a</i> , <i>p</i>	233°	<i>d</i> 18.8	MF, 9" diameter, nebulous spot, fades at edges.
<i>b</i> ,	326	19.9	MF, 8" diameter, nebulous spot, fades at edges.
<i>c</i> ,	229	13.7	MF, 10" diameter, nebulous spot, gbM.
<i>d</i> ,	229	12.2	MF, 6" diameter, nebulous spot, gbM.
<i>e</i> ,	312	11.1	F, 7"×2", <i>p</i> 135°, nebulous patch.
<i>f</i> ,	262	8.0	MF, 7"×2", <i>p</i> 50°, nebulous spot.
<i>g</i> ,	331	15.8	MF, 5" diameter, nebulous spot, gbM.
<i>h</i> ,	346	12.5	F, 4" diameter, nebulous spot, gbM.
<i>i</i> ,	349	13.3	F, 4" diameter, nebulous spot, gbM.
<i>j</i> ,	190	10.6	MF, 5" diameter, nebulous spot, gbM.
<i>k</i> ,	350	7.3	F, 5" diameter, nebulous spot, gbM.
<i>l</i> ,	353	11.2	MF, 11" diameter, nebulous spot, gbM.
<i>m</i> ,	357	9.5	MF, 3" diameter, nebulous spot, gbM.
<i>n</i> ,	178	5.3	MB, 35"×6", <i>p</i> 65°, spindle, stellar Nu.
<i>o</i> ,	87	1.8	F, 10"×2", <i>p</i> 23°, thread.
<i>p</i> ,	55	2.5	MF, 10"×8", <i>p</i> 9°, nebulous spot, gbM.
<i>q</i> ,	141	7.6	MB, 8" diameter, almost a nebulous star.
<i>r</i> ,	73	7.0	F, 5" diameter, nebulous spot, gbM.
<i>s</i> ,	90	13.6	B, 9" diameter, nebulous star.
<i>t</i> ,	55	17.4	MB, 7" diameter, nebulous spot.

#### N.G.C. 1491, Perseus

$\alpha = 3^{\text{h}}57^{\text{m}}21^{\text{s}}$ ,  $\delta = +51^{\circ}5'6''$  (1920);  $\lambda = 118^{\circ}$ ,  $\beta = -1^{\circ}$

Plate No. 308, 1917, October 20, 45<sup>m</sup>. Cramer Crown.

Images small and round

Plate No. 355, 1919, December 22, 160<sup>m</sup>. S 23. Images small and round. Illustrated Plate XVc

A tuft of wispy nebulosity, roughly triangular in shape, about 3' on a side. The effect is produced by three principal V-shaped streamers or filaments, included angle 80°–90°, pointing *p* 225°. They are displaced with respect to one another and thus cross. A star of magnitude 10–11 lies in the fainter nebulosity filling the V.

#### N.G.C. 1555, Taurus

$\alpha = 4^{\text{h}}17^{\text{m}}17^{\text{s}}$ ,  $\delta = +19^{\circ}20'1''$  (1920);  $\lambda = 144^{\circ}$ ,  $\beta = -20^{\circ}$

Plate No. 312, 1917, November 17, 195<sup>m</sup>. S 27. Images small and elongated

Plate No. 322, 1918, February 11, 110<sup>m</sup>; 12, 100<sup>m</sup>; 13, 110<sup>m</sup>. Total 320<sup>m</sup>. S 27.

Images medium and round

Plate No. 326, 1919, March 1, 90<sup>m</sup>. S 30. Images small and round

For previous descriptions and chart see *Mount Wilson Contribution*, No. 127; *Astrophysical Journal*, 45, 89, 1917. All three plates show nebulosity *A* remaining about the same, nebulosity *C* extending farther to the W and N. Traces of *G* show as before, while dark regions not sketched show S and E of *K* and *H*.

### N.G.C. 1699, 1700, Eridanus

N.G.C. 1699,  $\alpha = 4^{\text{h}}53^{\text{m}}3^{\text{s}}$ ,  $\delta = -4^{\circ}52'8''$  } (1920);  $\lambda = 172^{\circ}$ ,  $\beta = -26^{\circ}$   
 N.G.C. 1700,  $\alpha = 4^{\text{h}}53^{\text{m}}0^{\text{s}}$ ,  $\delta = -4^{\circ}59'3''$  }

Plate No. 314, 1917, November 18, 120<sup>m</sup>. S 27. Large images, fairly round  
 Plate No. 3 (Hoge), 1919, December 24, 110<sup>m</sup>. S 30. Small round images

N.G.C. 1700 has a very bright center fading away in several gradual steps and forming an ellipse  $50'' \times 30''$ ,  $p\ 92^{\circ}$ . The entire mass is soft, having no detail or structure other than the changes in intensity between center and edge. A 23-hour exposure made with the focal-plane spectrograph on the 60-inch reflector gave a spectrum of sufficient strength to show that the type is Go or later, and that the nebula has large positive radial velocity.

There are two other nebulae on the plate whose positions are given with respect to the nucleus of N.G.C. 1700.

- a*, N.G.C. 1699,  $p\ 6^{\circ}$ ,  $d\ 6'.6$ , MB,  $30'' \times 17''$ ,  $p\ 161^{\circ}$ . Almost uniform left-handed spiral, vs B Nu. Position given in N.G.C. is incorrect.  
*b*, 129, 13.6 MF,  $15'' \times 10''$ ,  $p\ 9^{\circ}$  lbM, vs B Nu.

### N.G.C. 2024, Auriga

$\alpha = 5^{\text{h}}37^{\text{m}}49^{\text{s}}$ ,  $\delta = +51^{\circ}5'6''$  (1920);  $\lambda = 174^{\circ}$ ,  $\beta = -15^{\circ}$

Plate No. 316, 1917, November 19, 30<sup>m</sup>. Cramer Crown.

Images large and round

Comparison of this plate with Keeler's photograph, taken June 28, 1902, shows no apparent change in the nebula (*Lick Observatory Publications*, 8, Plate 13).

### N.G.C. 2146, Camelopard

$\alpha = 6^{\text{h}}5^{\text{m}}53^{\text{s}}$ ,  $\delta = +78^{\circ}23'$  (1920);  $\lambda = 102^{\circ}$ ,  $\beta = +25^{\circ}$

Plate No. 358, 1919, December 23, 258<sup>m</sup>. S 23. Images medium and a little elongated. Illustrated Plate XVf

A most remarkable nebula, best described in parts, although actually all blended together. (1) An irregular mass of nebulosity  $3'.5 \times 1'$ ,  $p\ 150^{\circ}$  greatly differing in intensity, with dark

markings in the direction of its elongation. The nucleus lies a little S of the center of this mass; the nebulosity is brightest around the nucleus. Superimposed on this bright mass is a dark marking in the form of a hand, with four talon-like fingers stretching Sp and with three stars standing out upon it. (2) A lobe in the form of an elongated ellipse  $3'.3 \times 1'$ ,  $p \ 125^\circ$ , with greatest density along the periphery. This extends about  $1'.4$  beyond the S end of (1) and its axis produced would intersect (1) at its N end. The interior is filled with soft nebulosity, has a line of bright knots toward its N end, and some tufts projecting over its f side. (3) A spiral arm leaving the Np point of (1) and sweeping to the S in such a way as to give the effect of a left-handed spiral. It ends  $p \ 200^\circ$ ,  $d \ 2'$ , with respect to the nucleus.

One might describe the system as a spiral with abnormal center, attached to a single arm or to double arms in the latter case, the lobe forming one of the arms. In the former case a single arm emerges from the S corner of (1), sweeping around the f side and under the N end of (1), and emerging on the p side as (3). In either case the major axis of the arm or arms would be  $5'.2$  long and lie in  $p \ 120^\circ$ . At the extremities there is the effect of a turn in the arm, but there is no increase in density where the single arm and element (1) are superimposed.

A medium-bright right-handed spiral,  $8' \times 2'$ ,  $p \ 30^\circ$  lies  $p \ 54^\circ$ ,  $d \ 19'$  with respect to nucleus of N.G.C. 2146. The plate shows many small nebulae.

#### N.G.C. 2245, Monoceros

$\alpha = 6^h 28^m 17^s$ ,  $\delta = +10^\circ 13' 2''$  (1920);  $\lambda = 169^\circ$ ,  $\beta = +2^\circ$

Plate No. 323, 1918, February 14, 60<sup>m</sup>. S 27. Poor seeing.

Large round images

Plate No. 329, 1919, March 28, 95<sup>m</sup>. S 30. Excellent seeing.

Small round images. Illustrated Plate XVIa

A fan-shaped nebula fading away irregularly from an almost stellar point toward the circumference, beyond which extends, torch fashion, nebulosity similar to that of the Orion nebula. A few seconds from its apex and almost at right angles to its axis is a line of nebulosity  $30''$ – $40''$  long. Alongside this line, away

from the nebula, is a fan-shaped dark area, appearing to be a shadow cast by an opaque portion of the line, the light source being the fan itself. Evidently the whole region is nebulous, as detail can be seen in the shadow, particularly a looped thread formation. The two photographs appear to show a striking difference about the head, but this may be due to the differences in the plates. The 1918 plate shows a round stellar nucleus standing out from the nebulosity, while the 1919 plate shows an almost solid mass completely covering the nucleus. Further observations will be made.

**N.G.C. 2247, Monoceros**

$\alpha = 6^h 28^m 45^s$ ,  $\delta = +10^\circ 22' 8''$  (1920);  $\lambda = 169^\circ$ ,  $\beta = +2^\circ$

Plate No. 323, 1918, February 14, 60<sup>m</sup>. S 27. Poor seeing.

Large round images

Plate No. 329, 1919, March 28, 95<sup>m</sup>. S 30. Excellent seeing. Small round images. Illustrated Plate XVIa

This nebula lies 9'.9 N of and 5'.7 f N.G.C. 2245 involving centrally the star B.D. +10° 1172. It surrounds the star irregularly, streamers radiating 2' to 3' from the center. In addition to the streamers there is a small patch 1' N and a line about 1' S. Both N.G.C. 2245 and N.G.C. 2247 lie in a dark lane. While Hubble's variable N.G.C. 2261 is related to a variable star, neither of these stars has been mentioned as variable.

The position given in the N.G.C. is not correct. Swift's original description is so exactly like that surrounding B.D. +10° 1172 that there is no question of this being the object. The position given is that of the B.D. star.

**N.G.C. 2274, 2275, Gemini**

N.G.C. 2274,  $\alpha = 6^h 42^m 2^s$ ,  $\delta = +33^\circ 39' 0''$   
N.G.C. 2275,  $\alpha = 6^h 42^m 3^s$ ,  $\delta = +33^\circ 41' 0''$  } (1920);  $\lambda = 149^\circ$ ,  $\beta = +15^\circ$

Plate No. 313, 1917, November 17, 20<sup>m</sup>. Cramer Crown. Poor seeing.

Images medium and elongated

Plates Nos. 100-137, 1919, December 19, 30<sup>m</sup>. S 23. Images small and comate

N.G.C. 2274. Nebulosity 7" diameter, gradually brighter toward the middle, with bright almost stellar nucleus. There is trace of a wing Np.

N.G.C. 2275. Nebulosity 10'' diameter, gradually brighter toward the middle, with bright stellar nucleus. There are traces of surrounding nebulosity 30'' in diameter.

**N.G.C. 2288, 2289, 2290, 2291, and 2294, Gemini**

N.G.C. 2288,	$a = 6^h 45^m 28^s$ ,	$\delta = +33^\circ 29' 1''$	} (1920); $\lambda = 149^\circ$ , $\beta = +15^\circ$
N.C.C. 2289,	$a = 6\ 45\ 29$ ,	$\delta = +33\ 30\ 9$	
N.G.C. 2290,	$a = 6\ 45\ 33$ ,	$\delta = +33\ 27\ 7$	
N.G.C. 2291,	$a = 6\ 45\ 35$ ,	$\delta = +33\ 33\ 0$	
N.G.C. 2294,	$a = 6\ 45\ 47$ ,	$\delta = +33\ 33\ 2$	

Plate No. 311, 1917, November 16, 90<sup>m</sup>. Cramer Crown. Good plate.  
Small images

Plate No. 315, 1917, November 18, 70<sup>m</sup>; 19, 140<sup>m</sup>. Total 210<sup>m</sup>. S 27. Poor seeing. Large images. Illustrated Plate XVa

This group is mentioned by Lord Rosse in his *Observations* and is shown by the photographs to be composed of spirals with a background of ill-defined nebulae of similar character.

The following is a brief description of all the nebulae on the plates. The positions are referred to the nucleus of N.G.C. 2290.

N.G.C. 2288,  $p\ 325^\circ$ ,  $d\ 1'8$ , MB nebulosity, 7'' diameter. B Nu. almost stellar.

N.G.C. 2289,  $p\ 343$ ,  $d\ 2'6$ ,  $15'' \times 10''$ ,  $p\ 100^\circ$ . gbM, B almost stellar Nu.

N.G.C. 2290, MF ring 5'' to 15'' wide, broken in places, outside diameter  $1'10 \times 0'54$  and mean diameter  $0'9 \times 0'45$ . B stellar Nu. in MB nebulosity 10'' diameter connecting with outer ring. Almost certainly a left-handed spiral.

N.G.C. 2291,  $p\ 3^\circ$ ,  $d\ 5'3$ , B almost stellar Nu. in F, R, nebulosity 35'' diameter showing traces of rings, almost certainly spiral.

N.G.C. 2294,  $p\ 28^\circ$ ,  $d\ 6'2$ , B almost uniform spindle  $27'' \times 9''$ ,  $p\ 7'5$ . Surrounded by faint nebulosity  $40'' \times 10''$  and having a vs B diffuse elongated Nu.

$a$ ,  $p\ 263^\circ$ ,  $d\ 16'2$  F Patch, 8'' diameter.

$b$ , 285 11.9 F 3'' diameter, gbM, Nu.

$c$ , 220 11.7 MB 10'' diameter, gbM, Nu.

$d$ , 349 11.0 Semicircular, 10'' radius, MB on curve, fades back of Nu. From vertex to central Nu. is a bright line 2'' wide,  $p\ 137^\circ$ .

$e$ , 96 5.2 F Sliver,  $10'' \times 5''$ ,  $p\ 130^\circ$ .

$f$ , 95 5.4 F Spot, 3'' diameter.

$g$ , 108 6.0 F Diffuse spot, 8'' diameter.

<i>h</i> ,	130	8.7	F	20''×5'', <i>p</i> 116'', MB Nu. near <i>f</i> end.
<i>i</i> ,	146	12.9	MB	Nebulous star.
<i>j</i> ,	96	7.5	F	15''×10'', <i>p</i> 85° elongated diffuse spot.
<i>k</i> ,	127	9.4		15''×8'', <i>p</i> 32° gbM Nu., looks S-shaped.
<i>l</i> ,	67	13.5	F	Diffuse patch, 15'' diameter.

**N.G.C. 2359, Canis Major**

$$\alpha = 7^{\text{h}}13^{\text{m}}50^{\text{s}}, \delta = -13^{\circ}4'1'' (1920); \lambda = 197^{\circ}, \beta = 0^{\circ}$$

Plate No. 320, 1917, December 17, 60<sup>m</sup>; 18, 150<sup>m</sup>. Total 210<sup>m</sup>. S 23.

Images large and round. Illustrated Plate XVIb

The brighter parts of the nebula agree closely with the drawings by the earlier observers. Sir John Herschel pictured it as resembling a bust, while Lassell drew it as like a balloon, with a long neck twisted in the *Sp* direction. The balloon or head is approximately 5' in diameter; the neck is to the S, with nebulosity about 1' wide extending 8' *p*, concave on the N and gradually narrowing and fading out. From the top (N) of the head a symmetrical streamer concave to S extends in *p* direction. The radius of curvature of the two streamers is roughly 15' and their ends are about 8' apart. A second streamer about 1' wide extends *f* from the top of the head to a distance of 9'.

**N.G.C. 2403,\* Camelopard**

$$\alpha = 7^{\text{h}}29^{\text{m}}7^{\text{s}}, \delta = +65^{\circ}46'5'' (1920); \lambda = 118^{\circ}, \beta = +30^{\circ}$$

Plate No. 307, 1917, October 19, 100<sup>m</sup>. Cramer Crown.

Images small and round

The illustration of N.G.C. 2403 (*Mount Wilson Contribution*, No. 132, Plate Xc; *Astrophysical Journal*, 46, 35, 1917, Plate V) was made from Plate No. 307, and not from No. 169 as there stated.

The nebulous spot *p* 50°, *d* 3'.4, with respect to the center of the nebula is probably a flaw, as there is a difference in character between it and the rest of the nebulosity on the plate.

**N.G.C. 2537, Lynx**

$$\alpha = 8^{\text{h}}7^{\text{m}}35^{\text{s}}, \delta = +46^{\circ}14' (1920); \lambda = 141^{\circ}, \beta = +33^{\circ}$$

Plate No. 2968 (Shapley), 1916, March 27, 30<sup>m</sup>. S 27

Plate No. 359, 1919, December 23, 60<sup>m</sup>. S 30. Images small and elongated

Nebulosity of the form of a horseshoe or a semi-elliptical line, major axis N-S, concave to the S, together with a line of



nebulosity  $30''$  long lying in the center of the ellipse on the major axis. Two faint lines of nebulosity extend from the N end of this line to the outer nebulosity, the included angle being about  $150^\circ$ . The axes of the complete ellipse would measure  $75'' \times 45''$ . The nebulosity is of the mixed type, there being a number of well-defined knots in it.

I.C.II 2233 falls near the edge of the plates and appears to be a faint edge-on spiral  $4' \times 10''$ ,  $p\ 170^\circ \pm$ , with faint stellar nucleus. A faint patch  $20''$  diameter lies  $4.6 f$  N.G.C. 2357.

#### N.G.C. 2964, Leo Minor

$$\alpha = 9^h 38^m 11^s, \delta = +32^\circ 12.8' (1920); \lambda = 162^\circ, \beta = +50^\circ$$

Plate No. 321, 1917, December 18, 60<sup>m</sup>. Cramer Crown. Images small and round

Plate No. 324, 1919, February 28, 210<sup>m</sup>. S 30. Images small and round

A right-handed spiral, with bright inner arms extending to  $75'' \times 45''$ ,  $p\ 90^\circ$ , and exterior arms to  $2.5 \times 1.2$ . The inner arms are dotted with bright condensations, the outer are faint and soft. Several peculiar details suggest a drift of the component parts relative to each other; among these may be noted the winged knots on the  $p$  side, the disjunction of the nucleus and the  $f$  arm, and a left-handed wisp crossing the  $p$  arm N of the nucleus.

#### N.G.C. 2968, Leo Minor

$$\alpha = 9^h 38^m 28^s, \delta = +32^\circ 17.7' (1920); \lambda = 162^\circ, \beta = +50^\circ$$

Plate No. 321, 1917, December 18, 60<sup>m</sup>. Cramer Crown. Images small and round

Plate No. 324, 1919, February 28, 210<sup>m</sup>. S 30. Images small and round

Probably an edge-on spiral, since it shows an irregular ellipse of nebulosity  $1.2 \times 7'$ ,  $p\ 31^\circ$ , gradually increasing in brightness toward the central nucleus  $2''$  diameter, and has an absorption streak running irregularly along the major axis.

The plate shows many small nebulae; measures were made of 15 with the nucleus of N.G.C. 2968 as a center.

- a,  $p\ 305^\circ$ ,  $d\ 13.4$  MB, uniform ellipse,  $7'' \times 3''$ ,  $p\ 142^\circ$ .  
 b, 247 11.3 MB, uniform ellipse,  $8'' \times 4''$ ,  $p\ 140^\circ$ , sbM.  
 c, 282 10.0 MF, uniform,  $3''$  diameter.

<i>d</i> ,	196	9.2	F,	spindle, 20"×6", <i>p</i> 129°, F Nu.
<i>e</i> ,	329	2.7	MF,	uniform patch, 9"×4", <i>p</i> 48°.
<i>f</i> ,	242	0.8	MB,	10"×2", <i>p</i> 179°, gbM.
<i>g</i> ,	4	14.1	MB,	10" diameter, gbM.
<i>h</i> ,	166	6.5	MB,	10" diameter, <i>f</i> side stronger.
<i>i</i> ,	168	13.6	MB,	gbM, 11"×8", <i>p</i> 60°.
<i>j</i> ,	154	7.7	F,	uniform, 12"×3", <i>p</i> 132°.
<i>k</i> ,	61	4.9	MB,	sbM, 12"×6", <i>p</i> 75°.
<i>l</i> ,	19	13.0	MF,	spindle, gbM, 10"×4", <i>p</i> 23°.
<i>m</i> ,	124	13.7	MF,	nebulous star, 4" diameter.
<i>n</i> ,	56	14.0	F,	uniform, lbM, 10"×3", <i>p</i> 23°.
<i>o</i> ,	47	15.9	MF,	gbM, Nu, 10"×3", <i>p</i> 29°.

**N.G.C. 2970, Leo Minor**

$\alpha=9^{\text{h}}38^{\text{m}}48^{\text{s}}$ ,  $\delta=+32^{\circ}20'7''$  (1920);  $\lambda=162^{\circ}$ ,  $\beta=+50^{\circ}$

Plate No. 321, 1917, December 18, 60<sup>m</sup>. Cramer Crown. Images small and elongated

Plate No. 324, 1919, February 28, 210<sup>m</sup>. S 30. Images small and round

Bright nebulosity gradually fading away, 15"×10", *p* 80°, with a bright stellar nucleus about 5" diameter centrally located.

**N.G.C. 3310, Ursa Major**

$\alpha=10^{\text{h}}33^{\text{m}}48^{\text{s}}$ ,  $\delta=+53^{\circ}55'1''$  (1920);  $\lambda=124^{\circ}$ ,  $\beta=+55^{\circ}$

Plate No. 356, 1919, December 22, 12<sup>m</sup> and 90<sup>m</sup>. Exp. on same plate. S 30. Images small and round

A left-handed spiral, 90"×50", *p* 170°. The short exposure shows a bright nucleus surrounded by a bright elliptical ring, 22"×15", *p* 140°, from which springs an arm of much smaller density in *p* 130°, bending to the north and running for a length of about 25". A faint star with faint surrounding nebulosity lies just adjoining the ring at *p* 230°, *d* 14", from the center. The long exposure shows a mass 30"×25", *p* 130°, with the arm emerging as above and ending at *p* 20°, *d* 25". The nucleus, ring, and two stars show plainly. There are traces of other arms lying around the bright mass, particularly one emerging opposite the strong arm running southward and ending at *p* 165°, *d* 30". The ring is strongest in its N and S sections.

**N.G.C. 3367, Leo Major**

$\alpha = 10^h 42^m 21^s$ ,  $\delta = +14^\circ 10' 2''$  (1920);  $\lambda = 200^\circ$ ,  $\beta = +59^\circ$

Plate No. 289, 1917, April 22, 70<sup>m</sup>. S 23. Images small and comate

Plate No. 327, 1919, March 1, 150<sup>m</sup>. S 30. Small round images.

Illustrated Plate XV<sub>e</sub>

A left-handed spiral about 1'.8 diameter, almost circular, with a bright sharp stellar nucleus. The periphery is well defined on the *p* side but lacking on the *f*. It is similar in type to N.G.C. 5921<sup>1</sup> in that an almost straight bar crosses the center *p* 70°, from the ends of which emerge arms almost at right angles to the bar, a single arm at one end, a double one at the other. The bar is slightly concave on the N side and its *f* end continues in a series of condensations across the arm to the periphery. The arm emerges from the bar 14" from the nucleus and turns to the N. The *p* end of the bar spreads into soft nebulosity and just touches the arm from the *f* end; the arm on the *p* end leaves at about 16" from the nucleus, turns to the south, and at about 10" spreads into two parallel arms with nebulosity between them, which run parallel for about 90°; the outer one then fades away into the rim, while the inner one continues and is merged in the *p* rim. There are a number of branching and crossing threads, and a bright knot *p* 267°, *d* 47", from the nucleus lying in the periphery. The greatest extent of the nebulosity is 60", *p* 40°. The double arm brightens at a point just *f* the nucleus. The plate shows a number of nebulous spots, the more prominent of which are as follows, the measures referring to the nucleus of 3367.

<i>a</i> ,	<i>p</i> 269°, <i>d</i> 14'.4	5" diameter, uniform.
<i>b</i> ,	193    11.0	3" diameter, gbM, B, stellar Nu.
<i>c</i> ,	151    4.9	3" diameter, stellar Nu.
<i>d</i> ,	149    13.0	11"×5", <i>p</i> 126°, gbM.
<i>e</i> ,	150    15.0	10"×4", <i>p</i> 145°, lbM.
<i>f</i> ,	25    18.1	5" diameter, gbM.
<i>g</i> ,	34    14.3	5" diameter, lbM.
<i>h</i> ,	45    17.7	4" diameter, lbM.
<i>i</i> ,	57    15.3	5" diameter, gbM.
N.G.C. 3377	49    21.8	

<sup>1</sup> *Publications of the Astronomical Society of the Pacific*, 24, 227, 1912.

- N.G.C. 3371      Should lie about one-third the distance from  
3367 to 3377, but there is nothing on the plate.
- N.G.C. 3373      Should lie in the region *f* 3367 and a little S,  
but there is nothing on the plate.

**N.G.C. 3377, Leo Major**

$$\alpha = 10^h 43^m 28^s, \quad \delta = 14^\circ 24' 4'' (1920); \quad \lambda = 201^\circ, \quad \beta = +60^\circ$$

Plate No. 289, 1917, April 22, 70<sup>m</sup>. S 23. Small astigmatic images

Plate 327, 1919, March 1, 150<sup>m</sup>. S 30. Small comate images

A diffuse ellipse  $90'' \times 30''$ ,  $p$   $40^\circ$ , gradually increasing in brightness toward the center, where there is a great increase in brightness in an elongated nucleus  $20'' \times 13''$ . A number of faint nebulae not listed under N.G.C. 3367 appear in the field. The measures refer to the nucleus of N.G.C. 3377.

- |             |     |                   |      |   |
|-------------|-----|-------------------|------|---|
| <i>a</i> ,  | $p$ | $315^\circ$ , $d$ | 9.1  | Very faint, 1' diameter.  |
| <i>b</i> ,  |     | 60                | 8.2  | MF, uniform, 10'' diameter.   |
| <i>c</i> ,  |     | 110               | 12.9 | MF, uniform, $12'' \times 4''$ , $p$ $129^\circ$ .  |
| <i>d</i> ,  |     | 64                | 19.4 | MF, lbM, 8'' diameter.  |
| N.G.C. 3391 | 52  | 22.9              |      | ( $10^h 44^m 45^s$ , $+14^\circ 38' 6''$ ) (1920); appears on the corner of plate 289. The image is bright, $20'' \times 11''$ , $p$ $26^\circ$ , and suggestive of spiral formation, but the image is too comate to say for certain. |

**N.G.C. 3379, Leo Major**

$$\alpha = 10^h 43^m 37^s, \quad \delta = +13^\circ 0' 2'' (1920); \quad \lambda = 203^\circ, \quad \beta = +59^\circ$$

Plate No. 290, 1917, April 23, 75<sup>m</sup>. S 23. Small, slightly elongated image

Plate No. 334, 1919, March 30, 120<sup>m</sup>. S 23. Small, slightly elongated image.

Illustrated Plate XVIIa

A nebula which long since attracted attention, owing to its resemblance to an unresolved star cluster. It has a very bright nucleus  $10''$ – $12''$  diameter, surrounded by a bright atmosphere,  $30''$  diameter, which gradually fades away at  $90''$  diameter. The nebula differs from many others, such as N.G.C. 4374 (M 84) and N.G.C. 4402, in having a planet-like nucleus, whereas usually the nebulosity gradually increases toward the center, with a possible sudden increase in brightness to form a semi-diffuse nucleus. A spectrogram<sup>1</sup> made with the focal-plane spectrograph at the

<sup>1</sup> *Publications of the Astronomical Society of the Pacific*, 30, 255, 1918.

Newtonian focus of the 60-inch reflector shows the nucleus to be G5 or later, and to have a radial velocity of about +850 km/sec. Slipher obtained a value of 780 km/sec. Faint traces of the outer nebulosity show a maximum of continuous spectrum corresponding to the nucleus.

#### N.G.C. 3384, Leo Major

$$\alpha = 10^{\text{h}}44^{\text{m}}4^{\text{s}}, \quad \delta = +13^{\circ}3'1'' (1920); \quad \lambda = 203^{\circ}, \quad \beta = +59^{\circ}$$

Plate 290, 1917, April 23, 75<sup>m</sup>. S 23. Small, slightly comate images

Plate 334, 1919, March 30, 120<sup>m</sup>. S 23. Small, lightly comate images.

Illustrated plate XVIIa

An astonishing nebula consisting of a bright center 40'' diameter, on which are superimposed a very bright elongated nucleus 19'' $\times$ 10'',  $p$  45°, crossed by a second bright nucleus 40'' $\times$ 5'',  $p$  130°, presenting a Saturn-like appearance. Finally, from this mass wings or branches extend in  $p$  53° on either side, to a distance of 1'.5 The wings gradually broaden to a width of 1' at 1' from the center, where they are rounded off.

The three nebulae, N.G.C. 3379, 3384, 3389, appearing on the same plate present very different features. N.G.C. 3389 is a well-defined spiral, N.G.C. 3384 presents spiral and planetary characteristics, while N.G.C. 3379 leads one to believe it a very distant, unresolved cluster or group of spirals.

#### N.G.C. 3389, Leo Major

$$\alpha = 10^{\text{h}}44^{\text{m}}14^{\text{s}}, \quad \delta = +12^{\circ}57'0'' (1920); \quad \lambda = 204, \quad \beta = +60^{\circ}.$$

Plate No. 290, 1917, April 23, 75<sup>m</sup>. S 23. Small slightly comate images

Plate No. 334, 1919, March 30, 120<sup>m</sup>. S 23. Small slightly elongated images. Illustrated Plate XVIIa

A medium-bright right-handed spiral 110'' $\times$ 52'',  $p$  107°, having a very small stellar nucleus. The arms are fairly dense, with condensations along them, but are not strictly regular in form.

#### N.G.C. 3395-3396, Leo Minor

$$\left. \begin{array}{l} \text{N.G.C. 3395, } \alpha = 10^{\text{h}}45^{\text{m}}23^{\text{s}}, \quad \delta = +33^{\circ}24'4'' \\ \text{N.G.C. 3396, } \alpha = 10^{\text{h}}45^{\text{m}}28^{\text{s}}, \quad \delta = +33^{\circ}24'9'' \end{array} \right\} (1920); \quad \lambda = 160^{\circ}, \quad \beta = +64^{\circ}$$

Plate No. 286, 1917, March 26, 120<sup>m</sup>. S 23. Small round images.

Illustrated Plate XVIIIa

Plate No. 332, 1919, March 29, 110<sup>m</sup>. S 30. Small round images

N.G.C. 3395 is a right-handed spiral with its major axis in  $p\ 32^\circ$ . Its *Sp* portion is well defined and extends about  $52''$  along the major axis from the nucleus. The *Nf* portion is markedly deficient in size and in density of material. N.G.C. 3396 lies  $p\ 66^\circ$ ,  $d\ 73''$  *Nf* with respect to the nucleus of 3395. It is composed of a bright elongated nucleus  $10'' \times 5''$ ,  $p\ 97^\circ$ , with which is blended a knot about  $3''$  diameter  $9''$  *f* and a short line diagonally opposite. Surrounding this is a mass whose general axis is in  $p\ 94^\circ$  and which extends  $42''$  *f* the nucleus. Between the two nebulae is evidence of a great disturbance, since material which would ordinarily belong to the *Nf* arm of 3395 is absent, while stream lines indicate its presence about 3396. It remains to be ascertained whether the formation is the result of two separate centers or whether 3395 has separated from 3396, or, finally, whether 3396 has wrenched material away from 3395. The stream line of 3395 suggests a right-hand twist. There is more than enough material in 3396 to make up for that lost in the arm of 3395; in fact, it is just about equal to the complete arm of 3395.

There are many small nebulae on the plates, the more prominent of which are the following, the measures referring to the nucleus of N.G.C. 3395:

I.C.II 2603			Not on plates.
a,	$p\ 278^\circ, d\ 15.9$	$10'' \times 4'', p\ 56^\circ$	bM.
Big. 270			Not on plates.
b,	280	11.1	MF, $5''$ diameter, bM.
c,	210	15.2	MF, $10'' \times 5'', p\ 99^\circ$ , lbM.
I.C.II 2604	203	13.8	MB, Irr. R, $50''$ diameter, RH spiral.
d,	339	11.9	MF, $6''$ diameter, lbM.
e,	330	4.3	MF, $6''$ diameter, lbM.
f,	342	5.4	MB, $2''$ diameter, stellar.
I.C.II 2605 } Big. 402 }			Part of arm of N.G.C. 3395.
I.C.II 2608	157	14.1	MB, $45'' \times 6'', p\ 118^\circ$ , B Nu., spindle.
g,	40	13.0	MB, $10''$ diameter, lbM.
h,	98	9.2	MF, $3''$ diameter, lbM.
i,	46	17.4	MF, $4''$ diameter, lbM.
j,	80	12.7	F, $9'' \times 5'', p\ 116^\circ$ , lbM.
k,	124	23.2	MB, $60'' \times 10'', p\ 170^\circ$ , B Nu., spindle.

## N.G.C. 3786, 3788, Ursa Major

N.G.C. 3786,  $\alpha = 11^h 35^m 29^s$ ,  $\delta = +32^\circ 21' 3''$  }  
 N.G.C. 3788,  $\alpha = 11^h 35^m 32^s$ ,  $\delta = +32^\circ 22' 8''$  } (1920);  $\lambda = 159^\circ$ ,  $\beta = +75^\circ$

Plate No. 337, 1919, April 29, 30<sup>m</sup>. S 23. Images small  
and slightly elongated

Plate No. 338, 1919, April 29, 135<sup>m</sup>. S 27. Images large  
and fairly round. Illustrated Plate XVb

N.G.C. 3786 is a right-handed spiral with a bright nucleus, a fairly bright central part  $60'' \times 30''$ ,  $p$   $67^\circ$ , and a faint interrupted ring, not strictly elliptical,  $2' \times 1'$ ,  $p$   $75^\circ$ , which is probably an extended arm. The central part is weaker on the N side, which shows an irregular dark marking. The outer ring just touches a faint prolongation from the S end of N.G.C. 3788.

N.G.C. 3788 is a right-handed elliptical spiral  $92'' \times 20''$ ,  $p$   $179^\circ$ , very similar to N.G.C. 5545 lying  $p$   $18^\circ$ ,  $d$   $1' 4''$  N of N.G.C. 3788. The nebulosity on and between the arms is soft, with traces of condensation near the center. The brightest spot is a knot  $p$   $40^\circ$ ,  $d$   $10''$ . The center and the N end of the major axis in the curve of the arm are bright.

N.G.C. 3791 and 3793 do not appear on the plates. Plate No. 338 is literally covered with small nebulae, some of them spindles, and many of them merely rounded masses with relatively bright ill-defined centers. Presumably these are related to the spiral family. The measures of some of them, referred to the nucleus of N.G.C. 3786, are as follows:

<i>a</i> , $p$ $314^\circ$ , $d$ $22' 4''$	MF, R, $7''$ , lbM.
<i>b</i> , $311$ $16.6$	F, $9'' \times 4''$ , $p$ $135^\circ$ .
<i>c</i> , $285$ $12.4$	F, Irr. R, $6''$ .
<i>d</i> , $273$ $11.0$	MF, R, $7''$ , lbM.
<i>e</i> , $330$ $17.4$	MF, R, $4''$ , lbM.
<i>f</i> , $325$ $14.4$	MB, R, $5''$ , BM.
<i>g</i> , $331$ $16.7$	F, Irr. R, $8''$ .
<i>h</i> , $336$ $18.5$	MB, R, $7''$ , BM.
<i>i</i> , $331$ $14.9$	F, Irr. R, $6''$ , lbM.
<i>j</i> , $322$ $11.4$	MF, R, $5''$ , bM.
<i>k</i> , $238$ $6.1$	MF, Irr. R, $9''$ , lb near end.
<i>l</i> , $226$ $4.8$	MF, $20'' \times 4''$ , $p$ $132^\circ$ , knots at middle and ends.
<i>l'</i> , $225$ $4.7$	MB, $8'' \times 3''$ , $p$ $87^\circ$ , other F nebulosity <i>f</i> .

<i>m</i> ,	285	2.9	F, Irr. R, 6", uniform.
<i>n</i> ,	351	16.0	MF, R, 5", bM.
<i>o</i> ,	210	1.4	MB, 10"×3", $p$ 139°, BM.
<i>p</i> ,	181	10.5	MF, R, 6", lbM.
<i>q</i> ,	6	8.4	MB, R, 6", bM.
<i>r</i> ,	167	8.5	MF, R, 5", lbM.
<i>s</i> ,	10	11.4	MF, R, 4", bM.
<i>t</i> ,	70	4.6	MF, 14"×4", $p$ 3°, bM, spindle.
<i>u</i> ,	44	10.7	MF, R, 4", lbM.
<i>v</i> ,	115	8.6	F, Irr. R, 4", lbM.
<i>w</i> ,	34	15.0	MF, 10"×2", $p$ 135°, lbM.
<i>x</i> ,	115	11.4	F, In R, 6", lbM.
<i>y</i> ,	60	12.4	F, R, 2".
<i>z</i> ,	112	15.3	MF, Irr. R, 10", uniform.

#### N.G.C. 4395, 4399, 4400, 4401, Canes Venatici

N.G.C. 4395,	$\alpha = 12^h 21^m 51^s$ ,	$\delta = +33^\circ 59' 4''$	} (1920); $\lambda = 121^\circ$ , $\beta = +82^\circ$
N.G.C. 4399,	$\alpha = 12 \ 22 \ \pm$	$\delta = +34 \ 0 \pm$	
N.G.C. 4400,	$\alpha = 12 \ 22 \ \pm$	$\delta = +34 \ 0 \pm$	
N.G.C. 4401,	$\alpha = 12 \ 22 \ 1$	$\delta = +33 \ 57.5$	

Plate No. 330, 1919, March 28, 270<sup>m</sup>. S 23. Images small and elongated

Plate No. 331, 1919, March 28, 20<sup>m</sup>. S 30. Images small and round

Plate No. 333, 1919, March 29, 30, 450<sup>m</sup>. S 30. Images small and slightly elongated. Illustrated Plate XVIIb

These four nebulae, together with a large amount of fainter nebulosity, form a remarkable spiral. The configuration is approximately circular in outline, with indications of a three-armed spiral or pinwheel and a two-armed spiral with one detached arm (similar to N.G.C. 3395-3396), all of which are blended and not simply superimposed. The brightest nebulosity is not at the center of either, but lies in the *Sf* portion of the whole. Aside from these predominating features, large faint whorls are also seen which indicate that the nebula is roughly spherical in form. N.G.C. 4395 is the two-armed portion, N.G.C. 4399 the *Sf* arm of the pinwheel, and N.G.C. 4401 the brightest knot of the whole. The nebula as a whole is roughly 12'×10', elongated in  $p$  128°, with N.G.C. 4395 as center; beyond this, and in fact scattered over the plate, are many small nebulous stars or spots similar to those within the



nebula. The plates are not strong enough to show definitely the relation of the component parts, and further descriptions will be reserved for a longer exposure.

### N.G.C. 4656-4657, Canes Venatici

N.G.C. 4656,  $\alpha = 12^h 40^m 5^s$ ,  $\delta = +32^\circ 36' 2''$  } (1920);  $\lambda = 90^\circ$ ,  $\beta = +86^\circ$   
 N.G.C. 4657,  $\alpha = 12^h 40^m 14^s$ ,  $\delta = +32^\circ 39' 4''$

Plate No. 336, 1919, April 28, 20<sup>m</sup>. S 27. Images comate

Plate No. 339, 1919, April 29, 140<sup>m</sup>. S 27. Images medium and elongated

Plates Nos. 100-145, 1920, February 16, 240<sup>m</sup>. S 30. Images small and round. Illustrated Plate XVIIIb

The objects listed as N.G.C. 4656 and 4657 constitute a most interesting single right-handed spiral. It appears as though a section were scaling off from a streamer of nebulosity which extends across the plate for a distance of 20'. The nebulosity strongly resembles that of N.G.C. 4449. There is no well-defined center or nucleus, but the inner end of the stronger arm is relatively bright, and this is taken as the center in the discussion. The strong Nf arm consists of well-defined soft nebulosity dotted with about 50 condensations and having much fainter material lying on its concave side. The position angle at the center is about 26°, but the direction changes rapidly, the arm becomes concave on the f side and turns south at  $p\ 50^\circ$ ,  $d\ 3' 6''$  from the center, and after a return of 25'' stops. The width is from 20'' to 30''. The Sp arm is not as well defined and the material is distributed in several bands. It consists of a  $p$  member emerging from the center in  $p\ 220^\circ$  to a distance of 3' 4'', which then branches, one branch continuing straight on, the other curving slightly concave N for a distance of 5'. The second member starts in  $p\ 185^\circ$ , runs straight for 2', then gradually curves for about 5', ending in  $p\ 223^\circ$ . There are traces of other lines of material extending to a distance of 8'.

In addition to a number of very small nebulae on the plate there is a well-defined two-armed right-handed spiral  $p\ 260^\circ$ ,  $d\ 3' 4''$  with respect to the center of 4656-7; it is  $30'' \times 20''$ ,  $p\ 10^\circ$ .

**N.G.C. 5257, 5258, Virgo**

N.G.C. 5257,  $\alpha = 13^h 35^m 49^s$ ,  $\delta = +1^\circ 14' 7''$  }  
 N.G.C. 5258,  $\alpha = 13 \ 35 \ 53$ ,  $\delta = +1 \ 14.3$  } (1920);  $\lambda = 298^\circ$ ,  $\beta = +61^\circ$

Plate No. 345, 1919, June 27, 50<sup>m</sup>. S 30. Images small and elongated. Illustrated Plate XIX*b*

N.G.C. 5257 is a left-handed spiral with two principal arms, each making a complete revolution before fading out. It forms an irregular ellipse  $80'' \times 40''$ ,  $p \ 120^\circ$  (no trail). For a length of  $20''$ , beginning a half-turn from the center, there are several bright knots in line in each arm. Beyond this the nebulosity is soft and spreads into brushes at the ends. The curvature at the ends is very small, and there is indication that the  $f$  one extends to N.G.C. 5258.

N.G.C. 5258 is a left-handed spiral whose brighter parts lie within an ellipse  $60'' \times 18''$ ,  $p \ 30^\circ$  (no trail), from the extremities of which spring the two main opposite arms forming a letter S, the arms themselves being opposite arcs of a circle of  $30''$  radius. The central nucleus is brighter than that of N.G.C. 5257, and two knots as bright as the nucleus lie one to the N end and one to the S. The arms are soft and brushy, as in N.G.C. 5257.

**N.G.C. 5278-5279, Ursa Major**

N.G.C. 5278,  $\alpha = 13^h 38^m 40^s$ ,  $\delta = +56^\circ 4' 3''$  }  
 N.G.C. 5279,  $\alpha = 13 \ 38 \ 45$ ,  $\delta = +56 \ 4.5$  } (1920);  $\lambda = 74^\circ$ ,  $\beta = +60^\circ$

Plate No. 341, 1919, May 28, 30<sup>m</sup>. S 30. Fair images

Plate No. 342, 1919, June 25, 160<sup>m</sup>. S 30. Fair images. Illustrated Plate XIX*a*

These separately listed objects are parts of the same nebula, consisting of a stellar center and a ribbon of nebulosity which encircles the nucleus for a little more than one turn, then abruptly decreases in intensity and widens out, and continuing in a curve, concave to the S, ends abruptly in a bright twist or hook, at about  $p \ 70^\circ$ ,  $d \ 40''$ . The first coil is roughly  $30'' \times 20''$ ,  $p \ 60^\circ$ , and the whole lies within an ellipse  $65'' \times 30''$ ,  $p \ 60^\circ$ . The curl on the end forms a semicircle of about  $7''$  radius and points  $p \ 320^\circ$ .

This nebula appears on the same plates as the group of objects listed by Barnard under I.C. 917 to 928; the illustration is from Plate No. 342 where it appears near the edge.

**N.G.C. 5544,\* 5545,\* 5557, Boötes**

N.G.C. 5544,  $\alpha = 14^h 13^m 40^s$ ,  $\delta = +36^\circ 56' 5''$   
 N.G.C. 5545,  $\alpha = 14 \ 13 \ 41$ ,  $\delta = +36 \ 56 \ 8$   
 N.G.C. 5557,  $\alpha = 14 \ 15 \ 5$ ,  $\delta = +36 \ 51 \ 6$  } (1920);  $\lambda = 32^\circ$ ,  $\beta = +68^\circ$

Plate No. 127, 1912, June 13, 180<sup>m</sup>. S 23

Plate No. 260, 1916, April 30, 50<sup>m</sup>. S 23. Images small and round

Plate No. 261, 1916, May 1, 2, 3, 4, 5, 360<sup>m</sup>. S 27. Images small. Illustrated Plate XXb

In *Mount Wilson Contribution*, No. 132, the orientation of these plates is in error  $180^\circ$ , consequently the descriptions of N.G.C. 5544 and 5545 are interchanged and Plate XIIIc is shown S at top and f at right. The positions in N.G.C. are incorrect, as that of 5545 is S of 5544, while actually it is to the N. Bigourdan's value (*Annales Observatoire de Paris, Observations*, 1899) for N.G.C. 5544 is  $\alpha = 14^h 12^m 50^s.62$ ,  $\delta = +37^\circ 2' 7''.2$  (1900), the relative position of the nebulae  $p \ 244^\circ \pm$ ,  $d \ 37''$ , but he states that the measures are uncertain and difficult. The corrected description is as follows:

N.G.C. 5544 and 5545 are two overlapping spirals, the former in plan, the latter very much inclined to the line of sight.

N.G.C. 5544 consists of a bright stellar nucleus, a nebular ring about  $5''$  wide and  $28''$  outside diameter, a fainter diametral streak crossing the nucleus in  $p \ 130^\circ$  and an outer ring of about the same intensity as the inner one, irregularly round,  $8''$  wide and  $45''$  outside diameter; both rings are slightly elongated in  $p \ 115^\circ$ . The nebulosity is entirely soft.

N.G.C. 5545 is a left-handed spiral  $70'' \times 15''$ ,  $p \ 60^\circ$ , its  $p$  end just tangent to the  $f$  point of the nucleus of N.G.C. 5544. The nucleus is faint and stellar. The arms are about equal in intensity where they start from the nucleus, but that on the  $p$  side continues bright for a much greater distance, being interrupted, however, at several points. Several knots and condensations

appear. Its extremely small, bright nucleus lies in  $p\ 68^\circ$ ,  $d\ 36''$ , with respect to nucleus of N.G.C. 5544.

N.G.C. 5557 appears at the  $f$  side of the plates; it is so distorted that one cannot more than suspect it to be a spiral. Its position with respect to N.G.C. 5544 is  $p\ 105^\circ$ ,  $d\ 17.4$  and, allowing for distortion, seems to be a bright mass  $18'' \times 14''$  surrounded with fainter nebulosity  $40''$  diameter.

The plates are covered with a multitude of faint nebulae, a number of which are as follows, their positions being given with respect to the nucleus of N.G.C. 5544:

<i>a</i> ,	$p\ 235^\circ$ ,	$d\ 20.7$	MB, Irr. R, $12''$ diameter BM (edge of plate).
<i>b</i> ,	216	21.3	F, nebulous spot, $5''$ diameter (edge of plate).
<i>c</i> ,	329	9.8	F, uniform sliver, $20'' \times 2''$ , $p\ 24^\circ$ .
<i>d</i> ,	205	7.5	MB, elongated Nu., $4'' \times 2''$ , $p\ 4^\circ$ , in MF nebulosity, $11''$ diameter.
<i>e</i> ,	228	3.8	F, $5''$ diameter, gbM.
<i>f</i> ,	356	6.6	Faint, MF at center, $10'' \times 3''$ , $p\ 42^\circ$ .
<i>g</i> ,	179	4.8	Bright Nu., $2''$ to $3''$ diameter, surrounded by F nebulosity, $13''$ diameter, $p\ 79^\circ$ .
<i>h</i> ,	173	16.1	MF center, $10'' \times 2''$ , $p\ 145^\circ$ , in F nebulosity $15'' \times 5''$ .
<i>i</i> ,	23	7.8	Two F slivers each $11''$ long lying $p\ 37^\circ$ and $52^\circ$ intersecting to form a V on $Sp$ end.
<i>j</i> ,	139	18.5	F, $8''$ diameter, gbM.
<i>k</i> ,	97	13.0	F, $10'' \times 2''$ , $p\ 130^\circ$ .
<i>l</i> ,	124	16.0	F, Wisp, $13'' \times 3''$ , $p\ 76^\circ$ .
<i>m</i> ,	130	23.1	Nebulous spot, $10'' \times 5''$ , $p\ 51^\circ$ (edge of plate).

### N.G.C. 5868, 5869, Serpens

N.G.C. 5868,  $\alpha = 15^h 5^m 44^s$ ,  $\delta = +0^\circ 50'.2$  } (1920);  $\lambda = 328^\circ$ ,  $\beta = +47^\circ$   
 N.G.C. 5869,  $\alpha = 15.5\ 45$ ,  $\delta = +0\ 46.6$  }

Plate No. 328, 1919, March 1, 50<sup>m</sup>, S 23. Images small and almost round

Plate No. 335, 1919, March 30, 30<sup>m</sup>, S 30. Images small and elongated

N.G.C. 5868 is a medium bright, semi-diffuse stellar nucleus  $2''$ – $3''$  diameter with a faint halo  $5''$  diameter.

N.G.C. 5869 is a medium bright, diffuse stellar nucleus  $5'' \times 4''$ ,  $p\ 133^\circ$ , surrounded with nebulosity gradually fading away at  $10'' \times 7''$ .

N.G.C. 5865 and N.G.C. 5871, for which positions are given in this vicinity, do not appear on the plates.

There is a very faint diffuse spot roughly  $7''$  diameter,  $p\ 116^\circ$ ,  $d\ 1'9$ , with respect to the nucleus of 5868.

#### N.G.C. 6014, 6017, Serpens

N.G.C. 6014,  $\alpha = 15^h 52^m 1^s$ ,  $\delta = +6^\circ 9'7''$  (1920);  $\lambda = 341^\circ$ ,  $\beta = +39^\circ$   
 N.G.C. 6017,  $\alpha = 15\ 53\ 19$ ,  $\delta = +6\ 13.6$

Plate No. 325, 1919, February, 28, 30<sup>m</sup>. S 30. Images small and slightly elongated

N.G.C. 6014. Medium bright stellar nucleus lying centrally in faint nebulosity  $30''$  diameter, showing traces of rings. It is probably a spiral. There is a faint nebula of the same character,  $15''$  diameter, at  $p\ 51^\circ$ ,  $d\ 11'0$ , with respect to N.G.C. 6014.

N.G.C. 6017. A faint elliptical nebula  $18'' \times 6''$ ,  $p\ 133^\circ$ , with bright nucleus  $7'' \times 5''$ .

#### N.G.C. 6703,\* Lyra

$\alpha = 18^h 45^m 0^s$ ,  $\delta = +45^\circ 27'7''$  (1920);  $\lambda = 42^\circ$ ,  $\beta = +18^\circ$

Plate No. 344 (Duncan and Hoge), 1919, June 26, 315<sup>m</sup>. S 30.  
 Images medium and elongated

This plate was taken for classification, but the results are not conclusive and the type must be settled spectroscopically. The nucleus is lost in the very strong central part,  $30''$  in diameter. The ring,  $80''$  diameter, shows more plainly, and there is nebulosity between the ring and the central mass; but it is not clear whether the nebula is a planetary or a spiral in plan. Ten small faint nebulae, in addition to the six mentioned previously, are shown on the plate.

#### N.G.C. 6820, Vulpes

$\alpha = 19^h 39^m 3^s$ ,  $\delta = +22^\circ 53'3''$  (1920);  $\lambda = 27^\circ$ ,  $\beta = -1^\circ$

Plate No. 298, 1917, July 23, 90<sup>m</sup>. S 23. Images small and nearly round

The nebula lies in a rich region of the Milky Way. It has a stellar nucleus lying eccentrically to the south in a mass of soft, irregular, patchy nebulosity, roughly  $30''$  in diameter.

N.G.C. 6823, an open cluster, appears on the Nf corner of the plate.

**N.G.C. 6846, Cygnus**

$\alpha = 19^{\text{h}}53^{\text{m}}22^{\text{s}}$ ,  $\delta = +32^{\circ}8'4''$  (1920);  $\lambda = 37^{\circ}$ ,  $\beta = +1^{\circ}$

Plate No. 295, 1917, July 20, 150<sup>m</sup>. S 23. Images small and elongated

A small group of twelve stars, approximate magnitude 17, in a very rich region of the Milky Way, clustered about three stars of magnitude 15.

**N.G.C. 6888, Cygnus**

$\alpha = 20^{\text{h}}9^{\text{m}}33^{\text{s}}$ ,  $\delta = +38^{\circ}9'1''$  (1920);  $\lambda = 43^{\circ}$ ,  $\beta = +1^{\circ}$

Plate No. 299, 1917, August 21, 60<sup>m</sup>. S 23. Images small and slightly elongated

Plate No. 301, 1917, August 22, 60<sup>m</sup>. S 27. Images small and slightly elongated

Plate No. 348, 1919, July 25, 300<sup>m</sup>. S 30. Images medium. Illustrated Plate XXc

A network nebula in the heart of the Milky Way, about  $13^{\circ}$  Np N.G.C. 6960 and 6992, which it resembles in shape and character of nebulosity. It is roughly elliptical,  $18' \times 9'$ ,  $p\ 42^{\circ}$ . The N, Np, and Sp edges include the bulk of the nebulosity, which gives it a crescent form, the bowl of which is filled with faint and scattered nebulosity.

**N.G.C. 6906, Sagitta**

$\alpha = 20^{\text{h}}19^{\text{m}}36^{\text{s}}$ ,  $\delta = +6^{\circ}12'3''$  (1920);  $\lambda = 18^{\circ}$ ,  $\beta = -18^{\circ}$

Plate No. 352 (Benioff), 1919, August 27, 120<sup>m</sup>. Images small and nearly round

A right-handed spiral lying at the edge of the Milky Way where the star density, for this plate, is five to six stars per square minute of arc. The nebula measures  $90'' \times 35''$ ,  $p\ 35^{\circ}$ , the arms are soft and delicate, though increased exposure may show parts to be granular. A short line  $12''$  long projects equally beyond the nucleus in  $p\ 165^{\circ}$  and  $345^{\circ}$ .

**N.G.C. 6927, 6928, 6930, Delphin**

N.G.C. 6927,  $\alpha = 20^{\text{h}}28^{\text{m}}46^{\text{s}}$ ,  $\delta = +9^{\circ}38'6''$   
 N.G.C. 6928,  $\alpha = 20\ 28\ 58$ ,  $\delta = +9\ 39.2$   
 N.G.C. 6930,  $\alpha = 20\ 29\ 7$ ,  $\delta = +9\ 34.6$  } (1920);  $\lambda = 22^{\circ}$ ,  $\beta = -18^{\circ}$

Plate No. 347 (Duncan and Hoge), 1919, June 27, 60<sup>m</sup>. Images small and elongated

Plate No. 350, 1919, August 21, 140<sup>m</sup>. S 23. Images small and elongated

These plates show three N.G.C. nebulae in addition to the several small nebulae given below. The foregoing positions have been corrected from Bigourdan's observations.

The following measures refer to the brightest spot of N.G.C. 6928.

<i>a</i> ,	<i>p</i> 231°, <i>d</i> 4.2	10"×5", <i>p</i> 20°, gbM, BM.
N.G.C. 6927	257 3.0	18"×8", <i>p</i> 10°, gbM, BM.
N.G.C. 6928		100"×28", <i>p</i> 110°, left-handed spiral, two arms making about three-fourths of a turn each. Brightest in the middle where the two arms join with a slight offset, forming a bent line 35" long.
<i>b</i> ,	161 1.6	MF, nebulous spot, 4" diameter.
N.G.C. 6930	146 3.9	30"×12", <i>p</i> 9°, left-handed spiral nebula with slight traces of outside arms at end of major axis.
<i>c</i> ,	139 5.6	Nebulous spot, 3" diameter.
<i>d</i> ,	126 13.2	20"×6", <i>p</i> 70°, lbM.

#### N.G.C. 7023, Draco

$$\alpha = 21^{\text{h}}0^{\text{m}}37^{\text{s}}, \delta = +67^{\circ}51' (1920); \lambda = 72^{\circ}, \beta = +14^{\circ}$$

Plate No. 343, 1919, June 25, 160<sup>m</sup>. S 23. Images small and slightly elongated

Comparison of this plate with No. 12 (1911, July 23, 149<sup>m</sup>, S 23) in the stereocomparator gave no indication of change.

#### N.G.C. 7048, Cygnus

$$\alpha = 21^{\text{h}}11^{\text{m}}23^{\text{s}}, \delta = +45^{\circ}57'4 (1920); \lambda = 57^{\circ}, \beta = -2^{\circ}$$

Plate No. 296, 1917, July 20, 60<sup>m</sup>. S 23. Images round and large

A planetary resembling the Dumb-bell nebula, about 1' diameter, weak axis in *p* 170°. The central star is very faint. A longer exposure is necessary to bring out the detail.

#### N.G.C. 7240, 7242, Lacerta

$$\left. \begin{array}{l} \text{N.G.C. 7240, } \alpha = 22^{\text{h}}11^{\text{m}}53^{\text{s}}, \delta = +36^{\circ}52'7 \\ \text{N.G.C. 7242, } \alpha = 22^{\text{h}}12^{\text{m}}10^{\text{s}}, \delta = +36^{\circ}53'7 \end{array} \right\} (1920); \lambda = 59^{\circ}, \beta = -17^{\circ}$$

Plate No. 292, 1917, June 21, 22, 195<sup>m</sup>. S 23. Images round and medium

Plate No. 354, 1919, December 22, 50<sup>m</sup>. S 23. Images round and small

Plate No. 357, 1919, December 23, 145<sup>m</sup>. S 23. Images small and elongated

A group including twenty in addition to the six nebulae described by Barnard in *A.N.*, 137, 717, 1906. The measures refer to the nucleus of N.G.C. 7242.

N.G.C. 7240 <i>p</i>	0°d 0'	18"×5", <i>p</i> 108°, gbM, B stellar Nu., Barnard <i>c</i> .
N.G.C. 7242	73 3.6	12"×6", <i>p</i> 33°, gbM, B stellar Nu., Barnard <i>a</i> .
<i>a</i> ,	217 8.7	MB, 9"×1'5, <i>p</i> 178°, gbM.
<i>b</i> , I.C.II 5191?	287 4.1	Spindle, 45"×6", <i>p</i> 66°, BNu., Barnard <i>f</i> .
<i>c</i> ,	214 6.0	F, 3" diameter
<i>d</i> ,	203 8.2	F, 8"×2", <i>p</i> 170°.
<i>e</i> ,	217 3.6	B, 3" diameter, almost stellar, F wings <i>p</i> 58°.
<i>f</i> , I.C.II 5192?	251 1.8	12"×6", <i>p</i> 160°, gbM, Barnard <i>d</i> .
<i>g</i> ,	193 6.5	F, 2" diameter, bM.
<i>h</i> , I.C.I 1441	332 1.4	Spiral, 30"×15", <i>p</i> 40°, Barnard <i>e</i> , Bigourdan 233.
<i>i</i> ,	171 4.6	F, 4"×2", <i>p</i> 140°.
<i>j</i> ,	4 9.7	F, 10"×2", <i>p</i> 143°.
<i>k</i> ,	15 4.1	MB, 4" diameter, stellar.
<i>l</i> ,	175 14.0	MB, 3" diameter.
<i>m</i> ,	95 2.3	F, 2" diameter.
<i>n</i> ,	157 6.2	Spindle, 20"×6", <i>p</i> 120°, B stellar Nu.
<i>o</i> ,	141 4.1	F, 6"×3", <i>p</i> 100°.
<i>p</i> , I.C.II 5195	71 4.0	B, 4" diameter, gbM, almost stellar.
<i>q</i> ,	140 5.7	F, 3" diameter, Nu.
<i>r</i> , I.C.II 5194?	119 4.8	10" diameter, gbM, B stellar Nu., Barnard <i>b</i> .
<i>s</i> ,	41 6.3	F, 3" diameter.
<i>t</i> ,	68 7.3	B, 3" diameter, almost stellar.
<i>u</i> ,	40 15.4	F, 20"×6", <i>p</i> 124°, B stellar Nu.
<i>v</i> ,	51 12.5	F, 2" diameter.
<i>w</i> ,	83 10.0	F, 2" diameter.
<i>x</i> ,	117 13.6	18"×5", <i>p</i> 118°, stellar Nu.

### N.G.C. 7435, 7436, Pegasus

N.G.C. 7435,  $\alpha = 22^h 54^m 6^s$ ,  $\delta = +25^\circ 42' 2''$  } (1920);  $\lambda = 62^\circ$ ,  $\beta = -31^\circ$   
 N.G.C. 7436,  $\alpha = 22^h 54^m 6^s$ ,  $\delta = +25^\circ 43' 3''$  }

Plate No. 293, 1917, June 23, 120<sup>m</sup>. S 23. Images small and round

The plate shows a rich field of small nebulae consisting of elongated masses with bright almost stellar nuclei. They are probably spiral.

N.G.C. 7431,  $\alpha = 22^h 53^m 47^s$ ,  $\delta = +25^\circ 44' 2''$  (1920), is a star with faint companion *f*.

N.G.C. 7433,  $\alpha = 22^h 54^m 2^s$ ,  $\delta = +25^\circ 43' 2''$  (1920), does not appear on the plate.



N.G.C. 7436 has a bright stellar nucleus surrounded by faint nebulosity, 7" diameter.

The positions of the following nebulae are referred to N.G.C. 7436.

<i>a</i> , <i>p</i>	239°, <i>d</i> 14.9	MB, 20"×8", <i>p</i> 40°, lbM.
<i>b</i> ,	273 7.9	F, 15"×5", <i>p</i> 150, lbM.
<i>c</i> ,	249 7.2	MB, 30"×8", <i>p</i> 140, spindle, bM.
<i>d</i> ,	332 12.6	F, 15"×10", <i>p</i> 30, lbM.
<i>e</i> ,	238 5.7	F, 20"×10", <i>p</i> 150, lbM.
<i>f</i> ,	334 5.8	MF, 10"×5", <i>p</i> 150, spindle, stellar Nu.
<i>g</i> ,	313 3.5	MF, 5" diameter, stellar Nu.
<i>h</i> ,	300 1.6	MB, 30"×10", <i>p</i> 45, ellipse, stellar Nu.
<i>i</i> ,	232 1.0	MB, 30"×10", <i>p</i> 160, spiral, stellar Nu.
<i>j</i> ,	187 2.4	MB, 5" diameter.
<i>k</i> ,	270 0.4	B, 20"×6", <i>p</i> 95, spindle, stellar Nu.
<i>l</i> ,	168 1.1	MF, 4" diameter stellar nucleus, N.G.C. 7435.
<i>m</i> ,	136 7.3	MB, 20"×10", <i>p</i> 130.
<i>n</i> ,	141 9.4	F, 30"×8", <i>p</i> 40, uniform.
<i>o</i> ,	47 8.9	MF, 6" diameter, bM.

**N.G.C. 7611, 7615, 7617, 7619, 7621, 7623, 7626, 7631, Pegasus**

N.G.C. 7611,	$\alpha = 23^h 15^m 33^s$ , $\delta = +7^\circ 22.5'$	} (1920); $\lambda = 56^\circ$ , $\beta = -51^\circ$
N.G.C. 7615,	$\alpha = 23 15 53$ , $\delta = +7 58.5$	
N.G.C. 7617,	$\alpha = 23 16 2$ , $\delta = +7 43.7$	
N.G.C. 7619,	$\alpha = 23 16 12$ , $\delta = +7 46.0$	
N.G.C. 7621,	$\alpha = 23 16 20$ , $\delta = +7 55.7$	
N.G.C. 7623,	$\alpha = 23 16 27$ , $\delta = +7 57.5$	
N.G.C. 7626,	$\alpha = 23 16 39$ , $\delta = +7 46.7$	
N.G.C. 7631,	$\alpha = 23 17 24$ , $\delta = +7 46.7$	

Plate No. 351, 1919, August 21, 130<sup>m</sup>. S 23. Images small and round

N.G.C. 7611, B, stellar Nu., 10" diameter in F nebulosity. 60"×15", *p* 140°, edge of plate.

N.G.C. 7615, MF, uniform, 40"×20", *p* 140°.

N.G.C. 7617, B, stellar Nu., 8"×5", *p* 32°.

N.G.C. 7619, B, Nu., 12"×10", *p* 32°, in F nebulosity.

N.G.C. 7621, Stellar Nu., 3" diameter in nebulosity 20"×5", *p* 170°.

N.G.C. 7623, B, stellar Nu., 8"×6", *p* 170°, in F nebulosity 15" diameter.

N.G.C. 7626, B, stellar Nu., 8" diameter, in F nebulosity 40" diameter.

N.G.C. 7631, MF, stellar Nu., 3" diameter, in F nebulosity 90"×30", *p* 80°.

There are many other small nebulae on the plate, which will be listed when a duplicate plate has been made.

### N.G.C. 7722, Pegasus

$\alpha = 23^h 34^m 41^s$ ,  $\delta = +15^\circ 31' 0''$  (1920);  $\lambda = 68^\circ$ ,  $\beta = -44^\circ$

Plate No. 353, 1919, August 27, 27<sup>m</sup>. S 23. Images small, almost round

The exposure is sufficient to show a spiral with bright nucleus and strong absorption streak *f* the nucleus. The portion shown on the plate covers  $45'' \times 30''$ ,  $p\ 150^\circ$  (no trail).

### I.C.I 922, 928, 931, Ursa Major, and a Group of 72 Others

I.C.I 922,  $\alpha = 13^h 40^m 17^s$ ,  $\delta = +56^\circ 0' 4''$  }  
 I.C.I 928,  $\alpha = 13\ 40\ 43$ ,  $\delta = +56\ 1.2$  } (1920);  $\lambda = 73^\circ$ ,  $\beta = +59^\circ$   
 I.C.I 931,  $\alpha = 13\ 40\ 49$ ,  $\delta = +56\ 1.3$  }

Plate No. 341, 1919, May 28, 30<sup>m</sup>. S 30. Fair images

Plate No. 342, 1919, June 25, 160<sup>m</sup>. S 30. Fair images

Barnard originally called attention to this group in *A.N.*, 125, 379, 1890, and numbers from 917 to 938 (with a few exceptions) were assigned to it in the *Index Catalogue*. Of the seventy-five nebulae shown on the plates only three (not including N.G.C. 5278-5279, which appear among them) have been identified, namely, I.C.I 922, 928, 931. Many of the objects are almost stellar, but they have been listed because of some peculiarity of appearance which distinguishes them from the neighboring star images. Measurements were made on the plate relative to B.D. +56° 1677, for which the reduced co-ordinates are  $\alpha = 13^h 37^m 19^s 6$ ,  $\delta = +56^\circ 25' 2''$  (1860). Positions are given for right ascension and declination 1860. Hubble's paper<sup>1</sup> on this field which has just been published identifies twenty-five of the objects given here; they are indicated as H22, etc.

<sup>1</sup> E. P. Hubble, "Photographic Investigations of Faint Nebulae," *Publications of the Yerkes Observatory*, 4, Part II, 1919.

Description		a 1860	§ 1860
MB, Spindle, 30"×9", $p$ 10°, lbM.....		13 <sup>b</sup> 36 <sup>m</sup> 7°0	+56°22.4
MF, 7", gbM.....	H22	9.1	15.9
B, 14",×8", $p$ 70°.....		11.6	20.4
MB, 7", gbM.....		19.6	25.5
B, Nucleus, N.G.C. 5278.....		27.2	22.0
B, Tail, N.G.C. 5279.....		31.5	22.2
MF, 10", patch.....	H31	47.3	28.8
MB, 5",.....		52.5	36.3
MF, 5", lbM.....		56.7	36.0
F, 10", patch.....		37 4.6	8.9
MF, 5", lbM.....		5.6	19.9
MF, 12" diameter, patch.....		13.0	40.6
MB, 12"×8", $p$ 135°, spindle, gbM.....		13.7	31.1
F, 6", lbM.....		14.1	14.7
MB, 10", gbM.....	H34	14.1	8.9
MF, 20"×5", $p$ 170°, uniform.....		16.7	31.2
B, B.D.+56° 1677.....		19.6	25.2
MF, 12"×8", $p$ 100°, lbM.....	H35	21.9	14.0
MF, 12"×8", $p$ 70°, lbM.....		23.2	10.2
MB, 4",.....		23.5	15.9
B, 20"×8", $p$ 100°, gbM.....	H36	26.1	13.8
MB, 12"×8", $p$ 135°, gbM.....	H37	34.3	12.6
MF, 4",.....		38.7	24.8
B, 6", stellar.....	H40	45.1	17.8
F, 8", patch.....		46.9	10.2
MF, 10", lbM.....		47.1	40.1
MB, 10", patch.....		48.2	35.1
MB, 12"×4", $p$ 60°, uniform.....		48.5	33.0
MB, 8"×4", $p$ 135°, lbM.....	H41	52.0	22.0
MF, 5", lbM.....		53.7	26.8
MB, 5", lbM.....		54.6	17.4
MB, 8", I.C.I 922, gbM.....	H42	38 02.7	18.6
B, 5", gbM.....	H43	3.4	17.7
MB, 20"×5", $p$ 100°, spindle, gbM.....	H44	5.4	18.5
F, 5", patch.....		7.5	13.7
MF, 5", lbM.....		8.9	17.4
B.D.+56° 1679.....		14.8	19.7
B, 5", stellar.....		16.0	28.1
F, Patch 8".....		16.0	14.7
MF, Patch 8".....		19.0	14.6
MB, 10"×4", $p$ 90°, patch.....		26.1	16.7
MB, 3",.....		28.0	20.4
B, 8"×4", $p$ 120°, gbM, I.C.I 928.....		29.2	19.4
MF, 6", gbM.....		32.0	24.8
MF, 8", patch.....		32.7	16.7
MB, 10"×8", $p$ 90°, lbM.....		33.0	25.3
B, 5", I.C.I 931, stellar.....	H48	34.8	19.5
MB, 7"×3", $p$ 30°, lbM.....		35.2	30.4
B, 4", almost stellar.....	H49	35.5	20.3
B, Star?.....		36.6	15.8
B, Star? 4".....	H51	37.3	15.6
MF, 10"×4", $p$ 140°, lbM.....		38.9	24.3
B, 5", almost stellar.....		39.4	18.9
B, 6", almost stellar.....	H53	41.4	20.3
MB, 4", almost stellar.....		42.7	20.9
F, 7", lbM.....		43.1	15.0

Description		$\alpha$ 1860	$\delta$ 1860
F, 8"×4", $p$ 95°		13 <sup>h</sup> 38 <sup>m</sup> 47. <sup>s</sup> 2	+56°19'.4
F, 10"×5", $p$ 135°	H56	51.0	15.5
B.D. +56° 1682		56.4	19.6
B, 8"×5", $p$ 40°, gbM.		58.9	25.4
B, 15"×6", $p$ 90°, gbM.	H59	59.2	23.8
MF, 7" patch, lbM.		39 0.0	28.3
B, 30"×6", $p$ 80°, BNu., spindle	H60	12.7	32.8
F, 6" patch		13.6	11.4
B, 30"×6", $p$ 30°, gbM.	H61	13.7	38.9
F, 5" patch		14.0	12.1
B, 8"×5", $p$ 135°		19.6	19.3
B, 10"×6", $p$ 150°	H62	25.5	19.1
MB, 25" patch, gbM.	H63	31.6	41.2
B, 15"×10", $p$ 40°, patch	H64	33.5	34.8
F, 30"×4", $p$ 10°, sliver.		33.5	34.1
MB, 4", almost stellar.		36.1	22.4
MB, 4", almost stellar.		37.3	23.1
F, 5"		40.8	28.7
MF, 3"		41.5	19.7
F, 11"×6", $p$ 135°		47.5	11.1
MF, 8" patch, lbM.		51.6	24.5
MF, 8"×4", $p$ 40°, patch		53.6	24.3
MB, 10"×4", $p$ 130°, spindle, bM.	H66	55.0	16.1

## I.C.I 1470, Cassiopeia

$$\alpha = 23^{\text{h}}1^{\text{m}}51^{\text{s}}, \delta = +59^{\circ}48'9'' (1920); \lambda = 78^{\circ}, \beta = -1^{\circ}$$

Plate No. 297, 1917, July 21, 190<sup>m</sup>. S 23. Images intermediate and fairly round. Illustrated Plate XXa

A gaseous nebula lying in a rich region of the Milky Way. Its prominent feature is a bright thread of nebulosity irregularly triangular in shape, superimposed on the fainter nebulosity. The sides of the triangle are roughly 30" long; the north side lies in  $p$  88° and is straight, except for an abrupt bend to the N around a star directly in its middle; the  $f$  side in  $p$  60° is shaped like an integral sign, while the  $p$  side,  $p$  140°, is V-shaped, points inward, and has a faint star at its apex. The N and  $p$  sides do not quite join. The faint nebulosity is roughly 70"×45" and is quite full of markings, which a longer exposure will show to advantage. A dark marking cuts across the nebula north of the triangle.

Three nebulous stars appear in the plate:

$a$ ,	314°	14'.8	Three stars involved in F nebulosity.
$b$ ,	197	10.7	Bright star in group of 5, involved in nebulosity.
$c$ ,	84	6.2	Two stars involved in nebulosity.

**I.C.II 2233, Lynx**

$\alpha = 8^{\text{h}} 8^{\text{m}} 19^{\text{s}}$ ,  $\delta = +45^{\circ} 59'.5$  (1920);  $\lambda = 141^{\circ}$ ,  $\beta = +35^{\circ}$

Plate No. 2968 (Shapley), 1916, March 27, 30<sup>m</sup>. S 27

Plate No. 359, 1919, December 23, 60<sup>m</sup>. S 30. Images elliptical

The nebula falls near the edge of the plates of N.G.C. 2537 and appears to be a faint edge-on spiral  $240'' \times 10''$ ,  $p$   $170^{\circ}$  (no trail), with a faint stellar nucleus.

**I.C.II 5146, Cygnus**

$\alpha = 21^{\text{h}} 50^{\text{m}} 25^{\text{s}}$ ,  $\delta = +46^{\circ} 53'.2$  (1920);  $\lambda = 62^{\circ}$ ,  $\beta = -7^{\circ}$

Plate No. 276, 1916, August 4, 60<sup>m</sup>. S 23. Images small and round.

Plate No. 349, 1919, July 26, 300<sup>m</sup>. S 23. Images small and elongated.

Illustrated Plate XIXc

This well-known nebula lies at the end of a dark lane which is well shown on Plate No. 349 and on the various published photographs of Barnard, Curtis, Franks, and Wolf. It surrounds the star B.D.  $+46^{\circ} 3474$   $9^{\text{M}}5$ , and its strong parts are  $12'$  in diameter, while extensions run to the boundaries of the dark region in which it lies. Two of these extensions end at stars involved in nebulosity,  $a$ ,  $p$  257,  $d$   $9'.7$ , which is preceded by a bright patch, and  $b$ ,  $p$  156<sup>o</sup>,  $d$   $9'.8$ , where the nebulosity brightens on the preceding side of the star. The nebula is a wonderful array of dark and light markings and cannot be likened to any other object, although counterparts of certain configurations may be found in some of the other large gaseous nebulae. For example, the dark birdlike or torchlike dark markings in the  $S_p$  section, of which there are two, are similar to a marking in the  $p$  section of M 16; two dark indentations on the  $N_p$  side resemble some of the indentations about the rim of M 8; and some of the canopied structure resembles the outlying parts of the Orion nebula.

MOUNT WILSON OBSERVATORY

April 1920

ERRATA in *Mount Wilson Contr.*, No. 132,

*Astrophysical Journal*, 46, 24, 1917

Page 35: N.G.C. 2403, Plate Vc was made from negative No. 307 (of the present series) instead of No. 169.

Page 41: N.G.C. 4594, the equation should read  $V = -2.78x + 1180$ .

Plate VIIIc: N.G.C. 5544-5545, orientation of the plate is S at top,  $f$  at right; identification of nebulae in text is not correct; true description is found in the present series.

Page 42: N.G.C. 4900,  $\alpha = 12^{\text{h}} 56^{\text{m}} 28^{\text{s}}$ .

## REVIEWS

*Problems of Cosmogony and Stellar Dynamics.* By J. H. JEANS.  
Cambridge: University Press, 1919. American Agents, G. P.  
Putnam's Sons, New York. Large royal 8vo. Pp. vii+293,  
figs. 44 and 5 plates. \$6.50.

### ABSTRACT

*Equilibrium of a freely rotating single mass.*—After giving the equilibrium equations for a rotating system and deriving a new and more exact expression for the potential of any slightly distorted ellipsoidal figure, Jeans discusses the stability of: (1) an incompressible fluid mass; (2) a compressible fluid mass; (3) an incompressible fluid nucleus surrounded by an atmosphere rotating with it; and (4) a gaseous mass in adiabatic equilibrium.

*Equilibrium of a system of two masses.*—The tides raised on a non-rotating sphere of incompressible fluid by an approaching rigid sphere are shown to be great enough to cause fission if the approach is sufficiently close. An atmosphere around the sphere would elongate toward the tide-raising body and might in case of near approach stream out in a pulsating manner. The problem of a double star system consisting of two fluid masses revolving in a rigid configuration is a very difficult one. Jeans's conclusion is that beyond stability a ring of broken fragments may be formed.

*Origin of spiral nebulae.*—Jeans's theory of their formation as a result of contraction accompanied by rotation which leads to equatorial breaking up is far from convincing. He relies on tidal forces which are admittedly infinitesimal and he neglects the possible effects of strong internal energy and of initial irregularities.

*Origin of our galaxy.*—Jeans's supposition that our galaxy is derived from a rotating nebula whose original radius of 30 parsecs increased to 2000 parsecs after the break-up, involves an age of only 500 million years and an expansion which the reviewer proves to be dynamically impossible. The reviewer points out that the excessively small chance of the close approach of two stars taken in conjunction with certain evidences of an approach to statistical equilibrium in our galaxy suggests an age which is beyond any order of time hitherto accepted.

*Origin of binary and multiple stars.*—Jeans's assumption that binary stars originate from nebulae by fission leads to deductions which can be reconciled with the facts only with the aid of arbitrary hypotheses. His picture of the cataclysmic birth of binaries is purely imaginary and very improbable.

*Origin of the solar system.*—As the Laplacian theory is clearly unsatisfactory, Jeans suggests a tidal theory, according to which the sun, originally a nebulous mass extending out to Neptune, was broken up by purely tidal action. The chief objection to this theory, aside from the improbability of the necessary encounters, is that it adopts the contraction hypothesis as to the origin of the sun's heat, a hypothesis

which is inconsistent with the conclusions of geologists and physicists as to the age of the earth and which is almost wholly unsupported by astronomical evidence.

*Theory of cosmic origins.*—While recognizing *Jeans's contributions* to the purely gravitational theory, the reviewer vigorously attacks the idea that stars and galaxies have their origin in the contraction of nebulae. The dynamics of our galaxy and the evidences of geology sharply deny the adequacy of this source of stellar energy. Unfortunately Jeans has accepted this contraction theory without question and is, therefore, led to make improbable assumptions necessary to reconcile certain points with that theory. His book is not, accordingly, a broad, open-minded discussion of the problems of cosmogony.

The English-speaking mathematical world is again under obligations to Professor Jeans for a careful and dispassionate exposition of a certain aspect of the physical world, his former works *Mathematical Theory of Electricity and Magnetism* and *Dynamical Theory of Gases* being already widely known. The labor of organizing into a coherent whole the many and diverse results which have been obtained in a given field, of adding to these results a sensible quantum, and finally of presenting a clear picture in an acceptable style is very great. The least that we, who have the benefit of all this labor for a small financial outlay, can do is to express our appreciation and grant such recognition as the work merits. From the point of view which he has adopted we believe that Jeans has succeeded in presenting as complete and strong a case as could be made; that point of view being a purely gravitational theory of cosmic evolution—a continuation, as Jeans puts it, of the work of Laplace, MacLaurin, Roche, Kelvin, Jacobi, Poincaré, and Darwin in the effort to interpret the cosmic forms through the agencies of the laws of motion and of gravitation alone.

The various forms in which interest centers are enumerated in chapter i. They are binary stars, spiral and other nebulae, and star clusters. Information with regard to these objects has been gleaned from many sources, and in concluding his review of these objects Jeans says: "The aim of a scientific cosmogony must be to trace these and other uniformities to their sources. When we find a formation repeated many times with only slight variations, we may feel confident that its origin is in every case the same. The problem of cosmogony is to discover these origins and to prove that they would lead to the observed formations."

Under the heading "Theories of Cosmogony" is given a brief review of the ideas of Laplace and Kant, together with certain modifications and criticisms of a later date. Under the subtitle "Tidal-Action Theory"

is included the planetesimal hypothesis. The description of this theory as given here is so different from that given by the authors, Chamberlin and Moulton, that we are compelled to believe that Jeans has not taken the trouble to inform himself as to what the theory really is, and when he concludes the description with the statement, "But whether all this can happen or not can only be decided by exhaustive mathematical investigations," we cannot avoid wondering what it is he is proposing to do.

The mathematical discussions begin with chapter ii, which opens with a statement of the conditions necessary and sufficient for a configuration of equilibrium in a system at rest. A clear and vivid exposition of Poincaré's notion of a series of such figures as a function of a parameter is given both descriptively and with the proper analysis. Diagrams illustrating the branch points, where one series of figures crosses another, help the reader very much in gaining an insight into the nature of the ideas and arguments involved, particularly into the difference in character of these branch points, which are always critical points in the stability of the series. The discussion of the conditions for equilibrium of systems in rotation yields the equations which the author wishes to use throughout the book for the figures of equilibrium of rotating fluid masses.

In the following chapter is presented an analysis for the figures of equilibrium of an incompressible fluid mass. Three classes of problems are recognized for which the analysis is fundamentally the same, but which differ vitally in their complications. The first problem is that of a freely rotating single mass. The analysis for the MacLaurin spheroids and Jacobi's ellipsoids is given, together with tables of numerical data and a discussion, following Poincaré, of stability along a certain series for which the density is constant. It is found that the MacLaurin spheroids are stable up to the point where they first meet the Jacobi ellipsoids, after which the stability passes to the ellipsoids. The ellipsoidal figures are stable up to the point where the pear-shaped figures begin.

The second problem is that of the tides raised on a spherical fluid mass by a distant heavy spherical body. When the tide-raising potential is limited to terms of the second order, two series of figures are found corresponding to the MacLaurin spheroids and the Jacobi ellipsoids. The ellipsoidal figures being physically impossible, there remains only a series of prolate spheroids which are stable up to  $e=0.88$ , for which the polar diameter is a little more than twice the equatorial.



In the double-star problem Jeans supposes two fluid masses revolving about one another in a rigid configuration; and of this problem there are two types: Roche's problem, in which one of the bodies is supposed spherical, and Darwin's problem, in which both bodies yield to the tidal forces. Here is given Roche's theorem that a small fluid satellite revolving about a very large spherical primary cannot be in equilibrium in any configuration whatever if its distance from the center of the primary is less than 2.455 times the radius of the primary. The results obtained by Darwin seem to prove that Roche's limit is altered by less than  $2\frac{1}{2}$  per cent, whatever be the ratio in which the total mass is distributed between the two bodies.

The discussion of the stability mentioned above involves only such variations as are along an ellipsoidal series. A complete discussion requires a knowledge of the variations when the ellipsoidal figure is slightly distorted in any manner, and this requires a knowledge of the potential of any slightly distorted ellipsoidal figure. The author states that Poincaré's method of expansion in powers of a parameter with coefficients which are ellipsoidal harmonics cannot be readily carried out to the third power of this parameter, although the nature of the difficulty is not stated. As the second-order terms are not sufficient fully to determine the stability, the third-order terms must be obtained in order to effect a determination. Jeans has developed a method of his own for computing the third-order terms, and chapter iv is devoted to an exposition of this method and the attaining of the desired expression for the potential.

The solution of the question of stability is made possible by a sufficiently exact expression for the potential, and chapter v is devoted to an analysis for the stability. There is no difficulty in the tidal and double-star problems, for the spheroidal or ellipsoidal figures become unstable before the pear-shaped figure is reached, so that the pear-shaped figures for these cases are unstable. For the pear-shaped figures in the rotational problem, however, the matter is much more difficult, the ellipsoidal figures being stable right up to the point of bifurcation. Darwin's analysis in 1902 had indicated that these figures were stable, while Liapounoff's analysis in 1905 seemed to show that they were unstable. Thus the matter stood until 1915, when Jeans carried out the analysis which is outlined in chapters iv and v of the present volume. This computation shows that the pear-shaped figures are unstable at and near the point of bifurcation. Notwithstanding the fact that these figures of equilibrium are unstable, Jeans believes they are of great

importance in the subsequent dynamical motion, and that it is worth while, therefore, to trace the sequence of these figures of equilibrium. The labor of working out the three-dimensional figures is so great that he turned to the two-dimensional. He says:

A problem which admits of very much easier solution is the two-dimensional problem of tracing out the sequence of configurations of a rotating cylinder of liquid. So far as the three-dimensional case has been solved, the analogy between the two-dimensional and the three-dimensional cases is so very close that we can reasonably hope that it will persist beyond. If this is so, we can discover the general nature of the solution of the three-dimensional problem by examining the much simpler two-dimensional problem. We accordingly turn to a discussion of the two-dimensional problem.

The analysis for the rotating cylinder is carried out in sufficient detail to be clear, and concludes with a series of figures, three of which are from computations showing how a very narrow constriction, or neck, is formed, and a fourth figure, which seems to be conjectural, showing separation into two quite unequal masses, and the paragraph:

Thus we may with fair confidence assert that the two-dimensional series ends by fission into two detached masses, and in view of the close parallelism which we have discovered between the two-dimensional and the three-dimensional problems, it seems highly probable that the three-dimensional series will end by a similar fission into detached masses.

Since there are no stable figures of equilibrium in any of the problems considered beyond the spheroids and ellipsoids, the question naturally arises, What does happen? The answer is that the statical problem gives way to a dynamical one. Obviously when equilibrium is impossible motion occurs, and with considerable courage Jeans starts in pursuit of the tidal problem in chapter vi. The first approximation to the idealized tidal problem might be stated as follows: What would happen to a non-rotating spherical fluid mass, aside from mere translation, if a second large, rigid, spherical mass were made to approach within a certain distance of the first mass and then recede, the motion occurring along a straight line through the center of the first mass? The answer is that if the approach is sufficiently slow so that the primary can adjust itself to the figures of equilibrium, it will assume the shape of a prolate spheroid, continually lengthening until the final figure of equilibrium is reached in which the ratio of the major and minor axes is approximately 17:8; after this, the motion begins in a rapid lengthening of the axis of the prolate spheroid, which may or may not cease when the secondary begins to recede. In case the approach and recession of

the secondary is so rapid that the action may be regarded as impulsive, the primary oscillates along a series of prolate spheroids, provided the impulse is not too great. If the impulse is sufficiently great for the eccentricity of the prolate spheroid to pass 0.948, instability sets in, and a series of diagrams is given on which Jeans remarks: "Fig. 23 shews rough drawings (partly conjectural) of spheroids with the furrows produced on passing the earlier points of bifurcation. Little doubt will be felt that such figures will in time break up into a number of separate detached pieces."

The discussion is closed with a brief account of the effect of the forward motion of the secondary in an actual orbit. One effect is to set the primary into rotation, and another is to distort the primary into a boomerang shape. No account is taken of any original rotation of the primary, and no one will censure Jeans for this omission; the difficulties are far too great, but that it would effect a very serious modification in the results can scarcely be doubted. Perhaps a few paragraphs calling attention to this omission, particularly with respect to its effects upon the application of his results to cosmic processes, would have been in order. The direct and unmodified application of these results to a rotating mass would seem to be highly misleading.

The nature of the motion which occurs in the rotational problem beyond the series of Jacobi ellipsoids cannot be stated. One conjecture is that the incompressible fluid mass divides into two masses, the smaller being less than one-third of the larger mass, and that they continue to rotate as a rigid body as in the double-star problem. There are other possibilities, however.

The double-star problem, after stability ceases, is even more intractable than the rotational problem. The satellite is stable beyond a distance which corresponds closely to Roche's limit, but it cannot be followed mathematically for smaller distances. After a consideration of the various factors the author says: "Whichever way we approach the problem, the final result of the motion must be a ring of broken fragments, each fragment being so small that its forces of cohesion can resist the mechanical tendency to disintegration. Roche has suggested that Saturn's rings may have been formed in this way. . . ."

The problem of compressible and non-homogeneous fluids is taken up in chapter vii. For matter of uniform composition Jeans shows that the figures of equilibrium can be specified by their boundaries alone, and that therefore the series of such figures must be a linear one, after the manner of the incompressible problem. Corresponding to the

MacLaurin spheroids there is a series of pseudo-spheroidal figures which become exactly spheroidal at the point where they branch into the Jacobi ellipsoids; then a series of pseudo-ellipsoidal figures which become exactly ellipsoidal again at the end of this series. The stability of these figures cannot be predicted from general principles for the rotational problem, but Jeans regards it as possible that the rotating mass may divide up into a number of detached masses instead of only two as in the incompressible case. The general case of incompressibility being too complicated and difficult, Roche's model is taken up. This model goes to the far extreme of compressibility in having a spherical rigid nucleus and an atmosphere of zero density. The simplicity of this model admits of the potential being written down at once, the upper boundary of the atmosphere being one of the equipotential surfaces. For a fixed volume of atmosphere and an increasing rate of rotation the upper boundary of the atmosphere finally develops a cusp or sharp edge at the equator, and for higher rates of rotation the atmosphere must escape at the edge, since the volume of the atmosphere decreases. A slight improvement upon Roche's model is made by assuming that the nucleus, instead of being a rigid sphere, is an incompressible fluid having the same rate of rotation as the atmosphere. This change does not alter the character of the results from the Roche model until the figure of the nucleus becomes ellipsoidal and the corresponding equipotential surfaces become pointed, so that the atmosphere escapes in two streams from these two points.

The same thing happens for the Roche model in the tidal problem. The equipotential surfaces become pointed first on the side toward the tide-rising body and then, if the tidal forces increase with sufficient rapidity, at both ends; and the atmosphere streams out from these ends in a pulsatory manner. In the double-star problem the two atmospheres merely unite, as would be expected.

The very wide gap between the incompressible model (A) on the one hand and Roche's model (B) and the modified Roche's model (C) on the other is filled for the rotational problem by the adiabatic model (D), which consists of a "mass of gas in adiabatic equilibrium, so that the pressure and density are connected at every point by the relation  $p = \kappa \rho^\gamma$ , where  $\kappa$  and  $\gamma$  retain the same values throughout the mass." The results of the analysis for this model are summarized by the author in the following paragraphs:

It follows that as we pass along either of the chains of models C and D which connect A and B, or along any other chain of models connecting A and

B, there must be some point on each at which fissional break-up gives place to rotational<sup>1</sup> break-up. At such a point the two methods of break-up must be about to begin simultaneously with the same rotation. Thus the condition determining such a point is that the centrifugal force shall be precisely equal to gravity on the equator of that configuration at which the rotation reaches such a value that a figure of revolution is no longer a stable form for the mass.

We have determined this critical point on each of the two chains of models C and D. Of these the adiabatic chain D is the more important. As we pass along this chain from A to B the value of  $\gamma$  varies from  $\infty$  to 1.2; the critical point is approximately given by  $\gamma = 2.2$ . Thus a mass of gas or other compressible matter in adiabatic equilibrium will break up by fission if  $\gamma$  is greater than 2.2; it will break up equatorially if  $\gamma$  lies between 1.2 and 2.2. This latter range of course includes the values of  $\gamma$  for all gases whose density is so low that Boyle's law is approximately satisfied; for these  $\gamma$  is always less than 1.66.

Similarly as we pass along the C chain of generalized Roche's models, the value of  $s$ , the ratio of the volume of the nucleus to that of the atmosphere varies from  $\infty$  to 0. The critical point is found to occur at about  $s$  equal to one third. Thus when the atmosphere is less than a third of the volume of the nucleus, the mass will break up by fission; when the atmosphere is greater than this the mass will break up equatorially.

Chapter viii is devoted to a discussion of the problem of von Helmholtz, viz., the flow of energy associated with a contracting, and therefore radiating, mass of gas. Under the assumption that the laws of an ideal gas are obeyed, that the ratio of the specific heats and the opacity are constant throughout the mass and throughout the process of contraction, and that the mass contracts along a series of figures in thermal equilibrium, and certain other assumptions of more or less importance, it is shown that the temperature varies inversely as the radius of the sphere, a law which was first announced by Lane in 1870; and the conclusion is reached that the rate of radiation of energy is a constant, although Jeans does not wish to stand by this conclusion in its application to the sun. It is assumed that eventually the mass arrives at a stage where the density is so great that the laws of an ideal gas are not obeyed, and the rate of radiation falls. Finally, further contraction becomes impossible, and the mass merely cools off in accordance with Stefan's law.

As the application of the abstract theory of rotating masses to the cosmic forms proceeds, the argument becomes less mathematical and frankly more speculative. Thus in chapter ix a serious effort is made

<sup>1</sup> This word should evidently be "equatorial" instead of "rotational," as in the preceding paragraph it is stated that the method of break-up which occurs in Roche's model will be referred to as "equatorial" break-up.

to show that the spiral nebulae have developed out of vastly extended masses of gas. Since the observed spiral nebulae are obviously dissimilar in their details, a purely mathematical theory of them is impossible; their striking similarities, however, suggest a common process which must have a mathematical theory. The argument threads its way through a very complicated and difficult field. It contains many points that are speculative and highly debatable; but it is better to limit ourselves here to the picture which Jeans describes.

Since, as he says, every permanent astronomical body must contract, our extended nebula, once in existence, will do so also. The heavier elements will find their way to the center; and when a rotating figure of equilibrium has been attained the equilibrium will be intermediate between an isothermal equilibrium, for which  $\gamma$ , the ratio of the specific heats, is unity, and an adiabatic equilibrium, for which  $\gamma$  might be equal to  $5/3$ . Inside of this range of values for  $\gamma$  the mass in its process of contraction must arrive eventually at the point of equatorial break-up. The maximum value of  $\gamma$  for which equatorial break-up is possible is  $\gamma = 2.2$ . Diagrams showing a meridional cross-section for  $\gamma = 1.2$  and  $\gamma = 2.2$ , just as the process of break-up is about to begin, are given and are compared with photographs of nebulae seen edgewise. In two of these photographs fair resemblance to the case  $\gamma = 2.2$  is clear, but a rather meager resemblance for the case  $\gamma = 1.2$ . The photographs suggest diamond rather than lenticular shapes. Balancing the probabilities as to the values of  $\gamma$ , the author arrives at the equation  $\omega^2 = 0.035 \times 2\pi$  for the relation between the angular velocity and the mean density at the time when the cuspidal edge is formed. The photographs evidently represent a stage beyond this critical stage. Furthermore they cannot be supposed to represent rigid bodies as do the diagrams. The author himself departs from the equilibrium theory in assuming that the outer parts of the nebula are rotating faster than the inner, and the effect of this departure is to modify the diagram in the general direction of the photographs.

Just what happens after the critical stage sets in is the interesting thing, and unfortunately no one can say. Jeans extends a theorem of Laplace and proves that if a ring is formed it must have a density greater than  $1/3$  of the mean density of the nucleus. This disposes finally of the Laplacian idea as to the formation of the planets in the solar system, if there is anyone who still has any lingering doubts about it.

If a ring cannot form, what can happen? Here Jeans appeals to the tidal forces of the rest of creation, which are admitted to be

infinitesimally small, and assumes that these forces would tend to fix two points on the equator at which and only at which matter would stream forth. Once a stream of matter has begun to issue forth, the tidal forces will be reinforced by the matter already ejected, so that the stream presumably will increase. The matter will not issue forth uniformly; rather it will come in waves, and the interval between the waves is defined by the very simple relation  $c = k\omega$ , where  $c$  is the molecular velocity, and  $\omega$  is the angular rate of rotation. In order that this filament may not simply scatter into space, its line density must be comparable with  $2/3(c^2/k^2)$ , where  $k^2$  is the constant of gravitation. Given the line densities and the length of the waves, it is possible to compute the mass of each of the waves. Using what seem to be probable values, their mass turns out to be eight times the mass of the sun, so that the nuclei in the arms of the spiral nebulae are comparable with the mass of the sun.

It is difficult to believe that the tidal forces mentioned above would act in the way which Jeans describes. Inasmuch as they were in existence before the critical stage set in it seems more probable that they would set up infinitesimal waves of distortion in the rotating mass, for the direction of the tidal forces would be a fixed direction. These waves of distortion might be effective in determining the course of evolution after the critical stage set in, but they could hardly have the effect of pulling out streams of matter from the rotating mass. The molecules at the sharp edge are, in effect, satellites revolving in circular orbits about the primary mass. The effect of the tidal forces would be merely to slightly perturb their orbits. Presumably these perturbative forces would be very much smaller than the perturbative action of the sun on the moon, and yet the moon shows no tendency to rush straight out toward or away from the sun. Such effects as Jeans describes might perhaps occur if a non-rotating mass were held in equilibrium in one of the lenticular figures by suitable fictitious forces. But once a molecule is freed from a rotating primary it takes to orbital motion, and the tidal forces would be merely perturbative. It must be borne in mind that Jeans does not invoke the highly active internal forces which are a vital element of the planetesimal hypothesis of Chamberlin and Moulton, to which Jeans's hypothesis bears a strong superficial resemblance. His primary mass is a quiescent one, and the forces of ejection are tidal. The omission of a strong internal energy seems to be a fatal one.

Chapter x is devoted to a statistical study of stellar systems with particular application to our own galaxy and to globular star clusters.

Our own galaxy<sup>1</sup> is supposed to have been derived from such a rotating nebula as is described in chapter ix. At the stage of break-up of the nebula the equatorial radius was about thirty parsecs, and the period of rotation was of the order of 160,000 years. After the break-up into the units which are now the stars, a process of expansion is assumed to have set in which enlarged the system to its present dimensions of 2000 parsecs radius, and presumably the galaxy is still in the process of expansion. Obviously such an expansion must have occurred if the hypothesis as to its origin is admitted, for the present dimensions are some sixty-six times the supposed original one. The fact that such an expansion is dynamically impossible, however, merely shows that the hypothesis as to its origin is inadmissible.

The proof of this impossibility is very simple. At the moment when instability of the rotating mass set in the relation  $2T_0 + W_0 = 0$  existed, where  $T_0$  is the kinetic energy and  $W_0$  the potential energy; thus  $T_0 = -\frac{1}{2}W_0$ , and the total energy  $T_0 + W_0$  was equal to  $+\frac{1}{2}W_0$ . Suppose now that the process of radiation ceased altogether, and that all of the kinetic energy was absorbed in the process of expansion. Under these assumptions, which are the most favorable possible for a maximum expansion, the total energy,  $E = T + W$ , would be constant, and equal to  $\frac{1}{2}W_0$ . Let the subscript 1 indicate the value at the end of a process of uniform expansion. Then  $\frac{1}{2}W_0 = T_1 + W_1$ . But if  $T_1$  is zero, then  $W_1 = \frac{1}{2}W_0$ . Since the configuration has remained unaltered the relation  $W_1 = \frac{1}{2}W_0$  says that the size of the configuration has merely doubled, and that every molecule is at rest. If the configuration has altered, which is actually assumed in Jeans's hypothesis, it must still be true that  $W = \frac{1}{2}W_0$ , and any increase in the radius beyond two must be offset by a corresponding increase in the density near the center. In other words, only such configurations are admissible as will change  $W$  into  $W_1$  without any work. Now our galaxy at the present time is by no means without kinetic energy, and there is no evidence whatever of a strong central condensation such as would result if the outer boundary had expanded many diameters. We can only conclude, therefore, that an expansion to 66 diameters is wholly impossible.

If we assume that a system of stars moves in such a way that  $W = -k^2/\sqrt{I}$ , where  $k^2$  is a constant factor of proportionality, and  $I$  is the moment of inertia with respect to the center of mass, and such would be the case for any configuration which merely altered its linear

<sup>1</sup> Throughout the volume Jeans has used the word "universe" as synonymous with the word "galaxy"; obviously, the galaxy is but a part of the universe.



dimensions, then Eddington's equation  $d^2I/dt^2 = 4T + 2W$  can be written  $d^2I/dt^2 = 4E + 2k^2/\sqrt{I}$ . For any permanent system the energy,  $E = T + W$ , is a negative constant, and the integration of the foregoing equation shows that  $I$  oscillates with a period equal to  $2\pi k^2/(-2E)^{3/2}$ . So far as these assumptions are applicable to spiral nebulae, and the assumptions seem fairly reasonable ones if the spiral form is anything like a permanent one, then, unless the size is a constant one, it can merely oscillate—sometimes expanding, sometimes contracting. On the assumptions that our galaxy is an oblate spheroid the axes of which are in the ratio of 10 to 3 and the equatorial radius 2000 parsecs, that there are  $1.5 \times 10^9$  stars uniformly distributed and of such mass that the mean density of the spheroid is  $5 \times 10^{-23}$ , and that the average star has a velocity of 25 kilometers per second, and these are the figures actually adopted by Jeans, then if the galaxy is expanding at the present time its period of oscillation is 25 million years, and at the end of this period it must have returned to the condition from which it started. This period would be increased to 100 million years if the density were only  $1/5$  of that previously assumed and the velocities were increased from 25 to 40 kilometers per second. According to Jeans's hypothesis the process of expansion has been going on for something like 500 million years and is still continuing. The entire period of oscillation, therefore, must be well over 1000 million years, and such a period is inconsistent with our present astronomical data.

The frequency of close approach of stars is the next topic discussed, and the effects which these individual encounters have in diverting the path of a star from a straight line; in other words, in developing a cross-velocity. Inasmuch as this cross-velocity amounts to only 1 kilometer per second after 40,000 million years in our own system, it is clear that the effects of individual encounters in a period of 500 million years, which Jeans regards as the order of astronomical time, would be negligible; and the motion of a star depends almost entirely on the massed action of all the stars of the entire system. As Jeans puts it, "the problem of stellar dynamics is the same as the problem of the kinetic theory of gases with the collisions left out," and is therefore very much simpler.

The study of the distribution of the stars, particularly with respect to steady states of motion, shows that, except for certain artificial cases, "the only possible configuration for a cluster of stars moving freely under their own gravitation in steady motion are those in which the stars either form a spherically symmetric figure or a figure of revolution which is symmetrical with respect to an axis." With respect to

our own system of stars the indications are that we are approaching a steady state but have not yet reached it. After an examination of the rate of approach the author states: "Thus it appears that after an interval of 10,000,000 years the courses of the stars will be little altered; their orbits over 10,000,000 years are not far removed from the straight lines they would describe if gravitation were suddenly annihilated. It is clear that the approach to a steady state is an excessively slow process." In order to reconcile this perfectly obvious conclusion with the apparently obvious conclusion that our system of stars has already approached a steady state of motion in the not-at-all obvious period of 500 million years, recourse is had to the previous notion that in the early stages of the process the radius of the galaxy was only 30 parsecs, and consequently the stellar density was about 300,000 times as great as at present. In this condensed condition the time requirements would be very much less severe, and "what gravitation fails to accomplish now in 10 million years may have been accomplished in 10,000 years when the system was young and the stars closely packed together." As the assumption that the system has expanded in the previously described manner cannot be granted, the reconciliation has not been effected, and we are forced to the conclusion that the period of 500 million years is very seriously in error.

Other interesting conclusions of this statistical study are that the phenomenon of star-streaming does not exist when the steady state of motion has been attained; that a steady state of motion can never be perfectly attained by a stellar system; and that in our system the stars of types A, F, G, K, and M seem to be approximately in a steady state, while the B-type stars do not.

Chapter xi is devoted to a consideration of the origin and evolution of binary and multiple stars. It is taken for granted, without question or argument, that binary stars have originated from a single nebula by a process of fission, although in the last paragraph of the chapter the possibility is recognized that a binary star may have originated in some exceptional cases from what might be called a double nebula. The preliminary considerations in which the gas is thought of as an adiabatic mass of air leads to the following conclusions:

- a) No binary star which has formed by fission can have a density of less than about  $\frac{1}{4}$ .
- b) No giant binary can have been formed by fission.
- c) The temperature of a binary star which has been formed by fission must decrease as its evolution progresses.

These conclusions being out of harmony with observations Jeans finds it necessary to revise his data. The justification of this revision is sought in the high internal temperatures of the stars, which, according to Emden and Eddington, may be as high as 10,000,000 degrees. This high temperature may modify the properties of the gas so that fission becomes possible. In short, Jeans assumes that, since the star is double, fission must have occurred. Jeans's process of fission is different from that of Darwin in that Darwin thought of it as a statical process, while Jeans thinks of it as cataclysmic, i.e., the two components were separated with considerable relative velocity. Owing to their elliptic motion, however, they must continually collide at periastron with a diminution of eccentricity at each collision. These repeated collisions keep getting milder and milder until finally the two stars just graze one another at periastron, the eccentricity being reduced not quite to zero, and the process of fission is complete.

The foregoing process is largely an imaginary one, as it is far too complicated to follow with an exact analysis. If the two stars were just in contact one would infer from the analysis of chapter vii that the figure of the smaller mass was unstable, for it would have been unstable for both the incompressible model and the modified Roche model. To assign an eccentricity to the relative orbit of the smaller body would seem to make matters worse, for, even if the figure was stable but very close to instability, a collision due to the eccentricity would probably precipitate another cataclysm and result in the scattering of the material of the smaller body in the form of a ring. It does not seem possible to get the smaller mass outside of the Roche limit in safety, and it is very hard to see how a double star can result from the process of fission. If this difficulty is in reality an insuperable one, it would seem that Moulton was correct in his opinion that Darwin overestimated the importance of these forms of equilibrium from an astronomical point of view.

Laying aside this difficulty, however, we proceed to the effects of tidal action on the subsequent evolution, and it is to Darwin that we owe the foundations of this study. One of the first conclusions reached is that the tidal action increases both the eccentricity and the mean distance. But it is very quickly found that for homogeneous masses the latus rectum cannot be doubled, however long the tidal action may have continued. The range is still less for compressible masses, provided the ratio of the masses does not exceed  $2\frac{1}{2}$  to 1. As for the period, it is found that the maximum increase is 13.6 times; for most binaries however the maximum is 4.4 times. Furthermore Jeans concludes:

Thus under no circumstances can the semi-latus rectum of a binary system in which  $M/M' < 2\frac{1}{2}$  exceed the mean radius of the primitive nebula at the instant at which the spheroidal form became unstable. . . . If we suppose the spectroscopic binaries to have originated by fission the problem of explaining why it is that short period binaries are generally of small eccentricity of orbit and of early spectral type, the reverse being true of long period binaries, admits of no answer so long as we regard a binary star as a self contained dynamical system.

In 1909 the Carnegie Institution of Washington published a volume, entitled *The Tidal and Other Problems*, which contained two papers by F. R. Moulton on the formation of binary stars by the process of fission and their subsequent separation by tidal action as imagined by Darwin. The results of these papers were again summarized by Moulton in his *Introduction to Astronomy* (second edition, 1916, p. 543). Neither of these publications is referred to by Jeans, although they contain most of the conclusions which he has reached in his discussion and many others. On the whole, these conclusions, first arrived at by Moulton and later by Jeans, are against the hypothesis that binary stars originated from a single star by a process of fission due to rapid rotation, without, however, completely disproving it. It appears from both discussions that if the fission occurred at all it must have occurred while the star was still in a very tenuous nebulous state; and to the reviewer it seems that the formation of two stars from a single nebula was due, if it occurred at all, to irregularities in the density of the nebula rather than to the process of fission as described by Darwin.

In order to give the fission theory the benefit of every possible doubt, however, Jeans next takes into account the influence of the other stars on the supposedly new-born binary star. The general effect of the mass of all the stars upon the system is merely tidal, resulting in minute perturbations. The secular effect is infinitesimal, so that there remains only the effect of the individual encounters. Any single encounter might result in any kind of an effect, owing to the great variety of circumstances and conditions under which the encounter might take place. The statistical effect of very large numbers of encounters, as implied by the equipartition of energy, is to make the eccentricity tend toward the definite value  $e=0.637$  and to increase the major axis. "Any group of stars which has experienced a large number of stellar encounters will have orbits in which the eccentricities are ranged according to the law  $2e de$  round a mean value of  $2/3$ , while the periods will depend on

the mass of the star, being of the order of a year for stars of the average mass 1.7 times the mass of the sun."

Thus the effect of stellar encounters with the binary system is to bring the fission hypothesis and the subsequent evolution into harmony with Campbell's table, which exhibits the relations between the various types of stars and their periods and eccentricities. A very interesting point which is not discussed is the survival of a binary system as a result of the first few encounters when the binary is still struggling to maintain its dual character. What proportion of them would survive, and what proportion of them would experience another cataclysm? Apparently 35 to 40 per cent of the stars are binary. The only star which we can observe directly has a very low rate of rotation, suggesting naturally that many other stars are in a similar state of poverty as to rotation. Bearing this fact in mind, and the further fact that a binary once formed was subject to many vicissitudes in its struggle to maintain duality if it was formed by the process of fission, it must be admitted that the number of stars that actually are binary is surprisingly large.

There remains one more difficulty in Jeans's appeal to the equipartition of energy, viz., the interval of time necessary for many encounters. An encounter as close as Neptune is to the sun would occur once on an average in an interval of time which is of the order of a million million years, and to have any statistical effect very many such intervals must have elapsed. The effect of a single encounter at this distance upon a close and rapidly revolving binary would be very small, as is clear from the fact that the presence of the sun lengthens the moon's period by about one hour only, and even this effect would be greatly reduced if the moon were almost in contact with the earth, as would be the case in a binary newly formed by fission. The average time interval for an encounter as close as the sun is to the earth is of the order a million billion ( $10^{15}$ ) years. It is clear, therefore, that if the dynamics of our galaxy are such as would be expected from the use of statistical methods, and it is becoming more apparent year by year that this is approximately true, then the age of the galaxy must be great beyond any order of time which has hitherto been commonly entertained. Jeans's hypothesis that the process was relatively much more rapid a few hundred million years ago because the system was at that time very much condensed cannot be admitted, since the energy of the system is definitely against it. We are face to face with a new conception of the order of astronomical time.

Just as a single star divides by the process of fission into a binary, so a binary at a later stage may subdivide into a triple or multiple system. If it does so the density at the second division must have been greater than 342 times the density at the first division, and the periods will be of the order of 18 to 1. An interesting summary of a statistical study of triple systems by Russell is given. From this study it is concluded that systems in which the separation of the components is less than 1000 years' proper motion may have formed by fission, while systems in which the separation is greater than 1000 years' proper motion may have had a different origin, possibly from a double nebula.

The last chapter of the book, chapter xii, deals with the origin and evolution of the solar system. Naturally the rotational picture as described by Laplace receives the first consideration. The weight of modern opinion is rather decidedly adverse to the Laplacian system of rings, and, with perhaps a mild reservation, Jeans agrees with this decision. In addition to other difficulties, many of which are carefully analyzed, this hypothesis implies that the sun should have divided into a binary, which it has failed to do.

The only other hypothesis considered is what Jeans calls the tidal hypothesis, which bears a very close resemblance to the planetesimal hypothesis, though not identical with it. The tidal hypothesis considers the break-up of a gaseous mass by purely tidal action, and for this purpose a vastly distended condition of the sun, even out to the orbit of Neptune, is considered most favorable. The planetesimal hypothesis, on the other hand, presupposes a sun much the same as our present sun, with a very high order of internal energy, the tidal action serving merely to release and direct the action of this internal energy. In the early stages the two ideas are quite different, although in the later stages the two types of evolution are much the same.

The general harmony of our actual system with this idea is first noted, and then the details are brought before the bar for examination. Obviously the first objection is the improbability of a close encounter happening. In the present state of the galaxy an approach to within three times the distance of Neptune would occur only once on an average in 300,000 million years, although in the earlier hypothetically condensed condition of the galaxy this interval would be reduced to 3 million years. For an expanded state of the sun Jeans might have made this objection much stronger, for if his former conclusion that the rate of radiation is constant is correct, and if the present rate of radiation is the

same as the earlier rate, then the sun would have shrunk from an infinitely distended state in periods given in the following table:

Distance	Years	Distance	Years
Neptune.....	2940	Mars.....	58,000
Uranus.....	4600	Earth.....	88,000
Saturn.....	9250	Venus.....	122,000
Jupiter.....	16,000	Mercury.....	228,000

Present size, 18,900,000

Thus the improbability of the event depends, even for the condensed condition of the galaxy, upon the size of the sun which is adopted. Under the most favorable assumptions there would be only one chance in a thousand for the conditions which Jeans considers most favorable for tidal action. In this respect a sun of the present size, as postulated by the planetesimal hypothesis, has a great advantage; but for a purely tidal theory this condensed condition of the sun would require a much closer approach of the secondary sun and consequently a very much more extended time interval, the time interval varying inversely as the square of the distance of closest approach.

We shall not follow Jeans through the detailed examination of this hypothesis, which is more or less familiar to those who are interested in this subject. It will be sufficient to quote his final paragraph:

This vague sketch of the tidal theory will, it is hoped, be read as an indication of the possibilities open to the tidal theory, rather than as an attempt to advocate the theory or present it in a final form. The theory is beset with difficulties, and in some respects appears to be definitely unsatisfactory. To the author it appears more acceptable than the rotational theory, or any other theory so far offered of the genesis of the solar system; but an enormous amount of mathematical research appears to be needed before the theory can either be advocated with confidence or finally abandoned.

To the reviewer the planetesimal hypothesis, as set forth by Chamberlin and Moulton, seems much preferable to the purely tidal theory as discussed by Jeans, for the questions of density of the detached masses are far less troublesome. Furthermore the planetesimal hypothesis will survive even though the idea that the sun has condensed from a vastly distended nebula be discarded; while the purely tidal hypothesis apparently will not.

The last topic discussed by Jeans is the time scale. The gravitational theory of the sun's heat provides for 20 million years, and

the radioactive sources do not add much to this. The estimates of the geologists as to the age of the earth seem to converge to a period of some 250 million years. As for the galaxy, only ten oscillations of a star across the galaxy require 3000 million years, and hardly less than that would suffice for the present distributions of the stars and their velocities. These estimates are discordant, but the time for the galaxy can be reduced by supposing that it was once in a much-condensed condition, so that the time of an oscillation was much smaller. He states that the age of the sun can be much lengthened by supposing that three-fourths of the sun's energy has been radiated in the last 15 million years, while the remaining one-fourth was dissipated during an interval of 200 million years, notwithstanding that this last supposition violates the former conclusion that the rate of dissipation should be a constant. Balancing up these various estimates he concludes that the age of the galaxy is of the order of 500 million years, and that there are no difficulties of a serious nature on the score of time.

The volume is brought to a close with a brief résumé of the ideas which have just been discussed, and a statement that these ideas merely seem more probable than others in the present state of our knowledge. No final decision is as yet possible.

Human nature is cautious and conservative when considered in the mass. An idea, once well established, continues to survive generation after generation, even long after its usefulness has ceased. A sort of intellectual inertia preserves its existence, much in the same fashion as a religious dogma. During the early part of the nineteenth century the Laplacian nebular hypothesis made a wonderful appeal to the scientific imagination of that era. Its beauty and simplicity and apparent harmony with the observed facts established it in a position of security and confidence, so that it modified very profoundly the scientific thought of the entire century. By the middle of the century ideas had become much cleared with respect to the doctrine of energy, and in particular the mechanical equivalence of heat had been established. This enabled von Helmholtz to make a great contribution to the nebular hypothesis, and indeed the only essentially new idea that has ever been added to it, by showing how the heat of the sun could be supposed to have been maintained by the process of contraction; and that this source would be sufficient to provide the sun with energy at its present rate of emission for about 20 million years.



By this time the doctrine of evolution in its entire generality had been established by Herbert Spencer, and a highly developed special doctrine in the field of biology by Charles Darwin. The geologists were accepting the doctrine of uniformity in the geological processes instead of their previous notions of geological catastrophes. Gradually the geologists and biologists began to find themselves cramped by the limitations on time which the astronomers and physicists were imposing upon them. Unable to come to any agreement with the astronomers and physicists on the questions of time, the geologists and biologists went their own way and ignored the astronomers and physicists altogether. The evidences close at hand in their own fields were far more certain, more tangible, and more numerous than the mere speculations of the astronomers as to the sources of the sun's heat. The implications of these evidences could not be ignored. Gradually the geologists extended their time estimates from a few millions of years to a few hundreds of millions. Increasing geological evidence has uniformly pushed upward their time estimates, until now there are reliable estimates as high as 1600 millions of years.<sup>1</sup> That these estimates are out of harmony with the Laplacian doctrine is nothing to them; let the astronomers look after their own troubles. In this attitude the geologists are strictly correct, for they are following their own lines of evidence.

The discovery of the radioactive processes some twenty years ago seemed for a time to offer the astronomers a way out of their embarrassment, but at best the relief was but a partial one, and their time estimates are far below the demands of the geologists. But worse was still to come, from the Laplacian point of view. Not only have the geologists attacked the Laplacian implication as to time, but they have also attacked the Laplacian implication as to a once molten earth. Professor T. C. Chamberlin finds the evidences of earth structure out of harmony with a once molten condition, and in collaboration with

<sup>1</sup> In a very careful study of the various lines of evidence as to the age of the earth Arthur Holmes (*The Age of the Earth*, 1913) showed that there are only two that have stood the tests of destructive criticism; one is the geological and the other the radioactive. The geological methods rest upon measurements of the amount of salt in the oceans, the thickness of the sedimentary strata, and the deposits of calcium carbonate. These three lines are not independent but are intimately related. The estimates from them are concordant, 100 million to 300 million years, but they stand or fall together. The radioactive method, which commands a higher confidence on the part of the geologists, leads to estimates as high as 1600 million years for the age of some of the oldest rocks, and evidently the earth itself is still older. The reconciliation between the two methods is effected by showing that the geological methods lead to minimum estimates only.

Professor F. R. Moulton has offered a hypothesis as to the origin of the planetary system which is more acceptable than the Laplacian hypothesis, not only to many geologists but also to many astronomers. The formulation of the planetesimal hypothesis by Chamberlin and Moulton has necessarily involved renewed attacks upon the Laplacian hypothesis, so that even Jeans casts his vote against it so far as the formation of the planetary system is concerned.

These attacks upon the origin of the planetary system have not, however, directly involved the question of the origin of the sun. Except that they insist upon having their allotted interval of time, the geologists are quite willing that the astronomers should let their suns condense out of nebulae if they wish to; but the geologists must have plenty of time. This is precisely the condition which the condensation hypothesis will not permit. On the hypothesis that the energy of the sun is due to its contraction, and that the rate of radiation is constant, the age of the sun cannot exceed 20 million years. To suppose, as Jeans has done, that this period can be extended to 250 million years by imagining that the rate has been constant during the last 15 million years, and only one-fortieth as great as at present during the remainder of the time, is merely playing with words, for the actual effect would be to reduce the geological period to 15 million years, and not to extend it to 250 million years, because if the earth received only one-fortieth of its present quota of energy it would be a solidly frozen waste. Any other hypothesis as to a reduced rate of radiation in the past encounters the same trouble—it reduces the geologic period instead of extending it. The conclusion is therefore unavoidable on geologic grounds that the energy of the sun does not come essentially from the process of contraction, and that the entire Laplacian conception of the origin of stars from contracting nebulae is incorrect.

It is not necessary for the astronomers to go to the geologists for this conclusion. The structure of the stellar systems has implications as to time as certainly as has the structure of the earth. On the general principle that the whole is greater than a part one would naturally expect the order of astronomic time to be vastly greater than the order of geologic time. This anticipation is amply justified by the dynamics of the galaxy. The close approach of two stars is an event of fundamental importance in the system; and if one astronomical unit be the order of approach the expectation of any one star is of the order of a million billion ( $10^{15}$ ) years. At the distance of Neptune it is of the order of a million million years. Jeans has shown in the present volume

that a cross-velocity of one kilometer per second would be generated by the more distant encounters in a period of something like 40,000 million years. He is furthermore in agreement with Charlier that the cross-velocity would be of the same order of magnitude as the velocity itself in a period which is of the order  $10^{15}$  years. He states also that the galaxy is well along toward a state of steady motion, and that in the present state of the galaxy the rate at which this steady state is being approached is an excessively slow one. In these statements we are in hearty accord, and we are perfectly willing to accept their logical implication that the age of the galaxy is excessively great.

This conclusion is in harmony with what we see at present. It is not in harmony with the contraction hypothesis as to the origin of the stellar energies. Indeed, there is but little that is in harmony with this hypothesis save the law of gravitation itself, and there is nothing in this single harmony to compel us to believe that it is an essential factor in the case. Observational astronomy does not support it. There are no examples to which one can point with any certainty by way of illustration. There is no sequence of figures showing the various stages of a process that is supposed to be universal. There are many nebulae in the sky, but they show no tendency toward spherical shapes, and even the planetary nebulae fail to stimulate our hopes. The galaxy should be full of masses of stellar dimensions which are dead and cold and solid, but there is no evidence of any such. The earth is the largest body, of which we have any certain knowledge, that is solid. Jupiter and Saturn are almost certainly purely gaseous, while Uranus and Neptune seem to be neither purely solid nor purely gaseous. The range of masses of the stars, so far as we know them, is not great, while under the condensation hypothesis we have no reason to anticipate any limits at all. The relatively large number of runaway stars forbids us to believe that they are merely ejected members of our own system, and if they have come from other galaxies we are forced to believe that they, at least, are very old. The almost incredibly large number of temporary stars tells us unmistakably that the cosmos knows of other things than the law of gravitation and the kinetic theory of gases. In fact, in whatever direction we may push our inquiries, we find little or nothing to encourage our faith in the hypothesis of contraction.

The spectral types of the stars fitted in with it fairly well, but it is a case of fitting in with it rather than a case of lending it any support. In the way of genuine support of an observational character there is virtually nothing. It has had a highly respected past because the

simplicity of the idea has attracted to it the talents of great mathematicians. The name of Laplace gave it standing from the beginning. Von Helmholtz rescued it from an early grave by showing that the contraction would produce vast amounts of heat; while Lane showed that the production of heat was greater than the radiation, and that therefore the temperature would rise. Darwin suggested that an excess of angular momentum might cause a mass to divide into two masses. Not only would this process of fission explain the origin of our own moon, but it could also be called into service to explain the existence of binary and multiple stars. This idea seems to have fascinated Poincaré, and it was the inspiration of his great paper on the figures of equilibrium of rotating fluid masses.

This very brief review of its history shows that the mathematicians have had a grand time with the hypothesis that the stars have had their origin in the contraction of a nebular mass. It challenged their powers without ever wholly discouraging their efforts. The early successes of Laplace, Helmholtz, and Lane and the partial success of Darwin have given the hypothesis an almost universal currency, so that Jeans accepts it as a fundamental postulate without even a question. To him "the problem of cosmogony is to discover these origins [of astronomical forms] and to prove [by means of the contraction hypothesis?] that they would lead to the observed formations." If this be accepted as a definition of the scope of cosmogony, then cosmogony is merely a subtitle in the more general subject of cosmology, which might be defined as the study of the transformations of energy throughout the cosmos, the study of origins being of no more interest than the study of dissolutions; the study of forms, however, is vital, as they are our only observational means of determining the transformations of energy which are occurring.

Looked at from this point of view the contraction hypothesis is seen to be a very one-sided affair. It postulates the existence of the necessary nebulae with no inquiry as to the origin of the nebula, a matter which is just as important as the star itself. It is satisfied to bring the picture down to date and to ignore altogether the question of dissolution. There are some hundreds of thousands of spiral nebulae which, as many believe, may be galaxies like our own. They are in varying states of development; but if the radiation of their stars is limited to some such period as 1000 million years, which is a very generous estimate for the contraction hypothesis, we cannot help but wonder how so many of them got started all at once, for 1000 million years is a very brief time, so far as we can see, in the total physical existence of a galaxy. In a

few hundreds of millions of years they will all be cold and dead and literally petrified. But they still exist, even though the light of the skies be all gone. For millions of billions of years they plow their way through darkness. Even a collision of two galaxies would not result in a catastrophe, though it might result in a slight scattering of the dead stars. The period of light and luminescence is as but a flash of lightning as compared with the period of darkness and death, a period which would seem to be so long that we are almost tempted to call it permanent.

It would scarcely seem possible that anyone could entertain so dismal a picture, and yet it is a logical implication of the contraction hypothesis.

So much for the future of the astronomical forms which we see! What becomes of the radiant energy which the stars are pouring into space at such an extravagant rate? Are we to suppose that it too pursues an endless journey with no further incidents than an occasional reduction in wave-length as a consequence of its interception by some physical mass? As the contraction hypothesis says nothing whatever on this subject we are at liberty to believe what we please, for we are in the fields of cosmology, and not cosmogony.

More strictly, to the domain of cosmogony belongs the question as to the origin of molecules, atoms, and electrons. In the days of Laplace and von Helmholtz the atom was a fundamental and permanent physical unit; there was no need of considering its origin. Today we recognize that it has an organized structure—a unit that has been built up, as have all the other units, and likewise susceptible to destruction. Their vast numbers are comparable, so to speak, only with the vastness of astronomical space; for if the mass of the solar system were uniformly distributed over the sun's share of space there would be approximately 10 cubic centimeters of space for each atom, and relatively to their sizes they would be as far apart as are the stars. The energy required for their organization also is very great, so that one can scarcely avoid the conclusion that their origin is an astronomical affair. If this speculation is correct, then the problems of cosmogony are very largely extended. Not only must the stars and galaxies be accounted for, but also the electrons, atoms, molecules, and nebulae. Fortunately our information with respect to the physical units, from electrons to galaxies, is very rapidly advancing. In the domain of cosmology facts are outstripping theory. We are very greatly in need of intelligent speculations, particularly speculations which will co-ordinate the physical processes of the cosmos and make intelligible the ebb and flow of energy as it surges

up and down the series of physical units. It was this service that the contraction hypothesis rendered to the scientific thought of the first half of the last century. But it is not sufficiently comprehensive in its scope nor sufficiently in agreement with our interpretations of observations to be any longer acceptable.

Jeans has made a splendid exposition of the theory in the present volume, and we are grateful to him for illuminating many points which have not hitherto been clear. But the real value of his analysis has been obscured by two unfortunate errors: the first of these was the attempt to harmonize the age of the galaxy with the age of the sun, by supposing that the galaxy was formerly in a very much condensed condition so that the process of the distribution of the velocities of the stars proceeded much more rapidly than at present; the second was the attempt to harmonize the age of the sun with the geological estimates of the age of the earth by a mere play upon words. It would have been much better had he regarded the contraction theory as a hypothesis to be tested rather than as a postulate into which other things must necessarily fit. Had he done so, he would not have left with the reader the impression that the process of fission satisfactorily accounts for the binary stars, and that the gravitational source of the sun's heat is quite adequate for all purposes. The facts, as we see them, are quite the contrary, and a frank recognition of these difficulties would have compelled an equally frank rejection of the condensation hypothesis, thereby clearing the way for newer pictures which will not only take into account the discoveries of modern physics with respect to the structure and elemental properties of matter but will also harmonize with the equally wonderful advances of the astronomers in their studies of the structure of the cosmos.

W. D. MACMILLAN

UNIVERSITY OF CHICAGO  
April 1920

# INDEX TO VOLUME LI

## SUBJECTS

	PAGE
Absorption Bands of Halogen Acids, Fine Structure of the Near Infra-Red. <i>Walter F. Colby</i> . . . . .	230
Abstracts, Preparation of . . . . .	190, 255
Acids, Fine Structure of the Near Infra-Red Absorption Bands of the Halogen. <i>Walter F. Colby</i> . . . . .	230
Air Lines in Spark Spectra from $\lambda$ 5927 to $\lambda$ 8719. <i>Paul W. Merrill</i> . . . . .	236
Barium, in Region of Greater Wave-Length, Electric Furnace Spectrum of. <i>Arthur S. King</i> . . . . .	179
Barium, Revision of Series in Spectrum of. <i>F. A. Saunders</i> . . . . .	23
Boss 5026, Orbits of the Spectroscopic Components of. <i>W. E. Harper</i> . . . . .	187
Boss 1517, Parallax of the Star. <i>J. Votile</i> . . . . .	254
Brightness Ratio, Gold-Point Palladium-Point. <i>Edward P. Hyde</i> and <i>W. E. Forsythe</i> . . . . .	244
Calcium in Region of Greater Wave-Length, Electric Furnace Spectrum of. <i>Arthur S. King</i> . . . . .	179
Catalogue of 848 Stars in Messier 3, Photometric. <i>Harlow Shapley</i> and <i>Helen N. Davis</i> . . . . .	140
$\delta$ Cephei Variables, Problem of the. <i>J. G. Hagen</i> . . . . .	62
Clusters, Studies Based on Colors and Magnitudes in Stellar. Fifteenth Paper: Photometric Analysis of Globular System Messier 68. <i>Harlow Shapley</i> . . . . .	49
Sixteenth Paper: Photometric Catalogue of 848 Stars in Messier 3. <i>Harlow Shapley</i> and <i>Helen N. Davis</i> . . . . .	140
Clusters in Sagittarius and Scutum, Bright Nebulae and Star. <i>John C. Duncan</i> . . . . .	4
Cobalt in the Region of Greater Wave-Length, Electric Furnace Spectrum of. <i>Arthur S. King</i> . . . . .	179
Comet 1919b and on the Rejection of a Comet's Tail. <i>E. E. Barnard</i> . . . . .	102
Diffraction of Telescopic Objective in Case of a Circular Source of Light. <i>H. Nagaoka</i> . . . . .	73
Double Stars, Application of Michelson's Interferometer Method to Measurement of Close. <i>J. A. Anderson</i> . . . . .	263
Eclipse of May 29, 1919, Observations of Total Solar. <i>C. G. Abbot</i> and <i>A. F. Moore</i> . . . . .	1
Electron Theory of Dispersion to Account for Change of Refractive Index with Temperature, A Modification of the. <i>E. O. Hulburt</i> . . . . .	223
Errata . . . . .	308

	PAGE
Gold-Point Palladium-Point Brightness Ratio. <i>Edward P. Hyde and W. E. Forsythe</i> . . . . .	244
Gratings, Polarization of Radiation by. <i>L. R. Ingersoll</i> . . . . .	129
Halogen Acids, Fine Structure of Near Infra-Red Absorption Bands of. <i>Walter F. Colby</i> . . . . .	230
Interference Methods to Astronomical Measurements, Application of. <i>A. A. Michelson</i> . . . . .	257
Interferometer Method to Measurement of Close Double Stars, Application of Michelson's. <i>J. A. Anderson</i> . . . . .	263
Kayser, Note Concerning Retirement of Professor . . . . .	128
Magnitudes in Stellar Clusters, Studies Based on the Colors and. Fifteenth Paper: A Photometric Analysis of the Globular System Messier 68. <i>Harlow Shapley</i> . . . . .	49
Sixteenth Paper: Photometric Catalogue of 848 Stars in Messier 3. <i>Harlow Shapley and Helen N. Davis</i> . . . . .	140
Messier 68, Photometric Analysis of Globular System. <i>Harlow Shapley</i> . . . . .	49
Messier 3, Photometric Catalogue of 848 Stars in. <i>Harlow Shapley and Helen N. Davis</i> . . . . .	140
Michelson's Interferometer Method to Measurement of Close Double Stars, Application of. <i>J. A. Anderson</i> . . . . .	263
Nebulae and Star Clusters in Sagittarius and Scutum, Bright. <i>John C. Duncan</i> . . . . .	4
Nebulae with 60-Inch Reflector, 1917-1919, Photographs of. <i>Francis G. Pease</i> . . . . .	276
Nickel in Region of Greater Wave-Length, Electric Furnace Spectrum of. <i>Arthur S. King</i> . . . . .	179
Note Concerning Retirement of Professor Kayser . . . . .	128
Notice to Contributors . . . . .	192
Nova Ophiuchi 1919, Spectrum of. <i>Walter S. Adams and Cora G. Burwell</i> . . . . .	121
Objective in Case of Circular Source of Light, Diffraction of a Telescopic. <i>H. Nagaoka</i> . . . . .	73
Ophiuchi 1919, Spectrum of Nova. <i>Walter S. Adams and Cora G. Burwell</i> . . . . .	121
Orbits of Spectroscopic Components of Boss 5026. <i>W. E. Harper</i> . . . . .	187
$\pi^s$ Orionis, Ellipsoidal Variable Star. <i>Joel Stebbins</i> . . . . .	218
Palladium-Point Brightness Ratio, Gold-Point. <i>Edward P. Hyde and W. E. Forsythe</i> . . . . .	244
Parallax of the B-Star Boss 1517. <i>J. Voûte</i> . . . . .	254
Photometric Analysis of Globular System Messier 68. <i>Harlow Shapley</i> . . . . .	49
Polarization of Radiation by Gratings. <i>L. R. Ingersoll</i> . . . . .	129
Radial Velocities, Five Oe5 Stars with Variable. <i>W. Carl Rufus</i> . . . . .	252
Radiation by Gratings, Polarization of. <i>L. R. Ingersoll</i> . . . . .	129
Refractive Index with Temperature, A Modification of Electron Theory of Dispersion to Account for Change of. <i>E. O. Hulburt</i> . . . . .	223



Reviews:	PAGE
Eccles, J. R. <i>Advanced Lecture Notes on Light</i> (Edwin B. Frost) . . . . .	128
Jeans, J. H. <i>Problems of Cosmogony and Stellar Dynamics</i> (W. D. MacMillan) . . . . .	309
March, Arthur. <i>Theorie der Strahlung und der Quanten</i> (A. C. Lunn). . . . .	127
Ricco, Annibale, 1844-1919. <i>Giorgio Abetti</i> . . . . .	65
Sagittarius, Bright Nebulae and Star Clusters in. <i>John C. Duncan</i> . . . . .	4
Scutum, Bright Nebulae and Star Clusters. <i>John C. Duncan</i> . . . . .	4
Spectra from $\lambda$ 5927 to $\lambda$ 8719, Note on Air Lines in Spark. <i>Paul W. Merrill</i> . . . . .	236
Spectra of Cobalt, Nickel, Barium, Strontium, and Calcium in Region of Greater Wave-Length, Observations of Electric Furnace. <i>Arthur S. King</i> . . . . .	179
Spectra, Preliminary Observations of Zeeman Effect for Electric Furnace. <i>Arthur S. King</i> . . . . .	107
Spectra Produced by Electric Furnace, Absorption. <i>Arthur S. King</i> . . . . .	13
Spectroscopic Components of Boss 5026, Orbits of the. <i>W. E. Harper</i> . . . . .	187
Spectrum of Barium, Revision of Series in. <i>F. A. Saunders</i> . . . . .	23
Spectrum of Electrically Exploded Wires. <i>J. A. Anderson</i> . . . . .	37
Spectrum of Nova Ophiuchi 1919. <i>Walter S Adams and Cora G. Burwell</i> . . . . .	121
Star Boss 1517, Parallax of the B-. <i>J. Volte</i> . . . . .	254
Star Boss 5026, Orbits of Spectroscopic Components of. <i>W. E. Harper</i> . . . . .	187
Star $\pi^5$ Orionis, Ellipsoidal Variable. <i>Joel Stebbins</i> . . . . .	218
Star $\lambda$ Tauri, Eclipsing Variable. <i>Joel Stebbins</i> . . . . .	193
Stars, Application of Michelson's Interferometer Method to Measurement of Close Double. <i>J. A. Anderson</i> . . . . .	263
Stars in Messier 3, Photometric Catalogue of 848. <i>Harlow Shapley and Helen N. Davis</i> . . . . .	140
Stars with Variable Radial Velocities, Five Oe5. <i>W. Carl Rufus</i> . . . . .	252
Strontium in Region of Greater Wave-Length, Electric Furnace Spectrum of. <i>Arthur S. King</i> . . . . .	179
Studies Based on Colors and Magnitudes in Stellar Clusters.	
Fifteenth Paper: Photometric Analysis of Globular System Messier 68. <i>Harlow Shapley</i> . . . . .	49
Sixteenth Paper: Photometric Catalogue of 848 Stars in Messier 3. <i>Harlow Shapley and Helen N. Davis</i> . . . . .	140
$\lambda$ Tauri, Eclipsing Variable Star. <i>Joel Stebbins</i> . . . . .	193
Temperature, Modification of Electron Theory of Dispersion to Account for Change of Refractive Index with. <i>E. O. Hulburt</i> . . . . .	223
Variable Star $\lambda$ Tauri, Eclipsing. <i>Joel Stebbins</i> . . . . .	193
Variable Star $\pi^5$ Orionis, Ellipsoidal. <i>Joel Stebbins</i> . . . . .	218
Variables, Problem of $\delta$ Cephei. <i>J. G. Hagen</i> . . . . .	62
Zeeman Effect for Electric Furnace Spectra, Preliminary Observations of. <i>Arthur S. King</i> . . . . .	107

## INDEX TO VOLUME LI

### AUTHORS

	PAGE
ABBOT, C. G., and A. F. MOORE, Observations of the Total Solar Eclipse of May 29, 1919 . . . . .	I
ABETTI, GIORGIO. Annibale Riccò, 1844-1919 . . . . .	65
ADAMS, WALTER S., and CORA G. BURWELL. Spectrum of Nova Ophiuchi 1919 . . . . .	121
ANDERSON, J. A. Spectrum of Electrically Exploded Wires . . . . .	37
Application of Michelson's Interferometer Method to the Measurement of Close Double Stars . . . . .	263
BARNARD, E. E. Comet 1919b and on the Rejection of a Comet's Tail	102
BURWELL, CORA G., and WALTER S. ADAMS. Spectrum of Nova Ophiuchi 1919 . . . . .	121
COLBY, WALTER F. Fine Structure of the Near Infra-Red Absorption Bands of the Halogen Acids . . . . .	230
DAVIS, HELEN N., and HARLOW SHAPLEY. Studies Based on the Colors and Magnitudes in Stellar Clusters.	
Sixteenth Paper: Photometric Catalogue of 848 Stars in Messier 3	140
DUNCAN, JOHN C. Bright Nebulae and Star Clusters in Sagittarius and Scutum Photographed with 60-Inch Reflector . . . . .	4
FORSYTHE, W. E., and EDWARD P. HYDE. Gold-Point Palladium-Point Brightness Ratio . . . . .	244
FROST, EDWIN B. Review of: <i>Advanced Lecture Notes on Light</i> , J. R. Eccles . . . . .	128
HAGEN, J. G. Problem of the $\delta$ Cephei Variables . . . . .	62
HARPER, W. E. Orbits of the Spectroscopic Components of Boss 5026	187
HULBURT, E. O. A Modification of the Electron Theory of Dispersion to Account for the Change of the Refractive Index with Temperature . . . . .	223
HYDE, EDWARD P., and W. E. FORSYTHE. Gold-Point Palladium-Point Brightness Ratio . . . . .	244
INGERSOLL, L. R. Polarization of Radiation by Gratings . . . . .	129
KING, ARTHUR S. Characteristics of Absorption Spectra Produced by the Electric Furnace . . . . .	13
Observations of the Electric Furnace Spectra of Cobalt, Nickel, Barium, Strontium, and Calcium in the Region of Greater Wave-Length. . . . .	179
Preliminary Observations of the Zeeman Effect for Electric Furnace Spectra . . . . .	107

	PAGE
LUNN, A. C. Review of: <i>Theorie der Strahlung und der Quanten</i> , Arthur March . . . . .	127
MACMILLAN, W. D. Review of: <i>Problems of Cosmogony and Stellar Dynamics</i> , J. H. Jeans . . . . .	309
MERRILL, PAUL W. Note on the Air Lines in Spark Spectra from $\lambda$ 5927 to $\lambda$ 8719 . . . . .	236
MICHELSON, A. A. On the Application of Interference Methods to Astronomical Measurements . . . . .	257
MOORE, A. F., and C. G. ABBOT. Observations of the Total Solar Eclipse of May 29, 1919. . . . .	I
NAGAOKA, H. Diffraction of a Telescopic Objective in the Case of a Circular Source of Light . . . . .	73
PEASE, FRANCIS G. Photographs of Nebulae with the 60-Inch Reflector, 1917-1919 . . . . .	276
RUFUS, W. CARL. Five Oe5 Stars with Variable Radial Velocities . . . . .	252
SAUNDERS, F. A. Revision of the Series in the Spectrum of Barium . . . . .	23
SHAPLEY, HARLOW. Studies Based on the Colors and Magnitudes in Stellar Clusters. Fifteenth Paper: A Photometric Analysis of the Globular System Messier 68 . . . . .	49
SHAPLEY, HARLOW, and HELEN N. DAVIS. Studies Based on the Colors and Magnitudes in Stellar Clusters. Sixteenth Paper: Photometric Catalogue of 848 Stars in Messier 3 . . . . .	140
STEBBINS, JOEL. Eclipsing Variable Star $\lambda$ Tauri . . . . .	193
Ellipsoidal Variable Star $\pi^s$ Orionis . . . . .	218
VOÛTE, J. Parallax of the B-Star Boss 1517 . . . . .	254

PAGE

127

100

36

157

1

73

76

52

23

19

10

15

8

4













This book should be returned to the Library on or before the last date stamped below.

A fine of five cents a day is imposed by retaining it beyond the specified time.

Please return promptly.





3 2044 059 981 837